Radio-Frequency and Microwave Communication Circuits: Analysis and Design
Devendra K. Misra

ISBNs: 0-471-41253-8 (Hardback); 0-471-22435-9 (Electronic)

RADIO-FREQUENCY AND MICROWAVE COMMUNICATION CIRCUITS

RADIO-FREQUENCY AND MICROWAVE COMMUNICATION CIRCUITS

ANALYSIS AND DESIGN

DEVENDRA K. MISRA

A WILEY–INTERSCIENCE PUBLICATION
JOHN WILEY & SONS, INC.
New York • Chichester • Weinheim • Brisbane • Singapore • Toronto

ISBN 0-471-22435-9

This title is also available in print as ISBN 0-471-41253-8.

For more information about Wiley products, visit our web site at www.Wiley.com.

CONTENTS

PREFACE

Wireless technology has been growing tremendously, with new applications reported almost every day. Besides the traditional applications in communication, such as radio and television, RF and microwaves are being used in cordless phones, cellular communication, local area networks (LANs), and personal communication systems (PCSs). Keyless door entry, radio frequency identification (RFID), monitoring of patients in a hospital or a nursing home, and cordless mice or keyboards for computers are some of the other areas where RF technology is being employed. While some of these applications have traditionally used infrared (IR) technology, radio frequency circuits are continuously taking over because of their superior performance. The current rate of growth in RF technology is expected to continue in the foreseeable future. These advances require personnel trained in radio frequency and microwave engineering. Therefore, besides regular courses as a part of electrical engineering curricula, short courses and workshops are regularly conducted in these areas for practicing engineers. I also introduced a course in this area over ten years ago to address the needs of local industry. Since the available textbooks generally assumed that students had more background in electrical circuits and electromagnetic fields than our curriculum provided, I developed the lecture notes for this class. Based on the input from our alumni, I added a second course as well. This book is based on the lecture notes that evolved over the past several years.

As mentioned above, the presentation of this book assumes only a basic course in electronic circuits as a prerequisite. Instead of using electromagnetic fields as most of the microwave engineering books do, the subject is introduced via circuit concepts. Further, an overview of communication systems is presented in the beginning to provide the reader with an overall perspective of the various building blocks involved.

The book is organised into twelve chapters and seven appendices, using a top-down approach. It begins with an introduction to frequency bands, RF and microwave devices, and applications in communication, radar, industrial, and biomedical areas. The introduction also includes a brief description of microwave transmission lines—waveguides, strip lines, and microstrip lines. Modern wireless communication systems, such as terrestrial and satellite communication systems and RF wireless services, are briefly discussed in Chapter 2. After introducing antenna terminology, effective isotropic radiated power (EIRP), the Friis transmission formula, and the radar range equation are presented. The final section of the chapter introduces noise and distortion associated with communication systems.

Chapter 3 starts with distributed circuits and the construction of solutions to the transmission line equation. Topics presented in this chapter include RF circuit analysis, phase and group velocities, sending end impedance, reflection coefficient, return loss, insertion loss, experimental determination of characteristic impedance and propagation constant, voltage standing wave ratio (VSWR), and measurement of impedance. The final section of this chapter includes a description of the Smith chart and its application in analysis of transmission line circuits.

Resonant circuits are discussed in Chapter 4, which begins with series and parallel resistance-inductance-capacitance (RLC) circuits. This is followed by a section on transformer-coupled circuits. The final two sections of this chapter are devoted to transmission line resonant circuits and microwave resonators. The next two chapters of the book deal with impedance matching techniques. Single reactive element or stub, double-stub, and lumped-element matching techniques are discussed in Chapter 5 while Chapter 6 is devoted to multisection transmission line impedance transformers. Chapter 6 includes binomial and Chebyshev sections as well as impedance tapers.

Chapter 7 introduces circuit parameters associated with two-port networks. Impedance, admittance, hybrid, transmission, scattering, and chain-scattering parameters are presented along with examples that illustrate their characteristic behaviors. Chapter 8 begins with the image parameter method for the design of passive filter circuits. The insertion loss technique is introduced next to synthesize Butterworth- and Chebyshev-type low-pass filters. It includes impedance and frequency scaling techniques to realize high-pass, band-pass, and band-stop networks. The chapter concludes with a section on microwave transmission line filter design.

Concepts of signal flow graph analysis are introduced in Chapter 9 along with a representation of voltage source and passive devices. It facilitates the formulation of power gain relations that are needed in the amplifier design discussed in the following chapter. Chapter 10 starts with stability considerations using scattering parameters of a two-port network. Design techniques of different amplifiers are then presented.

Chapter 11 presents basic concepts and design of various oscillator circuits. Concepts of the phase-locked loop and its application in the design of frequency synthesizers are also summarized. The final section of this chapter includes analysis and design of microwave transistor oscillators using s-parameters. Chapter 12 includes fundamentals of frequency division multiplexing, amplitude modulation,

radio frequency detection, frequency-modulated signals, and mixer circuits. The book ends with seven appendices that include a discussion of logarithmic units (dB, dBm, dBW, dBc, and neper), design equations for selected transmission lines (coaxial line, strip line, and microstrip line), and a list of abbreviations used in the communications area.

Some of the highlights of the book are as follows.

- The presentation starts with an overview of frequency bands, RF and microwave devices, and their applications in various areas. Communication systems are presented next in Chapter 2, which motivates students. It includes terrestrial and satellite systems, wireless services, antenna terminology, the Friis transmission formula, radar equation, and Doppler radar. Thus, students learn about the systems using blocks of amplifiers, oscillators, mixers, filters, and so on. Student response here has strongly supported this *top-down approach.*
- Since students are assumed to have had only one semester of electrical circuits, the resonant circuits and two-port networks are included in this book. Concepts of network parameters (impedance, admittance, hybrid, transmission, and scattering) and their characteristics are introduced via examples.
- A separate chapter on oscillator design includes concepts of feedback, Hartley oscillator, Colpitts oscillator, Clapp oscillator, crystal oscillators, PLL and frequency synthesizers, transistor oscillator design using s-parameters, and 3-port s-parameter description of transistors and their use in feedback network design.
- There is a separate chapter on the detectors and mixers that includes AM and FM signal characteristics and their detection schemes, single diode mixers, RF detectors, double-balanced mixers, conversion loss, intermodulation distortion in diode ring mixers, and FET mixers.
- Appendices include logarithmic units, design equations for selected transmission lines, and a list of abbreviations used in the communication area.
- There are over 130 solved examples with step-by-step explanations. Practicing engineers will find this text useful for self-study as well.
- There are nearly 200 class-tested problems. Supplementary material is available to instructors adopting the book. This includes an instructor's manual and access to a web page containing useful material, such as downloadable files used for solving the problems, reference material, and URLs of other useful sites.

ACKNOWLEDGMENTS

I learned this subject from engineers and authors who are too many to include in this short space. I would like to gratefully acknowledge their contributions. I would like to thank my anonymous reviewers, and my former students, who made several constructive suggestions to improve the presentation. I deeply appreciate the support I received from my wife Ila and son Shashank during the course of this project. This book became a reality only because of the enthusiastic support I received from Senior Editor Dr. Philip Meyler and his staff at John Wiley & Sons.

DEVENDRA K. MISRA

Radio-Frequency and Microwave Communication Circuits: Analysis and Design
Devendra K. Misra

ISBNs: 0-471-41253-8 (Hardback); 0-471-22435-9 (Electronic)

1

INTRODUCTION

Scientists and mathematicians of the nineteenth century laid the foundation of telecommunication and wireless technology, which has affected all facets of modern society. In 1864, James C. Maxwell put forth fundamental relations of electromagnetic fields that not only summed up the research findings of Laplace, Poisson, Faraday, Gauss, and others but also predicted the propagation of electrical signals through space. Heinrich Hertz subsequently verified this in 1887 and Guglielmo Marconi successfully transmitted wireless signals across the Atlantic Ocean in 1900. Interested readers may find an excellent reference on the historical developments of radio frequencies (RF) and microwaves in the *IEEE Transactions on Microwave Theory and Technique* (Vol. MTT-32, September 1984).

Wireless communication systems require high-frequency signals for the efficient transmission of information. There are several factors that lead to this requirement. For example, an antenna radiates efficiently if its size is comparable to the signal wavelength. Since the signal frequency is inversely related to its wavelength, antennas operating at radio frequencies and microwaves have higher radiation efficiencies. Further, their size is relatively small and hence convenient for mobile communication. Another factor to favor RF and microwaves is that the transmission of broadband information signals requires a high-frequency carrier signal. In the case of a single audio channel, the information bandwidth is about 20 kHz. If amplitude modulation is used to superimpose this information on a carrier then it requires at least this much bandwidth on one side of the spectrum. Further, commercial AM transmission requires a separation of 10 kHz between the two transmitters. On the other hand, the required bandwidth increases significantly if frequency modulation is used. Each FM transmitter typically needs a bandwidth of 200 kHz for audio transmission. Similarly, each television channel requires about

TABLE 1.1 Frequency Bands Used in Commercial Broadcasting

	Channels	Frequency Range	Wavelength Range
AM	107	535 kHz–1605 kHz	186.92 m–560.75 m
TV	2–4	54 MHz–72 MHz	4.17 m–5.56 m
	5–6	76 MHz–88 MHz	3.41 m–3.95 m
FM	100	88 MHz–108 MHz	2.78 m–3.41 m
TV	7–13	174 MHz–216 MHz	1.39 m–1.72 m
	14–83	470 MHz–890 MHz	33.7 cm–63.83 cm

6 MHz bandwidth to carry the video information as well. Table 1.1 shows the frequency bands used for commercial radio and television broadcasts.

In the case of digital transmission, a standard monochrome television picture is sampled over a grid of 512×480 elements that are called pixels. Eight bits are required to represent 256 shades of the gray display. In order to display motion, 30 frames are sampled per second. Thus, it requires about 59 Mb/s ($512 \times 480 \times 8 \times 30 = 58{,}982{,}400$). Color transmission requires even higher bandwidth (on the order of 90 Mb/s).

Wireless technology has been expanding very fast, with new applications reported every day. Besides the traditional applications in communication, such as radio and television, RF and microwave signals are being used in cordless phones, cellular communication, LAN, WAN, MAN, and PCS. Keyless door entry, radio-frequency identification (RFID), monitoring of patients in a hospital or a nursing home, and cordless mice or keyboards for computers are some of the other areas where RF technology is being applied. While some of these applications have traditionally used infrared (IR) technology, current trends are moving toward RF. The fact is that RF is superior to infrared technology in many ways. Unlike RF, infrared technology requires unobstructed line-of-sight connection. Although RF devices are more expensive in comparison with IR, this is expected to change soon as their production and use increases.

TABLE 1.2 IEEE Frequency Band Designations

Band Designation	Frequency Range	Wavelength Range (in free-space)
VLF	3–30 kHz	10 km–100 km
LF	30–300 kHz	1 km–10 km
MF	300–3000 kHz	100 m–1 km
HF	3–30 MHz	10 m–100 m
VHF	30–300 MHz	1 m–10 m
UHF	300–3000 MHz	10 cm–1 m
SHF	3–30 GHz	1 cm–10 cm
EHF	30–300 GHz	0.1 cm–1 cm

TABLE 1.3 Microwave Frequency Band Designations

Frequency Bands	Old (still widely used)	New (not so commonly used)
500–1000 MHz	UHF	C
1–2 GHz	L	D
2–4 GHz	S	E
3–4 GHz	S	F
4–6 GHz	C	G
6–8 GHz	C	H
8–10 GHz	X	I
10–12.4 GHz	X	J
12.4–18 GHz	Ku	J
18–20 GHz	K	J
20–26.5 GHz	K	K
26.5–40 GHz	Ka	K

The electromagnetic frequency spectrum is divided into bands as shown in Table 1.2. Hence, AM radio transmission operates in the medium frequency (MF) band; television channels 2–12 operate in the very high frequency (VHF) band; and channels 18–90 operate in ultra high frequency (UHF) band. Table 1.3 shows the band designations in the microwave frequency range.

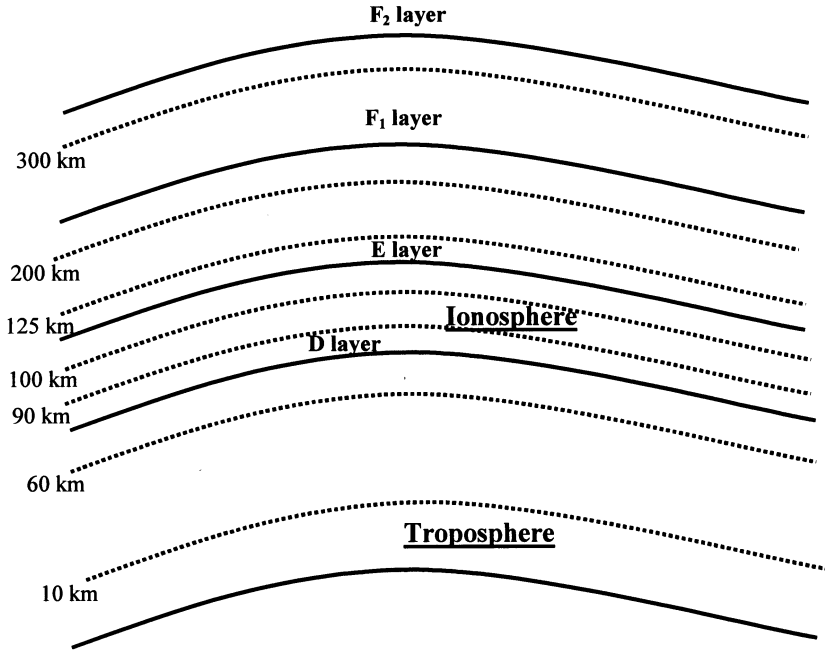

Figure 1.1 Atmosphere surrounding the earth.

Besides the natural and human-made changes, electrical characteristics of the atmosphere affect the propagation of electrical signals. Figure 1.1 shows various layers of the ionosphere and the troposphere that are formed due to the ionization of atmospheric air. As illustrated in Figure 1.2(a) and (b), a radio frequency signal can reach the receiver by propagating along the ground or after reflection from the ionosphere. These signals may be classified as *ground* and *sky waves*, respectively. Behavior of the sky wave depends on the season, day or night, and solar radiation. The ionosphere does not reflect microwaves and the signals propagate line-of-sight, as shown in Figure 1.2(c). Hence, curvature of the earth limits the range of a microwave communication link to less than 50 km. One way to increase the range is to place a human-made reflector up in the sky. This kind of arrangement is called the *satellite communication system*. Another way to increase the range of a microwave link is to place the repeaters at periodic intervals. This is known as the *terrestrial communication system*.

Figures 1.3 and 1.4 list selected devices used at RF and microwave frequencies. Solid-state devices as well as vacuum tubes are used as active elements in RF and microwave circuits. Predominant applications for microwave tubes are in radar, communications, electronic countermeasures (ECM), and microwave cooking. They are also used in particle accelerators, plasma heating, material processing, and power transmission. Solid-state devices are employed mainly in the RF region and in low-power microwave circuits, such as low-power transmitters for LAN, and receiver circuits. Some of the applications of solid-state devices are listed in Table 1.4.

Figure 1.5 lists some applications of microwaves. Besides terrestrial and satellite communications, microwaves are used in radar systems as well as in various industrial and medical applications. Civilian applications of radar include air-traffic control, navigation, remote sensing, and law enforcement. Its military uses include surveillance, guidance of weapons, and C^3 (command, control, and communication). Radio frequency and microwave energy is also used in industrial heating as well as household cooking. Since this process does not use a conduction mechanism for the heat transfer, it can improve the quality of certain products significantly. For example, the hot air used in a printing press to dry the ink adversely affects the paper and shortens its life span. On the other hand, only the ink portion is heated in microwave drying and the paper is barely affected by it. Microwaves are also used in material processing, telemetry, imaging, and hyperthermia.

1.1 MICROWAVE TRANSMISSION LINES

Figure 1.6 shows selected transmission lines used in RF and microwave circuits. The most common transmission line used in the RF and microwave range is the coaxial line. A low-loss dielectric material is used in these transmission lines to minimize the signal loss. Semirigid coaxial lines with continuous cylindrical conductors outside perform well in microwave range. In order to ensure single-mode transmission, the cross-section of a coaxial line must be much smaller in comparison with the signal wavelength. However, this limits the power capacity of these lines. In high-power

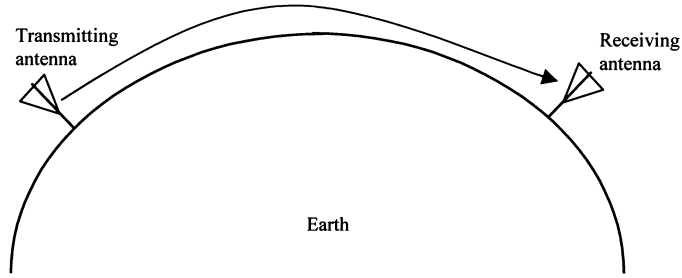

(a) Signal propagation along the ground

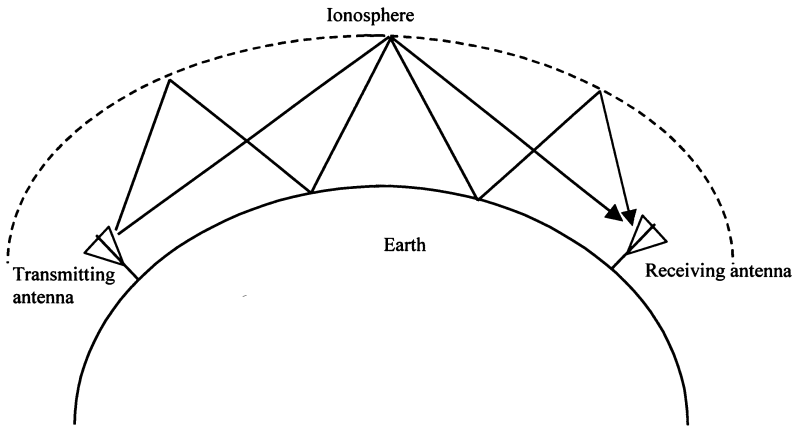

(b) Propagation of the sky wave

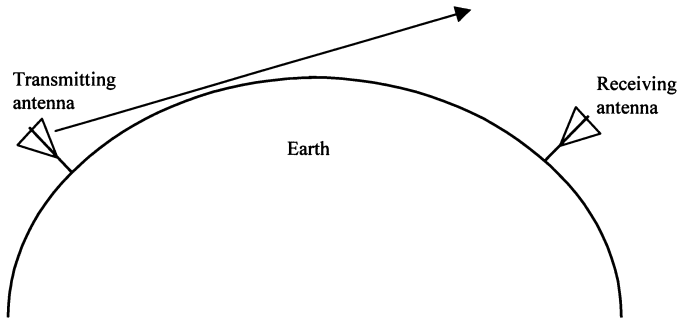

(c) Line-of-sight propagation

Figure 1.2 Modes of signal propagation.

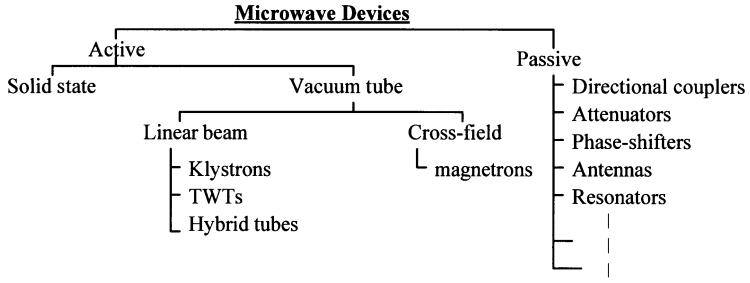

Figure 1.3 Microwave devices.

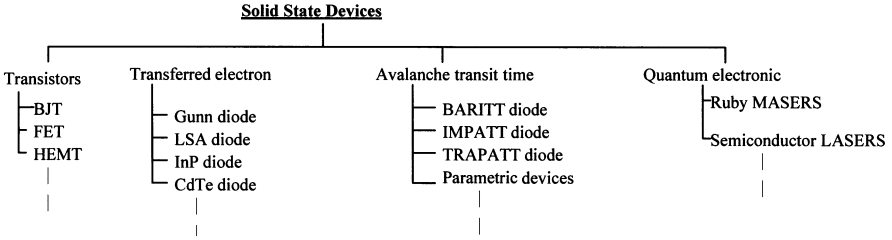

Figure 1.4 Solid-state devices used at RF and microwave frequencies.

TABLE 1.4 Selected Applications of Microwave Solid-State Devices

Devices	Applications	Advantages
Transistors	L-band transmitters for telemetry systems and phased-array radar systems; transmitters for communication systems	Low cost, low power supply, reliable, high CW power output, lightweight
TED	C, X, and Ku-band ECM amplifiers for wideband systems; X and Ku-band transmitters for radar systems, such as traffic control	Low power supply (12 V), low cost, lightweight, reliable, low noise, high gain
IMPATT	Transmitters for mm-wave communication	Low power supply, low cost, reliable, high CW power, lightweight
TRAPATT	S-band pulsed transmitter for phased-array radar systems	High peak and average power, reliable, low power supply, low cost
BARITT	Local oscillators in communication and radar receivers	Low power supply, low cost, low noise, reliable

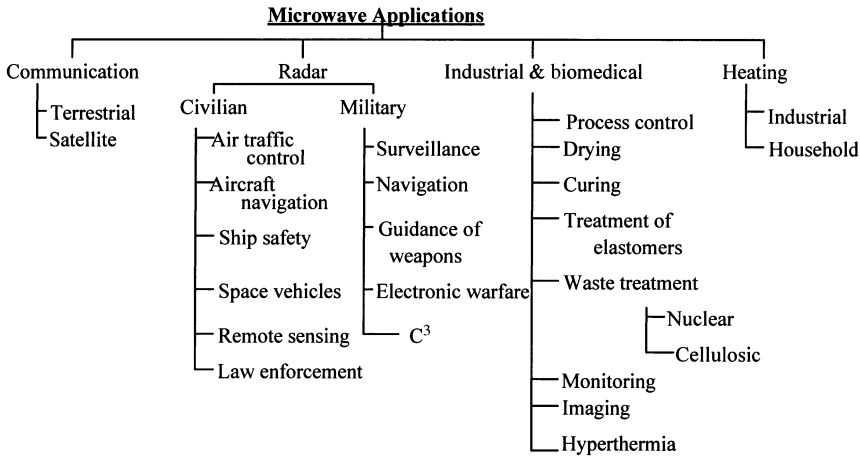

Figure 1.5 Some applications of microwaves.

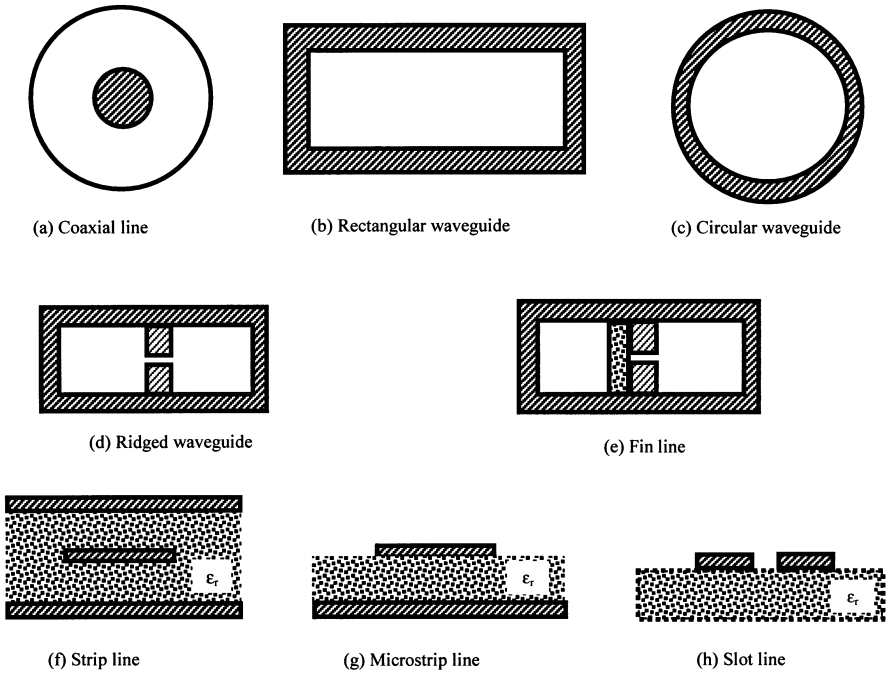

Figure 1.6 Transmission lines used in RF and microwave circuits.

microwave circuits, waveguides are used in place of coaxial lines. Rectangular waveguides are commonly employed for connecting the high-power microwave devices because these are easy to manufacture in comparison with circular waveguides. However, certain devices (such as rotary joints) require a circular cross-section. The ridged waveguide provides broadband operation in comparison with the rectangular one. The fin line shown in Figure 1.6 (e) is commonly used in the mm-wave band. Physically, it resembles a combination of slot line enclosed in a rectangular waveguide.

The transmission lines illustrated in Figure 1.6 (f)–(h) are most convenient in connecting the circuit components on a printed circuit board (PCB). The physical dimensions of these transmission lines are dependent on the dielectric constant ε_r of insulating material and on the operating frequency band. The characteristics and design formulas of selected transmission lines are given in the appendices. Chapter 2 provides an overview of wireless communication systems and their characteristics.

Radio-Frequency and Microwave Communication Circuits: Analysis and Design
Devendra K. Misra

ISBNs: 0-471-41253-8 (Hardback); 0-471-22435-9 (Electronic)

2

COMMUNICATION SYSTEMS

Modern communication systems require radio frequency and microwave signals for the wireless transmission of information. These systems employ oscillators, mixers, filters, and amplifiers to generate and process various kinds of signals. The transmitter communicates with the receiver via antennas placed on each side. Electrical noise associated with the systems and the channel affects the performance. A system designer needs to know about the channel characteristics and system noise in order to estimate the required power levels. This chapter begins with an overview of microwave communication systems and the radio frequency wireless services to illustrate the applications of circuits and devices that are described in the following chapters. It also gives an idea to the reader about the placement of different building blocks in a given system.

A short discussion on antennas is included to help in understanding the signal behavior when it propagates from transmitter to receiver. The Friis transmission formula and the radar range equation are important in order to understand effects of frequency, range, and operating power levels on the performance of a communication system. Note that radar concepts now find many other applications, such as proximity or level sensing in an industrial environment. Therefore, a brief discussion on Doppler radar is also included in this chapter. Noise and distortion characteristics play a significant role in analysis and design of these systems. Minimum detectable signal (MDS), gain compression, intercept-point, and the dynamic range of an amplifier (or the receiver) are subsequently introduced. Other concepts associated with noise and distortion characteristics are also introduced in this chapter.

2.1 TERRESTRIAL COMMUNICATION

As mentioned in the preceding chapter, microwave signals propagate along the line-of-sight. Therefore, the earth-curvature limits the range over which a microwave communication link can be established. A transmitting antenna sitting on a 25-foot-high tower can typically communicate only up to a distance of about 50 km. The repeaters can be placed at regular intervals to extend the range. Figure 2.1 illustrates the block diagram of a typical repeater.

The repeater system operates as follows. A microwave signal arriving at antenna A works as input to port 1 of the circulator. It is directed to port 2 without loss, assuming that the circulator is ideal. Then it passes through the receiver protection circuit that limits the magnitude of large signals but passes those of low intensity with negligible attenuation. The purpose of this circuit is to block excessively large signals from reaching the receiver input. The mixer following it works as a down-converter that transforms a high-frequency signal to a low frequency one, typically in the range of 70 MHz. The Schottky diode is generally employed in the mixer because of its superior noise characteristics. This frequency conversion facilitates amplification of the signal economically. A band-pass filter is used at the output of the mixer to stop undesired harmonics. An intermediate frequency (IF) amplifier is

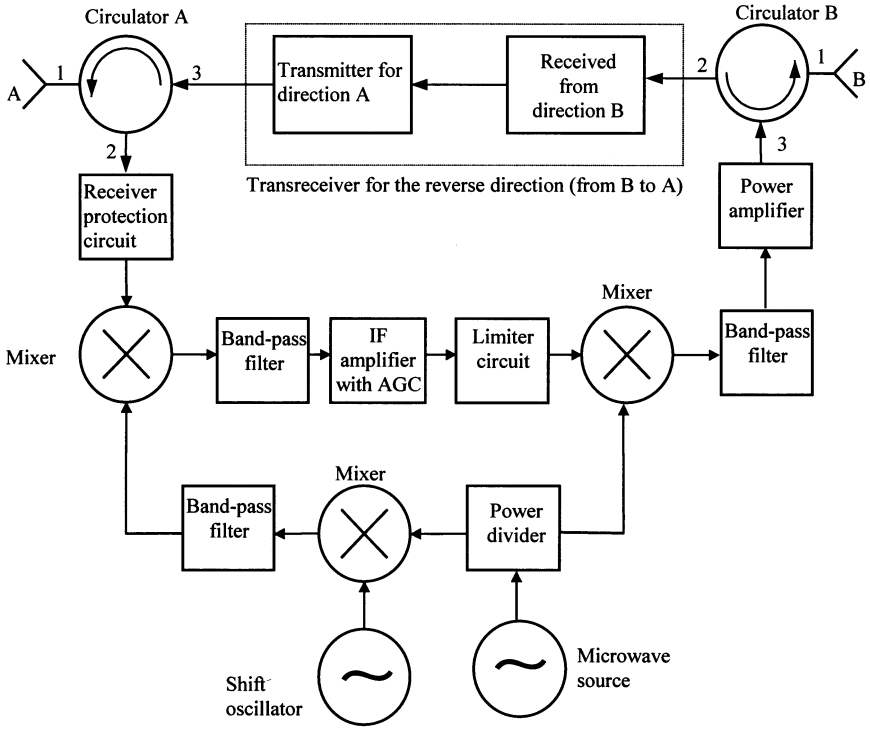

Figure 2.1 Block arrangement of a repeater system.

then used to amplify the signal. It is generally a low-noise solid-state amplifier with ultralinear characteristics over a broadband. The amplified signal is mixed again with another signal for up-conversion of frequency. After filtering out undesired harmonics introduced by the mixer it is fed to a power amplifier stage that feeds circulator B for onward transmission through antenna B. This up-converting mixer circuit generally employs the varactor diode. Circulator B directs the signal entering at port 3 to the antenna connected at its port 1. Similarly, the signal propagating upstream is received by antenna B and the circulator directs it toward port 2. It then goes through the processing as described for the downstream signal and is radiated by antenna A for onward transmission. Hence, the downstream signal is received by antenna A and transmitted in the forward direction by antenna B. Similarly, the upstream signal is received by antenna B and forwarded to the next station by antenna A. The two circulators help channel the signal in the correct direction.

A parabolic antenna with tapered horn as primary feeder is generally used in microwave links. This kind of composite antenna system, known as the hog-horn, is fairly common in high-density links because of its broadband characteristics. These microwave links operate in the frequency range of 4–6 GHz, and signals propagating in two directions are separated by a few hundred megahertz. Since this frequency range overlaps with the C-band satellite communication, their interference needs to be taken into design consideration. A single frequency can be used twice for transmission of information using vertical and horizontal polarization.

2.2 SATELLITE COMMUNICATION

The ionosphere does not reflect microwaves as it does radio frequency signals. However, one can place a conducting object (satellite) up in the sky that reflects them back to earth. A satellite can even improve the signal quality using on-board electronics before transmitting it back. The gravitational force needs to be balanced somehow if this object is to stay in position. An orbital motion provides this balancing force. If a satellite is placed at low altitude then greater orbital force will be needed to keep it in position. These low- and medium-altitude satellites are visible from a ground station only for short periods. On the other hand, a satellite placed at an altitude of about 36,000 km over the equator is visible from its shadow all the time. These are called *geosynchronous* or *geostationary satellites*.

C-band geosynchronous satellites use between 5725 MHz and 7075 MHz for their uplinks. The corresponding downlinks are between 3400 MHz and 5250 MHz. Table 2.1 lists the downlink center frequencies of a 24-channel transponder. Each channel has a total bandwidth of 40 MHz; 36 MHz of that carries the information and the remaining 4 MHz is used as a guard-band. It is accomplished with a 500-MHz bandwidth using different polarization for the overlapping frequencies. The uplink frequency plan may be found easily after adding 2225 MHz to these downlink frequencies. Figure 2.2 illustrates the simplified block diagram of a C-band satellite transponder.

TABLE 2.1 C-Band Downlink Transponder Frequencies

Horizontal Polarization		Vertical Polarization	
Channel	Center Frequency (MHz)	Channel	Center Frequency (MHz)
1	3720	2	3740
3	3760	4	3780
5	3800	6	3820
7	3840	8	3860
9	3880	10	3900
11	3920	12	3940
13	3960	14	3980
15	4000	16	4020
17	4040	18	4060
19	4080	20	4100
21	4120	22	4140
23	4160	24	4180

A 6-GHz signal received from the earth station is passed through a band-pass filter before amplifying it through a low-noise amplifier (LNA). It is then mixed with a local oscillator (LO) signal to bring down its frequency. A band-pass filter that is connected right after the mixer filters out the unwanted frequency components. This signal is then amplified by a traveling wave tube (TWT) amplifier and transmitted back to the earth.

Another frequency band in which satellite communication has been growing continuously is the Ku-band. The geosynchronous Fixed Satellite Service (FSS) generally operates between 10.7 and 12.75 GHz (space to earth) and 13.75 to 14.5 GHz (earth to space). It offers the following advantages over the C-band:

- The size of the antenna can be smaller (3 feet or even smaller with higher-power satellites) against 8 to 10 feet for C-band.
- Because of higher frequencies used in the up- and downlinks, there is no interference with C-band terrestrial systems.

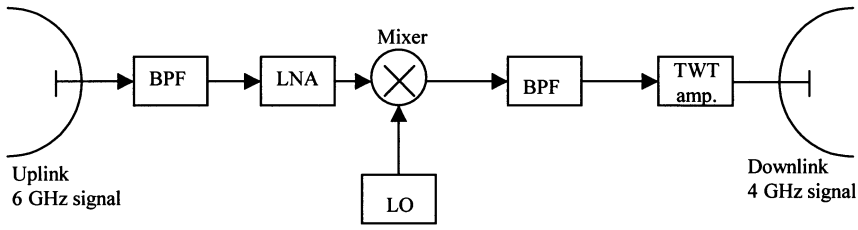

Figure 2.2 Simplified block-diagram of a transponder.

Since higher-frequency signals attenuate faster while propagating through adverse weather (rain, fog, etc.), Ku-band satellites suffer from this major drawback. Signals with higher powers may be used to compensate for this loss. Generally, this power is of the order of 40 to 60 W. The high-power direct broadcast satellite (DBS) system uses power amplifiers in the range of 100 to 120 W.

The National Broadcasting Company (NBC) has been using the Ku-band to distribute its programming to its affiliates. Also, various news-gathering agencies have used this frequency band for some time. Convenience stores, auto parts distributors, banks, and other businesses have used the very small aperture terminal (VSAT) because of its small antenna size (typically, on the order of three feet in diameter). It offers two-way satellite communication; usually back to hub or headquarters. The Public Broadcasting Service (PBS) uses VSATs for exchanging information among the public schools.

Direct broadcast satellites (DBSs) have been around since 1980, but early DBS ventures failed for various reasons. In 1991, Hughes Communications entered into the direct-to-home (DTH) television business. DirecTV was formed as a unit of GM Hughes, with DBS-1 launched in December 1993. Its longitudinal orbit is at 101.2°W and it employs a left-handed circular polarization. Subsequently, DBS-2 was launched in August 1994. It uses a right-handed circular polarization and its orbital longitude is at 100.8°W. DirecTV employs a digital architecture that can utilize video and audio compression techniques. It complies with the MPEG-2 (Motion Picture Experts Group). By using compression ratios 5 to 7, over 150 channels of programs are available from the two satellites. These satellites include 120-W traveling wave tube (TWT) amplifiers that can be combined to form eight pairs at 240 W power. This higher power can also be utilized for high-definition television (HDTV) transmission. Earth-to-satellite link frequency is 17.3 to 17.8 GHz while satellite-to-earth link uses the 12.2- to 12.7-GHz band. Circular polarization is used because it is less affected by rain than linear orthogonal (HP and VP) polarization.

Several communication services are now available that use low-earth-orbit satellites (LEOS) and medium-earth-orbit satellites (MEOS). LEOS altitudes range from 750 km to 1500 km while MEOS systems have an altitude around 10350 km. These services compete with or supplement the cellular systems and geosynchronous earth-orbit satellites (GEOS). The GEOS systems have some drawbacks due to the large distances involved. They require relatively large powers and the propagation time-delay creates problems in voice and data transmissions. The LEOS and MEOS systems orbit the earth faster because of being at lower altitudes and, therefore, these are visible only for short periods. As Table 2.2 indicates, several satellites are used in a personal communication system to solve this problem.

Three classes of service can be identified for mobile satellite services:

1. Data transmission and messaging from very small, inexpensive satellites
2. Voice and data communications from big LEOS
3. Wideband data transmission

TABLE 2.2 Specifications of Certain Personal Communication Satellites

	Iridium (LEO)†	Globalstar (LEO)	Odyssey (MEO)
No. of satellites	66	48	12
Altitude (km)	755	1,390	10,370
Uplink (GHz)	1.616–1.6265	1.610–1.6265	1.610–1.6265
Downlink (GHz)	1.616–1.6265	2.4835–2.500	2.4835–2.500
Gateway terminal uplink	27.5–30.0 GHz	C-band	29.5–30.0 GHz
Gateway terminal downlink	18.8–20.2 GHz	C-band	19.7–20.2 GHz
Average sat. connect time	9 min.	10–12 min.	2 hrs.
Features of handset			
Modulation	QPSK	QFPSK	QPSK
BER	1E-2 (voice)	1E-3 (voice)	1E-3 (voice)
	1E-5 (data)	1E-5 (data)	1E-5 (data)
Supportable data rate	4.8 (voice)	1.2–9.6 (voice & data)	4.8 (voice)
(Kbps)	2.4 (data)		1.2–9.6 (data)

† It is going out-of-service because of its excessive operational costs.

Another application of L-band microwave frequencies (1227.60 MHz and 1575.42 MHz) is in the global positioning system (GPS). It uses a constellation of 24 satellites to determine a user's geographical location. Two services are available: the standard positioning service (SPS) for civilian use, utilizing a single frequency course/acquisition (C/A) code, and the precise positioning service (PPS) for the military, utilizing a dual-frequency P-code (protected). These satellites are at an altitude of 10,900 miles above the earth with their orbital period of 12 hours.

2.3 RADIO FREQUENCY WIRELESS SERVICES

A lot of exciting wireless applications are reported frequently that use voice and data communication technologies. Wireless communication networks consist of microcells that connect people with truly global, pocketsize communication devices, telephones, pagers, personal digital assistants, and modems. Typically, a cellular system employs a 100-W transmitter to cover a cell of 0.5 to 10 miles in radius. The handheld transmitter has a power of less than 3 W. Personal communication networks (PCN/PCS) operate with a 0.01- to 1-W transmitter to cover a cell radius of less than 450 yards. The handheld transmitter power is typically less than 10 mW. Table 2.3 shows the cellular telephone standards of selected systems.

There have been no universal standards set for wireless personal communication. In North America, cordless has been CT-0 (an analog 46/49 MHz standard) and cellular AMPS (Advanced Mobile Phone Service) operating at 800 MHz. The situation in Europe has been far more complex; every country has had its own standard. While cordless was nominally CT-0, different countries used their own frequency plans. This led to a plethora of new standards. These include, but are not

TABLE 2.3 Selected Cellular Telephones

		Analog Cellular		Digital Cellular Phones			
Standard		AMP	ETACS	NADC (IS-54)	NADC (IS-95)	GSM	PDC
Frequency range	Tx	824–849	871–904	824–849	824–849	890–915	940–956 1177–1501
(MHz)	Rx	869–894	916–949	869–894	869–894	935–960	810–826 1429–1453
Transmitter's power (max.)				600 mW	200 mW	1 W	
Multiple access		FDMA	FDMA	TDMA/FDM	CDMA/FDM	TDMA/FDM	TDMA/FDM
Number of channels		832	1000	832	20	124	1600
Channel spacing (kHz)		30	25	30	1250	200	25
Modulation		FM	FM	$\pi/4$ DQPSK	BPSK/0QPSK	GMSK	$\pi/4$ DQPSK
Bit rate (kb/s)		–	–	48.6	1228.8	270.833	42

TABLE 2.4 Selected Cordless Telephones

	Analog Cordless		Digital Cordless Phones		
Standards	CT-0	CT-1 & CT-1+	CT-2 & CT-2+	DECT	PHS (Formerly PHP)
Frequency range (MHz)	46/49	CT-1: 915/960 CT-1+: 887–932	CT-1: 864–868 CT-2+: 930/931 940/941	1880–1990	1895–1907
Transmitter's power (max.)			10 mW & 80 mW	250 mW	80 mW
Multiple access	FDMA	FDMA	TDMA/FDM	TDMA/FDM	TDMA/FDM
Number of channels	10–20	CT-1: 40 CT-1+: 80	40	10 (12 users per channel)	300 (4 users per channels)
Channel spacing (kHz)	40	25	100	1728	300
Modulation	FM	FM	GFSK	GFSK	$\pi/4$ DQPSK
Bit rate (kb/s)	–	–	72	1152	384

limited to, CT-1, CT-1+, DECT (Digital European Cordless Telephone), PHP (Personal Handy Phone, in Japan), E-TACS (Extended Total Access Communication System, in UK), NADC (North American Digital Cellular), GSM (Global System for Mobile Communication), and PDC (Personal Digital Cellular). Specifications of selected cordless telephones are given in Table 2.4.

2.4 ANTENNA SYSTEMS

Figure 2.3 illustrates some of the antennas that are used in communication systems. These can be categorized into two groups—wire antennas and the aperture-type antennas. Electric dipole, monopole, and loop antennas belong to the former group whereas horn, reflector, and lens belong to the latter category. The aperture antennas can be further subdivided into primary and secondary (or passive) antennas. Primary antennas are directly excited by the source and can be used independently for transmission or reception of signals. On the other hand, a secondary antenna requires another antenna as its feeder. Horn antennas fall in first category whereas the reflector and lens belong to the second. Various kinds of horn antennas are commonly used as feeders in reflector and lens antennas.

When an antenna is energized, it generates two types of electromagnetic fields. Part of the energy stays nearby and part propagates outward. The propagating signal represents the radiation fields while the nonpropagating is reactive (capacitive or inductive) in nature. Space surrounding the antenna can be divided into three regions. The reactive fields dominate in the nearby region but reduce in strength at a faster rate in comparison with those associated with the propagating signal. If the largest dimension of an antenna is D and the signal wavelength is λ then reactive fields dominate up to about $0.62\sqrt{(D^3/\lambda)}$ and diminish after $2D^2/\lambda$. The region beyond $2D^2/\lambda$ is called the far field (or radiation field) region.

Power radiated by an antenna per unit solid angle is known as the radiation intensity U. It is a far field parameter that is related to power density (power per unit area) W_{rad} and distance r as follows:

$$U = r^2 W_{\text{rad}} \tag{2.4.1}$$

Directive Gain and Directivity

If an antenna radiates uniformly in all directions then it is called an *isotropic antenna*. This is a hypothetical antenna that helps in defining the characteristics of a real one. The directive gain D_{G} is defined as the ratio of radiation intensity due to the test antenna to that of an isotropic antenna. It is assumed that total radiated power remains the same in the two cases. Hence,

$$D_{\text{G}} = \frac{U}{U_{\text{o}}} = \frac{4\pi U}{P_{\text{rad}}} \tag{2.4.2}$$

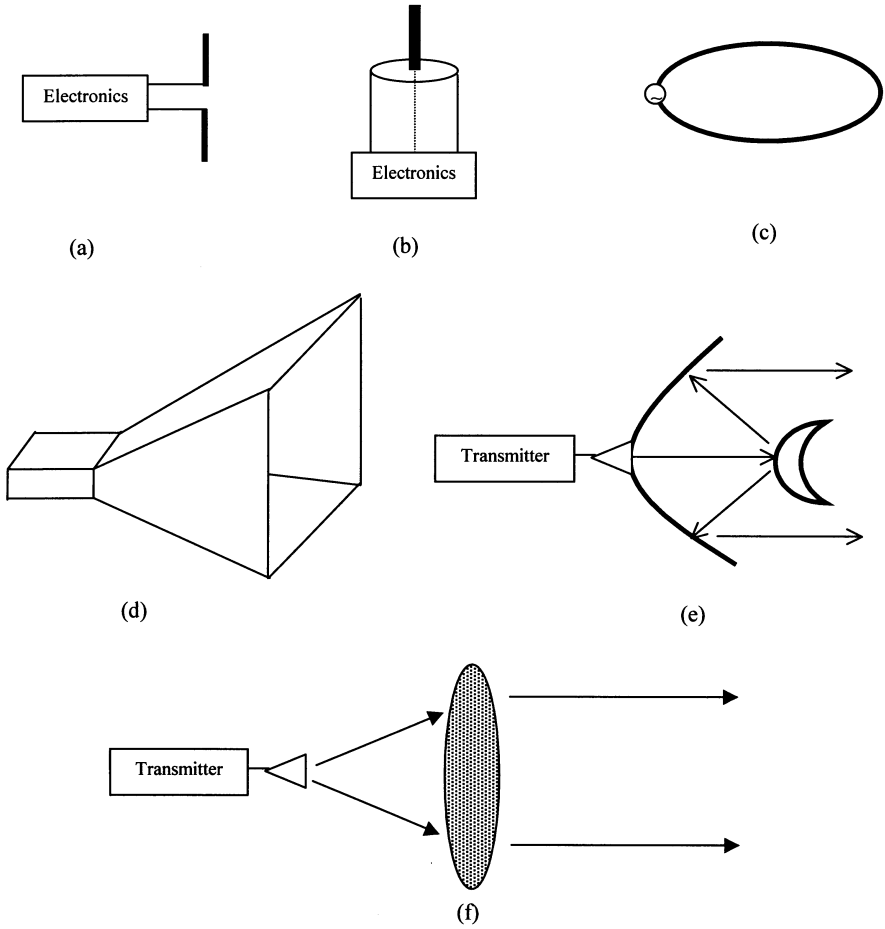

Figure 2.3 Some commonly used antennas: (a) electric dipole, (b) monopole, (c) loop, (d) pyramidal horn, (e) cassegrain reflector, and (f) lens.

where

U = radiation intensity due to the test antenna, in watts-per-unit solid angle
U_o = radiation intensity due to the isotropic antenna, in watts-per-unit solid angle
P_{rad} = total radiated power in watts

Since U is a directional dependent quantity, the directive gain of an antenna depends on the angles θ and ϕ. If the radiation intensity assumes its maximum value

then the directive gain is called the directivity D_o. That is,

$$D_o = \frac{U_{max}}{U_o} = \frac{4\pi U_{max}}{P_{rad}} \tag{2.4.3}$$

Gain of an Antenna

Power gain of an antenna is defined as the ratio of its radiation intensity at a point to the radiation intensity that results from a uniform radiation of the same input power. Hence,

$$\text{Gain} = 4\pi \frac{\text{Radiation intensity}}{\text{Total input power}} = 4\pi \frac{U(\theta, \phi)}{P_{in}} \tag{2.4.4}$$

Most of the time, we deal with relative gain. It is defined as a ratio of the power gain of the test antenna in a given direction to the power gain of a reference antenna. Both antennas must have the same input power. The reference antenna is usually a dipole, horn, or any other antenna whose gain can be calculated or is known. However, the reference antenna is a lossless isotropic source in most cases. Hence,

$$\text{Gain} = 4\pi \frac{U(\theta, \phi)}{P_{in}(\text{Lossless isotropic antenna})} \tag{2.4.5}$$

When the direction is not stated, the power gain is usually taken in the direction of maximum radiation.

Radiation Patterns and Half-Power Beam Width (HPBW)

Far-field power distribution at a distance r from the antenna depends upon the spatial coordinates θ and ϕ. Graphical representations of these distributions on the orthogonal plane (θ-plane or ϕ-plane) at a constant distance r from the antenna are called its radiation patterns. Figure 2.4 illustrates the radiation pattern of the vertical dipole antenna with θ. Its ϕ-plane pattern can be found after rotating it about the vertical axis. Thus, a three-dimensional picture of the radiation pattern of a dipole is doughnut shaped. Similarly, the power distributions of other antennas generally show peaks and valleys in the radiation zone. The highest peak between the two valleys is known as the *main lobe* while the others are called the *side-lobes*. The total angle about the main peak over which power reduces by 50 percent of its maximum value is called the *half-power beam width* on that plane.

The following relations are used to estimate the power gain G and the half-power beam width HPBW (or BW) of an aperture antenna

$$G = \frac{4\pi}{\lambda^2} A_e = \frac{4\pi}{\lambda^2} A\kappa \tag{2.4.6}$$

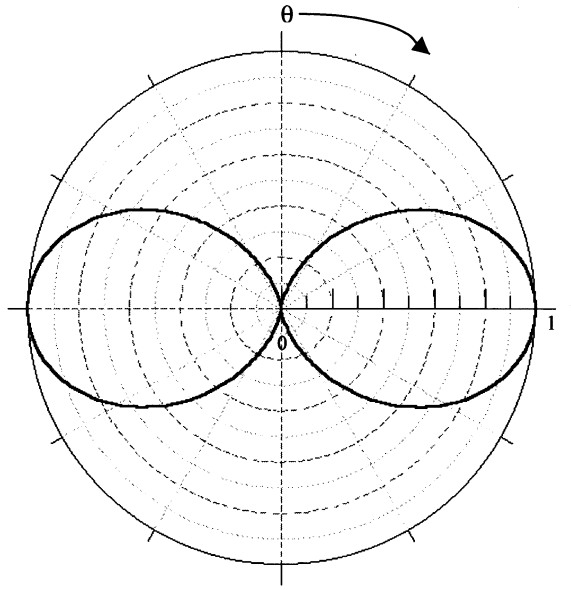

Figure 2.4 Radiation pattern of a dipole in the vertical (θ) plane.

and,

$$BW \text{ (in degree)} = \frac{65 \times \lambda}{d} \tag{2.4.7}$$

where A_e is the effective area of the radiating aperture in square meters; A is its physical area ($\pi \times d^2/4$, for a reflector antenna dish with its diameter d); κ is the efficiency of the antenna (ranges from 0.6 to 0.65); and λ is the signal wavelength in meters.

Example 2.1: Calculate the power gain (in dB) and the half-power beam width of a parabolic dish antenna of 30 m in diameter that is radiating at 4 GHz.

Signal wavelength and area of the aperture are

$$\lambda = \frac{3 \times 10^8}{4 \times 10^9} = 0.075 \text{ m}$$

and

$$A = \frac{\pi d^2}{4} = \pi \frac{30^2}{4} = 706.8584 \text{ m}^2$$

Assuming that the aperture efficiency is 0.6, the antenna gain and the half-power beam width are found as follows:

$$G = \frac{4\pi}{(0.075)^2} \times 706.8584 \times 0.6 = 947482.09 = 10\log_{10}(947482.09)$$
$$= 59.76 \approx 60 \text{ dB}$$
$$BW = \frac{65 \times 0.075}{30} = 0.1625 \text{ deg.}$$

Antenna Efficiency

If an antenna is not matched with its feeder then a part of the signal available from the source is reflected back. It is considered as the reflection (or mismatch) loss. The reflection (or mismatch) efficiency is defined as a ratio of power input to the antenna to that of power available from the source. Since the ratio of reflected power to that of power available from the source is equal to the square of the magnitude of voltage reflection coefficient, the reflection efficiency e_r is given by

$$e_r = 1 - |\Gamma|^2$$
$$\Gamma = \text{Voltage reflection coefficient} = \frac{Z_A - Z_o}{Z_A + Z_o}$$

where Z_A is the antenna impedance and Z_o is the characteristic impedance of the feeding line.

Besides mismatch, the signal energy may dissipate in an antenna due to imperfect conductor or dielectric material. These efficiencies are hard to compute. However, the combined conductor and dielectric efficiency e_{cd} can be experimentally determined after measuring the input power P_{in} and the radiated power P_{rad}. It is given as

$$e_{cd} = \frac{P_{rad}}{P_{in}}$$

The overall efficiency e_o is a product of the above efficiencies. That is,

$$e_o = e_r e_{cd} \tag{2.4.8}$$

Example 2.2: A 50-Ω transmission line feeds a lossless one-half-wavelength-long dipole antenna. Antenna impedance is 73 Ω. If its radiation intensity, $U(\theta, \phi)$, is given as follows, find the maximum overall gain.

$$U = B_o \sin^3(\theta)$$

The maximum radiation intensity, $U_{\max}$, is B_o that occurs at $\theta = \pi/2$. Its total radiated power is found as follows:

$$P_{\text{rad}} = \int_0^{2\pi} \int_0^{\pi} B_o \sin^3 \theta \sin\theta \, d\theta \, d\phi = \frac{3}{4}\pi^2 B_o$$

Hence,

$$D_o = 4\pi \frac{U_{\max}}{P_{\text{rad}}} = \frac{4\pi B_o}{\frac{3}{4}\pi^2 B_o} = \frac{16}{3\pi} = 1.6977$$

or,

$$D_o(\text{dB}) = 10 \log_{10}(1.6977)\text{dB} = 2.2985 \text{ dB}$$

Since the antenna is lossless, the radiation efficiency e_{cd} is unity (0 dB). Its mismatch efficiency is computed as follows.

Voltage reflection coefficient at its input (it is formulated in the following chapter) is

$$\Gamma = \frac{Z_A - Z_o}{Z_A + Z_o} = \frac{73 - 50}{73 + 50} = \frac{23}{123}$$

Therefore, the mismatch efficiency of the antenna is

$$e_r = 1 - (23/123)^2 = 0.9650 = 10 \log_{10}(0.9650)\text{dB} = -0.1546 \text{ dB}$$

The overall gain G_o (in dB) is found as follows:

$$G_o(\text{dB}) = 2.2985 - 0 - 0.1546 = 2.1439 \text{ dB}$$

Bandwidth

Antenna characteristics, such as gain, radiation pattern, impedance, and so on, are frequency dependent. The bandwidth of an antenna is defined as the frequency band over which its performance with respect to some characteristic (HPBW, directivity, etc.) conforms to a specified standard.

Polarization

Polarization of an antenna is same as the polarization of its radiating wave. It is a property of the electromagnetic wave describing the time varying direction and relative magnitude of the electric field vector. The curve traced by the instantaneous

electric field vector with time is the polarization of that wave. The polarization is classified as follows:

- *Linear polarization:* If the tip of the electric field intensity traces a straight line in some direction with time then the wave is linearly polarized.
- *Circular polarization:* If the end of the electric field traces a circle in space as time passes then that electromagnetic wave is circularly polarized. Further, it may be right-handed circularly polarized (RHCP) or left-handed circularly polarized (LHCP), depending on whether the electric field vector rotates clockwise or counterclockwise.
- *Elliptical polarization:* If the tip of the electric field intensity traces an ellipse in space as time lapses then the wave is elliptically polarized. As in the preceding case, it may be right-handed or left-handed elliptical polarization (RHEP and LHEP).

In a receiving system, the polarization of the antenna and the incoming wave need to be matched for maximum response. If this is not the case then there will be some signal loss, known as *polarization loss*. For example, if there is a vertically polarized wave incident on a horizontally polarized antenna then the induced voltage available across its terminals will be zero. In this case, the antenna is *cross-polarized with incident wave*. The square of the cosine of the angle between wave-polarization and antenna-polarization is a measure of the polarization loss. It can be determined by squaring the scalar product of unit vectors representing the two polarizations.

Example 2.3: The electric field intensity of an electromagnetic wave propagating in a lossless medium in z-direction is given by

$$\vec{E}(\vec{r}, t) = \hat{x}E_{\mathrm{o}}(x,\ y)\cos(\omega t - kz)\ \mathrm{V/m}$$

It is incident upon an antenna that is linearly polarized as follows:

$$\vec{E}_{\mathrm{a}}(\vec{r}) = (\hat{x} + \hat{y})E(x,\ y,\ z)\ \mathrm{V/m}$$

Find the polarization loss factor.

In this case, the incident wave is linearly polarized along the x-axis while the receiving antenna is linearly polarized at 45° from it. Therefore, one-half of the incident signal is cross-polarized with the antenna. It is determined mathematically as follows.

The unit vector along the polarization of incident wave is

$$\hat{u}_{\mathrm{i}} = \hat{x}$$

The unit vector along the antenna polarization may be found as

$$\hat{u}_a = \frac{1}{\sqrt{2}}(\hat{x} + \hat{y})$$

Hence, the polarization loss factor is

$$|\hat{u}_i \bullet \hat{u}_a|^2 = 0.5 = -3.01 \text{ dB}$$

Effective Isotropic Radiated Power (EIRP)

EIRP is a measure of power gain of the antenna. It is equal to the power needed by an isotropic antenna that provides the same radiation intensity at a given point as the directional antenna. If power input to the feeding line is P_t and the antenna gain is G_t then EIRP is defined as follows:

$$\text{EIRP} = \frac{P_t G_t}{L} \tag{2.4.10}$$

where L is the input-to-output power ratio of transmission line that is connected between the output of the final power amplifier stage of the transmitter and the antenna. It is given by

$$L = \frac{P_t}{P_{ant}} \tag{2.4.10}$$

Alternatively, the EIRP can be expressed in dBw as follows:

$$\text{EIRP(dBw)} = P_t(\text{dBw}) - L(\text{dB}) + G(\text{dB}) \tag{2.4.11}$$

Example 2.4: In a transmitting system, output of its final high-power amplifier is 500 W and the line feeding its antenna has an attenuation of 20 percent. If gain of the transmitting antenna is 60 dB, find EIRP in dBw.

$$P_t = 500 \text{ W} = 26.9897 \text{ dBw}$$
$$P_{ant} = 0.8 \times 500 = 400 \text{ W}$$
$$G = 60 \text{ dB} = 10^6$$

and,

$$L = \frac{500}{400} = 1.25 = 10 \log_{10}(1.25) = 0.9691 \text{ dB}$$

Hence,

$$\text{EIRP(dBw)} = 26.9897 - 0.9691 + 60 = 86.0206 \text{ dBw}$$

or,

$$\text{EIRP} = \frac{500 \times 10^6}{1.25} = 400 \times 10^6 \text{ W}$$

Space Loss

The transmitting antenna radiates in all directions depending upon its radiation characteristics. However, the receiving antenna receives only the power that is incident on it. Hence, the rest of the power is not used and is lost in space. It is represented by the *space loss*. It can be determined as follows.

Power density w_t of a signal transmitted by an isotropic antenna is given by

$$w_t = \frac{P_t}{4\pi R^2} \text{ W/m}^2 \tag{2.4.12}$$

where P_t is the transmitted power in watts and R is the distance from the antenna in meters. The power received by a unity gain antenna located at R is found to be

$$P_r = w_t A_{eu} \tag{2.4.13}$$

where A_{eu} is the effective area of an isotropic antenna.

From (2.4.6), for an isotropic antenna

$$G = \frac{4\pi}{\lambda^2} A_{eu} = 1$$

or,

$$A_{eu} = \frac{\lambda^2}{4\pi}$$

Hence, (2.4.12) can be written as

$$P_r = \frac{P_t}{4\pi R^2} \times \frac{\lambda^2}{4\pi} \tag{2.4.14}$$

and the space loss ratio is found to be

$$\frac{P_r}{P_t} = \left(\frac{\lambda}{4\pi R}\right)^2 \tag{2.4.15}$$

It is usually expressed in dB as follows:

$$\text{Space loss ratio} = 20\log_{10}\left(\frac{\lambda}{4\pi R}\right)\text{dB} \tag{2.4.16}$$

Example 2.5: A geostationary satellite is 35 860 km away from the earth's surface. Find the space loss ratio if it is operating at 4 GHz.

$$R = 35860000 \text{ m}$$

and,

$$\lambda = \frac{3 \times 10^8}{4 \times 10^9} = 0.075 \text{ m}$$

Hence,

$$\text{Space loss ratio} = \left(\frac{4\pi \times 35860000}{0.075}\right)^2 = 2.77 \times 10^{-20} = -195.5752 \text{ dB}$$

Friis Transmission Formula and the Radar Range Equation

Analysis and design of communication and monitoring systems often require an estimation of transmitted and received powers. Friis transmission formula and the radar range equation provide the means for such calculations. The former is applicable to a one-way communication system where the signal is transmitted at one end and is received at the other end of the link. In the case of the radar range equation, the transmitted signal hits a target and the reflected signal is generally received at the location of the transmitter. We consider these two formulations here.

Friis Transmission Equation

Consider a simplified communication link as illustrated in Figure 2.5. A distance R separates the transmitter and the receiver. Effective apertures of transmitting and

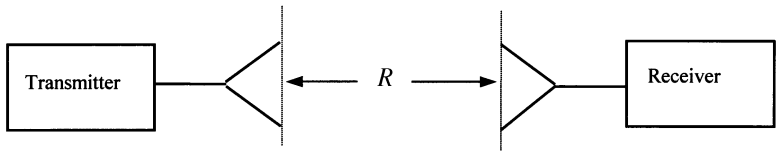

Figure 2.5 Simplified block diagram of the communication link.

receiving antennas are A_{et} and A_{er}, respectively. Further, the two antennas are assumed to be polarization matched.

If power input to the transmitting antenna is P_t then isotropic power density w_o at a distance R from the antenna is given as follows:

$$w_o = \frac{P_t e_t}{4\pi R^2} \tag{2.4.17}$$

where e_t is the radiation efficiency of the transmitting antenna.

For a directional transmitting antenna, the power density w_t can be written as follows:

$$w_t = \frac{P_t G_t}{4\pi R^2} = \frac{P_t e_t D_t}{4\pi R^2} \tag{2.4.18}$$

where G_t is the gain and D_t is the directivity of transmitting antenna.

Power collected by the receiving antenna is

$$P_r = A_{er} w_t \tag{2.4.19}$$

From (2.4.6),

$$A_{er} = \frac{\lambda^2}{4\pi} G_r \tag{2.4.20}$$

where the receiving antenna gain is G_r.

Therefore, we find that

$$P_r = \frac{\lambda^2}{4\pi} G_r w_t = \frac{\lambda^2}{4\pi} G_r \frac{P_t G_t}{4\pi R^2}$$

or

$$\frac{P_r}{P_t} = \left(\frac{\lambda}{4\pi R}\right)^2 G_r G_t = e_t e_r \left(\frac{\lambda}{4\pi R}\right)^2 D_r D_t \tag{2.4.21}$$

If signal frequency is f then for a free-space link,

$$\frac{\lambda}{4\pi R} = \frac{3 \times 10^8}{4\pi f R}$$

where f is in Hz and R is in meters.

Generally, the link distance is long and the signal frequency is high such that kilometer and megahertz will be more convenient units than the usual meter and hertz, respectively. For R in km and f in MHz, we find that

$$\frac{\lambda}{4\pi R} = \frac{3 \times 10^8}{4\pi \times 10^6 \times f_{\text{MHz}} \times 10^3 \times R_{\text{km}}} = \frac{0.3}{4\pi} \times \frac{1}{f_{\text{MHz}} R_{\text{km}}}$$

Hence, from (2.4.21),

$$P_{\text{r}}(\text{dBm}) = P_{\text{t}}(\text{dBm}) + 20\log_{10}\left(\frac{0.3}{4\pi}\right) - 20\log_{10}(f_{\text{MHz}} R_{\text{km}}) + G_{\text{t}}(\text{dB}) + G_{\text{r}}(\text{dB})$$

or,

$$P_{\text{r}}(\text{dBm}) = P_{\text{t}}(\text{dBm}) + G_{\text{t}}(\text{dB}) + G_{\text{r}}(\text{dB}) - 20\log_{10}(f_{\text{MHz}} R_{\text{km}}) - 32.4418 \tag{2.4.22}$$

where the transmitted and received powers are in dBm while the two antenna-gains are in dB.

Example 2.6: A 20-GHz transmitter on board the satellite uses a parabolic antenna that is 45.7 cm in diameter. The antenna gain is 37 dB and its radiated power is 2 W. The ground station that is 36941.031 km away from it has an antenna gain of 45.8 dB. Find the power collected by the ground station. How much power would be collected at the ground station if there were isotropic antennas on both sides?

The transmitted power, $P_{\text{t}}(\text{dBm}) = 10\log_{10}(2000) = 33.0103$ dBm and

$$20\log_{10}(f_{\text{MHz}} R_{\text{km}}) = 20\log_{10}(20 \times 10^3 \times 36941.031) = 177.3708 \text{ dB}$$

Hence, the power received at the earth station is found as follows:

$$P_{\text{r}}(\text{dBm}) = 33.0103 + 37 + 45.8 - 177.3708 - 32.4418 = -94.0023 \text{ dBm}$$

or,

$$P_{\text{r}} = 3.979 \times 10^{-10} \text{ mW}$$

If the two antennas are isotropic then $G_{\text{t}} = G_{\text{r}} = 1$ (or, 0 dB) and therefore,

$$P_{\text{r}}(\text{dBm}) = 33.0103 + 0 + 0 - 177.3708 - 32.4418 = -176.8023 \text{ dBm}$$

or,

$$P_{\text{r}} = 2.0882 \times 10^{-18} \text{ mW}$$

Radar Equation

In the case of a radar system, the transmitted signal is scattered by the target in all possible directions. The receiving antenna collects part of the energy that is scattered back toward it. Generally, a single antenna is employed for both the transmitter and the receiver, as shown in Figure 2.6.

If power input to the transmitting antenna is P_t and its gain is G_t then power density w_{inc} incident on the target is

$$w_{inc} = \frac{P_t G_t}{4\pi R^2} = \frac{P_t A_{et}}{\lambda^2 R^2} \tag{2.4.25}$$

where A_{et} is the effective aperture of the transmitting antenna.

The radar cross-section σ of an object is defined as the area intercepting that amount of power that, when scattered isotropically, produces at the receiver a power density that is equal to that scattered by the actual target. Hence,

$$\text{Radar cross-section} = \frac{\text{Scattered power}}{\text{Incident power density}} \text{ sq. m}$$

or,

$$\sigma = \frac{4\pi r^2 w_r}{w_{inc}} \tag{2.4.26}$$

where w_r is isotropically back-scattered power density at a distance r and w_{inc} is power density incident on the object.

Hence, the radar cross-section of an object is its effective area that intercepts an incident power density w_{inc} and gives an isotropically scattered power of $4\pi r^2 w_r$ for a back-scattered power density. Radar cross-sections of selected objects are listed in Table 2.5.

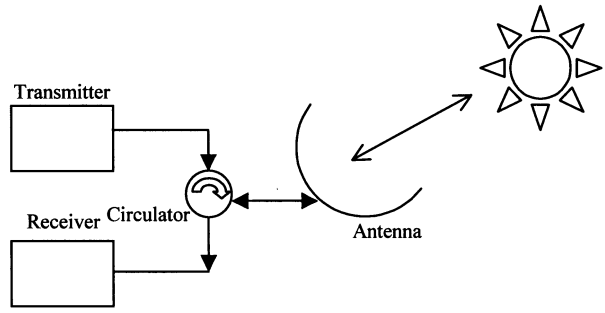

Figure 2.6 A radar system.

TABLE 2.5 Radar Cross-Sections of Selected Objects

Object	Radar Cross-Section (m^2)
Pickup truck	200
Automobile	100
Jumbo-jet airliner	100
Large bomber	40
Large fighter aircraft	6
Small fighter aircraft	2
Adult male	1
Conventional winged missile	0.5
Bird	0.01
Insect	0.00001
Advanced tactical fighter	0.000001

Using the radar cross-section of a target, the power intercepted by it can be found as follows:

$$P_{\text{inc}} = \sigma w_{\text{inc}} = \frac{\sigma P_{\text{t}} G_{\text{t}}}{4\pi R^2} \tag{2.4.27}$$

Power density arriving back at the receiver is

$$w_{\text{scatter}} = \frac{P_{\text{inc}}}{4\pi R^2} \tag{2.4.28}$$

and power available at the receiver input is

$$P_{\text{r}} = A_{\text{er}} w_{\text{scatter}} = \frac{G_{\text{r}} \lambda^2 \sigma P_{\text{t}} G_{\text{t}}}{4\pi (4\pi R^2)^2} = \frac{\sigma A_{\text{er}} A_{\text{et}} P_{\text{t}}}{4\pi \lambda^2 R^4} \tag{2.4.29}$$

Example 2.7: A distance of $100\,\lambda$ separates two lossless X-band horn antennas. Reflection coefficients at the terminals of transmitting and receiving antennas are 0.1 and 0.2, respectively. Maximum directivities of the transmitting and receiving antennas are 16 dB and 20 dB, respectively. Assuming that the input power in a lossless transmission line connected to the transmitting antenna is 2 W, and that the two antennas are aligned for maximum radiation between them and are polarization

matched, find the power input to the receiver.

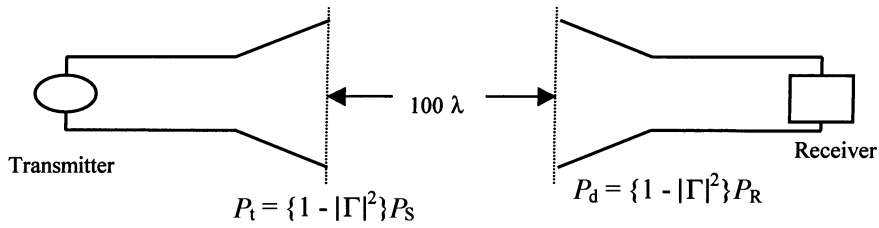

As discussed in the next chapter, impedance discontinuity generates an echo signal very similar to that of an acoustical echo. Hence, signal power available beyond the discontinuity is reduced. The ratio of the reflected signal voltage to that of the incident is called the *reflection coefficient*. Since the power is proportional to square of the voltage, power reflected from the discontinuity is equal to the square of the reflection coefficient times the incident power. Therefore, power transmitted in the forward direction will be given by

$$P_t = [1 - |\Gamma|^2]P_{in}$$

Therefore, the power radiated by the transmitting antenna is found to be

$$P_t = (1 - 0.1^2)2 = 1.98 \text{ W}$$

Since the Friis transmission equation requires the antenna gain as a ratio instead of in dB, G_t and G_r are calculated as follows.

$$G_t = 16 \text{ dB} = 10^{1.6} = 39.8107$$
$$G_r = 20 \text{ dB} = 10^{2.0} = 100$$

Hence, from (2.4.21),

$$P_r = \left(\frac{\lambda}{4\pi \times 100\lambda}\right)^2 \times 100 \times 39.8107 \times 1.98$$

or,

$$P_r = 5 \text{ mW}$$

and power delivered to the receiver, P_d, is

$$P_d = (1 - 0.2^2)5 = 4.8 \text{ mW}$$

Example 2.8: A radar operating at 12 GHz transmits 25 kW through an antenna of 25 dB gain. A target with its radar cross-section at 8 m^2 is located at 10 km from the radar. If the same antenna is used for the receiver, determine the received power.

$$P_t = 25 \text{ kW}$$
$$f = 12 \text{ GHz} \rightarrow \lambda = \frac{3 \times 10^8}{12 \times 10^9} = 0.025 \text{ m}$$
$$G_r = G_t = 25 \text{ dB} \rightarrow 10^{2.5} = 316.2278$$
$$R = 10 \text{ km}$$
$$\sigma = 8 \text{ m}^2$$

Hence,

$$P_r = \frac{G_r G_t P_t \sigma \lambda^2}{(4\pi)^3 R^4} = \frac{316.2278^2 \times 25000 \times 8 \times 0.025^2}{(4\pi)^3 \times (10^4)^4} = 6.3 \times 10^{-13} \text{ W}$$

or,

$$P_r = 0.63 \text{ pW}$$

Doppler Radar

An electrical signal propagating in free-space can be represented by a simple expression as follows:

$$v(z, t) = A \cos(\omega t - kz) \tag{2.4.30}$$

The signal frequency is ω radians per second and k is its wavenumber (equal to ω/c, where c is speed of light in free-space) in radian per meter. Assume that there is a receiver located at $z = R$, as shown in Figure 2.5 and R is changing with time (the receiver may be moving toward or away from the transmitter). In this situation, the receiver response v_o(t) is given as follows.

$$v_o(t) = V \cos(\omega t - kR) \tag{2.4.31}$$

The angular frequency, ω_o, of $v_o(t)$ can be easily determined after differentiating the argument of the cosine function with respect to time. Hence,

$$\omega_o = \frac{d}{dt}(\omega t - kR) = \omega - k\frac{dR}{dt} \tag{2.4.32}$$

Note that k is time independent, and the time derivative of R represents the velocity, v_r, of the receiver with respect to the transmitter. Hence, (2.4.32) can be written as follows:

$$\omega_o = \omega - \frac{\omega v_r}{c} = \omega\left(1 - \frac{v_r}{c}\right) \tag{2.4.33}$$

If the receiver is closing in then v_r will be negative (negative slope of R) and, therefore, the received signal will indicate a signal frequency higher than ω. On the other hand, it will show a lower frequency if R is increasing with time. It is the Doppler frequency shift that is employed to design the Doppler radar.

Consider a simplified block-diagram of the radar, as illustrated in Figure 2.7. A microwave signal generated by the oscillator is split into two parts via the power divider. The circulator feeds one part of this power to the antenna that illuminates a target while the mixer uses the remaining fraction as its reference signal. Further, the antenna intercepts a part of the signal that is scattered by the object. It is then directed to the mixer through the circulator. Output of the mixer includes a difference frequency signal that can be filtered out for further processing. Two inputs to the mixer will have the same frequency if the target is stationary and, therefore, the Doppler shift $\delta\omega$ will be zero. On the other hand, the mixer output will have Doppler frequency if the target is moving. Note that the signal travels twice over the same distance and, therefore, the Doppler frequency shift in this case will be twice that found via (2.4.33). Mathematically,

$$\omega_o = \omega\left(1 - \frac{2v_r}{c}\right) \tag{2.4.34}$$

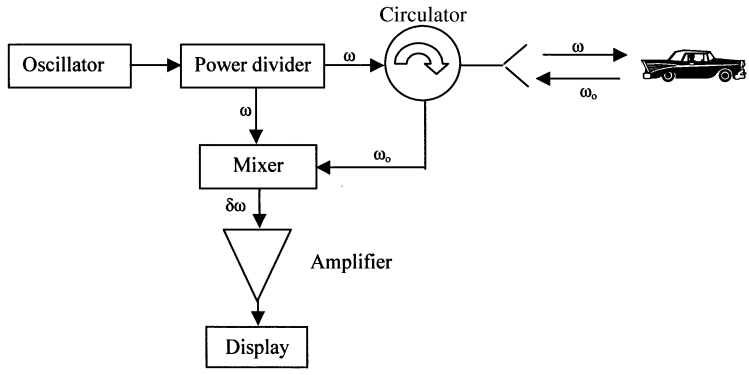

Figure 2.7 Simplified block-diagram of a Doppler radar.

and

$$\delta\omega = \frac{2\omega v_r}{c} \tag{2.4.35}$$

2.5 NOISE AND DISTORTION

Random movement of charges or charge carriers in an electronic device generates currents and voltages that vary randomly with time. In other words, the amplitude of these electrical signals cannot be predicted at any time. However, it can be expressed in terms of probability density functions. These signals are termed *noise*. For most applications, it suffices to know the mean square or root-mean-square value. Since the square of the current or the voltage is proportional to the power, mean-square noise voltage and current values are generally called *noise power*. Further, noise power is normally a function of frequency and the power-per-unit frequency (W per Hz) is defined as the power spectral density of noise. If the noise power is the same over the entire frequency band of interest then it is called *white noise*. There are several mechanisms that can cause noise in an electronic device. Some of these are as follows:

- *Thermal noise:* This is the most basic type of noise, which is caused by thermal vibration of bound charges. Johnson studied this phenomenon in 1928 and Nyquist formulated an expression for spectral density around the same time. Therefore, it is also known as *Johnson noise* or *Nyquist noise*. In most electronic circuits, thermal noise dominates; therefore, it will be described further because of its importance.
- *Shot noise:* This is due to random fluctuations of charge carriers that pass through the potential barrier in an electronic device. For example, electrons emitted from the cathode of thermionic devices or charge carriers in Schottky diodes produce a current that fluctuates about the average value I. The mean-square current due to shot noise is generally given by the following equation:

$$\langle i_{\text{Sh}}^2 \rangle = 2eIB \tag{2.5.1}$$

  where e is electronic charge (1.602×10^{-19} C) and B is the bandwidth in Hz.
- *Flicker noise:* This occurs in solid-state devices and vacuum tubes operating at low frequencies. Its magnitude decreases with the increase in the frequency. It is generally attributed to chaos in the dynamics of the system. Since the flicker noise power varies inversely with frequency, it is often called $1/f$ *noise*. Sometimes it is referred to as *pink noise*.

Thermal Noise

Consider a resistor R that is at a temperature of T K. Electrons in this resistor are in random motion with a kinetic energy that is proportional to the temperature T. These random motions produce small, random voltage fluctuations across its terminals. This voltage has a zero average value, but a nonzero mean-square value $\langle v_n^2 \rangle$. It is given by Planck's black-body radiation law, as follows:

$$\langle v_n^2 \rangle = \frac{4hfRB}{\exp(hf/kT) - 1} \tag{2.5.2}$$

where h is Planck's constant (6.546×10^{-34} J-Sec); k is the Boltzmann constant (1.38×10^{-23} J/K); T is temperature in Kelvin; B is bandwidth of the system in Hz; and f is center frequency of the bandwidth in Hz.

For frequencies below 100 GHz, the product hf will be smaller than 6.546×10^{-23} J and kT will be greater than 1.38×10^{-22} J if T stays above 10 K. Therefore, kT will be larger than hf for such cases. Hence, the exponential term in equation (2.5.2) can be approximated as follows:

$$\exp\left(\frac{hf}{kT}\right) \approx 1 + \frac{hf}{kT}$$

Therefore,

$$\langle v_n^2 \rangle \approx \frac{4hfRB}{hf/kT} = 4BRkT \tag{2.5.3}$$

This is known as the Rayleigh-Jeans approximation.

A Thevenin-equivalent circuit can replace the noisy resistor, as shown in Figure 2.8. As illustrated, it consists of a noise equivalent voltage source in series with the noise-free resistor. This source will supply a maximum power to a load of resistance R. The power delivered to that load in a bandwidth B is found as follows:

$$P_n = \frac{\langle v_n^2 \rangle}{4R} = kTB \tag{2.5.4}$$

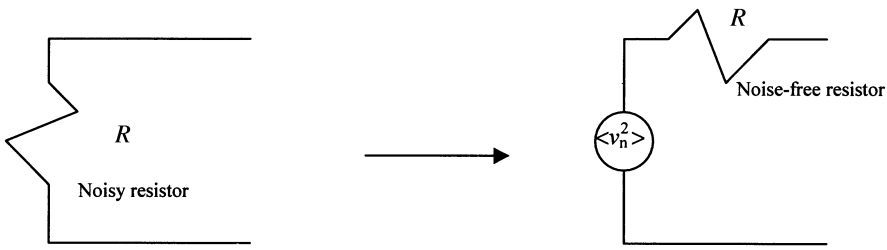

Figure 2.8 Noise equivalent circuit of a resistor.

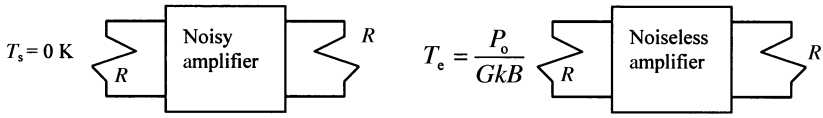

Figure 2.9 Noise-equivalent representation of an amplifier.

Conversely, if an arbitrary white noise source with its driving point impedance R delivers a noise power P_S to a load R then it can be represented by a noisy resistor of value R that is at temperature T_e. Hence,

$$T_e = \frac{P_S}{kB} \tag{2.5.5}$$

where T_e is an equivalent temperature selected so that the same noise power is delivered to the load.

Consider a noisy amplifier as shown in Figure 2.9. Its gain is G over the bandwidth B. Let the amplifier be matched to the noiseless source and the load resistors. If the source resistor is at a hypothetical temperature of $T_S = 0$ K, then the power input to the amplifier P_i will be zero and the output noise power P_o will be only due to noise generated by the amplifier. We can obtain the same noise power at the output of an ideal noiseless amplifier by raising the temperature T_S of the source resistor to T_e, as follows:

$$T_e = \frac{P_o}{GkB} \tag{2.5.6}$$

Hence, the output power in both cases is $P_o = GkT_eB$. The temperature T_e is known as the equivalent noise temperature of the amplifier.

Measurement of Noise Temperature by the Y-Factor Method

According to definition, the noise temperature of an amplifier (or any other two-port network) can be determined by setting the source resistance R at 0 K and then measuring the output noise power. However, a temperature of 0 K cannot be achieved in practice. We can circumvent this problem by repeating the experiment at two different temperatures. This procedure is known as the *Y-factor method*.

Consider an amplifier with power gain G over the frequency band B Hz. Further, its equivalent noise temperature is T_e K. The input port of the amplifier is terminated by a matched resistor R while a matched power meter is connected at its output, as illustrated in Figure 2.10. With R at temperature T_h, the power meter measures the noise output as P_1. Similarly, the noise power is found to be P_2 when the temperature of R is set at T_c. Hence,

$$P_1 = GkT_hB + GkT_eB$$

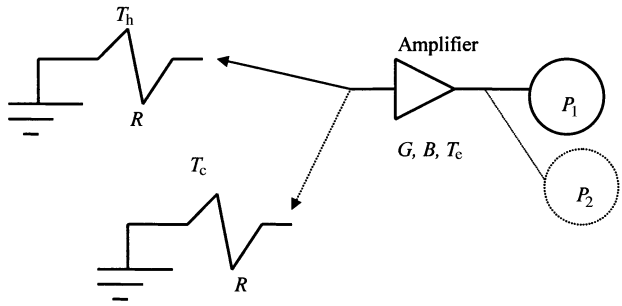

Figure 2.10 Experimental setup for measurement of the noise temperature.

and

$$P_2 = GkT_cB + GkT_eB$$

For T_h higher than T_c, the noise power P_1 will be larger than P_2.

Therefore,

$$\frac{P_1}{P_2} = Y = \frac{T_h + T_e}{T_c + T_e}$$

or,

$$T_e = \frac{T_h - YT_c}{Y - 1} \tag{2.5.7}$$

For T_h larger than T_c, Y will be greater than unity. Further, measurement accuracy is improved by selecting two temperature settings that are far apart. Therefore, T_h and T_c represent hot and cold temperatures, respectively.

Example 2.9: An amplifier has a power gain of 10 dB in the 500-MHz to 1.5-GHz frequency band. The following data is obtained for this amplifier using the *Y*-factor method:

$$\begin{aligned} &\text{At} \quad T_h = 290\ \text{K}, \qquad P_1 = -70\ \text{dBm} \\ &\text{At} \quad T_c = 77\ \text{K}, \qquad P_2 = -75\ \text{dBm} \end{aligned}$$

Determine its equivalent noise temperature. If this amplifier is used with a source that has an equivalent noise temperature of 450 K, find the output noise power in dBm.

Since P_1 and P_2 are given in dBm, the difference of these two values will give Y in dB. Hence,

$$Y = (P_1 - P_2)\text{dBm} = (-70) - (-75) = 5 \text{ dB}$$

or,

$$Y = 10^{0.5} = 3.1623$$
$$\therefore \quad T_e = \frac{290 - (3.1623)(77)}{3.1623 - 1} = 21.51 \text{ K}$$

If a source with an equivalent noise temperature of $T_S = 450$ K drives the amplifier, the noise power input to this will be kT_SB. Total noise power at the output of the amplifier will be

$$P_o = GkT_SB + GkT_eB = 10 \times 1.38 \times 10^{-23} \times 10^9 \times (450 + 21.51)$$
$$= 6.5068 \times 10^{-11} \text{ W}$$

Therefore,

$$P_o = 10 \log(6.5068 \times 10^{-8}) = -71.8663 \text{ dBm}$$

Noise Factor and Noise Figure

Noise factor of a two-port network is obtained by dividing the signal-to-noise ratio at its input port by the signal-to-noise ratio at its output. Hence,

$$\text{Noise factor, } F = \frac{S_i/N_i}{S_o/N_o}$$

where S_i, N_i, S_o, and N_o represent the power in input signal, input noise, output signal, and output noise, respectively. If the two-port network is noise-free then signal-to-noise ratio at its output will be the same as its input, resulting in a noise factor of unity. In reality, the network will add its own noise while the input signal and noise will be altered by the same factor (gain or loss). It will lower the output signal-to-noise ratio, resulting in a higher noise factor. Therefore, the noise factor of a two-port network is generally greater than unity. By definition, the input noise power is assumed to be the noise power resulting from a matched resistor at $T_o = 290$ K, i.e., $N_i = kT_oB$. Using the circuit arrangement illustrated in Figure 2.11, the noise factor of a noisy two-port network can be defined as follows:

$$\text{Noise factor} = \frac{\text{Total output noise in } B \text{ when input source temperature is 290 K}}{\text{Output noise of source (only) at 290 K}}$$

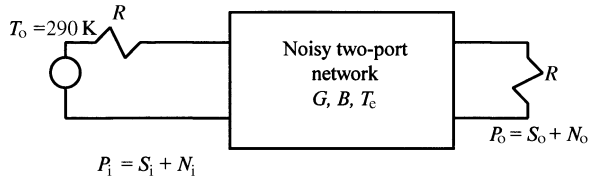

Figure 2.11 Circuit arrangement for the determination of noise factor of a noisy two-port network.

or,

$$F = \frac{kT_oBG + P_{int}}{kT_oBG} = 1 + \frac{P_{int}}{kT_oBG} \tag{2.5.8}$$

where P_{int} represents output noise power that is generated by the two-port network internally. It can be expressed in terms of noise factor as follows:

$$P_{int} = k(F-1)T_oBG = kT_eBG \tag{2.5.9}$$

where T_e is known as the equivalent noise temperature of a two-port network. It is related to the noise factor as follows:

$$T_e = (F-1)T_o \tag{2.5.10}$$

When the noise factor is expressed in decibels, it is commonly called the *noise figure* (NF). Hence,

$$\text{NF} = 10\log_{10}(F)\text{dB} \tag{2.5.11}$$

Example 2.10: Power gain of an amplifier is 20 dB in the frequency band of 10 GHz to 12 GHz. If its noise figure is 3.5 dB, find the output noise power in dBm.

$$\text{Output noise power} = kT_oBG + P_{int} = FkT_oBG = N_o$$

$$F = 3.5 \text{ dB} = 10^{0.35} = 2.2387$$

$$G = 20 \text{ dB} = 10^2 = 100$$

Therefore,

$$N_o = 2.2387 \times 1.38 \times 10^{-23} \times 290 \times 2 \times 10^9 \times 100 = 1.7919 \times 10^{-9} \text{ W}$$

or,

$$N_o = 10\log_{10}(1.7919 \times 10^{-6} \text{ mW})\text{dBm} = -57.4669 \text{ dBm} \approx -57.5 \text{ dBm}$$

Noise in Two-Port Networks

Consider a noisy two-port network as shown in Figure 2.12 (a). $Y_s = G_s + jB_s$ is source admittance that is connected at port 1 of the network. The noise it generates is represented by the current source i_s with its root-mean-square value as I_s. This noisy two-port can be replaced by a noise-free network with a current source i_n and a voltage source v_n connected at its input, as shown in Figure 2.12 (b). I_n and V_n represent the corresponding root-mean-square current and voltage of the noise. It is assumed that the noise represented by i_s is uncorrelated with that represented by i_n and v_n. However, a part of i_n, i_{nc}, is assumed to be correlated with v_n via the correlation admittance $Y_c = G_c + jX_c$ while the remaining part i_{nu} is uncorrelated. Hence,

$$I_s^2 = \langle i_s^2 \rangle = 4kTBG_S \tag{2.5.12}$$

$$V_n^2 = \langle v_n^2 \rangle = 4kTBR_n \tag{2.5.13}$$

and,

$$I_{nu}^2 = \langle i_{nu}^2 \rangle = 4kTBG_{nu} \tag{2.5.14}$$

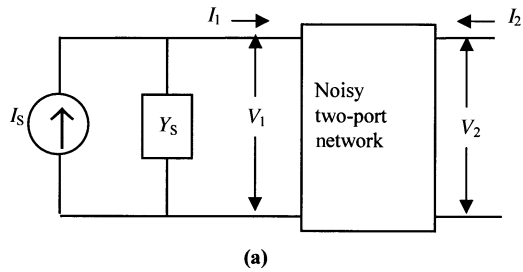

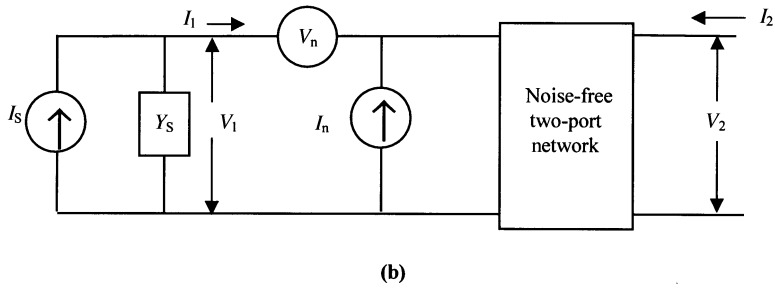

Figure 2.12 A noisy two-port network (a), and its equivalent circuit (b).

Now we find a Norton equivalent for the circuit that is connected at the input of a noise-free two-port network in Figure 2.12 (b). Since these are random variables, the mean square noise current $\langle i_{eq}^2 \rangle$ is found as follows:

$$\begin{aligned}\langle i_{eq}^2 \rangle &= \langle i_s^2 \rangle + \langle | \, i_n + Y_s v_n \, |^2 \rangle = \langle i_s^2 \rangle + \langle | \, i_{nu} + i_{nc} + Y_s v_n \, |^2 \rangle \\ &= \langle i_s^2 \rangle + \langle | \, i_{nu} + (Y_c + Y_s) v_n \, |^2 \rangle\end{aligned}$$

or,

$$\langle i_{eq}^2 \rangle = \langle i_s^2 \rangle + \langle i_{nu}^2 \rangle + | \, Y_c + Y_n \, |^2 \langle v_n^2 \rangle \tag{2.5.15}$$

Hence, the noise factor F is

$$F = \frac{\langle i_{eq}^2 \rangle}{\langle i_s^2 \rangle} = 1 + \frac{\langle i_{nu}^2 \rangle}{\langle i_s^2 \rangle} + | \, Y_c + Y_s \, |^2 \frac{\langle v_n^2 \rangle}{\langle i_s^2 \rangle} = 1 + \frac{G_{nu}}{G_s} + | \, Y_c + Y_s \, |^2 \frac{R_n}{G_s}$$

or,

$$F = 1 + \frac{G_{nu}}{G_S} + \frac{R_n}{G_S} \left\{ (G_S + G_c)^2 + (x_S + X_c)^2 \right\} \tag{2.5.16}$$

For a minimum noise factor, F_{min},

$$\frac{\partial F}{\partial G_S} = 0 \Rightarrow G_S^2 = G_c^2 + \frac{G_{nu}}{R_n} = G_{opt}^2 \tag{2.5.17}$$

and,

$$\frac{\partial F}{\partial X_S} = 0 \Rightarrow X_S = -X_c = X_{opt} \tag{2.5.18}$$

From (2.5.17),

$$G_{nu} = R_n (G_{opt}^2 - G_c^2) \tag{2.5.19}$$

Substituting (2.5.18) and (2.5.19) into (2.5.16), minimum noise factor is found as

$$F_{min} = 1 + 2R_n (G_{opt} + G_c) \tag{2.5.20}$$

Using (2.5.18)–(2.5.20), (2.5.16) can be expressed as follows:

$$F = F_{min} + \frac{R_n}{G_S} | Y_S - Y_{opt} |^2 \tag{2.5.21}$$

Noise Figure of a Cascaded System

Consider a two-port network with gain G_1, noise factor F_1, and equivalent noise temperature T_{e1}. It is connected in cascade with another two-port network, as shown in Figure 2.13 (a). The second two-port network has gain G_2, noise factor F_2, and noise temperature T_{e2}. Our goal is to find the noise factor F and the equivalent noise temperature T_e of the overall system illustrated in Figure 2.13 (b).

Assume that the noise power input to the first two-port network is N_i. Its equivalent noise temperature is T_i. Output noise power of the first system is N_1 whereas it is N_o after the second system. Hence,

$$N_1 = G_1 kT_i B + G_1 kT_{e1} B \tag{2.5.22}$$

and,

$$\begin{aligned} N_o &= G_2 N_1 + G_2 kT_{e2} B = G_2[G_1 kB(T_i + T_{e1})] + G_2 kT_{e2} B \\ &= G_1 G_2 kB[T_i + T_{e1} + T_{e2}/G_1] \end{aligned}$$

or,

$$N_o = G_1 G_2 kB[T_e + T_i] = GkB[T_e + T_i] \tag{2.5.23}$$

Therefore, the noise temperature of a cascaded system is

$$T_e = T_{e1} + \frac{T_{e2}}{G_1}$$

and, from $T_{e1} = (F_1 - 1)T_i$; $T_{e2} = (F_2 - 1)T_i$; $T_e = (F - 1)T_i$, we get

$$F = F_1 + \frac{F_2 - 1}{G_1}$$

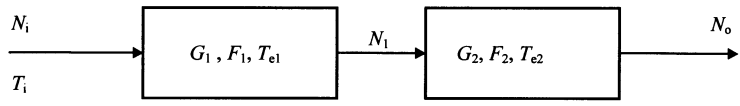

(a)

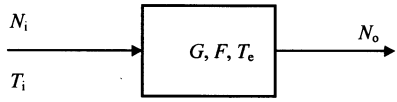

(b)

Figure 2.13 Two networks connected in cascade (a) and its equivalent system (b).

The above equations for T_e and F can be generalized as follows:

$$T_e = T_{e1} + \frac{T_{e2}}{G_1} + \frac{T_{e3}}{G_1 G_2} + \frac{T_{e4}}{G_1 G_2 G_3} + \cdots \tag{2.5.24}$$

and

$$F = F_1 + \frac{F_2 - 1}{G_1} + \frac{F_3 - 1}{G_1 G_2} + \frac{F_4 - 1}{G_1 G_2 G_3} + \cdots \tag{2.5.25}$$

Example 2.11: A receiving antenna is connected to an amplifier through a transmission line that has an attenuation of 2 dB. Gain of the amplifier is 15 dB and its noise temperature is 150 K over a bandwidth of 100 MHz. All the components are at an ambient temperature of 300 K.

(a) Find the noise figure of this cascaded system.
(b) What would be the noise figure if the amplifier were placed before the transmission line?

First we need to determine the noise factor of the transmission line alone. The formulas derived in the preceding section can then provide the desired noise figures for the two cases.

Consider a transmission line that is matched terminated at both its ends by resistors R_o, as illustrated in Figure 2.14. Since the entire system is in thermal equilibrium at T K, noise powers delivered to the transmission line and that available at its output are kTB. Mathematically,

$$P_o = kTB = GkTB + GN_{added}$$

where N_{added} is noise generated by the line as it appears at its input terminals. G is output-to-input power ratio and B is bandwidth of the transmission line. Note that input noise is attenuated in a lossy transmission line but there is noise generated by it as well. Hence,

$$N_{added} = \frac{1}{G}(1 - G)kTB = \left(\frac{1}{G} - 1\right)kTB = kT_eB$$

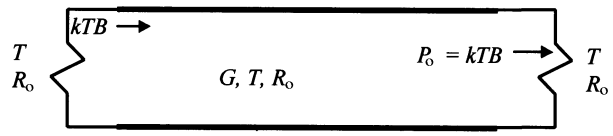

Figure 2.14 A lossy transmission line matched terminated at its ends.

An expression for the equivalent noise temperature T_e of the transmission line is found from it as follows:

$$T_e = \left(\frac{1}{G} - 1\right)T$$

and,

$$F = 1 + \frac{T_e}{T_o} = 1 + \left(\frac{1}{G} - 1\right)\frac{T}{T_o}$$

Gain of the amplifier, $G_{amp} = 15$ dB $= 10^{1.5} = 31.6228$. For the transmission line, $1/G = 10^{0.2} = 1.5849$.

Hence, the noise factor of the line is $1 + (1.5849 - 1)300/290 = 1.6051$. The corresponding noise figure is 2.05 dB. Similarly, the noise factor of the amplifier is found to be $1 + 150/290 = 1.5172$. Its noise figure is 1.81 dB.

(a) In this case, the noise figure of the cascaded system, $F_{cascaded}$, is found as

$$F_{cascaded} = F_{line} + \frac{F_{amp} - 1}{G_{line}} = 1.6051 + \frac{1.5172 - 1}{1/1.5849} = 2.4248 = 3.8468 \text{ dB}$$

(b) If the amplifier is connected before the line, i.e., the amplifier is placed right at the antenna, then

$$F_{cascaded} = F_{amp} + \frac{F_{line} - 1}{G_{amp}} = 1.5172 + \frac{1.6051 - 1}{31.6228} = 11.5363 = 1.8649 \text{ dB}$$

Note that the amplifier alone has a noise figure of 1.81 dB. Hence, the noisy transmission line connected after it does not alter the noise figure significantly.

Example 2.12: Two amplifiers, each with 20-dB gain, are connected in cascade as shown below. The noise figure of amplifier A_1 is 3 dB while that of A_2 is 5 dB. Calculate the overall gain and noise figure for this arrangement. If the order of two amplifiers is changed in the system, find its resulting noise figure.

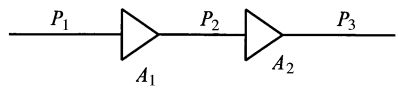

The noise factors and gains of two amplifiers are:

$$F_1 = 3 \text{ dB} = 10^{0.3} = 2$$
$$F_2 = 5 \text{ dB} = 10^{0.5} = 3.1623$$
$$G_1 = G_2 = 20 \text{ dB} = 10^2 = 100$$

Therefore, the overall gain and noise figure of the cascaded system is found as follows:

$$G = \frac{P_3}{P_1} = \frac{P_3}{P_2} \times \frac{P_2}{P_1} = 100 \times 100 = 10000 = 40 \text{ dB}$$

and,

$$F = F_1 + \frac{F_2 - 1}{G_1} = 2 + \frac{3.1623 - 1}{100} = 2.021623 = 3.057 \text{ dB}$$

If the order of amplifiers is changed then the overall gain will stay the same. However, the noise figure of new arrangement will change as follows:

$$F = F_2 + \frac{F_1 - 1}{G_2} = 3.1623 + \frac{2 - 1}{100} = 3.1723 = 5.013743 \text{ dB}$$

Minimum Detectable Signal (MDS)

Consider a receiver circuit with gain G over bandwidth B. Assume that its noise factor is F. P_I and P_o represent power at its input and output ports, respectively. N_I is input noise power and N_o is total noise power at its output as illustrated in Figure 2.15. Hence,

$$N_o = kT_oFBG \tag{2.5.26}$$

This constitutes the noise floor of the receiver. A signal weaker than this will be lost in noise. N_o can be expressed in dBW as follows:

$$N_o(\text{dBW}) = 10\log_{10}(kT_o) + F(\text{dB}) + 10\log_{10}(B) + G(\text{dB}) \tag{2.5.27}$$

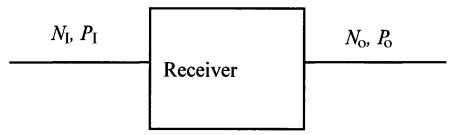

Figure 2.15 Signals at the two ports of a receiver with a noise figure of F dB.

The minimum detectable signal must have power higher than this. Generally, it is taken as 3 dB above this noise floor. Further,

$$10\log_{10}(kT_o) = 10\log_{10}(1.38 \times 10^{-23} \times 290) \approx -204 \text{ dBW per Hz}$$

Hence, the minimum detectable signal $P_{o\,MDS}$ at the output is

$$P_{o\,MDS} = -201 + F(\text{dB}) + 10\log_{10}(B_{\text{Hz}}) + G(\text{dB}) \tag{2.5.28}$$

The corresponding signal power $P_{I\,MDS}$ at its input is

$$P_{I\,MDS}(\text{dBW}) = -201 + F(\text{dB}) + 10\log_{10}(B_{\text{Hz}}) \tag{2.5.29}$$

Alternatively, $P_{I\,MDS}$ can be expressed in dBm as follows:

$$P_{I\,MDS}(\text{dBm}) = -111 + F(\text{dB}) + 10\log_{10}(B_{\text{MHz}}) \tag{2.5.30}$$

Example 2.13: The noise figure of a communication receiver is found as 10 dB at room temperature (290 K). Determine the minimum detectable signal power if (a) $B = 1$ MHz, (b) $B = 1$ GHz, (c) $B = 10$ GHz, and (d) $B = 1$ kHz.

From (2.5.30),

$$P_{I\,MDS} = -111 + F(\text{dB}) + 10\log_{10}(B_{\text{MHz}})\text{dBm}$$

Hence,

(a) $P_{I\,MDS} = -111 + 10 + 10\log_{10}(1) = -101 \text{ dBm} = 7.94 \times 10^{-11} \text{ mW}$
(b) $P_{I\,MDS} = -111 + 10 + 10\log_{10}(10^3) = -71 \text{ dBm} = 7.94 \times 10^{-8} \text{ mW}$
(c) $P_{I\,MDS} = -111 + 10 + 10\log_{10}(10^4) = -61 \text{ dBm} = 7.94 \times 10^{-7} \text{ mW}$

and,

(d) $P_{I\,MDS} = -111 + 10 + 10\log_{10}(10^{-3}) = -131 \text{ dBm} = 7.94 \times 10^{-14} \text{ mW}$

These results show that the receiver can detect a relatively weak signal when its bandwidth is narrow.

Intermodulation Distortion

The electrical noise of a system determines the minimum signal level that it can detect. On the other hand, the signal will be distorted if its level is too high. This occurs because of the nonlinear characteristics of electrical devices such as diodes, transistors, and so on. In this section, we analyze the distortion characteristics and introduce the associated terminology.

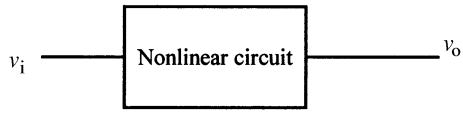

Figure 2.16 Nonlinear circuit with input signal v_i that produces v_o at its output.

Consider the nonlinear system illustrated in Figure 2.16. Assume that its nonlinearity is frequency independent and can be represented by the following power series

$$v_o = k_1 v_i + k_2 v_i^2 + k_3 v_i^3 + \cdots \tag{2.5.31}$$

For simplicity, we assume that the k_i are real and the first three terms of this series are sufficient to represent its output signal. Further, it is assumed that the input signal has two different frequency components that can be expressed as follows:

$$v_i = a\cos(\omega_1 t) + b\cos(\omega_2 t) \tag{2.5.32}$$

Therefore, the corresponding output signal can be written as

$$\begin{aligned} v_o \approx\ & k_1[a\cos(\omega_1 t) + b\cos(\omega_2 t)] + k_2[a\cos(\omega_1 t) + b\cos(\omega_2 t)]^2 \\ & + k_3[a\cos(\omega_1 t) + b\cos(\omega_2 t)]^3 \end{aligned}$$

After simplifying and rearranging it we get

$$\begin{aligned} v_o = {} & k_1[a\cos(\omega_1 t) + b\cos(\omega_2 t)] + k_2\left[\frac{a^2}{2}\left\{1 + \cos\left\{2\omega_1 t\right\}\right\} + \frac{b^2}{2}\left\{1 + \cos(2\omega_2 t)\right\}\right. \\ & \left. + \frac{ab}{2}\left\{\cos(\omega_1 + \omega_2)t + \cos(\omega_1 - \omega_2)t\right\}\right] + k_3\left[\frac{3}{4}a^3\cos(\omega_1 t) + \frac{3}{2}ab^2\cos(\omega_1 t)\right. \\ & + \frac{a^3}{4}\cos(3\omega_1 t) + \frac{3}{4}ab^2\cos(\omega_1 - 2\omega_2)t + \frac{3}{4}a^2 b\cos(2\omega_1 - \omega_2)t \\ & + \frac{3}{2}a^2 b\cos(\omega_2 t) + \frac{3}{4}b^3\cos(\omega_2 t) + \frac{b^3}{4}\cos(3\omega_2 t) + \frac{3}{4}a^2 b\cos(2\omega_1 + \omega_2)t \\ & \left. + \frac{3}{4}ab^2\cos(\omega_1 + 2\omega_2)t\right] \end{aligned} \tag{2.5.33}$$

Therefore, the output signal has several frequency components in its spectrum. Amplitudes of various components are listed in Table 2.6.

Figure 2.17 illustrates the input–output characteristic of an amplifier. If input signal is too low then it may be submerged under the noise. Output power rises linearly above the noise as the input is increased. However, it deviates from the linear

TABLE 2.6 Amplitudes of Various Harmonics in the Output

Harmonic Components	Amplitude
ω_1	$k_1 a + k_3\left(\frac{3}{4}a^3 + \frac{3}{2}ab^2\right)$
ω_2	$k_1 b + k_3\left(\frac{3}{4}b^3 + \frac{3}{2}a^2 b\right)$
$\omega_1 - \omega_2$	$k_2 \dfrac{ab}{2}$
$\omega_1 + \omega_2$	$k_2 \dfrac{ab}{2}$
$2\omega_1$	$k_2 \dfrac{a^2}{2}$
$2\omega_2$	$k_2 \dfrac{b^2}{2}$
$3\omega_1$	$k_3 \dfrac{a^3}{4}$
$3\omega_2$	$k_3 \dfrac{b^3}{4}$
$2\omega_1 - \omega_2$	$\frac{3}{4}k_3 a^2 b$
$\omega_1 - 2\omega_2$	$\frac{3}{4}k_3 ab^2$
$2\omega_1 + \omega_2$	$\frac{3}{4}k_3 a^2 b$
$\omega_1 + 2\omega_2$	$\frac{3}{4}k_3 ab^2$

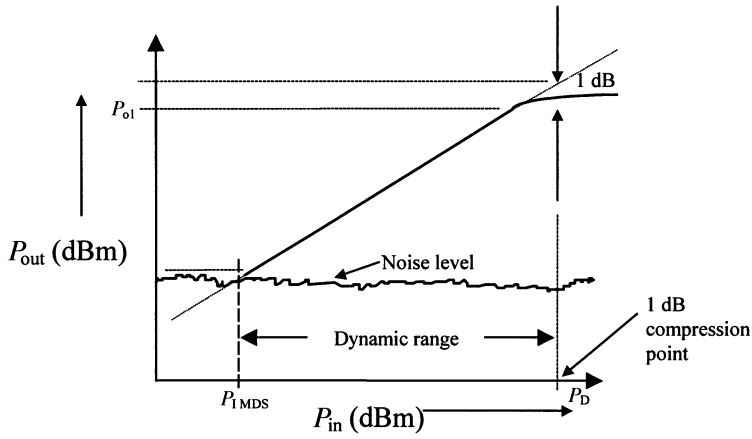

Figure 2.17 Gain characteristics of an amplifier.

characteristic after a certain level of input power. In the linear region, output power can be expressed in dBm as follows:

$$P_{\text{out}}(\text{dBm}) = P_{\text{in}}(\text{dBm}) + G(\text{dB})$$

The input power for which output deviates by 1 dB below its linear characteristic is known as 1-dB compression point. In this figure, it occurs at an input power of P_{D} dBm that produces an output of P_{o1} dBm. From the above relation, we find that

$$P_{\text{o1}}(\text{dBm}) + 1 = P_{\text{D}}(\text{dBm}) + G(\text{dB})$$

or,

$$P_{\text{D}}(\text{dBm}) = P_{\text{o1}}(\text{dBm}) + 1 - G(\text{dB}) \tag{2.5.34}$$

The difference between the input power at 1-dB compression point and the minimum detectable signal defines the dynamic range (DR). Hence,

$$\text{DR} = P_{\text{D}}(\text{dBm}) - P_{\text{I MDS}}$$

From (2.5.30) and (2.5.34), we find that

$$\text{DR} = P_{\text{o1}}(\text{dBm}) + 112 - G(\text{dB}) - F(\text{dB}) - 10\log_{10}(B_{\text{MHz}}) \tag{2.5.35}$$

Gain Compression

Nonlinear characteristics of the circuit (amplifier, mixer, etc.) compress its gain. If there is only one input signal, i.e., b is zero in (2.5.32), then the amplitude a_1 of $\cos(\omega_1 t)$ in its output is found from Table 2.6 to be

$$a_1 = k_1 a + \frac{3}{4} k_3 a^3 \tag{2.5.36}$$

The first term of a_1 represents the linear (ideal) case while its second term results from the nonlinearity. Generally, k_3 is a negative constant. Therefore, it tends to reduce a_1, resulting in lower gain. The single-tone gain compression factor may be defined as follows:

$$A_{1C} = \frac{a_1}{k_1 a} = 1 + \frac{3k_3}{4k_1} a^2 \tag{2.5.37}$$

Let us now consider the case when both of the input signals are present in (2.5.32). Amplitude of $\cos(\omega_1 t)$ in the output now becomes $k_1 a + k_3\left(\frac{3}{4}a^3 + \frac{3}{2}ab^2\right)$. If b is large in comparison with a then the term with k_3 may dominate (undesired) over the first (desired) one.

Second Harmonic Distortion

Second harmonic distortion occurs due to k_2. If b is zero, then the amplitude of the second harmonic will be $k_2(a^2/2)$. Since power is proportional to the square of the voltage, the desired term in the output can be expressed as

$$P_1 = 10\log_{10}\left(\varsigma k_1 \frac{a}{2}\right)^2 = 20\log_{10}(a) + C_1 \tag{2.5.38}$$

where ς is the proportionality constant and

$$C_1 = 20\log\left(\frac{\varsigma k_1}{2}\right)$$

Similarly, power in the second harmonic component can be expressed as

$$P_2 = 10\log_{10}\left(\varsigma k_2 \frac{a^2}{2}\right)^2 = 40\log_{10}(a) + C_2 \tag{2.5.39}$$

while the input power is

$$P_{\text{in}} = 10\log_{10}\left(\varsigma \frac{a}{2}\right)^2 = 20\log_{10}(a) + C_3 \tag{2.5.40}$$

Proportionality constants ς and k_2 are imbedded in C_2 and C_3.

From (2.5.38)–(2.5.40), we find that

$$P_1 = P_{\text{in}} + D_1 \tag{2.5.41}$$

and

$$P_2 = 2P_{\text{in}} + D_2 \tag{2.5.42}$$

where D_1 and D_2 replace C_1–C_3 and C_2–$2C_3$, respectively.

Equations (2.5.41) and (2.5.42) indicate that both the fundamental as well as the second harmonic signal in the output are linearly related with input power. However, the second harmonic power increases at twice the rate of the fundamental (the desired) component.

Intermodulation Distortion Ratio

From Table 2.6, we find that the cubic term produces intermodulation frequencies $2\omega_1 \pm \omega_2$ and $2\omega_2 \pm \omega_1$. If ω_1 and ω_2 are very close then $2\omega_1 + \omega_2$ and $2\omega_2 + \omega_1$ will be far away from the desired signals, and, therefore, these can be filtered out easily. However, the other two terms, namely, $2\omega_1 - \omega_2$ and $2\omega_2 - \omega_1$, will be so close to ω_1 and ω_2 that these components may be within the pass-band of the system. It will distort the output. This characteristic of a nonlinear circuit is specified via the intermodulation distortion. It is obtained after dividing the amplitude of one of the intermodulation terms by the desired output signal. For an input signal with

both ω_1 and ω_2 (i.e., a two-tone input), intermodulation distortion ratio (IMR) may be found as

$$\text{IMR} = \frac{\frac{3}{4}k_3a^2b}{k_1a} = \frac{3k_3}{4k_1}ab \tag{2.5.43}$$

Intercept Point (IP)

Since power is proportional to the square of the voltage, intermodulation distortion power may be defined as

$$P_{\text{IMD}} = \varsigma\frac{\left(\frac{3}{4}k_3a^2b\right)^2}{2} \tag{2.5.44}$$

where ς is the proportionality constant.

If the two input signals are equal in amplitude then $a = b$, and the expression for intermodulation distortion power simplifies to

$$P_{\text{IMD}} = \varsigma\frac{\left(\frac{3}{4}k_3a^3\right)^2}{2} \tag{2.5.45}$$

Similarly, the power in one of the input signal components can be expressed as follows:

$$P_{\text{in}} = \varsigma\frac{(a)^2}{2}$$

Therefore, the intermodulation distortion power can be expressed as

$$P_{\text{IMD}} = \alpha P_{\text{in}}^3$$

where α is another constant.

The ratio of intermodulation distortion power (P_{IMD}) to the desired output power $P_{\text{o}}(P_{\text{o}} = k_1^2P_{\text{in}})$ for the case where two input signal amplitudes are the same is known as the intermodulation distortion ratio. It is found to be

$$P_{\text{IMR}} = \frac{P_{\text{IMD}}}{P_{\text{o}}} = \alpha_1P_{\text{in}}^2 \tag{2.5.46}$$

Note that P_{IMD} increases as the cube of input power while the desired signal power P_{o} is linearly related with P_{in}. Hence, P_{IMD} increases three times as fast as P_{o} on a log–log plot (or both of them are expressed in dBm before displaying on a linear graph). In other words, for a change of 1 dBm in P_{in}, P_{o} changes by 1 dBm whereas P_{IMD} changes by 3 dBm. The value of the input power for which P_{IMD} is equal to P_{o}

is referred to as the intercept point (IP). Hence, P_{IMR} is unity at the intercept point. If P_{IP} is input power at IP then

$$P_{\text{IMR}} = 1 = \alpha_1 P_{\text{IP}}^2 \Rightarrow \alpha_1 = \frac{1}{P_{\text{IP}}^2} \tag{2.5.47}$$

Therefore, the intermodulation distortion ratio P_{IMR} is related with P_{IP} as follows:

$$P_{\text{IMR}} = \left(\frac{P_{\text{in}}}{P_{\text{IP}}}\right)^2 \tag{2.5.48}$$

Example 2.14: The intercept point in the transfer characteristic of a nonlinear system is found to be 25 dBm. If a −15-dBm signal is applied to this system, find the intermodulation ratio:

$$\begin{aligned} P_{\text{IMR}} = \left(\frac{P_{\text{in}}}{P_{\text{IP}}}\right)^2 &\rightarrow P_{\text{IMR}}(\text{dB}) = 2[P_{\text{in}}(\text{dBm}) - P_{\text{IP}}(\text{dBm})] \\ &= 2[-15 - 25] = -80 \text{ dB} \end{aligned}$$

Dynamic Range

As mentioned earlier, noise at one end and distortion at the other limit the range of detectable signals of a system. The amount of distortion that can be tolerated depends somewhat on the type of application. If we set the upper limit that a system can detect as the signal level at which the intermodulation distortion is equal to the minimum detectable signal then we can formulate an expression for its dynamic range. Thus, the ratio of the signal power that causes distortion power (in one frequency component) to be equal to the noise floor to that of the minimum detectable signal is the dynamic range (DR) of the system (amplifier, mixer, or receiver).

Since the ideal power output P_{o} is linearly related to input as follows:

$$P_{\text{o}} = k_1^2 P_{\text{in}} \tag{2.5.49}$$

the distortion power with reference to input can be expressed as

$$P_{\text{di}} = \frac{P_{\text{IMD}}}{k_1^2} \tag{2.5.50}$$

Therefore,

$$P_{\text{IMR}} = \frac{P_{\text{IMD}}}{P_{\text{o}}} = \frac{k_1^2 P_{\text{di}}}{k_1^2 P_{\text{in}}} = \frac{P_{\text{di}}}{P_{\text{in}}} = \left(\frac{P_{\text{in}}}{P_{\text{IP}}}\right)^2 \tag{2.5.51}$$

If $P_{\text{di}} = N_{\text{f}}$ (noise floor at the input) then

$$\frac{N_{\text{f}}}{P_{\text{in}}} = \left(\frac{P_{\text{in}}}{P_{\text{IP}}}\right)^2 \Rightarrow P_{\text{in}}^3 = P_{\text{IP}}^2 N_{\text{f}} \Rightarrow P_{\text{in}} = (P_{\text{IP}}^2 N_{\text{f}})^{1/3} \tag{2.5.52}$$

and the dynamic range is

$$\text{DR} = \frac{(P_{\text{IP}}^2 N_{\text{f}})^{1/3}}{N_{\text{f}}} = \left(\frac{P_{\text{IP}}}{N_{\text{f}}}\right)^{2/3} \tag{2.5.53}$$

or,

$$\text{DR(dB)} = \tfrac{2}{3}\left\{P_{\text{IP}}(\text{dBm}) - N_{\text{f}}(\text{dBm})\right\} \tag{2.5.54}$$

Example 2.15: A receiver is operating at 900 MHz with its bandwidth at 500 kHz and the noise figure at 8 dB. If its input impedance is 50 Ω and IP is 10 dBm then find its dynamic range

$$\begin{aligned} N_{\text{f}} = kT_{\text{o}}BF \Rightarrow N_f(\text{dBm}) &= 10\log_{10}(1.38 \times 10^{-23} \times 290 \times 500 \times 10^3 \times 10^3) + 8 \\ &= -108.99 \text{ dBm} \\ \therefore \quad \text{DR} &= \tfrac{2}{3}(10 + 108.99) = 79.32 \text{ dBm} \end{aligned}$$

SUGGESTED READING

C. A. Balanis, *Antenna Theory*. New York: Wiley, 1997.

J. Y. C. Cheah, Introduction to wireless communications applications and circuit design. In *RF and Microwave Circuit Design for Wireless Communications*, L. E. Larsen (ed). Boston: Artech House, 1996.

B. Razavi, *RF Microelectronics*. Englewood Cliffs, NJ: Prentice Hall, 1998.

Jochen H. Schiller, *Mobile Communication*. Reading, MA: Addison-Wesley, 2000.

J. R. Smith, *Modern Communication Circuits*. New York: McGraw Hill, 1997.

W. L. Stutzman and G. A. Thiele, *Antenna Theory and Design*. New York: Wiley, 1998.

PROBLEMS

1. **(a)** What is the gain in decibels of an amplifier with a power gain of 4?
   (b) What is the power gain ratio of a 5-dB amplifier?
   (c) Express 2 kW power in terms of dBm and dBw.

2. The maximum radiation intensity of a 90 percent efficiency antenna is 200 mW per unit solid angle. Find the directivity and gain (dimensionless and in dB) when the

(a) Input power is 40π mW.

(b) Radiated power is 40π mW.

3. The normalized far-zone field pattern of an antenna is given by

$$E = \begin{cases} \sqrt{\sin(\theta)\cos^2(\phi)} & 0 \le \theta \le \pi \text{ and } 0 \le \phi \le \pi/2,\ 3\pi/2 \le \phi \le 2\pi \\ 0 & \text{elsewhere} \end{cases}$$

Find the directivity of this antenna.

4. For an X-band (8.2–12.4 GHz) rectangular antenna, with aperture dimensions of 5.5 and 7.4 cm, find its maximum effective aperture (in cm^2) when its gain is

(a) 14.8 dB at 8.2 GHz

(b) 16.5 dB at 10.3 GHz

(c) 18.0 dB at 12.4 GHz

5. Transmitting and receiving antennas operating at 1 GHz with gains of 20 and 15 dB, respectively, are separated by a distance of 1 km. Find the maximum power delivered to the load when the input power is 150 W, assuming that the antennas are polarization matched.

6. An antenna with a total loss resistance of 1 ohm is connected to a generator whose internal impedance is $50 + j25$ ohm. Assuming that the peak voltage of the generator is 2 V and the impedance of antenna is $74 + j42.5$ ohm, find the power

(a) Supplied by the source (real power)

(b) Radiated by antenna

(c) Dissipated by antenna

7. The antenna connected to a radio receiver induces 9 μV of root-mean-square voltage into its input impedance that is 50 Ω. Calculate the input power in watts, dBm, and dBW. If the signal is amplified by 127 dB before it is fed to an 8-Ω speaker, find the output power.

8. The electric field radiated by a rectangular aperture, mounted on an infinite ground plane with z perpendicular to the aperture, is given by

$$\vec{E} = [\hat{\theta}\cos(\phi) - \hat{\phi}\sin(\phi)\cos(\theta)]\, f(r, \theta, \phi)$$

where $f(r, \theta, \phi)$ is a scalar function that describes the field variation of the antenna. Assuming that the receiving antenna is linearly polarized along the x-axis, find the polarization loss factor.

9. A radar receiver has a sensitivity of 10^{-12} W. If the radar antenna's effective aperture is 1 m^2 and the wavelength is 10 cm, find the transmitter power

required to detect an object at a distance of 3 km with a radar cross-section of $5\,m^2$.

10. Two space vehicles are separated by 10^8 m. Each has an antenna with D = 1000 operating at 2.5 GHz. If vehicle A's receiver requires 1 pW for a 20-dB signal-to-noise ratio, what transmitter power is required on vehicle B to achieve this signal-to-noise ratio?

11. **(a)** Design an earth-based radar system that receives 10^{-15} W of peak echo power from Venus. It is to operate at 10 GHz with a single antenna to be used for both transmitting and receiving. Specify the effective aperture of the antenna and the peak transmitter power. Assume that the Earth to Venus distance is 3 light-minutes; the diameter of Venus is $13 \bullet 10^6$ m; and the radar cross-section of Venus is 15 percent of its physical cross-section.

(b) If the system of (a) is used to observe the moon, determine the power received. Assume that the moon diameter is $3.5 \bullet 10^6$ m; its radar cross-section is 15 percent of the physical cross-section; and earth-to-moon distance is 1.2 light-seconds.

12. Consider an imaging satellite that sends closeup pictures of the planet Neptune. It uses a 10-W transmitter operating at 18 GHz and a 2.5-m diameter parabolic dish antenna. What earth-station system temperature is required to provide a signal-to-noise ratio of 3 dB for reception of a picture with $3 \bullet 10^6$ pixels (picture-elements) in 2 min if earth-station antenna diameter is 75 m? Assume aperture efficiencies of 70 percent and the Earth–Neptune distance as 4 light-hours. One pixel is equal to one bit and two bits per second has a bandwidth of 1 Hz.

13. Two receivers are shown below for a design trade-off study. The components have the following specifications:

(i)

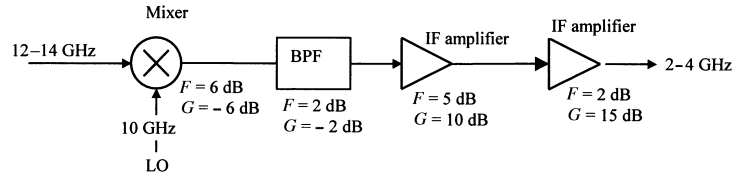

(ii)

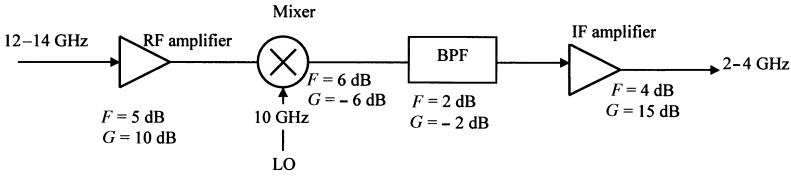

(a) Calculate the noise figure for the two systems.

(b) Calculate the overall gain of the two systems.

(c) Calculate the minimum detectable signal at the input of the two systems.

(d) If the output power at 1 dB compression point is 10 mW for both systems, calculate the dynamic range for the two systems.

14. Calculate the input minimum detectable signal in mW at room temperature for a receiver with (a) BW = 1 GHz, F = 5 dB; and (b) BW = 100 MHz, F = 10 dB.

15. (a) What is the rms noise voltage produced in a 10-kΩ resistance when its temperature is 45°C and the effective bandwidth is 100 MHz?

(b) A 50-kΩ resistance is connected in parallel with the 10-kΩ resistance of (a). What is the resulting rms noise voltage?

16. The intercept point in the transfer characteristic of a nonlinear system is found to be 33 dBm. If a −18-dBm signal is applied to this system, find the intermodulation ratio.

17. A receiver is operating at 2455 MHz with its bandwidth at 500 kHz and the noise figure at 15 dB. If its input impedance is 50 Ω and IP is 18 dBm then find its dynamic range.

Radio-Frequency and Microwave Communication Circuits: Analysis and Design
Devendra K. Misra

ISBNs: 0-471-41253-8 (Hardback); 0-471-22435-9 (Electronic)

3

TRANSMISSION LINES

Transmission lines are needed for connecting various circuit elements and systems together. Open-wire and coaxial lines are commonly used for circuits operating at low frequencies. On the other hand, coaxial line, stripline, microstrip line, and waveguides are employed at radio and microwave frequencies. Generally, the low-frequency signal characteristics are not affected as it propagates through the line. However, radio frequency and microwave signals are affected significantly because of the circuit size being comparable to the wavelength. A comprehensive understanding of signal propagation requires analysis of electromagnetic fields in a given line. On the other hand, a generalized formulation can be obtained using circuit concepts on the basis of line parameters.

This chapter begins with an introduction to line parameters and a distributed model of the transmission line. Solutions to the transmission line equation are then constructed in order to understand the behavior of the propagating signal. This is followed by the concepts of sending end impedance, reflection coefficient, return loss, and insertion loss. A quarter-wave impedance transformer is also presented along with a few examples to match resistive loads. Impedance measurement via the voltage standing wave ratio is then discussed. Finally, the Smith chart is introduced to facilitate graphical analysis and design of transmission line circuits.

3.1 DISTRIBUTED CIRCUIT ANALYSIS OF TRANSMISSION LINES

Any transmission line can be represented by a distributed electrical network, as shown in Figure 3.1. It comprises series inductors and resistors and shunt capacitors and resistors. These distributed elements are defined as follows:

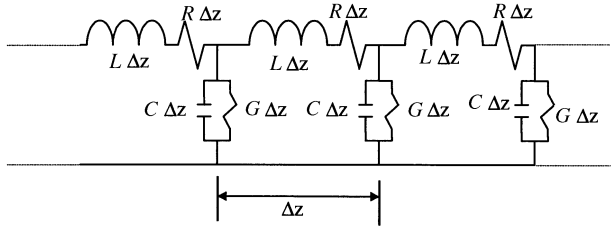

Figure 3.1 Distributed network model of a transmission line.

$L =$ Inductance per unit length (H/m)
$R =$ Resistance per unit length (ohm/m)
$C =$ Capacitance per unit length (F/m)
$G =$ Conductance per unit length (S/m)

L, R, C, and G are called the *line parameters*, which are determined theoretically by electromagnetic field analysis of the transmission line. These parameters are influenced by their cross-section geometry and the electrical characteristics of their constituents. For example, if a line is made up of an ideal dielectric and a perfect conductor then its R and G will be zero. If it is a coaxial cable with inner and outer radii a and b, respectively, as shown in Figure 3.2, then,

$$C = \frac{55.63\varepsilon_r}{\ln(b/a)} \quad \text{pF/m} \tag{3.1.1}$$

and,

$$L = 200\ln(b/a) \quad \text{nH/m} \tag{3.1.2}$$

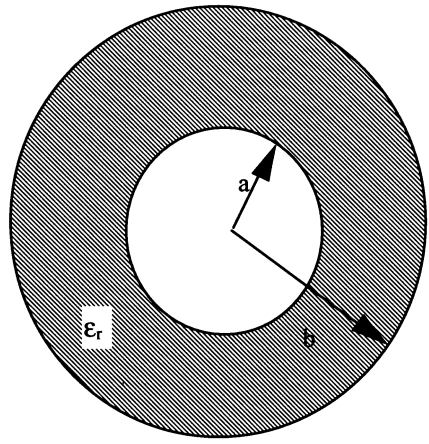

Figure 3.2 Coaxial line geometry.

where ε_r is the dielectric constant of the material between two coaxial conductors of the line.

If the coaxial line has small losses due to imperfect conductor and insulator, its resistance and conductance parameters can be calculated as follows:

$$R \approx 10\left[\frac{1}{a}+\frac{1}{b}\right]\sqrt{\frac{f_{(\mathrm{GHz})}}{\sigma}} \quad \text{ohm/m} \tag{3.1.3}$$

and,

$$G = \frac{0.3495\varepsilon_r f_{(\mathrm{GHz})} \tan(\delta)}{\ln(b/a)} \quad \text{S/m} \tag{3.1.4}$$

where $\tan(\delta)$ is loss-tangent of the dielectric material; σ is the conductivity (in S/m) of the conductors, and $f_{(\mathrm{GHz})}$is the signal frequency in GHz.

Characteristic Impedance of a Transmission Line

Consider a transmission line that extends to infinity, as shown in Figure 3.3. The voltages and the currents at several points on it are as indicated. When a voltage is divided by the current through that point, the ratio is found to remain constant. This ratio is called the characteristic impedance of the transmission line. Mathematically,

$$\text{Characteristic impedance} = Z_o = V_1/I_1 = V_2/I_2 = V_3/I_3 = \text{--------} = V_n/I_n$$

In actual electrical circuits, length of the transmission lines is always finite. Hence, it seems that the characteristic impedance has no significance in the real world. However, that is not the case. When the line extends to infinity, an electrical signal continues propagating in a forward direction without reflection. On the other hand, it may be reflected back by the load that terminates a transmission line of finite length. If one varies this termination, the strength of the reflected signal changes. When the transmission line is terminated by a load impedance that absorbs all the incident signal, the voltage source sees an infinite electrical length. Voltage-to-current ratio at any point on this line is a constant equal to the terminating impedance. In other words, there is a unique impedance for every transmission

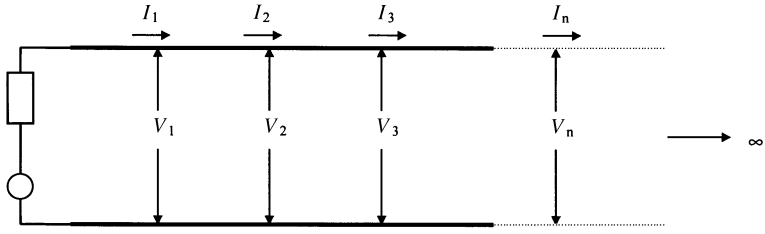

Figure 3.3 An infinitely long transmission line and a voltage source.

line that does not produce an echo signal when the line is terminated by it. The terminating impedance that does not produce echo on the line is equal to its characteristic impedance.

If

$$Z = R + j\omega L = \text{Impedance per unit length}$$
$$Y = G + j\omega C = \text{Admittance per unit length}$$

then, using the definition of characteristic impedance and the distributed model shown in Figure 3.1, we can write,

$$Z_o = \frac{(Z_o + Z\Delta z)\left(\frac{1}{Y\Delta z}\right)}{Z_o + Z\Delta z + \frac{1}{Y\Delta z}} = \frac{Z_o + Z\Delta z}{1 + Y\Delta z(Z_o + Z\Delta z)} \Rightarrow Z_o Y(Z_o + Z\Delta z) = Z$$

For $\Delta z \to 0$,

$$Z_o = \sqrt{\frac{Z}{Y}} = \sqrt{\frac{R + j\omega L}{G + j\omega C}} \tag{3.1.5}$$

Special Cases:

1. For a dc signal, $Z_o^{dc} = \sqrt{\frac{R}{G}}$.
2. For $\omega \to \infty$, $\omega L \gg R$ and $\omega C \gg G$, therefore, $Z_o(\omega \to \text{large}) = \sqrt{\frac{L}{C}}$.
3. For a lossless line, $R \to 0$ and $G \to 0$, and therefore, $Z_o = \sqrt{\frac{L}{C}}$.

Thus, a lossless semirigid coaxial line with $2a = 0.036$ inch, $2b = 0.119$ inch, and ε_r as 2.1 (Teflon-filled) will have $C = 97.71$ pF/m and $L = 239.12$ nH/m. Its characteristic impedance will be 49.5 ohm. Since conductivity of copper is 5.8×10^7 S/m and the loss-tangent of Teflon is 0.00015, $Z = 3.74 + j1.5 \times 10^3$ ohm/m, and $Y = 0.092 + j613.92$ mS/m at 1 GHz. The corresponding characteristic impedance is $49.5 - j0.058$ ohm, that is, very close to the approximate value of 49.5 ohm.

Example 3.1: Calculate the equivalent impedance and admittance of a one-meter-long line that is operating at 1.6 GHz. The line parameters are: $L =$

0.002 μH/m, $C = 0.012$ pF/m, $R = 0.015$ ohm/m, and $G = 0.1$ mS/m. What is the characteristic impedance of this line?

$$\begin{aligned} Z &= R + j\omega L = 0.015 + j2\pi \times 1.6 \times 10^9 \times 0.002 \times 10^{-6}\,\Omega/\text{m} \\ &= 0.015 + j20.11\,\Omega/\text{m} \\ Y &= G + j\omega C = 0.0001 + j2\pi \times 1.6 \times 10^9 \times 0.012 \times 10^{-12}\,\text{S/m} \\ &= 0.1 + j0.1206\,\text{mS/m} \\ Z_o &= \sqrt{\frac{Z}{Y}} = 337.02 + j121.38\,\Omega \end{aligned}$$

Transmission Line Equations

Consider the equivalent distributed circuit of a transmission line that is terminated by a load impedance Z_L, as shown in Figure 3.4. The line is excited by a voltage source $v(t)$ with its internal impedance Z_S. We apply Kirchhoff's voltage and current laws over a small length, Δz, of this line as follows:

For the loop, $v(z, t) = L\Delta z \dfrac{\partial i(z, t)}{\partial t} + R\Delta z i(z, t) + v(z + \Delta z, t)$
or,

$$\frac{v(z + \Delta z, t) - v(z, t)}{\Delta z} = -Ri(z, t) - L\frac{\partial i(z, t)}{\partial t}$$

Under the limit $\Delta z \to 0$, the above equation reduces to

$$\frac{\partial v(z, t)}{\partial z} = -\left[R \times i(z, t) + L\frac{\partial i(z, t)}{\partial t}\right] \tag{3.1.6}$$

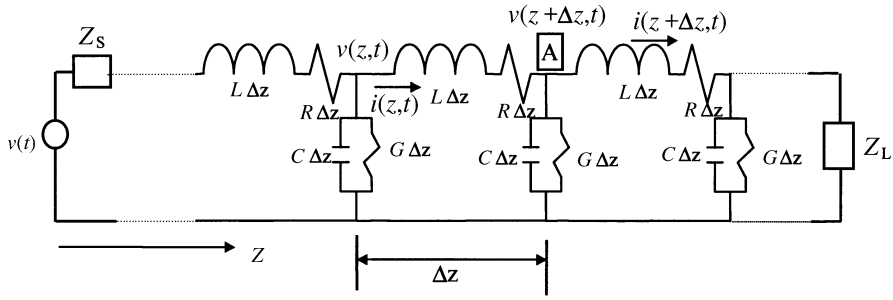

Figure 3.4 Distributed circuit model of a transmission line.

Similarly, at node A,

$$i(z,t) = i(z+\Delta z,t) + G\Delta z v(z+\Delta z,t) + C\Delta z \frac{\partial v(z+\Delta z,t)}{\partial t}$$

or,

$$\frac{i(z+\Delta z,t) - i(z,t)}{\Delta z} = -\left[G \times v(z+\Delta z,t) + C\frac{\partial v(z+\Delta z,t)}{\partial t}\right]$$

Again, under the limit $\Delta z \to 0$, it reduces to

$$\frac{\partial i(z,t)}{\partial z} = -G \times v(z,t) - C\frac{\partial v(z,t)}{\partial t} \tag{3.1.7}$$

Now, from equations (3.1.6) and (3.1.7) $v(z,t)$ or $i(z,t)$ can be eliminated to formulate the following:

$$\frac{\partial^2 v(z,t)}{\partial z^2} = RGv(z,t) + (RC+LG)\frac{\partial v(z,t)}{\partial t} + LC\frac{\partial^2 v(z,t)}{\partial t^2} \tag{3.1.8}$$

and,

$$\frac{\partial^2 i(z,t)}{\partial z^2} = RGi(z,t) + (RC+LG)\frac{\partial i(z,t)}{\partial t} + LC\frac{\partial^2 i(z,t)}{\partial t^2} \tag{3.1.9}$$

Special Cases:

1. For a lossless line, R and G will be zero, and these equations reduce to well-known homogeneous scalar wave equations,

$$\frac{\partial^2 v(z,t)}{\partial z^2} = LC\frac{\partial^2 v(z,t)}{\partial t^2} \tag{3.1.10}$$

and,

$$\frac{\partial^2 i(z,t)}{\partial z^2} = LC\frac{\partial^2 i(z,t)}{\partial t^2} \tag{3.1.11}$$

Note that the velocity of these waves is $\dfrac{1}{\sqrt{LC}}$.

2. If the source is sinusoidal with time (i.e., time-harmonic), we can switch to phasor voltages and currents. In that case, equations (3.1.8) and (3.1.9) can be

simplified as follows:

$$\frac{d^2V(z)}{dz^2} = ZYV(z) = \gamma^2 V(z) \tag{3.1.12}$$

and,

$$\frac{d^2I(z)}{dz^2} = ZYI(z) = \gamma^2 I(z) \tag{3.1.13}$$

where $V(z)$ and $I(z)$ are phasor quantities; Z and Y are impedance per unit length and admittance per unit length, respectively, as defined earlier. $\gamma = \sqrt{ZY} = \alpha + j\beta$, is known as the *propagation constant* of the line. α and β are called the *attenuation constant* and the *phase constant*, respectively.

Equations (3.1.12) and (3.1.13) are referred to as homogeneous Helmholtz equations.

Solution of Helmholtz Equations

Note that both of the differential equations have the same general format. Therefore, we consider the solution to the following generic equation here. Expressions for voltage and current on the line can be constructed on the basis of that.

$$\frac{d^2f(z)}{dz^2} - \gamma^2 f(z) = 0 \tag{3.1.14}$$

Assume that $f(z) = Ce^{\kappa z}$, where C and κ are arbitrary constants. Substituting it into (3.1.14), we find that $\kappa = \pm\gamma$. Therefore, a complete solution to this equation may be written as follows:

$$f(z) = C_1 e^{-\gamma z} + C_2 e^{\gamma z} \tag{3.1.15}$$

where C_1 and C_2 are integration constants that are evaluated through the boundary conditions.

Hence, complete solutions to equations (3.1.12) and (3.1.13) can be written as follows:

$$V(z) = V_{\text{in}} e^{-\gamma z} + V_{\text{ref}} e^{\gamma z} \tag{3.1.16}$$

and,

$$I(z) = I_{\text{in}} e^{-\gamma z} + I_{\text{ref}} e^{\gamma z} \tag{3.1.17}$$

where V_{in}, V_{ref}, I_{in}, and I_{ref} are integration constants that may be complex, in general. These constants can be evaluated from the known values of voltages and currents at

two different locations on the transmission line. If we express the first two of these constants in polar form as follows,

$$V_{\text{in}} = v_{\text{in}} e^{j\phi} \quad \text{and} \quad V_{\text{ref}} = v_{\text{ref}} e^{j\varphi}$$

the line voltage, in time domain, can be evaluated as follows:

$$\begin{aligned} v(z, t) &= \text{Re}[V(z) e^{j\omega t}] \\ &= \text{Re}[V_{\text{in}} e^{-(\alpha + j\beta)z} e^{j\omega t} + V_{\text{ref}} e^{+(\alpha + j\beta)z} e^{j\omega t}] \end{aligned}$$

or,

$$v(z, t) = v_{\text{in}} e^{-\alpha z} \cos(\omega t - \beta z + \phi) + v_{\text{ref}} e^{+\alpha z} \cos(\omega t + \beta z + \varphi) \tag{3.1.18}$$

At this point, it is important to analyze and understand the behavior of each term on the right-hand side of this equation. At a given time, the first term changes sinusoidally with distance, z, while its amplitude decreases exponentially. It is illustrated in Figure 3.5 (a). On the other hand, the amplitude of the second sinusoidal term increases exponentially. It is shown in Figure 3.5 (b). Further, the argument of cosine function decreases with distance in the former while it increases in the latter case. When a signal is propagating away from the source along $+z$-axis, its phase should be delayed. Further, if it is propagating in a lossy medium, its amplitude should decrease with distance z.

Thus, the first term on the right-hand side of equation (3.1.16) represents a wave traveling along $+z$-axis (an incident or outgoing wave). Similarly, the second term represents a wave traveling in the opposite direction (a reflected or incoming wave).

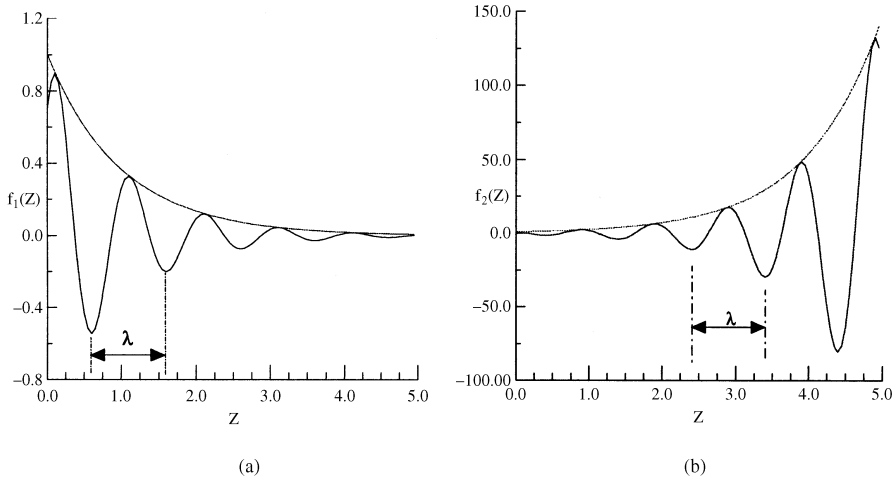

Figure 3.5 Behavior of two solutions to the Helmholtz equation with distance.

This analysis is also applied to equation (3.1.17). Note that I_{ref} is reflected current that will be 180° out-of-phase with incident current I_{in}.

Hence,

$$\frac{V_{in}}{I_{in}} = -\frac{V_{ref}}{I_{ref}} = Z_o$$

and, therefore, equation (3.1.17) may be written as follows:

$$I(z) = \frac{V_{in}}{Z_o} e^{-\gamma z} - \frac{V_{ref}}{Z_o} e^{\gamma z} \tag{3.1.19}$$

Incident and reflected waves change sinusoidally with both space and time. Time duration over which the phase angle of a wave goes through a change of 360° (2 π radians) is known as its *time-period*. Inverse of the time-period in seconds is the signal frequency in Hz. Similarly, the distance over which the phase angle of the wave changes by 360° (2 π radians) is known as its *wavelength* (λ). Therefore, the phase constant β is equal to 2 π divided by the wavelength in meters.

Phase and Group Velocities

The velocity with which the phase of a time-harmonic signal moves is known as its *phase velocity*. In other words, if we tag a phase point of the sinusoidal wave and monitor its velocity then we obtain the *phase velocity*, v_p, of this wave. Mathematically,

$$v_p = \frac{\omega}{\beta}$$

A transmission line has no dispersion if the phase velocity of a propagating signal is independent of frequency. Hence, a graphical plot of ω versus β will be a straight line passing through the origin. This kind of plot is called the *dispersion diagram* of a transmission line. An information-carrying signal is composed of many sinusoidal waves. If the line is dispersive then each of these harmonics will travel at a different velocity. Therefore, the information will be distorted at the receiving end. Velocity with which a group of waves travels is called the *group velocity*, v_g. It is equal to the slope of the dispersion curve of the transmission line.

Consider two sinusoidal signals with angular frequencies $\omega + \delta\omega$ and $\omega - \delta\omega$, respectively. Assume that these waves of equal amplitudes are propagating in z-direction with corresponding phase constants $\beta + \delta\beta$ and $\beta - \delta\beta$. The resultant wave can be found as follows.

$$\begin{aligned} f(z, t) &= \mathrm{Re}\{Ae^{j((\omega+\delta\omega)t-(\beta+\delta\beta)z)} + Ae^{j((\omega-\delta\omega)t-(\beta-\delta\beta)z)}\} \\ &= 2A\cos(\delta\omega t - \delta\beta z)\cos(\omega t - \beta z) \end{aligned}$$

Hence, the resulting wave, $f(z, t)$, is amplitude modulated. The envelope of this signal moves with the group velocity,

$$v_g = \frac{\delta\omega}{\delta\beta}$$

Example 3.2: A signal generator has an internal resistance of 50 Ω and an open-circuit voltage $v(t) = 3\cos(2\pi \times 10^8 t)$ V. It is connected to a 75-Ω lossless transmission line that is 4 m long and terminated by a matched load at the other end. If the signal propagation velocity on this line is 2.5×10^8 m/s, find the instantaneous voltage and current at an arbitrary location on the line.

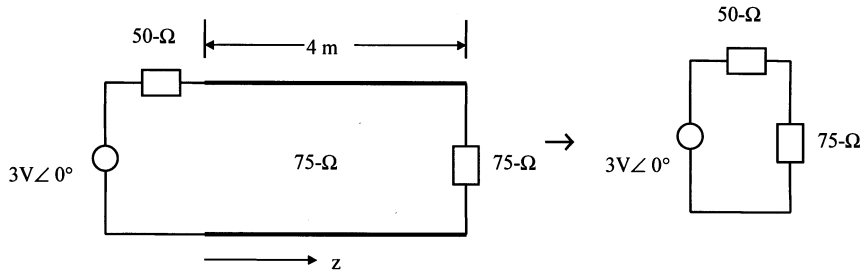

Since the transmission line is terminated by a load that is equal to its characteristic impedance, there will be no echo signal. Further, an equivalent circuit at its input end may be drawn, as shown in the illustration. Using the voltage division rule and Ohm's law, incident voltage and current can be determined as follows.

$$\text{Incident voltage at the input end, } V_{in}(z = 0) = \frac{75}{50 + 75} 3\angle 0^\circ = 1.8\angle 0^\circ \text{ V}$$

$$\text{Incident current at the input end, } I_{in}(z = 0) = \frac{3\angle 0^\circ}{50 + 75} = 0.024\angle 0^\circ \text{A}$$

and,

$$\beta = \frac{\omega}{v_p} = \frac{2\pi \times 10^8}{2.5 \times 10^8} = 0.8\pi \quad \text{rad/m}$$

$$\therefore\ V(z) = 1.8e^{-j0.8\pi z} V, \text{ and, } I(z) = 0.024e^{-j0.8\pi z} \text{A}$$

Hence,

$$v(z, t) = 1.8\cos(2\pi \times 10^8 t - 0.8\pi z)\text{V}, \text{ and } i(z, t) = 0.024\cos(2\pi \times 10^8 t - 0.8\pi z)\text{A}$$

Example 3.3: The parameters of a transmission line are:

$$R = 2\,\text{ohm/m},\ G = 0.5\,\text{mS/m},\ L = 8\,\text{nH/m},\ \text{and}\ C = 0.23\,\text{pF/m}$$

If the signal frequency is 1 GHz, calculate its characteristic impedance (Z_o) and the propagation constant (γ).

$$Z_o = \sqrt{\frac{R + j\omega L}{G + j\omega C}} = \sqrt{\frac{2 + j2\pi \times 10^9 \times 8 \times 10^{-9}}{0.5 \times 10^{-3} + j2\pi \times 10^9 \times 0.23 \times 10^{-12}}}\ \text{ohm}$$

$$= \sqrt{\frac{2 + j50.2655}{0.5 \times 10^{-3} + j1.4451 \times 10^{-3}}}\ \text{ohm} = \sqrt{\frac{50.31\angle 1.531\,\text{rad}}{15.29 \times 10^{-4}\angle 1.2377\,\text{rad}}}\ \text{ohm}$$

$$= 181.39\,\text{ohm}\angle 8.4^\circ = 179.44 + j26.51\,\text{ohm}$$

and $$\gamma = \sqrt{ZY} = \sqrt{(50.31\angle 1.531\,\text{rad.}) \times (15.29 \times 10^{-4}\angle 1.2377\,\text{rad.})}$$

$$= 0.2774\angle 79.31^\circ \text{m}^{-1} = 0.0514 + j0.2726\,\text{m}^{-1} = \alpha + j\beta$$

Therefore, $\alpha = 0.0514\,\text{Np/m}$, and $\beta = 0.2726\,\text{rad/m}$.

Example 3.4: Two antennas are connected through a quarter-wavelength-long lossless transmission line, as shown in the circuit illustrated here. However, the characteristic impedance of this line is unknown. The array is excited through a 50-Ω line. Antenna A has an impedance of $80 + j35\,\Omega$ while antenna B has $56 + j28\,\Omega$. Currents (peak values) through these antennas are found to be $1.5\angle 0^\circ$ A and $1.5\angle 90^\circ$ A, respectively. Determine characteristic impedance of the line connecting these two antennas, and the value of a reactance connected in series with antenna B.

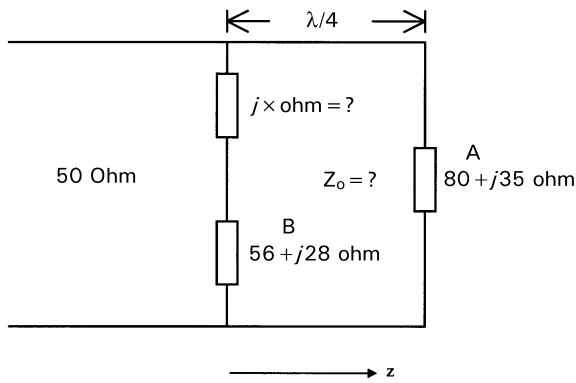

Assume that V_{in} and V_{ref} are the incident and reflected phasor voltages, respectively, at antenna A. Therefore, the current, I_A, through this antenna is

$$I_A = (V_{in} - V_{ref})/Z_o = 1.5\angle 0^\circ \text{A} \Rightarrow V_{in} - V_{ref} = Z_o I_A = Z_o 1.5\angle 0^\circ \text{ V}$$

Since the connecting transmission line is a quarter-wavelength long, incident and reflected voltages across the transmission line at the location of B will be jV_{in} and $-jV_{ref}$, respectively. Therefore, total voltage, V_{TBX}, appearing across antenna B and the reactance jX combined will be equal to $j(V_{in} - V_{ref})$.

$$V_{TBX} = j(V_{in} - V_{ref}) = jZ_o I_A = j1.5Z_o = 1.5Z_o\angle 90^\circ$$

Ohm's law can be used to find this voltage as follows.

$$V_{TBX} = (56 + j28 + jX)1.5\angle 90^\circ$$

Therefore, $X = -28\,\Omega$ and $Z_o = 56\,\Omega$.

Note that the unknown characteristic impedance is a real quantity because the transmission line is lossless.

3.2 SENDING END IMPEDANCE

Consider a transmission line of length ℓ and characteristic impedance Z_o. It is terminated by a load impedance Z_L, as shown in Figure 3.6. Assume that the incident and reflected voltages at its input ($z = 0$) are V_{in} and V_{ref}, respectively. The corresponding currents are represented by I_{in} and I_{ref}.

If $V(z)$ represents total phasor voltage at point z on the line and $I(z)$ is total current at that point, then

$$V(z) = V_{in}e^{-\gamma z} + V_{ref}e^{\gamma z} \tag{3.2.1}$$

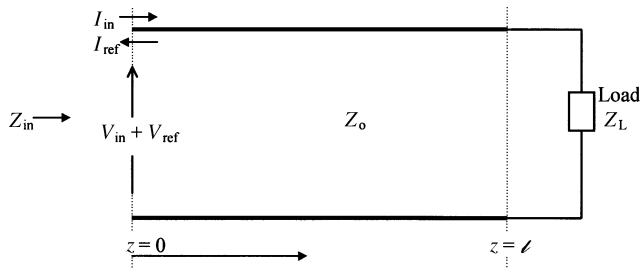

Figure 3.6 Transmission line terminated by a load impedance.

and,

$$I(z) = I_{\text{in}} e^{-\gamma z} + I_{\text{ref}} e^{\gamma z} \tag{3.2.2}$$

where V_{in}, V_{ref}, I_{in}, and I_{ref} are incident voltage, reflected voltage, incident current, and reflected current at $z = 0$, respectively.

Impedance at the input of this transmission line, Z_{in}, can be found after dividing total voltage by the total current at $z = 0$. Thus,

$$Z_{\text{in}} = \frac{V(z=0)}{I(z=0)} = \frac{V_{\text{in}} + V_{\text{ref}}}{I_{\text{in}} + I_{\text{ref}}} = \frac{V_{\text{in}} + V}{\frac{V_{\text{in}}}{Z_{\text{o}}} - \frac{V_{\text{ref}}}{Z_{\text{o}}}} = Z_{\text{o}} \frac{V_{\text{in}} + V_{\text{ref}}}{V_{\text{in}} - V_{\text{ref}}}$$

or,

$$Z_{\text{in}} = Z_{\text{o}} \frac{1 + \frac{V_{\text{ref}}}{V_{\text{in}}}}{1 - \frac{V_{\text{ref}}}{V_{\text{in}}}} = Z_{\text{o}} \frac{1 + \Gamma_{\text{o}}}{1 - \Gamma_{\text{o}}} \tag{3.2.3}$$

where $\Gamma_{\text{o}} = \rho e^{j\phi}$ is known as the *input reflection coefficient*.

Further,

$$Z_{\text{in}} = Z_{\text{o}} \frac{1 + \Gamma_{\text{o}}}{1 - \Gamma_{\text{o}}} \Rightarrow \frac{Z_{\text{in}}}{Z_{\text{o}}} = \overline{Z}_{\text{in}} = \frac{1 + \Gamma_{\text{o}}}{1 - \Gamma_{\text{o}}}$$

where $\overline{Z}_{\text{in}}$ is called the *normalized input impedance*.

Similarly, voltage and current at $z = \ell$ are related through load impedance as follows:

$$\begin{aligned} Z_{\text{L}} &= \frac{V(z=\ell)}{I(z=\ell)} = \frac{V_{\text{in}} e^{-\gamma\ell} + V_{\text{ref}} e^{+\gamma\ell}}{I_{\text{in}} e^{-\gamma\ell} + I_{\text{ref}} e^{+\gamma\ell}} \\ &= Z_{\text{o}} \frac{V_{\text{in}} e^{-\gamma\ell} + V_{\text{ref}} e^{+\gamma\ell}}{V_{\text{in}} e^{-\gamma\ell} - V_{\text{ref}} e^{+\gamma\ell}} = Z_{\text{o}} \frac{e^{-\gamma l} + \Gamma_{\text{o}} e^{+\gamma\ell}}{e^{-\gamma\ell} - \Gamma_{\text{o}} e^{+\gamma\ell}} \end{aligned}$$

Therefore,

$$\overline{Z}_{\text{L}} = \frac{e^{-\gamma\ell} + \Gamma_{\text{o}} e^{\gamma\ell}}{e^{-\gamma\ell} - \Gamma_{\text{o}} e^{+\gamma\ell}} \Rightarrow \Gamma_{\text{o}} = \frac{\overline{Z}_{\text{L}} - 1}{\overline{Z}_{\text{L}} + 1} e^{-2\gamma\ell} \tag{3.2.4}$$

and equation (3.2.3) can be written as follows:

$$\overline{Z}_{\text{in}} = \frac{1 + \dfrac{\overline{Z}_{\text{L}} - 1}{\overline{Z}_{\text{L}} + 1} e^{-2\gamma\ell}}{1 - \dfrac{\overline{Z}_{\text{L}} - 1}{\overline{Z}_{\text{L}} + 1} e^{-2\gamma\ell}} = \frac{\overline{Z}_{\text{L}}[1 + e^{-2\gamma\ell}] + [1 - e^{-2\gamma\ell}]}{\overline{Z}_{\text{L}}[1 - e^{2\gamma\ell}] + [1 + e^{-2\gamma\ell}]}$$

since,

$$\frac{1 - e^{-2\gamma\ell}}{1 + e^{-2\gamma\ell}} = \frac{e^{+\gamma l} - e^{-\gamma l}}{e^{+\gamma l} + e^{-\gamma l}} = \frac{\sinh(\gamma\ell)}{\cosh(\gamma\ell)} = \tanh(\gamma\ell)$$

$$\overline{Z}_{\text{in}} = \frac{\overline{Z}_{\text{L}} + \tanh(\gamma\ell)}{1 + \overline{Z}_{\text{L}} \tanh(\gamma\ell)}$$

or,

$$Z_{\text{in}} = Z_{\text{o}} \frac{Z_{\text{L}} + Z_{\text{o}} \tanh(\gamma\ell)}{Z_{\text{o}} + Z_{\text{L}} \tanh(\gamma\ell)} \tag{3.2.5}$$

For a lossless line, $\gamma = \alpha + j\beta = j\beta$, and therefore, $\tanh(\gamma\ell) = \tanh(j\beta\ell) = j\tan(\beta\ell)$. Hence, equation (3.2.5) simplifies as follows.

$$Z_{\text{in}} = Z_{\text{o}} \frac{Z_{\text{L}} + jZ_{\text{o}} \tan(\beta\ell)}{Z_{\text{o}} + jZ_{\text{L}} \tan(\beta\ell)} \tag{3.2.6}$$

Note from this equation that Z_{in} repeats periodically every one-half wavelength on the transmission line. In other words, input impedance on a lossless transmission line will be the same at points $d \pm n\lambda/2$, where n is an integer. It is due to the fact that

$$\beta\ell = \frac{2\pi}{\lambda}\left(d \pm \frac{n\lambda}{2}\right) = \frac{2\pi d}{\lambda} \pm n\pi$$

and $\tan(\beta\ell) = \tan\left(\dfrac{2\pi d}{\lambda} \pm n\pi\right) = \tan\left(\dfrac{2\pi d}{\lambda}\right)$.

Special Cases:

1. $Z_{\text{L}} = 0$ (i.e., a lossless line is short circuited) $\Rightarrow Z_{\text{in}} = jZ_{\text{o}} \tan(\beta\ell)$.
2. $Z_{\text{L}} = \infty$ (i.e., a lossless line has an open circuit at the load) $\Rightarrow Z_{\text{in}} = -jZ_{\text{o}} \cot(\beta\ell)$.
3. $\ell = \lambda/4$ and, therefore, $\beta\ell = \pi/2 \Rightarrow Z_{\text{in}} = Z_{\text{o}}^2/Z_{\text{L}}$.

According to the first two of these cases, a lossless line can be used to synthesize an arbitrary reactance. The third case indicates that a quarter-wavelength-long line of suitable characteristic impedance can be used to transform a load impedance Z_{L} to a

new value of Z_{in}. This kind of transmission line is called an *impedance transformer* and is useful in impedance-matching application. Further, this equation can be rearranged as follows:

$$\overline{Z}_{in} = \frac{1}{\overline{Z}_L} = \overline{Y}_L$$

Hence, normalized impedance at a point a quarter-wavelength away from the load is equal to the normalized load admittance.

Example 3.5: A transmission line of length d and characteristic impedance Z_o acts as an impedance transformer to match a 150-Ω load to a 300-Ω line (see illustration). If the signal wavelength is 1 m, find (a) d, (b) Z_o, and (c) the reflection coefficient at the load.

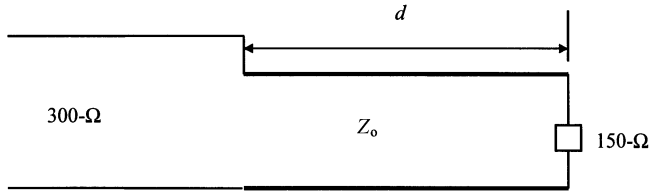

(a) $d = \lambda/4 \rightarrow \mathrm{d} = 0.25\,\mathrm{m}$.

(b) $Z_o = \sqrt{Z_{in}Z_L} \rightarrow Z_o = (150 \times 300)^{1/2} = 212.132\,\mathrm{ohm}$.

(c) $\Gamma_L = \dfrac{\overline{Z}_L - 1}{\overline{Z}_L + 1} = \dfrac{Z_L - Z_o}{Z_L + Z_o} = \dfrac{150 - 212.132}{150 + 212.132} = 0.1716.$

Example 3.6: Design a quarter-wavelength transformer to match a 20-Ω load to the 45-Ω line at 3 GHz. If this transformer is made from a Teflon-filled ($\varepsilon_r = 2.1$) coaxial line, calculate its length (in cm). Also, determine the diameter of its inner conductor if the inner diameter of the outer conductor is 0.5 cm. Assume that the impedance transformer is lossless.

$$Z_o = \sqrt{Z_{in}Z_L} = \sqrt{45 \times 20} = 30\,\Omega$$

and,

$$Z_o = \sqrt{\frac{L}{C}} = \sqrt{\frac{200 \times 10^{-9}}{55.63 \times \varepsilon_r \times 10^{-12}}}\ln(b/a) = 30$$

$$\therefore\ \ln(b/a) = \frac{30}{41.3762} = 0.7251$$

Therefore,

$$\frac{b}{a} = \frac{2b}{2a} = e^{0.7251} = 2.0649 \Rightarrow 2a = \frac{2b}{2.0649} = \frac{0.5}{2.0649} = 0.2421\,\text{cm}$$

Phase constant $\beta = \omega\sqrt{LC}$

$$\begin{aligned}\beta = \frac{2\pi}{\lambda} \Rightarrow \frac{1}{\lambda} &= \frac{\omega}{2\pi}\sqrt{LC} = f \times \sqrt{200 \times 55.63 \times \varepsilon_r \times 10^{-21}} \\ &= 3 \times 10^9 \times 10^{-10} \times \sqrt{200 \times 55.63 \times 2.1 \times 0.1} \\ &= 14.5011\,\text{m}^{-1}\end{aligned}$$

Therefore, $\lambda = 0.06896$ m, and $d = \dfrac{\lambda}{4} = 0.01724\,\text{m} = 1.724\,\text{cm}$.

Example 3.7: Design a quarter-wavelength microstrip impedance transformer to match a patch antenna of 80 Ω with a 50-Ω line. The system is to be fabricated on a 1.6-mm-thick substrate ($\varepsilon_r = 2.3$) that operates at 2 GHz (see illustration).

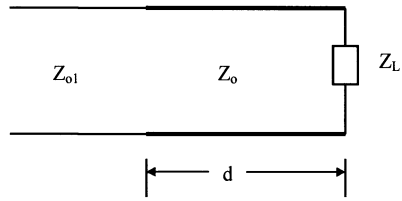

Characteristic impedance of the microstrip line impedance transformer must be

$$Z_o = \sqrt{Z_{o1}Z_L} = 63.2456\,\Omega$$

Design formulas for a microstrip line are given in the appendix. Assume that the strip thickness t is less than 0.096 mm and dispersion is negligible for the time being at the operating frequency.

$$A = \frac{63.2456}{60}\left(\frac{2.3+1}{2}\right)^{1/2} + \left(\frac{2.3-1}{2.3+1}\right) \times \left(0.23 + \frac{0.11}{2.3}\right) = 1.4635$$

$$B = \frac{60\pi^2}{63.2456\sqrt{2.3}} = 6.1739$$

Since $A \leq 1.52$,

$$\frac{w}{h} = \frac{2}{\pi}\left\{6.1739 - 1 - \ln(2 \times 6.1739 - 1) + \frac{2.3-1}{2 \times 2.3}\left[\ln(6.1739 - 1) + 0.39 - \frac{0.62}{2.3}\right]\right\}$$
$$= \frac{2 \times 3.2446}{\pi} = 2.0656 \Rightarrow w = 3.3\,\text{mm}$$

At this point, we can check if the dispersion in the line is really negligible. For that, we determine the effective dielectric constant as follows:

$$F\left(\frac{w}{h}\right) = \left(1 + 12\frac{h}{w}\right)^{-1/2} = \left(1 + \frac{12}{2.0656}\right)^{-1/2} = 0.383216$$

Assuming that $\frac{t}{h} = 0.005$,

$$\varepsilon_e = \frac{2.3+1}{2} + \frac{2.3-1}{2} \times 0.383216 - \frac{2.3-1}{4.6} \times \frac{0.005}{\sqrt{2.0656}} = 1.8981 \approx 1.9$$

and,

$$F = \frac{4h\sqrt{\varepsilon_r - 1}}{\lambda_o}\left\{0.5 + \left[1 + 2 \times \log\left(1 + \frac{w}{h}\right)\right]^2\right\} = 0.213712$$

$$\varepsilon_e(f) = \left(\frac{\sqrt{2.3} - \sqrt{1.9}}{1 + 4 \times F^{-1.5}} + \sqrt{1.9}\right)^2 = 1.909192$$

Since $\varepsilon_e(f)$ is very close to ε_e, dispersion in the line can be neglected.

$$\therefore \lambda = \frac{3 \times 10^8}{2 \times 10^9 \times \sqrt{1.9}}\text{m} = 10.8821\,\text{cm} \Rightarrow \text{length of line} = \frac{10.8821}{4} = 2.72\,\text{cm}$$

Reflection Coefficient, Return Loss, and Insertion Loss

The voltage reflection coefficient is defined as the ratio of reflected to incident phasor voltages at a location in the circuit. In the case of a transmission line terminated by load Z_L, the voltage reflection coefficient is given by equation (3.2.4). Hence,

$$\Gamma = \frac{V_{ref}}{V_{in}} = \frac{Z_L - Z_o}{Z_L + Z_o}e^{-2\gamma\ell} = \rho_L e^{j\theta}e^{-2(\alpha+j\beta)\ell} = \rho_L e^{-2\alpha\ell}e^{-j(2\beta\ell-\theta)} \qquad (3.2.7)$$

where $\rho_L e^{j\theta} = \frac{Z_L - Z_o}{Z_L + Z_o}$ is called the *load reflection coefficient.*

Equation (3.2.7) indicates that the magnitude of reflection coefficient decreases by a factor of $e^{-2\alpha\ell}$ as the observation point moves away from the load. Further, its phase angle changes by $-2\beta\ell$. A polar (magnitude and phase) plot of it will look like a spiral, as shown in Figure 3.7 (a). However, the magnitude of reflection coefficient will not change if the line is lossless. Therefore, the reflection coefficient point will be moving clockwise on a circle of radius equal to its magnitude, as the linelength is increased. As illustrated in Figure 3.7 (b), it makes one complete revolution for each half-wavelength distance away from load (because $-2\beta\lambda/2 = -2\pi$).

Similarly, the current reflection coefficient, Γ_c, is defined as a ratio of reflected to incident signal-current phasors. It is related to the voltage reflection coefficient as follows.

$$\Gamma_c = \frac{I_{ref}}{I_{in}} = \frac{-V_{ref}/Z_o}{V_{in}/Z_o} = -\Gamma$$

Return loss of a device is defined as the ratio of reflected power to incident power at its input. Since the power is proportional to the square of the voltage at that point, it may be found as

$$\text{Return loss} = \frac{\text{Reflected power}}{\text{Incident power}} = \rho^2$$

Generally, it is expressed in dB, as follows:

$$\text{Return loss} = 20\log_{10}(\rho)\text{dB} \tag{3.2.8}$$

Insertion loss of a device is defined as the ratio of transmitted power (power available at the output port) to that of power incident at its input. Since transmitted power is equal to the difference of incident and reflected powers for a lossless device, the insertion loss can be expressed as follows.

$$\text{Insertion loss of a lossless device} = 10\log_{10}(1-\rho^2)\text{dB} \tag{3.2.9}$$

Low-Loss Transmission Lines

Most practical transmission lines possess very small loss of propagating signal. Therefore, expressions for the propagation constant and the characteristic impedance can be approximated for such lines as follows.

$$\gamma = \sqrt{ZY} = \sqrt{(R+j\omega L)(G+j\omega C)} = \sqrt{-\omega^2 LC\left(1+\frac{R}{j\omega L}\right)\left(1+\frac{G}{j\omega C}\right)}$$

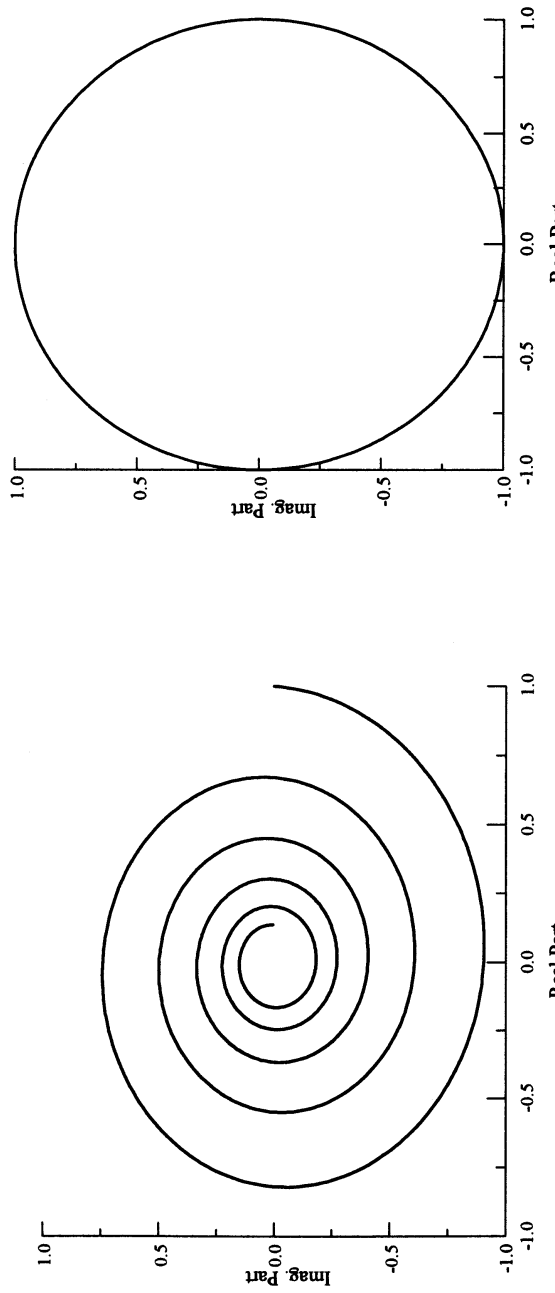

Figure 3.7 Reflection coefficient on (a) a lossy, and (b) a lossless transmission line.

For $R \ll \omega L$ and $G \ll \omega C$, a first-order approximation is

$$\gamma = \alpha + j\beta \approx j\omega\sqrt{LC}\left(1 + \frac{R}{j2\omega L}\right)\left(1 + \frac{G}{j2\omega C}\right) \approx j\omega\sqrt{LC}\left(1 + \frac{R}{j2\omega L} + \frac{G}{j2\omega C}\right)$$

Therefore,

$$\alpha \approx \frac{1}{2}\left(R\sqrt{\frac{C}{L}} + G\sqrt{\frac{L}{C}}\right)\text{Np/m} \tag{3.2.10}$$

and,

$$\beta \approx \omega\sqrt{LC}\ \text{rad/m} \tag{3.2.11}$$

$$Z_o = \sqrt{\frac{R + j\omega L}{G + j\omega C}} = \sqrt{\frac{L}{C}}\left(1 + \frac{R}{j\omega L}\right)^{1/2}\left(1 + \frac{G}{j\omega C}\right)^{-1/2}$$

Hence,

$$\begin{aligned} Z_o &\approx \sqrt{\frac{L}{C}\left(1 + \frac{R}{j2\omega L}\right)\left(1 - \frac{G}{j2\omega C}\right)} \approx \sqrt{\frac{L}{C}\left(1 + \frac{R}{j2\omega L} - \frac{G}{j2\omega C}\right)} \\ &= \sqrt{\frac{L}{C}}\left(1 + \frac{1}{j2\omega}\left(\frac{R}{L} - \frac{G}{C}\right)\right) \end{aligned} \tag{3.2.12}$$

Thus, the attenuation constant of a low-loss line is independent of frequency while its phase constant is linear, as in the case of a lossless line. However, the frequency dependency of its characteristic impedance is of concern to communication engineers, because it will distort the signal. If $RC = GL$, the frequency dependent term will go to zero. This kind of low-loss line is called the *distortionless line*. Hence,

$$\gamma = \sqrt{ZY} = \sqrt{(R + j\omega L)(G + j\omega C)} = (R + j\omega L)\sqrt{\frac{C}{L}} = \alpha + j\beta, \quad \left(\because\ G = \frac{RC}{L}\right) \tag{3.2.13}$$

Example 3.8: A signal propagating through a 50-Ω distortionless transmission line attenuates at the rate of 0.01 dB per meter. If this line has a capacitance of 100 pF per meter, find (a) R, (b) L, (c) G, and (d) v_p.

Since the line is distortionless,

$$Z_o = \sqrt{\frac{L}{C}} = 50$$

and,

$$\alpha = 0.01\,\text{dB/m} \approx 0.01/8.69\,\text{Np/m} = 1.15 \times 10^{-3}\,\text{Np/m}$$

Hence,

(a) $R = \alpha\sqrt{\dfrac{L}{C}} = 1.15 \times 10^{-3} \times 50 = 0.057\,\Omega/\text{m}$

(b) $L = CZ_o^2 = 10^{-10} \times 50^2\,\text{H/m} = 0.25\,\mu\text{H/m}$

(c) $G = \dfrac{RC}{L} = \dfrac{R}{Z_o^2} = \dfrac{0.057}{50^2}\,\text{S/m} = 22.8\,\mu\text{S/m}$

(d) $v_p = \dfrac{1}{\sqrt{LC}} = 2 \times 10^8\,\text{m/s}$

Experimental Determination of Characteristic Impedance and Propagation Constant of a Transmission Line

The given transmission line of length d is kept open at one end, and the impedance at its other end is measured using an impedance bridge. Assume that it is Z_{oc}. The process is repeated after placing a short circuit at its open end and this impedance is recorded as Z_{sc}. Using equation (3.2.5), one can write

$$Z_{oc} = Z_o \coth(\gamma d) \tag{3.2.14}$$

and,

$$Z_{sc} = Z_o \tanh(\gamma d) \tag{3.2.15}$$

Therefore,

$$Z_o = \sqrt{Z_{oc}Z_{sc}} \tag{3.2.16}$$

and,

$$\tanh(\gamma d) = \sqrt{\frac{Z_{sc}}{Z_{oc}}} \Rightarrow \gamma = \frac{1}{d}\tanh^{-1}\left(\sqrt{\frac{Z_{sc}}{Z_{oc}}}\right) \tag{3.2.17}$$

These two equations can be solved to determine Z_o and γ. The following identity can be used to facilitate the evaluation of the propagation constant.

$$\tanh^{-1}(Z) = \frac{1}{2}\ln\left(\frac{1+Z}{1-Z}\right)$$

The following examples illustrate this procedure.

Example 3.9: Impedance at one end of the transmission line is measured to be $Z_{in} = 30 + j60$ ohm using an impedance bridge, while its other end is terminated by a load Z_L. The experiment is repeated twice with the load replaced first by a short

circuit and then by an open circuit. This data is recorded as $j53.1$ ohm and $-j48.3$ ohm, respectively. Find the characteristic resistance of this line and the load impedance.

$$Z_o = \sqrt{Z_{sc} \times Z_{oc}} = \sqrt{j53.1 \times (-j48.3)} = 50.6432\,\Omega$$

$$Z_{in} = Z_o \frac{Z_L + jZ_o \tan(\beta\ell)}{Z_o + jZ_L \tan(\beta\ell)} = Z_o \frac{Z_L + Z_{sc}}{Z_o + jZ_L \tan(\beta\ell)}$$

$$= \frac{Z_o}{j\tan(\beta\ell)} \times \frac{Z_L + Z_o}{Z_L + \dfrac{Z_o}{j\tan(\beta\ell)}}$$

$$\therefore Z_{in} = Z_{oc} \frac{Z_L + Z_{sc}}{Z_L + Z_{oc}} \Rightarrow Z_L = Z_{oc} \frac{Z_{sc} - Z_{in}}{Z_{in} - Z_{oc}}$$

$$= -j48.3 \times \frac{j53.1 - (30 + j60)}{30 + j60 - (-j48.3)}$$

Therefore,

$$Z_L = 11.6343 + j6.3\,\Omega$$

Example 3.10: Measurements are made on a 1.5-m-long transmission line using an impedance bridge. After short-circuiting at one of its ends, impedance at the other end is found to be $j103$ ohm. Repeating the experiment with the short circuit now replaced by an open circuit gives $-j54.6$ ohm. Determine the propagation constant and the characteristic impedance of this line.

$$Z_o = \sqrt{Z_{oc} Z_{sc}} = \sqrt{-j54.6 \times j103} = 74.99 \approx 75\,\Omega$$

$$\tanh(1.5\gamma) = \sqrt{\frac{j103}{-j54.3}} = j1.8969 \Rightarrow 1.5\gamma = \tanh^{-1}(j1.8969) = \frac{1}{2}\ln\left(\frac{1 + j1.8969}{1 - j1.8969}\right)$$

$$1.5\gamma = \frac{1}{2}\ln\left(\frac{1 + j1.8969}{1 - j1.8969}\right) = \frac{1}{2}\ln(1\angle 2.1713\,\text{rad}) = \frac{1}{2}\ln(e^{j2.1713})$$

$$= j1.08565$$

$$\text{and, } \gamma = j0.7238\,\text{m}^{-1}.$$

Example 3.11: A 10-m long, 50-ohm lossless transmission line is terminated by a load, $Z_L = 100 + j50$ ohm. It is driven by a signal generator that has an open-circuit voltage V_s at $100\angle 0^\circ$ V and source impedance Z_s at 50 ohm. The propagating signal

has a phase velocity of 200 m/μS at 26 MHz. Determine the impedance at its input end and the phasor voltages at both its ends (see illustration).

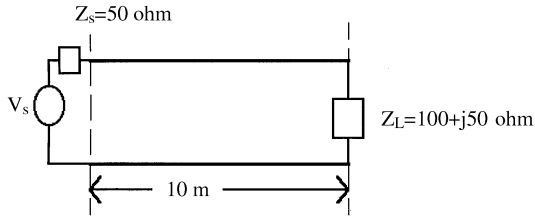

$$Z_{\text{in}} = Z_{\text{o}} \frac{Z_{\text{L}} + jZ_{\text{o}} \tan(\beta\ell)}{Z_{\text{o}} + jZ_{\text{L}} \tan(\beta\ell)} \text{ and } \beta = \frac{\omega}{v_p} = \frac{2\pi \times 26 \times 10^6}{200 \times 10^6} = 0.8168 \text{ rad/m}$$

$$\therefore Z_{\text{in}} = \frac{100 + j50 + j50 \tan(8.168)}{50 + j(100 + j50) \tan(8.168)} = 19.5278\,\Omega \angle 0.181 \text{ rad} = 19.21 + j3.53\,\Omega$$

The equivalent circuits at its input and at the load can be drawn as in the illustration.

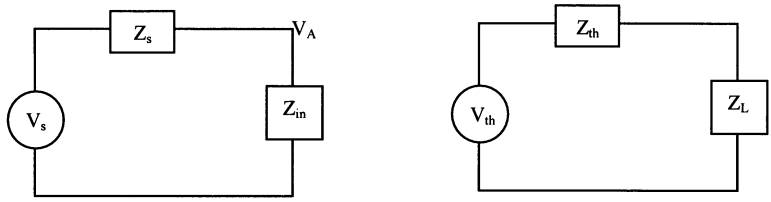

Voltage at the input end, $V_{\text{A}} = \dfrac{V_{\text{S}}}{Z_{\text{S}} + Z_{\text{in}}} Z_{\text{in}} = \dfrac{100 \times 19.5278 \angle 0.18 \text{ rad}}{50 + 19.21 + j3.52} \text{V}$

or,

$$V_{\text{A}} = \frac{1952.78 \angle 0.181 \text{ rad}}{69.2995 \angle 0.0508 \text{ rad}} = 28.1788 \angle 0.1302 \text{ rad V} = 28.1788 \angle 7.46^\circ \text{ V}$$

For determining voltage at the load, a Thevenin equivalent circuit can be used as follows:

$$Z_{\text{th}} = Z_{\text{o}} \frac{Z_{\text{s}} + jZ_{\text{o}} \tan(\beta\ell)}{Z_{\text{o}} + jZ_{\text{s}} \tan(\beta\ell)} = Z_{\text{o}}, \quad \because Z_{\text{s}} = Z_{\text{o}} = 50\,\Omega$$

and,

$$V_{\text{th}} = (V_{\text{in}} + V_{\text{ref}})_{\text{at,o.c.}} = (2 \times V_{\text{in}})_{\text{at o.c.}} = 100 \text{ V} \angle -8.168 \text{ rad}$$

$$\therefore V_{\text{L}} = \frac{V_{\text{th}}}{Z_{\text{th}} + Z_{\text{L}}} Z_{\text{L}} = \frac{100 \angle -8.168 \text{ rad}}{50 + 100 + j50} \times (100 + j50) \text{ V}$$

or,

$$V_L = 70.71 V\angle -8.0261\,\text{rad} = 70.71\angle -459.86^\circ\,\text{V} = 70.71\angle -99.86^\circ\,\text{V}$$

Alternatively,

$$V(z) = V_{in}e^{-j\beta z} + V_{ref}e^{j\beta z} = V_{in}(e^{-j\beta z} + \Gamma e^{j\beta z})$$

where V_{in} is incident voltage at $z = 0$ while Γ is the input reflection coefficient.

$$V_{in} = 50\,\text{V}\angle 0^\circ$$

and,

$$\Gamma = \frac{19.21 + j3.52 - 50}{19.21 + j3.52 + 50} = 0.4472\angle 2.9769\,\text{rad}$$

Hence,

$$\begin{aligned} V_L = V(z = 10\,\text{m}) &= 50(e^{-j8.168} + 0.4472e^{j(2.9769+8.168)}) \\ &= 50 \times 1.4142\,\text{V}\angle -1.742\,\text{rad} \end{aligned}$$

or,

$$V_L = 70.7117\,\text{V}\angle -99.8664^\circ$$

Example 3.12: Two identical signal generators are connected in parallel through a quarter-wavelength-long lossless 50-Ω transmission line. Each of these generators has an open-circuit voltage of $12\angle 0^\circ$ V and a source impedance of 50 Ω. It drives a 10-Ω load through another quarter-wavelength-long similar transmission line as illustrated here. Determine the power dissipated by the load.

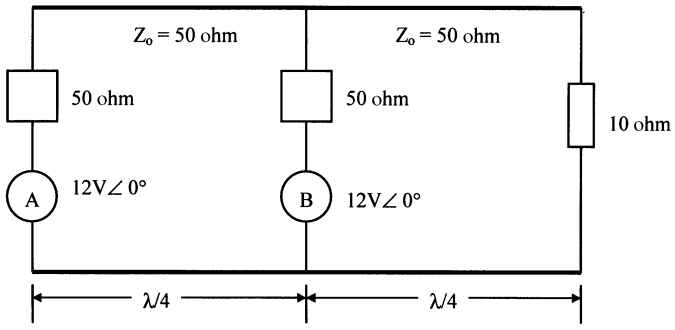

The signal generator connected at the left (source A), and the quarter-wavelength-long line connecting it, can be replaced by a Thevenin equivalent voltage source of $12\,\text{V}\angle -90^\circ$ with its internal resistance at 50 ohm. This voltage source can be combined with $12\angle 0^\circ\,\text{V}$ (source B) already there, which also has an internal resistance of 50 ohm. The resulting source will have a Thevenin voltage of $6 - j6\,\text{V} = 6\sqrt{2}\,\text{V}\angle -45^\circ$ and an internal resistance of 25 Ω (i.e., two 50-Ω resistances connected in parallel). The load will transform to $50 \times 50/10 = 250$ ohm at the location of source B. Therefore, a simplified circuit can be drawn as in the illustration.

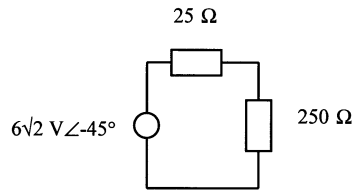

Voltage across 250 ohm will be equal to

$$250 \times (6 - j6)/275\,\text{V} = 60\sqrt{2}/11\angle -45^\circ\,\text{V}$$

Thus, the dissipated power, P_d, can be calculated as follows:

$$P_d = \frac{60^2 \times 2}{11^2 \times 2 \times 250} = 0.119008\,\text{W} = 119.008\,\text{mW}$$

3.3 STANDING WAVE AND STANDING WAVE RATIO

Consider a lossless transmission line that is terminated by a load impedance Z_L, as shown below in Figure 3.8. Incident and reflected voltage phasors at its input (i.e., at

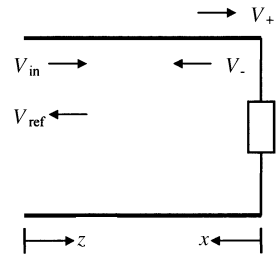

Figure 3.8 A lossless transmission line with termination.

$z = 0$) are assumed to be V_{in} and V_{ref}, respectively. Therefore, total voltage $V(z)$ can be expressed as follows:

$$V(z) = V_{\text{in}} e^{-j\beta z} + V_{\text{ref}} e^{+j\beta z}$$

Alternatively, $V(x)$ can be written as

$$V(x) = V_{+} e^{+j\beta x} + V_{-} e^{-j\beta x} = V_{+}[e^{+j\beta x} + \Gamma e^{-j\beta x}]$$

or,

$$V(x) = V_{+}[e^{+j\beta x} + \rho e^{-j(\beta x - \phi)}] \tag{3.3.1}$$

where,

$$\Gamma = \rho e^{j\phi} = \frac{V_{-}}{V_{+}}$$

V_{+} and V_{-} represent incident and reflected wave voltage phasors, respectively, at the load point (i.e., at $x = 0$).

Let us first consider two extreme conditions at the load. In one case, the transmission line has an open circuit, while in the other it has a short-circuit termination. Therefore, magnitude of the reflection coefficient, ρ, is unity in both cases. However, the phase angle, ϕ, is zero for the former, while it becomes π for the latter. Phasor diagrams for these two cases are depicted in Figure 3.9 (a) and (b), respectively. As distance x from the load increases, phasor $e^{j\beta x}$ rotates counter-clockwise because of the increase in its phase angle βx. On the other hand, phasor $e^{-j\beta x}$ rotates clockwise by the same amount. Therefore, the phase angle of the

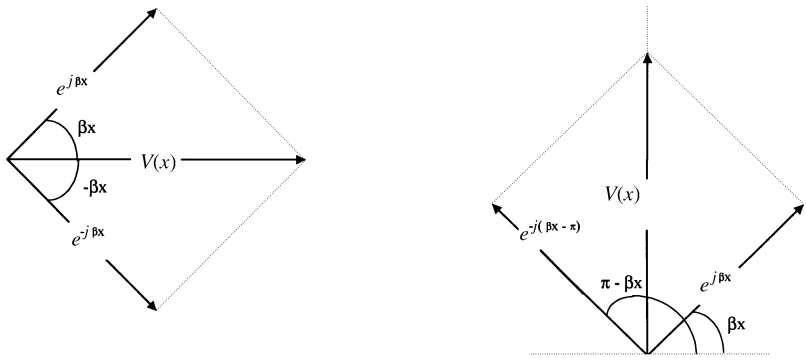

(a) with an open-circuit termination

(b) with a short-circuit termination

Figure 3.9 Phasor diagrams of line voltage with (a) an open-circuit (b) a short-circuit termination.

resultant voltage, $V(x)$, remains constant with space coordinate x while its magnitude varies sinusoidally between $\pm 2V_+$. Since the phase angle of the resultant signal $V(x)$ does not change with distance, it does not represent a propagating wave. Note that there are two waves propagating on this line in opposite directions. However, the resulting signal represents a *standing wave*.

When the terminating load is of an arbitrary value that is different from the characteristic impedance of the line there are still two waves propagating in opposite directions. The interference pattern of these two signals is stationary with time. Assuming that V_+ is unity, a phasor diagram for this case is drawn as shown in Figure 3.10. Magnitude of the resultant signal, $V(x)$, can be determined using the law of parallelogram, as follows.

$$|V(x)| = |V_+|\{1 + \rho^2 + 2\rho\cos(2\beta x - \phi)\}^{1/2} \tag{3.3.2}$$

The reflection coefficient, $\Gamma(x)$, can be expressed as follows.

$$\Gamma(x) = \frac{V_- e^{-j\beta x}}{V_+ e^{j\beta x}} = \rho e^{-j(2\beta x - \phi)} \tag{3.3.3}$$

Hence, the magnitude of this standing wave changes with location on the transmission line. Since x appears only in the argument of cosine function, the voltage magnitude has an extreme value whenever this argument is an integer multiple of π. It has a maximum whenever the reflected wave is in phase with the incident signal, and that requires that the following condition be satisfied:

$$(2\beta x - \phi) = \pm 2n\pi, \quad n = 0, 1, 2, \ldots \tag{3.3.4}$$

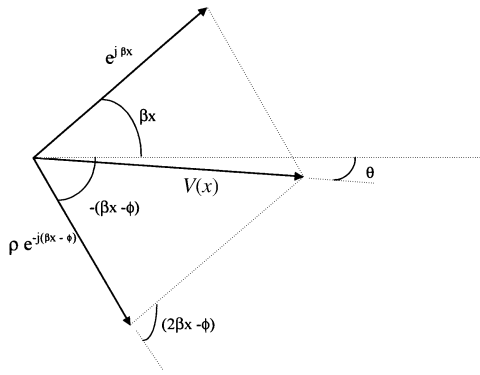

Figure 3.10 Phasor diagram of line voltage with an arbitrary termination.

On the other hand, $V(x)$ has a minimum value where the reflected and incident signals are out of phase. Hence, x satisfies the following condition at a minimum of the interference pattern.

$$(2\beta x - \phi) = \pm(2m + 1)\pi, \quad m = 0, 1, 2, \ldots \tag{3.3.5}$$

Further, these extreme values of the standing waves are

$$|V(x)|_{\max} = |V_+|\{1 + \rho\} \tag{3.3.6}$$

and,

$$|V(x)|_{\min} = |V_+|\{1 - \rho\} \tag{3.3.7}$$

The ratio of maximum to minimum values of voltage $V(x)$ is called the *voltage standing wave ratio* (VSWR). Therefore,

$$VSWR = S = \frac{|V(x)|_{\max}}{|V(x)|_{\min}}. = \frac{1 + \rho}{1 - \rho} \tag{3.3.8}$$

Since $0 \leq \rho \leq 1$ for a passive load, minimum value of the VSWR will be unity (for a matched load) while its maximum value can be infinity (for total reflection, with a short circuit or an open circuit as the load).

Assume that there is a voltage minimum at x_1 from the load and if one keeps moving toward the source then the next minimum occurs at x_2. In other words, there are two consecutive minimums at x_1 and x_2 with $x_2 > x_1$. Hence,

$$2(\beta x_1 - \phi) = (2\mathrm{m}_1 + 1)\pi$$

and,

$$2(\beta x_2 - \phi) = [2(\mathrm{m}_1 + 1) + 1]\pi$$

Subtracting the former equation from the latter, one finds

$$2\beta(x_2 - x_1) = 2\pi \Rightarrow x_2 - x_1 = \frac{\lambda}{2}$$

where $(x_2 - x_1)$ is separation between the two consecutive minimums.

Similarly, it can be proved that two consecutive maximums are a half-wavelength apart and also that separation between the consecutive maximum and minimum is a quarter-wavelength. This information can be used to measure the wavelength of a propagating signal. In practice, the location of a minimum is preferred over that of a maximum. This is because minimums are sharper in comparison with maximums, as illustrated in Figure 3.11. Further, a short (or open circuit) must be used as load for best accuracy in the measurement.

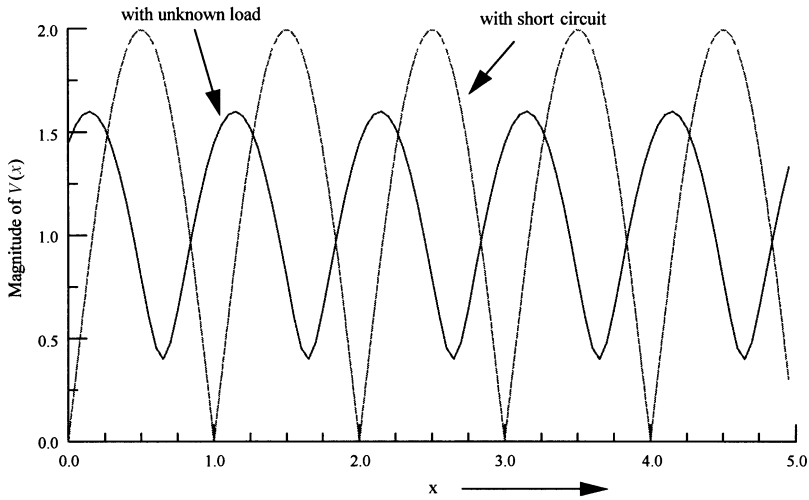

Figure 3.11 Standing wave pattern on a lossless transmission line.

Measurement of Impedance

Impedance of a one-port microwave device can be determined from measurement on the standing wave at its input. Those required parameters are the VSWR and the location of first minimum (or maximum) from the load. A slotted line that is equipped with a detector probe is connected before the load to facilitate the measurement. Since the output of a detector is proportional to power, the square root of the ratio is taken to find the VSWR. Since it may not be possible in most cases to probe up to the input terminals of the load, the location of the first minimum is determined as follows. An arbitrary minimum is located on the slotted line with unknown load. The load is then replaced by a short circuit. As a result, there is a shift in minimum, as shown in Figure 3.11. Shift of the original minimum away from the generator is equal to the location of the first minimum from the load.

Since reflected voltage is out of phase with that of the incident signal at the minimum of the standing wave pattern, a relation between the reflection coefficient, $\Gamma_1 = -\rho$, and impedance Z_1 at this point may be written as follows:

$$\Gamma_1 = -\rho = \frac{\overline{Z}_1 - 1}{\overline{Z}_1 + 1}$$

where $\overline{Z}_1$ is normalized impedance at the location of the first minimum of the voltage standing wave.

Since VSWR $S = \dfrac{1+\rho}{1-\rho}$,

$$\rho = \frac{S-1}{S+1},$$

and, therefore,

$$-\frac{S-1}{S+1}=\frac{\overline{Z}_1-1}{\overline{Z}_1+1}\Rightarrow \overline{Z}_1=\frac{1}{S}$$

This normalized impedance is equal to the input impedance of a line that is terminated by load Z_L and has a length of d_1. Hence,

$$\overline{Z}_1=\frac{1}{S}=\frac{\overline{Z}_L+j\tan(\beta d_1)}{1+j\overline{Z}_L\tan(\beta d_1)}\Rightarrow \overline{Z}_L=\frac{1-jS\tan(\beta d_1)}{S-j\tan(\beta d_1)}$$

Similarly, the reflected voltage is in phase with the incident signal at the maximum of the standing wave. Assume that the first maximum is located at a distance d_2 from the unknown load and that the impedance at this point is Z_2. One can write,

$$\Gamma_2=\rho=\frac{\overline{Z}_2-1}{\overline{Z}_2+1}=\frac{S-1}{S+1}\Rightarrow \overline{Z}_2=S$$

and,

$$\overline{Z}_L=\frac{\overline{Z}_2-j\tan(\beta d_2)}{1-j\overline{Z}_2\tan(\beta d_2)}$$

Since the maximum and minimum are measured on a lossless line that feeds the unknown load, magnitude of the reflection coefficient ρ does not change at different points on the line.

Example 3.13: A load impedance of $73-j42.5$ ohm terminates a transmission line of characteristic impedance $50+j0.01$ ohm. Determine its reflection coefficient and the voltage standing wave ratio.

$$\begin{aligned}\Gamma&=\frac{Z_L-Z_o}{Z_L+Z_o}=\frac{73-j42.5-(50+j0.01)}{73-j42.5+(50+j0.001)}\\&=\frac{23-j42.51}{123-j42.49}=\frac{48.3332\angle -1.0749\,\text{rad}}{130.1322\angle -0.3326\,\text{rad}}\\&=0.3714\angle -0.7423\,\text{rad}=0.3714\angle -42.53^\circ\end{aligned}$$

and,

$$VSRW=\frac{1+\rho}{1-\rho}=\frac{1+0.3714}{1-0.3714}=2.1817$$

Note that this line is lossy and, therefore, the reflection coefficient and VSWR will change with distance from the load.

Example 3.14: A 100-ohm transmission line is terminated by the load Z_L. Measurements indicate that it has a VSWR of 2.4 and the standing wave minimums are 100 cm apart. The scale reading at one of these minimums is found to be 275 cm. When the load is replaced by a short circuit, the minimum moves away from the generator to a point where the scale shows 235 cm. Find the signal wavelength and the load impedance.

Since the minimum are 100 cm apart, the signal wavelength $\lambda = 2 \times 100 = 200\,\text{cm} = 2\,\text{m}$.

$$\beta = \pi\,\text{rad/m and } d_1 = 275 - 235 = 40\,\text{cm}$$

Hence,

$$\overline{Z}_L = \frac{1 - j2.4\tan(0.4\pi)}{2.4 - j\tan(0.4\pi)} = 1.65 - j0.9618$$

or,

$$Z_L = 165 - j96.18\,\text{ohm}$$

3.4 SMITH CHART

Normalized impedance at a point in the circuit is related to its reflection coefficient as follows:

$$\overline{Z} = \bar{R} + j\bar{X} = \frac{1+\Gamma}{1-\Gamma} = \frac{1+\Gamma_r + j\Gamma_i}{1-\Gamma_r - j\Gamma_i} \tag{3.4.1}$$

where Γ_r and Γ_i represent real and imaginary parts of the reflection coefficient, while $\bar{R}$ and $\bar{X}$ are real and imaginary parts of the normalized impedance, respectively. This complex equation can be split into two, after equating real and imaginary components on its two sides. Hence,

$$\left(\Gamma_r - \frac{\bar{R}}{1+\bar{R}}\right)^2 + \Gamma_i^2 = \left(\frac{1}{1+\bar{R}}\right)^2 \tag{3.4.2}$$

and,

$$(\Gamma_r - 1)^2 + \left(\Gamma_i - \frac{1}{\bar{X}}\right)^2 = \left(\frac{1}{\bar{X}}\right)^2 \tag{3.4.3}$$

These two equations represent a family of circles on the complex Γ-plane. The circle in (3.4.2) has its center at $\left(\frac{\bar{R}}{1+\bar{R}}, 0\right)$ and a radius of $\frac{1}{1+\bar{R}}$. For $\bar{R} = 0$, it is centered at the origin with unity radius. As $\bar{R}$ increases, the center of the constant resistance circle moves on a positive real axis and its radius decreases. When $\bar{R} = \infty$, the radius reduces to zero and the center of the circle moves to (1, 0). These plots are shown in Figure 3.12. Note that for passive impedance, $0 \le \bar{R} \le \infty$ while $-\infty \le \bar{X} \le +\infty$.

Similarly, (3.4.3) represents a circle that is centered at $\left(1, \frac{1}{\bar{X}}\right)$ with a radius of $\frac{1}{\bar{X}}$. For $\bar{X} = 0$, its center lies at $(1, \infty)$ with an infinite radius. Hence, it is a straight line along the Γ_r-axis. As $\bar{X}$ increases on the positive side (that is, $0 \le \bar{X} \le \infty$), the center of the circle moves toward point (1, 0) along a vertical line defined by $\Gamma_r = 1$ and its radius becomes smaller and smaller in size. For $\bar{X} = \infty$, it becomes a point that is located at (1,0). Similar characteristics are observed for $0 \ge \bar{X} \ge -\infty$. As shown in Figure 3.12, a graphical representation of these two equations for all possible normalized resistance and reactance values is known as the *Smith chart*. Thus, a normalized impedance point on the Smith chart represents the corresponding reflection coefficient in polar coordinates on the complex Γ-plane. According to (3.2.7), the magnitude of the reflection coefficient on a lossless transmission line remains constant as ρ_L while its phase angle decreases as $-2\beta\ell$. Hence, it represents

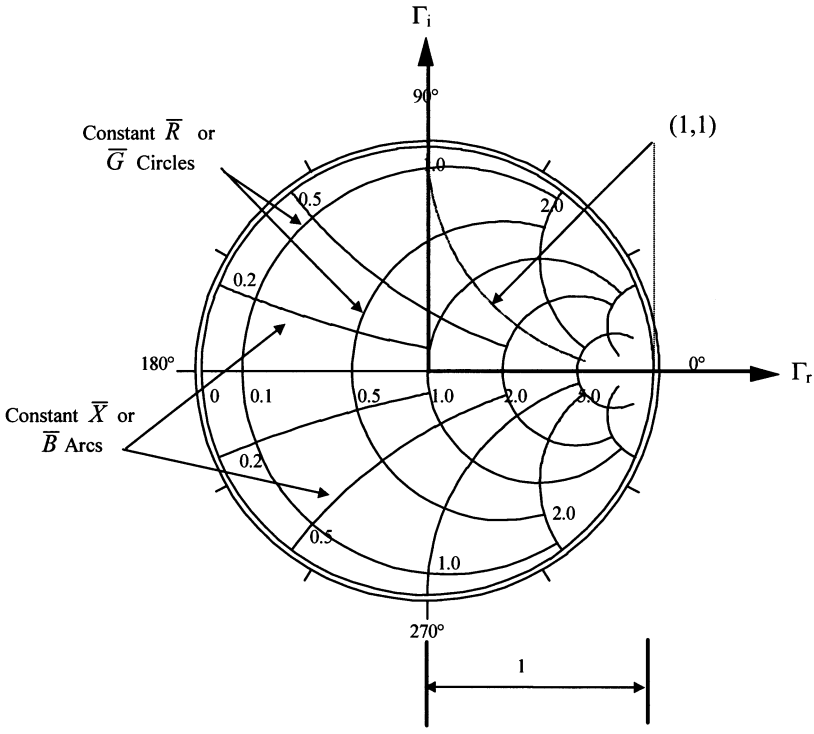

Figure 3.12 The Smith chart.

a circle of radius ρ_L. As one moves away from the load (that is, toward the generator), the reflection coefficient point moves clockwise on this circle. Since the reflection coefficient repeats periodically at every half-wavelength, the circumference of the circle is equal to $\lambda/2$. For a given reflection coefficient, normalized impedance may be found using the impedance scale of the Smith chart. Further, $\bar{R}$ in (3.4.1) is equal to the VSWR for $\Gamma_r > 0$ and $\Gamma_i = 0$. On the other hand, it equals the inverse of VSWR for $\Gamma_r < 0$ and $\Gamma_i = 0$. Hence, $\bar{R}$ values on the positive Γ_r-axis also represent the VSWR.

Since admittance represents the inverse of impedance, we can write,

$$\bar{Y} = \frac{1}{\bar{Z}} = \frac{1-\Gamma}{1+\Gamma},$$

Hence, a similar analysis can be performed with the normalized admittance instead of impedance. It results in a same kind of chart except that the normalized conductance circles replace normalized resistance circles while the normalized susceptance arcs replace normalized reactance.

Normalized resistance (or conductance) of each circle is indicated on the Γ_r-axis of the Smith chart. Normalized positive reactance (or susceptance) arcs are shown in the upper half while negative reactance (or susceptance) arcs are seen in the lower half. The Smith chart in conjunction with equation (3.2.7) facilitates the analysis and design of transmission line circuits.

Example 3.15: A load impedance of $50 + j100$ ohm terminates a lossless, quarter-wavelength-long transmission line. If characteristic impedance of the line is 50 ohm then find the impedance at its input end, the load reflection coefficient, and the VSWR on this transmission line.

This problem can be solved using equations (3.2.6), (3.2.7), and (3.3.8), or the Smith chart. Let us try it both ways.

$$\beta\ell = \frac{2\pi}{\lambda} \times \frac{\lambda}{4} = \frac{\pi}{2} = 90^\circ$$

$$Z_{in} = Z_o \frac{Z_L + jZ_o \tan(\beta\ell)}{Z_o + jZ_L \tan(\beta\ell)} = 50 \frac{(50 + j100) + j50 \tan(90^\circ)}{50 + j(50 + j100)\tan(90^\circ)}$$

$$\text{or, } Z_{in} = 50 \frac{j50}{j(50 + j100)} = \frac{2500}{50 + j100} = 10 - j20 \text{ ohm}$$

$$\Gamma = \frac{Z_L - Z_o}{Z_L + Z_o} = \frac{50 + j100 - 50}{50 + j100 + 50} = \frac{j100}{100 + j100} = \frac{100\angle 90^\circ}{100 \times \sqrt{2}\angle 45^\circ}$$

$$= 0.7071\angle 45^\circ$$

$$\text{VWSR} = \frac{1 + |\Gamma|}{1 - |\Gamma|} = \frac{1 + 0.7071}{1 - 0.7071} = \frac{1.7071}{0.2929} = 5.8283$$

To solve this problem graphically using the Smith chart, normalized load impedance is determined as follows.

$$\overline{Z}_{\mathrm{L}} = \frac{Z_{\mathrm{L}}}{Z_{\mathrm{o}}} = \frac{50 + j100}{50} = 1 + j2$$

This point is located on the Smith chart as shown in Figure 3.13. A circle that passes through $1 + j2$ is then drawn with point $1 + j0$ as its center. Since the radius of the Smith chart represents unity magnitude, the radius of this circle is equal to the magnitude of the reflection coefficient ρ_{L}. In other words, the normalized radius of this circle (i.e., the radius of this circle divided by the radius of the Smith chart) is equal to ρ_{L}. Note that a clockwise movement on this circle corresponds to a movement away from the load on the transmission line. Hence, a point d meters away from the load is located at $-2\beta d$ on the chart. Therefore, the input port of the line that is a quarter-wavelength away from the load (i.e., $d = \lambda/4$) can be located on

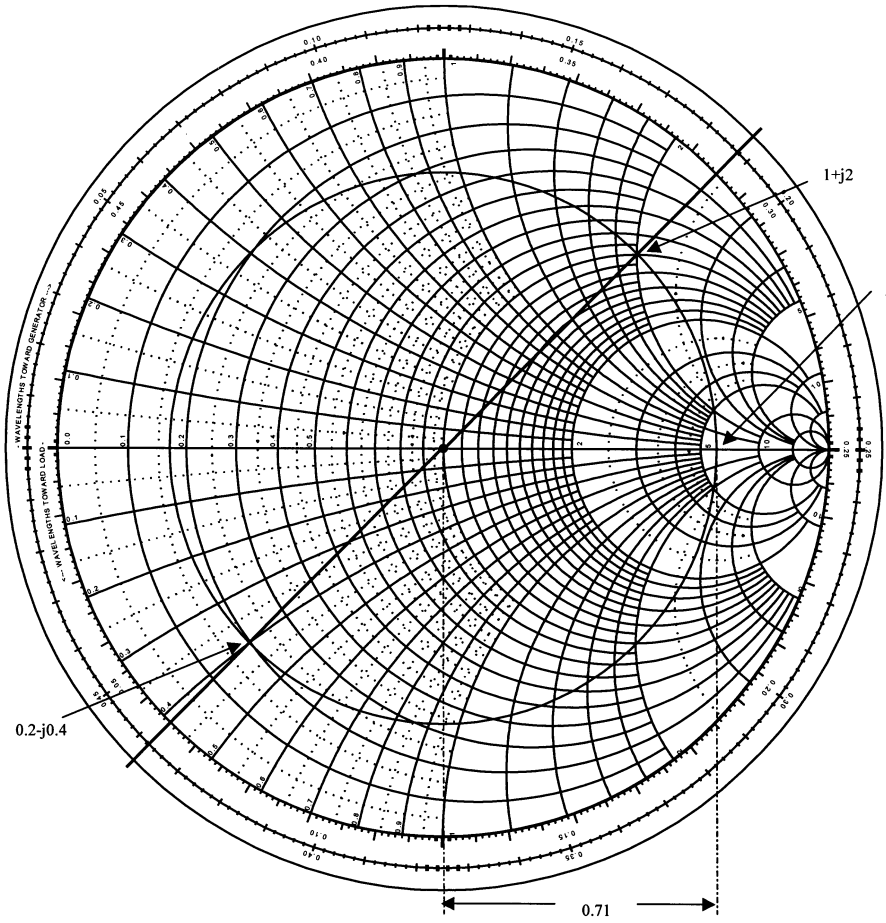

Figure 3.13 Solution to Example 3.15 using a Smith chart.

this circle after moving by $-\pi$ to a point at $0.438\,\lambda$ on "wavelengths toward generator" scale.

Thus, from the Smith chart, VSWR $= 5.8$, $\Gamma_L = 0.71\angle 45^\circ$, and $\overline{Z}_{in} = 0.2 - j0.4$.

$$Z_{in} = 50(0.2 - j0.4) = 10 - j20\,\text{ohm}$$

Example 3.16: A lossless 75-ohm transmission line is terminated by an impedance of $150 + j150$ ohm. Using the Smith chart, find (a) Γ_L, (b) VSWR, (c) Z_{in} at a distance of $0.375\,\lambda$ from the load, (d) the shortest length of the line for which impedance is purely resistive, and (e) the value of this resistance.

$$\overline{Z}_L = \frac{150 + j150}{75} = 2 + j2$$

After locating this normalized impedance point on the Smith chart, the constant VSWR circle is drawn as shown in Figure 3.14.

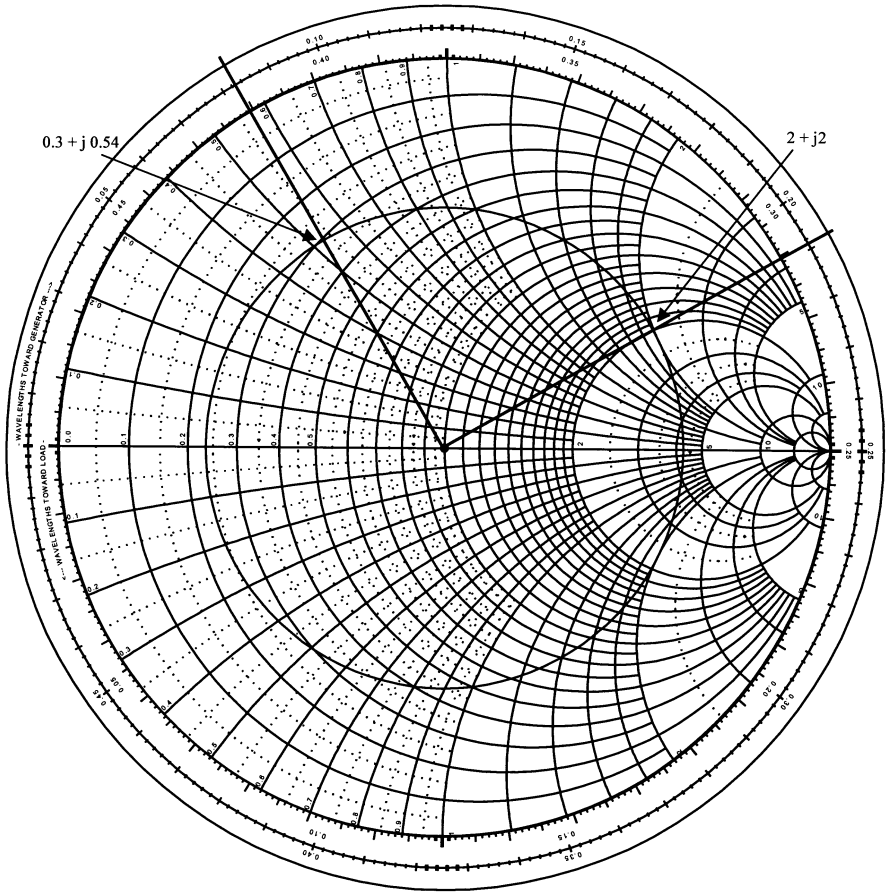

Figure 3.14 Solution to Example 3.16 using a Smith chart.

(a) Magnitude of the reflection coefficient is equal to the radius of the VSWR circle (with the radius of the Smith chart as unity). The angle made by the radial line that connects the load impedance point with the center of the chart is equal to the phase angle of reflection coefficient. Hence,

$$\Gamma_L = 0.62\angle 30^\circ$$

(b) VSWR is found to be 4.25 from the scale reading for the point where the circle intersects the $+\Gamma_r$ axis.

(c) For $d = 0.375\,\lambda$, $-2\beta d = -4.7124$ radians $= -270^\circ$ (clockwise from the load). This point is located after moving on the VSWR circle by $0.375\,\lambda$ from the load (at $0.084\,\lambda$ on "wavelengths toward generator" scale). The corresponding normalized impedance is found to be $0.3 + j0.54$. Therefore,

$$Z_{in}(\ell = 0.375\,\lambda) = 75(0.3 + j0.54) = 22.5 + j40.5 \text{ ohm}$$

(d) While moving clockwise from the load point, the VSWR circle crosses the Γ_r-axis for the first time at $0.25\,\lambda$. The imaginary part of impedance is zero at this intersection point. Therefore, $d = (0.25 - 0.208)\,\lambda = 0.042\,\lambda$. Normalized impedance at this point is 4.25. The next point on the transmission line where the impedance is purely real occurs a quarter-wavelength from it (i.e., $0.292\,\lambda$ from load). Normalized impedance at this point is 0.23.

(e) Normalized resistance and VSWR are the same at this point. Therefore,

$$R = 75 \times 4.25 = 318.75 \text{ ohm}$$

Example 3.17: A lossless 100-ohm transmission line is terminated by an impedance of $100 + j100$ ohm as illustrated here. Find the location of the first V_{max}, first V_{min}, and the VSWR if the operating wavelength is 5 cm.

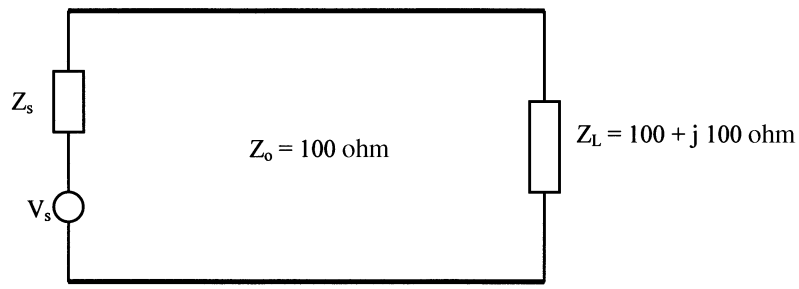

$$\overline{Z}_L = \frac{100 + j100}{100} = 1 + j1$$

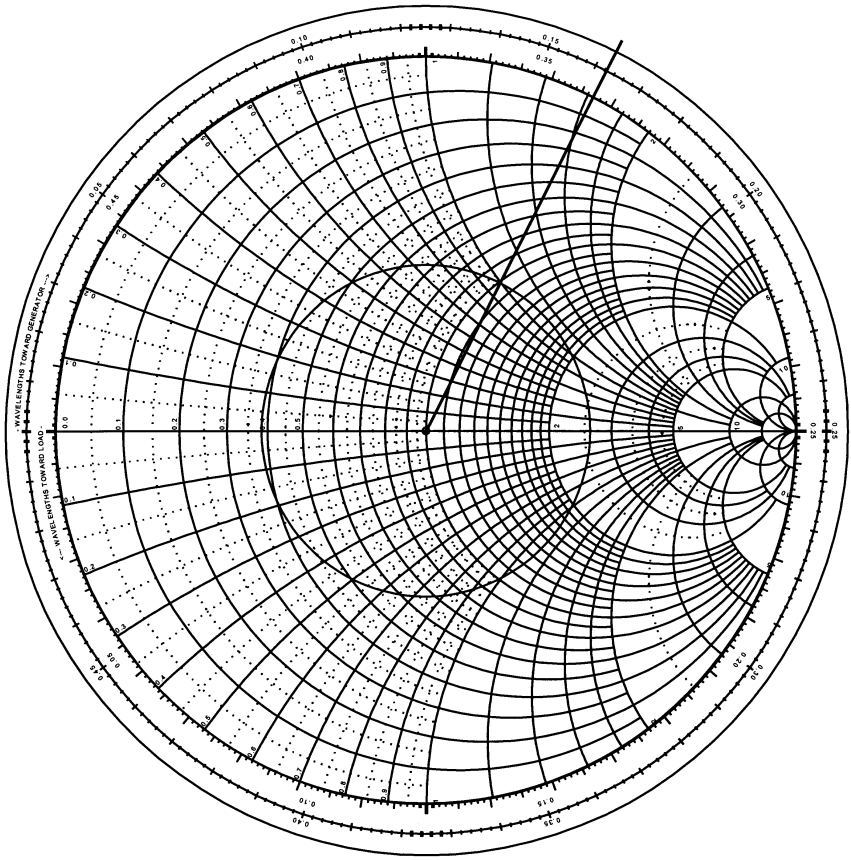

Figure 3.15 Solution to Example 3.17 using a Smith chart.

As shown in Figure 3.15, this point is located on the Smith chart and the VSWR circle is drawn. From the chart, VSWR = 2.6.

Scale reading on the "wavelengths toward generator" is 0.162 λ at the load point. When one moves away from this point clockwise (toward generator) on this VSWR circle, the voltage maximum is found first at 0.25 λ and then a minimum at 0.5 λ. If the first voltage maximum is at $d_{\max}$ from the load, then $d_{\max} = (0.25 - 0.162)\lambda = 0.088\,\lambda = 0.44$ cm from load.

The first minimum is a quarter-wavelength away from the point of voltage maximum. Hence, $d_{\min} = (0.5 - 0.162)\lambda = 0.338\,\lambda = 1.69$ cm.

Example 3.18: A 150-ohm load terminates a 75-ohm line. Find impedance at points 2.15 λ and 3.75 λ from the termination.

$$\overline{Z}_{\mathrm{L}} = \frac{150}{75} = 2$$

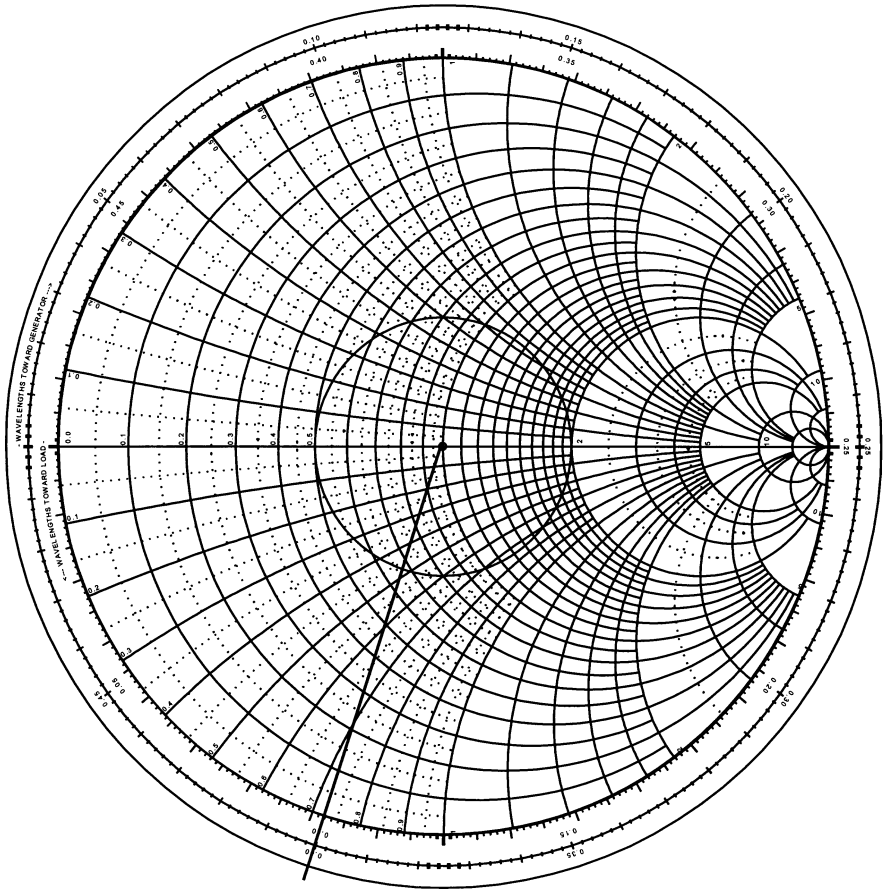

Figure 3.16 Solution to Example 3.18 using a Smith chart.

As illustrated in Figure 3.16, this point is located on the Smith chart and the VSWR circle is drawn. Note that the VSWR on this line is 2 and the load reflection coefficient is about $0.33\angle 0°$.

As one moves on the transmission line toward the generator, the phase angle of reflection coefficient changes by $-2\beta d$, where d is the distance away from the load. Hence, one revolution around the VSWR circle is completed for every half-wavelength. Therefore, normalized impedance will be 2 at every integer multiple of a half-wavelength from the load. It will be true for a point located at $2\,\lambda$ as well as at $3.5\,\lambda$. For the remaining $0.15\,\lambda$, the impedance point is located on the VSWR circle at $0.40\,\lambda$ (i.e., $0.25 + 0.15$) on the "wavelengths toward generator" scale. Similarly, the point corresponding to $3.75\,\lambda$ from the load is found at $0.5\,\lambda$.

From the Smith chart, normalized impedance at $2.15\,\lambda$ is $0.68 - j0.48$, while it is 0.5 at $3.75\,\lambda$. Therefore,

$$\text{Impedance at } 2.15\,\lambda, Z_1 = (0.68 - j0.48) \times 75 = 51 - j36 \text{ ohm}$$

and,

$$\text{Impedance at } 3.75\,\lambda Z_2 = (0.5) \times 75 = 37.5 \text{ ohm.}$$

Example 3.19: A lossless 100-ohm transmission line is terminated by an admittance of $0.0025 - j0.0025$ S. Find the impedance at a point $3.15\,\lambda$ away from load and the VSWR on this line.

$$\bar{Y}_L = \frac{Y_L}{Y_o} = Y_L \times Z_o = 0.25 - j0.25$$

As before, this normalized admittance point is located on the Smith chart and the VSWR circle is drawn. It is shown in Figure 3.17. There are two choices available at this point. The given normalized load admittance is converted to corresponding impedance by moving to a point on the diametrically opposite side of the VSWR circle. It shows a normalized load impedance as $2 + j2$. Moving from this point by $3.15\,\lambda$ toward the generator, normalized impedance is found as $0.55 - j1.08$. Alternatively, we can first move from the normalized admittance point by $3.15\,\lambda$ toward the generator to a normalized admittance point $0.37 + j0.75$. This is then converted to normalized impedance by moving to the diametric opposite point on the VSWR circle.

Thus, the normalized impedance at a point $3.15\,\lambda$ away from the load is $0.55 - j1.08$. The impedance at this point is $100 \times (0.55 - j1.08) = 55 - j108$ ohm, and the VSWR is approximately 4.3.

Example 3.20: An experiment is performed using the circuit illustrated here. First, a load Z_L is connected at the end of a 100-ohm transmission line and its VSWR is found to be 2. After that, the detector probe is placed at one of the minimums on the line. It is found that this minimum shifts toward the load by 15 cm when the load is replaced by a short circuit. Further, two consecutive minimums are found to be 50 cm apart. Determine the load impedance.

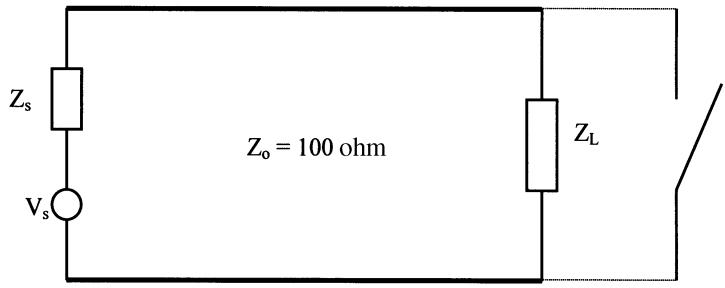

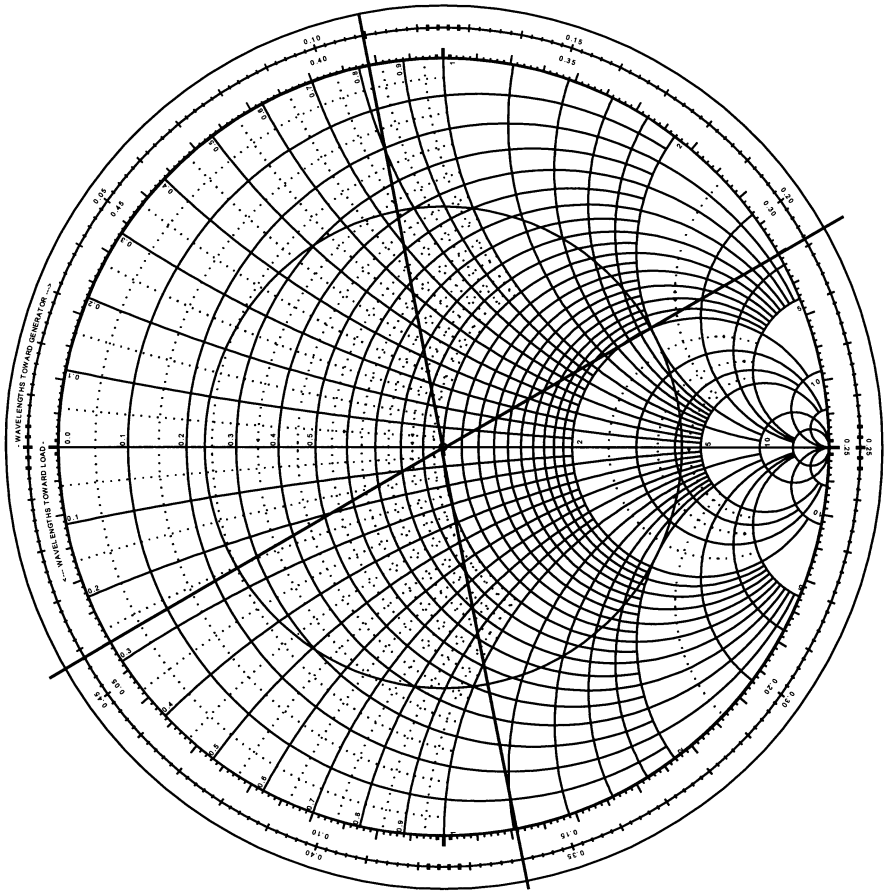

Figure 3.17 Solution to Example 3.19 using a Smith chart.

Since the separation between consecutive minimums is 50 cm, the signal wavelength on the line is 100 cm. Therefore, first minimum of the standing wave pattern occurs at $0.15\,\lambda$ from the load.

Since VSWR on the line is measured as 2, this circle is drawn on the Smith chart as illustrated in Figure 3.18. As explained in the preceding section, a minimum in a voltage standing wave occurs when the phase angle of the reflection coefficient is 180°. It is located on the Smith chart at a point where the VSWR circle intersects the $-\Gamma_r$ axis. From this point, we move toward the load by $0.15\,\lambda$ (i.e., counterclockwise) to locate the normalized load impedance point. It is found to be $1 - j0.7$. Therefore,

$$Z_L = 100 \times (1 - j0.7) = 100 - j70\,\text{ohm}$$

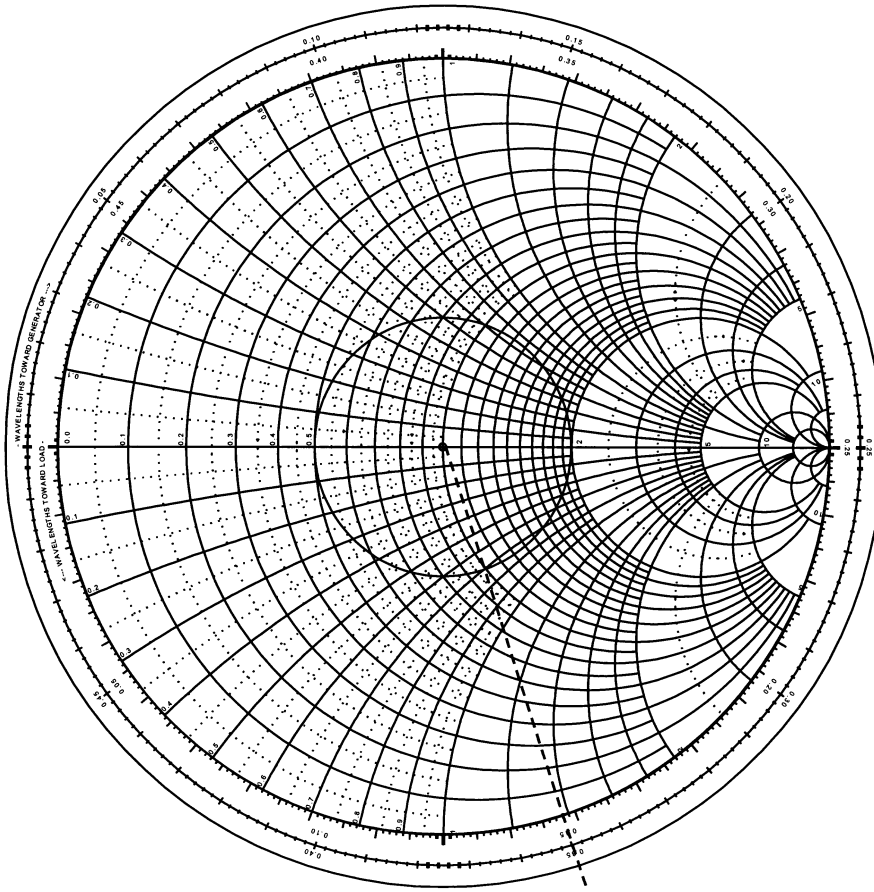

Figure 3.18 Solution to Example 3.20 using a Smith chart.

SUGGESTED READING

Robert E. Collin, *Foundations for Microwave Engineering*. New York: McGraw Hill, 1992.

K. C. Gupta and I. J. Bahl, *Microstriplines and slotlines*. Boston: Artech House, 1979.

T. Edwards, *Foundations for Microstrip Circuit Design*. New York: Wiley, 1992.

P. C. Magnusson, G. C. Alexander, and V. K. Tripathi, *Transmission Lines and Wave Propagation*. Boca Raton: CRC Press, 1992.

D. M. Pozar, *Microwave Engineering*. New York: Wiley, 1998.

S. Ramo. J. R. Whinnery, and T. Van Duzer, *Fields and Waves in Communication Electronics*. New York: Wiley, 1994.

Peter A. Rizzi, *Microwave Engineering*. Englewood Cliffs, NJ: Prentice Hall, 1988.

W. Sinnema, *Electronic Transmission Technology.* Englewood Cliffs, NJ: Prentice Hall, 1988.

PROBLEMS

1. A lossless semirigid coaxial line has its inner and outer conductor radii as 1.325 mm and 4.16 mm, respectively. Find the line parameters, characteristic impedance, and the propagation constant for a signal frequency of 500 MHz ($\varepsilon_r = 2.1$).

2. Calculate the magnitude of the characteristic impedance and the propagation constant for a coaxial line at 2 GHz. Assume that $b = 3$ cm, $a = 0.5$ cm, and $\varepsilon = \varepsilon_o(2.56 - j0.005)$.

3. A certain telephone line has the following electrical parameters:

$$R = 40\Omega \text{ per mile},\ L = 1.1 \text{ mH per mile},\ G \approx 0,\ \text{and } C = 0.062\ \mu\text{F per mile}$$

Loading coils are added which provide an additional inductance of 30 mH per mile as well as an additional resistance of 8 Ω per mile. Obtain the attenuation constant and phase velocities at frequencies of 300 Hz and 3.3 kHz.

4. A given transmission line has the following parameters:

$$Z_o = 600\angle 6^\circ\ \Omega,\ \alpha = 2.0 \cdot 10^{-5}\ \text{dB/m},\ v_p = 2.97 \cdot 10^8\ \text{m/s},\ \text{and } f = 1.0\ \text{kHz}$$

Write phasor $V(z)$ and $I(z)$, and the corresponding instantaneous values for a wave traveling in the z-direction, if the maximum value of the current wave at $z = 0$ is 0.3 mA and it has maximum positive value with respect to time at $t = 0$.

5. A 30-km-long transmission line is terminated by a $100 + j200\ \Omega$ load. A sinusoidal source with its output voltage $v(t) = 15\cos(8000\pi t)$ V and internal resistance 75 Ω is connected at its other end. Characteristic impedance of the line is 75 Ω and phase velocity of the signal is 2.5×10^8 m/s. Find total voltage across its input end and the load.

6. A 2.5-m-long transmission line is short circuited at one end and then the impedance at its other end is found to be $j5\ \Omega$. When the short is replaced by an open circuit, impedance at the other end changes to $-j500\ \Omega$. A 1.9-MHz sinusoidal source is used in this experiment and the transmission line is less than a quarter-wavelength long. Determine characteristic impedance of the line and phase velocity of the signal.

7. A lossless 75-Ω transmission line is connected between the load impedance of $37.5 - j15\ \Omega$ and a signal generator with internal impedance of 75 Ω. Find (a) the reflection coefficient at $0.15\ \lambda$ from the load, (b) VSWR on the line, and (c) input impedance at $1.3\ \lambda$ from the load.

8. Two antennas are connected through a quarter-wavelength-long lossless transmission line, as shown in the circuit below. However, the characteristic impedance of this line is unknown. The array is excited through a 50-Ω line.

Antenna A has impedance of $80 - j80\,\Omega$ while the antenna B has $75 - j55\,\Omega$. Peak voltage across antenna A is found to be $113.14\angle -45^\circ$ V and peak current through antenna B is $1.0\angle 90^\circ$ A. Determine the characteristic impedance of the line connecting the two antennas, and the value of a reactance connected in series with antenna B.

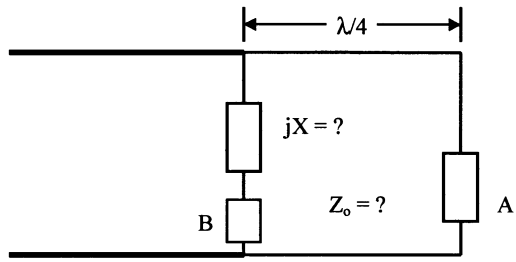

9. Measurements are made on a 1-m-long coaxial line (with negligible loss) using an impedance bridge that operates at 100 MHz. First, one of its ends is short circuited and the impedance at the other end is measured as $-j86.6025\,\Omega$. Repeating the measurements with an open circuit in place of a short circuit shows an impedance of $j28.8675\,\Omega$. Find the characteristic impedance of the line and the propagation constant. If the coaxial line is Teflon-filled ($\varepsilon_r = 2.1$) and the inner diameter of its outer conductor is 0.066 cm, determine the diameter of its inner conductor.

10. A lossless 75-ohm transmission line is terminated by a load impedance of $150 + j150$ ohm. Find the shortest length of line that results in (a) $Z_{in} = 75 - j120$ ohm, (b) $Z_{in} = 75 - j75$ ohm, and (c) $Z_{in} = 17.6$ ohm.

11. The open-circuit and short-circuit impedances measured at the input terminals of a lossless transmission line of length 1.5 m, which is less than a quarter-wavelength, are $-j54.6\,\Omega$ and $j103\,\Omega$, respectively.

(a) Find characteristic impedance, Z_o and propagation constant, γ, of the line.

(b) Without changing the operating frequency, find the input impedance of a short-circuited line that is twice the given length.

(c) How long should the short-circuited line be in order for it to appear as an open circuit at the input terminals?

12. At a frequency of 100 MHz, the following values are appropriate for a certain transmission line: $L = 0.25\,\mu H/m$, $C = 80\,pF/m$, $R = 0.15\,\Omega/m$, and $G = 8\,\mu S/m$. Calculate (a) the propagation constant, $\gamma = \alpha + j\beta$, (b) the signal wavelength, (c) the phase velocity, and (d) the characteristic impedance.

13. Open-circuit and short-circuit impedances measured at the input terminals of a 3-m-long (i.e., is greater than a quarter-wavelength but less than one-half wavelength) lossless transmission line are $j24.2\,\Omega$ and $-j232.4\,\Omega$ respectively.

(a) Find the characteristic impedance and propagation constant of this line.

(b) How long should the open-circuited line be in order for it to appear as a short circuit at the input terminals?

14. A 2.25-λ-long lossless transmission line with its characteristic impedance at 75 Ω is terminated in a load of 300 Ω. It is energized at the other port by a signal generator that has an open-circuit voltage of 20 V (peak value) and internal impedance of 75 Ω.

(a) Find the impedance at the input end of the line.

(b) Determine the total voltage across the load.

15. A 22.5-m-long lossless transmission line with $Z_o = 50\,\Omega$ is short circuited at one end and a voltage source $V_s = 20\cos(4\pi \times 10^6 t - 30^\circ)$ V is connected at its input terminals, as shown below. If the source impedance is 50 Ω and the phase velocity on the line is 1.8×10^8 m/s, find the total currents at its input and through the short circuit.

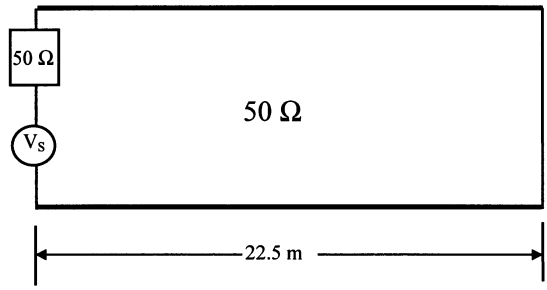

16. Determine the characteristic impedance and the phase velocity of a 25-cm long loss-free transmission line from the following experimental data: $Z_{SC} = -j90$ ohm, $Z_{OC} = j40$ ohm, and $f = 300$ MHz. Assume that $\beta\ell$ is less than π radians.

17. A lossless line is terminated in a load resistance of 50 Ω. Calculate the two possible values of characteristic impedance Z_o if one-fourth of the incident voltage wave is reflected back.

18. Measurements on a 0.6-m-long lossless coaxial cable at 100 kHz show a capacitance of 54 pF when the cable is open circuited and an inductance of 0.3 μH when it is short circuited. Determine the characteristic impedance of the line and the phase-velocity of this signal on the line. (Assume that the line length is less than a quarter-wavelength.)

19. For the reflection coefficients and characteristic impedances given, find the reflecting impedance in each case: (a) $\Gamma = 0.7\angle 30^\circ, Z_o = 50\,\Omega$; (b) $\Gamma = 0.9\angle -35^\circ$, $Z_o = 100\,\Omega$; (c) $\Gamma = 0.1 - j0.2, Z_o = 50\,\Omega$; (d) $\Gamma = 0.5 - j0$, $Z_o = 600\,\Omega$.

20. A 75-ohm lossless line is terminated by a load impedance $Z_L = 100 + j150$ ohm. Using the Smith chart, determine (a) the load reflection coefficient, (b) the VSWR, (c) the load admittance, (d) Z_{in} at 0.4λ from the load, (e) the location of V_{max} and V_{min} with respect to load if the line is 0.6λ long, and (f) Z_{in} at the input end.

21. A lossless 50-Ω line is terminated by $25 - j60\,\Omega$ load. Find (a) reflection coefficient at the load, (b) VSWR on the line, (c) impedance at 3.85λ from the load, (d) the shortest length of the line for which impedance is purely resistive, and (e) the value of this resistance.

22. An antenna of input impedance $Z_L = 75 + j150\,\Omega$ at 2 MHz is connected to a transmitter through a 100-m-long section of coaxial line, which has the following distributed constants:

$$R = 153\,\Omega \text{ per km},$$
$$L = 1.4 \text{ mH per km},$$
$$G = 0.8\,\mu\text{S per km, and}$$
$$C = 0.088\,\mu\text{F per km}.$$

Determine the characteristic impedance, the propagation constant, and the impedance at the input end of this line.

23. A lossless $50\,\Omega$ transmission line is terminated in $25 + j50\,\Omega$. Find (a) the voltage reflection coefficient, (b) impedance at 0.3λ from the load, (c) the shortest length of the line for which impedance is purely resistive, and (d) the value of this resistance.

24. A uniform transmission line has constants $R = 15\,\text{m}\Omega/\text{m}$, $L = 2\,\mu\text{H/m}$, $G = 1.2\,\mu\text{S/m}$, and $C = 1.1\,\text{nF/m}$. The line is 1 km long and it is terminated in a resistive load of $80\,\Omega$. At 8 kHz, find (a) the input impedance, (b) the attenuation in dB, and (c) the characteristic impedance.

25. A microwave transmitter is fabricated on a GaAs substrate. An antenna used in the system offers a resistive load of $40\,\Omega$. The electronic circuit has output impedance of $1\,\text{k}\Omega$. Design a microstrip $\lambda/4$ impedance transformer to match the system. The operating frequency is 4 GHz and the substrate thickness is 0.05 mm. ε_r of the GaAs substrate is 12.3.

26. A microstrip line is designed on a 0.1-mm-thick GaAs substrate ($\varepsilon_r = 14$). The strip thickness is 0.0001 mm and its width is 0.01 mm. Compute (a) the characteristic impedance and (b) the effective dielectric constant.

27. For the transmission line shown, find the (a) reflection coefficient (Γ_{in}) at the input end, (b) VSWR on the line, and (c) input admittance (Y_{in}).

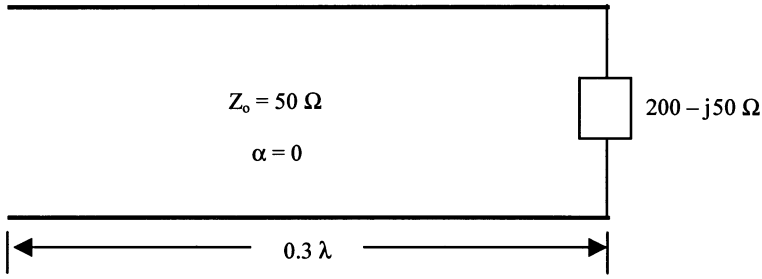

28. A lossless transmission line has characteristic impedance of $50\,\Omega$ and is terminated with an unknown load. The standing wave ratio on the line is 3.0. Successive voltage minimums are 20 cm apart, and the first minimum is 5 cm from the load.

(a) Determine the value of terminating load.

(b) Find the position and value of a reactance that might be added in series with the line at some point to eliminate reflections of waves incident from the source end.

29. A lossless 50-Ω line is connected to a load as shown below. The input reflection coefficient Γ_{in} at $1.45\,\lambda$ from the load is found at $0.3\angle -60°$. Find (a) the load impedance in ohm, (b) the VSWR, (c) shortest length of the line from the load for which the impedance is purely resistive, and (d) the value of this resistance in ohm.

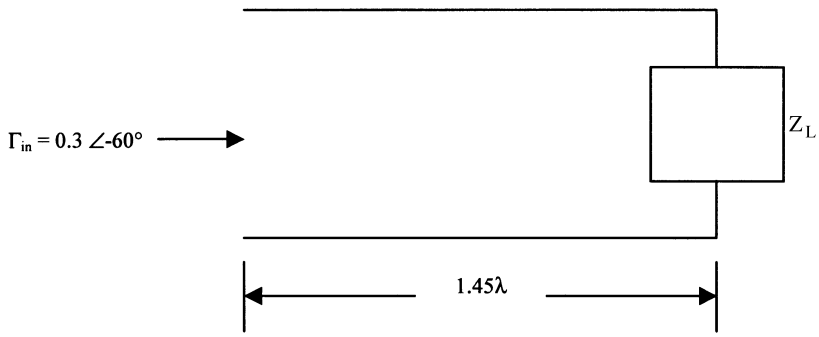

30. A lossless 100-ohm transmission line is terminated in $50 + j150\,\Omega$ load. Find (a) reflection coefficient at the load, (b) VSWR, and (c) $Z_{in}(z = 0.35\,\lambda)$.

31. A lossless 50-ohm transmission line is terminated by a $25 - j50$-ohm load. Find (a) Γ_L, (b) VSWR, (c) Z_{in} at $2.35\,\lambda$ from the load, (d) the shortest length of the line where impedance is purely resistive, and (e) the value of this resistance.

32. For the transmission line circuit shown below, find (a) the load reflection coefficient, (b) the impedance seen by the generator, (c) the VSWR on the transmission line, (d) the fraction of the input power delivered to the load.

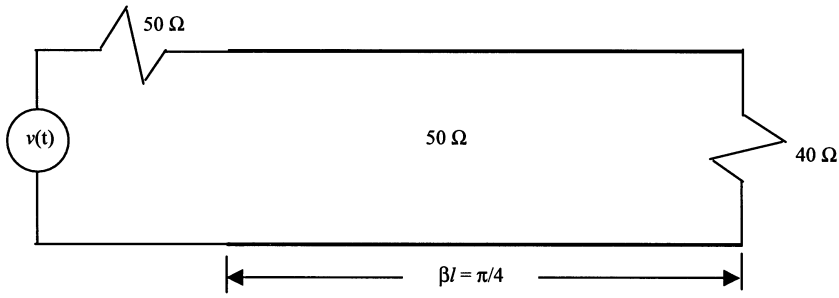

33. For the transmission line circuit shown below, find the required value of Z_o that will match the 20-ohm load resistance to the generator. The generator internal resistance is 60 ohm. Find VSWR on the transmission line. Is the load resistance matched to the transmission line?

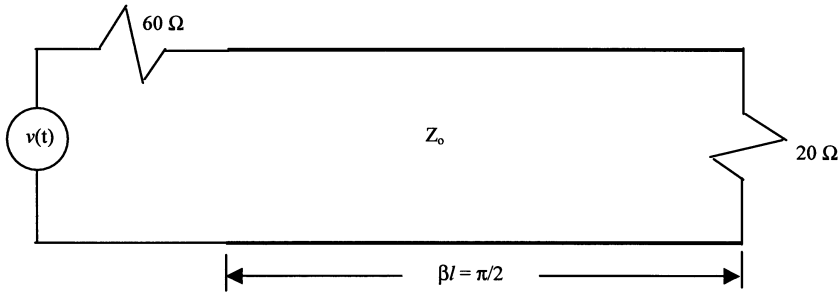

34. Use a Smith chart to find the following for the transmission line circuit shown below:

(a) Reflection coefficient at the load

(b) Reflection coefficient at the input

(c) VSWR on the line

(d) Input impedance

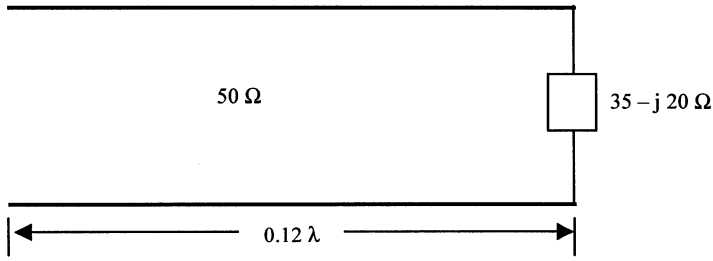

35. A lossless 40-ohm line is terminated in a 20-ohm load. Find the shortest line length that results in (a) $Z_{in} = 40 - j28$ ohm, (b) $Z_{in} = 48 + j16$ ohm. Use the Smith chart rather than the impedance transformation equation.

36. A 30-m-long lossless transmission line with $Z_o = 50\,\Omega$ operating at 2 MHz is terminated with a load $Z_L = 60 + j40\,\Omega$. If phase velocity on the line is $1.8 \cdot 10^8$ m/s, find:

(a) Load reflection coefficient

(b) Standing wave ratio

(c) Input impedance

37. A 50-ohm transmission line is terminated by an unknown load. Total voltage at various points of the line is measured and found to be as displayed below. Determine (a) the magnitude of reflection coefficient, (b) the VSWR, and (c) the signal wavelength in meters.

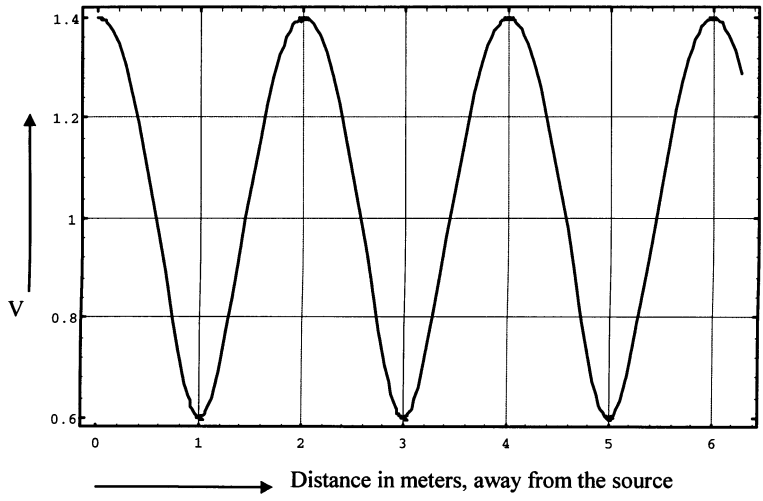

Radio-Frequency and Microwave Communication Circuits: Analysis and Design
Devendra K. Misra

ISBNs: 0-471-41253-8 (Hardback); 0-471-22435-9 (Electronic)

4

RESONANT CIRCUITS

A communication circuit designer frequently requires means to select (or reject) a band of frequencies from a wide signal spectrum. Resonant circuits provide such filtering. There are well-developed, sophisticated methodologies to meet virtually any specification. However, a simple circuit suffices in many cases. Further, resonant circuits are an integral part of the frequency-selective amplifier as well as of the oscillator designs. These networks are also used for impedance transformation and matching.

This chapter describes the analysis and design of these simple frequency-selective circuits, and presents the characteristic behaviors of series and parallel resonant circuits. Related parameters, such as quality factor, bandwidth, and input impedance, are introduced that will be used in several subsequent chapters. Transmission lines with an open or short circuit at their ends are considered next and their relationships with the resonant circuits are established. Transformer-coupled parallel resonant circuits are briefly discussed because of their significance in the radio frequency range. The final section summarizes the design procedure for rectangular and circular cylindrical cavities, and the dielectric resonator.

4.1 SERIES RESONANT CIRCUITS

Consider the series *R-L-C* circuit shown in Figure 4.1. Since the inductive reactance is directly proportional to signal frequency, it tries to block the high-frequency contents of the signal. On the other hand, capacitive reactance is inversely proportional to the frequency. Therefore, it tries to stop its lower frequencies. Note that the voltage across an ideal inductor leads the current by 90° (i.e., the phase angle of an

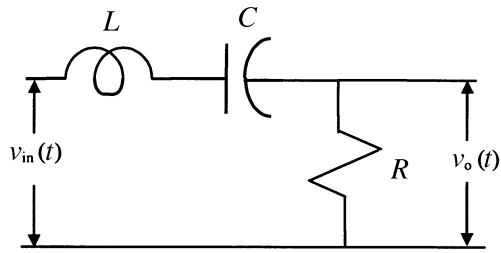

Figure 4.1 A series *R-L-C* circuit with input-output terminals.

inductive reactance is 90°). In the case of a capacitor, voltage across its terminals lags behind the current by 90° (i.e., the phase angle of a capacitive reactance is −90°). That means it is possible that the inductive reactance will be canceled out by the capacitive reactance at some intermediate frequency. This frequency is called the *resonant frequency* of the circuit. If the input signal frequency is equal to the resonant frequency, maximum current will flow through the resistor and it will be in phase with the input voltage. In this case, the output voltage V_o will be equal to the input voltage V_{in}. It can be analyzed as follows.

From Kirchhoff's voltage law,

$$\frac{L}{R}\frac{dv_o(t)}{dt} + \frac{1}{RC}\int_{-\infty}^{t} v_o(t)dt + v_o(t) = v_{in}(t) \tag{4.1.1}$$

Taking the Laplace transform of this equation with initial conditions as zero (i.e., no energy storage initially), we get

$$\left(\frac{sL}{R} + \frac{1}{sRC} + 1\right)V_o(s) = V_i(s) \tag{4.1.2}$$

where s is the complex frequency (Laplace variable).

The transfer function of this circuit, $T(s)$, is given by

$$T(s) = \frac{V_o(s)}{V_i(s)} = \frac{1}{\dfrac{sL}{R} + \dfrac{1}{sRC} + 1} = \frac{sR}{s^2L + sR + \dfrac{1}{C}} \tag{4.1.3}$$

Therefore, the transfer function of this circuit has a zero at the origin of the complex s-plane and also it has two poles. The location of these poles can be determined by solving the following quadratic equation.

$$s^2L + sR + \frac{1}{C} = 0 \tag{4.1.4}$$

Two possible solutions to this equation are as follows.

$$s_{1,2} = -\frac{R}{2L} \pm \sqrt{\left(\frac{R}{2L}\right)^2 - \frac{1}{LC}} \tag{4.1.5}$$

The circuit response will be influenced by the location of these poles. Therefore, these networks can be characterized as follows.

- If $\frac{R}{2L} > \frac{1}{\sqrt{LC}}$, i.e., $R > 2\sqrt{\frac{L}{C}}$, both of these poles will be real and distinct, and the circuit is *overdamped*.
- If $\frac{R}{2L} = \frac{1}{\sqrt{LC}}$, i.e., $R = 2\sqrt{\frac{L}{C}}$, the transfer function will have double poles at $s = -\frac{R}{2L} = -\frac{1}{\sqrt{LC}}$. The circuit is *critically damped*.
- If $\frac{R}{2L} < \frac{1}{\sqrt{LC}}$, i.e., $R < 2\sqrt{\frac{L}{C}}$, the two poles of $T(s)$ will be complex conjugate of each other. The circuit is *underdamped*.

Alternatively, the transfer function may be rearranged as follows:

$$T(s) = \frac{sCR}{s^2LC + sRC + 1} = \frac{sCR\omega_o^2}{s^2 + 2\zeta\omega_o s + \omega_o^2} \tag{4.1.6}$$

where

$$\zeta = \frac{R}{2}\sqrt{\frac{C}{L}} \tag{4.1.7}$$

$$\omega_o = \frac{1}{\sqrt{LC}} \tag{4.1.8}$$

ζ is called the *damping ratio*, and ω_o is the *undamped natural frequency.*

Poles of $T(s)$ are determined by solving the following equation.

$$s^2 + 2\zeta\omega_o s + \omega_o^2 = 0 \tag{4.1.9}$$

For $\zeta < 1$, $s_{1,2} = -\zeta\omega_o \pm j\omega_o\sqrt{1-\zeta^2}$. As shown in Figure 4.2, the two poles are complex conjugate of each other. Output transient response will be oscillatory with a ringing frequency of $\omega_o(1-\zeta^2)$ and an exponentially decaying amplitude. This circuit is underdamped.

For $\zeta = 0$, the two poles move on the imaginary axis. Transient response will be oscillatory. It is a critically damped case.

For $\zeta = 1$, the poles are on the negative real axis. Transient response decays exponentially. In this case, the circuit is overdamped.

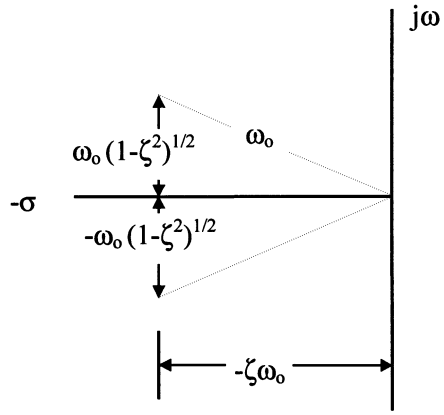

Figure 4.2 Pole-zero plot of the transfer function.

Consider the unit step function shown in Figure 4.3. It is like a direct voltage source of one volt that is turned on at time $t = 0$. If it represents input voltage $v_{in}(t)$ then the corresponding output $v_o(t)$ can be determined via Laplace transform technique.

The Laplace transform of a unit step at the origin is equal to $1/s$. Hence, output voltage, $v_o(t)$, is found as follows.

$$v_o(t) = L^{-1}V_o(s) = L^{-1}\frac{sCR\omega_o^2}{s^2 + 2\zeta\omega_o s + \omega_o^2} \times \frac{1}{s} = L^{-1}\frac{CR\omega_o^2}{(s + \zeta\omega_o)^2 + (1 - \zeta^2)\omega_o^2}$$

where L^{-1} represents inverse Laplace transform operator. Therefore,

$$v_o(t) = \frac{2\varsigma}{\sqrt{1 - \zeta^2}} e^{-\varsigma\omega_o t} \sin\left(\omega_o t\sqrt{1 - \zeta^2}\right) u(t)$$

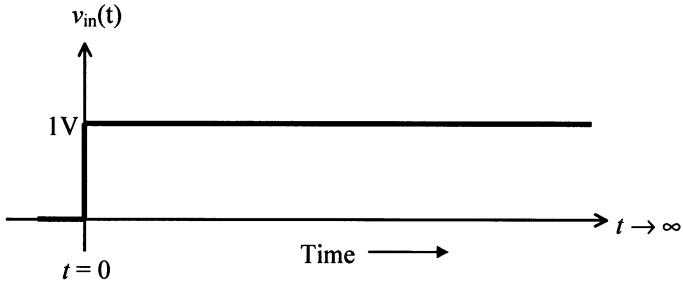

Figure 4.3 A unit-step input voltage.

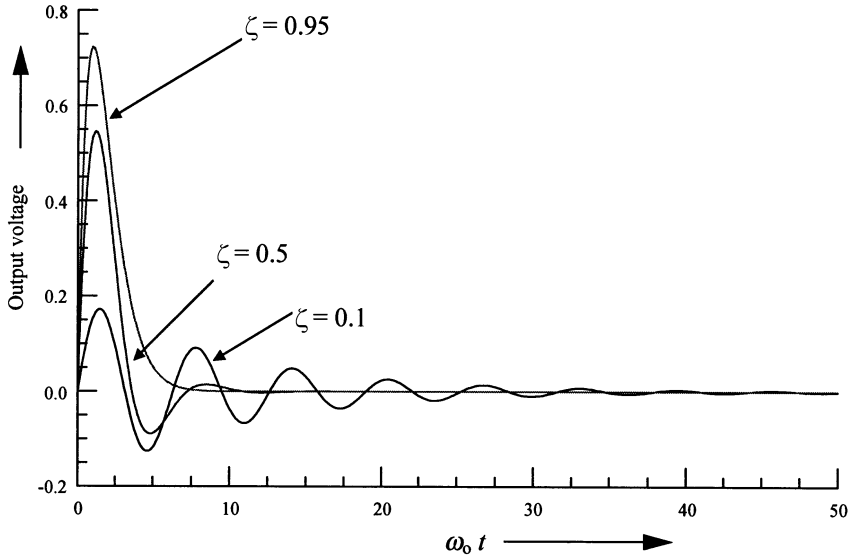

Figure 4.4 Response of a series *R-L-C* circuit to a unit step input for three different damping factors.

This response is illustrated in Figure 4.4 for three different damping factors. As can be seen, initial ringing lasts longer for a lower damping factor.

A sinusoidal steady-state response of the circuit can be easily determined after replacing s by $j\omega$, as follows:

$$V_o(j\omega) = \frac{V_i(j\omega)}{\frac{j\omega L}{R} + \frac{1}{j\omega RC} + 1} = \frac{V_i(j\omega)}{1 + \frac{j}{RC}\left(LC\omega - \frac{1}{\omega}\right)}$$

or,

$$V_o(j\omega) = \frac{V_i(j\omega)}{1 + \frac{j}{RC}\left(\frac{\omega}{\omega_o^2} - \frac{1}{\omega}\right)} = \frac{V_i(j\omega)}{1 + \frac{j}{\omega_o RC}\left(\frac{\omega}{\omega_o} - \frac{\omega_o}{\omega}\right)}$$

The *quality factor*, Q, of the resonant circuit is a measure of its frequency selectivity. It is defined as follows.

$$Q = \omega_o \frac{\text{Average stored energy}}{\text{Power loss}} \tag{4.1.10}$$

Hence,

$$Q = \omega_o \frac{\frac{1}{2}LI^2}{\frac{1}{2}I^2R} = \frac{\omega_o L}{R}$$

Since $\omega_o L = \dfrac{1}{\omega_o C}$,

$$Q = \frac{\omega_o L}{R} = \frac{1}{\omega_o RC} = \frac{\sqrt{LC}}{RC} = \frac{1}{R}\sqrt{\frac{L}{C}} = \frac{1}{2\zeta} \tag{4.1.11}$$

Therefore,

$$V_o(j\omega) = \frac{V_i(j\omega)}{\left(1 + jQ\left(\dfrac{\omega}{\omega_o} - \dfrac{\omega_o}{\omega}\right)\right)} \tag{4.1.12}$$

Alternatively,

$$\frac{V_o(j\omega)}{V_i(j\omega)} = A(j\omega) = \frac{1}{\left(1 + jQ\left(\dfrac{\omega}{\omega_o} - \dfrac{\omega_o}{\omega}\right)\right)} \tag{4.1.13}$$

The magnitude and phase angle of (4.1.13) are illustrated in Figures 4.5 and 4.6, respectively. Figure 4.5 shows that the output voltage is equal to the input for a signal frequency equal to the resonant frequency of the circuit. Further, phase angles of the two signals in Figure 4.6 are the same at this frequency, irrespective of the quality factor of the circuit. As signal frequency moves away from this point on either side, the output voltage decreases. The rate of decrease depends on the quality factor of the circuit. For higher Q, the magnitude is sharper, indicating a higher selectivity of the circuit. If signal frequency is below the resonant frequency then output voltage leads the input. For a signal frequency far below the resonance, output leads the input almost by 90°. On the other hand, it lags behind the input for higher frequencies. It converges to $-90°$ as the signal frequency moves far beyond the resonant frequency. Thus, the phase angle changes between $\pi/2$ and $-\pi/2$, following a sharper change around the resonance for high-Q circuits. Note that the voltage across the series-connected inductor and capacitor combined has inverse characteristics to those of the voltage across the resistor. Mathematically,

$$V_{LC}(j\omega) = V_{in}(j\omega) - V_o(j\omega)$$

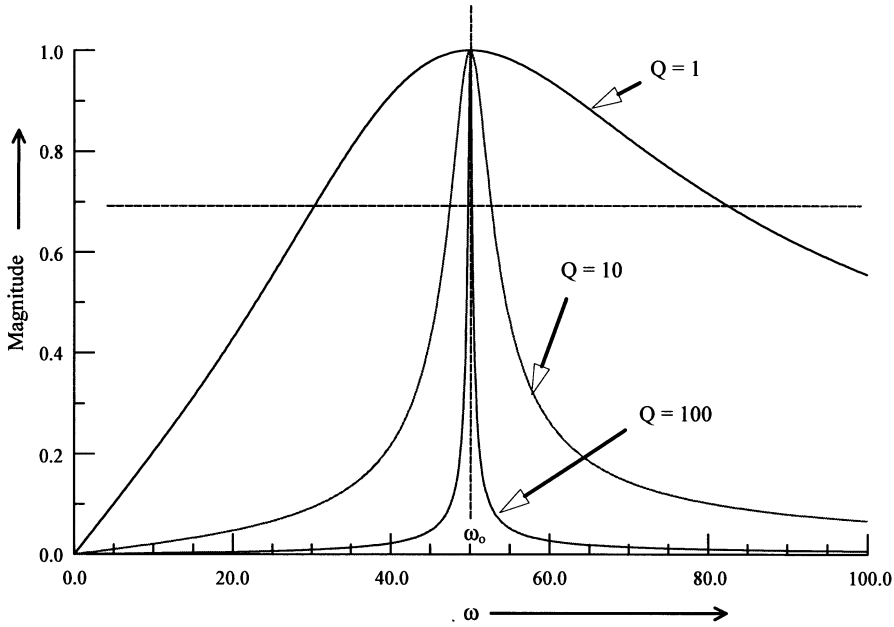

Figure 4.5 Magnitude of $A(j\omega)$ as a function of ω.

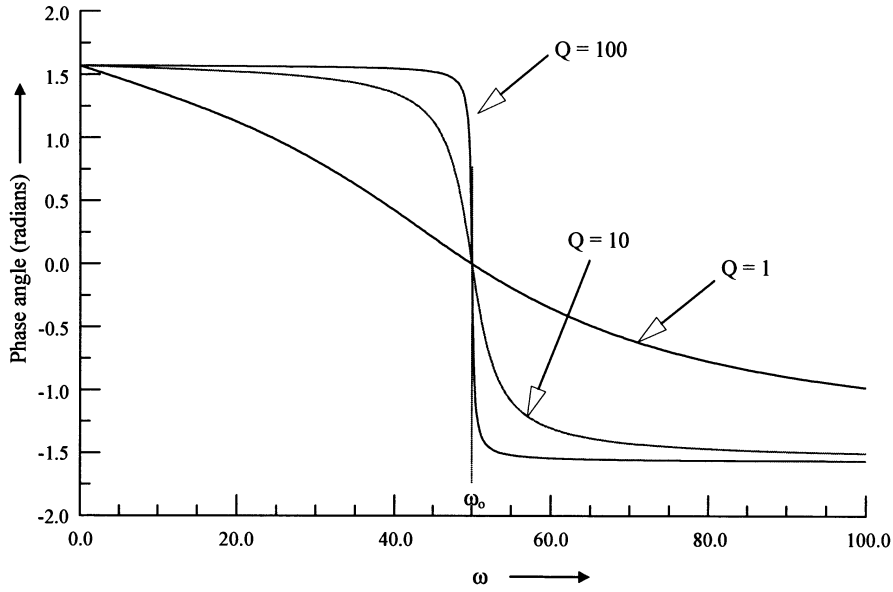

Figure 4.6 The phase angle of $A(j\omega)$ as a function of ω.

where $V_{LC}(j\omega)$ is the voltage across the inductor and capacitor combined. In this case, sinusoidal steady-state response can be obtained as follows.

$$\frac{V_{LC}(j\omega)}{V_{in}(j\omega)} = 1 - \frac{V_o(j\omega)}{V_{in}(j\omega)} = 1 - \frac{1}{\left(1 + jQ\left(\frac{\omega}{\omega_o} - \frac{\omega_o}{\omega}\right)\right)} = \frac{jQ\left(\frac{\omega}{\omega_o} - \frac{\omega_o}{\omega}\right)}{\left(1 + jQ\left(\frac{\omega}{\omega_o} - \frac{\omega_o}{\omega}\right)\right)}$$

Hence, this configuration of the circuit represents a band-rejection filter.

Half-power frequencies ω_1 and ω_2 of a band-pass circuit can be determined from (4.1.13) as follows:

$$\frac{1}{2} = \frac{1}{1 + Q^2\left(\frac{\omega}{\omega_o} - \frac{\omega_o}{\omega}\right)^2} \Rightarrow 2 = 1 + Q^2\left(\frac{\omega}{\omega_o} - \frac{\omega_o}{\omega}\right)^2$$

Therefore,

$$Q\left(\frac{\omega}{\omega_o} - \frac{\omega_o}{\omega}\right) = \pm 1$$

Assuming that $\omega_1 < \omega_o < \omega_2$,

$$Q\left(\frac{\omega_1}{\omega_o} - \frac{\omega_o}{\omega_1}\right) = -1$$

and,

$$Q\left(\frac{\omega_2}{\omega_o} - \frac{\omega_o}{\omega_2}\right) = 1$$

Therefore,

$$\frac{\omega_2}{\omega_o} - \frac{\omega_o}{\omega_2} = -\left(\frac{\omega_1}{\omega_o} - \frac{\omega_o}{\omega_1}\right)$$

or,

$$\omega_2 - \frac{\omega_o^2}{\omega_2} = -\omega_1 + \frac{\omega_o^2}{\omega_1} \Rightarrow (\omega_2 + \omega_1) = \frac{\omega_o^2}{\omega_1} + \frac{\omega_o^2}{\omega_1} = \omega_o^2\left(\frac{1}{\omega_1} + \frac{1}{\omega_2}\right)$$

or,

$$\omega_o^2 = \omega_1\omega_2 \tag{4.1.14}$$

and,

$$\left(\frac{\omega_1}{\omega_o} - \frac{\omega_o}{\omega_1}\right) = -\frac{1}{Q} \Rightarrow \omega_1 - \frac{\omega_o^2}{\omega_1} = -\frac{\omega_o}{Q}$$

or,

$$\omega_1 - \omega_2 = -\frac{\omega_o}{Q} \Rightarrow Q = \frac{\omega_o}{\omega_2 - \omega_1} \tag{4.1.15}$$

Example 4.1: Determine the element values of a resonant circuit that passes all the sinusoidal signals from 9 MHz to 11 MHz. This circuit is to be connected between a voltage source with negligible internal impedance and a communication system with its input impedance at 50 Ω. Plot its characteristics in a frequency band of 1 to 20 MHz.

From (4.1.14),

$$\omega_o = \sqrt{\omega_1 \times \omega_2} \rightarrow f_o = \sqrt{f_1 \times f_2} = \sqrt{9 \times 11} = 9.949874 \text{ MHz}$$

From (4.1.11) and (4.1.15),

$$Q = \frac{\omega_o L}{R} = \frac{\omega_o}{\omega_1 - \omega_2} \rightarrow L = \frac{R}{\omega_1 - \omega_2} = \frac{50}{2 \times \pi \times 10^6 \times (11 - 9)}$$
$$= 3.978874 \times 10^{-6} \text{ H} \approx 4\ \mu\text{H}$$

From (4.1.8),

$$\omega_o = \frac{1}{\sqrt{LC}} \Rightarrow C = \frac{1}{L\omega_o^2} = 6.430503 \times 10^{-11} \text{ F} \approx 64.3 \text{ pF}$$

The circuit arrangement is shown in Figure 4.7. Its magnitude and phase characteristics are displayed in Figure 4.8.

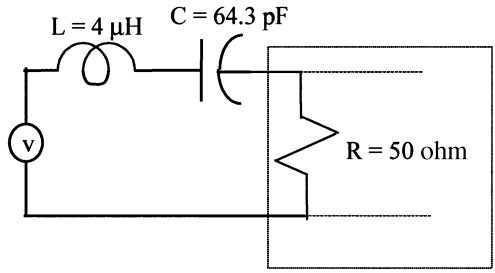

Figure 4.7. The filter circuit arrangement for Example 4.1.

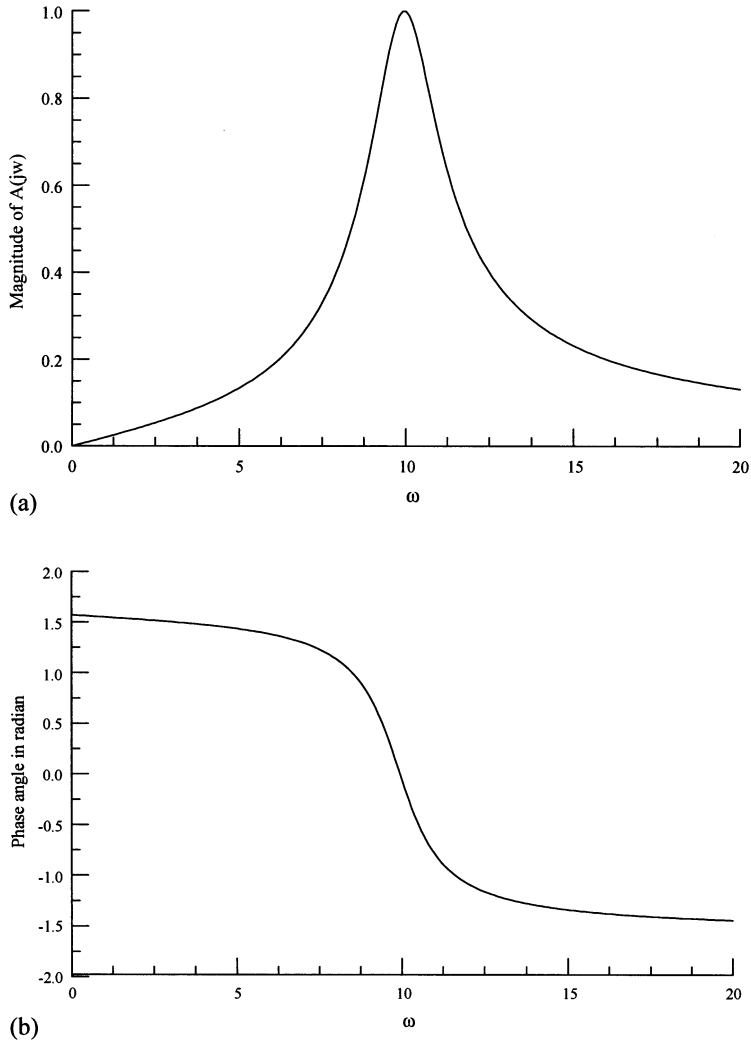

Figure 4.8 Magnitude (a) and phase (b) plots of A ($j\omega$) for the circuit in Figure 4.7.

Input Impedance

Impedance across the input terminals of a series *R-L-C* circuit can be determined as follows.

$$Z_{\text{in}} = R + j\omega L + \frac{1}{j\omega C} = R + j\omega L\left(1 - \frac{\omega_o^2}{\omega^2}\right) \tag{4.1.16}$$

At resonance, the inductive reactance cancels out the capacitive reactance. Therefore, the input impedance reduces to total resistance of the circuit. If signal frequency changes from the resonant frequency by $\pm\delta\omega$, the input impedance can be approximated as follows.

$$Z_{\text{in}} = R + j\omega L\frac{(\omega+\omega_{\text{o}})(\omega-\omega_{\text{o}})}{\omega^2} \approx R + j2\delta\omega L = R + j\frac{2QR\delta\omega}{\omega_{\text{o}}} \tag{4.1.17}$$

Alternatively,

$$\begin{aligned} Z_{\text{in}} &\approx R + j2\delta\omega L = \frac{\omega_{\text{o}}L}{Q} + j2(\omega-\omega_{\text{o}})L = j2\left(\omega-\omega_{\text{o}}+\frac{\omega_{\text{o}}}{j2Q}\right)L \\ &= j2\left(\omega-\omega_{\text{o}}\left(1+j\frac{1}{2Q}\right)\right)L \end{aligned} \tag{4.1.18}$$

Therefore, a series resonant circuit can be analyzed with R as zero (i.e., assuming that the circuit is lossless). The losses can be included subsequently by replacing a real resonant frequency, ω_{o}, by the complex frequency, $\omega_{\text{o}}\left(1+j\frac{1}{2Q}\right)$.

At resonance, current through the circuit, I_{r},

$$I_{\text{r}} = \frac{V_{\text{in}}}{R} \tag{4.1.19}$$

Therefore, voltages across the inductor, V_{L}, and the capacitor, V_{c}, are

$$V_{\text{L}} = j\omega_{\text{o}}L\frac{V_{\text{in}}}{R} = jQV_{\text{in}} \tag{4.1.20}$$

and,

$$V_{\text{C}} = \frac{1}{j\omega_{\text{o}}C}\frac{V_{\text{in}}}{R} = -jQV_{\text{in}} \tag{4.1.21}$$

Hence, the magnitude of voltage across the inductor is equal to the quality factor times input voltage while its phase leads 90°. Magnitude of the voltage across the capacitor is the same as that across the inductor. However, it is 180° out of phase because it lags behind the input voltage by 90°.

4.2 PARALLEL RESONANT CIRCUITS

Consider an *R-L-C* circuit in which the three components are connected in parallel, as shown in Figure 4.9. A subscript p is used to differentiate the circuit elements from those used in the series circuit of the preceding section. A current source, $i_{\text{in}}(t)$,

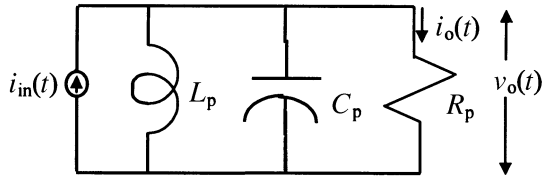

Figure 4.9 A parallel *R-L-C* circuit.

is connected across its terminals and $i_o(t)$ is current through the resistor R_p. Voltage across this circuit is $v_o(t)$. From Kirchhoff's current law,

$$i_{in}(t) = \frac{1}{L_p}\int_{-\infty}^{t} R_p i_o(t)dt + C_p \frac{d(R_p i_o(t))}{dt} + i_o(t) \tag{4.2.1}$$

Assuming that there was no energy stored in the circuit initially, we take the Laplace transform of (4.2.1). It gives

$$I_{in}(s) = \left(\frac{R_p}{sL_p} + sR_pC_p + 1\right) I_o(s)$$

Hence,

$$\frac{I_o(s)}{I_{in}(s)} = \frac{\dfrac{sL_p}{R_p}}{\left(s^2 L_p C_p + s\dfrac{L_p}{R_p} + 1\right)} \tag{4.2.2}$$

Note that this equation is similar to (4.1.6) of the preceding section. It changes to $T(s)$ if RC replaces L_p/R_p. Therefore, results of the series resonant circuit can be used for this parallel resonant circuit, provided

$$\zeta = \frac{1}{2\omega_o R_p C_p}$$

and,

$$\omega_o = \frac{1}{\sqrt{L_p C_p}} \tag{4.2.3}$$

Hence,

$$\zeta = \frac{1}{2\omega_o R_p C_p} = \frac{1}{2R_p}\sqrt{\frac{L_p}{C_p}} \tag{4.2.4}$$

The quality factor, Q_p, and the impedance, Z_p, of the parallel resonant circuit can be determined as follows:

$$Q_{\text{series}} = \frac{\omega_o L}{R} = \frac{1}{\omega_o RC} \Rightarrow Q_p = \omega_o R_p C_p = \frac{R_p}{\omega_o L_p} \tag{4.2.5}$$

$$Z_p = \frac{V_o(j\omega)}{I_{in}(i\omega)} = \frac{I_o(j\omega)R_p}{I_{in}(j\omega)} = \frac{j\omega L_p}{\left(-\omega^2 L_p C_p + j\omega \frac{L_p}{R_p} + 1\right)} \tag{4.2.6}$$

Input Admittance

Admittance across input terminals of the parallel resonant circuit (i.e., the admittance seen by the current source) can be determined as follows.

$$Y_{in} = \frac{1}{Z_p} = \frac{1}{R_p} + j\omega C_p + \frac{1}{j\omega L_p} = \frac{1}{R_p} + j\omega C_p \left(1 - \frac{\omega_o^2}{\omega^2}\right) \tag{4.2.7}$$

Hence, input admittance will be equal to $1/R_p$ at the resonance. It will become zero (that means the impedance will be infinite) for a lossless circuit. It can be approximated around the resonance, $\omega_o \pm \delta\omega$, as follows.

$$Y_{in} \approx \frac{1}{R_p} + j2\delta\omega C_p = \frac{1}{R_p} + j\frac{2\delta\omega Q}{\omega_o R_p} \tag{4.2.8}$$

The corresponding impedance is

$$Z_p \approx \frac{R_p}{1 + j\frac{2Q\delta\omega}{\omega_o}} \tag{4.2.9}$$

Current through the capacitor, I_c, at the resonance is

$$I_c = j\omega_o C_p R_p I_{in} = jQI_{in} \tag{4.2.10}$$

and current through the inductor, I_L, is

$$I_L = \frac{1}{j\omega_o L_p} R_p I_{in} = -jQI_{in} \tag{4.2.11}$$

Thus, current through the inductor is equal in magnitude but opposite in phase to that through the capacitor. Further, these currents are larger than the input current by a factor of Q.

Quality Factor of a Resonant Circuit

If resistance R represents losses in the resonant circuit, Q given by the preceding formulas is known as the *unloaded Q*. If the power loss due to external load coupling

is included through an additional resistance R_L then the *external* Q_e is defined as follows:

$$Q_e = \begin{cases} \dfrac{\omega_o L}{R_L} & \text{for series resonant circuit} \\ \dfrac{R_L}{\omega_o L_p} & \text{for parallel resonant circuit} \end{cases} \tag{4.2.12}$$

The loaded Q, Q_L, of a resonant circuit includes internal losses as well as the power extracted by the external load. It is defined as follows:

$$Q_L = \begin{cases} \dfrac{\omega_o L}{R_L + R} & \text{for series resonant circuit} \\ \dfrac{R_L \| R_p}{\omega_o L_p} & \text{for parallel resonant circuit} \end{cases} \tag{4.2.13}$$

where,

$$R_L \| R_p = \frac{R_L R_p}{R_L + R_p}$$

Hence, the following relation holds good for both kinds of resonant circuits (see Table 4.1).

$$\frac{1}{Q_L} = \frac{1}{Q_e} + \frac{1}{Q} \tag{4.2.14}$$

Example 4.2: Consider the loaded parallel resonant circuit illustrated here. Compute the resonant frequency in radians per second, unloaded Q, and the loaded Q of this circuit.

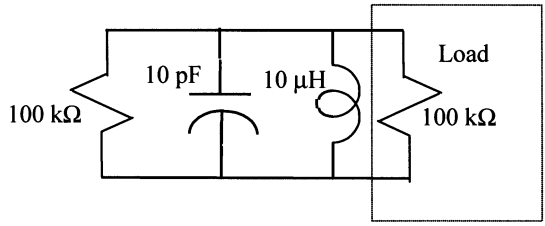

$$\omega_o = \frac{1}{\sqrt{L_p C_p}} = \frac{1}{\sqrt{10^{-5} \times 10^{-11}}} = 10^8 \text{ rad/s}$$

The unloaded $Q = \dfrac{R_p}{\omega_o L_p} = \dfrac{10^5}{10^8 \times 10^{-5}} = 100.$

TABLE 4.1 Relations for Series and Parallel Resonant Circuits

	Series	Parallel
ω_o	$\frac{1}{\sqrt{LC}}$	$\frac{1}{\sqrt{L_pC_p}}$
Damping factor, ζ	$\frac{R}{2}\sqrt{\frac{C}{L}}$	$\frac{1}{2R_p}\sqrt{\frac{L_p}{C_p}}$
Unloaded Q	$\frac{\omega_o L}{R}=\frac{1}{\omega_o RC}$	$\frac{R_p}{\omega_o L_p}=\omega_o R_p C_p$
External $Q=Q_e$	$\frac{\omega_o L}{R_L}=\frac{1}{\omega_o R_L C}$	$\frac{R_L}{\omega_o L_p}=\omega_o R_L C_p$
Loaded $Q=Q_L$	$\frac{Q\times Q_e}{Q+Q_e}$	$\frac{Q\times Q_e}{Q+Q_e}$
Input impedance, Z_{in}, around resonance	$R+j\frac{2RQ\delta\omega}{\omega_o}$	$\frac{R}{1+j\frac{2Q\delta\omega}{\omega_o}}$

The external Q, $Q_e=\dfrac{R_L}{\omega_o L_p}=\dfrac{10^5}{10^8\times 10^{-5}}=100.$

The loaded Q, $Q_L=\dfrac{R_p\|R_L}{\omega_o L_p}=\dfrac{QQ_e}{Q+Q_e}=\dfrac{50\times 10^3}{10^8\times 10^{-5}}=50$.

4.3 TRANSFORMER-COUPLED CIRCUITS

Transformers are used as a means of coupling as well as of impedance transforming in electronic circuits. Transformers with tuned circuits in one or both of their sides are employed in voltage amplifiers and oscillators operating at radio frequencies. This section presents an equivalent model and an analytical procedure for the transformer-coupled circuits.

Consider a load impedance Z_L that is coupled to the voltage source V_s via a transformer as illustrated in Figure 4.10. Source impedance is assumed to be Z_s. The transformer has a turn ratio of n:1 between its primary (the source) and secondary (the load) sides.

Using the notations as indicated, equations for various voltages and currents can be written in phasor form as follows.

$$V_1 = j\omega L_1 I_1 + j\omega M I_2 \tag{4.3.1}$$

$$V_2 = j\omega M I_1 + j\omega L_2 I_2 \tag{4.3.2}$$

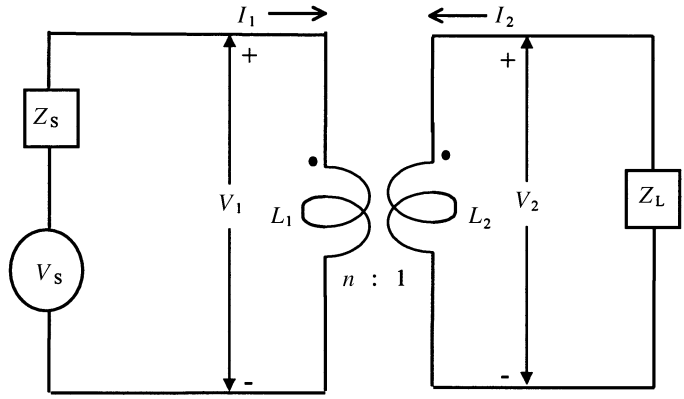

Figure 4.10 A transformer-coupled circuit.

where M is the mutual inductance between the two sides of the transformer. Standard convention with a dot on each side is used. Hence, magnetic fluxes reinforce each other for the case of currents entering this terminal on both sides, and M is positive.

The following relations hold for an ideal transformer operating at any frequency.

$$V_1 = nV_2 \tag{4.3.3}$$

$$I_1 = -\frac{I_2}{n} \tag{4.3.4}$$

and,

$$\frac{V_1}{I_1} = Z_1 = \frac{nV_2}{-I_2/n} = n^2 \frac{V_2}{-I_2} = n^2 Z_2 \tag{4.3.5}$$

There are several equivalent circuits available for a transformer. We consider one of these that is most useful in analyzing the communication circuits. This equivalent circuit is illustrated in Figure 4.11 below. The following equations for phasor voltages and currents may be formulated using the notations indicated in Figure 4.11.

$$V_1 = j\omega(1-\xi)L_1 I_1 + j\omega\xi L_1\left(I_1 + \frac{I_2}{n}\right) = j\omega L_1 I_1 + j\omega\xi L_1 \frac{I_2}{n} \tag{4.3.6}$$

and,

$$V_2 = \frac{1}{n}\left(\, j\omega\xi L_1\left(I_1 + \frac{I_2}{n}\right)\right) \tag{4.3.7}$$

If the circuit shown in Figure 4.11 is equivalent to that shown in Figure 4.10 then these two equations represent the same voltages as those of (4.3.1) and (4.3.2).

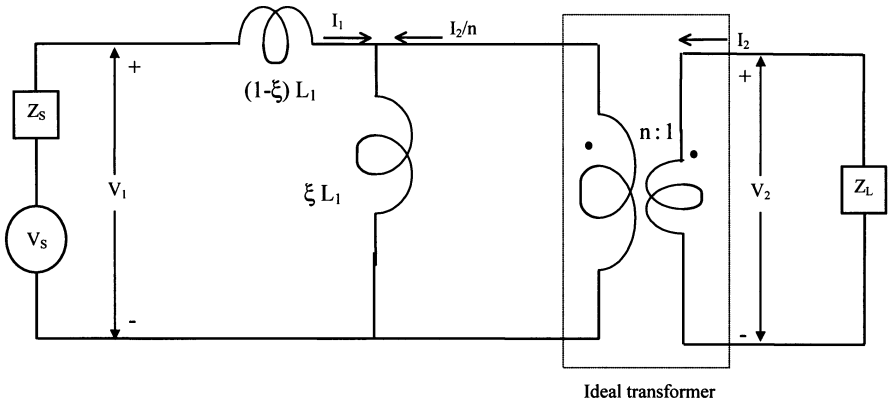

Figure 4.11 Equivalent model of the transformer-coupled circuit shown in Figure 4.10.

Hence,

$$\frac{\xi L_1}{n} = M \tag{4.3.8}$$

and,

$$\frac{\xi L_1}{n^2} = L_2 \tag{4.3.9}$$

In other words,

$$n = \sqrt{\frac{\xi L_1}{L_2}} \tag{4.3.10}$$

and,

$$\xi = \frac{nM}{L_1} = \frac{M\sqrt{\xi}}{\sqrt{L_1 L_2}} \Rightarrow \sqrt{\xi} = \frac{M}{\sqrt{L_1 L_2}} = \kappa \tag{4.3.11}$$

where κ is called the *coefficient of coupling*. It is close to unity for a tightly coupled transformer, and close to zero for a loose coupling.

Example 4.3: A tightly coupled transformer is used in the circuit shown in Figure 4.12. Inductances of its primary and secondary sides are 320 nH and 20 nH, respectively. Find its equivalent circuit, the resonant frequency, and the Q of this circuit.

Since the transformer is tightly coupled, $\kappa \approx 1$. Therefore, $\xi \approx 1$, $(1 - \xi) \approx 0$, and its equivalent circuit simplifies as shown in Figure 4.13. From (4.3.10),

$$n = \sqrt{\frac{\xi L_1}{L_2}} \approx \sqrt{\frac{320}{20}} = 4$$

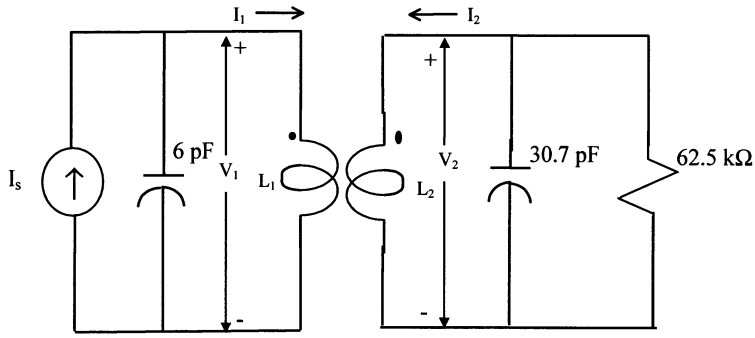

Figure 4.12 A transformer-coupled resonant circuit.

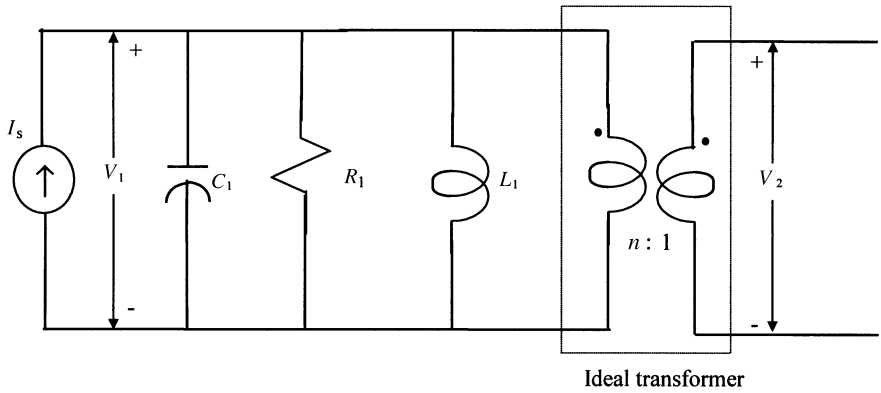

Figure 4.13 An equivalent model of the transformer-coupled circuit shown in Figure 4.12.

and, from (4.3.5),

$$Z_1 = n^2 Z_2 \Rightarrow Y_1 = \frac{Y_2}{n^2} = \frac{1}{n^2}\left(\frac{1}{R_2} + j\omega C_2\right)$$

Therefore,

$$R_1 = n^2 R_2 = 16 \times 62.5\ k\Omega = 1\text{M}\Omega$$

$$C_1 = 6 + \frac{1}{4^2}30.7\ \text{pF} = 6 + 1.91875 \approx 7.92\ \text{pF}$$

$$\omega_o = \frac{1}{\sqrt{L_1 C_1}} = \frac{1}{\sqrt{320 \times 10^{-9} \times 7.92 \times 10^{-12}}} = 628.1486 \times 10^6\ \text{rad/s}$$

$$f_o = \frac{\omega_o}{2\pi} = 99.97\ \text{MHz} \approx 100\ \text{MHz}$$

and,

$$Q = \frac{R_1}{\omega_o L_1} = \frac{10^6}{628.1486 \times 10^6 \times 320 \times 10^{-9}} = 4974.9375$$

Example 4.4: A transformer-coupled circuit is shown in Figure 4.14. Draw its equivalent circuit using an ideal transformer. (a) If the transformer is tuned only to its secondary side (that is, R_1 and C_1 are removed), determine its resonant frequency and impedance seen by the current source. (b) Determine the current transfer function (I_o/I_s) for the entire circuit (that is, R_1 and C_1 are included in the circuit). If the transformer is loosely coupled, and both sides have identical quality factors as well as the resonant frequencies, determine the locations of the poles of the current transfer function on the complex ω-plane.

Following the preceding analysis and Figure 4.11, the equivalent circuit can be drawn easily, as shown in Figure 4.15. Using notations as indicated in the figure,

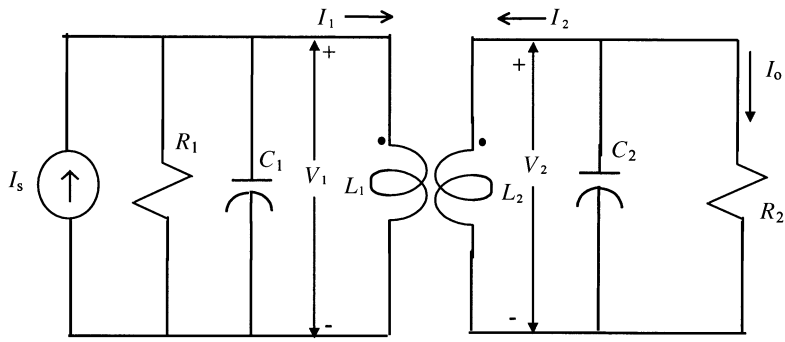

Figure 4.14 A double-tuned transformer-coupled circuit.

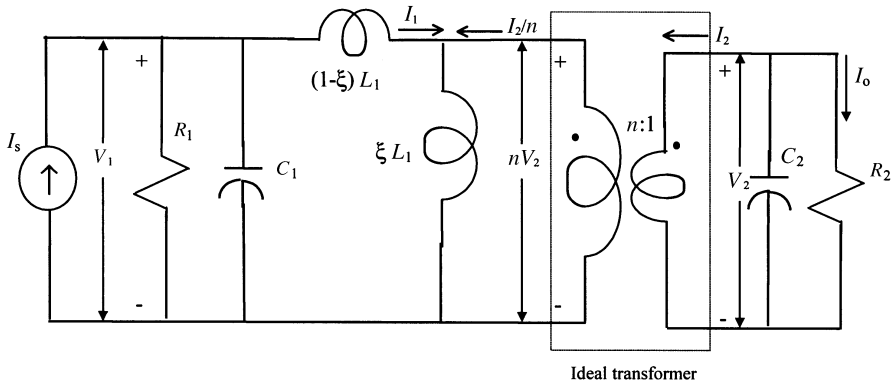

Figure 4.15 An equivalent representation for the circuit shown in Figure 4.14.

circuit voltages and currents can be found as follows.

$$nV_2 = s\xi L_1\left(I_1 + \frac{I_2}{n}\right) \tag{4.3.12}$$

$$V_2 = -I_2\frac{R_2}{1 + sR_2C_2} = R_2I_o \tag{4.3.13}$$

$$I_s = I_1 + \left(\frac{1}{R_1} + sC_1\right)(nV_2 + s(1-\xi)L_1I_1) \tag{4.3.14}$$

From (4.3.12), (4.3.13), and (4.3.10), we find that

$$\left(1 + \frac{s^2\xi L_1R_2C_2 + s\xi L_1}{n^2R_2}\right)V_2 = \left(1 + s^2L_2C_2 + \frac{sL_2}{R_2}\right)R_2I_o = \frac{s\xi L_1}{n}I_1$$

or,

$$\frac{I_o}{I_1} = \frac{\dfrac{s\xi L_1}{nR_2}}{1 + s^2L_2C_2 + \dfrac{sL_2}{R_2}} \tag{4.3.15}$$

- When R_1 and C_1 are absent, I_1 will be equal to I_s, and (4.3.15) will represent the current transfer characteristics. This equation is similar to (4.2.2). Hence the resonant frequency is found as follows:

$$\omega_o = \frac{1}{\sqrt{L_2C_2}} \tag{4.3.16}$$

Note that the resonant frequency in this case depends only on L_2 and C_2. It is independent of inductance L_1 of the primary side.

The impedance seen by the current source, with R_1 and C_1 removed, is determined as follows:

$$Z_{in}(s) = \frac{V_1}{I_1} = sL_1(1-\xi) + \frac{n^2sL_2}{s^2L_2C_2 + s\dfrac{L_2}{R_2} + 1} \tag{4.3.17}$$

At resonance,

$$Z_{in}(j\omega_o) = j\omega_oL_1(1-\xi) + n^2R_2 \tag{4.3.18}$$

and, if the transformer is tightly coupled, $\xi \approx 1$

$$Z_{\text{in}}(j\omega_{\text{o}}) = n^2 R_2 \tag{4.3.19}$$

- When R_1 and C_1 are included in the circuit, (4.3.12)–(4.3.14) can be solved to obtain a relationship between I_{o} and I_{s}. The desired current transfer function can be obtained as follows.

$$\frac{I_{\text{o}}}{I_s} = \frac{\dfrac{s\xi L_1}{nR_2}}{\left(s^2 L_2 C_2 + s\dfrac{L_2}{R_2} + 1\right) \times \left\{1 + s(1-\xi)L_1\left(\dfrac{1}{R_1} + sC_1\right)\right\} + s\xi L_1\left(\dfrac{1}{R_1} + sC_1\right)} \tag{4.3.20}$$

Note that the denominator of this equation is now a polynomial of the fourth degree. Hence, this current ratio has four poles on the complex ω-plane. If the transformer is loosely coupled, ξ will be negligible. In that case, the denominator of (4.3.20) can be approximated as follows.

$$\frac{I_{\text{o}}}{I_s} \approx \frac{\dfrac{s\xi L_1}{nR_2}}{\left(s^2 L_2 C_2 + s\dfrac{L_2}{R_2} + 1\right) \times \left\{1 + sL_1\left(\dfrac{1}{R_1} + sC_1\right)\right\} + s\xi L_1\left(\dfrac{1}{R_1} + sC_1\right)} \tag{4.3.21}$$

For $\omega_1 = \omega_2 = \omega_{\text{o}}$, and $Q_1 = Q_2 = Q_{\text{o}}$,

$$L_1 C_1 = L_2 C_2 = \frac{1}{\omega_{\text{o}}^2}$$

and,

$$\frac{R_1}{L_1} = \frac{R_2}{L_2} = \omega_{\text{o}} Q_{\text{o}}.$$

Hence, (4.3.21) may be written as follows.

$$\frac{I_{\text{o}}}{I_{\text{s}}} \approx \frac{\dfrac{s\xi L_1}{nR_2}}{\left(\dfrac{s^2}{\omega_{\text{o}}^2} + \dfrac{s}{\omega_{\text{o}} Q} + 1\right)^2 + \xi\left(\dfrac{s^2}{\omega_{\text{o}}^2} + \dfrac{s}{\omega_{\text{o}} Q}\right)} \tag{4.3.22}$$

Poles of (4.3.22) are determined by solving the following equation.

$$\left(\frac{s^2}{\omega_o^2}+\frac{s}{\omega_o Q}+1\right)^2+\xi\left(\frac{s^2}{\omega_o^2}+\frac{s}{\omega_o Q}\right)=0 \tag{4.3.23}$$

Roots of this equation are found to be

$$s \approx -\frac{\omega_o}{2Q_o} \pm j\omega_o\sqrt{(1\mp\sqrt{\xi})-\left(\frac{1}{2Q_o}\right)^2} \tag{4.3.24}$$

4.4 TRANSMISSION LINE RESONANT CIRCUITS

Transmission lines with open or short-circuited ends are frequently used as resonant circuits in the UHF and microwave range. We consider such networks in this section. Since the quality factor is an important parameter of these circuits, we need to include the finite (even though small) loss in the line. There are four basic types of these networks as illustrated in Figure 4.16.

It can be easily found by analyzing the input impedance characteristics around the resonant wavelength, λ_r, that the circuits of Figure 4.16(a) and (d) behave like a series *R-L-C* circuit. On the other hand, the other two transmission lines possess the characteristics of a parallel resonant circuit. A quantitative analysis of these circuits is presented below for n as unity.

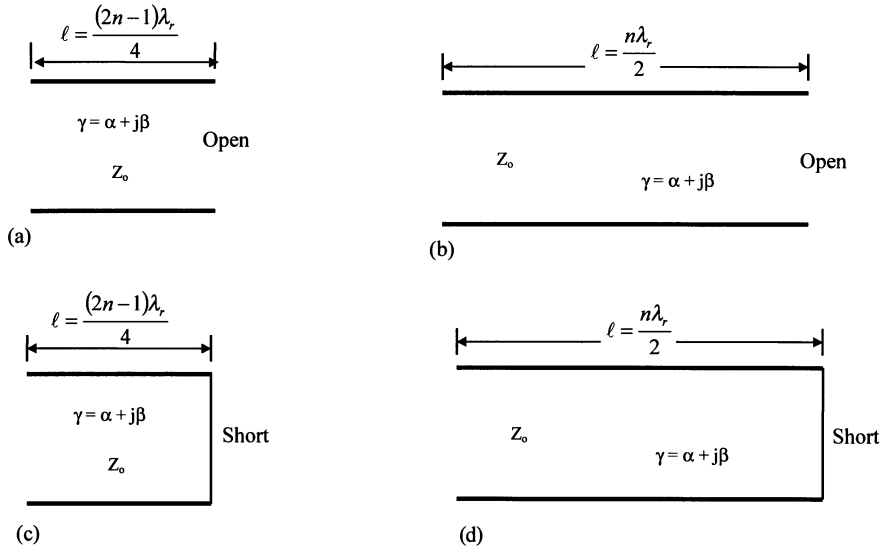

Figure 4.16 Four basic types of transmission line resonant circuits, $n = 1, 2, \ldots$.

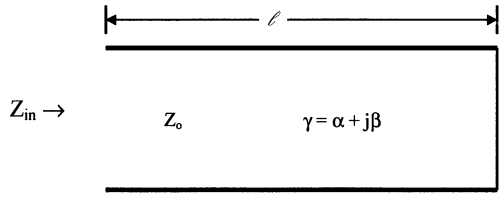

Figure 4.17 A short-circuited lossy transmission line.

Short-Circuited Line

Consider a transmission line of length ℓ and characteristic impedance Z_o. It has a propagation constant, $\gamma = \alpha + j\beta$. The line is short circuited at one of its ends as shown in Figure 4.17. The impedance at its other end, Z_{in}, can be determined from (3.2.5) as follows.

$$Z_{in} = Z_o \tanh(\gamma\ell) = Z_o \tanh(\alpha + j\beta)\ell = Z_o \frac{\tanh(\alpha\ell) + j\tan(\beta\ell)}{1 + j\tanh(\alpha\ell)\tan(\beta\ell)} \tag{4.4.1}$$

For $\alpha\ell \ll 1$, $\tanh(\alpha\ell) \approx \alpha\ell$, and assuming that the line supports only the TEM mode, we find that $\beta\ell = \dfrac{\omega\ell}{v_p}$. Hence, it can be simplified around the resonant frequency, ω_o, as follows:

$$\beta\ell = \frac{\omega\ell}{v_p} = \frac{\omega_0\ell}{v_p} + \frac{\delta\omega\ell}{v_p} = \beta_r\ell + \frac{\delta\omega\ell}{v_p} \tag{4.4.2}$$

where β_r is the phase constant at the resonance.

If the transmission line is one-half-wavelength long at the resonant frequency then

$$\beta_r\ell = \pi, \text{ and } \frac{\ell}{v_p} = \frac{\pi}{\omega_o}.$$

Therefore, $\tan(\beta\ell)$ can be approximated as follows:

$$\tan(\beta\ell) = \tan\left(\pi + \frac{\delta\omega\ell}{v_p}\right) = \tan\left(\pi + \frac{\pi\delta\omega}{\omega_o}\right) = \tan\left(\frac{\pi\delta\omega}{\omega_o}\right) \approx \frac{\pi\delta\omega}{\omega_o}$$

and,

$$Z_{\text{in}} \approx Z_{\text{o}} \frac{\alpha\ell + j\dfrac{\pi\delta\omega}{\omega_{\text{o}}}}{1 + j(\alpha\ell)\left(\dfrac{\pi\delta\omega}{\omega_{\text{o}}}\right)} \approx Z_{\text{o}}\left(\alpha\ell + j\frac{\pi\delta\omega}{\omega_{\text{o}}}\right) \tag{4.4.3}$$

It is assumed in (4.4.3) that $(\alpha\ell)\left(\dfrac{\pi\delta\omega}{\omega_{\text{o}}}\right) \ll 1$.

For a series resonant circuit, $Z_{\text{in}} \approx R + j2\ \delta\omega\ L$. Hence, a half-wavelength-long transmission line with short-circuit termination is similar to a series resonant circuit. The equivalent circuit parameters are found as follows (assuming that losses in the line are small such that the characteristic impedance is a real number):

$$R \approx Z_{\text{o}}\alpha\ell = \frac{1}{2}Z_{\text{o}}\alpha\lambda_{\text{r}} \tag{4.4.4}$$

$$L \approx \frac{\pi}{2} \times \frac{Z_{\text{o}}}{\omega_{\text{o}}} \tag{4.4.5}$$

$$C \approx \frac{1}{\pi\omega_{\text{o}}Z_{\text{o}}} \tag{4.4.6}$$

and,

$$Q = \frac{\omega_{\text{o}}L}{R} \approx \frac{\pi}{2\alpha\ell} = \frac{\beta_{\text{r}}}{2\alpha} \tag{4.4.7}$$

On the other hand, if the transmission line is a quarter-wavelength long at the resonant frequency then $\beta_{\text{r}}\ell = \pi/2$, and $\dfrac{\ell}{v_{\text{p}}} = \dfrac{\pi}{2\omega_{\text{o}}}$. Therefore,

$$\tan(\beta\ell) = \tan\left(\frac{\pi}{2} + \frac{\delta\omega\ell}{v_{\text{p}}}\right) = \tan\left(\frac{\pi}{2} + \frac{\pi\delta\omega}{2\omega_{\text{o}}}\right) = -\cot\left(\frac{\pi\delta\omega}{2\omega_{\text{o}}}\right) \approx -\frac{2\omega_{\text{o}}}{\pi\delta\omega} \tag{4.4.8}$$

and,

$$Z_{\text{in}} \approx Z_{\text{o}} \frac{-j\dfrac{2\omega_{\text{o}}}{\pi\delta\omega}}{1 - j\alpha\ell\dfrac{2\omega_{\text{o}}}{\pi\delta\omega}} = \frac{\dfrac{Z_{\text{o}}}{\alpha\ell}}{1 + j\dfrac{\pi}{\alpha\ell} \times \dfrac{\delta\omega}{2\omega_{\text{o}}}} \tag{4.4.9}$$

This expression is similar to the one obtained for a parallel resonant circuit in (4.2.9). Therefore, this transmission line is working as a parallel resonant circuit with equivalent parameters as follows:

$$R_{\mathrm{p}} \approx \frac{Z_{\mathrm{o}}}{\alpha \ell} = \frac{4Z_{\mathrm{o}}}{\alpha \lambda_{\mathrm{r}}} \tag{4.4.10}$$

$$L_{\mathrm{p}} \approx \frac{4Z_{\mathrm{o}}}{\pi \omega_{\mathrm{o}}} \tag{4.4.11}$$

$$C_{\mathrm{p}} \approx \frac{\pi}{4\omega_{\mathrm{o}} Z_{\mathrm{o}}} \tag{4.4.12}$$

and,

$$Q = \frac{\pi}{4\alpha \ell} = \frac{\beta_{\mathrm{r}}}{2\alpha} \tag{4.4.13}$$

Open-Circuited Line

The analysis of the open-circuited transmission line shown in Figure 4.18 can be performed following a similar procedure. These results are summarized in the following.

From (3.2.5),

$$Z_{\mathrm{in}}|_{Z_{\mathrm{L}}=\infty} = \frac{Z_{\mathrm{o}}}{\tanh(\gamma \ell)} \tag{4.4.14}$$

For a transmission line that is a half-wavelength long, the input impedance can be approximated as follows:

$$Z_{\mathrm{in}} \approx Z_{\mathrm{o}} \frac{1 + j(\alpha \ell)\left(\dfrac{\pi \delta \omega}{\omega_{\mathrm{o}}}\right)}{\alpha \ell + j\dfrac{\pi \delta \omega}{\omega_{\mathrm{o}}}} \approx \frac{Z_{\mathrm{o}}}{\alpha \ell + j\dfrac{\pi \delta \omega}{\omega_{\mathrm{o}}}} \tag{4.4.15}$$

This is similar to (4.2.9). Therefore, a half-wavelength-long open-circuited transmission line is similar to a parallel resonant circuit with equivalent parameters

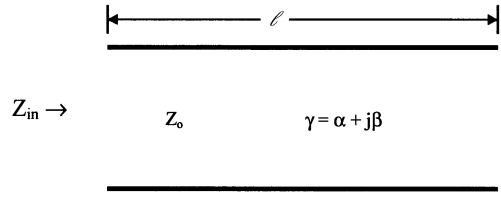

Figure 4.18 An open-circuited transmission line.

as follows:

$$R_{\mathrm{p}} \approx \frac{Z_{\mathrm{o}}}{\alpha\ell} = \frac{2Z_{\mathrm{o}}}{\alpha\lambda_{\mathrm{r}}} \tag{4.4.16}$$

$$L_{\mathrm{p}} \approx \frac{2Z_{\mathrm{o}}}{\pi\omega_{\mathrm{o}}} \tag{4.4.17}$$

$$C_{\mathrm{p}} \approx \frac{\pi}{2\omega_{\mathrm{o}}Z_{\mathrm{o}}} \tag{4.4.18}$$

and,

$$Q = \frac{\pi}{2\alpha\ell} = \frac{\beta_{\mathrm{r}}}{2\alpha} \tag{4.4.19}$$

If the line is only a quarter-wavelength long, the input impedance can be approximated as follows:

$$Z_{\mathrm{in}} \approx Z_{\mathrm{o}} \frac{1 - j(\alpha\ell)\left(\dfrac{2\omega_{\mathrm{o}}}{\pi\delta\omega}\right)}{\alpha\ell - j\dfrac{2\omega_{\mathrm{o}}}{\pi\delta\omega}} \approx Z_{\mathrm{o}}\left(\alpha\ell + j\frac{\pi\delta\omega}{2\omega_{\mathrm{o}}}\right) \tag{4.4.20}$$

Since (4.4.20) is similar to (4.1.17), this transmission line works as a series resonant circuit. Its equivalent circuit parameters are found as follows (see Table 4.2):

$$R \approx Z_{\mathrm{o}}\alpha\ell = \frac{1}{4}Z_{\mathrm{o}}\alpha\lambda_{\mathrm{r}} \tag{4.4.21}$$

$$L \approx \frac{\pi Z_{\mathrm{o}}}{4\omega_{\mathrm{o}}} \tag{4.4.22}$$

$$C \approx \frac{4}{\pi\omega_{\mathrm{o}}Z_{\mathrm{o}}} \tag{4.4.23}$$

TABLE 4.2 Equivalent Circuit Parameters of the Resonant Lines for $n = 1$

	Quarter-Wavelength Line		Half-Wavelength Line	
	Open Circuit	Short Circuit	Open Circuit	Short Circuit
Resonance	Series	Parallel	Parallel	Series
R	$\frac{1}{4}Z_{\mathrm{o}}\alpha\lambda_{\mathrm{r}}$	$\dfrac{4Z_{\mathrm{o}}}{\alpha\lambda_{\mathrm{r}}}$	$\dfrac{2Z_{\mathrm{o}}}{\alpha\lambda_{\mathrm{r}}}$	$\frac{1}{2}Z_{\mathrm{o}}\alpha\lambda_{\mathrm{r}}$
L	$\dfrac{\pi Z_{\mathrm{o}}}{4\omega_{\mathrm{o}}}$	$\dfrac{4Z_{\mathrm{o}}}{\pi\omega_{\mathrm{o}}}$	$\dfrac{2Z_{\mathrm{o}}}{\pi\omega_{\mathrm{o}}}$	$\dfrac{\pi Z_{\mathrm{o}}}{2\omega_{\mathrm{o}}}$
C	$\dfrac{4}{\pi Z_{\mathrm{o}}\omega_{\mathrm{o}}}$	$\dfrac{\pi}{4Z_{\mathrm{o}}\omega_{\mathrm{o}}}$	$\dfrac{\pi}{2Z_{\mathrm{o}}\omega_{\mathrm{o}}}$	$\dfrac{2}{\pi Z_{\mathrm{o}}\omega_{\mathrm{o}}}$
Q	$\dfrac{\beta_{\mathrm{r}}}{2\alpha}$	$\dfrac{\beta_{\mathrm{r}}}{2\alpha}$	$\dfrac{\beta_{\mathrm{r}}}{2\alpha}$	$\dfrac{\beta_{\mathrm{r}}}{2\alpha}$

and,

$$Q = \frac{\pi Z_o}{4R} = \frac{\pi}{4\alpha\ell} = \frac{\beta_o}{2\alpha} \tag{4.4.24}$$

Example 4.5: Design a half-wavelength-long coaxial line resonator that is short-circuited at its ends. Its inner conductor radius is 0.455 mm and the inner radius of the outer conductor is 1.499 mm. The conductors are made of copper. Compare the Q of an air-filled to that of a Teflon-filled resonator operating at 5 GHz. The dielectric constant of Teflon is 2.08 and its loss tangent is 0.0004.

From the relations for coaxial lines given in the appendix,

$$R_s = \sqrt{\frac{\omega\mu_o}{2\sigma}} = \sqrt{\frac{2\pi \times 5 \times 10^9 \times 4\pi \times 10^{-7}}{2 \times 5.813 \times 10^7}} = 0.018427\ \Omega$$

$$\alpha_c = \frac{R_s}{2\sqrt{\frac{\mu_o}{\varepsilon_o}}\ln\left(\frac{b}{a}\right)}\left(\frac{1}{a}+\frac{1}{b}\right) = \frac{0.018427}{2 \times 376.7343 \times \ln\left(\frac{1.499}{0.455}\right)}\left(\frac{1000}{0.455}+\frac{1000}{1.499}\right)$$

$$= 0.058768\ \text{Np/m}$$

With Teflon-filling,

$$\alpha_c = \frac{R_s}{2\sqrt{\frac{\mu_o}{\varepsilon_o\varepsilon_r}}\ln\left(\frac{b}{a}\right)}\left(\frac{1}{a}+\frac{1}{b}\right) = \frac{0.018427 \times \sqrt{2.08}}{2 \times 376.7343 \times \ln\left(\frac{1.499}{0.455}\right)}\left(\frac{100}{0.455}+\frac{100}{1.499}\right)$$

$$= 0.084757\ \text{Np/m}$$

$$\alpha_d = \frac{\omega}{2}\sqrt{\mu_o\varepsilon_o\varepsilon_r}\tan\delta = \pi \times 5 \times 10^9 \times 3 \times 10^8 \times \sqrt{2.08} \times 0.0004 = 0.030206$$

$$\beta_o = \frac{2 \times \pi \times 5 \times 10^9}{3 \times 10^8} = 104.719755\ \text{rad/m}$$

$$\beta_d = \frac{2 \times \pi \times 5 \times 10^9 \times \sqrt{2.08}}{3 \times 10^8} = 151.029\ \text{rad/m}$$

$$Q_{\text{air}} = \frac{\beta_o}{2\alpha} = \frac{104.719755}{2 \times 0.058768} = 890.96$$

$$Q_{\text{teflon}} = \frac{\beta_d}{2\alpha} = \frac{151.029}{2 \times (0.084757 + 0.030206)} = 656.8629$$

Example 4.6: Design a half-wavelength-long microstrip resonator using a 50-ohm line that is short circuited at its ends. The substrate thickness is 0.159 cm with its dielectric constant 2.08 and the loss tangent 0.0004. The conductors are of copper.

Compute the length of the line for resonance at 2 GHz and Q of the resonator. Assume that thickness t of the microstrip is 0.159 μm.

Design equations for the microstrip line (from the appendix) are

$$\frac{w}{h} = \begin{cases} \dfrac{8e^A}{e^{2A}-2} & \text{for } A > 1.52 \\ \dfrac{2}{\pi}\left[B - 1 - \ln(2B-1) + \dfrac{\varepsilon_r - 1}{2\varepsilon_r}\left\{\ln(B-1) + 0.39 - \dfrac{0.61}{\varepsilon_r}\right\}\right] & \text{for } A \le 1.52 \end{cases}$$

where,

$$A = \frac{Z_o}{60}\left(\frac{\varepsilon_r + 1}{2}\right)^{1/2} + \frac{\varepsilon_r - 1}{\varepsilon_r + 1}\left(0.23 + \frac{0.11}{\varepsilon_r}\right)$$

and,

$$B = \frac{60\pi^2}{Z_o\sqrt{\varepsilon_r}}$$

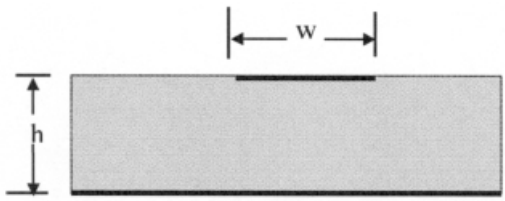

Therefore,

$$A = \frac{50}{60}\left(\frac{2.08 + 1}{2}\right)^{1/2} + \frac{2.08 - 1}{2.08 + 1}\left(0.23 + \frac{0.11}{2.08}\right) = 1.1333$$

Since A is smaller than 1.52, we need B to determine the width of microstrip. Hence,

$$B = \frac{60\pi^2}{50 \times \sqrt{2.08}} = 8.212$$

$$\frac{w}{h} = \frac{2}{\pi}\left[8.212 - 1 - \ln(2 \times 8.212 - 1) + \frac{2.08 - 1}{2 \times 2.08}\left\{\ln(8.212 - 1) + 0.39 - \frac{0.61}{2.08}\right\}\right]$$
$$= 3.1921$$

Therefore,

$$w = 0.507543 \text{ cm} \approx 0.51 \text{ cm}$$

Further,

$$\varepsilon_e = 0.5\left(2.08 + 1 + (2.08 - 1) \times \frac{1}{\sqrt{1 + \dfrac{12}{3.192094}}}\right) - \frac{(2.08 - 1)0.0001}{4.6\sqrt{3.1921}} = 1.7875$$

Therefore, the length of the resonator can be determined as follows:

$$\ell = \frac{\lambda}{2} = \frac{v_p/f}{2} = \frac{c}{2f\sqrt{\varepsilon_e}} = \frac{3 \times 10^{10}}{2 \times 2 \times 10^9 \times \sqrt{1.7875}}\text{cm} = 5.6096 \text{ cm}$$

Since $\sigma_{\text{copper}} = 5.813 \times 10^7$ S/m, the quality factor of this resonator is determined as follows. For $\dfrac{w}{h} \geq \dfrac{1}{2\pi}$,

$$\frac{w_e}{h} = \frac{w}{h} + 0.3979\frac{t}{h}\left\{1 + \ln\left(2\frac{h}{t}\right)\right\} = 3.1923$$

and,

$$\zeta = 1 + \frac{h}{w_e}\left(1 - \frac{1.25t}{\pi h} + \frac{1.25}{\pi}\ln\left(2\frac{h}{t}\right)\right) = 2.5476$$

Therefore, for $\dfrac{w}{h} \geq 1$, α_c is found to be

$$\alpha_c = 44.1255 \times 10^{-5}\frac{\zeta Z_o \varepsilon_{re}}{h}\sqrt{\frac{f_{(\text{GHz})}}{\sigma}}\left\{\frac{w_e}{h} + \frac{0.667\left(\dfrac{w_e}{h}\right)}{\dfrac{w_e}{h} + 1.444}\right\} \text{ Neper/m}$$

$$= 0.0428 \text{ Neper/m}$$

Similarly, α_d is found from (A2.28) as follows:

$$\alpha_d = 10.4766\frac{\varepsilon_r}{\varepsilon_r - 1}\frac{\varepsilon_{re} - 1}{\sqrt{\varepsilon_{re}}}f_{(\text{GHZ})}\tan\delta \text{ Neper/m} = 0.0095 \text{ Neper/m}$$

and,

$$\beta = \frac{2\pi}{\lambda} = \frac{2\pi}{2\ell} = \frac{2\pi}{2 \times \dfrac{5.6096}{100}} \text{ rad/m} = 56.0035 \text{ rad/m}$$

Hence, Q of the resonator is found as follows.

$$Q = \frac{\beta}{2\alpha} = \frac{56.0035}{2 \times (0.0428 + 0.0095)} = 535.4$$

4.5 MICROWAVE RESONATORS

Cavities and dielectric resonators are commonly employed as resonant circuits at frequencies above 1 GHz. These resonators provide much higher Q than the lumped elements and transmission line circuits. However, the characterization of these devices requires analysis of associated electromagnetic fields. Characteristic relations of selected microwave resonators are summarized in this section. Interested readers can find several excellent references and textbooks analyzing these and other resonators.

Rectangular Cavities

Consider a rectangular cavity made of conducting walls with dimensions $a \times b \times c$, as shown in Figure 4.19. It is filled with a dielectric material of dielectric constant ε_r and the relative permeability μ_r. In general, it can support both TE_{mnp} and TM_{mnp} modes, which may be degenerate. The cutoff frequency of TE_{mn} and TM_{mn} modes can be determined from the following formula.

$$f_c(\text{MHz}) = \frac{300}{\sqrt{\mu_r \varepsilon_r}} \sqrt{\left[\left(\frac{m}{2a}\right)^2 + \left(\frac{n}{2b}\right)^2\right]} \text{ MHz}$$

Resonant frequency f_r of a rectangular cavity operating in either TE_{mnp} or TM_{mnp} mode can be determined as follows.

$$f_r(\text{MHz}) = \frac{300}{\sqrt{\mu_r \varepsilon_r}} \sqrt{\left[\left(\frac{m}{2a}\right)^2 + \left(\frac{n}{2b}\right)^2 + \left(\frac{p}{2c}\right)^2\right]} \text{ MHz} \tag{4.5.1}$$

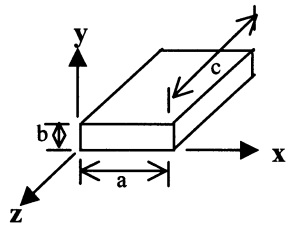

Figure 4.19 Geometry of the rectangular cavity resonator.

If the cavity is made of a perfect conductor and filled with a perfect dielectric then it will have infinite Q. However, it is not possible in practice. In the case of cavity walls having a finite conductivity (instead of infinite for the perfect conductor) but filled with a perfect dielectric (no dielectric loss) then its quality factor Q_c for TE_{10p} mode is given by

$$Q_c|_{10p} = \frac{60b(ac\omega\sqrt{\mu\varepsilon})^3}{\pi R_s(2p^2a^3b + 2bc^3 + p^2a^3c + ac^3)}\sqrt{\frac{\mu_r}{\varepsilon_r}} \tag{4.5.2}$$

Permittivity and permeability of the dielectric filling are given by ε and μ, respectively; ω is angular frequency; and R_s is the surface resistivity of walls which is related to the skin depth δ_s and the conductivity σ as follows.

$$R_s = \frac{1}{\sigma\delta_s} = \sqrt{\frac{\omega\mu}{2\sigma}} \tag{4.5.3}$$

On the other hand, if the cavity is filled with a dielectric with its loss tangent as $\tan\delta$ while its walls are made of a perfect conductor then the quality factor Q_d is given as

$$Q_d = \frac{1}{\tan\delta} \tag{4.5.4}$$

When there is power loss both in the cavity walls as well as in the dielectric filling, the quality factor Q is found from Q_c and Q_d as follows:

$$\frac{1}{Q} = \frac{1}{Q_c} + \frac{1}{Q_d} \tag{4.5.5}$$

Example 4.7: An air-filled rectangular cavity is made from a piece of copper WR-90 waveguide. If it resonates at 9.379 GHz in TE_{101} mode, find the required length c and the Q of this resonator.

Specifications of WR-90 can be found in the appendix, as follows:

$$a = 0.9 \text{ in} = 2.286 \text{ cm}$$

and,

$$b = 0.4 \text{ in} = 1.016 \text{ cm}$$

From (4.5.1),

$$\frac{1}{2c} = \sqrt{\left(\frac{9379}{300}\right)^2 - \left(\frac{1}{2a}\right)^2} = 22.3383 \Rightarrow c = 2.238 \text{ cm}$$

Next, the surface resistance, R_s, is determined from (4.5.3) as 0.0253 Ω and the Q_c is found from (4.5.2) to be about 7858.

Example 4.8: A rectangular cavity made of copper has inner dimensions $a = 1.6$ cm, $b = 0.71$ cm, and $c = 1.56$ cm. It is filled with Teflon ($\varepsilon_r = 2.05$ and $\tan\delta = 2.9268 \times 10^{-4}$). Find the TE_{101} mode resonant frequency and Q of this cavity.

From (4.5.1),

$$f_r = \frac{300}{\sqrt{2.05}}\sqrt{\left(\frac{1}{2\cdot 0.016}\right)^2 + \left(\frac{1}{2\cdot 0.0156}\right)^2} \approx 9379 \text{ MHz} = 9.379 \text{ GHz}$$

Since power dissipates both in the dielectric filling as well as in the sidewalls, overall Q will be determined from (4.5.5).

From (4.5.2) and (4.5.4), Q_c and Q_d are found to be 5489 and 3417, respectively. Substituting these into (4.5.5), Q of this cavity is found to be 2106.

Circular Cylindrical Cavities

Figure 4.20 shows the geometry of a circular cylindrical cavity of radius r and height h. It is filled with a dielectric material of relative permeability μ_r and dielectric constant ε_r. Its resonant frequency f_r in megahertz is given as

$$f_r(\text{MHz}) = \frac{300}{2\pi\sqrt{\mu_r\varepsilon_r}}\sqrt{\left(\frac{\chi_{nm}}{r}\right)^2 + \left(\frac{p\pi}{h}\right)^2} \text{ MHz} \tag{4.5.6}$$

where,

$$\chi_{nm} = \begin{cases} P_{nm} & \text{for TM modes} \\ p'_{nm} & \text{for TE modes} \end{cases} \tag{4.5.7}$$

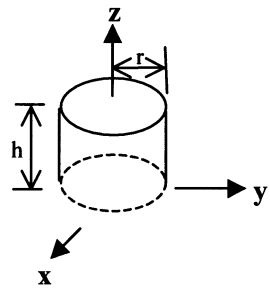

Figure 4.20 Geometry of the circular cylindrical cavity resonator.

TABLE 4.3 Zeros of $J_n(x)$ and $J_n'(x)$

n	p_{n1}	p_{n2}	p_{n3}	p'_{n1}	p'_{n2}	p'_{n3}
0	2.405	5.520	8.654	3.832	7.016	10.173
1	3.832	7.016	10.173	1.841	5.331	8.536
2	5.136	8.417	11.620	3.054	6.706	9.969

where p_{nm} represents the mth zero of the Bessel function of the first kind and order n while p'_{nm} represents the mth zero of the derivative of the Bessel function. In other words, these represent roots of the following equations, respectively (see Table 4.3).

$$J_n(x) = 0 \tag{4.5.8}$$

and

$$\frac{dJ_n(x)}{dx} = 0 \tag{4.5.9}$$

The Q_{c} of a circular cylindrical cavity operating in TE_{nmp} mode and filled with a lossless dielectric can be found from the following formula.

$$Q_{\mathrm{c}} = \frac{47.7465}{\delta_{\mathrm{s}} f_{\mathrm{r}}(\mathrm{MHz})} \frac{\left[1 - \left(\frac{n}{p'_{\mathrm{nm}}}\right)^2\right]\left[(p'_{\mathrm{nm}})^2 + \left(\frac{p\pi r}{h}\right)^2\right]^{1.5}}{\left[\left\{p'^2_{\mathrm{nm}} + \left(\frac{2r}{h}\right)\left(\frac{p\pi r}{h}\right)^2\right\} + \left\{1 - \left(\frac{2r}{h}\right)\left(\frac{np\pi r}{p'_{\mathrm{nm}} h}\right)^2\right\}\right]} \tag{4.5.10}$$

In the case of $\mathrm{TM}_{\mathrm{nmp}}$ mode, Q_{c} is given by

$$Q_{\mathrm{c}} = \frac{47.7456}{\delta_{\mathrm{s}} f_{\mathrm{r}}(\mathrm{MHz})} \frac{\sqrt{\left[p^2_{\mathrm{nm}} + \left(\frac{p\pi r}{h}\right)^2\right]}}{1 + \left(\frac{2r}{h}\right)}, \quad p > 0 \tag{4.5.11}$$

For $p = 0$,

$$Q_{\mathrm{c}} \approx \frac{47.7465}{\delta_{\mathrm{s}} f_{\mathrm{r}}(\mathrm{MHz})} \frac{p_{\mathrm{nm}}}{1 + \left(\frac{r}{h}\right)}, \quad p = 0 \tag{4.5.12}$$

The quality factor Q_{d} due to dielectric loss and the overall Q are determined as before from (4.5.4), (4.5.5) with appropriate Q_{c}.

Example 4.9: Determine the dimensions of an air-filled circular cylindrical cavity that resonates at 5 GHz in TE_{011} mode. It should be made of copper and its height should be equal to its diameter. Find Q of this cavity, given that $n = 0$, $m = p = 1$, and $h = 2r$.

From (4.5.6), with χ_{01} as 3.832 from Table 4.3, we get

$$r = \sqrt{\frac{3.832^2 + \left(\frac{\pi}{2}\right)^2}{\left(5000 \cdot \frac{2\pi}{300}\right)^2}} = 0.03955 \text{ m}$$

and,

$$h = 2r = 0.0791 \text{ m}$$

Since

$$\delta_s = \sqrt{\frac{2}{\omega\mu\sigma}} = \sqrt{\frac{2}{2\pi \cdot 5 \cdot 10^9 \cdot 4\pi \cdot 10^{-7} \cdot 5.8 \cdot 10^7}} = 9.3459 \cdot 10^{-7} \text{ m}$$

Q of the cavity can be found from (4.5.10) as

$$Q_c = \frac{47.7465 \cdot 10^6}{9.3459 \cdot 10^{-7} \cdot 5 \cdot 10^9} \times \frac{\left[3.832^2 + \left(\frac{\pi}{2}\right)^2\right]^{1.5}}{\left\{3.832^2 + \left(\frac{\pi}{2}\right)^2\right\} + 1} = 39984.6$$

Further, there is no loss of power in air ($\tan\delta \approx 0$) Q_d is infinite, and therefore, Q is the same as Q_c.

Dielectric Resonators (DR)

Dielectric resonators, made of high-permittivity ceramics, provide high Q with smaller size. These resonators are generally a solid sphere or cylinder of circular or rectangular cross-section. High-purity TiO_2 ($\varepsilon_r \approx 100$, $\tan\delta \approx 0.0001$) was used in early dielectric resonators. However, it was found to be intolerably dependent on the temperature. With the development of new ceramics, temperature dependence of DR can be significantly reduced.

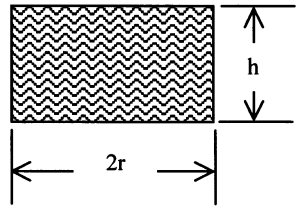

Figure 4.21 Geometry of an isolated circular cylindrical dielectric resonator (DR).

Figure 4.21 shows an isolated circular cylindrical DR. Its analysis is beyond the scope of this book. Its $TE_{01\delta}$-mode resonant frequency, f_r in GHz, can be found from the following formula:

$$f_r(\text{GHz}) = \frac{34}{r\varepsilon_r}\left(3.45 + \frac{r}{h}\right) \text{GHz} \tag{4.5.13}$$

where r and h are in millimeters. This relation is found to be accurate within ± 2 percent if

$$2 > \frac{r}{h} > 0.5 \tag{4.5.14}$$

and,

$$50 > \varepsilon_r > 30 \tag{4.5.15}$$

An isolated DR is of almost no use in practive. A more practical situation is illustrated in Figure 4.22 where it is coupled with a microstrip line in a conducting enclosure. Assume that dielectric constants of the DR and the substrate are ε_r and ε_s, respectively. With various dimensions as shown (all in meters), the following formulas can be used to determine its radius r and the height h. If r is selected between the following bounds then the formulas presented in this section are found to have a tolerance of no more than 2 percent:[1]

$$\frac{1.2892 \times 10^8}{f_r\sqrt{\varepsilon_s}} > r > \frac{1.2892 \times 10^8}{f_r\sqrt{\varepsilon_r}} \tag{4.5.16}$$

where f_r is resonant frequency in Hz.

The height of the DR is then found as

$$h = \frac{1}{\beta}\left[\tan^{-1}\left\{\frac{\alpha_1}{\beta\tanh(\alpha_1 t)}\right\} + \tan^{-1}\left\{\frac{\alpha_2}{\beta\tanh(\alpha_2 d)}\right\}\right] \tag{4.5.17}$$

[1]D. Kajfez and P. Guillon, *Dielectric Resonators*. Dedham MA: Artech House, 1986.

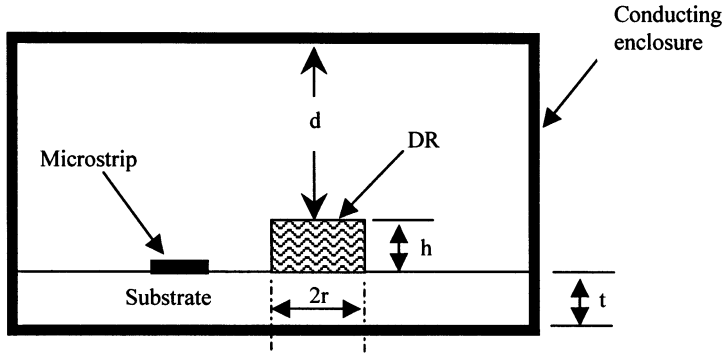

Figure 4.22 Geometry of a circular cylindrical dielectric resonator (DR) in MIC configuration.

where,

$$\alpha_1 = \sqrt{k'^2 - k_o^2 \varepsilon_s} \tag{4.5.18}$$

$$\alpha_2 = \sqrt{k'^2 - k_o^2} \tag{4.5.19}$$

$$\beta = \sqrt{k_o^2 \varepsilon_r - k'^2} \tag{4.5.20}$$

$$k' = \frac{2.405}{r} + \frac{y}{2.405r\left[1 + \left(\frac{2.43}{y}\right) + 0.291y\right]} \tag{4.5.21}$$

$$y = \sqrt{(k_o r)^2(\varepsilon_r - 1) - 5.784} \tag{4.5.22}$$

and,

$$k_o = \omega\sqrt{\mu_o \varepsilon_o} \tag{4.5.23}$$

Example 4.10: Design a $TE_{01\delta}$-mode cylindrical dielectric resonator for use at 35 GHz in the microstrip circuit shown in Figure 4.22. The substrate is 0.25 mm thick and its dielectric constant is 9.9. The dielectric constant of the material available for DR is 36. Further, the top of the DR should have a clearance of 1 mm from the conducting enclosure.

Since

$$\frac{1.2892 \times 10^8}{f_r\sqrt{\varepsilon_s}} = 1.171 \times 10^{-3}\,\text{m}$$

and,

$$\frac{1.2892 \times 10^8}{f_r\sqrt{\varepsilon_r}} = 6.139 \times 10^{-4}\,\text{m}$$

radius r of the DR may be selected as 0.835 mm.

Height h of the DR is then determined from (4.5.17)–(4.5.22), as follows:

$$y = \sqrt{(k_o r)^2(\varepsilon_r - 1) - 5.784} = 2.707$$

$$k' = \frac{2.405}{r} + \frac{y}{2.405r\left[1 + \left(\frac{2.43}{y}\right) + 0.291y\right]} = 3.382 \times 10^3$$

$$\alpha_1 = \sqrt{k'^2 - k_o^2\varepsilon_s} = 2.474 \times 10^3$$

$$\alpha_2 = \sqrt{k'^2 - k_o^2} = 3.302 \times 10^3$$

and,

$$\beta = \sqrt{k_o^2\varepsilon_r - k'^2} = 2.812 \times 10^3$$

After substituting these numbers into (4.5.17), h is found to be

$$h = \frac{1}{\beta}\left[\tan^{-1}\left\{\frac{\alpha_1}{\beta\tanh(\alpha_1 t)}\right\} + \tan^{-1}\left\{\frac{\alpha_2}{\beta\tanh(\alpha_2 d)}\right\}\right] = 6.683 \times 10^{-4}\,\text{m} = 0.668\ \text{mm}$$

SUGGESTED READING

I. Bahl and P. Bhartia, *Microwave Solid State Circuit Design*. New York: Wiley, 1988.

R. E. Collin, *Foundations for Microwave Engineering*. New York: McGraw Hill, 1992.

R. S. Elliott, *An Introduction to Guided Waves and Microwave Circuits*, Englewood Cliffs, NJ: Prentice Hall, 1993.

D. Kajfez and P. Guillon, *Dielectric Resonators*. Dedham MA: Artech House, 1986.

D. M. Pozar, *Microwave Engineering*. New York: Wiley, 1998.

S. Ramo. J. R. Whinnery, and T. Van Duzer, *Fields and Waves in Communication Electronics*. New York: Wiley, 1994.

Peter A. Rizzi, *Microwave Engineering*. Englewood Cliffs, NJ: Prentice Hall, 1988.

J. R. Smith, *Modern Communication Circuits*. New York: McGraw Hill, 1998.

PROBLEMS

1. Determine the resonant frequency, bandwidth, and Q of the following circuit.

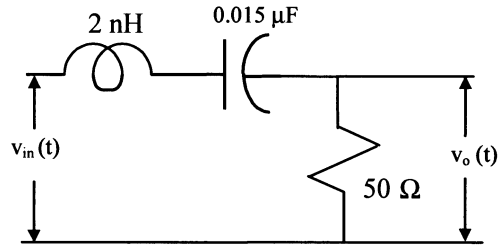

2. Quality factor of a 100-nH inductor is 150 at 100 MHz. It is used in a series resonant circuit with a 50-Ω load resistor. Find the capacitor required to resonate this circuit at 100 MHz. Find loaded Q of the circuit.

3. Find capacitance C in the following series R-L-C circuit if it is resonating at 1200 rad/s. Compute output voltage $v_o(t)$ when $v_{in}(t) = 4\cos(\omega t + 0.2\ \pi)$ V for ω as 1200 rad/s, 300 rad/s, and 4800 rad/s.

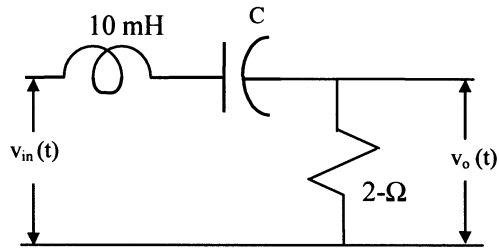

4. Magnitude of input impedance in the following series R-L-C circuit is found to be 3 Ω at the resonant frequency of 1600 rad/s. Find the inductance L, Q, and the bandwidth.

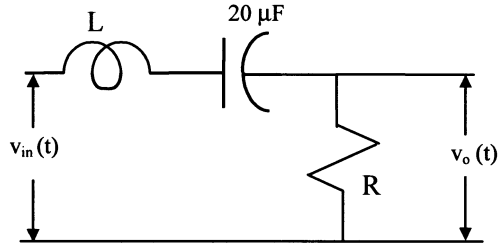

5. Determine the element values of a resonant circuit to filter all the sinusoidal signals from 100 MHz to 130 MHz. This filter is to be connected between a

voltage source with negligible internal impedance and a communication system that has input impedance of 50 ohm. Plot its response over the frequency range of 50 to 200 MHz.

6. Calculate the resonant frequency, Q, and bandwidth of the parallel resonant circuit shown below.

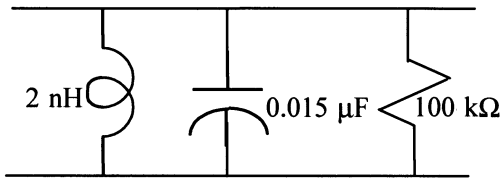

7. Find the resonant frequency, unloaded Q, and loaded Q of the following parallel resonant circuit.

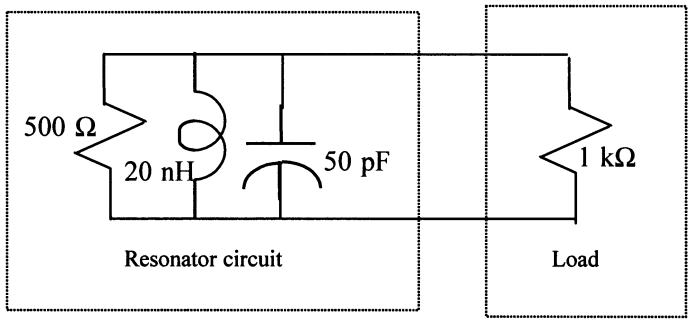

8. The parallel *R-L-C* circuit shown below is resonant at 20,000 radian/s. If its admittance has a magnitude of 1 mS at the resonance then find the values of R and L.

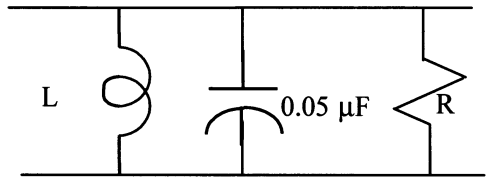

9. Consider the loaded parallel resonant circuit shown below. Compute the resonant frequency in radians per second, unloaded Q, and the loaded Q of this circuit.

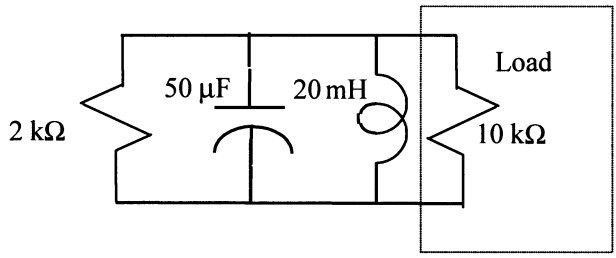

10. Resistance R in a parallel R-L-C circuit is 200 Ω. The circuit has a bandwidth of 80 rad/s with lower half-power frequency at 800 rad/s. Find inductance and capacitance of the circuit.

11. A parallel R-L-C circuit is resonant at 2×10^6 rad/s and it has a bandwidth of 20,000 rad/s. If its impedance at resonance is 2000 Ω, find the circuit parameters.

12. A resonator is fabricated from a 2-λ-long transmission line that is short-circuited at its ends. Find its Q.

13. A 3-cm-long 100-Ω air-filled coaxial line is used to fabricate a resonator. It is short circuited at one end while a capacitor is connected at the other end to obtain the resonance at 6 GHz. Find the value of this capacitor.

14. A 100-Ω air-filled coaxial line of length l is used to fabricate a resonator. It is terminated by $10 - j5000$ Ω at its ends. If the signal wavelength is 1 m, find the required length for the first resonance and the Q of this resonator.

15. Design a half-wavelength-long coaxial line resonator that is short circuited at its ends. Its inner conductor radius is 0.455 mm and the inner radius of the outer conductor is 1.499 mm. The conductors are made of copper. Compare the Q of an air-filled to that of a Teflon-filled resonator operating at 800 MHz. The dielectric constant of Teflon is 2.08 and its loss tangent is 0.0004.

16. Design a half-wavelength-long microstrip resonator using a 50-ohm line that is short circuited at its ends. The substrate thickness is 0.12 cm with its dielectric constant 2.08 and the loss tangent 0.0004. The conductors are of copper. Compute the length of the line for resonance at 900 MHz and the Q of the resonator.

17. Secondary side of a tightly coupled transformer is terminated by a 2 kΩ in parallel with capacitor C_2. A current source $I = 10 \cos(4 \times 10^6)$ mA is connected on its primary side. The inductance L_1 of its primary is 0.30 μH, mutual inductance $M = 3$ μH, and the unloaded Q of the secondary coil is 70.

Determine the value of C_2 such that this circuit resonates at 4×10^6 rad/s. Find its input impedance and also the output voltage at the resonant frequency. What is the circuit bandwidth?

18. A 16-Ω resistor terminates the secondary side of a tightly coupled transformer. A 40-μF capacitor is connected in series with its primary coil that has an inductance L_1 at 100 mH. If the secondary coil has an inductance L_2 at 400 mH, then find the resonant frequency and the Q of this circuit.

19. A 16-Ω resistor terminates the secondary side of a tightly coupled transformer. A 30-μF capacitor is connected in series with its primary coil that has an inductance of 25 mH. If the circuit Q is 50 find the inductance L_2 of the secondary coil.

20. An air-filled rectangular cavity is made from a piece of copper WR-430 waveguide. If it resonates at 2 GHz in TE_{101} mode, find the required length c and the Q of this resonator.

21. Design an air-filled circular cylindrical cavity that resonates at 9 GHz in TE_{011} mode. It should be made of copper and its height should be equal to its diameter. Find Q of this cavity.

22. Design a $TE_{01\delta}$ mode cylindrical dielectric resonator for use at 4.267 GHz in the microstrip circuit shown in Figure 4.22. The substrate is 0.7 mm thick and its dielectric constant is 9.6. Dielectric constant of the material available for DR is 34.19. Further, the top of the DR should have a clearance of 0.72 mm from the conducting enclosure.

Radio-Frequency and Microwave Communication Circuits: Analysis and Design
Devendra K. Misra

ISBNs: 0-471-41253-8 (Hardback); 0-471-22435-9 (Electronic)

5

IMPEDANCE MATCHING NETWORKS

One of the most critical requirements in the design of high-frequency electronic circuits is that the maximum possible signal energy is transferred at each point. In other words, the signal should propagate in a forward direction with a negligible echo (ideally, zero). Echo signal not only reduces the power available but also deteriorates the signal quality due to the presence of multiple reflections. As noted in the preceding chapter, impedance can be transformed to a new value by adjusting the turn ratio of a transformer that couples it with the circuit. However, it has several limitations. This chapter presents a few techniques to design other impedance transforming networks. These circuits include transmission line stubs, and resistive and reactive networks. Further, the techniques introduced are needed in active circuit design at RF and microwave frequencies.

As shown in Figure 5.1, impedance matching networks are employed at the input and the output of an amplifier circuit. These networks may also be needed to perform some other tasks, such as filtering the signal and blocking or passing the dc bias voltages. This chapter begins with a section on the impedance matching techniques that use a single reactive element or stub connected in series or in shunt. Theoretical

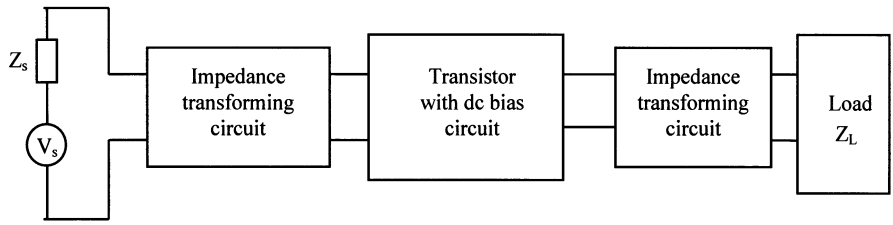

Figure 5.1 Block diagram of an amplifier circuit.

principles behind the technique are explained, and the graphical procedure to design these circuits using the Smith chart is presented. Principles and procedures of the double-stub matching are discussed in the following section. The chapter ends with sections on resistive and reactive L-section matching networks. Both analytical as well as graphical procedures to design these networks using ZY-charts are included.

5.1 SINGLE REACTIVE ELEMENT OR STUB MATCHING

When a lossless transmission line is terminated by an impedance Z_L, the magnitude of the reflection coefficient (and hence, the VSWR) on it remains constant but its phase angle can be anywhere between $+180^\circ$ and -180°. As we have seen in Chapter 3, it represents a circle on the Smith chart and a point on this circle represents the normalized load. As one moves away from the load, impedance (or the admittance) value changes. This movement is clockwise on the VSWR circle. The real part of the normalized impedance (or the normalized admittance) becomes unity at certain points on the line. Addition of a single reactive element or a transmission line stub at this point can eliminate the echo signal and reduce the VSWR to unity beyond this point. A finite-length transmission line with its other end open or short circuit is called the *stub* and behaves like a reactive element as explained in Chapter 3.

In this section, we discuss the procedure for determining the location on a lossless feeding line where a stub or a reactive element can be connected to eliminate the echo signal. Two different possibilities, a series or a shunt element, are considered. Mathematical equations as well as the graphical methods are presented to design the circuits.

A Shunt Stub or Reactive Element

Consider a lossless transmission line of characteristic impedance Z_o that is terminated by a load admittance Y_L, as shown in Figure 5.2. Corresponding normalized input admittance at a point d_s away from the load can be found from (3.2.6) as follows:

$$\bar{Y}_{in} = \frac{\bar{Y}_L + j\tan(\beta d_s)}{1 + j\bar{Y}_L \tan(\beta d_s)} \tag{5.1.1}$$

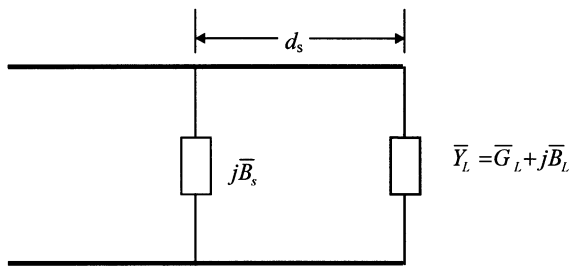

Figure 5.2 Transmission line with a shunt matching element.

In order to obtain a matched condition at d_s, the real part of the input admittance must be equal to the characteristic admittance of the line; i.e., the real part of (5.1.1) must be unity. This requirement is used to determine d_s. The parallel susceptance B_s is then connected at d_s to cancel out the imaginary part of Y_{in}. Hence,

$$d_s = \frac{1}{\beta}\tan^{-1}\left(\frac{\bar{B}_L \pm \sqrt{\bar{B}_L^2 - A(1-\bar{G}_L)}}{A}\right) \tag{5.1.2}$$

where $A = \bar{G}_L(\bar{G}_L - 1) + \bar{B}_L^2$.

The imaginary part of the normalized input admittance at d_s is found as follows.

$$\bar{B}_{in} = \frac{\{\bar{B}_L + \tan(\beta d_s)\} \times \{1 - \bar{B}_L \tan(\beta d_s)\} - \bar{G}_L^2 \tan(\beta d_s)}{\{\bar{G}_L \tan(\beta d_s)\}^2 + \{1 - \bar{B}_L \tan(\beta d_s)\}^2} \tag{5.1.3}$$

The other requirement to obtain a matched condition is

$$\bar{B}_s = -\bar{B}_{in} \tag{5.1.4}$$

Hence, a shunt inductor is needed at d_s if the input admittance is found capacitive (i.e., B_{in} is positive). On the other hand, it will require a capacitor if Y_{in} is inductive at d_s. As mentioned earlier, a lossless transmission line section can be used in place of this inductor or capacitor. Length of this transmission line section is determined according to the susceptance needed by (5.1.4) and the termination (i.e., an open circuit or a short circuit) at its other end. This transmission line section is called a stub. If ℓ_s is the stub length that has a short circuit at its other end, then

$$\ell_s = \frac{1}{\beta}\cot^{-1}(-\bar{B}_s) = \frac{1}{\beta}\cot^{-1}(\bar{B}_{in}) \tag{5.1.5}$$

On the other hand, if there is an open circuit at the other end of the stub, then

$$\ell_s = \frac{1}{\beta}\tan^{-1}(\bar{B}_s) = \frac{1}{\beta}\tan^{-1}(-\bar{B}_{in}) \tag{5.1.6}$$

A Series Stub or Reactive Element

If a reactive element (or a stub) needs to be connected in series as shown in Figure 5.3, the design procedure can be developed as follows. The normalized input impedance at d_s is

$$\bar{Z}_{in} = \frac{\bar{Z}_L + j\tan(\beta d_s)}{1 + j\bar{Z}_L \tan(\beta d_s)} \tag{5.1.7}$$

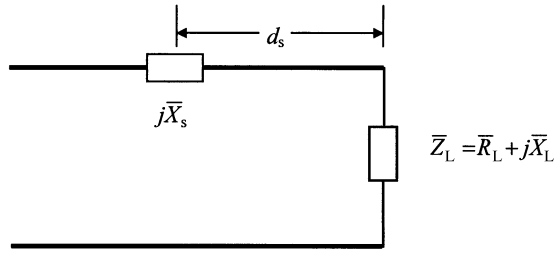

Figure 5.3 Transmission line with a matching element connected in series.

In order to obtain a matched condition at d_s, the real part of the input impedance must be equal to the characteristic impedance of the line; i.e., the real part of (5.1.7) must be unity. This condition is used to determine d_s. A reactance X_s is then connected in series at d_s to cancel out the imaginary part of Z_{in}. Hence,

$$d_s = \frac{1}{\beta}\tan^{-1}\left(\frac{\bar{X}_L \pm \sqrt{\bar{X}_L^2 - A_z(1-\bar{R}_L)}}{A_z}\right) \tag{5.1.8}$$

where, $A_z = \bar{R}_L(\bar{R}_L - 1) + \bar{X}_L^2$.

The imaginary part of the normalized input impedance at d_s is found as follows:

$$\bar{X}_{in} = \frac{\{\bar{X}_L + \tan(\beta d_s)\} \times \{1 - \bar{X}_L \tan(\beta d_s)\} - \bar{R}_L^2 \tan(\beta d_s)}{\{\bar{R}_L \tan(\beta d_s)\}^2 + \{1 - \bar{X}_L \tan(\beta d_s)\}^2} \tag{5.1.9}$$

In order to obtain a matched condition at d_s, the reactive part X_{in} must be eliminated by adding an element of opposite nature. Hence,

$$\bar{X}_s = -\bar{X}_{in} \tag{5.1.10}$$

Therefore, a capacitor will be needed in series if the input impedance is inductive. It will require an inductor if input reactance is capacitive. As before, a transmission line stub can be used instead of an inductor or a capacitor. Length of this stub with an open circuit at its other end can be determined as follows.

$$\ell_s = \frac{1}{\beta}\cot(-\bar{X}_s) = \frac{1}{\beta}\cot(\bar{X}_{in}) \tag{5.1.11}$$

However, if the stub has a short circuit at its other end, its length will be a quarter-wavelength shorter (or longer, if the resulting number becomes negative) than this value. It can be found as

$$\ell_s = \frac{1}{\beta}\tan(\bar{X}_s) = \frac{1}{\beta}\tan(-\bar{X}_{in}) \tag{5.1.12}$$

Note that the location d_s and the stub length ℓ_s are periodic in nature in both cases. It means that the matching conditions will also be satisfied at points one-half wavelength apart. However, the shortest possible values of d_s and ℓ_s are preferred because those provide the matched condition over a broader frequency band.

Graphical Method

These matching networks can also be graphically designed using a Smith chart. The procedure is similar for both series as well as shunt-connected elements, except that the former is based on the normalized impedance while the latter works with normalized admittance. It can be summarized in the following steps.

1. Determine the normalized impedance of the load and locate that point on the Smith chart.
2. Draw the constant VSWR circle. If the stub needs to be connected in parallel, move a quarter-wavelength away from the load impedance point. This point is located at the other end of the diameter that connects the load point with the center of the circle. For a series-stub, stay at the normalized impedance point.
3. From the point found in step 2, move toward the generator (clockwise) on the VSWR circle until it intersects the unity resistance (or conductance) circle. Distance traveled to at this intersection point from the load is equal to d_s. There will be at least two such points within one-half wavelength from the load. A matching element can be placed at either one of these points.
4. If the admittance in the previous step is $1 + j\bar{B}$, then a susceptance of $-j\bar{B}$ in shunt is needed for matching. This can be a discrete reactive element (inductor or capacitor, depending upon a negative or positive susceptance value) or a transmission line stub.
5. In the case of a stub, the required length is determined as follows. Since its other end will have an open or a short, VSWR on it will be infinite. It is represented by the outermost circle of the Smith chart. Locate the desired susceptance point (i.e., $0 - j\bar{B}$) on this circle and then move toward load (counterclockwise) until an open circuit (i.e., a zero susceptance) or a short circuit (an infinite susceptance) is found. This distance is equal to the stub length ℓ_s.

For a series reactive element or stub, steps 4 and 5 will be same except that the normalized reactance replaces the normalized susceptance.

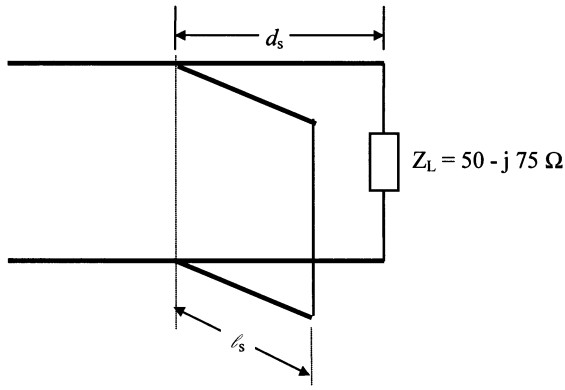

Figure 5.4 A shunt stub matching network.

Example 5.1: A uniform, lossless 100-ohm line is connected to a load of $50 - j75$ ohm, as illustrated in Figure 5.4. A single stub of 100-ohm characteristic impedance is connected in parallel at a distance d_s from the load. Find the shortest values of d_s and stub length ℓ_s for a match.

As mentioned in the preceding analysis, design equations (5.1.2), (5.1.3), (5.1.5), and (5.1.6) for a shunt stub use admittance parameters. On the other hand, the series connected stub design uses impedance parameters in (5.1.8), (5.1.9), (5.1.11), and (5.1.12). Therefore, d_s and ℓ_s can be theoretically determined as follows.

$$\bar{Y}_L = \frac{Y_L}{Y_o} = \frac{Z_o}{Z_L} = \frac{100}{50 - j75} = 0.6154 + j0.9231$$

$$A = \bar{G}_L(\bar{G}_L - 1) + \bar{B}_L^2 = 0.6154(0.6154 - 1) + 0.9231^2 = 0.6154$$

From (5.1.2), the two possible values of d_s are

$$d_s = \frac{\lambda}{2\pi}\tan^{-1}\left(\frac{-0.75 + \sqrt{(-0.75)^2 - 0.6154(1 - 0.5)}}{0.6154}\right) = 0.1949\,\lambda$$

and,

$$d_s = \frac{\lambda}{2\pi}\tan^{-1}\left(\frac{-0.75 - \sqrt{(-0.75)^2 - 0.6154(1 - 0.5)}}{0.6154}\right) = 0.0353\,\lambda$$

At $0.1949\,\lambda$ from the load, the real part of the normalized admittance is unity while its imaginary part is -1.2748. Hence, the stub should provide $j1.2748$ to

cancel it out. Length of a short-circuited stub, ℓ_s, is calculated from (5.1.5) as follows.

$$\ell_s = \frac{1}{\beta}\cot^{-1}(-1.2748) = 0.3941\lambda$$

On the other hand, normalized admittance is $1 + j1.2748$ at $0.0353\,\lambda$ from the load. In order to obtain a matched condition, the stub at this point must provide a normalized susceptance of $-j1.2748$. Hence,

$$\ell_s = \frac{1}{\beta}\cot^{-1}(1.2748) = 0.1059\,\lambda$$

Thus, there are two possible solutions to this problem. In one case, a short-circuited 0.3941-λ-long stub is needed at $0.1949\,\lambda$ from the load. The other design requires a $0.1059\,\lambda$ long short-circuited stub at $0.0353\,\lambda$ from the load. It is preferred over the former design because of its shorter lengths.

The following steps are needed for solving this example graphically with the Smith chart.

1. Determine the normalized load admittance.

$$\bar{Z}_L = \frac{50 - j75}{100} = 0.5 - j0.75$$

2. Locate the normalized load impedance point on the Smith chart. Draw the VSWR circle as shown in Figure 5.5.
3. From the load impedance point, move to the diametrically opposite point and locate the corresponding normalized load admittance. It is point $0.62 + j0.91$ on the chart.
4. Locate the point on the VSWR circle where the real part of the admittance is unity. There are two such points with normalized admittance values $1 + j1.3$ (say, point A) and $1 - j1.3$ (say, point B), respectively.
5. Distance d_s of $1 + j1.3$ (point A) from the load admittance can be determined as $0.036\,\lambda$ (i.e., $0.170\,\lambda - 0.134\,\lambda$) and for point B ($1 - j1.3$) as $0.195\,\lambda$ (i.e., $0.329\,\lambda - 0.134\,\lambda$).
6. If a susceptance of $-j1.3$ is added at point A or $j1.3$ at point B, the load will be matched.
7. Locate the point $-j1.3$ along the lower circumference of the chart and from there move toward the load (counterclockwise) until the short circuit (infinity on the chart) is reached. Separation between these two points is as $0.25\,\lambda - 0.146\,\lambda = 0.104\,\lambda$. Hence a 0.104-$\lambda$-long transmission line with a short circuit at its rear end will have the desired susceptance for point A.
8. For a matching stub at point B, locate the point $j1.3$ on the upper circumference of the chart and then move toward the load up to the short circuit (i.e., the

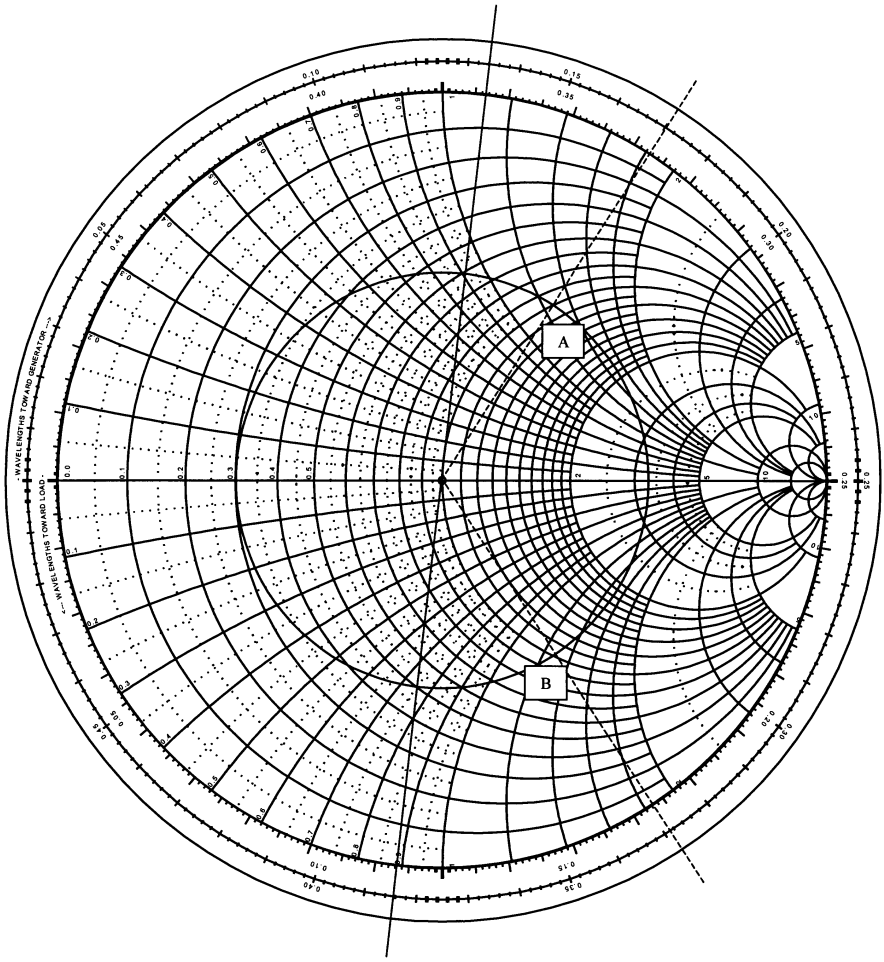

Figure 5.5 Graphical design of matching circuit for Example 5.1.

right-hand end of the chart). Hence, the stub length ℓ_s for this case is determined as $0.025\,\lambda + 0.146\,\lambda = 0.396\,\lambda$.

Therefore, a 0.104-λ-long stub at $0.036\,\lambda$ from the load (point A) or a 0.396-λ-long stub at $0.195\,\lambda$ (point B) from the load will match the load. These values are comparable to those obtained earlier.

As mentioned earlier, point A is preferred over point B in matching network design because it is closer to the load, and also the stub length in this case is shorter. In order to compare the frequency response of these two designs, the input reflection coefficient is calculated for the network. Its magnitude plot is shown in Figure 5.6. Since various lengths in the circuit are known in terms of wavelength, it is assumed that the circuit is designed for a signal wavelength of λ_d. As signal frequency is

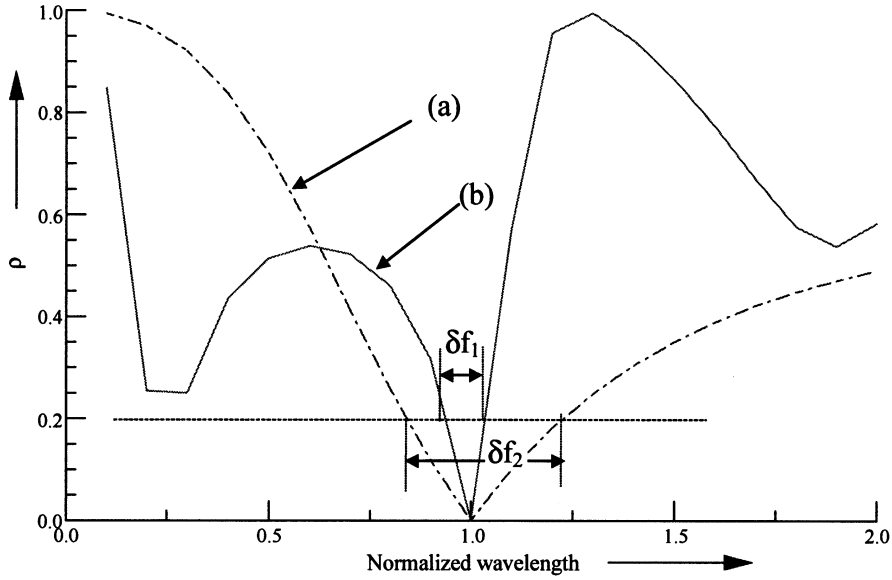

Figure 5.6 Magnitude of the reflection coefficient as a function of signal frequency.

changed, its wavelength changes to λ. The normalized wavelength used for this plot is equal to λ_d/λ. Since the wavelength is inversely related to the propagation constant, the horizontal scale may also be interpreted as a normalized frequency scale, with 1 being the design frequency.

Plot (a) in Figure 5.6 corresponds to design A (that requires a shorter stub closer to the load) while plot (b) represents design B (a longer stub and away from the load). At the normalized wavelength of unity, both of these curves go to zero. As signal frequency is changed on either side (i.e., decreased or increased from this setting), reflection coefficient increases. However, this change in plot (a) is gradual in comparison with that in plot (b). In other words, for an allowed reflection coefficient of 0.2, bandwidth for design A is δf_2, which is much wider in comparison with δf_1 of design B.

Example 5.2: A lossless 100-Ω line is to be matched with a $100/[2 + j3.732]\ \Omega$ load by means of a lossless short-circuited stub, as shown in Figure 5.7. Characteristic impedance of the stub is $200\,\Omega$. Find the position closest to the load and the length of the stub using a Smith chart.

1. In this example, it will be easier to determine the normalized load admittance directly, as follows.

$$\bar{Y}_L = \frac{1}{\bar{Z}_L} = \frac{Z_o}{Z_L} = 2 + j3.732$$

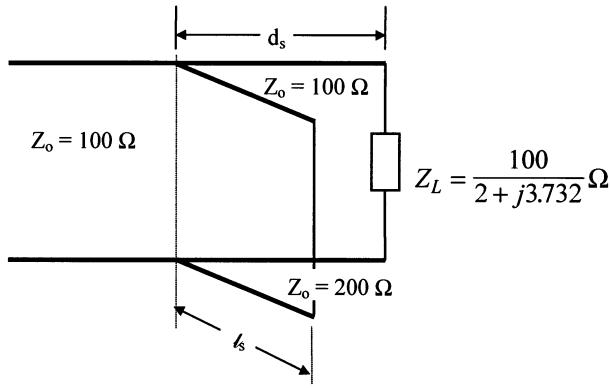

Figure 5.7 Matching circuit for Example 5.2.

2. Locate this normalized admittance point on the Smith chart and draw the VSWR circle. It is illustrated in Figure 5.8.
3. Move toward the generator (clockwise) on the VSWR circle until the real part of the admittance is unity. One such point is $1 - j2.7$ and the other is $1 + j2.7$. Since the former is closer to the load, the stub must be placed at this point. Hence,

$$d_s = (0.3 - 0.217)\lambda = 0.083\,\lambda$$

4. Normalized susceptance needed for matching at this point is $j2.7$. However, it is normalized with $100\,\Omega$, while characteristic impedance of the stub is $200\,\Omega$. This means that the normalization must be corrected before determining the stub length ℓ_s. It can be done as follows.

$$j\bar{B}_s = \frac{j2.7 \times 200}{100} = j5.4$$

5. Point $j5.4$ is located on the upper scale of the Smith chart. Moving from this point toward the load (that is counterclockwise), open-circuit admittance (zero) is found first. Moving further in the same direction, the short-circuit admittance point is found next. This means that the stub length will be shorter with an open circuit at its other end. However, a short-circuited stub is used in Figure 5.7. Hence,

$$\ell_s = 0.22\,\lambda + 0.25\,\lambda = 0.47\,\lambda$$

Example 5.3: A load reflection coefficient is given as $0.4\angle -30^\circ$. It is desired to get a load with reflection coefficient at $0.2\angle 45^\circ$. There are two different circuits given in Figure 5.9. However, the information provided for these circuits is incomplete.

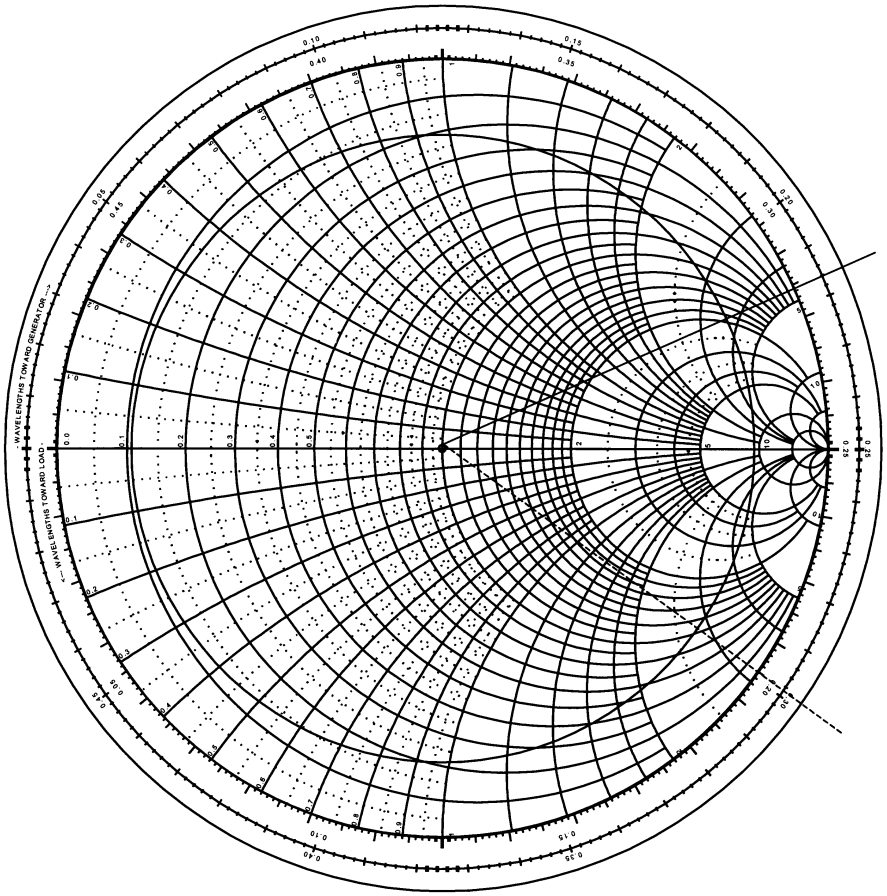

Figure 5.8 Graphical solution of Example 5.2.

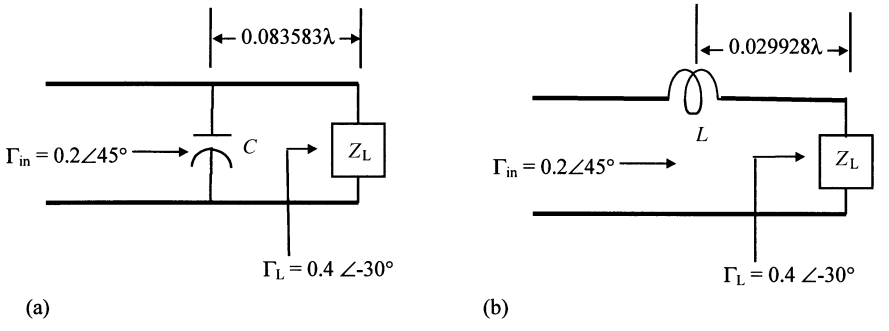

Figure 5.9 The two circuit designs for Example 5.3.

Complete or verify the designs at 4 GHz. Assume that characteristic impedance is 50 Ω.

This example can be solved using equations (3.2.4) and (3.2.6) of Chapter 3. Alternatively, a graphical procedure can be adopted. Both of these methods are illustrated in the following.

From (3.2.4), the given load and the desired normalized impedance or admittance can be calculated as follows. The normalized load impedance is

$$\bar{Z}_{\mathrm{L}} = \frac{1+\Gamma_{\mathrm{L}}}{1-\Gamma_{\mathrm{L}}} = \frac{1+0.4\angle -30^{\circ}}{1-0.4\angle -30^{\circ}} = 1.7980 - j0.8562$$

The desired normalized input impedance is

$$\bar{Z}_{\mathrm{in}} = \frac{1+\Gamma_{\mathrm{in}}}{1-\Gamma_{\mathrm{in}}} = \frac{1+0.2\angle 45^{\circ}}{1-0.2\angle 45^{\circ}} = 1.2679 + j0.3736$$

and the corresponding normalized input admittance is

$$\bar{Y}_{\mathrm{in}} = \frac{1-\Gamma_{\mathrm{in}}}{1+\Gamma_{\mathrm{in}}} = \frac{1-0.2\angle 45^{\circ}}{1+0.2\angle 45^{\circ}} = 0.7257 - j0.2138$$

- From (3.2.6), the normalized input admittance at $\ell = 0.0836\,\lambda$ from the load is

$$\bar{Y}_{\mathrm{in}} = \frac{1}{\bar{Z}_{\mathrm{in}}} = \frac{1+j\bar{Z}_{\mathrm{L}}\tan(\beta\ell)}{\bar{Z}_{\mathrm{L}}+j\tan(\beta\ell)} = 0.7257 + j0.6911$$

  Hence, the real part of this admittance is equal to the desired value. However, its imaginary part is off by $-j0.9049$. A negative susceptance is inductive while the given circuit has a capacitor that adds a positive susceptance. Therefore, the desired reflection coefficient cannot be obtained by the circuit given in Figure 5.9 (a).
- In the circuit shown in Figure 5.9 (b), components are connected in series. Therefore, it will be easier to solve this problem using impedance instead of admittance. From (3.2.6), the normalized impedance at $\ell_2 = 0.0299\,\lambda$ from the load is

$$\bar{Z}_{\mathrm{in}} = \frac{\bar{Z}_{\mathrm{L}}+j\tan(\beta\ell_2)}{1+j\bar{Z}_{\mathrm{L}}\tan(\beta\ell_2)} = 1.2679 - j0.9456$$

  Hence, its real part is equal to the desired value. However, its imaginary part needs modification by $j1.3192$ to get $j0.3736$. Hence, an inductor is required at

this point. The circuit given in Figure 5.9 (b) has a series inductor. Therefore, this circuit will have the desired reflection coefficient provided its value is

$$L = \frac{1.3192 \times 50}{2 \times \pi \times 4 \times 10^9}\text{H} = 2.6245 \times 10^{-9}\text{H} \approx 2.62 \text{ nH}$$

Figure 5.10 illustrates the graphical procedure to solve this example using a Smith chart. VSWR circles are drawn for the given reflection coefficient magnitudes. Using the phase angle of load reflection coefficient, the normalized load impedance point is identified as $1.8 - j0.85$, which is close to the value calculated earlier. The process is repeated for the desired input reflection coefficient and the corresponding input impedance point is identified as $1.27 + j0.37$. For the circuit given in Figure 5.9 (a), the admittance (normalized) points are found as $0.45 + j0.22$ and $0.73 - j0.21$, respectively. Next, move from the normalized load admittance point

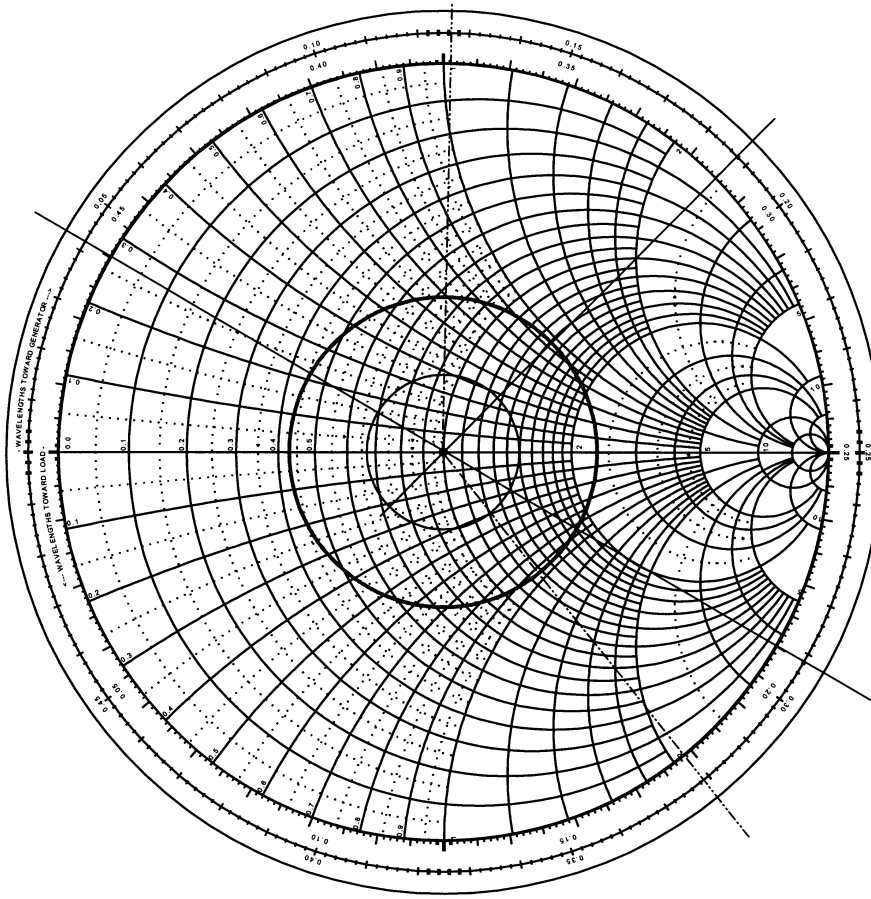

Figure 5.10 Graphical solution to Example 5.3.

toward the generator by a distance of $0.083583\,\lambda$ (i.e., $0.042\,\lambda + 0.084\,\lambda = 0.126\,\lambda$ of the scale "wavelengths toward generator"). The normalized admittance value of this point is found to be $0.73 + j0.69$. Hence, its real part is the same as that of the desired input admittance. However, its susceptance is $j0.69$, whereas the desired value is $-j0.2$. Hence, an inductor will be needed in parallel at this point. Since the given circuit has a capacitor, this design is not possible.

For the circuit shown in Figure 5.9 (b), elements are connected in series. Therefore, normalized impedance points need to be used in this case. Move from the load impedance $(1.8 - j0.85)$ point toward the generator by a distance of $0.029928\,\lambda$ (i.e., $0.292\,\lambda + 0.03\,\lambda = 0.322\,\lambda$ on the "wavelengths toward generator" scale). Normalized impedance value at this point is $1.27 - j0.95$. Thus, the resistance at this point is found to be equal to the desired value. However, its reactance is $-j0.95$, whereas the required value is $j0.37$. Therefore, a series reactance of $j1.32$ is needed at this point. The given circuit has an inductor that provides a positive reactance. Hence, this circuit will work. The required inductance L is found as follows.

$$L = \frac{1.32 \times 50}{2 \times \pi \times 4 \times 10^9}\text{H} = 2.626\ \text{nH}$$

5.2 DOUBLE-STUB MATCHING

The matching technique presented in the preceding section requires that a reactive element or stub be placed at a precise distance from the load. This point will shift with load impedance. Sometimes it may not be feasible to match the load using a single reactive element. Another possible technique to match the circuit employs two stubs with fixed separation between them. This device can be inserted at a convenient point before the load. The impedance is matched by adjusting the lengths of the two stubs. Of course, it does not provide a universal solution. As will be seen later in this section, separation between the two stubs limits the range of load impedance that can be matched with a given double-stub tuner.

Let ℓ_1 and ℓ_2 be the lengths of two stubs, as shown in Figure 5.11. The first stub is located at a distance ℓ from the load, $Z_\text{L} = R + jX$ ohm. Separation between the two stubs is d, and characteristic impedance of every transmission line is Z_o. In double-stub matching, load impedance Z_L is transformed to normalized admittance at the location of the first stub. Since the stub is connected in parallel, its normalized susceptance is added to that and then the resulting normalized admittance is transferred to the location of second stub. Matching conditions at this point require that the real part of this normalized admittance be equal to unity while its imaginary part is canceled by a conjugate susceptance of the second stub. Mathematically,

$$\frac{\bar{Y} + j(\bar{B}_1 + \tan(\beta d))}{1 + j(\bar{Y} + j\bar{B}_1)\tan(\beta d)} + j\bar{B}_2 = 1 \tag{5.2.1}$$

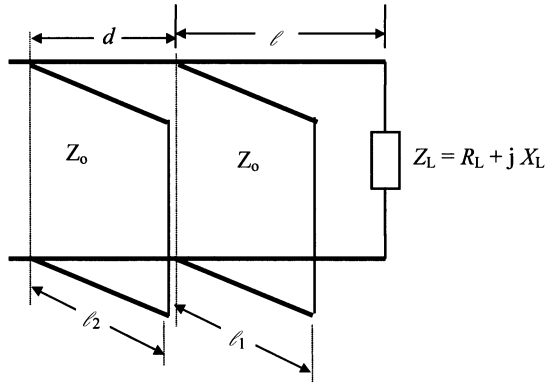

Figure 5.11 Double-stub matching network.

where,

$$\bar{Y} = \frac{1 + j\bar{Z}_L \tan(\beta\ell)}{\bar{Z}_L + j\tan(\beta\ell)} = \frac{\bar{Y}_L + j\tan(\beta\ell)}{1 + j\bar{Y}_L \tan(\beta\ell)} = \bar{G} + j\bar{B} \tag{5.2.2}$$

where jB_1 and jB_2 are the susceptance of the first and second stubs, respectively, and β is the propagation constant over the line.

For

$$\mathrm{Re}\frac{\bar{Y} + j(\bar{B}_1 + \tan(\beta d))}{1 + j(\bar{Y} + j\bar{B}_1)\tan(\beta d)} = 1$$

$$\bar{G}^2 \tan^2(\beta d) - \bar{G}\{1 + \tan^2(\beta d)\} + \{1 - (\bar{B} + \bar{B}_1)\tan(\beta d)\}^2 = 0 \tag{5.2.3}$$

Since conductance of the passive network must be a positive quantity, (5.2.3) requires that a given double stub can be used for matching only if the following condition is satisfied.

$$0 \le \bar{G} \le \csc^2(\beta d) \tag{5.2.4}$$

Two possible susceptances of the first stub that can match the load are determined by solving (5.2.3) as follows.

$$\bar{B}_1 = \cot(\beta d)\left[1 - \bar{B}\tan(\beta d) \pm \sqrt{\bar{G}\sec^2(\beta d) - \{\bar{G}\tan(\beta d)\}^2}\right] \tag{5.2.5}$$

Normalized susceptance of the second stub is determined from (5.2.1) as follows:

$$\bar{B}_2 = \frac{\bar{G}^2 \tan(\beta d) - \{\bar{B} + \bar{B}_1 + \tan(\beta d)\} \times \{1 - (\bar{B} + \bar{B}_1)\tan(\beta d)\}}{\{\bar{G}\tan(\beta d)\}^2 + \{1 - (\bar{B} + \bar{B}_1)\tan(\beta d)\}^2} \tag{5.2.6}$$

Once the susceptance of a stub is known, its short-circuit length can be determined easily as follows:

$$\ell_1 = \frac{1}{\beta}\cot^{-1}(-\bar{B}_1) \tag{5.2.7}$$

and,

$$\ell_2 = \frac{1}{\beta}\cot^{-1}(-\bar{B}_2) \tag{5.2.8}$$

Graphical Method

A two-stub matching network can also be graphically designed with the help of the Smith chart. This procedure follows the preceding analytical concepts. It can be summarized as follows.

1. Locate the normalized load-impedance point on the Smith chart and draw the VSWR circle. Move to the corresponding normalized admittance point. If the load is connected right at the first stub then go to the next step; otherwise, move toward the generator (clockwise) by $2\beta\ell$ on the VSWR circle. Assume that the normalized admittance of this point is $g + jb$.
2. Rotate the unity conductance circle counterclockwise by $2\beta d$. The conductance circle that touches this circle encloses the "forbidden region." In other words, this tuner can match only those $\bar{Y}$ that lie outside this circle. It is a graphical representation of the condition expressed by (5.2.4).
3. From $g + jb$, move on the constant conductance circle till it intersects the rotated unity conductance circle. There are at least two such points, providing two design possibilities. Let the normalized admittance of one of these points be $g + jb_1$.
4. The required normalized susceptance of the first stub is $j(b_1 - b)$.
5. Draw a VSWR circle through point $g + jb_1$ and move toward the generator (clockwise) by $2\beta d$ on it. This point will fall on the unity conductance circle of the Smith chart. Assume that this point is $1 + jb_2$.
6. The susceptance required from the second stub is $-jb_2$.
7. Once the stub susceptances are known, their lengths can be determined following the procedure used in the previous technique.

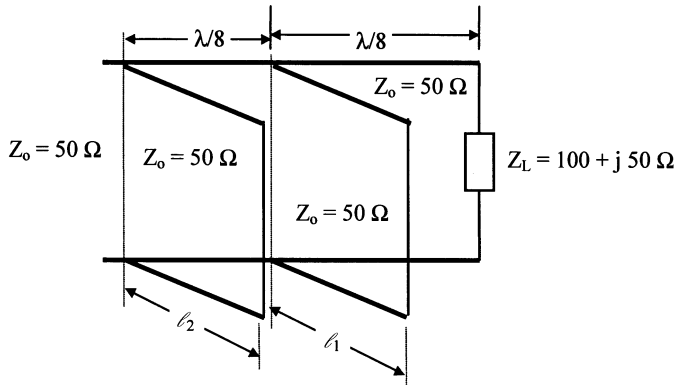

Figure 5.12 A two-stub matching network for Example 5.4.

Example 5.4: For the double-stub tuner shown in Figure 5.12, find the shortest values of ℓ_1 and ℓ_2 to match the load.

Since the two stubs are separated by $\lambda/8$, βd is equal to $\pi/4$ and the condition (5.2.4) gives

$$0 \leq \bar{G} \leq 2$$

That means the real part of the normalized admittance at the first stub (load side stub) must be less than 2 otherwise it cannot be matched.

The graphical procedure requires the following steps to find stub settings.

1. $\bar{Z}_L = \dfrac{100 + j50}{50} = 2 + j1.$
2. Locate this normalized load impedance on the Smith chart (point A) and draw the VSWR circle, as depicted in Figure 5.13. Move to the diametrically opposite side and locate the corresponding normalized admittance point B at $0.4 - j0.2$.
3. Rotate the unity conductance circle counterclockwise by $2\beta d = \pi/2 = 90^\circ$. This shows that this tuner can match only admittance with a real part less than 2 (because it touches the constant conductance circle of 2).
4. Move clockwise from point $0.4 - j0.2$ ($0.463\,\lambda$ on the "wavelengths toward generator" scale) by a distance of $2\beta\ell = \pi/2 = 90^\circ$ or $\lambda/8$ on the VSWR circle and locate the point C at $0.088\,\lambda$ ($0.463\,\lambda + 0.125\,\lambda = 0.588\,\lambda$) as the normalized admittance $0.5 - j0.5$ of the load transferred to the first stub's location.
5. From point C, move on the constant conductance circle until it intersects the rotated unity conductance circle. There are two such points, D and F. If point D is used for the design then the susceptance of the first stub must be equal to

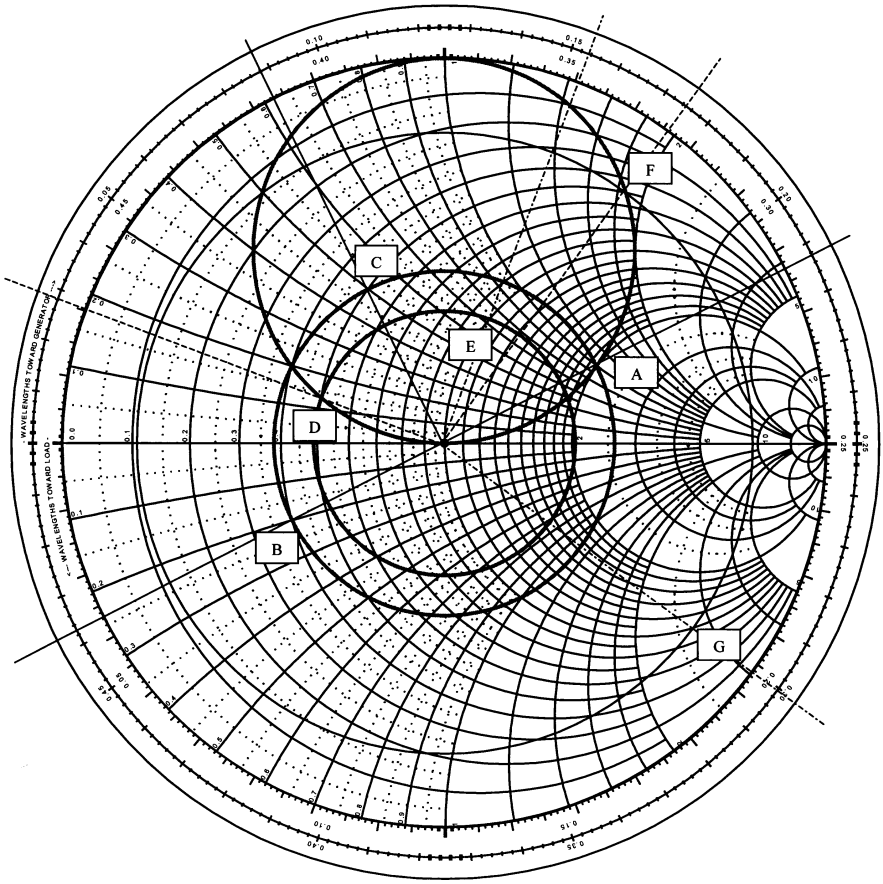

Figure 5.13 Smith chart solution to Example 5.4.

$-j0.37$ (i.e., $j0.13 - j0.5$). On the other hand, it will be $j1.36$ (i.e., $j1.86 - j0.5$) for point F.

6. Locate point $-j0.37$ and move toward the load along the circumference of the Smith chart until you reach the short circuit (infinite susceptance). This gives $\ell_1 = 0.194\,\lambda$. Similarly, ℓ_1 is found to be $0.4\,\lambda$ for $j1.36$.
7. Draw the VSWR circle through point D and move on it by $0.125\,\lambda$ (i.e., point $0.154\,\lambda$ on the "wavelengths toward generator" scale). The real part of the admittance at this point (point E) is unity while its susceptance is $j0.72$. Therefore, the second stub must be set for $-j0.72$ if the first one is set for $-j0.37$. Hence, the second stub is required to be $0.15\,\lambda$ long (i.e., $\ell_2 = 0.15\,\lambda$).
8. Draw the VSWR circle through point F and move on it by $0.125\,\lambda$ ($0.3\,\lambda$ on the "wavelengths toward generator" scale). The real part of the admittance at this point (point G) is unity while its susceptance is $-j2.7$. Therefore, the second

stub must be set for $j2.7$ if the first one is set for $j1.36$. In this case, the length of the second stub is found as $0.442\,\lambda$ (i.e., $\ell_2 = 0.442\,\lambda$).

9. Hence, the length of the first stub should be equal to $0.194\,\lambda$ and that of the second stub should be $0.15\,\lambda$. The other possible design, where the respective lengths are found to be $0.4\,\lambda$ and $0.442\,\lambda$, is not recommended.

Alternatively, the required stub susceptances and, hence, lengths ℓ_1 and ℓ_2 can be calculated from (5.2.2) to (5.2.8) as follows.

$$\bar{Y} = \bar{G} + j\bar{B} = 0.5 + j0.5$$
$$\bar{B}_1 = j1.366 \text{ or } -j0.366$$

For $\bar{B}_1 = j1.366$, $\bar{B}_2 = j2.7321$, and for $\bar{B}_1 = -j0.366$, $\bar{B}_2 = -j0.7321$. The corresponding lengths are found to be $0.3994\,\lambda$, $0.4442\,\lambda$, $0.1942\,\lambda$, and $0.1494\,\lambda$. These values are fairly close to those obtained graphically from the Smith chart.

5.3 MATCHING NETWORKS USING LUMPED ELEMENTS

The matching networks described so far may not be useful for certain applications. For example, the wavelength of a 100-MHz signal is 3 m and, therefore, it may not be practical to use the stub matching in this case because of its size on a printed circuit board. This section presents matching networks utilizing discrete components that can be useful especially in such cases. There are two different kinds of L-section matching circuits described here. This section begins with resistive matching circuits that can be used for broadband applications. However, these networks dissipate signal energy and also introduce thermal noise. This section ends with a presentation of the reactive matching networks that are almost lossless but the design is frequency dependent.

Resistive L-Section Matching Circuits

Consider a signal generator with internal resistance R_s. It feeds a load resistance R_L, as illustrated in Figure 5.14. Since source resistance is different from the load, a part of the signal is reflected back. Assume that R_s is larger than R_L and there is a resistive L-section introduced between the two. Further, voltages at its input and output ports are assumed to be V_{in} and V_o, respectively. If this circuit is matched at both its ports then the following two conditions must be true.

1. With R_L connected, resistance looking into the input port must be R_s.
2. With R_s terminating the input port, resistance looking into the output port must be R_L.

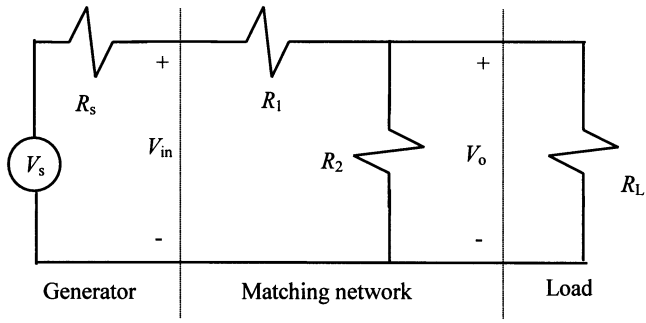

Figure 5.14 A resistive L-section matching circuit.

From the first condition,

$$R_s = R_1 + \frac{R_2 R_L}{R_2 + R_L} = \frac{R_1 R_2 + R_1 R_L + R_2 R_L}{R_2 + R_L} \tag{5.3.1}$$

and from the second,

$$R_L = \frac{R_2(R_1 + R_s)}{R_2 + R_1 + R_s} = \frac{R_1 R_2 + R_2 R_s}{R_2 + R_1 + R_s} \tag{5.3.2}$$

Equations (5.3.1) and (5.3.2) can be solved for R_1 and R_2 as follows:

$$R_1 = \sqrt{R_s(R_s - R_L)} \tag{5.3.3}$$

and,

$$R_2 = \sqrt{\frac{R_L^2 R_s}{R_s - R_L}} \tag{5.3.4}$$

The voltage across the load and the attenuation in the matching network are

$$V_0 = \frac{V_{in}}{R_1 + R_2 \| R_L} R_2 \| R_L \Rightarrow \frac{V_0}{V_{in}} = \frac{R_2 R_L}{R_1 R_2 + R_1 R_L + R_2 R_L} \tag{5.3.5}$$

and,

$$\text{Attenuation in dB} = 20 \log \left\{ \frac{R_2 R_L}{R_1(R_2 + R_L) + R_2 R_L} \right\} \tag{5.3.6}$$

Note that R_1 and R_2 are real only when R_s is greater than R_L. If this condition is not satisfied (i.e., $R_s < R_L$), the circuit shown in Figure 5.14 will require modifica-

tion. Flipping the L-section the other way around (i.e., R_1 connected in series with R_L and R_2 across the input) will match the circuit. Design equations for that case can be easily obtained.

Example 5.5: Internal resistance of a signal generator is 75 ohm. If it is being used to excite a 50-ohm transmission line then design a resistive network to match the two. Calculate the attenuation in dB that occurs in the inserted circuit.

Since $R_L = 50$ ohm and $R_s = 75$ ohm, R_s is greater than R_L, and therefore, the circuit shown in Figure 5.14 can be used.

$$R_1 = \sqrt{75(75-50)} = 43.3\,\Omega$$

$$R_2 = \sqrt{\frac{75 \cdot 50^2}{75-50}} = 86.6\,\Omega$$

and,

$$\text{Attenuation in dB} = 20\log\left(\frac{86.6 \cdot 50}{43.3(86.6+50)+86.6 \cdot 50}\right) = 20\log(0.4227)$$
$$= -7.48 \text{ dB}$$

The final circuit arrangement is shown in Figure 5.15.

Reactive L-Section Matching Circuits

As mentioned earlier, resistive matching circuits are frequency insensitive but dissipate a part of the signal power that adversely affects the signal-to-noise ratio. Here, we consider an alternative design using reactive components. In this case, power dissipation is ideally zero but the matching is frequency dependent.

Consider the two circuits shown in Figure 5.16. In one of these circuits, resistor R_s is connected in series with a reactance X_s, while in the other, resistor R_p is

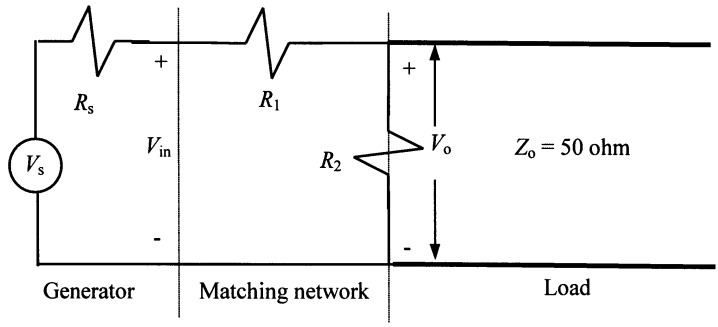

Figure 5.15 Resistive matching circuit for Example 5.5.

Figure 5.16 Series- and parallel-connected impedance circuits.

connected in parallel with a reactance X_p. If impedance of one circuit is complex conjugate of the other, then

$$|R_s + jX_s| = \left| \frac{jX_pR_p}{R_p + jX_p} \right|$$

or,

$$\sqrt{R_s^2 + X_s^2} = \frac{X_pR_p}{\sqrt{R_p^2 + X_p^2}} \tag{5.3.7}$$

The quality factor, Q, of a reactive circuit is defined in Chapter 4 as follows:

$$Q = \omega \frac{\text{Energy stored in the network}}{\text{Average power loss}}$$

where ω is angular frequency of the signal.

For a series circuit,

$$Q = \frac{X_s}{R_s} \tag{5.3.8}$$

and, for a parallel circuit,

$$Q = \frac{R_p}{X_p} \tag{5.3.9}$$

Assuming that the quality factors of these two circuits are equal, (5.3.7) can be simplified as follows.

$$\sqrt{R_s^2 + R_s^2Q^2} = \frac{\left(\frac{R_p}{Q}\right)R_p}{\sqrt{R_p^2 + \left(\frac{R_p}{Q}\right)^2}} \Rightarrow R_s\sqrt{1+Q^2} = \frac{R_p}{\sqrt{1+Q^2}}$$

Hence,

$$1 + Q^2 = \frac{R_p}{R_s} \tag{5.3.10}$$

The design procedure is based on equations (5.3.8)–(5.3.10). For a resistive load to be matched with another resistor (it may be a transmission line or generator), R_p and R_s are defined such that the former is greater. Q of the circuit is then calculated from (5.3.10). Respective reactances are subsequently determined from (5.3.8) and (5.3.9). If one reactance is selected capacitive then the other must be inductive. X_p will be connected in parallel with R_p and X_s will be in series with R_s. The following example illustrates the procedure.

Example 5.6: Design a reactive L-section that matches a 600-Ω resistive load to a 50-Ω transmission line. Determine component values if the matching is desired at 400 MHz.

Since R_p must be larger than R_s, the 600-Ω load is selected as R_p and 50-Ω line as R_s. Hence, from (5.3.10) we have

$$Q^2 + 1 = \frac{R_p}{R_s} = \frac{600}{50} = 12 \Rightarrow Q = \sqrt{11} = 3.3166$$

Now, from (5.3.8) and (5.3.9),

$$X_s = QR_s = 3.3166 \cdot 50 = 165.8312\,\Omega$$

$$X_p = \frac{R_p}{Q} = \frac{600}{3.3166} = 180.9068\,\Omega$$

Therefore, either one of the two circuits in Figure 5.17 can be used to match the load with the line.

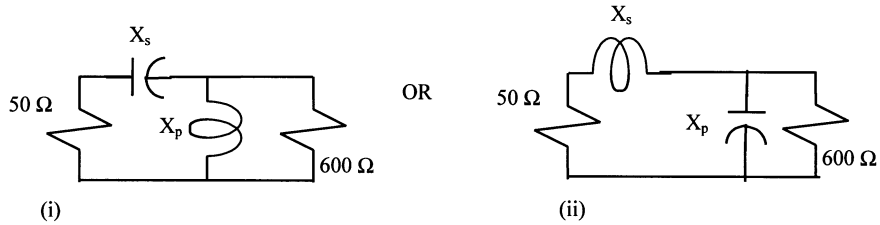

Figure 5.17 Design of two reactive matching circuits for Example 5.6.

For circuit (i) in Figure 5.17, component values are determined as follows.

$$X_s = 165.8312 = \frac{1}{\omega C_s}$$

$$\therefore C_s \frac{1}{2 \cdot \pi \cdot 400 \cdot 10^6 \cdot 165.8312} \approx 2.4 \cdot 10^{-12} F = 2.4 \text{ pF}$$

and,

$$X_p = 180.9068 = \omega L_p$$

$$\therefore L_p = \frac{180.9068}{2 \cdot \pi \cdot 400 \cdot 10^6} = 71.9805 \cdot 10^{-9} \text{H} \approx 72 \text{ nH}$$

Similarly, the component values for circuit (ii) in Figure 5.17 are

$$X_s = 165.8312 = \omega L_s$$

$$\therefore L_s = \frac{165.8312}{2 \cdot \pi \cdot 400 \cdot 10^6} = 65.9821 \cdot 10^{-9} \text{ H} \approx 66 \text{ nH}$$

and,

$$X_p = 180.9068 = \frac{1}{\omega C_p}$$

$$\therefore C_p = \frac{1}{2 \cdot \pi \cdot 400 \cdot 10^6 \cdot 180.9068} = 2.2 \cdot 10^{-12} \text{ F} = 22 \text{ pF}$$

Example 5.7: Consider the preceding example again and transform a 600-ohm resistive load to a 173.2-ohm by adjusting the Q of a matching circuit. Continue the transformation process to get 50 ohm from 173.2 ohm. Compare the frequency response (reflection coefficient versus frequency) of your circuits.

For the first part of this example, R_p is 600 ohm and R_s is 173.2 ohm. Hence, from (5.3.8)–(5.3.10),

$$Q = \sqrt{\frac{R_p}{R_s} - 1} = \sqrt{\frac{600}{173.2} - 1} = 1.569778$$

$$X_s = QR_s = 271.8856\Omega$$

and,

$$X_p = \frac{R_p}{Q} = 382.2196\Omega$$

Repeating the calculations with $R_p = 173.2\ \Omega$ and $R_s = 50\ \Omega$, for the second part of the problem, we get

$$Q = \sqrt{\frac{R_p}{R_s} - 1} = \sqrt{\frac{173.2}{50} - 1} = 1.5697$$

This value of Q is very close to that obtained earlier. This is because 173.2 is close to the geometric mean of 600 and 50.

Hence,

$$X_s = QR_s = 78.4857\,\Omega$$

and,

$$X_p = \frac{R_p}{Q} = 110.3386\,\Omega$$

Two of the possible circuits (iii and iv) are shown in Figure 5.18 along with their component values. For these circuits, the impedance that the 50-ohm transmission line sees can be determined. The reflection coefficient is then determined for each case. This procedure is repeated for the circuits obtained in Example 5.6 as well. Magnitude of the reflection coefficient for each of these four cases is displayed in Figure 5.19. Curves (a) and (b) are obtained for circuits (i) and (ii) of Figure 5.17, respectively. The frequency response of circuit (iii) in Figure 5.18 is illustrated by curve (c) of Figure 5.19 while curve (d) displays the frequency response of circuit (iv). The horizontal axis of Figure 5.19 represents the normalized frequency (i.e., the signal frequency divided by 400 MHz).

As Figure 5.19 indicates, the reflection coefficient is zero for all four circuits at a normalized frequency of unity. However, it increases if the signal frequency is changed on either side. Further, the rate of increase in reflection is higher for circuits obtained earlier in Example 5.6. For example, if a reflection coefficient of 0.2 is acceptable, circuits (iii) and (iv) can provide much wider bandwidth in comparison with those of the previous example. This concept can be used to shape the reflection coefficient characteristics over the desired frequency band.

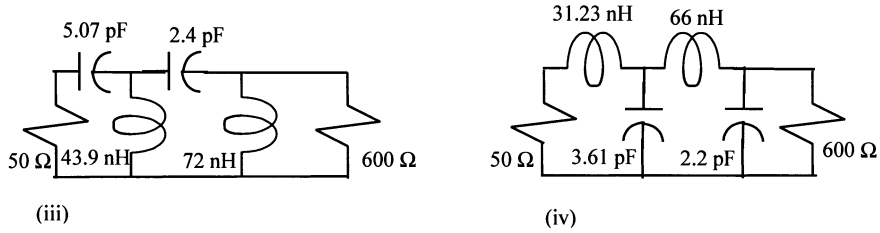

Figure 5.18 Design of reactive matching networks for Example 5.7.

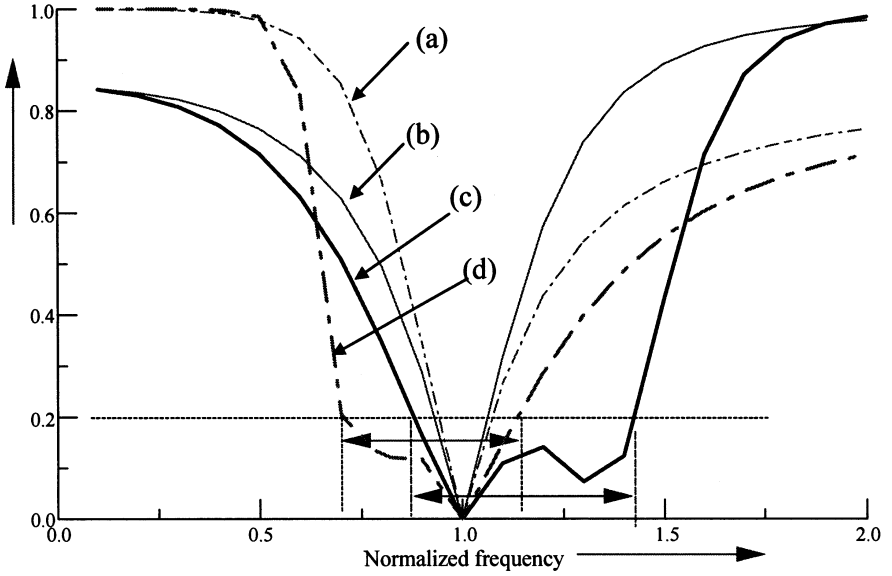

Figure 5.19 Reflection coefficient (magnitude) versus normalized frequency for the matching circuits designed in Examples 5.6 and 5.7.

Example 5.8: A 50-Ω transmission line is to be matched with a $10 + j10$-Ω load. Design two different L-section reactive circuits and find component values at 500 MHz.

Unlike the cases considered so far, the load is complex in this example. However, the same design procedure is still applicable. We consider only the real part of load impedance initially and take its imaginary part into account later in the design. Since characteristic impedance of the transmission line is greater than the real part of the load (that is, $50\ \Omega > 10\ \Omega$), R_p is 50 Ω while R_s is 10 Ω. Therefore,

$$Q^2 = \frac{50}{10} - 1 = 4 \Rightarrow Q = 2$$

X_s and X_p can be determined now from (5.3.8) and (5.3.9):

$$X_s = Q \cdot R_s = 2 \cdot 10 = 20\,\Omega$$

and,

$$X_p = \frac{R_p}{Q} = \frac{50}{2} = 25\,\Omega$$

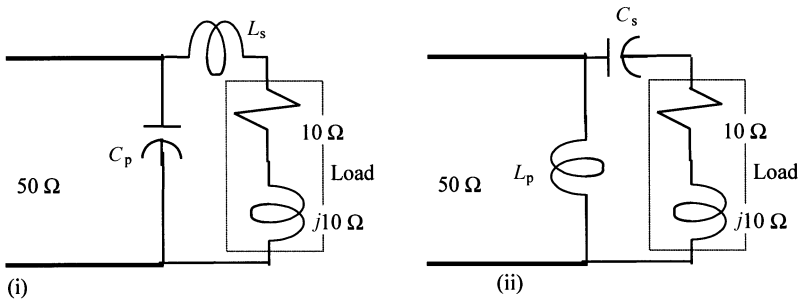

Figure 5.20 Reactive matching circuits for Example 5.8.

Reactance X_p is connected in parallel with the transmission line while X_s is in series with the load. These two matching circuits are shown in Figure 5.20. If X_p is a capacitive reactance of 25 Ω then X_s must be inductive 20 Ω. The reactive part that has not been taken into account so far needs to be included at this point in X_s. Since this reactive part of the load is inductive 10 Ω, another series inductor for the remaining 10 Ω is needed, as shown in circuit (i) of Figure 5.20. Hence,

$$\omega L_s = (20 - 10)$$
$$\therefore L_s = \frac{10}{2 \cdot \pi \cdot 500 \cdot 10^6} H = 0.3183 \cdot 10^{-8}\,\text{H} = 3.183\ \text{nH}$$

and,

$$\frac{1}{\omega C_p} = 25$$
$$\therefore C_p = \frac{1}{2 \cdot \pi \cdot 500 \cdot 10^6 \cdot 25} = 0.0127324 \cdot 10^{-9}\,\text{F} = 12.7324\ \text{pF}$$

In the second case, X_p is assumed inductive and, therefore, X_s needs to be capacitive. It is circuit (ii) as shown in Figure 5.20. Since the load has a 10-Ω inductive reactance, it must be taken into account in determining the required capacitance. Therefore,

$$\omega C_s = \frac{1}{(20 + 10)} \Rightarrow C_s = \frac{1}{2 \cdot \pi \cdot 500 \cdot 10^6 \cdot 30}\,\text{F} = 10.61\ \text{pF}$$

and,

$$\omega L_p = 25 \Rightarrow L_p = \frac{25}{2 \cdot \pi \cdot 500 \cdot 10^6}\,\text{H} = 7.9577\ \text{nH}$$

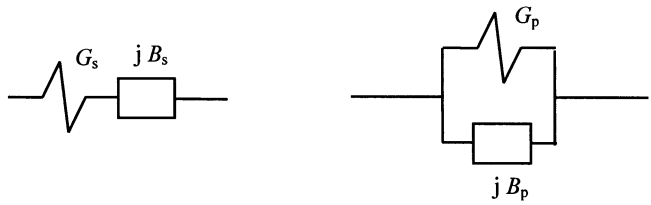

Figure 5.21 Series- and parallel-connected admittance circuits.

The matching procedure used so far is based on the transformation of series impedance to a parallel circuit of the same quality factor. Similarly, one can use an admittance transformation, as shown in Figure 5.21.

These design equations can be obtained easily following the procedure used earlier:

$$\frac{G_s}{G_p} = 1 + Q^2 \tag{5.3.11}$$

$$Q = \frac{G_s}{B_s} \tag{5.3.12}$$

and

$$Q = \frac{B_p}{G_p} \tag{5.3.13}$$

Note from (5.3.11) that G_s must be greater than G_p for a real Q.

Example 5.9: A load admittance, $Y_L = 8 - j12$ mS, is to be matched with a 50-ohm line. There are three different L-section matching networks given to you in Figure 5.22. Complete or verify each of these circuits. Find the element values at 1 GHz.

Since characteristic impedance of the line is 50 ohm, the corresponding conductance will be 0.02 S. The real part of the load admittance is 0.008 S. Therefore, G_s must be 0.02 S in (5.3.11). However, the given circuits in Figure 5.22 have a capacitor or an inductor connected in parallel with the 50-ohm line. Obviously, these design equations cannot be used here. Equations (5.3.8)–(5.3.10) use the impedance values. Hence, we follow the procedure outlined below.

$$Y_L = \frac{1}{Z_L} \Rightarrow Z_L = \frac{10^3}{8 - j12}\Omega = 38.4615 + j57.6923\,\Omega$$

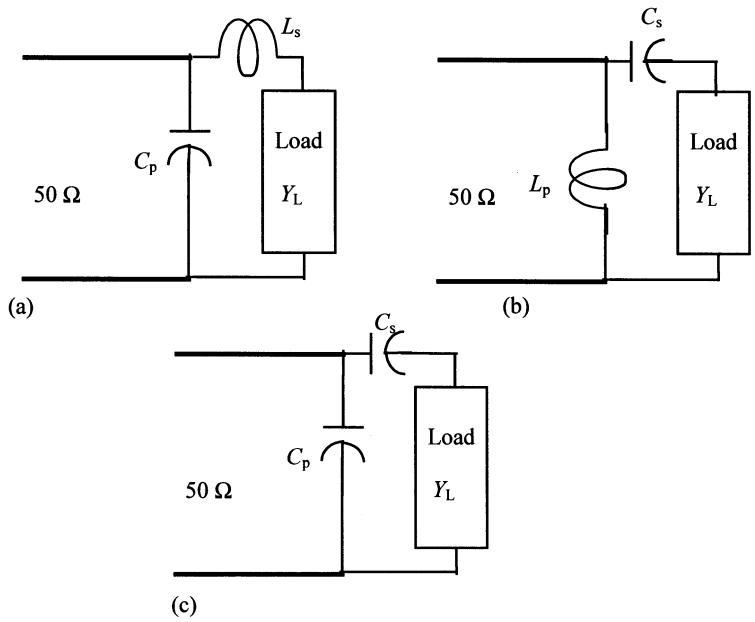

Figure 5.22 Three possible L-section matching circuits given in Example 5.9.

Therefore,

$$R_p = 50\,\Omega \text{ and } R_s = 38.4615\,\Omega \Rightarrow Q = \sqrt{\frac{50}{38.4615} - 1} = 0.5477$$

Now, from (5.3.8) and (5.3.9),

$$X_s = Q \cdot R_s = 0.5477 \cdot 38.4615 = 21.0654\,\Omega$$

and,

$$X_p = \frac{R_p}{Q} = \frac{50}{0.5477} = 91.2909\,\Omega$$

For circuit (a) in Figure 5.22, capacitor C_p can be selected, which provides 91.29-ohm reactance. It means that the inductive reactance on its right-hand-side must be 21.06 ohm. However, an inductive reactance of 57.69 ohm is already present there due to load. Another series inductor will increase it further, whereas it needs to be reduced to 21.06 ohm. Thus, we conclude that circuit (a) cannot be used.

In circuit (b) in Figure 5.22, there is an inductor in parallel with the transmission line. For a match, its reactance must be 91.29 Ω and overall reactance to the right

must be capacitive 21.06 Ω. Inductive reactance of 57.69 Ω of the load needs to be neutralized as well. Hence,

$$X_c = 57.6923 + 21.0654 = 78.7577\,\Omega$$
$$\therefore X_p = \frac{R_p}{Q} = \frac{50}{0.5477} = 91.2909\,\Omega$$

and,

$$X_p = 91.2909\,\Omega \Rightarrow L = \frac{91.2909}{2 \cdot \pi \cdot 10^9}\text{H} = 14.5294\text{ nH}$$

Circuit (c) in Figure 5.22 has a capacitor across the transmission line terminals. Assuming that its reactance is 91.29 ohm, reactance to the right must be inductive 21.06 ohm. As noted before, the reactive part of the load is an inductive 57.69 ohm. It can be reduced to the desired value by connecting a capacitor in series. Hence, the component values for circuit (c) are calculated as follows:

$$X_s = 57.6923 - 21.0654 = 36.6269\ \Omega$$
$$\therefore C_s = 4.3453\text{ pF}$$

and,

$$X_p = 91.29009\,\Omega \Rightarrow C_p = 1.7434\text{ pF}$$

Example 5.10: Reconsider the previous example where $Y_L = 8 - j12$ mS is to be matched with a 50-ohm line. Complete or verify the following L-section matching circuits at a signal frequency of 1 GHz.

As noted in the preceding example, G_s is 0.02 S while G_p is 8 mS. Looking over the given circuit configurations, it seems possible to complete or verify these circuits through (5.3.11)–(5.1.13). Hence,

$$Q = \sqrt{\frac{G_s}{G_p} - 1} = \sqrt{\frac{0.02}{0.008} - 1} = 1.2247$$
$$B_s = \frac{G_s}{Q} = \frac{0.02}{1.2247} = 0.0163\text{ S}$$

and,

$$B_p = Q \cdot G_p = 1.2247 \cdot 0.008 = 0.0097978 \approx 0.01\text{ S}$$

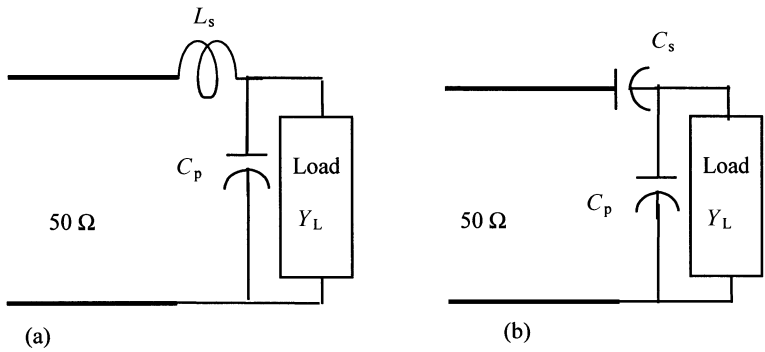

Figure 5.23 L-section matching networks given in Example 5.10.

If B_s is selected as an inductive susceptance then B_p must be capacitive. Since load has an inductive susceptance of 12 mS, the capacitor must neutralize that too. Hence, circuit (a) of Figure 5.23 will work provided that

$$B_s = 0.0163 \text{ S} \Rightarrow L_s = 9.746 \text{ nH}$$

and,

$$B_p = (0.01 + 0.012) \text{ S} = 0.022 \text{ S} \Rightarrow C_p = 3.501 \text{ pF}$$

In circuit (b) of Figure 5.23, a capacitor is connected in series with G_s. Therefore, B_p must be an inductive susceptance. Since it is 0.012 S while only 0.01 S is required for matching, a capacitor in parallel is needed. Hence,

$$B_s = 0.0163 \text{ S} \Rightarrow C_s = 2.599 \text{ pF}$$

and,

$$B_p = (0.012 - 0.01) = 0.002 \text{ S (capacitive)} \Rightarrow C_p = 0.3183 \text{ pF}$$

Thus, both of these circuits can work provided the component values are as found above.

Graphical Method

As described earlier, L-section reactive networks can be used for matching the impedance. One of these reactive elements appears in series with the load or the desired impedance while the other one is connected in parallel. Thus, the resistive part stays constant when a reactance is connected in series with impedance. Similarly, a change in the shunt-connected susceptance does not affect the conductive part of admittance. Consider normalized impedance point X on the Smith chart

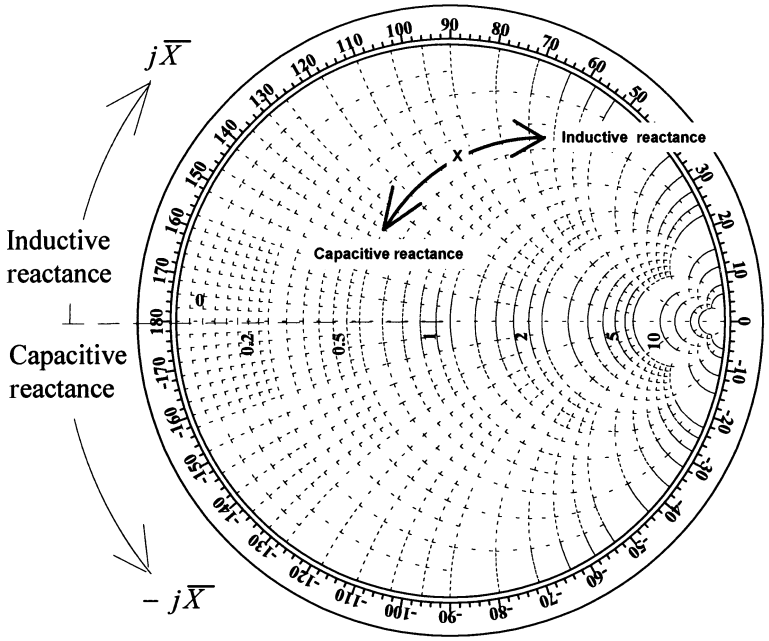

Figure 5.24 Impedance ($\bar{Z}$-) Smith chart.

shown in Figure 5.24. To distinguish it from others, it may be called the Z-Smith chart. If its resistive part needs to be kept constant at 0.5, one must stay on this constant resistance circle. A clockwise movement from this point increases the positive reactance. It means that the inductance increases in series with the impedance of X. On the other hand, the positive reactance decreases with a counterclockwise movement. A reduction in positive reactance means a decrease in series inductance or an increase in series capacitance. Note that this movement also represents an increase in negative reactance.

Now consider a Smith chart that is rotated by 180° from its usual position, as shown in Figure 5.25. It may be called a Y-Smith chart because it represents the admittance plots. In this case, addition (or subtraction) of a susceptance to admittance does not affect its real part. Hence, it represents a movement on the constant conductance circle. Assume that a normalized admittance is located at point X. The conductive part of this admittance is 0.5. If a shunt inductance is added then it moves counterclockwise on this circle. On the other hand, a capacitive susceptance moves this point clockwise on the constant conductance circle.

A superposition of Z- and Y-Smith charts is shown in Figure 5.26. It is generally referred to as a ZY-Smith chart because it includes impedance as well as admittance plots at the same time. A short-circuit impedance is zero while the corresponding admittance goes to infinity. A single point on the ZY-Smith chart represents it. Similarly, it may be found that other impedance points of the Z-chart coincide with

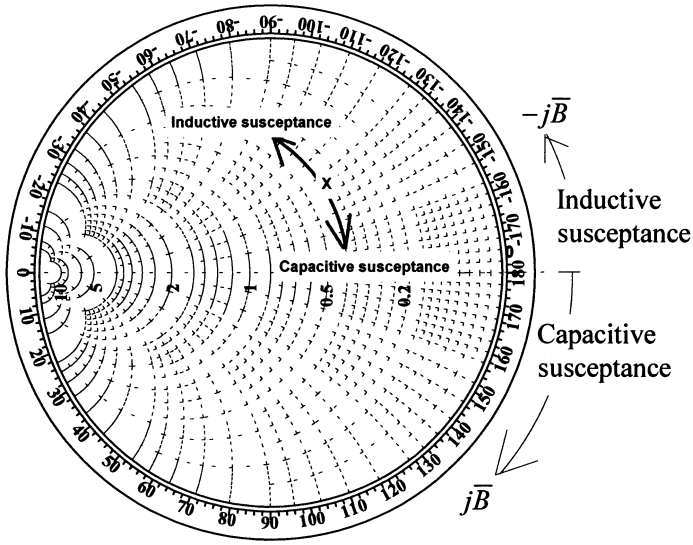

Figure 5.25 Admittance ($\bar{Y}$-) Smith chart.

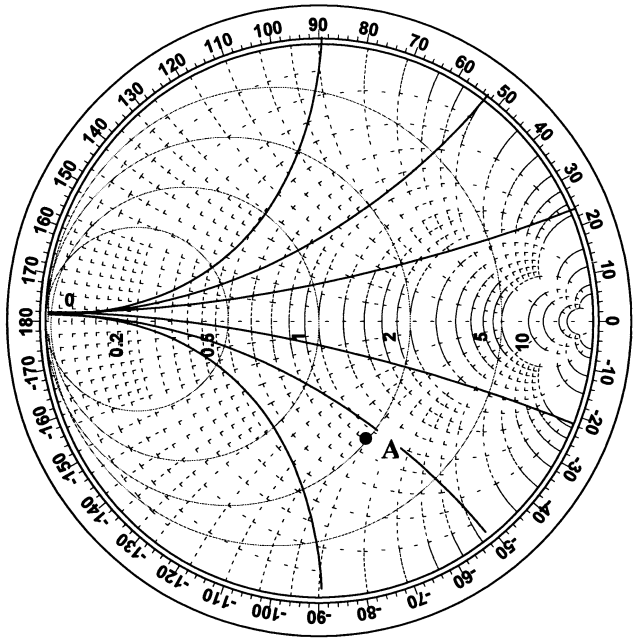

Figure 5.26 ZY-chart.

the corresponding admittance points of the Y-chart as well. Hence, impedance can be transformed to the corresponding admittance just by switching from the Z- to the Y-scales of a ZY-Smith chart. For example, a normalized impedance point of $0.9 - j1$ is located using the Z-chart scales as A in Figure 5.26. The corresponding admittance is read from the Y-chart as $0.5 + j0.55$.

Reactive L-section matching circuits can be easily designed using a ZY-Smith chart. Load and desired impedance points are identified on this chart using Z-scales. Y-scales may be used if either one is given as admittance. Note that the same characteristic impedance is used for normalizing these values. Now, move from the point to be transformed toward the desired point following a constant resistance or conductance circle. Movement on the constant conductance circle gives the required susceptance (i.e., a reactive element will be needed in shunt). It is determined by subtracting initial susceptance (the starting point) from the value reached. When moving on the conductance circle, use the Y-scale of the chart. Similarly, moving on a constant resistance circle will mean that a reactance must be connected in series. It can be determined using the Z-scale of the ZY-Smith chart.

Note from the ZY-chart that if a normalized load value falls inside the unity resistance circle then it can be matched with the characteristic impedance Z_o only after shunting it with an inductor or capacitor (a series-connected inductor or capacitor at the load will not work). Similarly, a series inductor or capacitor is required at the load if the normalized value is inside the unity conductance circle. Outside these two unity circles, if the load point falls in the upper half then the first component required for matching would be a capacitor that can be series or parallel connected. On the other hand, first an inductor will be needed at the load if the load point is located in the lower half and outside the unity circles.

Example 5.11: Use a ZY-Smith chart to design the matching circuits of Examples 5.9 and 5.10.

In this case, the given load admittance can be normalized by the characteristic admittance of the transmission line. Hence,

$$\bar{Y}_L = \frac{Y_L}{Y_o} = Y_L \times Z_o = 0.4 - j0.6$$

This point is found on the ZY-Smith chart as A in Figure 5.27. The matching requires that this admittance must be transformed to 1. This point can be reached through a unity conductance or resistance circle. Hence, a matching circuit can be designed if somehow we can reach one of these circles through constant resistance and conductance circles only. Since constant conductance circles intersect constant resistance circles, one needs to start on a constant resistance circle to get on the unity conductance circle or vice-versa. There are two circles (namely, 0.4 conductance and 0.78 resistance circles) passing through point A. Hence, it is possible to get on to the unity resistance circle via the 0.4 conductance circle. Alternatively, one can reach the unity conductance circle through the 0.78 resistance circle. In either case, a circuit

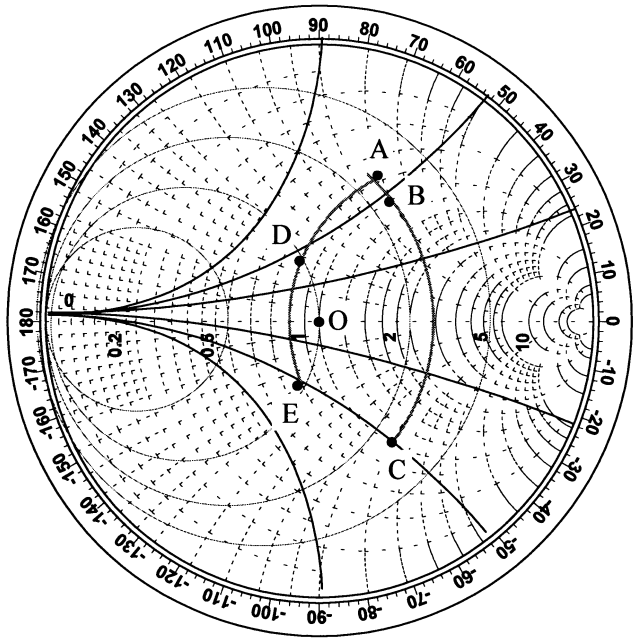

Figure 5.27 Graphical solution to Example 5.11.

can be designed. From point A, one can move on the 0.4 conductance circle (or 0.78 resistance circle) so that the real part of the admittance (or impedance) remains constant. If we start counterclockwise from A on the conductance circle, we end up at infinite susceptance without intersecting the unity resistance circle. Obviously, this does not yield a matching circuit. Similarly, a clockwise movement on the 0.78 resistance circle from A cannot produce a matching network. Hence, an inductor in parallel or in series with the given load cannot be used for the design of a matching circuit. This proves that the circuit shown in Figure 5.22 (a) cannot be designed.

There are four possible circuits. In one case, move from point A to B on the conductance circle (a shunt capacitor) and then from B to O on the unity resistance circle (a series capacitor). The second possibility is via A to C (a shunt capacitor) and then from C to O (a series inductor). A third circuit can be obtained following the path from A to D (a series capacitor) and then from D to O (a shunt capacitor). The last one can be designed by following the path from A to E (a series capacitor) and then from E to O (a shunt inductor).

A-E to E-O and A-D to D-O correspond to the circuits shown in Figures 5.22 (b) and 5.22 (c), respectively. Similarly, A-C to C-O and A-B to B-O correspond to circuits shown in Figures 5.23 (a) and 5.23 (b), respectively. Component values for each of these circuits are determined following the corresponding susceptance or reactance scales. For example, we move along a resistance circle from A to D. That means there will be a change in reactance. The required element value is determined after subtracting the reactance at A from the reactance at D. This difference is $j0.42$

$-j1.15 = -j0.73$. Negative reactance means it is a series capacitor. Note that $-j0.73$ is a normalized value. The actual reactance is $-j073 \times 50 = -j36.5$ ohm. It is close to the corresponding value of 36.6269 ohm obtained earlier. Other components can be determined as well.

Example 5.12: Two types of L-section matching networks are shown in Figure 5.28. Select one that can match the load $Z_L = 25 + j10$ ohm to a 50-ohm transmission line. Find the element values at 500 MHz.

First, let us consider circuit (a). R_p must be 50 ohm because it is required to be greater than R_s. However, the reactive element is connected in series with it. That will be possible only with R_s. Hence, this circuit cannot be designed using (5.3.8)–(5.3.10). The other set of design equations, namely (5.3.11)–(5.3.13), requires admittance instead of impedance. Therefore, the given impedances are inverted to find the corresponding admittances as follows.

$$Y_L = \frac{1}{Z_L} = \frac{1}{25 + j10} = 0.034483 - j0.01379 \text{ S}$$

and,

$$Y_o = \frac{1}{Z_o} = \frac{1}{50} = 0.02 \text{ S}$$

Since G_s must be larger than G_p, this set of equations produces a matching circuit that has a reactance in series with Y_L. Thus, we conclude that the circuit given in Figure 5.28 (a) cannot be designed.

Now, consider the circuit shown in Figure 5.28 (b). For (5.3.8)–(5.3.10), R_p is 50 ohm while R_s is 25 ohm. Hence, one reactance of the matching circuit will be connected across 50 ohm and the other one will go in series with Z_L. The circuit in Figure 5.28 (b) has this configuration. Hence, it will work. Its component values are calculated as follows.

$$Q = \sqrt{\frac{50}{25} - 1} = 1$$

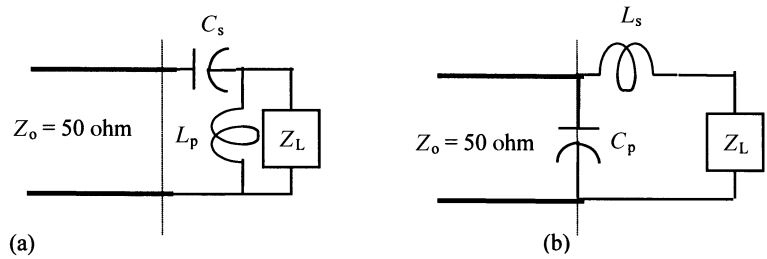

Figure 5.28 L-section matching circuits given for Example 5.12.

Therefore,

$$X_s = R_s = 25 \text{ ohm}$$

and,

$$X_p = R_p = 50 \text{ ohm}$$

For X_p to be capacitive, we have

$$\frac{1}{\omega C_p} = 50 \Rightarrow C_p = 6.366 \text{ pF}$$

And there is already 10 ohm inductive reactance included in the load. Therefore, another inductive 15 ohm will suffice. Thus,

$$\omega L_s = 25 - 10 = 15 \Rightarrow L_s = \frac{15}{\omega}\text{H} = 4.775 \text{ nH}$$

This example can be solved using a ZY-Smith chart as well. To that end, the load impedance is normalized with characteristic impedance of the line. Hence,

$$\bar{Z}_L = \frac{25 + j10}{50} = 0.5 + j0.2$$

This point is located on a ZY-Smith chart, as shown in Figure 5.29. It is point A on this chart. If we move on the conductance circle from A, we never reach the unity resistance circle. That means an L-section matching circuit that has a reactance (inductor or capacitor) in parallel with the load cannot be designed. Therefore, circuit (a) of Figure 5.28 is not possible.

Next, we try a reactance in series with the load. Moving on the constant resistance circle from A indicates that there are two possible circuits. Movement from A to B on the resistance circle and then from B to O on the unity conductance circle provides component values of circuit shown in Figure 5.28 (b).

The required normalized reactance is found to be $j0.3$ (i.e., $j0.5 - j0.2$). It is an inductor because of its positive value. Further, it will be connected in series with the load because it is found by moving on a constant resistance circle from A.

The required series inductance is determined as follows.

$$X_L = 0.3 \times 50 = 15 \Rightarrow L_s = \frac{15}{\omega}\text{H} = 4.775 \text{ nH}$$

Movement from B to O gives a normalized susceptance of $j1$. Positive susceptance is a capacitor in parallel with a 50-ohm line. Hence,

$$\omega C_p = \frac{1}{50} \Rightarrow C_p = 6.366 \text{ pF}$$

These results are found to be exactly equal to those found earlier analytically.

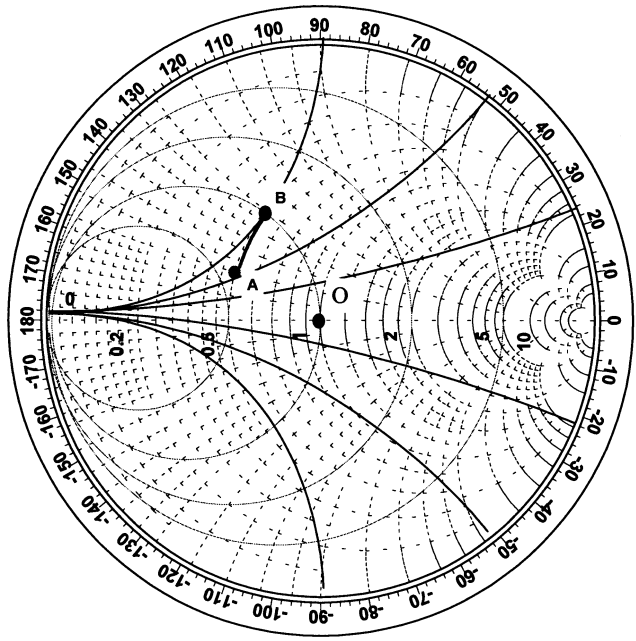

Figure 5.29 Graphical solution to Example 5.12.

SUGGESTED READING

I. Bahl and P. Bhartia, *Microwave Solid State Circuit Design*. New York: Wiley, 1988.

R. E. Collin, *Foundations for Microwave Engineering*. New York: McGraw Hill, 1992.

V. F. Fusco, *Microwave Circuits*. Englewood Cliffs, NJ: Prentice Hall, 1987.

D. M. Pozar, *Microwave Engineering*. New York: Wiley, 1998.

S. Ramo. J. R. Whinnery, and T. Van Duzer, *Fields and Waves in Communication Electronics*. New York: Wiley, 1994.

Peter A. Rizzi, *Microwave Engineering*. Englewood Cliffs, NJ: Prentice Hall, 1988.

W. Sinnema, *Electronic Transmission Technology*. Englewood Cliffs, NJ: Prentice Hall, 1988.

PROBLEMS

1. A 10-V (rms) voltage source in series with 50-Ω resistance represents a signal generator. It is to be matched with a 100-Ω load. Design a matching circuit that provides perfect matching over the frequency band of 1 kHz to 1 GHz. Determine power delivered to the load.

2. A 1000-Ω load is to be matched with a signal generator that can be represented by a 1-A (root-mean-square) current source in parallel with 100-Ω resistance. Design a resistive circuit to match it. Determine the power dissipated in the matching network.

3. Design a single-stub network to match a $800 - j300$-Ω load to a 400-Ω lossless line. The stub should be located as close to the load as possible and it is to be connected in parallel with the transmission line.

4. A $140 - j70$-Ω load is terminating a 70-Ω transmission-line, as shown below. Find the location and length of a short-circuited stub of 40-Ω characteristic impedance that will match the load with the line.

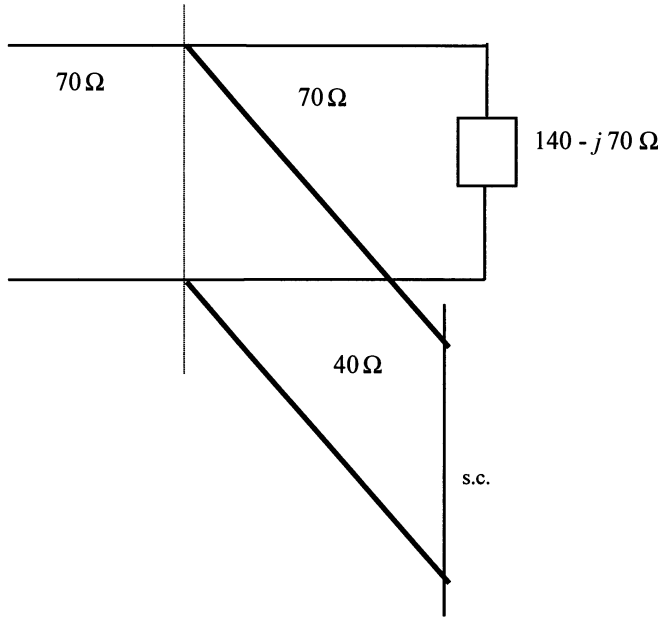

5. An antenna has impedance of $40 + j30$ ohm at its input. Match it with a 50-Ω line using short-circuited shunt stubs. Determine (a) required stub admittance, (b) distance between the stub and the antenna, (c) stub length, and (d) VSWR on each section of the circuit.

6. A lossless 100-Ω transmission line is to be matched with a $100 + j100$-Ω load using double-stub tuner. Separation between the two stubs is $\lambda/8$ and its characteristic impedance is 100 Ω. Load is connected right at the location of

the first stub. Determine the shortest possible lengths of the two stubs to obtain the matched condition. Also find VSWR between the two stubs.

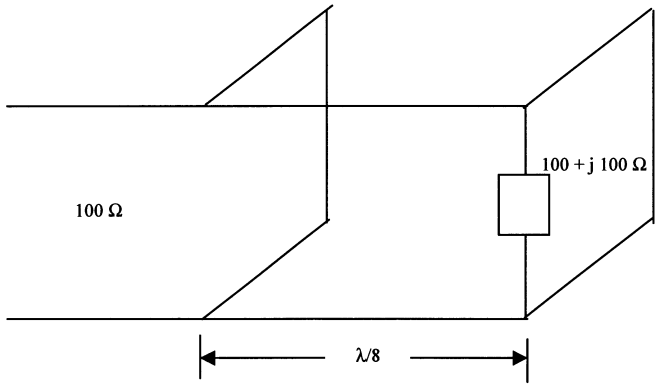

7. A lossless 75-ohm transmission line is to be matched with a $150 + j15$-Ω load using a shunt-connected double-stub tuner. Separation between the two stubs is $\lambda/8$ and its characteristic impedance is 75 ohm. The stub closest to the load (first stub) is $\lambda/2$ away from it. Determine the shortest possible lengths of the two stubs to obtain the matched condition. Also find the VSWR between the two stubs.

8. Complete or verify the following two interstage designs of 1 GHz.

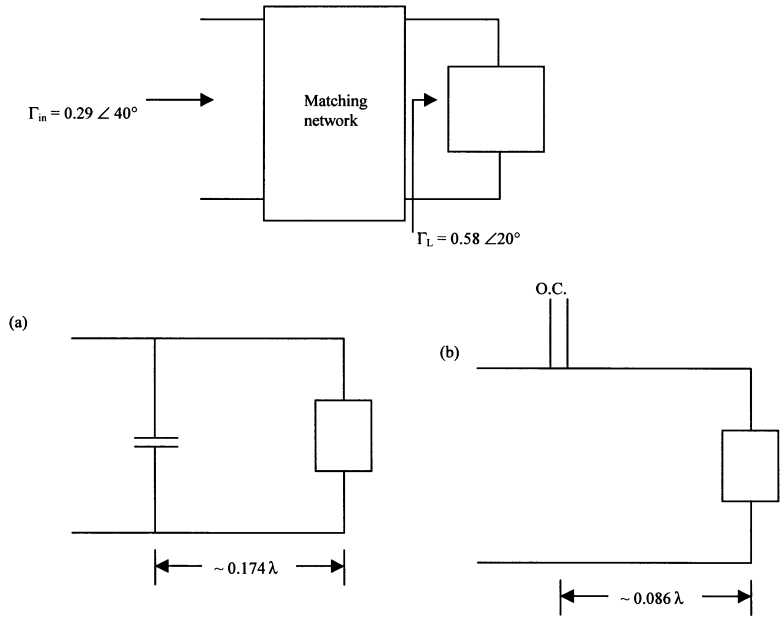

9. Complete or verify the following two interstage designs of 1 GHz. Assume that characteristic impedance is 50 ohm.

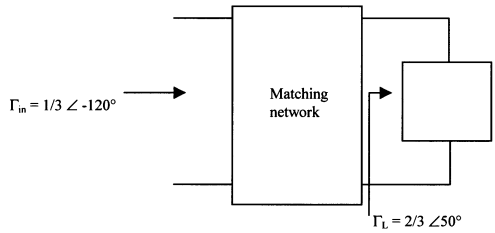

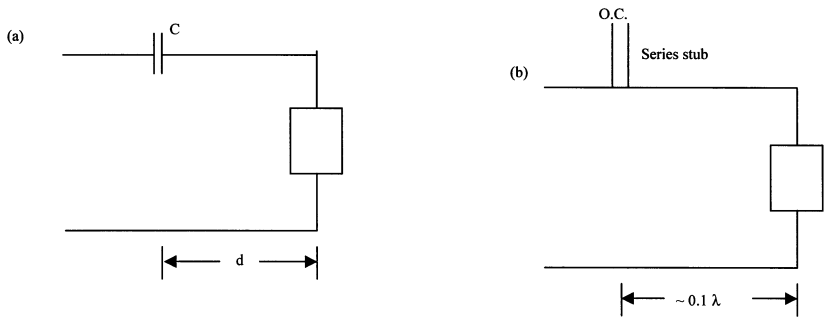

10. Complete or verify the following interstage designs at $f = 4$ GHz.

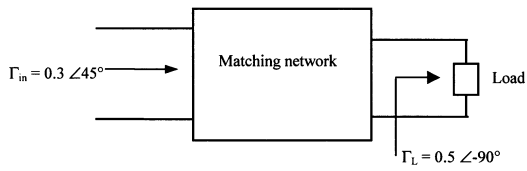

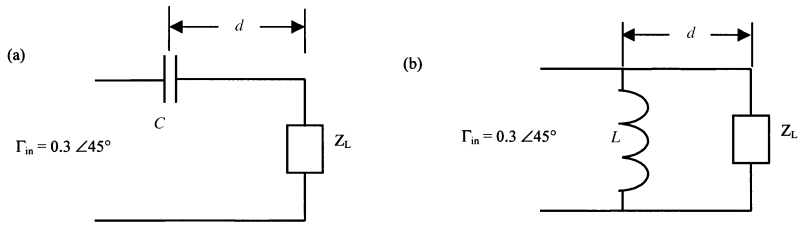

11. Complete or verify the following interstage designs at $f = 4$ GHz. The characteristic impedance is 50 Ω.

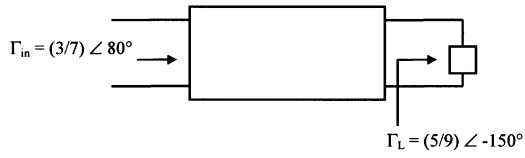

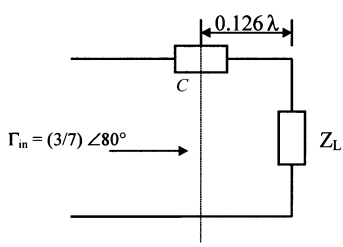

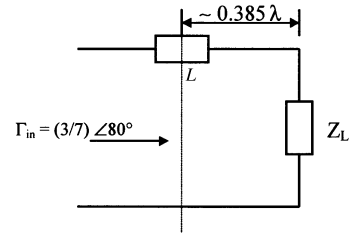

12. Two types of L-section matching networks are shown below. Select one that can match the load $Z_L = 20 - j100$ Ω to a 50-Ω transmission line. Find the element values at 500 MHz.

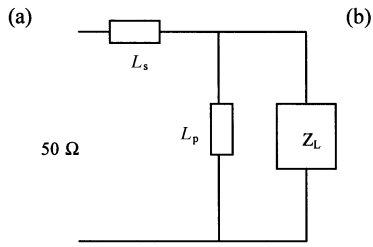

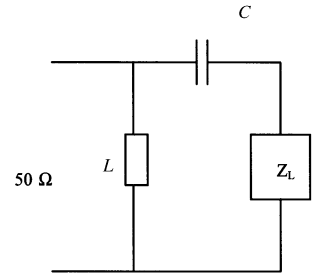

13. Two types of L-section matching networks are shown below. Select one that can match a $30 + j50$-Ω load to a 50-Ω line at 1 GHz.

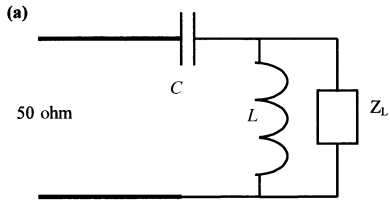

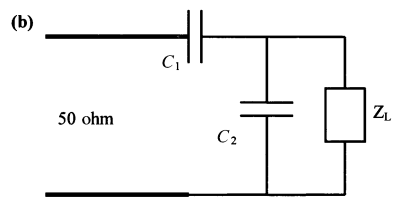

14. Design a matching network that will transform a $50 - j50$-ohm load to the input impedance of $25 + j25$ ohm.

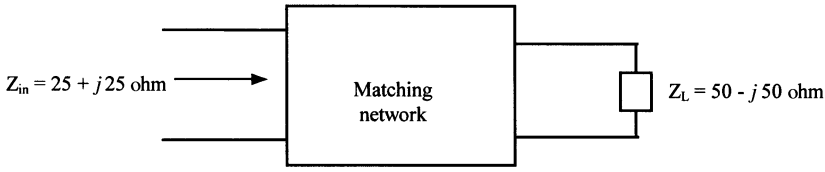

15. Match the following load to a 50-Ω generator using lumped elements. Assume the signal frequency at 4 GHz.

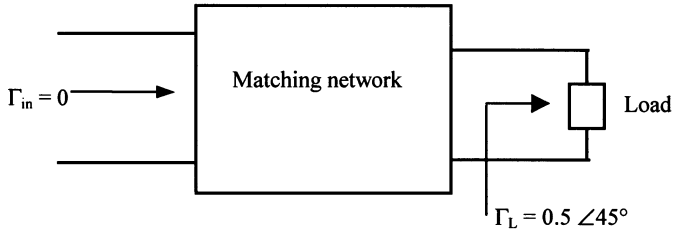

16. Two types of L-section matching networks are shown below. Select one that can match the load $Z_L = 60 - j20\ \Omega$ to a 50-Ω transmission line. Find the element values at 500 MHz.

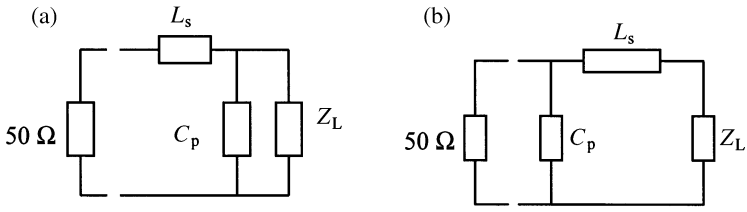

17. Design a lumped-element network that will provide a load $Z_L = 30 + j50$ ohm for the following amplifier operating at 2 GHz.

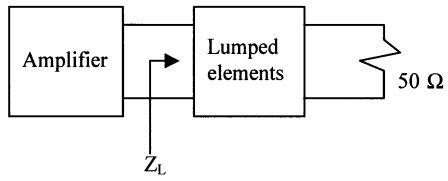

18. A 200-ohm load is to be matched with a 50-ohm line. Design (a) a resistive network and (b) a reactive network to match the load. (c) Compare the performance of the two designs.

Radio-Frequency and Microwave Communication Circuits: Analysis and Design
Devendra K. Misra

ISBNs: 0-471-41253-8 (Hardback); 0-471-22435-9 (Electronic)

6

IMPEDANCE TRANSFORMERS

In the preceding chapter, several techniques were considered to match a given load impedance at a fixed frequency. These techniques included transmission line stubs as well as lumped elements. Note that lumped-element circuits may not be practical at higher frequencies. Further, it may be necessary in certain cases to keep the reflection coefficient below a specified value over a given frequency band. This chapter presents transmission line impedance transformers that can meet such requirements. The chapter begins with the single-section impedance transformer that provides perfect matching at a single frequency. Matching bandwidth can be increased at the cost of a higher reflection coefficient. This concept is used to design multisection transformers. The characteristic impedance of each section is controlled to obtain the desired pass-band response.

Multisection binomial transformers exhibit almost flat reflection coefficient about the center frequency and increase gradually on either side. A wider bandwidth is achieved with an increased number of quarter-wave sections. Chebyshev transformers can provide even wider bandwidth with the same number of sections but the reflection coefficient exhibits ripples in its pass-band. This chapter includes a procedure to design these multisection transformers as well as transmission line tapers. The chapter concludes with a brief discussion on the Bode-Fano constraints, which provide an insight into the trade-off between the bandwidth and allowed reflection coefficient.

6.1 SINGLE SECTION QUARTER-WAVE TRANSFORMER

We considered a single-section quarter-wavelength transformer design problem earlier in Example 3.5. This section presents a detailed analysis of such circuits. Consider the load resistance R_L that is to be matched with a transmission line of characteristic impedance Z_o. Assume that a transmission line of length ℓ and characteristic impedance Z_1 is connected between the two, as shown in Figure 6.1. Its input impedance Z_{in} is found as follows.

$$Z_{in} = Z_1 \frac{R_L + jZ_1 \tan(\beta\ell)}{Z_1 + jR_L \tan(\beta\ell)} \tag{6.1.1}$$

For $\beta\ell = 90^\circ$ (i.e., $\ell = \lambda/4$) and $Z_1 = \sqrt{Z_o R_L}$, Z_{in} is equal to Z_o and, hence, there is no reflected wave beyond this point toward the generator. However, it reappears at other frequencies when $\beta\ell \neq 90^\circ$. The corresponding reflection coefficient Γ_{in} can be determined as follows.

$$\Gamma_{in} = \frac{Z_{in} - Z_o}{Z_{in} + Z_o} = \frac{Z_1 \dfrac{R_L + jZ_1 \tan(\beta\ell)}{Z_1 + jR_L \tan(\beta\ell)} - Z_o}{Z_1 \dfrac{R_L + jZ_i \tan(\beta\ell)}{Z_1 + jR_L \tan(\beta\ell)} + Z_o} = \frac{R_L - Z_o}{R_L + Z_o + j2\sqrt{Z_o R_L}\tan(\beta\ell)}$$

$$= \rho_{in} \exp(j\varphi)$$

$$\therefore \rho_{in} = \frac{R_L - Z_o}{\{(R_L + Z_o)^2 + 4Z_o R_L \tan^2(\beta\ell)\}^{1/2}} = \frac{1}{\left\{1 + \left(\dfrac{2\sqrt{Z_o R_L}}{R_L - Z_o}\sec(\beta\ell)\right)^2\right\}^{1/2}} \tag{6.1.2}$$

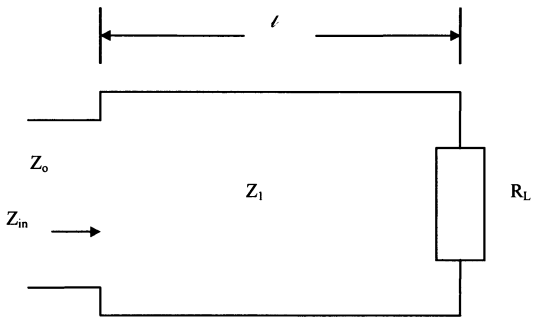

Figure 6.1 A single-section quarter-wave transformer.

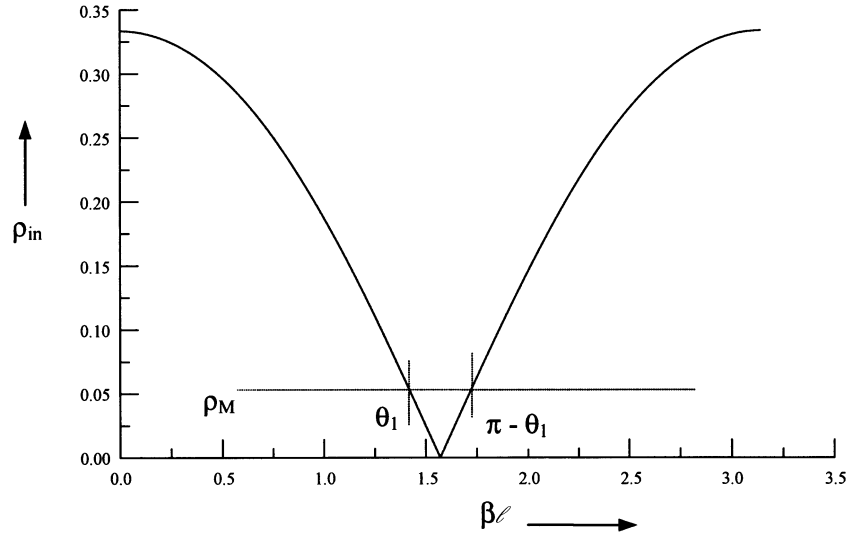

Figure 6.2 Reflection coefficient characteristics of a single section impedance transformer used to match a 100-Ω load to a 50-Ω line.

Variation in ρ_{in} with frequency is illustrated in Figure 6.2. For $\beta\ell$ near 90°, it can be approximated as follows:

$$\rho_{in} \approx \frac{|R_L - z_o|}{2\sqrt{Z_o R_L}\tan(\beta\ell)} \approx \frac{|R_L - Z_o|}{2\sqrt{Z_o R_L}}\cos(\beta\ell) \tag{6.1.3}$$

If ρ_M is the maximum allowable reflection coefficient at the input, then

$$\cos(\theta_1) = \left|\frac{2\rho_M\sqrt{Z_o R_L}}{(R_L - Z_o)\sqrt{1-\rho_M^2}}\right|; \quad \theta_1 < \pi/2 \tag{6.1.4}$$

In the case of a TEM wave propagating on the transmission line, $\beta\ell = \dfrac{\pi}{2}\times\dfrac{f}{f_o}$, where f_o is the frequency at which $\beta\ell = \dfrac{\pi}{2}$. In this case, the bandwidth $(f_2 - f_1) = \Delta f$ is given by

$$\Delta f = (f_2 - f_1) = 2(f_o - f_1) = 2\left(f_o - \frac{2f_o}{\pi}\theta_1\right) \tag{6.1.5}$$

and the fractional bandwidth is

$$\frac{\Delta f}{f_o} = 2 - \frac{4}{\pi}\cos^{-1}\left|\frac{2\rho_M\sqrt{Z_o R_L}}{(R_L - Z_o)\sqrt{1-\rho_M^2}}\right| \tag{6.1.6}$$

Example 6.1: Design a single-section quarter-wave impedance transformer to match a 100-Ω load to a 50-Ω air-filled coaxial line at 900 MHz. Determine the range of frequencies over which the reflection coefficient remains below 0.05.

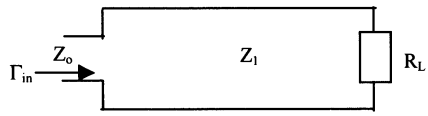

For $R_L = 100\,\Omega$ and $Z_o = 50\,\Omega$

$$Z_1 = \sqrt{100 \times 50} = 70.7106781\,\Omega$$

and,

$$\ell = \frac{\lambda}{4} = \frac{3 \times 10^8}{4 \times 900 \times 10^6}\,\text{m} = 8.33\,\text{cm}$$

Magnitude of the reflection coefficient increases as $\beta\ell$ changes from $\pi/2$ (i.e., the signal frequency changes from 900 MHz). If the maximum allowed ρ is $\rho_M = 0.05$(VSWR = 1.1053), then fractional bandwidth is found to be

$$\frac{\Delta f}{f_o} = 2 - \frac{4}{\pi}\cos^{-1}\left|\frac{2\rho_M\sqrt{Z_o R_L}}{(R_L - Z_o)\sqrt{1-\rho_M^2}}\right| = 0.180897$$

Therefore, 818.5964 MHz$\leq f \leq$981.4037 MHz or 1.4287$\leq \beta\ell \leq$1.7129.

6.2 MULTI-SECTION QUARTER-WAVE TRANSFORMERS

Consider an N-section impedance transformer connected between a transmission line of characteristic impedance of Z_o and load R_L, as shown in Figure 6.3. As indicated, the length of every section is the same while their characteristic impedances are different. Impedance at the input of Nth section can be found as follows:

$$Z_{in}^N = Z_N \frac{\exp(j\beta\ell) + \Gamma_N \exp(-j\beta\ell)}{\exp(j\beta\ell) - \Gamma_N \exp(-j\beta\ell)} \tag{6.2.1}$$

where

$$\Gamma_N = \frac{R_L - Z_N}{R_L + Z_N} \tag{6.2.2}$$

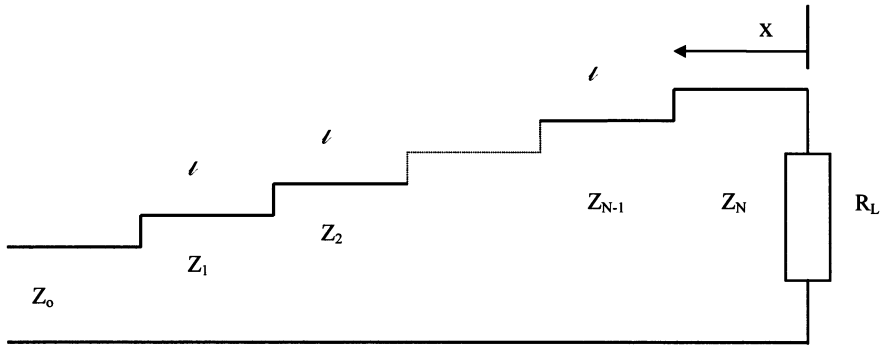

Figure 6.3 An N-section impedance transformer.

The reflection coefficient seen by the (N-1)st section is

$$\Gamma'_{N-1} = \frac{Z_{\text{in}}^N - Z_{N-1}}{Z_{\text{in}}^N + Z_{N-1}} = \frac{Z_N(e^{j\beta\ell} + \Gamma_N e^{-j\beta\ell}) - Z_{N-1}(e^{j\beta\ell} - \Gamma_N e^{-j\beta\ell})}{Z_N(e^{j\beta\ell} + \Gamma_N e^{-j\beta\ell}) + Z_{N-1}(e^{j\beta\ell} - \Gamma_N e^{-j\beta\ell})}$$

or,

$$\Gamma'_{N-1} = \frac{(Z_N - Z_{\text{N}-1})e^{j\beta\ell} + \Gamma_N(Z_N + Z_{\text{N}-1})e^{-j\beta\ell}}{(Z_N + Z_{\text{N}-1})e^{j\beta\ell} + \Gamma_N(Z_N - Z_{\text{N}-1})e^{-j\beta\ell}}$$

Therefore,

$$\Gamma'_{N-1} = \frac{\Gamma_{N-1} + \Gamma_N e^{-j2\beta\ell}}{1 + \Gamma_N \Gamma_{N-1} e^{-j2\beta\ell}} \tag{6.2.3}$$

where

$$\Gamma_{N-1} = \frac{Z_N - Z_{N-1}}{Z_N + Z_{N-1}} \tag{6.2.4}$$

If Z_N is close to R_{L} and Z_{N-1} is close to Z_N, then Γ_N and Γ_{N-1} are small quantities, and a first-order approximation can be assumed. Hence,

$$\Gamma'_{N-1} \approx \Gamma_{N-1} + \Gamma_N e^{-j2\beta\ell} \tag{6.2.5}$$

Similarly,

$$\Gamma'_{N-2} \approx \Gamma_{N-2} + \Gamma'_N e^{-j2\beta\ell} = \Gamma_{N-2} + \Gamma_{N-1} e^{-j2\beta\ell} + \Gamma_N e^{-j4\beta\ell}$$

Therefore, by induction, the reflection coefficient seen by the feeding line is

$$\Gamma \approx \Gamma_0 + \Gamma_1 e^{-j2\beta\ell} + \Gamma_2 e^{-j4\beta\ell} + \cdots + \Gamma_{N-1} e^{-j2(N-1)\beta\ell} + \Gamma_N e^{-j2N\beta\ell} \tag{6.2.6}$$

or,

$$\Gamma = \sum_{n=0}^{N} \Gamma_n e^{-j2n\beta\ell} \tag{6.2.7}$$

where

$$\Gamma_n = \frac{Z_{n+1} - Z_n}{Z_{n+1} + Z_n} \tag{6.2.8}$$

Thus, we need a procedure to select Γ_n so that Γ is minimized over the desired frequency range. To this end, we recast the above equation as follows:

$$\Gamma = \Gamma_0 + \Gamma_1 w + \Gamma_2 w^2 + \cdots + \Gamma_N w^N = \Gamma_N \prod_{n=1}^{N} (w - w_n) \tag{6.2.9}$$

where

$$\varphi = -2\beta\ell \tag{6.2.10}$$

and,

$$w = e^{j\varphi} \tag{6.2.11}$$

Note that for $\beta\ell = 0$ (i.e., $\lambda \to \infty$), individual transformer sections in effect have no electrical length and load R_L appears to be directly connected to the main line. Therefore,

$$\Gamma = \sum_{n=0}^{N} \Gamma_n = \frac{R_L - Z_o}{R_L + Z_o}, \quad (\because \ w = 1) \tag{6.2.12}$$

and, only N of the $N + 1$ section reflection coefficients can be selected independently.

6.3 TRANSFORMER WITH UNIFORMLY DISTRIBUTED SECTION REFLECTION COEFFICIENTS

If all of the section reflection coefficients are equal then (6.2.9) can be simplified as follows:

$$\frac{\Gamma}{\Gamma_N} = 1 + w + w^2 + w^3 + \cdots + w^{N-1} + w^N = \frac{w^{N+1} - 1}{w - 1} \tag{6.3.1}$$

or,

$$\frac{\Gamma}{\Gamma_N} = \frac{e^{j(N+1)\varphi} - 1}{e^{j\varphi} - 1} = e^{jN\varphi/2} \frac{\sin\left(\dfrac{N+1}{2}\varphi\right)}{\sin\left(\dfrac{\varphi}{2}\right)}$$

Hence,

$$|\Gamma| = \rho(\varphi) = \rho_N \left| \frac{\sin\left(\dfrac{N+1}{2}\varphi\right)}{\sin\left(\dfrac{\varphi}{2}\right)} \right| = (N+1)\rho_N \left| \frac{\sin\left(\dfrac{N+1}{2}\varphi\right)}{(N+1)\sin\left(\dfrac{\varphi}{2}\right)} \right| \tag{6.3.2}$$

and, from (6.2.12),

$$\sum_{n=0}^{N} \Gamma_n = (N+1)\rho_N = \frac{R_\mathrm{L} - Z_\mathrm{o}}{R_\mathrm{L} + Z_\mathrm{o}} \tag{6.3.3}$$

Therefore, equation (6.3.2) can be written as follows:

$$\rho(\beta\ell) = \left| \frac{R_\mathrm{L} - Z_\mathrm{o}}{R_\mathrm{L} + z_\mathrm{o}} \right| \cdot \left| \frac{\sin\{(N+1)\beta\ell\}}{(N+1)\sin(\beta\ell)} \right| \tag{6.3.4}$$

This can be viewed as an equation that describes magnitude ρ of the reflection coefficient as a function of frequency. As (6.3.4) indicates, a pattern of $\rho(\beta\ell)$ repeats periodically with an interval of π. It peaks at $n\pi$, where n is an integer including zero. Further, there are $N - 1$ minor lobes between two consecutive main peaks. The number of zeros between the two main peaks of $\rho(\beta\ell)$ is equal to the number of quarter-wave sections, N.

Consider that there are three quarter-wave sections connected between a 100-ohm load and a 50-ohm line. Its reflection coefficient characteristics can be found from (6.3.4), as illustrated in Figure 6.4. There are three zeros in it, one at $\beta\ell = \pi/2$ and the other two symmetrically located around this point. In other words, zeros occur at $\beta\ell = \pi/4$, $\pi/2$, and $3\pi/4$. When the number of quarter-wave sections is increased from 3 to 6, the $\rho(\beta\ell)$ plot changes as illustrated in Figure 6.5.

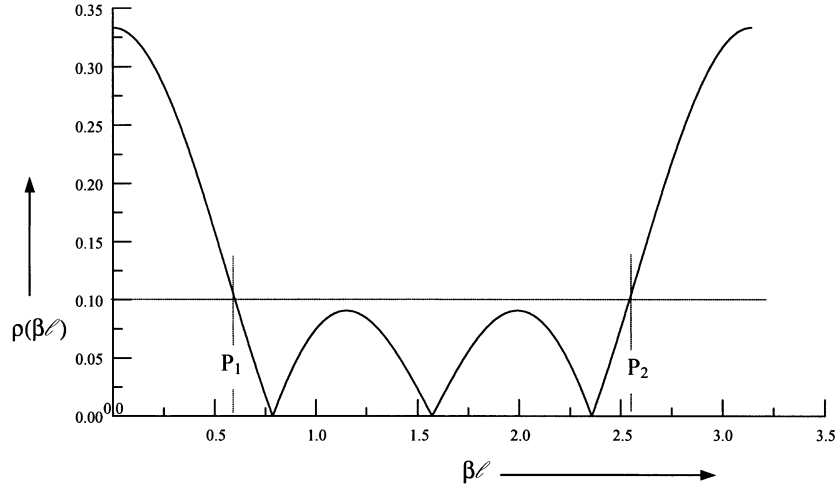

Figure 6.4 Reflection coefficient versus $\beta\ell$ of a three-section transformer with equal section reflection coefficients for $R_L = 100\,\Omega$ and $Z_o = 50\,\Omega$.

For a six-section transformer, Figure 6.5 shows five minor lobes between two main peaks of $\rho(\beta\ell)$. One of these minor lobes has its maximum value (peak) at $\beta\ell = \pi/2$. Six zeros of this plot are symmetrically located, $\beta\ell = n\pi/7$, $n = 1, 2, \ldots, 6$. Thus, characteristics of $\rho(\beta\ell)$ can be summarized as follows:

- Pattern of $\rho(\beta\ell)$ repeats with an interval of π.
- There are N nulls and $(N - 1)$ minor peaks in an interval.

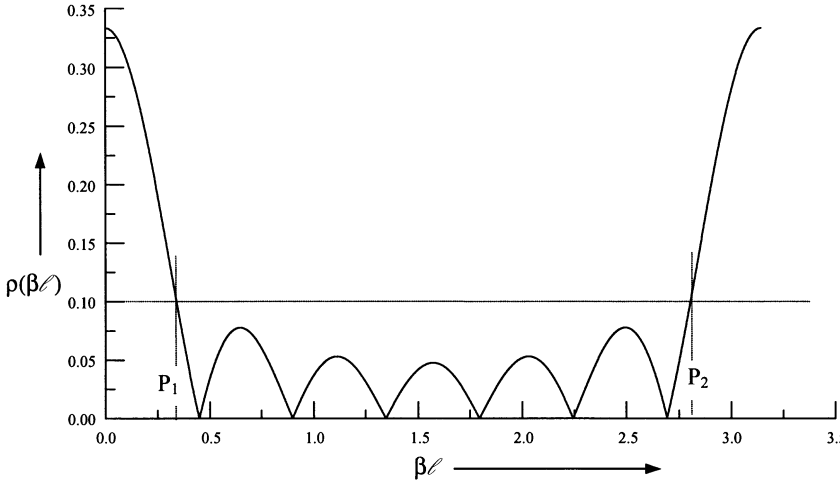

Figure 6.5 Reflection coefficient versus $\beta\ell$ for a six-section transformer with equal section reflection coefficients ($R_L = 100\,\Omega$ and $Z_o = 50\,\Omega$).

- When N is odd, one of the nulls occurs at $\beta\ell = \pi/2$ (i.e., $\ell = \lambda/4$).
- If ρ_M is specified as an upper bound on ρ to define the frequency band then points P_1 and P_2 bound the acceptable range of $\beta\ell$. This range becomes larger as N increases.

Since

$$w^{N+1} - 1 = \prod_{n=0}^{N} (w - w_n) \tag{6.3.5}$$

where

$$w_n = e^{j\frac{2\pi n}{(N+1)}}, \quad n = 1, 2, \ldots, N \tag{6.3.6}$$

(6.3.1) may be written as follows:

$$\frac{\Gamma}{\Gamma_N} = \prod_{n=1}^{N}(w - w_n) = \prod_{n=1}^{N}\left(w - e^{j\frac{2\pi n}{(N+1)}}\right) \tag{6.3.7}$$

This equation is of the form of (6.2.9). It indicates that when section reflection coefficients are the same, roots are equispaced around the unit circle on the complex w-plane with the root at $w = 1$ deleted. This is illustrated in Figure 6.6 for $N = 3$. It follows that

$$\frac{\rho}{\rho_N} = \left|\prod_{n=1}^{N}\left(w - e^{j\frac{2\pi n}{N+1}}\right)\right| = \prod_{n=1}^{N}\left|\left(w - e^{j\frac{2\pi n}{N+1}}\right)\right| \tag{6.3.8}$$

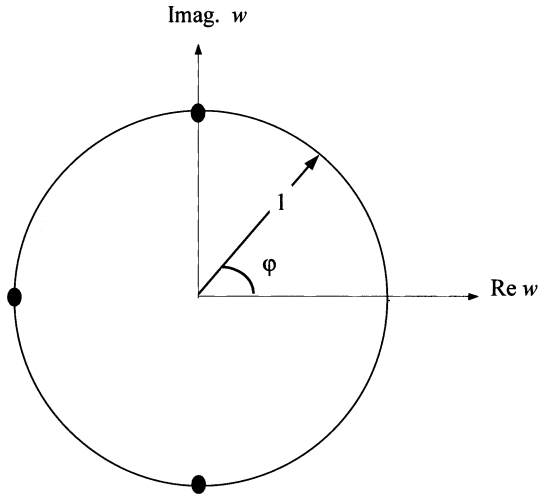

Figure 6.6 Location of zeros on a unit circle on the complex w-plane for $N = 3$.

Since $w = e^{j\varphi}$ is constrained to lie on the unit circle, distance between w and w_n is given by

$$d_n(\varphi) = \left| e^{j\varphi} - e^{j\frac{2\pi n}{N+1}} \right| \tag{6.3.9}$$

For the case of $N = 3$, $d_n(\varphi = 0)$ is illustrated in Figure 6.7. From (6.3.3), (6.3.8), and (6.3.9), we get

$$\rho(\varphi) = \frac{1}{N+1} \left| \frac{R_L - Z_o}{R_L + Z_o} \right| \prod_{n=1}^{N} d_n(\varphi) \tag{6.3.10}$$

Thus, as $\varphi = -2\beta\ell$ varies from 0 to 2 π, $w = e^{j\varphi}$ makes one complete traverse of the unit circle, and distances $d_1, d_2, \ldots, d_N$ vary with φ. If w coincides with the root w_n, then the distance d_n is zero. Consequently, the product of the distances is zero. Since the product of these distances is proportional to the reflection coefficient, $\rho(\varphi_n)$ goes to zero. It attains a local maximum whenever w is approximately halfway between successive roots.

Example 6.2: Design a four-section quarter-wavelength impedance transformer with uniform distribution of reflection coefficient to match a 100-Ω load to a 50-Ω air-filled coaxial line at 900 MHz. Determine the range of frequencies over which the reflection coefficient remains below 0.1. Compare this bandwidth with that obtained for a single-section impedance transformer.

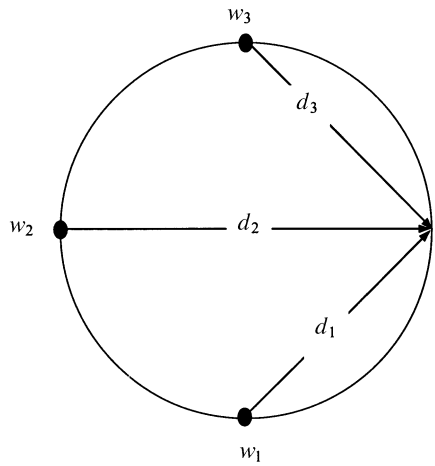

Figure 6.7 Graphical representation of (6.3.9) for $N = 3$ and $\varphi = 0$.

From (6.3.3) with $N = 4$ we have

$$\Gamma_4 = \frac{1}{5}\frac{100 - 50}{100 + 50} = \frac{1}{15}$$

and, from (6.2.2),

$$\frac{1}{15} = \frac{100 - Z_4}{100 + Z_4}$$

or,

$$100 + Z_4 = 1500 - 15 \cdot Z_4 \Rightarrow 16 \cdot Z_4 = 1400 \Rightarrow Z_4 = 87.5\,\Omega$$

Characteristic impedance of other sections can be determined from (6.2.8) as follows:

$$\frac{1}{15} = \frac{Z_4 - Z_3}{Z_4 + Z_3} \Rightarrow 87.5 + Z_3 = 15 \cdot 87.5 - 15 \cdot Z_3 \Rightarrow Z_3 = 76.5625\,\Omega$$

$$\frac{1}{15} = \frac{Z_3 - Z_2}{Z_3 + Z_2} \Rightarrow Z_2 = \frac{14 \cdot 76.5625}{16} = 66.9922\,\Omega \approx 67\,\Omega$$

and,

$$\frac{1}{15} = \frac{Z_2 - Z_1}{Z_2 + Z_1} \Rightarrow Z_1 = \frac{14 \cdot 67}{16} = 58.625\,\Omega$$

The frequency range over which reflection coefficient remains below 0.1 is determined from (6.3.4) as follows:

$$0.1 = \left|\frac{1}{3} \times \frac{\sin(5 \cdot \theta_m)}{5 \cdot \sin(\theta_m)}\right| \Rightarrow \left|\frac{\sin(5 \cdot \theta_m)}{\sin(\theta_m)}\right| = 1.5$$

where θ_m represents the value of $\beta\ell$ at which magnitude of reflection coefficient is equal to 0.1.

This is a transcendental equation that can be graphically solved. To that end, one needs to plot $|\sin(5\theta_m)|$ and $1.5|\sin(\theta_m)|$ versus θ_m on the same graph and look for the intersection of two curves. Alternatively, a numerical method can be employed to determine θ_m. Two solutions to this equation are found to be 0.476 and 2.665, respectively. Hence,

$$0.476 \leq \beta\ell \leq 2.665 \text{ or } 272.7 \text{ MHz} \leq f \leq 1.5269 \text{ Ghz}$$

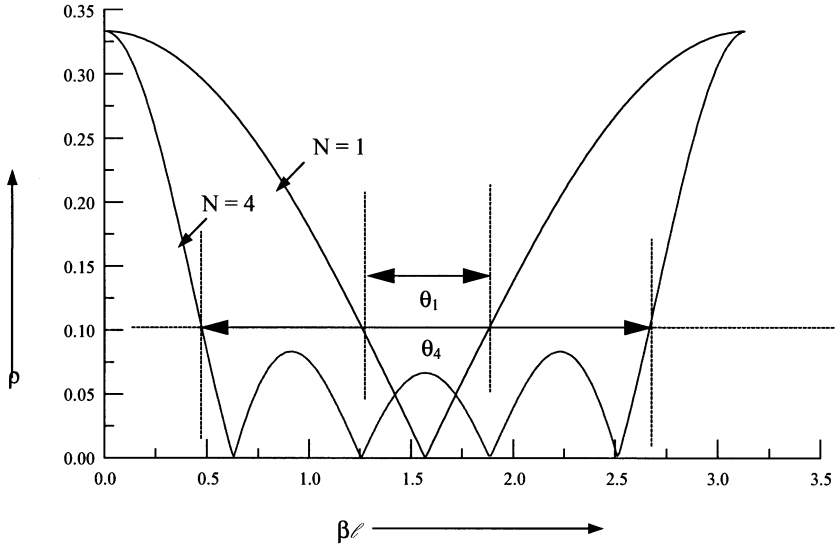

Figure 6.8 Reflection coefficient versus $\beta\ell$ for a four-section ($N = 4$) and a single-section ($N = 1$) impedance transformer.

Corresponding bandwidth with a single section can be evaluated as follows:

$$1.2841 \leq \beta\ell \leq 1.8575 \text{ or } 735.74\,\text{MHz} \leq f \leq 1.0643\,\text{GHz}$$

Reflection coefficient characteristics for two cases are displayed in Figure 6.8. Clearly, it has much wider bandwidth with four sections in comparison with that of a single section.

6.4 BINOMIAL TRANSFORMERS

As shown in Figures 6.4 and 6.5, there are peaks and nulls in the pass-band of a multisection quarter-wavelength transformer with uniform section reflection coefficients. This characteristic can be traced to equispaced roots on the unit circle. One way to avoid this behavior is to place all the roots at a common point w equal to -1. With this setting, distances d_n are the same for all cases and $\prod_{n=1}^{N}(w - w_n)$ goes to zero only once. It occurs for φ equal to $-\pi$, i.e., at $\beta\ell = \pi/2$. Thus, ρ is zero only for the frequency at which each section of the transformer is $\lambda/4$ long. With $w_n = -1$ for all n, equation (6.2.9) may be written as follows.

$$\frac{\Gamma}{\Gamma_N} = \prod_{n=1}^{N}(w - w_n) = (w + 1)^N = \sum_{m=0}^{N} \frac{N!}{m!(N-m)!} w^m \tag{6.4.1}$$

The following binomial expansion is used in writing (6.4.1).

$$(1+x)^m = \sum_{n=1}^{N} \frac{m!}{n!(m-n)!} x^n$$

A comparison of equation (6.4.1) with (6.2.7) indicates that

$$\frac{\Gamma_n}{\Gamma_N} = \frac{N!}{n!(N-n)!}; \quad n = 0, 1, 2, \ldots, N. \tag{6.4.2}$$

and therefore, the section reflection coefficients, normalized to Γ_N, are binomially distributed.

From equation (6.4.1),

$$\Gamma = \Gamma_N(w+1)^N \Rightarrow \Gamma(\beta\ell) = \Gamma_N(e^{-j2\beta\ell}+1)^N = \Gamma_N 2^N e^{-jN\beta\ell}[\cos(\beta\ell)]^N$$

or,

$$\rho(\beta\ell) = \rho_N 2^N |\cos(\beta\ell)|^N \tag{6.4.3}$$

For $\beta\ell = 0$, load R_L is effectively connected to input line. Therefore,

$$\rho(0) = \rho_N 2^N = \left|\frac{R_L - Z_o}{R_L + Z_o}\right| \tag{6.4.4}$$

and,

$$\rho(\beta\ell) = \left|\frac{R_L - Z_o}{R_L + Z_o}\right| \times |\cos(\beta\ell)|^N \tag{6.4.5}$$

Reflection coefficient characteristics of multisection binomial transformers versus $\beta\ell$ (in degrees) are illustrated in Figure 6.9. Reflection coefficient scale is normalized with the load reflection coefficient ρ_L. Unlike the preceding case of uniformly distributed section reflection coefficients, it shows a smooth characteristic without lobes.

Example 6.3: Design a four-section quarter-wavelength binomial impedance transformer to match a 100-Ω load to a 50-Ω air-filled coaxial line at 900 MHz. Determine the range of frequencies over which the reflection coefficient remains below 0.1. Compare this result with that obtained in Example 6.2.

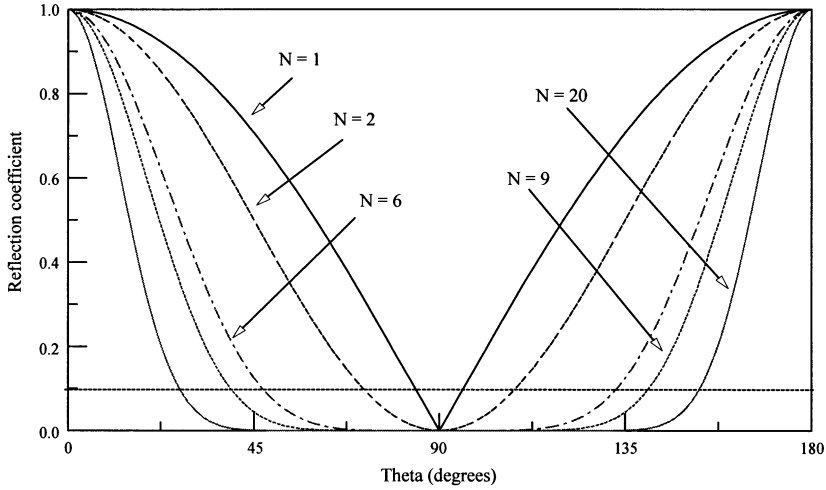

Figure 6.9 Reflection coefficient versus $\beta\ell$ for a multisection binomial transformer.

With $N = 4$ and $n = 0$, 1, and 2 in (6.4.2), we get

$$\frac{\Gamma_0}{\Gamma_4} = \frac{4!}{0!4!} = \frac{\Gamma_4}{\Gamma_4} \Rightarrow \Gamma_0 = \Gamma_4$$

$$\frac{\Gamma_1}{\Gamma_4} = \frac{4!}{1!3!} = \frac{\Gamma_3}{\Gamma_4} \Rightarrow \Gamma_1 = \Gamma_3 = 4 \times \Gamma_4$$

and,

$$\frac{\Gamma_2}{\Gamma_4} = \frac{4!}{2!2!} = 6 \Rightarrow \Gamma_2 = 6 \times \Gamma_4$$

From (6.4.4),

$$\rho(0) = \rho_N 2^N = \left|\frac{R_\mathrm{L} - Z_\mathrm{o}}{R_\mathrm{L} + Z_\mathrm{o}}\right| \Rightarrow \rho_4 = \frac{1}{2^4}\left|\frac{100 - 50}{100 + 50}\right| = \frac{1}{48} = 0.020833$$

and from (6.2.8),

$$\Gamma_\mathrm{n} = \frac{Z_{n+1} - Z_n}{Z_{n+1} + Z_n} \Rightarrow \rho_n(Z_{n+1} + Z_n) = Z_{n+1} - Z_n$$

Therefore,

$$Z_n = \frac{1 - \rho_n}{1 + \rho_n} \times Z_{n+1} \tag{6.4.6}$$

Alternatively,

$$Z_{n+1} = \frac{1+\rho_n}{1-\rho_n} \times Z_n \tag{6.4.7}$$

Characteristic impedance of each section can be determined from (6.4.6), as follows:

$$Z_4 = \frac{1-\frac{1}{48}}{1+\frac{1}{48}} \times 100 = 95.9184\,\Omega$$

$$Z_3 = \frac{1-\frac{4}{48}}{1+\frac{4}{48}} \times 95.9184 = 81.1617\,\Omega$$

$$Z_2 = \frac{1-\frac{6}{48}}{1+\frac{6}{48}} \times 81.1617 = 63.1258\,\Omega$$

and,

$$Z_1 = \frac{1-\frac{4}{48}}{1+\frac{4}{48}} \times 63.1258 = 53.4141\,\Omega$$

If we continue with this formula, we find that

$$Z_o = \frac{1-\frac{1}{48}}{1+\frac{1}{48}} \times 53.4141 = 51.2339\,\Omega$$

This is different from the given value of $50\,\Omega$. It happened because of approximation involved in the formula. Error keeps building up if the characteristic impedances are determined proceeding just one way. In order to minimize it, common practice is to determine the characteristic impedances up to half-way proceeding from the load side and then the remaining half from the input side. Thus, Z_1 and Z_2 should be determined from (6.4.7), as follows:

$$Z_1 = \frac{1+\frac{1}{48}}{1-\frac{1}{48}} \times 50 = 52.1277\,\Omega$$

and,

$$Z_2 = \frac{1+\dfrac{4}{48}}{1-\dfrac{4}{48}} \times 50 = 61.6054\,\Omega$$

The frequency range over which the reflection coefficient remains below 0.1 can be determined from (6.4.5) as follows.

$$0.1 = \tfrac{1}{3}\,|\cos(\vartheta_M)|^4 \Rightarrow \vartheta_M = 0.7376$$

Therefore,

$$0.7376 \leq \beta\ell \leq 2.404, \quad \text{or} \quad 422.61\ \text{MHz} \leq f \leq 1.3774\,\text{GHz}$$

Clearly, it has larger frequency bandwidth in comparison with that of a single section. However, it is less than the bandwidth obtained with uniformly distributed section reflection coefficients. Reflection coefficient as a function of $\beta\ell$ is illustrated in Figure 6.10.

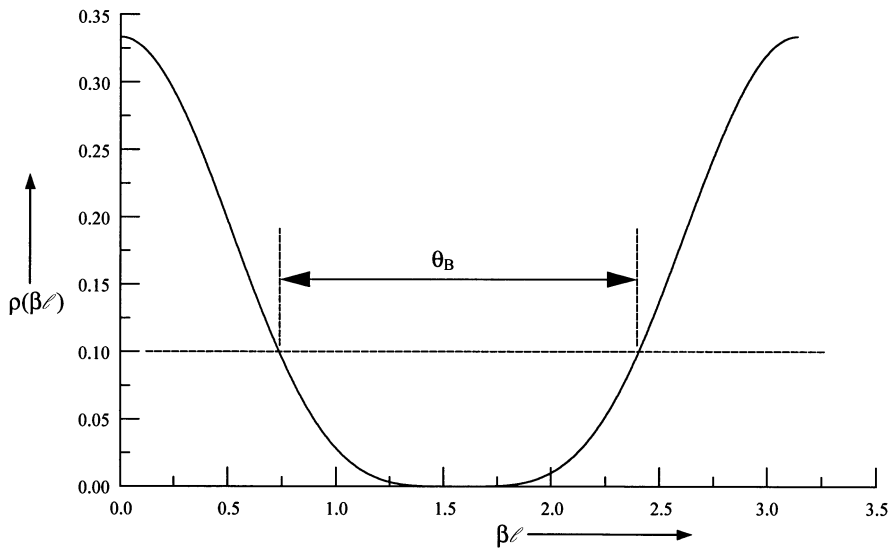

Figure 6.10 Reflection coefficient of a four-section binomial transformer versus $\beta\ell$.

6.5 CHEBYSHEV TRANSFORMERS

Consider again the case of a uniform three-section impedance transformer that is connected between a 50-ohm line and 100-ohm load. Distribution of zeros around the unit circle is shown in Figure 6.11 with solid points. Its frequency response is illustrated in Figure 6.12 as curve (a). Now, let us move two of these zeros to $\pm 120^\circ$ while keeping the remaining one fixed at 180°, as illustrated by unfilled points in Figure 6.11. With this change in the distribution of zeros on the complex w-plane, $\rho(\beta\ell)$ versus $\beta\ell$ varies as shown by curve (b) in Figure 6.12. It shows relatively much lower peaks of intervening lobes while widths as well as heights of the two main lobes increase. On the other hand, if we move the two zeros to $\pm 60^\circ$ then the main peaks go down while intervening lobes rise. This is illustrated by hatched points in Figure 6.11 and by curve (c) in Figure 6.12. In this case, minor lobes increase while the main lobes reduce in size. Note that zeros in this case are uniformly distributed around the unit circle and, therefore, its $\rho(\beta\ell)$ characteristic has identical lobes.

Thus, the heights of intervening lobes decrease at the cost of the main lobe when zeros are moved closer together. On the other hand, moving the zeros farther apart raises the level of intervening lobes but reduces the main lobe. However, we need a systematic method to determine the location of each zero for a maximum permissible reflection coefficient, ρ_M, and the number of quarter-wave sections, N. An optimal distribution of zeros around the unit circle will keep peaks of all pass-band lobes at the same height of ρ_M.

In order to have magnitudes of all minor lobes in the pass-band equal, section reflection coefficients are determined by the characteristics of Chebyshev functions,

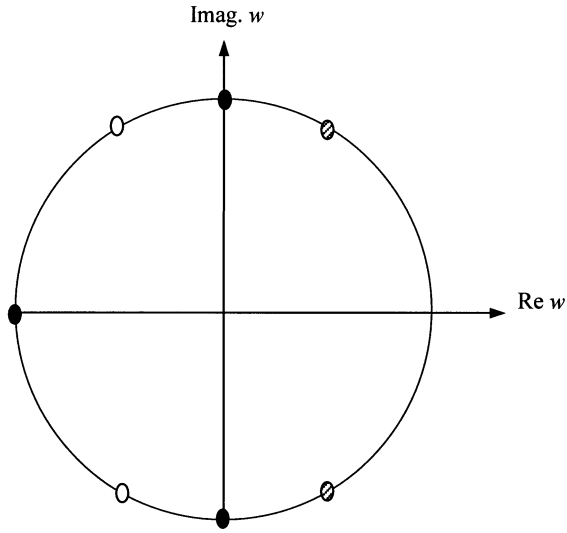

Figure 6.11 Distribution of zeros for a uniform three-section impedance transformer (solid), with two of those zeros moved to $\pm 120^\circ$ (unfilled), or to $\pm 60^\circ$ (hatched).

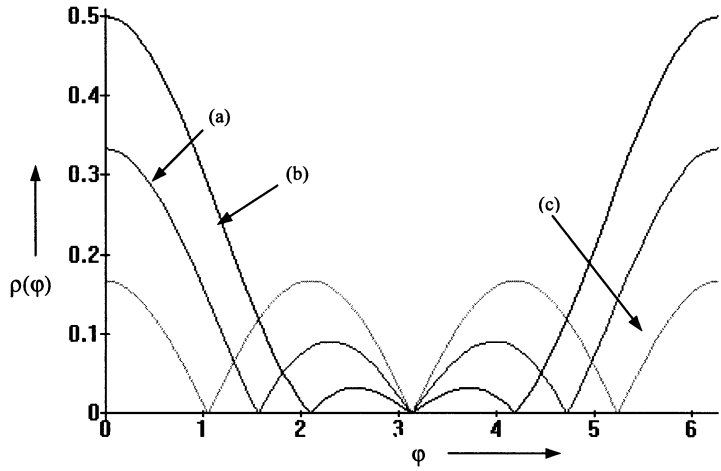

Figure 6.12 Reflection coefficient versus φ for (a) a uniform three-section transformer, (b) two zeros moved to $\pm 120^\circ$, and (c) two zeros moved to $\pm 60^\circ$.

named after a Russian mathematician who first studied them. These functions satisfy the following differential equation:

$$(1 - x^2)\frac{d^2 T_m(x)}{dx^2} - x\frac{dT_m(x)}{dx} + m^2 T_m(x) = 0 \tag{6.5.1}$$

Chebyshev functions of degree m, represented by $T_m(x)$, are mth degree polynomials that satisfy (6.5.1). The first four of these and a recurrence relation for higher-order Chebyshev polynomials are given as follows:

$$\begin{aligned} T_1(x) &= x \\ T_2(x) &= 2x^2 - 1 \\ T_3(x) &= 4x^3 - 3x \\ T_4(x) &= 8x^4 - 8x^2 + 1 \\ &\vdots \\ &\vdots \\ T_m(x) &= 2xT_{m-1}(x) - T_{m-2}(x) \end{aligned}$$

Alternatively,

$$T_m(x) = \begin{cases} \cos(m\cos^{-1}(x)) - 1 \le x \le 1 \\ \cosh(m\cosh^{-1}(x)) x \ge 1 \\ (-1)^m \cosh(m\cosh^{-1}|(x)|) x \le -1 \end{cases} \tag{6.5.2}$$

Note that, for $x = \cos(\theta)$,

$$T_m(\cos(\theta)) = \cos(m\theta) \tag{6.5.3}$$

Figure 6.13 depicts Chebyshev polynomials of degree 1 through 4. The following characteristics can be noted from it.

- Magnitudes of these polynomials oscillate between ± 1 for $-1 \leq x \leq 1$.
- For $|x| > 1$, $|T_m(x)|$ increases at a faster rate with x as m increases.
- Numbers of zeros are equal to the order of polynomials. Zeros of an even-order polynomial are symmetrically located about the origin, with one of the minor lobes' peak at $x = 0$.
- Polynomials of odd orders have one zero at $x = 0$ while the remaining zeros are symmetrically located.

These characteristics of Chebyshev polynomials are utilized to design an impedance transformer that has ripples of equal magnitude in its pass-band. The number of quarter-wave sections determines the order of Chebyshev polynomials and the distribution of zeros on the complex w-plane is selected according to that. With x_o properly selected, $|T_m(x)|$ precisely corresponds to $\rho(\beta\ell)$. This is done by linking $\beta\ell$ to x of Chebyshev polynomial as follows.

$$x = x_o \cos(\beta\ell) \tag{6.5.4}$$

Consider the design of a three-section equal-ripple impedance transformer. A Chebyshev polynomial of order three is appropriate for this case. Figure 6.14

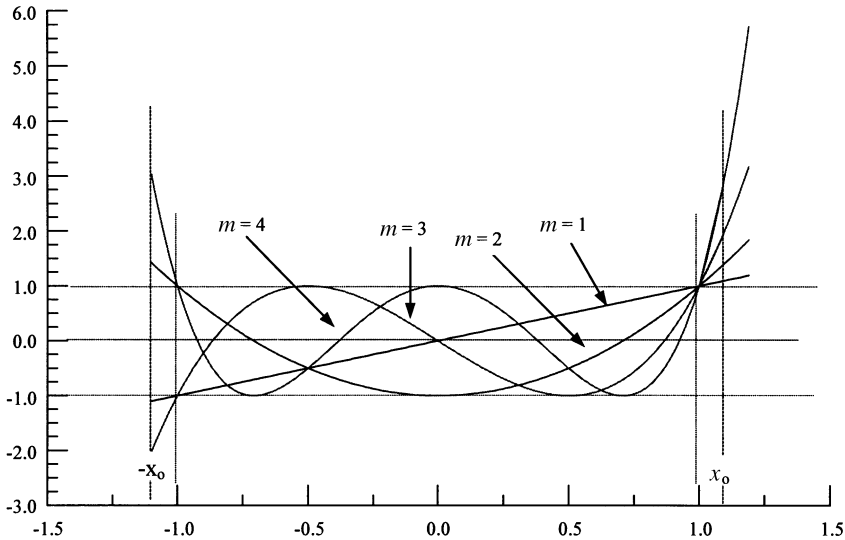

Figure 6.13 Chebyshev polynomials for $m = 1, 2, 3, 4$.

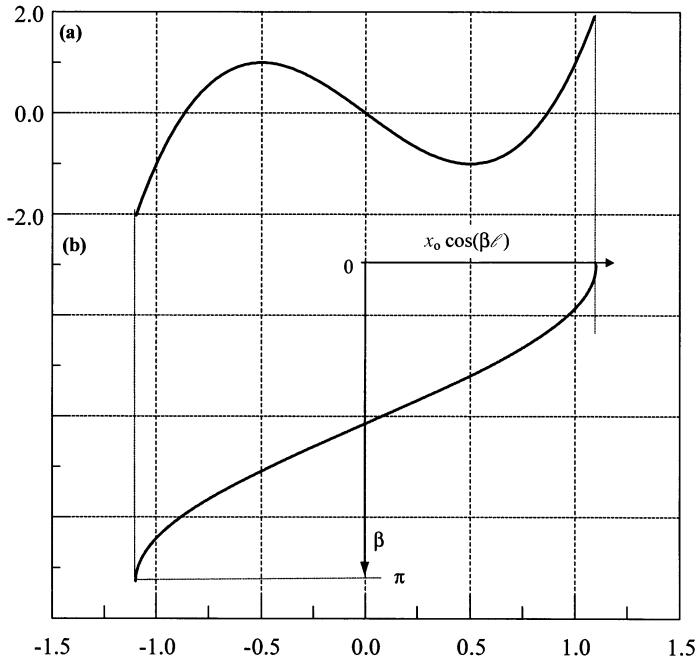

Figure 6.14 Third-order Chebyshev polynomial (a) and its variable, x versus $\beta\ell$ (b).

illustrates $T_3(x)$ together with (6.5.4). Note that Chebyshev variable x and angle φ on the complex w-plane are related through (6.5.4) because φ is equal to $-2\beta\ell$. As φ varies from 0 to -2π, x changes as illustrated in Figure 6.14 (b) and the corresponding $T_3(x)$ in Figure 6.14 (a). Figure 6.15 shows $|T_3(\varphi)|$ which can represent the desired $\rho(\varphi)$ provided that

$$\frac{T_3(\varphi = 0)}{1} = \frac{T_3(x_o)}{1} = \frac{|(R_L - Z_o)/(R_L + Z_o)|}{\rho_M} \tag{6.5.5}$$

where ρ_M is the maximum allowed reflection coefficient in the pass-band.

For an m-section impedance transformer, (6.5.5) can be written as follows:

$$T_m(x_o) = \left|\frac{R_L - Z_o}{R_L + Z_o}\right| \times \frac{1}{\rho_M} \tag{6.5.6}$$

Location x_o can now be determined from (6.5.2) as follows:

$$x_o = \cosh\left(\frac{1}{m} \times \cosh^{-1}(T_m(x_o))\right) \tag{6.5.7}$$

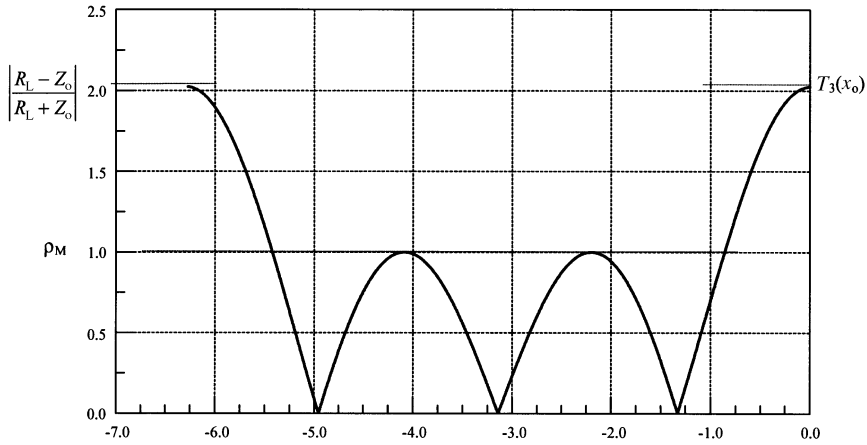

Figure 6.15 $|T_3(x)|$ versus φ and its relationship with the desired $\rho(\varphi)$.

With x_o determined from (6.5.7), $|T_m(x)|$ represents the desired $\rho(\beta\ell)$. Hence, zeros of reflection coefficient are the same as those of $T_m(x)$. Since Chebyshev polynomials have zeros in the range of $-1 < x < 1$, zeros of $\rho(\varphi)$ can be determined from (6.5.2).

Therefore,

$$T_m(x_n) = 0 \Rightarrow \cos(m \times \cos^{-1}(x_n)) = 0 = \pm\cos\left((2n-1)\frac{\pi}{2}\right), \quad n = 1, 2, \ldots$$

where x_n is the location of the nth zero.

Hence,

$$x_n = \pm\cos\left((2n-1)\frac{\pi}{2m}\right) \tag{6.5.8}$$

and corresponding φ_n can be evaluated from (6.5.4) as follows.

$$\varphi_n = 2 \times \cos^{-1}\left(\frac{x_n}{x_o}\right) \tag{6.5.9}$$

Zeros of $\rho(\varphi)$, w_n, on the complex w-plane are now known because $w_n = e^{i\varphi_n}$. Equation (6.2.9) can be used to determine the section reflection coefficient, Γ_n. Z_n is, in turn, determined from equation (6.2.8).

Bandwidth of the impedance transformer extends from $x = -1$ to $x = +1$. With $\beta\ell = \theta_M$ at $x = 1$, (6.5.4) gives

$$\cos(\theta_M) = \frac{1}{x_o}$$

Therefore, bandwidth of a Chebyshev transformer can be expressed as follows.

$$\cos^{-1}\left(\frac{1}{x_{\mathrm{o}}}\right) \leq \beta\ell \leq \pi - \cos^{-1}\left(\frac{1}{x_{\mathrm{o}}}\right) \tag{6.5.10}$$

Example 6.4: Reconsider the matching of a 100-Ω to a 50-Ω line. Design an equal-ripple four-section quarter-wavelength impedance transformer and compare its bandwidth with those obtained earlier for $\rho_{\mathrm{M}} = 0.1$.

From (6.5.6),

$$T_4(x_{\mathrm{o}}) = \left|\frac{100-50}{100+50}\right| \times \frac{1}{0.1} = \frac{1}{0.3} = 3.3333$$

Therefore, now x_{o} can be determined from (6.5.7) as follows.

$$x_{\mathrm{o}} = \cosh\left(\frac{1}{4} \times \cosh^{-1}(3.3333)\right)$$

In case inverse hyperbolic functions are not available on a calculator, the following procedure can be used to evaluate x_{o}. Assume that $y = \cosh^{-1}(3.3333) \Rightarrow 3.3333 = \cosh(y) = \dfrac{e^{y}+e^{-y}}{2}$. Hence,

$$e^{y} + e^{-y} = 2 \times 3.3333 = 6.6666$$

or,

$$e^{2y} - 6.6666 \times e^{y} + 1 = 0 \Rightarrow e^{y} = \frac{6.6666 \pm \sqrt{(6.6666)^2 - 4}}{2} = 6.5131 \text{ and } 0.1535$$

$$y = \ln(6.5131) = 1.8738$$

Therefore,

$$\frac{1}{4}\cosh^{-1}(3.3333) = \frac{1.8738}{4} = 0.4684$$

and,

$$x_{\mathrm{o}} = \cosh(0.4684) = \frac{e^{0.4684} + e^{-0.4684}}{2} = 1.1117$$

Note that the other solution of e^{y} produces $y = -1.874$ and $x_{\mathrm{o}} = 1.1117$. From (6.5.8) and (6.5.9), we get

$$x_n = \pm 0.9239, \quad \pm 0.3827$$

and,

$$\varphi_n = -67.61^\circ, \quad -139.71^\circ, \quad -220.29^\circ, \quad -292.39^\circ$$

Therefore,

$$w_1 = 0.381 - j0.925$$
$$w_2 = -0.763 - j0.647$$
$$w_3 = -0.763 + j0.647$$

and,

$$w_4 = 0.381 + j0.925$$

Now, from equation (6.2.9) we get

$$\Gamma = \Gamma_4(1 + 0.764 \times w + 0.837 \times w^2 + 0.764 \times w^3 + w^4)$$

Therefore,

$$\Gamma_o = \Gamma_4, \Gamma_1 = \Gamma_3 = 0.764 \times \Gamma_4, \quad \text{and } \Gamma_2 = 0.837 \times \Gamma_4$$

From equation (6.2.12) we have

$$\Gamma = \sum_{n=0}^{N} \Gamma_n = \frac{R_L - Z_o}{R_L + Z_o} \Rightarrow 4.365 \times \Gamma_4 = \frac{R_L - Z_o}{R_L + Z_o}$$

$$\Gamma_4 = \frac{1}{4.365} \times \frac{100 - 50}{100 + 50} = 0.076$$

Hence,

$$\Gamma_o = \Gamma_4 = 0.076, \Gamma_1 = \Gamma_3 = 0.058, \quad \text{and } \Gamma_2 = 0.064$$

Now, characteristic impedance of each section can be determined from (6.2.8) as follows:

$$\Gamma_4 = \frac{Z_L - Z_4}{Z_L + Z_4} \Rightarrow Z_4 = \frac{1 - \Gamma_4}{1 + \Gamma_4} Z_L = 85.87\,\Omega$$

$$\Gamma_3 = \frac{Z_4 - Z_3}{Z_4 + Z_3} \Rightarrow Z_3 = \frac{1 - \Gamma_3}{1 + \Gamma_3} Z_4 = 76.46\,\Omega$$

$$\Gamma_2 = \frac{Z_3 - Z_2}{Z_3 + Z_2} \Rightarrow Z_2 = \frac{1 - \Gamma_2}{1 + \Gamma_2} Z_3 = 67.26\,\Omega$$

and,

$$\Gamma_1 = \frac{Z_2 - Z_1}{Z_2 + Z_1} \Rightarrow Z_1 = \frac{1 - \Gamma_1}{1 + \Gamma_1} Z_2 = 59.89\,\Omega$$

In order to minimize the accumulating error in Z_n, it is advisable to calculate half of the impedance values from the load side and the other half from the input side. In other words, Z_1 and Z_2 should be determined as follows:

$$Z_1 = \frac{1 + \Gamma_o}{1 - \Gamma_o} Z_o = 58.2251\,\Omega$$

and

$$Z_2 = \frac{1 + \Gamma_1}{1 - \Gamma_1} Z_1 = 65.3951\,\Omega$$

Bandwidth is determined from (6.5.10) as follows.

$$\cos(\beta\ell) = \frac{1}{x_o} = 0.899 \Rightarrow \beta\ell = 0.452$$

$$\therefore\ 0.452 \leq \beta\ell \leq 2.6896$$

Thus, bandwidth is greater than what was achieved from either a uniform or a binomial distribution of Γ_n coefficients.

6.6 EXACT FORMULATION AND DESIGN OF MULTISECTION IMPEDANCE TRANSFORMERS

The analysis and design presented so far is based on the assumption that the section reflection coefficients are small, as implied by (6.2.5). If this is not the case, an exact expression for the reflection coefficient must be used. Alternatively, there are design tables available in the literature[1] that can be used to synthesize an impedance transformer. In case of a two- or three-section Chebyshev transformer, the design procedure summarized below may be used as well.

Exact formulation of the multisection impedance transformer is conveniently developed via the power loss ratio, P_{LR}, defined as follows:

$$P_{LR} = \text{Power loss ratio} = \frac{\text{Incident power}}{\text{Power delivered to the load}}$$

[1] G.L. Matthaei, L. Young, and E.M.T. Jones, *Microwave Filters, Impedance-Matching Networks, and Coupling Structures*, Dedham, MA: Artech House, 1980.

If P_{in} represents the incident power and ρ_{in} is the input reflection coefficient, then

$$P_{LR} = \frac{P_{in}}{(1-\rho_{in}^2)P_{in}} = \frac{1}{1-\rho_{in}^2} \Rightarrow \rho_{in} = \sqrt{\frac{P_{LR}-1}{P_{LR}}} \tag{6.6.1}$$

For any transformer, ρ_{in} can be determined from its input impedance Z_{in}. The power loss ratio P_{LR} can subsequently be evaluated from (6.6.1). This P_{LR} can be expressed in terms of $Q_{2N}(\cos\theta)$, an even polynomial of degree $2N$ in $\cos\theta$. Hence,

$$P_{LR} = 1 + Q_{2N}(\cos\theta) \tag{6.6.2}$$

Coefficients of $Q_{2N}(\cos\theta)$ are functions of various impedances Z_n. For an equal ripple characteristic in the pass-band, a Chebyshev polynomial can be used to specify P_{LR} as follows:

$$P_{LR} = 1 + k^2 T_N^2(\sec\theta_M \cos\theta) \tag{6.6.3}$$

where k^2 is determined from the maximum value of P_{LR} in the pass-band. θ_M represents the value of $\beta\ell$ that corresponds to the maximum allowed reflection coefficient ρ_M. Since $T_N^2(\sec\theta_M \cos\theta)$ has a maximum value of unity in the pass-band, the extreme value of P_{LR} will be $1 + k^2$. Various characteristic impedances are determined by equating (6.6.2) and (6.6.3). Further, (6.6.1) produces a relation between ρ_M and k^2, as follows.

$$\rho_M = \sqrt{\frac{k^2}{1+k^2}} \tag{6.6.4}$$

For the two-section impedance transformer shown in Figure 6.16, reflection coefficient characteristics as a function of θ are illustrated in Figure 6.17. Power loss ratio for this transformer is found to be

$$P_{LR} = 1 + \frac{(Z_L - Z_o)^2}{4Z_L Z_o} \times \frac{(\sec^2\theta_z \cos^2\theta - 1)^2}{\tan^4\theta_z} \tag{6.6.5}$$

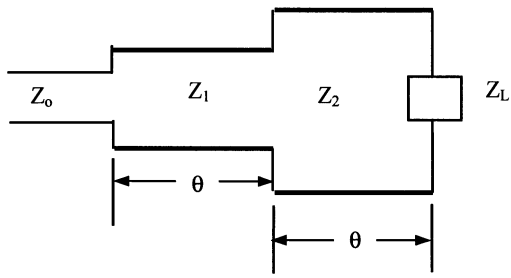

Figure 6.16 A two-section impedance transformer.

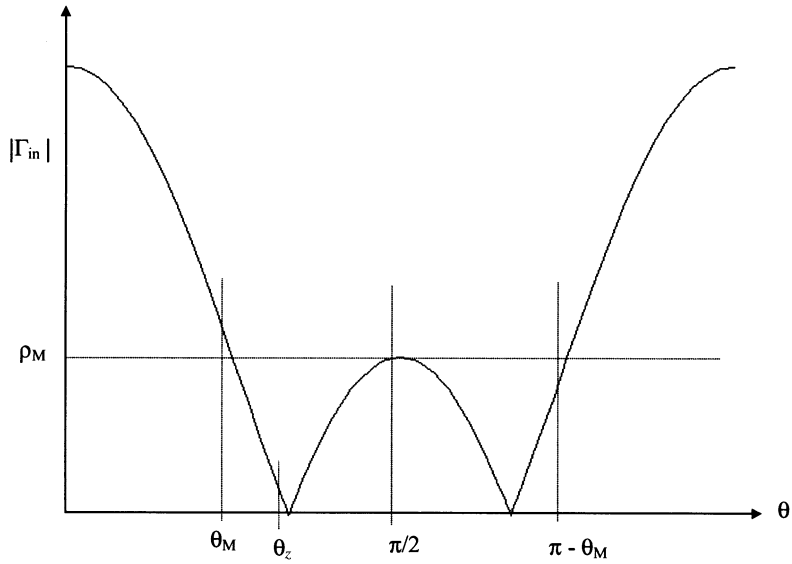

Figure 6.17 Reflection coefficient characteristics of a two-section Chebyshev transformer.

where θ_z is the value of θ at the lower zero (i.e., $\theta_z < \pi/2$), as shown in Figure 6.17.

Maximum power loss ratio, $P_{\text{LR Max}}$, is found to be

$$P_{\text{LR,Max}} = 1 + \frac{(Z_\text{L} - Z_\text{o})^2}{4Z_\text{L}Z_\text{o}} \cot^4 \theta_z \tag{6.6.6}$$

Hence,

$$k^2 = \frac{(Z_\text{L} - Z_\text{o})^2}{4Z_\text{L}Z_\text{o}} \cot^4 \theta_z \tag{6.6.7}$$

Required values of characteristic impedances, Z_1 and Z_2, are determined from the following equations:

$$Z_1^2 = Z_\text{o}^2 \left[\frac{(Z_\text{L} - Z_\text{o})^2}{4Z_\text{o}^2 \tan^4 \theta_z} + \frac{Z_\text{L}}{Z_\text{o}} \right]^{1/2} + \frac{(Z_\text{L} - Z_\text{o})Z_\text{o}}{2 \tan^2 \theta_z} \tag{6.6.8}$$

and,

$$Z_2 = \frac{Z_\text{L}}{Z_1} Z_\text{o} \tag{6.6.9}$$

Pass-band edge, θ_M, is given by

$$\theta_M = \cos^{-1}(\sqrt{2}\cos\theta_z) \tag{6.6.10}$$

Hence, bandwidth of this transformer is found as

$$\theta_M \le \theta = \beta\ell \le \pi - \theta_M \tag{6.6.11a}$$

For a TEM wave,

$$\frac{\Delta f}{f_o} = 2 - \frac{4\theta_M}{\pi} \tag{6.6.11b}$$

If bandwidth is specified in a design problem along with Z_L and Z_o, then θ_M is known. Therefore, θ_z can be determined from (6.6.10). Impedances Z_1 and Z_2 are determined subsequently from (6.6.8) and (6.6.9), respectively. The corresponding maximum reflection coefficient ρ_M can be easily evaluated following k^2 from (6.6.7). On the other hand, if ρ_M is specified instead of θ_M then k^2 is determined from (6.6.4). θ_z, in turn, is calculated from (6.6.7). Now, Z_1, Z_2, and θ_M can be determined from (6.6.8), (6.6.9), and (6.6.10), respectively.

In the limit $\theta_z \to \pi/2$, two zeros of ρ in Figure 6.17 come together to give a maximally flat transformer. In that case, (6.6.8) and (6.6.9) are simplified to give

$$Z_1 = Z_L^{1/4} \times Z_o^{3/4} \tag{6.6.12}$$

$$Z_2 = Z_L^{3/4} \times Z_o^{1/4} \tag{6.6.13}$$

and,

$$\theta_M = \cos^{-1}(\cot\theta_z) \tag{6.6.14}$$

Example 6.5: Use the exact theory to design a two-section Chebyshev transformer to match a 500-Ω load to a 100-Ω line. Required fractional bandwidth is 0.6. What is the resultant value of ρ_M.

From (6.6.10) and (6.6.11),

$$\frac{\Delta f}{f_o} = 2 - \frac{4}{\pi}\cos^{-1}(\sqrt{2}\cos\theta_z) \Rightarrow \cos\theta_z = \frac{1}{\sqrt{2}}\cos\left(\frac{2 - \dfrac{\Delta f}{f_o}}{\dfrac{4}{\pi}}\right)$$

$$= \frac{1}{\sqrt{2}}\cos\left(\frac{2 - 0.6}{4/\pi}\right) = 0.321$$

$$\therefore\ \theta_z = 1.244 \text{ radians}$$

and,

$$\theta_{\mathrm{M}} = \cos^{-1}(\sqrt{2}\cos\theta_z) = \cos^{-1}(\sqrt{2} \times 0.321) = 1.1$$

From (6.6.7),

$$k^2 = \frac{(Z_{\mathrm{L}} - Z_{\mathrm{o}})^2}{4Z_{\mathrm{L}}Z_{\mathrm{o}}}\cot^4\theta_z = \frac{(\bar{Z}_{\mathrm{L}} - 1)^2}{4\bar{Z}_{\mathrm{L}}}\cot^4\theta_z = 0.0106$$

Therefore, from (6.6.4),

$$\rho_{\mathrm{M}} = \sqrt{\frac{k^2}{1+k^2}} = 0.1022$$

Now, from (6.6.8),

$$Z_1^2 = Z_{\mathrm{o}}^2\left[\frac{(Z_{\mathrm{L}} - Z_{\mathrm{o}})^2}{4Z_{\mathrm{o}}^2\tan^4\theta_z} + \frac{Z_{\mathrm{L}}}{Z_{\mathrm{o}}}\right]^{1/2} + \frac{(Z_{\mathrm{L}} - Z_{\mathrm{o}})Z_{\mathrm{o}}}{2\tan^2\theta_z} \Rightarrow \bar{Z}_1^2 = \left[\frac{(\bar{Z}_{\mathrm{L}} - 1)^2}{4\tan^4\theta_z} + \bar{Z}_{\mathrm{L}}\right]^{1/2} + \frac{(\bar{Z}_{\mathrm{L}} - 1)}{2\tan^2\theta_z}$$

$$= 2.4776$$

$$\therefore \bar{Z}_1 = \sqrt{2.4776} = 1.57 \Rightarrow Z_1 = 157.41\Omega$$

and from (6.6.9),

$$Z_2 = \frac{Z_{\mathrm{L}}}{Z_1}Z_{\mathrm{o}} = 317.655\,\Omega$$

Check: For $\theta = \pi/2$,

$$\bar{Z}_{\mathrm{in}} = \frac{\bar{Z}_1^2}{\bar{Z}_2^2}\bar{Z}_{\mathrm{L}} = \frac{1.5741^2}{3.1765^2}5 = 1.2277$$

$$\Gamma = \frac{\bar{Z}_{\mathrm{in}} - 1}{\bar{Z}_{\mathrm{in}} + 1} = 0.1022 = \rho_m$$

Let us consider the design of a three-section impedance transformer. Figure 6.18 shows a three-section impedance transformer connected between the load Z_{L} and a transmission line of characteristic impedance Z_{o}. The reflection coefficient characteristic of such a Chebyshev transformer is illustrated in Figure 6.19. The power loss ratio, P_{LR}, of a three-section Chebyshev transformer is found to be

$$P_{\mathrm{LR}} = 1 + \frac{(Z_{\mathrm{L}} - Z_{\mathrm{o}})^2}{4Z_{\mathrm{L}}Z_{\mathrm{o}}} \times \frac{(\sec^2\theta_z\cos^2\theta - 1)^2 \times \cos^2\theta}{\tan^4\theta_z} \tag{6.6.15}$$

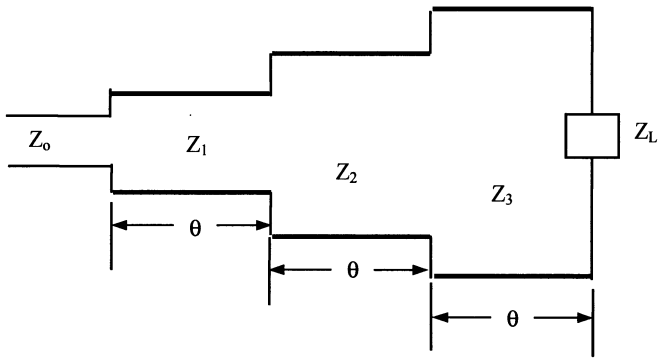

Figure 6.18 A three-section impedance transformer.

It attains the maximum allowed value at $\theta = \theta_M$, where

$$\theta_M = \cos^{-1}\left(\frac{2}{\sqrt{3}}\cos\theta_z\right) \tag{6.6.16}$$

Since the maximum power loss ratio must be equal to $1 + k^2$,

$$k^2 = \frac{(Z_L - Z_o)^2}{4Z_L Z_o}\left(\frac{2\cos\theta_z}{3\sqrt{3}\tan^2\theta_z}\right)^2 \tag{6.6.17}$$

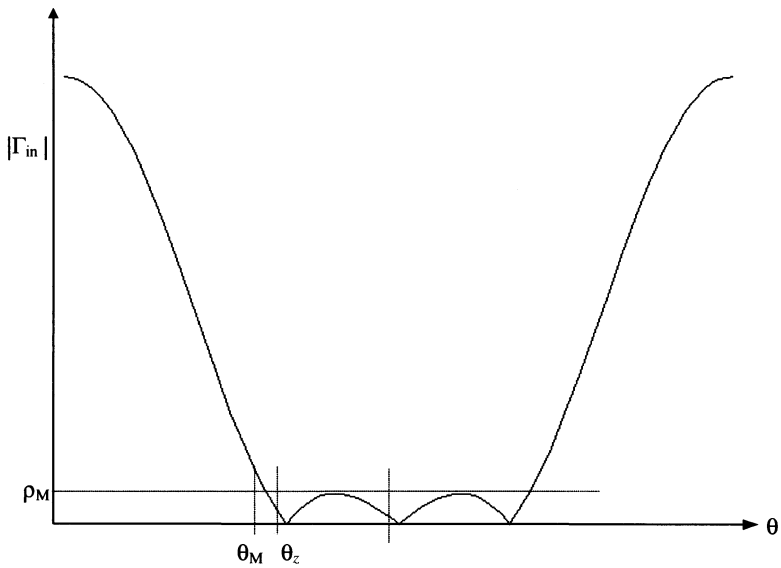

Figure 6.19 Reflection coefficient characteristics of a three-section Chebyshev transformer.

Characteristic impedance Z_1 is obtained by solving the following equation.

$$\frac{Z_L - Z_o}{\tan^2 \theta_z} = \frac{Z_1^2}{Z_o} + 2\left(\frac{Z_L}{Z_o}\right)^{1/2} Z_1 - \frac{Z_L Z_o^2}{Z_1^2} - 2\left(\frac{Z_L}{Z_o}\right)^{1/2} Z_1^{-1} Z_o^2 \tag{6.6.18}$$

The other two characteristic impedances, namely, Z_2 and Z_3, are then determined as follows:

$$Z_2 = \sqrt{Z_L Z_o} \tag{6.6.19}$$

and,

$$Z_3 = \frac{Z_L Z_o}{Z_1} \tag{6.6.20}$$

The range of the pass-band (bandwidth) is still given by (6.6.11) provided that θ_M is now computed from (6.6.16).

Example 6.6: Design a three-section Chebyshev transformer (exact theory) to match a 500-Ω load to a 100-Ω line. Required fractional bandwidth is 0.6. Compute ρ_M and compare it with that obtained in the previous example.

From (6.6.16) and (6.6.11),

$$\theta_M = \cos^{-1}\left(\frac{2}{\sqrt{3}}\cos\theta_z\right) \text{ and } \frac{\Delta f}{f_o} = 0.6 \Rightarrow \frac{\frac{\pi}{2} - \theta_M}{\frac{\pi}{2}} = 0.3 \Rightarrow \theta_M = \frac{\pi}{2}(1 - 0.3) = 1.1$$

$$\therefore \cos(\theta_z) = \frac{\sqrt{3}}{2}\cos\theta_M = 0.3932 \Rightarrow \theta_z = 1.17 \text{ radians}$$

Now, from (6.6.17),

$$k^2 = \frac{(Z_L - Z_o)^2}{4 Z_L Z_o}\left(\frac{2\cos\theta_z}{3\sqrt{3}\tan^2\theta_z}\right)^2 = \frac{(\bar{Z}_L - 1)^2}{4\bar{Z}_L}\left(\frac{2\cos\theta_z}{3\sqrt{3}\tan^2\theta_z}\right)^2 = 6.125 \times 10^{-4}$$

and, from (6.6.4),

$$\rho_M = \sqrt{\frac{k^2}{1 + k^2}} = 0.0247$$

which is approximately one-fourth of the previous (two-section transformer) case.

Z_1 is obtained by solving the equation (6.6.18) as follows,

$$\frac{Z_L - Z_o}{\tan^2\theta_z} = \frac{Z_1^2}{Z_o} + 2\left(\frac{Z_L}{Z_o}\right)^{1/2} Z_1 - \frac{Z_L Z_o^2}{Z_1^2} - 2\left(\frac{Z_L}{Z_o}\right)^{1/2} Z_1^{-1} Z_o^2$$

or,

$$\frac{\bar{Z}_L - 1}{\tan^2\theta_z} = \bar{Z}_1^2 + 2(\bar{Z}_L)^{1/2}\bar{Z}_1 - \frac{\bar{Z}_L}{\bar{Z}_1^2} - 2(\bar{Z}_L)^{1/2}\bar{Z}_1^{-1} = \frac{4}{\tan^2\theta_z} = 0.7314$$

$$\therefore\ \bar{Z}_1^2 + 2\sqrt{5}\bar{Z}_1 - \frac{5}{\bar{Z}_1^2} - \frac{2\sqrt{5}}{\bar{Z}_1} = 0.7314$$

or,

$$\bar{Z}_1^4 + 2\sqrt{5}\bar{Z}_1^3 - 0.7314\bar{Z}_1^2 - 2\sqrt{5}\bar{Z}_1 - 5 = 0$$

$$\therefore\ \bar{Z}_1 = -4.4679, (-0.6392 - j0.6854), (-0.6392 + j0.6854), \text{ and } 1.2742$$

Thus, only one of these solutions can be physically realized because the others have a negative real part. After selecting $Z_1 = 127.42\,\Omega$, (6.6.19) and (6.6.20) give

$$Z_3 = \frac{Z_L Z_o}{Z_1} = 392.4277\,\Omega$$

and,

$$Z_2 = \sqrt{Z_L Z_o} = 223.6068\,\Omega$$

If we use the approximate formulation and then following the procedure of Example 6.4 we find from (6.5.6) that

$$T_3(x_o) = \frac{500 - 100}{500 + 100} \times \frac{1}{0.02474} = 26.9458$$

Now, from (6.5.7),

$$x_o = \cosh\left[\frac{1}{3}\cosh^{-1}(26.9458)\right] = 2.0208$$

and from (6.5.8),

$$x_n = \pm\cos\left[(2n-1)\frac{\pi}{6}\right] = \pm 0.866,\quad 0$$

Using (6.5.9) we get,

$$\varphi_n = 2.2558, 3.1416, \text{ and } 4.0274$$

Since $w_n = e^{j\varphi_n}$, we find that,

$$w_1 = -0.6327 + j0.7744$$
$$w_2 = -0.6327 - j0.7744$$
$$w_3 = -1$$

and from (6.2.9),

$$\frac{\Gamma}{\Gamma_3} = (w - w_1)(w - w_2)(w - w_e) = w^3 + 2.2654w^2 + 2.2654w + 1$$

Hence,

$$\Gamma_o = \Gamma_3$$
$$\Gamma_1 = \Gamma_2 = 2.2654\Gamma_3$$

Now, from (6.2.12),

$$\Gamma_o + \Gamma_1 + \Gamma_2 + \Gamma_3 = 6.5307\Gamma_3 = (500 - 100)/(500 + 100)$$

Therefore,

$$\Gamma_3 = 0.1021 = \Gamma_o$$
$$\Gamma_1 = \Gamma_2 = 0.2313$$

Corresponding impedances are now determined from (6.2.8) as follows:

$$\left.\begin{aligned} \bar{Z}_1 &= \frac{1 + \Gamma_o}{1 - \Gamma_o} = 1.2274 \\ \bar{Z}_2 &= \frac{1 + \Gamma_1}{1 - \Gamma_1} = 2.4234 \end{aligned}\right\} \text{calculated from the input side.}$$

and,

$$\left.\bar{Z}_3 = \frac{1 - \Gamma_3}{1 + \Gamma_3}\bar{Z}_L = 4.0737\right\} \text{calculated from the load side.}$$

A comparison of these values with those obtained earlier using the exact formulation shows that the two sets are within 10 per cent of deviation for this example.

Note that for the fractional bandwidth of 0.6 with a single section, reflection coefficient ρ_M increases to 0.3762.

6.7 TAPERED TRANSMISSION LINES

Consider that the multisection impedance transformer of Figure 6.3 is replaced by a tapered transition of length L, as illustrated in Figure 6.20. Characteristic impedance of this transition is a continuous smooth function of distance, with its values at the two ends as Z_o and R_L. An approximate theory of such a matching section can be easily developed on the basis of analysis already presented in Section 6.2.

The continuously tapered line can be modeled by a large number of incremental sections of length δz. One of these sections, connected at z, has a characteristic impedance of $Z + \delta Z$ and the one before it has a characteristic impedance of Z, as shown in Figure 6.20. These impedance values are conveniently normalized by Z_o before obtaining the incremental reflection coefficient at distance z. Hence,

$$\delta\Gamma_o = \frac{\bar{Z} + \delta\bar{Z} - \bar{Z}}{\bar{Z} + \delta\bar{Z} + \bar{Z}} \approx \frac{\delta\bar{Z}}{2\bar{Z}} \tag{6.7.1}$$

As $\delta z \to 0$, it can be written as

$$d\Gamma_o = \frac{d\bar{Z}}{2\bar{Z}} = \frac{1}{2}\frac{d(\ln \bar{Z})}{dz}dz \tag{6.7.2}$$

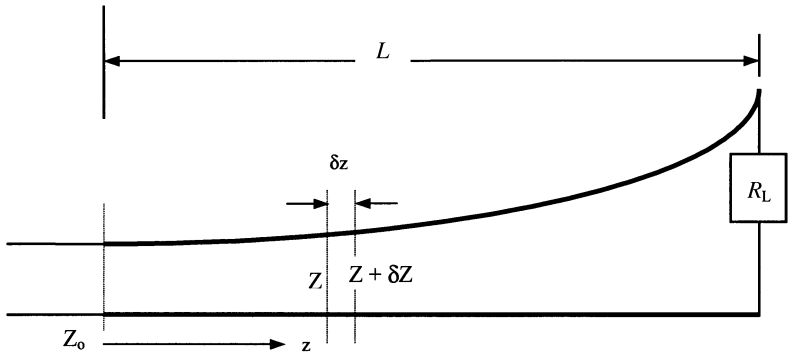

Figure 6.20 A tapered transition connected between load R_L and a transmission line of characteristic impedance Z_o.

The corresponding incremental reflection coefficient $d\Gamma_{in}$ at the input can be written as follows:

$$d\Gamma_{in} \approx e^{-j2\beta z} d\Gamma_o = e^{-j2\beta z} \cdot \frac{1}{2} \cdot \frac{d}{dz}(\ln \bar{Z}) dz$$

Total reflection coefficient, Γ_{in}, at the input of the tapered section can be determined by summing up these incremental reflections with their appropriate phase angles. Hence,

$$\Gamma_{in} = \int_0^L d\Gamma_{in} = \frac{1}{2} \int_0^L e^{-j2\beta z} \frac{d}{dz}(\ln \bar{Z}) dz \tag{6.7.3}$$

Therefore, Γ_{in} can be determined from (6.7.3) provided that $\bar{Z}(z)$ is given. However, the synthesis problem is a bit complex because, in that case, $\bar{Z}(z)$ is to be determined for a specified Γ_{in}. Let us first consider a few examples of evaluating Γ_{in} for the given distributions of $\frac{d}{dz}(\ln \bar{Z})$.

Case 1: $\frac{d}{dz}(\ln \bar{Z})$ is constant over the entire length of the taper.

Suppose that

$$\frac{d}{dz}(\ln \bar{Z}(z)) = C_1 \quad \ldots \quad 0 \le z \le L$$

where C_1 is a constant. On integrating this equation, we get

$$\ln(\bar{Z}(z)) = C_1 z + C_2$$

With $\bar{Z}(z = 0) = 1$ and $\bar{Z}(z = L) = \bar{R}_L$, constants C_1 and C_2 can be determined. Hence,

$$\ln(\bar{Z}) = \frac{z}{L} \ln(\bar{R}_L) \Rightarrow \bar{Z} = e^{(z/L)\ln(\bar{R}_L)} \tag{6.7.4}$$

Thus, the impedance is changing exponentially with distance. Therefore, this kind of taper is called an *exponential taper*. From (6.7.3), the total reflection coefficient is found as

$$\Gamma_{in} = \frac{1}{2} \int_0^L e^{-j2\beta z} \frac{d}{dz}\left[\frac{z}{L} \ln(\bar{R}_L)\right] dz = \frac{\ln(\bar{R}_L)}{2L} \int_0^L e^{-j2\beta z} dz = \frac{\ln(\bar{R}_L)}{2L} \cdot \frac{e^{-j2\beta z}}{-j2\beta} \Bigg|_0^L$$

or,

$$\Gamma_{\text{in}} = \frac{\ln(\bar{R}_{\text{L}})}{2L} \cdot \frac{e^{-j\beta L} - 1}{-j2\beta} = \frac{\ln(\bar{R}_{\text{L}})}{2} \cdot e^{-j\beta L} \cdot \frac{\sin(\beta L)}{\beta L} \Rightarrow \frac{2\rho_{\text{in}}}{\ln(\bar{R}_{\text{L}})} = \frac{\sin(\beta L)}{(\beta L)} \tag{6.7.5}$$

where $\rho_{\text{in}} = |\Gamma_{\text{in}}|$. It is assumed in this evaluation that $\beta = 2\pi/\lambda$ is not changing with distance z. The right-hand side of (6.7.5) is displayed in Figure 6.21 as a function of βL. Since L is fixed for a given taper and β is directly related to signal frequency, this plot also represents the frequency response of an exponential taper.

Case 2: $\dfrac{d}{dz}(\ln \bar{Z})$ is a triangular function.

If $\dfrac{d}{dz}(\ln \bar{Z})$ is a triangular function, defined as

$$\frac{d(\ln \bar{Z})}{dz} = \begin{cases} \dfrac{4z}{L^2} \ln \bar{R}_{\text{L}} & 0 \le z \le \dfrac{L}{2} \\ 4\left(\dfrac{1}{L} - \dfrac{z}{L^2}\right) \ln \bar{R}_{\text{L}} & \dfrac{L}{2} \le z \le L \end{cases} \tag{6.7.6}$$

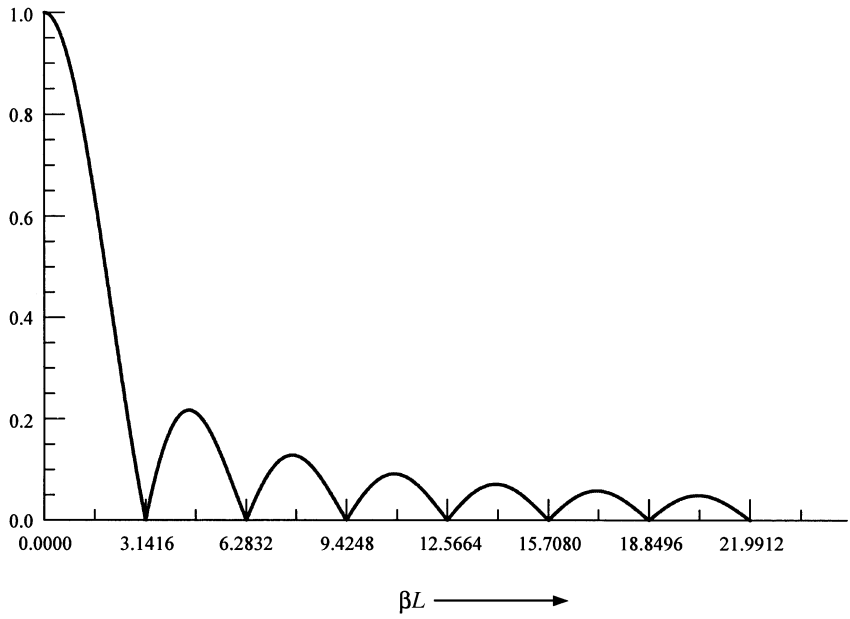

Figure 6.21 Frequency response of an exponential taper.

then,

$$\ln \bar{Z} = \begin{cases} \displaystyle\int_0^{L/2} \frac{4z}{L^2} \ln \bar{R}_{\mathrm{L}} dz & 0 \le z \le \frac{L}{2} \\ \displaystyle\int_{L/2}^{L} 4\left(\frac{1}{L} - \frac{z}{L^2}\right) \ln \bar{R}_{\mathrm{L}} dz & \frac{L}{2} \le z \le L \end{cases}$$

or,

$$\ln \bar{Z} = \begin{cases} \dfrac{2z^2}{L^2} \ln \bar{R}_{\mathrm{L}} + c_1 & 0 \le z \le \dfrac{L}{2} \\ 4\left(\dfrac{z}{L} - \dfrac{z^2}{2L^2}\right) \ln \bar{R}_{\mathrm{L}} + c_2 & \dfrac{L}{2} \le z \le L \end{cases}$$

Integration constants c_1 and c_2 are determined from the given conditions $Z(z=0) = 1$ and $Z(z=L) = \bar{R}_{\mathrm{L}}$. Hence,

$$\bar{Z} = \begin{cases} \exp\left\{\dfrac{2z^2}{L^2} \ln \bar{R}_{\mathrm{L}}\right\} & \cdots 0 \le z \le \dfrac{L}{2} \\ \exp\left\{\left(\dfrac{4z}{L} - \dfrac{2z^2}{L^2} - 1\right) \ln \bar{R}_{\mathrm{L}}\right\} & \cdots \dfrac{L}{2} \le z \le L \end{cases} \tag{6.7.7}$$

and therefore, total reflection coefficient is found from (6.7.3) as

$$\Gamma_{\mathrm{in}} = \frac{1}{2}\left[\int_0^{L/2} e^{-j2\beta z} \cdot \frac{4z}{L^2} \cdot \ln(\bar{R}_{\mathrm{L}}) dz + \int_{L/2}^{L} e^{-j2\beta z} \cdot \frac{4}{L^2} \cdot (L - z) \cdot \ln(\bar{R}_{\mathrm{L}}) dz\right]$$

or,

$$\Gamma_{\mathrm{in}} = \frac{2 \cdot \ln(\bar{R}_{\mathrm{L}})}{L^2}\left[\int_0^{L/2} z \cdot e^{-j2\beta z} dz + \int_{L/2}^{L} (L - z) \cdot e^{-j2\beta z} dz\right]$$

Since

$$\int z \cdot e^{-j2\beta z} dz = \frac{z \cdot e^{-j2\beta z}}{-j2\beta} - \frac{e^{-j2\beta z}}{(-j2\beta)^2}$$

and,

$$\int e^{-j2\beta z} dz = \frac{e^{-j2\beta z}}{-j2\beta}$$

Γ_{in} can be found as follows:

$$\Gamma_{in} = \frac{1}{2} \cdot e^{-j\beta L} \cdot \ln(\bar{R}_L) \cdot \left[\frac{\sin(\beta L/2)}{(\beta L/2)}\right]^2 \tag{6.7.8}$$

Figure 6.22 shows normalized magnitude of Γ_{in} as a function of βL. As before, it also represents the frequency response of this taper of length L. When we compare it with that of Figure 6.21 for an exponential taper, we find that the magnitude of minor lobes is reduced now but the main lobe has become relatively wider. It affects the cutoff frequency of a given taper. For example, if the maximum allowed normalized reflection coefficient is 0.2 then an exponential taper has a lower value of βL in comparison with that of a taper with triangular distribution. However, it is the other way around for a normalized reflection coefficient of 0.05. For a fixed-length L, βL is proportional to frequency and, hence, the lower value of βL has a lower cutoff frequency in comparison with the other case.

Figure 6.23 depicts variation in normalized characteristic impedance along the length of two tapers. A coaxial line operating in TEM mode can be used to design these tapers by varying the diameter of its inner conductor. Similarly, the narrow sidewall width of a TE_{10}-mode rectangular waveguide can be modified to get the desired taper while keeping its wide side constant.

Case 3: $\frac{d}{dz}(\ln \bar{Z})$ is a Gaussian distribution.

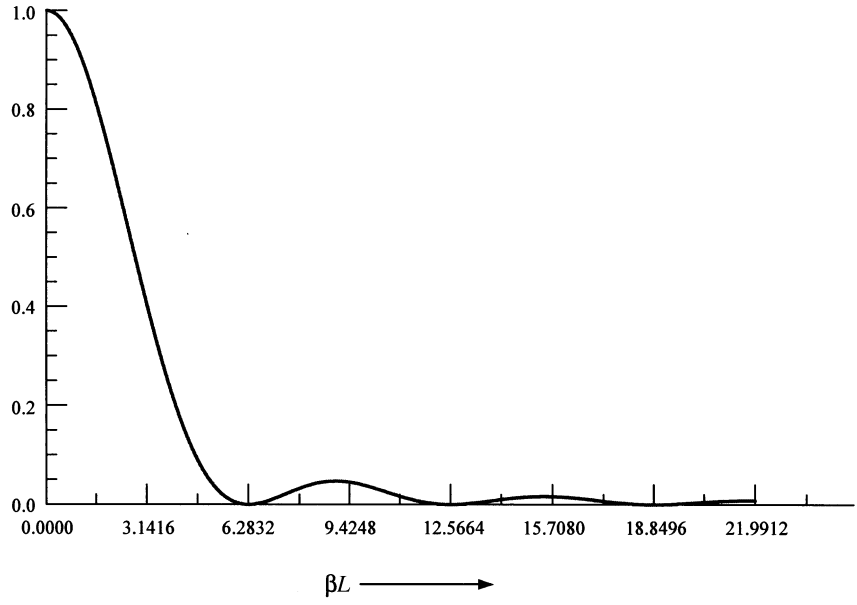

Figure 6.22 Frequency response of a taper with triangular distribution.

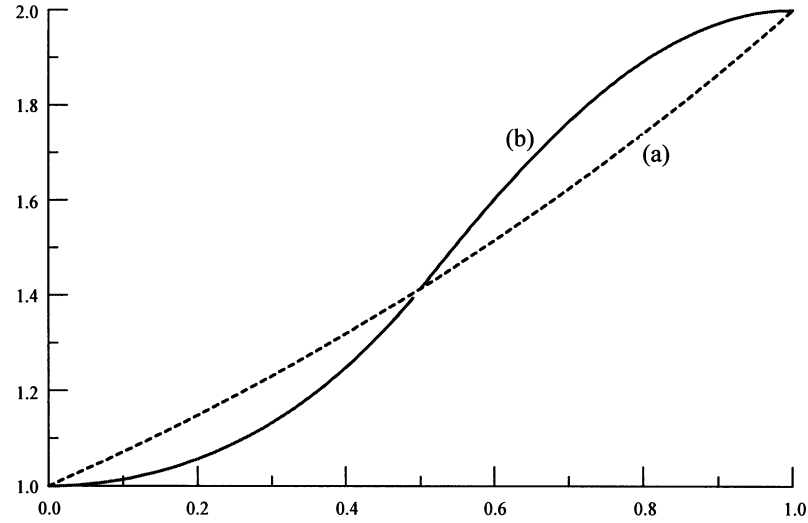

Figure 6.23 Distribution of normalized characteristic impedance along a tapered line terminated by $R_L = 2Z_o$ for (a) case 1, and (b) case 2.

Assume that

$$\frac{d}{dz}[\ln(\bar{Z})] = K_1 e^{-\alpha(z-L/2)^2} \tag{6.7.9}$$

This distribution is centered around the midpoint of the tapered section. Its falloff rate is governed by the coefficient α. Integrating it over distance z, we find that

$$\ln(\bar{Z}) = K_1 \int_0^z e^{-\alpha(z'-L/2)^2} dz' \tag{6.7.10}$$

Since $\bar{Z}(z = L) = \bar{R}_L$,

$$K_1 = \frac{\ln(\bar{R}_L)}{\int_0^L e^{-\alpha(z'-L/2)^2} dz'} \tag{6.7.11}$$

Therefore,

$$\ln(\bar{Z}) = \ln(\bar{R}_L) \cdot \frac{\int_0^z e^{-\alpha(z'-L/2)^2} dz'}{\int_0^L e^{-\alpha(z'-L/2)^2} dz'} \tag{6.7.12}$$

and,

$$\Gamma_{in} = \frac{1}{2} K_1 \int_0^L e^{-j2\beta z} \cdot e^{-\alpha(z-L/2)^2} dz \tag{6.7.13}$$

With the following substitution of variable and associated limits of integration in (6.7.11) and (6.7.13),

$$z - \frac{L}{2} = x$$

$$dz = dx$$

$$z = 0 \rightarrow x = -L/2$$

and,

$$z = L \rightarrow x = L/2$$

we get

$$\Gamma_{\text{in}} = \frac{1}{2} K_1 \int_{-L/2}^{L/2} e^{-j2\beta(x+\frac{L}{2})} \times e^{-\alpha x^2} dx = \frac{1}{2} K_1 \, e^{-j\beta L} \int_{-L/2}^{L/2} e^{-j2\beta x} \times e^{\alpha x^2} dx$$

or,

$$\Gamma_{\text{in}} = \frac{1}{2} \ln(\bar{R}_{\text{L}}) \, e^{-j\beta\ell} \frac{\int_{-L/2}^{L/2} e^{-j2\beta x} e^{-\alpha x^2} dx}{\int_{-L/2}^{L/2} e^{-\alpha x^2} dx} = \frac{1}{2} \ln(\bar{R}_{\text{L}}) \, e^{-j\beta\ell} \frac{\int_{0}^{L/2} \cos(2\beta x) \cdot e^{-\alpha x^2} dx}{\int_{0}^{L/2} e^{-\alpha x^2} dx} \tag{6.7.14}$$

It can be arranged after substituting $\sqrt{\alpha}x$ with y, and $\sqrt{\alpha}(L/2)$ with ξ as follows.

$$\Gamma_{\text{in}} = \frac{1}{2} \ln(\bar{R}_{\text{L}}) e^{-j\beta\ell} \frac{\int_{0}^{\xi} \cos\left(\left\{ \frac{\beta L}{\xi} \right\} y \right) \cdot e^{-y^2} dy}{\int_{0}^{\xi} e^{-y^2} dy} \tag{6.7.15}$$

Figure 6.24 shows the normalized magnitude of the reflection coefficient versus βL for two different values of ξ. It indicates that the main lobe becomes wider and the level of minor lobes goes down as ξ is increased.

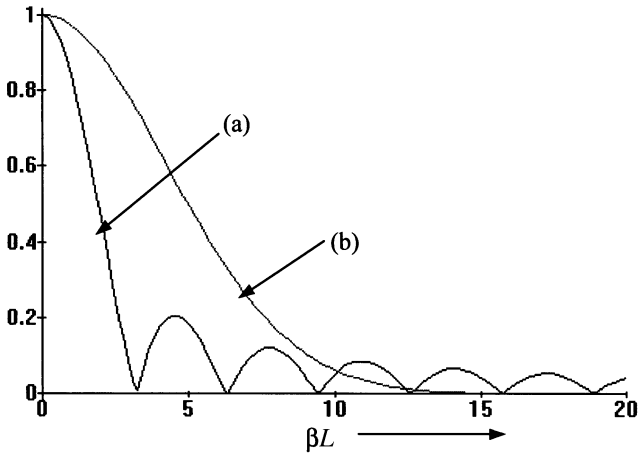

Figure 6.24 Frequency response of a tapered line with normal distribution of normalized characteristic impedance for (a) $\xi = 0.3$, and (b) $\xi = 3$.

6.8 SYNTHESIS OF TRANSMISSION LINE TAPERS

The frequency response of a transmission line taper can be easily determined from (6.7.3). However, the inverse problem of determining its impedance variation that provides the desired frequency response needs further consideration. To this end, assume that $F(\alpha)$ is the Fourier transform of a function $f(x)$. In other words,

$$F(\alpha) = \int_{-\infty}^{\infty} f(x) e^{-j\alpha x} dx \tag{6.8.1}$$

and,

$$f(x) = \frac{1}{2\pi} \int_{-\infty}^{\infty} F(\alpha) e^{j\alpha x} d\alpha \tag{6.8.2}$$

For convenience, we rewrite (6.7.3) as follows.

$$\Gamma_{\text{ni}}(2\beta) = \int_0^L \left\{ \frac{1}{2} \frac{d}{dz} (\ln \bar{Z}) \right\} e^{-j2\beta z} dz$$

If $\dfrac{1}{2} \dfrac{d(\ln \bar{Z})}{dz} = 0$ for $-\infty \leq z < 0$ and for $z > L$, then it may be written as

$$\Gamma_{\text{in}}(2\beta) = \int_{-\infty}^{\infty} \frac{1}{2} \frac{d}{dz} (\ln \bar{Z}) e^{-j2\beta z} dz \tag{6.8.3}$$

A comparison of (6.8.3) with (6.8.1) indicates that $\Gamma_{\text{in}}(2\beta)$ represents the Fourier transform of $\dfrac{1}{2} \dfrac{d(\ln \bar{Z}(z))}{dz}$. Hence, from (6.8.2),

$$\frac{1}{2} \frac{d(\ln \bar{Z})}{dz} = \frac{1}{2\pi} \int_{-\infty}^{\infty} \Gamma_{\text{in}}(2\beta) e^{j2\beta x} d(2\beta) \tag{6.8.4}$$

This equation can be used to design a taper that will have the desired reflection coefficient characteristics. However, only those $\Gamma_{\text{in}}(2\beta)$ that have an inverse Fourier transform limited to $0 \leq z \leq L$ (zero outside this range) can be realized. At this point, we can conveniently introduce the following normalized variables:

$$p = 2\pi \frac{z - (L/2)}{L} \tag{6.8.5}$$

and,

$$u = \frac{\beta L}{\pi} = \frac{2L}{\lambda} \tag{6.8.6}$$

Therefore,

$$z = \frac{L}{2\pi}(p + \pi)$$

and,

$$dz = \frac{L}{2\pi}dp$$

New integration limits are found as $-\pi \le p \le \pi$. Hence,

$$\Gamma_{\text{in}}(2\beta) = \frac{1}{2}\int_{-\pi}^{\pi} e^{-j2\beta\left(\frac{L}{2}+\frac{Lp}{2\pi}\right)} \cdot \frac{d}{dp}(\ln \bar{Z}) \cdot \frac{dp}{dz} \cdot \frac{L}{2\pi} \cdot dp$$

or,

$$\Gamma_{\text{in}}(2\beta) = \frac{1}{2}e^{-j\beta L}\int_{-\pi}^{\pi} e^{-jup} \cdot \frac{d}{dp}(\ln \bar{Z}) \cdot dp \tag{6.8.7}$$

Now, if we define $g(p) = \dfrac{d(\ln \bar{Z})}{dp}$, and $F(u) = \displaystyle\int_{-\pi}^{\pi} e^{-jup} g(p)dp$, then (6.8.7) can be expressed as follows:

$$\Gamma_{\text{in}}(2\beta) = \frac{1}{2}e^{-j\beta L}F(u)$$

or,

$$\rho_{\text{in}}(2\beta) = \frac{1}{2}|F(u)|$$

Further,

$$F(u = 0) = \ln(\bar{Z}_{\text{L}}) \tag{6.8.8}$$

Thus, $F(u)$ and $g(p)$ form the Fourier transform pair. Therefore,

$$g(p) = \frac{1}{2\pi}\int_{-\infty}^{\infty} e^{jup}F(u)du = \begin{cases} \text{nonzero} & \text{for } |p| < \pi \\ 0 & \text{for } |p| > \pi \end{cases} \tag{6.8.9}$$

In order to satisfy the conditions embedded in writing (6.8.3), only those $F(u)$ that produce $g(p)$ as zero for $|p| > \pi$ can be synthesized. Suitable restrictions on $F(u)$ can be derived after expanding $g(p)$ in a complex Fourier series as follows.

$$g(p) = \begin{cases} \sum_{n=-\infty}^{\infty} a_n e^{jnp} & -\pi \le p \le \pi \\ 0 & |p| > \pi \end{cases} \tag{6.8.10}$$

Since $g(p)$ is a real function, constants $a_n = a^*_{-n}$. Therefore,

$$F(u) = \int_{-\pi}^{\pi} e^{-jup} \times \sum_{n=-\infty}^{\infty} a_n e^{jnp} dp = \sum_{n=-\infty}^{\infty} a_n \int_{-\pi}^{\pi} e^{-j(u-n)p} dp = \sum_{n=-\infty}^{\infty} a_n \frac{e^{-j(u-n)p}}{-j(u-n)} \Bigg|_{-\pi}^{\pi}$$

or,

$$F(u) = \sum_{n=-\infty}^{\infty} a_n \frac{e^{-j(u-n)\pi} - e^{j(u-n)\pi}}{-j(u-n)} = 2\pi \sum_{n=-\infty}^{\infty} a_n \frac{\sin \pi(u-n)}{\pi(u-n)} \tag{6.8.11}$$

For $u = m$ (an integer),

$$\frac{\sin \pi(m-n)}{\pi(m-n)} = \begin{cases} 1 & \text{for } m = n \\ 0 & \text{for } m \ne n \end{cases}$$

Therefore,

$$F(n) = 2\pi a_n \Rightarrow a_n = \frac{F(n)}{2\pi}$$

and,

$$F(u) = \sum_{n=-\infty}^{\infty} F(n) \frac{\sin \pi(u-n)}{\pi(u-n)} \tag{6.8.12}$$

This is the well-known *sampling theorem* used in communication theory. It states that $F(u)$ is uniquely reconstructed from a knowledge of sample values of $F(u)$ at $u = n$, where n is an integer (positive or negative) including zero, i.e., $u = n = 0, \pm 1, \pm 2, \pm 3, \ldots$.

In order to have greater flexibility in selecting $F(u)$, let us assume that $a_n = 0$ for all $|n| > N$. Therefore,

$$g(p) = \sum_{n=-N}^{N} a_n e^{jnp} \tag{6.8.13}$$

and, from (6.8.11),

$$F(u) = 2\pi \sum_{n=-N}^{N} a_n(-1)^n \frac{\sin(\pi u)}{\pi(u-n)} = 2\pi \frac{\sin(\pi u)}{\pi u} \sum_{n=-N}^{N} a_n(-1)^n \frac{u}{(u-n)}$$

This series can be recognized as the partial-fraction expansion of a function and, therefore, $F(u)$ can be expressed as follows:

$$F(u) = 2\pi \frac{\sin(\pi u)}{\pi u} \times \frac{Q(u)}{\prod_{n=1}^{N}(u^2 - n^2)} \tag{6.8.14}$$

where $Q(u)$ is an arbitrary polynomial of degree $2N$ in u subject to the restriction $Q(-u) = Q^*(u)$ so that $a_n = a^*_{-n}$. Further, it contains an arbitrary constant multiplier.

In (6.8.14), $\sin(\pi u)$ has zeros at $u = \pm n$. However, the first $2N$ of these zeros are canceled by $(u^2 - n^2)$. These can be replaced by $2N$ new arbitrarily located zeros by proper choice of $Q(u)$.

Example 6.7: Design a transmission line taper to match a 100-Ω load to a 50-Ω line. The desired frequency response has a triple zero at $\beta L = \pm 2\pi$. Plot its frequency response and normalized characteristic impedance distribution.

The desired characteristic can be accomplished by moving zeros at ± 1 and ± 3 into the points $u = \pm 2$. Due to this triple zero, the reflection coefficient will remain small over a relatively wide range of βL around $\pm 2\pi$. Therefore,

$$Q(u) = C(u^2 - 4)^3$$

and,

$$F(u) = 2\pi C \frac{\sin(\pi u)}{\pi u} \times \frac{(u^2 - 4)^3}{(u^2 - 1) \times (u^2 - 4) \times (u^2 - 9)}$$

Since $u = \beta L/\pi$, $F(u)$ versus u represents the frequency response of this taper. Further, it can be normalized with $F(0)$ as follows.

$$\left|\frac{F(u)}{F(0)}\right| = \frac{9}{16} \times \frac{\sin(\pi u)}{\pi u} \times \frac{(u^2 - 4)^3}{(u^2 - 1) \times (u^2 - 4) \times (u^2 - 9)}$$

A plot of this equation is illustrated in Figure 6.25. It shows that the normalized magnitude is very small around $u = 2$.

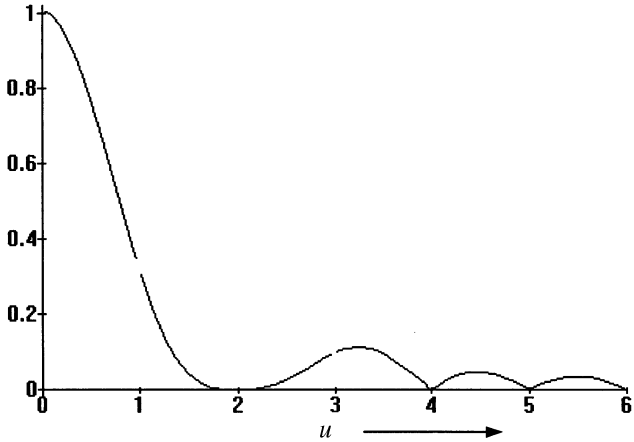

Figure 6.25 Normalized frequency response of the taper in Example 6.7.

Since $F(0)$ is given by (6.8.8), multiplying constant C in $F(u)$ can be easily determined. Hence,

$$F(0) = 2\pi C \times 1 \times \frac{(-4)^3}{(-1)\times(-4)\times(-9)} = 2\pi C \times \frac{16}{9} = \ln \bar{Z}_{\mathrm{L}} \Rightarrow C = \frac{9}{32\times\pi}\ln \bar{Z}_{\mathrm{L}}$$

Further,

$$F(1) = \frac{2\pi C}{\pi}\left(\frac{\sin \pi u}{u^2-1}\right)\Big|_{u=1} \times \frac{(1-4)^3}{(1-4)\times(1-9)} = C\pi\frac{9}{8} = \frac{9}{32\pi}\times \ln \bar{Z}_{\mathrm{L}} \times \pi\frac{9}{8}$$

$$= 0.3164 \times \ln \bar{Z}_{\mathrm{L}}$$

$$F(2) = 0$$

$$F(3) = \frac{2\pi C}{3\pi}\left(\frac{\sin \pi u}{u^2-9}\right)\Big|_{u=3} \times \frac{(9-4)^3}{(9-1)\times(9-4)} = -\frac{25}{72}C\pi$$

$$= \left(-\frac{25}{72}\pi\right) \times \frac{9}{32\pi} \times \ln \bar{Z}_L = 0.09766 \times \ln \bar{Z}_{\mathrm{L}}$$

and $F(n) = 0$ for $n > 3$. Therefore,

$$a_{\mathrm{o}} = \frac{1}{2\pi}F(0) = \frac{1}{2\pi}\ln \bar{Z}_{\mathrm{L}}$$

$$a_1 = a_{-1} = \frac{1}{2\pi}F(1) = \frac{0.3164}{2\pi}\ln \bar{Z}_{\mathrm{L}}$$

$$a_2 = a_2 = 0$$

$$a_3 = a_{-3} = \frac{1}{2\pi}F(3) = -\frac{0.09766}{2\pi}\ln \bar{Z}_{\mathrm{L}}$$

and,

$$a_n = a_{-n} = 0 \quad \text{for } n > 3$$

Hence,

$$g(p) = \frac{d(\ln \bar{Z})}{dp} = \frac{\ln \bar{Z}_L}{2\pi}(a_o + 2a_1 \cos(p) + 2a_3 \cos(3p))$$

$$= \frac{\ln \bar{Z}_L}{2\pi}(1 + 0.6328 \times \cos(p) - 0.1953 \times \cos(3p))$$

and,

$$\ln \bar{Z} = \frac{\ln \bar{Z}_L}{2\pi}(p + 0.6328 \times \sin(p) - 0.0651 \times \sin(3p)) + c_1$$

The integration constant c_1 can be evaluated as follows:

$$\ln \bar{Z} = 0 \text{ at } p = -\pi \text{ or } \ln \bar{Z} = \ln \bar{Z}_L \text{ at } p = \pi$$

Therefore,

$$c_1 = 0.5 \times \ln \bar{Z}_L$$

and,

$$\ln \bar{Z} = \frac{\ln \bar{Z}_L}{2\pi}(p + \pi + 0.6328 \times \sin(p) - 0.0651 \sin(3p))$$

where

$$p = \frac{2\pi}{L}\left(z - \frac{L}{2}\right)$$

Normalized impedance (Z) versus the length of the taper (z/L) is illustrated in Figure 6.26.

Example 6.8: Design a taper to match a 100-Ω load to a 50-Ω transmission line. Its reflection coefficient has double zeros at $\beta L = \pm 2\pi$, and $\pm 3\pi$. Plot its frequency response and normalized characteristic impedance versus normalized length of the taper.

This design can be achieved by moving the zeros at $u = \pm 1$ and ± 4 into the points ± 2 and ± 3, respectively. Hence,

$$Q(u) = C(u^2 - 2^2)^2(u^2 - 3^3)^2 = C(u^2 - 4)^2(u^2 - 9)^2$$

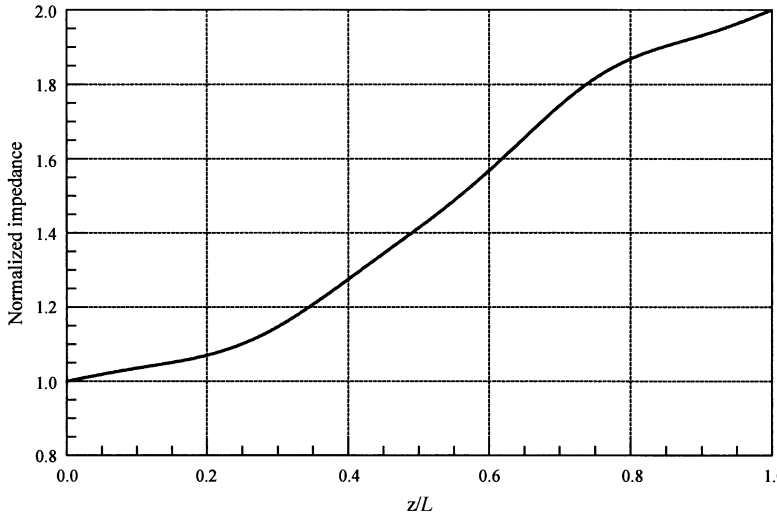

Figure 6.26 Normalized characteristic impedance variation along the length of the taper in Example 6.7.

and,

$$F(u) = C\frac{\sin(\pi u)}{\pi u} \times \frac{(u^2-4)^2 \times (u^2-9)^2}{(u^2-1) \times (u^2-4) \times (u^2-9) \times (u^2-16)}$$

Therefore,

$$F(0) = 2.25C;\ F(1) = 0.8C;\ F(2) = 0;\ F(3) = 0;\ F(4) = (7/40)C$$

and $F(n) = 0$ for $n > 4$. From (6.8.8),

$$F(0) = \ln \bar{Z}_{\mathrm{L}} \Rightarrow C = \frac{\ln \bar{Z}_{\mathrm{L}}}{2.25}$$

and,

$$g(p) = \frac{d(\ln \bar{Z})}{dp} = \sum_{n=-\infty}^{\infty} a_n e^{-jnp};\quad a_n = \frac{F(n)}{2\pi}$$

or,

$$\begin{aligned} g(p) &= \frac{2.25 \times C}{2\pi} + \frac{0.8 \times C}{2\pi}(e^{jp} + e^{-jp}) + \frac{7 \times C}{40 \times 2\pi}(e^{j4p} + e^{-j4p}) \\ &= \frac{\ln \bar{Z}_{\mathrm{L}}}{2\pi}[1 + 0.7111 \times \cos(p) + 0.1556 \times \cos(4p)] \end{aligned}$$

Therefore,

$$\ln \bar{Z} = \frac{\ln \bar{Z}_L}{2\pi}[p + 0.7111 \times \sin(p) + 0.0389 \times \sin(4p)] + c_1$$

since

$$\ln \bar{Z}|_{p=-\pi} = 0, \quad c_1 = \frac{\ln \bar{Z}_L}{2}$$

and,

$$\ln \bar{Z} = \frac{\ln \bar{Z}_L}{2\pi}[p + \pi + 0.7111 \times \sin(p) + 0.0389 \times \sin(4p)]$$

where

$$p = \frac{2\pi}{L}\left(z - \frac{L}{2}\right)$$

Frequency response and normalized characteristic impedance distribution are shown in Figures 6.27 and 6.28, respectively.

Klopfenstein Taper

The preceding procedure indicates infinite possibilities of synthesizing a transmission line taper. A designer naturally looks for the best design. In other words, which design gives the shortest taper for a given ρ_M? The answer to this question is the

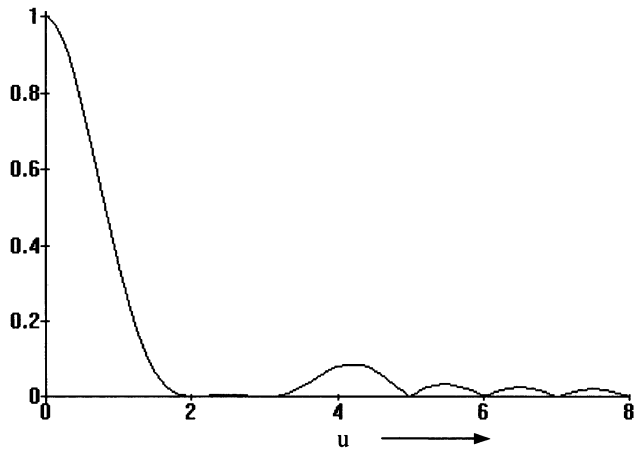

Figure 6.27 Frequency response of the taper in Example 6.8.

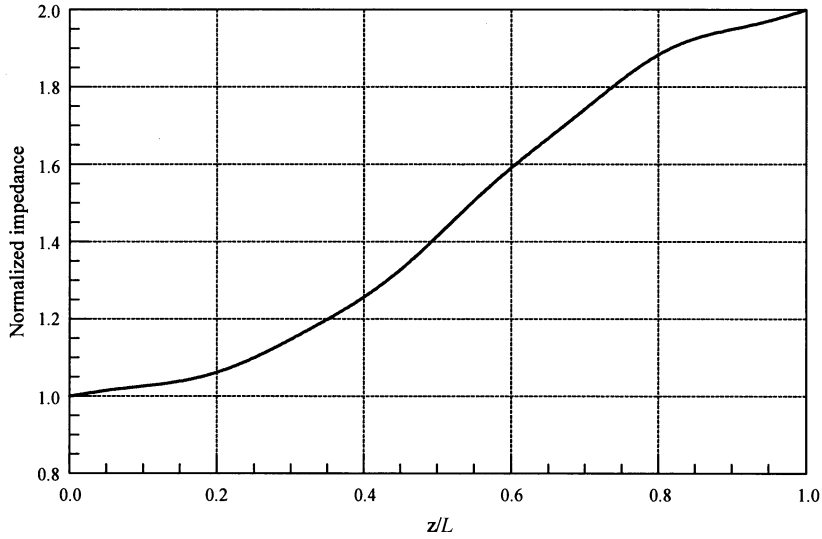

Figure 6.28 Normalized characteristic impedance variation of the taper in Example 6.8.

Klopfenstein taper, which is derived from a stepped Chebyshev transformer. The design procedure is summarized here without its derivation.

Characteristic impedance variation of this taper versus distance z is given by

$$Z(z) = \sqrt{Z_o R_L} \cdot e^{\kappa} \tag{6.8.15}$$

where,

$$\kappa = \frac{A^2 \Gamma_o}{\cosh(A)} f\left(\frac{2z}{L} - 1, A\right), \quad 0 \le z \le L \tag{6.8.16}$$

$$f(\zeta, A) = \int_0^{\zeta} \frac{I_1(A\sqrt{1-y^2})}{A\sqrt{1-y^2}} dy, \quad |x| \le 1 \tag{6.8.17}$$

$$\Gamma_o = \frac{R_L - Z_o}{R_L + Z_o} \tag{6.8.18}$$

Since the cutoff value of βL is equal to A, we have

$$A = \beta_o L \tag{6.8.19}$$

For a maximum ripple ρ_M in its pass-band, it can be determined as follows.

$$A = \cosh^{-1}\left(\frac{|\Gamma_o|}{\rho_M}\right) \tag{6.8.20}$$

$I_1(x)$ is the modified Bessel function of the first kind. $f(\zeta, \mathrm{A})$ needs to be numerically evaluated except for the following special cases:

$$f(0, A) = 0$$
$$f(x, 0) = \frac{x}{2}$$
$$f(1, A) = \frac{\cosh(A) - 1}{A^2}$$

The resulting input reflection coefficient as a function of βL (and hence, frequency) is given by

$$\Gamma_{\text{in}}(\beta L) = \Gamma_{\text{o}} e^{-j\beta L} \frac{\cosh\left(\sqrt{A^2 - (\beta L)^2}\right)}{\cosh(A)} \tag{6.8.21}$$

Note that the hyperbolic cosine becomes the cosine function for an imaginary argument.

Example 6.9: Design a Klopfenstein taper to match a 100-Ω load to a 50-Ω transmission line. Maximum allowed reflection coefficient in its pass-band is 0.1. Plot the characteristic impedance variation along its normalized length and the input reflection coefficient versus βL.

From (6.8.18),

$$\Gamma_{\text{o}} = \frac{R_{\text{L}} - Z_{\text{o}}}{R_{\text{L}} + Z_{\text{o}}} = \frac{100 - 50}{100 + 50} = \frac{1}{3}$$

From (6.8.20),

$$A = \cosh^{-1}\left(\frac{|\Gamma_{\text{o}}|}{\rho_{\text{M}}}\right) = \cosh^{-1}\left(\frac{1/3}{0.1}\right) = 1.87382$$

Equation (6.8.15) is used to evaluate $Z(z)$ numerically. These results are shown in Table 6.1. This data is also displayed in Figure 6.29. The reflection coefficient of this taper is depicted in Figure 6.30.

6.9 BODE-FANO CONSTRAINTS FOR LOSSLESS MATCHING NETWORKS

Various matching circuits described in this and the preceding chapter indicate that zero reflection is possible only at selected discrete frequencies. Examples 5.6 and 5.7 of previous chapter show that the bandwidth over which the reflection coefficient

TABLE 6.1 Characteristic Impedance of the Klopfenstein Taper (in Example 6.9) as a Function of its Normalized Length

Z/L	Impedance in Ohm
0	56.000896
0.05	57.030043
0.1	58.169255
0.15	59.412337
0.2	60.757724
0.25	62.202518
0.3	63.74238
0.35	65.371433
0.4	67.082194
0.45	68.865533
0.5	70.710678
0.55	72.605261
0.6	74.535428
0.65	76.486009
0.7	78.440749
0.75	80.382597
0.8	82.294063
0.85	84.157604
0.9	85.95606
0.95	87.673089
1	89.29361

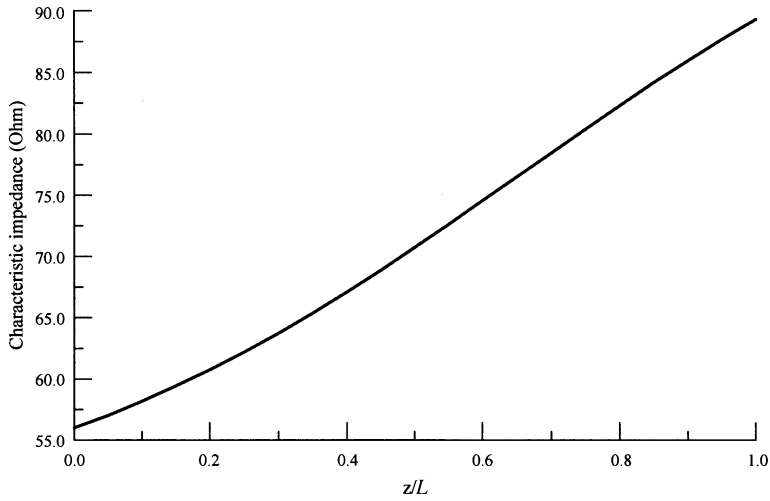

Figure 6.29 Characteristic impedance distribution along the normalized length of the Klopfenstein taper in Example 6.9.

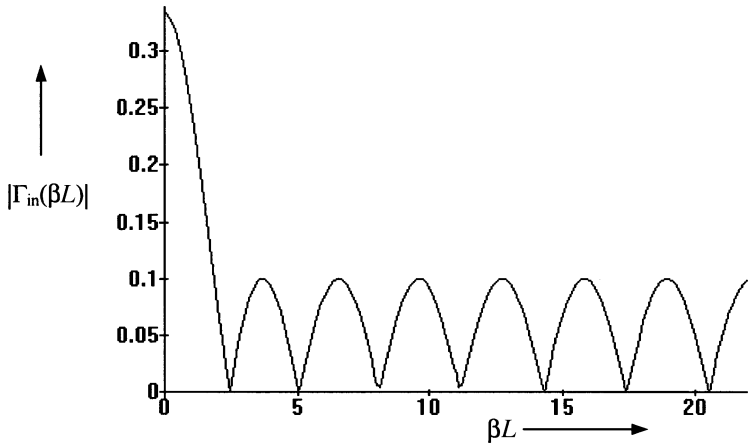

Figure 6.30 Reflection coefficient versus βL of the Klopfenstein taper in Example 6.9.

remains below a specified value is increased with the number of components. A circuit designer would like to know whether a lossless passive network could be designed for a perfect matching. Further, it will be helpful if associated constraints and design trade-offs are known. Bode-Fano constraints provide such means to the designer.

Bode-Fano criteria provide optimum results under ideal conditions. These results may require approximation to implement the circuit. Table 6.2 summarizes these constraints for selected *R-C* and *R-L* loads. The detailed formulations are beyond the scope of this book.

As an example, if it is desired to design a reactive matching network at the output of a transistor amplifier then this situation is similar to that depicted in the top row of the table. Further, consider the case in which magnitude ρ of the reflection coefficient remains constant at $\rho_m(\rho_m < 1)$ over the frequency band from ω_1 to ω_2, whereas it stays at unity outside this band. The constraint for this circuit is found to be

$$\int_0^\infty \ln\left(\frac{1}{\rho}\right)d\omega = \ln\left(\frac{1}{\rho_m}\right)\int_{\omega_1}^{\omega_2} d\omega = (\omega_2 - \omega_1)\ln\left(\frac{1}{\rho_m}\right) \leq \frac{\pi}{RC} \qquad (6.9.1)$$

This condition shows the trade-off associated with the bandwidth and the reflection coefficient. If R and C are given then the right-hand side of (6.9.1) is fixed. In this situation, wider bandwidth $(\omega_2 - \omega_1)$ is possible only at the cost of a higher reflection coefficient ρ_m. Further, ρ_m cannot go to zero unless the bandwidth $(\omega_2 - \omega_1)$ is zero. In other words, a perfect matching condition is achievable only at discrete frequencies.

TABLE 6.2 The Bode-Fano Constraints to Match Certain Loads Using a Passive Lossless Network

Circuit Arrangement	Constraint Relation
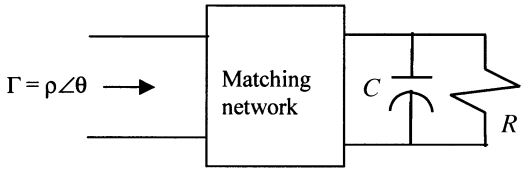	$\int_0^\infty \ln\left(\frac{1}{\rho}\right)d\omega \le \frac{\pi}{RC}$
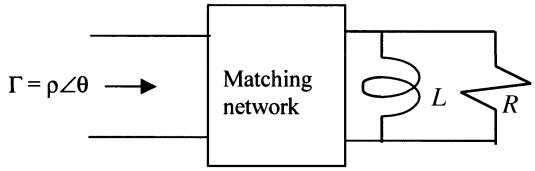	$\int_0^\infty \ln\left(\frac{1}{\rho}\right)d\omega \le \frac{\omega_o^2 \pi L}{R}$ (where ω_o is the center frequency)
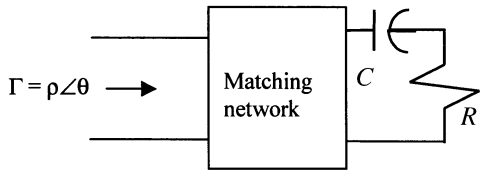	$\int_0^\infty \ln\left(\frac{1}{\rho}\right)d\omega \le \omega_o^2 \pi RC$ (where ω_o is the center frequency)
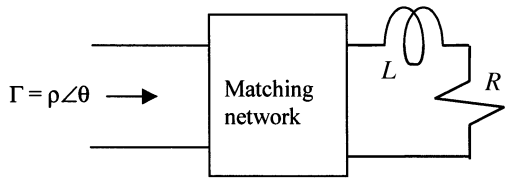	$\int_0^\infty \ln\left(\frac{1}{\rho}\right)d\omega \le \frac{\pi R}{L}$

SUGGESTED READING

I. Bahl and P. Bhartia, *Microwave Solid State Circuit Design.* New York: Wiley, 1988.

R. E. Collin, *Foundations for Microwave Engineering.* New York: McGraw Hill, 1992.

R. S. Elliott, *An Introduction to Guided Waves and Microwave Circuits*. Englewood Cliffs, NJ: Prentice Hall, 1993.

V. F. Fusco, *Microwave Circuits*. Englewood Cliffs, NJ: Prentice Hall, 1987.

G. L. Matthaei, L. Young, and E. M. T. Jones, *Microwave Filters, Impedance-Matching Networks, and Coupling Structures*. Dedham MA: Artech House, 1980.

D. M. Pozar, *Microwave Engineering*. New York: Wiley, 1998.

PROBLEMS

1. Output impedance of a microwave receiver is 50 Ω. Find the required length and characteristic impedance of a transmission line that will match a 100-Ω load to the receiver. Signal frequency and phase velocity are 10-GHz and 2.4×10^8 m/s, respectively. What is the frequency band over which the reflection coefficient remains below 0.1?

2. A quarter-wave impedance matching transformer is used to match a microwave source with internal impedance 10 Ω to a 50-Ω transmission line. If source frequency is 3 GHz and phase velocity on the line is equal to the speed of light in free-space, then find the following.
   (a) Required length and characteristic impedance of the matching section
   (b) Reflection coefficients at two ends of the matching section

3. A 0.7-m-long transmission line short circuited at one end has an input impedance of $-j68.8\,\Omega$. Signal frequency and phase velocity are 100 MHz and 2×10^8 m/s, respectively.
   (a) What is the characteristic impedance of the transmission line?
   (b) If a 200-Ω load is connected to the end of this line, what is the new input impedance?
   (c) A quarter-wave-matching transformer is to be used to match a 200-Ω load with the line. What will be the required length and characteristic impedance of the matching transformer?

4. Design a two-section binomial transformer to match a 100-Ω load to a 75-Ω line. What is the frequency band over which reflection coefficient remains below 0.1?

5. Design a three-section binomial transformer to match a 75-Ω load to a 50-Ω transmission line. What is the fractional bandwidth for a VSWR less than 1.1?

6. Using the approximate theory, design a two-section Chebyshev transformer to match a 100-Ω load to a 75-Ω line. What is the frequency band over which the reflection coefficient remains below 0.1? Compare the results with those obtained in Problem 4.

7. Design a four-section Chebyshev transformer to match a network with input impedance 60 Ω to a transmission line of characteristic impedance 40 Ω. Find the bandwidth if the maximum allowed VSWR in its pass-band is 1.2.

8. Using the exact theory, design a two-section Chebyshev transformer to match a 10-Ω load to a 75-Ω line. Find the bandwidth over which the reflection coefficient remains below 0.05.

9. Using the exact theory, design a three-section Chebyshev transformer to match a 10-Ω load to a 75-Ω line. Find the bandwidth over which the reflection coefficient remains below 0.05. Compare the results with those obtained in Problem 8.

10. Design a transmission line taper to match a 75-Ω load to a 50-Ω line. The desired frequency response has a double zero at $\beta L = \pm 2\pi$. Plot its frequency response and normalized characteristic impedance distribution.

11. Design a transmission line taper to match a 40-Ω load to a 75-Ω line. Its reflection coefficient has triple zeros at $\beta L = \pm 2\pi$. Plot its frequency response and normalized characteristic impedance distribution versus the normalized length of the taper.

12. Design a Klopfenstein taper to match a 40-Ω load to a 75-Ω line. Maximum allowed reflection coefficient in its pass-band is 0.1. Plot the characteristic impedance variation along its normalized length and the input reflection coefficient versus βL. Compare the results with those obtained in Problem 11.

Radio-Frequency and Microwave Communication Circuits: Analysis and Design
Devendra K. Misra

ISBNs: 0-471-41253-8 (Hardback); 0-471-22435-9 (Electronic)

7

TWO-PORT NETWORKS

Electronic circuits are frequently needed for processing a given electrical signal to extract the desired information or characteristics. This includes boosting the strength of a weak signal or filtering out certain frequency bands and so forth. Most of these circuits can be modeled as a black box that contains a linear network comprising resistors, inductors, capacitors, and dependent sources. Thus, it may include electronic devices but not the independent sources. Further, it has four terminals, two for input and the other two for output of the signal. There may be a few more terminals to supply the bias voltage for electronic devices. However, these bias conditions are embedded in equivalent dependent sources. Hence, a large class of electronic circuits can be modeled as two-port networks. Parameters of the two-port completely describe its behavior in terms of voltage and current at each port. These parameters simplify the description of its operation when the two-port network is connected into a larger system.

Figure 7.1 shows a two-port network along with appropriate voltages and currents at its terminals. Sometimes, port-1 is called the input while port-2 is the output port. The upper terminal is customarily assumed to be positive with respect to the lower one on either side. Further, currents enter the positive terminals at each port. Since

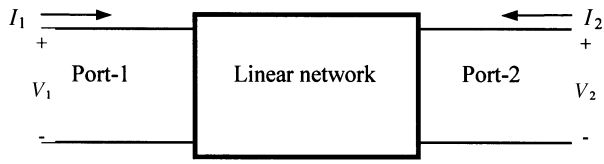

Figure 7.1 Two-port network.

the linear network does not contain independent sources, the same currents leave respective negative terminals. There are several ways to characterize this network. Some of these parameters and relations among them are presented in this chapter, including impedance parameters, admittance parameters, hybrid parameters, and transmission parameters. Scattering parameters are introduced later in the chapter to characterize the high-frequency and microwave circuits.

7.1 IMPEDANCE PARAMETERS

Consider the two-port network shown in Figure 7.1. Since the network is linear, the superposition principle can be applied. Assuming that it contains no independent sources, voltage V_1 at port-1 can be expressed in terms of two currents as follows:

$$V_1 = Z_{11}I_1 + Z_{12}I_2 \tag{7.1.1}$$

Since V_1 is in volts, and I_1 and I_2 are in amperes, parameters Z_{11} and Z_{12} must be in ohms. Therefore, these are called the *impedance parameters*.

Similarly, we can write V_2 in terms of I_1 and I_2 as follows:

$$V_2 = Z_{21}I_1 + Z_{22}I_2 \tag{7.1.2}$$

Using the matrix representation, we can write

$$\begin{bmatrix} V_1 \\ V_2 \end{bmatrix} = \begin{bmatrix} Z_{11} & Z_{12} \\ Z_{21} & Z_{22} \end{bmatrix} \begin{bmatrix} I_1 \\ I_2 \end{bmatrix} \tag{7.1.3}$$

or,

$$[V] = [Z][I] \tag{7.1.4}$$

where $[Z]$ is called the *impedance matrix* of two-port network.

If port-2 of this network is left open then I_2 will be zero. In this condition, (7.1.1) and (7.1.2) give

$$Z_{11} = \left.\frac{V_1}{I_1}\right|_{I_2=0} \tag{7.1.5}$$

and,

$$Z_{21} = \left.\frac{V_2}{I_1}\right|_{I_2=0} \tag{7.1.6}$$

Similarly, with a source connected at port-2 while port-1 is open circuit, we find that

$$Z_{12} = \left.\frac{V_1}{I_2}\right|_{I_1=0} \tag{7.1.7}$$

and,

$$Z_{22} = \left.\frac{V_2}{I_2}\right|_{I_1=0} \tag{7.1.8}$$

Equations (7.1.5) through (7.1.8) define the impedance parameters of a two-port network.

Example 7.1: Find impedance parameters for the two-port network shown here.

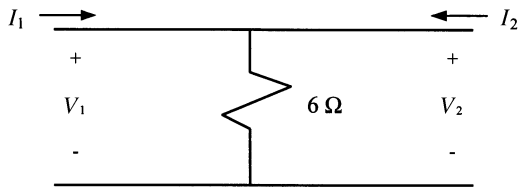

If I_2 is zero then V_1 and V_2 can be found from Ohm's law as 6 I_1. Hence, from (7.1.5) and (7.1.6),

$$Z_{11} = \left.\frac{V_1}{I_1}\right|_{I_2=0} = \frac{6I_1}{I_1} = 6\ \Omega$$

and,

$$Z_{21} = \left.\frac{V_2}{I_1}\right|_{I_2=0} = \frac{6I_1}{I_1} = 6\ \Omega$$

Similarly, when the source is connected at port-2 and port-1 has an open circuit, we find that

$$V_2 = V_1 = 6\ I_2$$

Hence, from (7.1.7) and (7.1.8),

$$Z_{12} = \left.\frac{V_1}{I_2}\right|_{I_1=0} = \frac{6I_2}{I_2} = 6\ \Omega$$

and,

$$Z_{22} = \left.\frac{V_2}{I_2}\right|_{I_1=0} = \frac{6I_2}{I_2} = 6\ \Omega$$

Therefore,

$$\begin{bmatrix} Z_{11} & Z_{12} \\ Z_{21} & Z_{22} \end{bmatrix} = \begin{bmatrix} 6 & 6 \\ 6 & 6 \end{bmatrix}$$

Example 7.2: Find impedance parameters of the two-port network shown here.

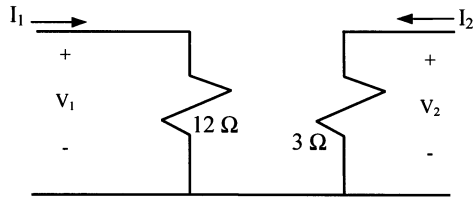

As before, assume that the source is connected at port-1 while port-2 is open. In this condition, $V_1 = 12\,I_1$ and $V_2 = 0$. Therefore,

$$Z_{11} = \left.\frac{V_1}{I_1}\right|_{I_2=0} = \frac{12I_1}{I_1} = 12\ \Omega$$

and,

$$Z_{21} = \left.\frac{V_2}{I_1}\right|_{I_2=0} = 0$$

Similarly, with a source connected at port-2 while port-1 has an open circuit, we find that

$$V_2 = 3\ I_2 \text{ and } V_1 = 0$$

Hence, from (7.1.7) and (7.1.8),

$$Z_{12} = \left.\frac{V_1}{I_2}\right|_{I_1=0} = 0$$

and,

$$Z_{22} = \left.\frac{V_2}{I_2}\right|_{I_1=0} = \frac{3I_2}{I_2} = 3\ \Omega$$

Therefore,

$$\begin{bmatrix} Z_{11} & Z_{12} \\ Z_{21} & Z_{22} \end{bmatrix} = \begin{bmatrix} 12 & 0 \\ 0 & 3 \end{bmatrix}$$

Example 7.3: Find impedance parameters for the two-port network shown here.

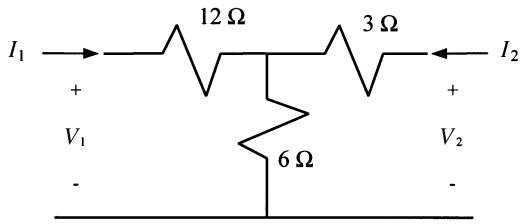

Assuming that the source is connected at port-1 while port-2 is open, we find that,

$$V_1 = (12 + 6)\, I_1 = 18\, I_1 \quad \text{and} \quad V_2 = 6\, I_1$$

Note that there is no current flowing through a 3-Ω resistor because port-2 is open. Therefore,

$$Z_{11} = \left.\frac{V_1}{I_1}\right|_{I_2=0} = \frac{18 I_1}{I_1} = 18\ \Omega$$

and,

$$Z_{21} = \left.\frac{V_2}{I_1}\right|_{I_2=0} = \frac{6 I_1}{I_1} = 6\ \Omega$$

Similarly, with a source at port-2 and port-1 open circuit,

$$V_2 = (6 + 3)\, I_2 = 9\, I_2 \quad \text{and} \quad V_1 = 6\, I_2$$

This time, there is no current flowing through a 12-Ω resistor because port-1 is open. Hence, from (7.1.7) and (7.1.8),

$$Z_{12} = \left.\frac{V_1}{I_2}\right|_{I_1=0} = \frac{6 I_2}{I_2} = 6\ \Omega$$

and,

$$Z_{22} = \left.\frac{V_2}{I_2}\right|_{I_1=0} = \frac{9 I_2}{I_2} = 9\ \Omega$$

Therefore,

$$\begin{bmatrix} Z_{11} & Z_{12} \\ Z_{21} & Z_{22} \end{bmatrix} = \begin{bmatrix} 18 & 6 \\ 6 & 9 \end{bmatrix}$$

An analysis of results obtained in Examples 7.1–7.3 indicates that Z_{12} and Z_{21} are equal for all three circuits. In fact, it is an inherent characteristic of these networks. It will hold for any reciprocal circuit. If a given circuit is symmetrical then Z_{11} will be equal to Z_{22} as well. Further, impedance parameters obtained in Example 7.3 are equal to the sum of the corresponding results found in Examples 7.1 and 7.2. This happens because if the circuits of these two examples are connected in series we end up with the circuit of Example 7.3. It is illustrated here.

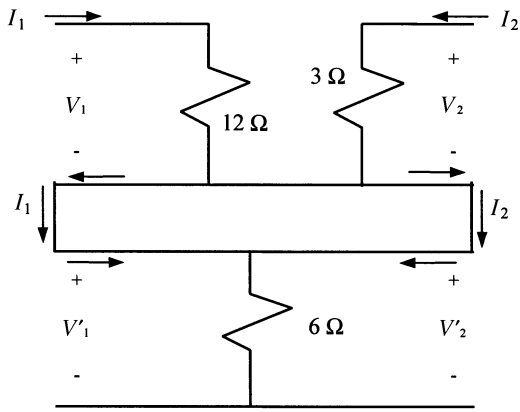

Example 7.4: Find impedance parameters for a transmission line network shown here.

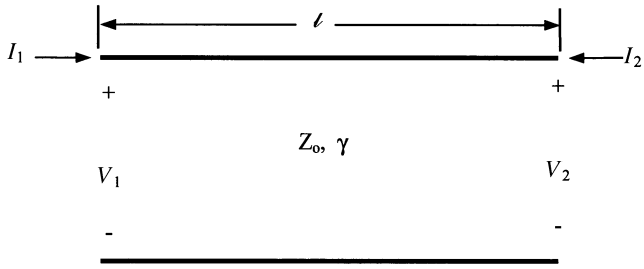

This circuit is symmetrical because interchanging port-1 and port-2 does not affect it. Therefore, Z_{22} must be equal to Z_{11}. Further, if current I at port-1 produces an open-circuit voltage V at port-2 then current I injected at port-2 will produce V at port-1. Hence, it is a reciprocal circuit. Therefore, Z_{12} will be equal to Z_{21}.

Assume that the source is connected at port-1 while the other port is open. If V_{in} is incident voltage at port-1 then $V_{in}\, e^{-\gamma\ell}$ is the voltage at port-2. Since the reflection coefficient of an open circuit is $+1$, the reflected voltage at this port is equal to the incident voltage. Therefore, the reflected voltage reaching port-1 is $V_{in}\, e^{-2\gamma\ell}$. Hence,

$$V_1 = V_{in} + V_{in}e^{-2\gamma\ell}$$
$$V_2 = 2\, V_{in}e^{-\gamma\ell}$$
$$I_1 = \frac{V_{in}}{Z_o}(1 - e^{2\gamma\ell})$$

and,

$$I_2 = 0$$

Therefore,

$$Z_{11} = \left.\frac{V_1}{I_1}\right|_{I_2=0} = \frac{V_{in}(1 + e^{-2\gamma\ell})}{\frac{V_{in}}{Z_o}(1 - e^{-2\gamma\ell})} = Z_o \frac{e^{+\gamma\ell} + e^{-\gamma\ell}}{e^{+\gamma\ell} - e^{-\gamma\ell}} = \frac{Z_o}{\tanh(\gamma\ell)} = Z_o \coth(\gamma\ell)$$

and,

$$Z_{21} = \left.\frac{V_2}{I_1}\right|_{I_2=0} = \frac{2V_{in}e^{-\gamma\ell}}{\frac{V_{in}}{Z_o}(1 - e^{-2\gamma\ell})} = Z_o \frac{2}{e^{+\gamma\ell} - e^{-\gamma\ell}} = \frac{Z_o}{\sinh(\gamma\ell)}$$

For a lossless line, $\gamma = j\beta$ and, therefore,

$$Z_{11} = \frac{Z_o}{j\tan(\beta\ell)} = -jZ_o \cot(\beta\ell)$$

and,

$$Z_{21} = \frac{Z_o}{j\sin(\beta\ell)} = -j\frac{Z_o}{\sin(\beta\ell)}$$

7.2 ADMITTANCE PARAMETERS

Consider again the two-port network shown in Figure 7.1. Since the network is linear, the superposition principle can be applied. Assuming that it contains no

independent sources, current I_1 at port-1 can be expressed in terms of two voltages as follows:

$$I_1 = Y_{11}V_1 + Y_{12}V_2 \tag{7.2.1}$$

Since I_1 is in amperes, and V_1 and V_2 are in volts, parameters Y_{11} and Y_{12} must be in siemens. Therefore, these are called the *admittance parameters*.

Similarly, we can write I_2 in terms of V_1 and V_2 as follows:

$$I_2 = Y_{21}V_1 + Y_{22}V_2 \tag{7.2.2}$$

Using the matrix representation, we can write

$$\begin{bmatrix} I_1 \\ I_2 \end{bmatrix} = \begin{bmatrix} Y_{11} & Y_{12} \\ Y_{21} & Y_{22} \end{bmatrix} \begin{bmatrix} V_1 \\ V_2 \end{bmatrix} \tag{7.2.3}$$

or,

$$[I] = [Y][V] \tag{7.2.4}$$

where $[Y]$ is called the *admittance matrix* of the two-port network.

If port-2 of this network has a short circuit then V_2 will be zero. In this condition, (7.2.1) and (7.2.2) give

$$Y_{11} = \left.\frac{I_1}{V_1}\right|_{V_2=0} \tag{7.2.5}$$

and,

$$Y_{21} = \left.\frac{I_2}{V_1}\right|_{V_2=0} \tag{7.2.6}$$

Similarly, with a source connected at port-2 and a short circuit at port-1,

$$Y_{12} = \left.\frac{I_1}{V_2}\right|_{V_1=0} \tag{7.2.7}$$

and,

$$Y_{22} = \left.\frac{I_2}{V_2}\right|_{V_1=0} \tag{7.2.8}$$

Equations (7.2.5) through (7.2.8) define the admittance parameters of a two-port network.

Example 7.5: Find admittance parameters of the circuit shown here.

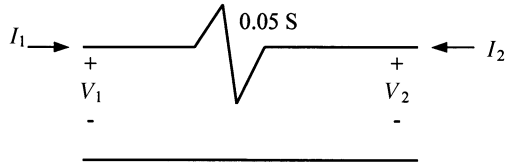

If V_2 is zero then I_1 is equal to 0.05 V_1 and I_2 is -0.05 V_1. Hence, from (7.2.5) and (7.2.6),

$$Y_{11} = \frac{I_1}{V_1}\bigg|_{V_2=0} = \frac{0.05V_1}{V_1} = 0.05 \text{ S}$$

and,

$$Y_{21} = \frac{I_2}{V_1}\bigg|_{V_2=0} = \frac{-0.05V_1}{V_1} = -0.05 \text{ S}$$

Similarly, with a source connected at port-2 and port-1 having a short circuit,

$$I_2 = -I_1 = 0.05\ V_2$$

Hence, from (7.2.7) and (7.2.8),

$$Y_{12} = \frac{I_1}{V_2}\bigg|_{V_1=0} = \frac{-0.05\ V_2}{V_2} = -0.05 \text{ S}$$

and,

$$Y_{22} = \frac{I_2}{V_2}\bigg|_{V_1=0} = \frac{0.05\ V_2}{V_2} = 0.05 \text{ S}$$

Therefore,

$$\begin{bmatrix} Y_{11} & Y_{12} \\ Y_{21} & Y_{22} \end{bmatrix} = \begin{bmatrix} 0.05 & -0.05 \\ -0.05 & 0.05 \end{bmatrix}$$

Again we find that Y_{11} is equal to Y_{22} because this circuit is symmetrical. Similarly, Y_{12} is equal to Y_{21} because it is reciprocal.

Example 7.6: Find admittance parameters for the two-port network shown here.

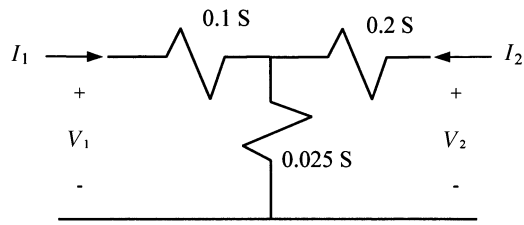

Assuming that a source is connected at port-1 while port-2 has a short circuit, we find that

$$I_1 = \frac{0.1(0.2 + 0.025)}{0.1 + 0.2 + 0.025} V_1 = \frac{0.0225}{0.325} V_1 \text{ A}$$

and if voltage across 0.2 S is V_N, then

$$V_N = \frac{I_1}{(0.2 + 0.025)} = \frac{0.0225}{0.225 \cdot 0.325} V_1 = \frac{V_1}{3.25} \text{ V}$$

Therefore,

$$I_2 = -0.2 V_N = -\frac{0.2}{3.25} V_1 \text{ A}$$

Hence, from (7.2.5) and (7.2.6),

$$Y_{11} = \left.\frac{I_1}{V_1}\right|_{V_2=0} = \frac{0.0225}{0.325} = 0.0692 \text{ S}$$

and,

$$Y_{21} = \left.\frac{I_2}{V_1}\right|_{V_2=0} = -\frac{0.2}{3.25} = -0.0615 \text{ S}$$

Similarly, with a source at port-2 and port-1 having a short circuit,

$$I_2 = \frac{0.2(0.1 + 0.025)}{0.2 + 0.1 + 0.025} V_1 = \frac{0.025}{0.325} V_2 \text{ A}$$

and if voltage across 0.1 S is V_M, then

$$V_M = \frac{I_2}{(0.1 + 0.025)} = \frac{0.025}{0.125 \cdot 0.325} V_2 = \frac{2V_2}{3.25} \text{ V}$$

Therefore,

$$I_1 = -0.1V_M = -\frac{0.2}{3.25}V_2 \text{ A}$$

Hence, from (7.2.7) and (7.2.8),

$$Y_{12} = \left.\frac{I_1}{V_2}\right|_{V_1=0} = -\frac{0.2}{3.25} = -0.0615 \text{ S}$$

and,

$$Y_{22} = \left.\frac{I_2}{V_2}\right|_{V_1=0} = \frac{0.025}{0.325} = 0.0769 \text{ S}$$

Therefore,

$$\begin{bmatrix} Y_{11} & Y_{12} \\ Y_{21} & Y_{22} \end{bmatrix} = \begin{bmatrix} 0.0692 & -0.0615 \\ -0.0615 & 0.0769 \end{bmatrix}$$

As expected, $Y_{12} = Y_{21}$ but $Y_{11} \neq Y_{22}$. This is because the given circuit is reciprocal but is not symmetrical.

Example 7.7: Find admittance parameters of the two-port network shown here.

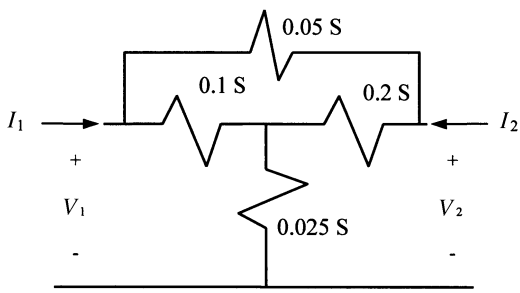

Assuming that a source is connected at port-1 while port-2 has a short circuit, we find that

$$I_1 = \left\{0.05 + \frac{0.1(0.2 + 0.025)}{0.1 + 0.2 + 0.025}\right\}V_1 = 0.1192V_1 \text{ A}$$

and if current through 0.05 S is I_N, then

$$I_N = \frac{0.05}{0.05 + \dfrac{0.1(0.2 + 0.025)}{0.1 + 0.2 + 0.025}}I_1 = 0.05\ V_1 \text{ A}$$

Current through 0.1 S is $I_1 - I_N = 0.0692V_1$. Using the current division rule, current I_M through 0.2 S is found as follows:

$$I_M = \frac{0.2}{0.2 + 0.025} 0.0692V_1 = 0.0615V_1 \text{ A}$$

Hence, $I_2 = -(I_N + I_M) = -0.1115V_1$ A.

Now, from (7.2.5) and (7.2.6),

$$Y_{11} = \left.\frac{I_1}{V_1}\right|_{V_2=0} = 0.1192 \text{ S}$$

and,

$$Y_{21} = \left.\frac{I_2}{V_1}\right|_{V_2=0} = -0.1115 \text{ S}$$

Similarly, with a source at port-2 and port-1 having a short circuit, current I_2 at port-2 is

$$I_2 = \left\{0.05 + \frac{0.2(0.1 + 0.025)}{0.2 + 0.1 + 0.025}\right\} V_2 = 0.1269V_2 \text{ A}$$

and current I_N through 0.05 S can be found as follows:

$$I_N = \frac{0.05}{0.05 + \dfrac{0.2(0.1 + 0.025)}{0.2 + 0.1 + 0.025}} I_2 = 0.05V_2 \text{ A}$$

Current through 0.2 S is $I_2 - I_N = 0.0769V_2$. Using the current division rule one more time, the current I_M through 0.1 S is found as follows:

$$I_M = \frac{0.1}{0.1 + 0.025} 0.0769V_2 = 0.0615V_2 \text{ A}$$

Hence, $I_1 = -(I_N + I_M) = -0.1115V_2$ A. Therefore, from (7.2.7) and (7.2.8),

$$Y_{12} = \left.\frac{I_1}{V_2}\right|_{V_1=0} = -0.1115 \text{ S}$$

and,

$$Y_{22} = \left.\frac{I_2}{V_2}\right|_{V_1=0} = 0.1269 \text{ S}$$

Therefore,

$$\begin{bmatrix} Y_{11} & Y_{12} \\ Y_{21} & Y_{22} \end{bmatrix} = \begin{bmatrix} 0.1192 & -0.1115 \\ -0.1115 & 0.1269 \end{bmatrix}$$

As expected, $Y_{12} = Y_{21}$ but $Y_{11} \neq Y_{22}$. This is because the given circuit is reciprocal but is not symmetrical. Further, we find that the admittance parameters obtained in Example 7.7 are equal to the sum of the corresponding impedance parameters of Examples 7.5 and 7.6. This is because when the circuits of these two examples are connected in parallel we end up with the circuit of Example 7.7. It is illustrated here.

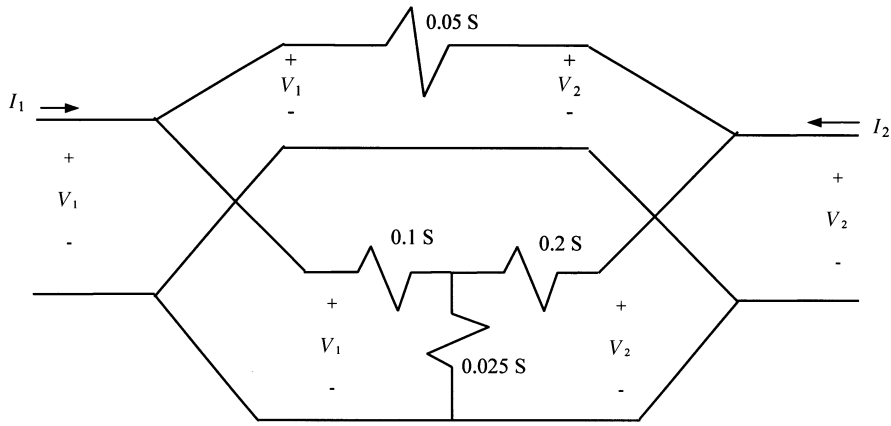

Example 7.8: Find admittance parameters of a transmission line of length ℓ, as shown here.

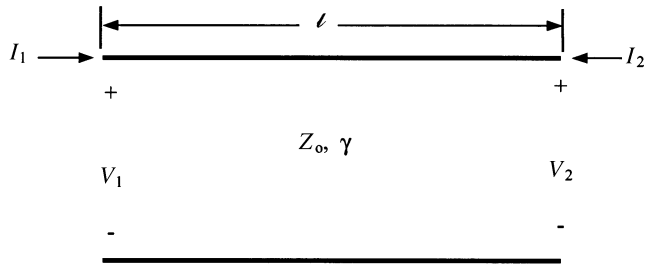

This circuit is symmetrical because interchanging port-1 and port-2 does not affect it. Therefore, Y_{22} must be equal Y_{11}. Further, if voltage V at port-1 produces a short-circuit current I at port-2 then voltage V at port-2 will produce current I at port-1. Hence, it is a reciprocal circuit. Therefore, Y_{12} will be equal to Y_{21}.

Assume that a source is connected at port-1 while the other port has a short circuit. If V_{in} is the incident voltage at port-1 then it will appear as $V_{in}\,e^{-\gamma\ell}$ at port-2. Since the reflection coefficient of a short circuit is equal to -1, reflected voltage at this port is 180° out of phase with incident voltage. Therefore, the reflected voltage reaching port-1 is $-V_{in}\,e^{-2\gamma\ell}$. Hence,

$$V_1 = V_{in} - V_{in}e^{-2\gamma\ell}$$
$$V_2 = 0$$
$$I_1 = \frac{V_{in}}{Z_o}(1 + e^{-2\gamma\ell})$$

and,

$$I_2 = -\frac{2V_{in}}{Z_o}e^{-\gamma\ell}$$

Therefore,

$$Y_{11} = \frac{I_1}{V_1}\bigg|_{V_2=0} = \frac{\frac{V_{in}}{Z_o}(1 + e^{-2\gamma\ell})}{V_{in}(1 - e^{-2\gamma\ell})} = \frac{e^{+\gamma\ell} + e^{-\gamma\ell}}{Z_o(e^{+\gamma\ell} - e^{-\gamma\ell})} = \frac{1}{Z_o \cdot \tanh(\gamma\ell)}$$

and,

$$Y_{21} = \frac{I_2}{V_1}\bigg|_{V_2=0} = \frac{-\frac{2V_{in}}{Z_o}e^{-\gamma\ell}}{V_{in}(1 - e^{-2\gamma\ell})} = -\frac{2}{Z_o(e^{+\gamma\ell} - e^{-\gamma\ell})} = -\frac{1}{Z_o \cdot \sinh(\gamma\ell)}$$

For a lossless line, $\gamma = j\beta$ and, therefore,

$$Y_{11} = \frac{1}{jZ_o \tan(\beta\ell)}$$

and

$$Y_{21} = -\frac{1}{jZ_o \sin(\beta\ell)} = j\frac{1}{Z_o \cdot \sin(\beta\ell)}$$

7.3 HYBRID PARAMETERS

Reconsider the two-port network of Figure 7.1. Since the network is linear, the superposition principle can be applied. Assuming that it contains no independent

sources, voltage V_1 at port-1 can be expressed in terms of current I_1 at port-1 and voltage V_2 at port-2 as follows:

$$V_1 = h_{11}I_1 + h_{12}V_2 \tag{7.3.1}$$

Similarly, we can write I_2 in terms of I_1 and V_2 as follows:

$$I_2 = h_{21}I_1 + h_{22}V_2 \tag{7.3.2}$$

Since V_1 and V_2 are in volts while I_1 and I_2 are in amperes, parameter h_{11} must be in ohms, h_{12} and h_{21} must be dimensionless, and h_{22} must be in siemens. Therefore, these are called *hybrid parameters*.

Using the matrix representation, we can write

$$\begin{bmatrix} V_1 \\ I_2 \end{bmatrix} = \begin{bmatrix} h_{11} & h_{12} \\ h_{21} & h_{22} \end{bmatrix} \begin{bmatrix} I_1 \\ V_2 \end{bmatrix} \tag{7.3.3}$$

Hybrid parameters are especially important in transistor circuit analysis. These parameters are determined as follows. If port-2 has a short circuit then V_2 will be zero. In this condition, (7.3.1) and (7.3.2) give

$$h_{11} = \left.\frac{V_1}{I_1}\right|_{V_2=0} \tag{7.3.4}$$

and,

$$h_{21} = \left.\frac{I_2}{I_1}\right|_{V_2=0} \tag{7.3.5}$$

Similarly, with a source connected at port-2 while port-1 is open,

$$h_{12} = \left.\frac{V_1}{V_2}\right|_{I_1=0} \tag{7.3.6}$$

and,

$$h_{22} = \left.\frac{I_2}{V_2}\right|_{I_1=0} \tag{7.3.7}$$

Thus, parameters h_{11} and h_{21} represent the input impedance and the forward current gain, respectively, when a short circuit is at port-2. Similarly, h_{12} and h_{22} represent the reverse voltage gain and the output admittance, respectively, when port-1 has an open circuit. Because of this mix, these are called hybrid parameters. In

transistor circuit analysis, these are generally denoted by h_i, h_f, h_r, and h_o, respectively.

Example 7.9: Find hybrid parameters of the two-port network shown here.

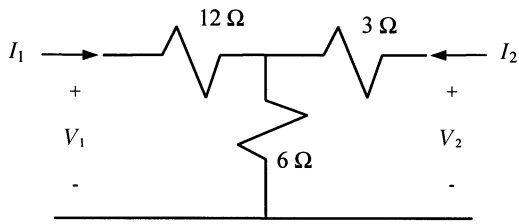

With a short circuit at port-2,

$$V_1 = I_1\left(12 + \frac{6 \cdot 3}{6+3}\right) = 14I_1$$

and, using the current divider rule, we find that

$$I_2 = -\frac{6}{6+3}I_1 = -\frac{2}{3}I_1$$

Therefore, from (7.3.4) and (7.3.5),

$$h_{11} = \left.\frac{V_1}{I_1}\right|_{V_2=0} = 14\ \Omega$$

and,

$$h_{21} = \left.\frac{I_2}{I_1}\right|_{V_2=0} = -\frac{2}{3}$$

Similarly, with a source connected at port-2 while port-1 has an open circuit,

$$V_2 = (3+6)I_2 = 9\ I_2$$

and,

$$V_1 = 6\ I_2$$

because there is no current flowing through a 12-Ω resistor.

Hence, from (7.3.6) and (7.3.7),

$$h_{12} = \left.\frac{V_1}{V_2}\right|_{I_1=0} = \frac{6I_2}{9I_2} = \frac{2}{3}$$

and,

$$h_{22} = \left.\frac{I_2}{V_2}\right|_{I_1=0} = \frac{1}{9}\text{S}$$

Thus,

$$\begin{bmatrix} h_{11} & h_{12} \\ h_{21} & h_{22} \end{bmatrix} = \begin{bmatrix} 14\ \Omega & \frac{2}{3} \\ -\frac{2}{3} & \frac{1}{9}\text{S} \end{bmatrix}$$

7.4 TRANSMISSION PARAMETERS

Reconsider the two-port network of Figure 7.1. Since the network is linear, the superposition principle can be applied. Assuming that it contains no independent sources, voltage V_1 and current I_1 at port-1 can be expressed in terms of current I_2 and voltage V_2 at port-2 as follows:

$$V_1 = AV_2 - BI_2 \tag{7.4.1}$$

Similarly, we can write I_1 in terms of I_2 and V_2 as follows:

$$I_1 = CV_2 - DI_2 \tag{7.4.2}$$

Since V_1 and V_2 are in volts while I_1 and I_2 are in amperes, parameters A and D must be dimensionless, B must be in ohms, and C must be in siemens.

Using the matrix representation, (7.4.2) can be written as follows.

$$\begin{bmatrix} V_1 \\ I_1 \end{bmatrix} = \begin{bmatrix} A & B \\ C & D \end{bmatrix} \begin{bmatrix} V_2 \\ -I_2 \end{bmatrix} \tag{7.4.3}$$

Transmission parameters (also known as *elements of chain matrix*) are especially important for analysis of circuits connected in cascade. These parameters are determined as follows.

If port-2 has a short circuit then V_2 will be zero. Under this condition, (7.4.1) and (7.4.2) give

$$B = \left.\frac{V_1}{-I_2}\right|_{V_2=0} \tag{7.4.4}$$

and,

$$D = \left.\frac{I_1}{-I_2}\right|_{V_2=0} \tag{7.4.5}$$

Similarly, with a source connected at the port-1 while port-2 is open, we find that

$$A = \left.\frac{V_1}{V_2}\right|_{I_2=0} \tag{7.4.6}$$

and,

$$C = \left.\frac{I_1}{V_2}\right|_{I_2=0} \tag{7.4.7}$$

Example 7.10: Determine transmission parameters of the network shown here.

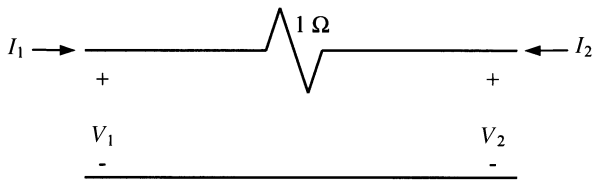

With a source connected at port-1 while port-2 has a short circuit (so that V_2 is zero),

$$I_2 = -I_1 \text{ and } V_1 = I_1 \text{ V}$$

Therefore, from (7.4.4) and (7.4.5),

$$B = \left.\frac{V_1}{-I_2}\right|_{V_2=0} = 1\ \Omega$$

and,

$$D = \left.\frac{I_1}{-I_2}\right|_{V_2=0} = 1$$

Similarly, with a source connected at port-1 while port-2 is open (so that I_2 is zero),

$$V_2 = V_1 \quad \text{and} \quad I_1 = 0$$

Now, from (7.4.6) and (7.4.7),

$$A = \left.\frac{V_1}{V_2}\right|_{I_2=0} = 1$$

and,

$$C = \left.\frac{I_1}{V_2}\right|_{I_2=0} = 0$$

Hence, the transmission matrix of this network is

$$\begin{bmatrix} A & B \\ C & D \end{bmatrix} = \begin{bmatrix} 1 & 1 \\ 0 & 1 \end{bmatrix}$$

Example 7.11: Determine transmission parameters of the network shown here.

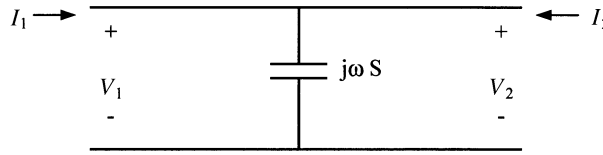

With a source connected at port-1 while port-2 has a short circuit (so that V_2 is zero),

$$I_2 = -I_1 \quad \text{and} \quad V_1 = 0 \text{ V}$$

Therefore, from (7.4.4) and (7.4.5),

$$B = \left.\frac{V_1}{-I_2}\right|_{V_2=0} = 0\ \Omega$$

and,

$$D = \left.\frac{I_1}{-I_2}\right|_{V_2=0} = 1$$

Similarly, with a source connected at port-1 while port-2 is open (so that I_2 is zero),

$$V_2 = V_1 \quad \text{and} \quad I_1 = j\omega\ V_1 \text{ A}$$

Now, from (7.4.6) and (7.4.7),

$$A = \left.\frac{V_1}{V_2}\right|_{I_2=0} = 1$$

and,

$$C = \left.\frac{I_1}{V_2}\right|_{I_2=0} = j\omega \text{ S}$$

Hence, the transmission matrix of this network is

$$\begin{bmatrix} A & B \\ C & D \end{bmatrix} = \begin{bmatrix} 1 & 0 \\ j\omega & 1 \end{bmatrix}$$

Example 7.12: Determine transmission parameters of the network shown here.

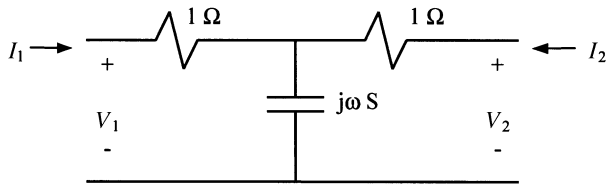

With a source connected at port-1 while port-2 has a short circuit (so that V_2 is zero), we find that

$$V_1 = \left(1 + \frac{1}{1+j\omega}\right) I_1 = \frac{2+j\omega}{1+j\omega} I_1$$

and,

$$I_2 = -\frac{\dfrac{1}{(j\omega)}}{\dfrac{1}{j\omega}+1} I_1 = -\frac{1}{1+j\omega} I_1$$

Therefore, from (7.4.4) and (7.4.5),

$$B = \left.\frac{V_1}{-I_2}\right|_{V_2=0} = 2 + j\omega\ \Omega$$

and,

$$D = \left.\frac{I_1}{-I_2}\right|_{V_2=0} = 1 + j\omega$$

Similarly, with a source connected at port-1 while port-2 is open (so that I_2 is zero),

$$V_1 = \left(1 + \frac{1}{j\omega}\right) I_1 = \left(\frac{1 + j\omega}{j\omega}\right) I_1$$

and,

$$V_2 = \frac{1}{j\omega} I_1$$

Now, from (7.4.6) and (7.4.7),

$$A = \left.\frac{V_1}{V_2}\right|_{I_2=0} = 1 + j\omega$$

and,

$$C = \left.\frac{I_1}{V_2}\right|_{I_2=0} = j\omega \text{ S}$$

Hence,

$$\begin{bmatrix} A & B \\ C & D \end{bmatrix} = \begin{bmatrix} 1 + j\omega & 2 + j\omega \\ j\omega & 1 + j\omega \end{bmatrix}$$

Example 7.13: Find transmission parameters of the transmission line shown here.

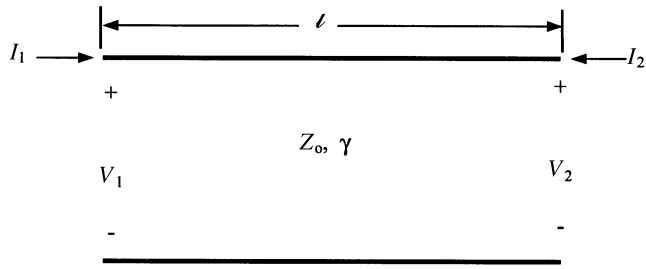

Assume that a source is connected at port-1 while the other port has a short circuit. If V_{in} is incident voltage at port-1 then it will be $V_{in}\, e^{-\gamma \ell}$ at port-2. Since the reflection coefficient of the short circuit is -1, reflected voltage at this port is 180°

out of phase with incident voltage. Therefore, reflected voltage reaching port-1 is $-V_{\text{in}}\, e^{-2\gamma\ell}$. Hence,

$$V_1 = V_{\text{in}} - V_{\text{in}} e^{-2\gamma\ell}$$
$$V_2 = 0$$
$$I_1 = \frac{V_{\text{in}}}{Z_{\text{o}}}(1 + e^{-2\gamma\ell})$$

and,

$$I_2 = -\frac{2V_{\text{in}}}{Z_{\text{o}}} e^{-\gamma\ell}$$

Therefore, from (7.4.4) and (7.4.5),

$$B = \left.\frac{V_1}{-I_2}\right|_{V_2=0} = \frac{Z_{\text{o}}}{2e^{-\gamma\ell}}(1 - e^{-2\lambda\ell}) = Z_{\text{o}}\left(\frac{e^{\gamma\ell} - e^{-\gamma\ell}}{2}\right)\Omega = Z_{\text{o}} \sinh(\gamma\ell)$$

and,

$$D = \left.\frac{I_1}{-I_2}\right|_{V_2=0} = \frac{1 + e^{-2\lambda}}{2e^{-\lambda\ell}} = \frac{e^{\gamma\ell} + e^{-\gamma\ell}}{2} = \cosh(\gamma\ell)$$

Now assume that port-2 has an open circuit while the source is still connected at port-1. If V_{in} is incident voltage at port-1 then $V_{\text{in}}\, e^{-\gamma\ell}$ is at port-2. Since the reflection coefficient of an open circuit is $+1$, reflected voltage at this port is equal to incident voltage. Therefore, the reflected voltage reaching port-1 is $V_{\text{in}}\, e^{-2\gamma\ell}$. Hence,

$$V_1 = V_{\text{in}} + V_{\text{in}} e^{-2\gamma\ell}$$
$$V_2 = 2\, V_{\text{in}} e^{-\gamma\ell}$$
$$I_1 = \frac{V_{\text{in}}}{Z_{\text{o}}}(1 - e^{-2\gamma\ell})$$

and,

$$I_2 = 0$$

Now, from (7.4.6) and (7.4.7),

$$A = \left.\frac{V_1}{V_2}\right|_{I_2=0} = \frac{1 + e^{-2\gamma\ell}}{2e^{-\gamma\ell}} = \cosh(\gamma\ell)$$

and,

$$C = \left.\frac{I_1}{V_2}\right|_{I_2=0} = \frac{1 - e^{-2\gamma\ell}}{2Z_o e^{-\gamma\ell}} = \frac{1}{Z_o}\sinh(\gamma\ell)$$

Hence, the transmission matrix of a finite-length transmission line is

$$\begin{bmatrix} A & B \\ C & D \end{bmatrix} = \begin{bmatrix} \cosh(\gamma\ell) & Z_o \sinh(\gamma\ell) \\ \dfrac{1}{Z_o}\sinh(\gamma\ell) & \cosh(\gamma\ell) \end{bmatrix}$$

For a lossless line, $\gamma = j\beta$, and therefore, it simplifies to

$$\begin{bmatrix} A & B \\ C & D \end{bmatrix} = \begin{bmatrix} \cos(\beta\ell) & jZ_o \sin(\beta\ell) \\ j\dfrac{1}{Z_o}\sin(\beta\ell) & \cos(\beta\ell) \end{bmatrix}$$

An analysis of results obtained in Examples 7.10–7.13 indicates that the following condition holds for all four circuits:

$$AD - BC = 1 \tag{7.4.8}$$

This is because these circuits are reciprocal. In other words, if a given circuit is known to be reciprocal then (7.4.8) must be satisfied. Further, we find that transmission parameter A is equal to D in all four cases. This always happens when a given circuit is reciprocal.

In Example 7.11, A and D are real, B is zero, and C is imaginary. For a lossless line in Example 7.13, A and D simplify to real numbers while C and D become purely imaginary. This characteristic of the transmission parameters is associated with any lossless circuit.

A comparison of the circuits in Examples 7.10 to 7.12 reveals that the two-port network of Example 7.12 can be obtained by cascading that of Example 7.10 on the two sides of Example 7.11, as shown here.

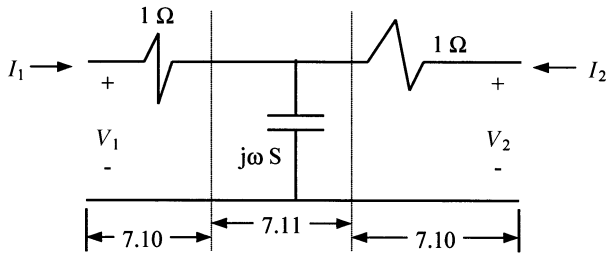

Therefore, the chain (or transmission) matrix for the network shown in Example 7.12 can be obtained after multiplying three chain matrices as follows:

$$\begin{bmatrix} 1 & 1 \\ 0 & 1 \end{bmatrix} \cdot \begin{bmatrix} 1 & 0 \\ j\omega & 1 \end{bmatrix} \cdot \begin{bmatrix} 1 & 1 \\ 0 & 1 \end{bmatrix} = \begin{bmatrix} 1 & 1 \\ 0 & 1 \end{bmatrix} \cdot \begin{bmatrix} 1 & 1 \\ j\omega & j\omega + 1 \end{bmatrix} = \begin{bmatrix} 1 + j\omega & 2 + j\omega \\ j\omega & 1 + j\omega \end{bmatrix}$$

This shows that chain matrices are convenient in analysis and design of networks connected in cascade.

7.5 CONVERSION OF THE IMPEDANCE, ADMITTANCE, CHAIN, AND HYBRID PARAMETERS

One type of network parameters can be converted into another via the respective defining equations. For example, the admittance parameters of a network can be found from its impedance parameters as follows.

From (7.2.3) and (7.1.3), we find

$$\begin{bmatrix} I_1 \\ I_2 \end{bmatrix} = \begin{bmatrix} Y_{11} & Y_{12} \\ Y_{21} & Y_{22} \end{bmatrix} \begin{bmatrix} V_1 \\ V_2 \end{bmatrix} = \begin{bmatrix} Z_{11} & Z_{12} \\ Z_{21} & Z_{22} \end{bmatrix}^{-1} \begin{bmatrix} V_1 \\ V_2 \end{bmatrix}$$

Hence,

$$\begin{bmatrix} Y_{11} & Y_{12} \\ Y_{21} & Y_{22} \end{bmatrix} = \begin{bmatrix} Z_{11} & Z_{12} \\ Z_{21} & Z_{22} \end{bmatrix}^{-1} = \frac{1}{Z_{11}Z_{22} - Z_{12}Z_{21}} \begin{bmatrix} Z_{22} & -Z_{12} \\ -Z_{21} & Z_{11} \end{bmatrix}$$

Similarly, (7.3.3) can be rearranged as follows:

$$\begin{bmatrix} I_1 \\ I_2 \end{bmatrix} = \begin{bmatrix} \dfrac{D}{B} & -\dfrac{(AD - BC)}{B} \\ -\dfrac{1}{B} & \dfrac{A}{B} \end{bmatrix} \begin{bmatrix} V_1 \\ V_2 \end{bmatrix}$$

Hence,

$$\begin{bmatrix} Y_{11} & Y_{12} \\ Y_{21} & Y_{22} \end{bmatrix} = \begin{bmatrix} \dfrac{D}{B} & -\dfrac{(AD - BC)}{B} \\ -\dfrac{1}{B} & \dfrac{A}{B} \end{bmatrix}$$

Relations between other parameters can be found following a similar procedure. These relations are given in Table 7.1.

TABLE 7.1 Conversions Among the Impedance, Admittance, Chain, and Hybrid Parameters

$Z_{11} = \frac{Y_{22}}{Y_{11}Y_{22} - Y_{12}Y_{21}}$	$Z_{11} = \frac{A}{C}$	$Z_{11} = \frac{h_{11}h_{22} - h_{12}h_{21}}{h_{22}}$
$Z_{12} = \frac{-Y_{12}}{Y_{11}Y_{22} - Y_{12}Y_{21}}$	$Z_{12} = \frac{AD - BC}{C}$	$Z_{12} = \frac{h_{12}}{h_{22}}$
$Z_{21} = \frac{-Y_{21}}{Y_{11}Y_{22} - Y_{12}Y_{21}}$	$Z_{21} = \frac{1}{C}$	$Z_{21} = \frac{-h_{21}}{h_{22}}$
$Z_{22} = \frac{Y_{11}}{Y_{11}Y_{22} - Y_{12}Y_{21}}$	$Z_{22} = \frac{D}{C}$	$Z_{22} = \frac{1}{h_{22}}$
$Y_{11} = \frac{Z_{22}}{Z_{11}Z_{22} - Z_{12}Z_{21}}$	$Y_{11} = \frac{D}{B}$	$Y_{11} = \frac{1}{h_{11}}$
$Y_{12} = \frac{-Z_{12}}{Z_{11}Z_{22} - Z_{12}Z_{21}}$	$Y_{12} = \frac{-(AD - BC)}{B}$	$Y_{12} = \frac{-h_{12}}{h_{11}}$
$Y_{21} = \frac{-Z_{21}}{Z_{11}Z_{22} - Z_{12}Z_{21}}$	$Y_{21} = \frac{-1}{B}$	$Y_{21} = \frac{h_{21}}{h_{11}}$
$Y_{22} = \frac{Z_{11}}{Z_{11}Z_{22} - Z_{12}Z_{21}}$	$Y_{22} = \frac{A}{B}$	$Y_{22} = \frac{h_{11}h_{22} - h_{12}h_{21}}{h_{11}}$
$A = \frac{Z_{11}}{Z_{21}}$	$A = \frac{-Y_{22}}{Y_{21}}$	$A = \frac{-(h_{11}h_{22} - h_{12}h_{21})}{h_{21}}$
$B = \frac{Z_{11}Z_{22} - Z_{12}Z_{21}}{Z_{21}}$	$B = \frac{-1}{Y_{21}}$	$B = \frac{-h_{11}}{h_{21}}$
$C = \frac{1}{Z_{21}}$	$C = \frac{-(Y_{11}Y_{22} - Y_{12}Y_{21})}{Y_{21}}$	$C = \frac{-h_{22}}{h_{21}}$
$D = \frac{Z_{22}}{Z_{21}}$	$D = \frac{-Y_{11}}{Y_{21}}$	$D = \frac{-1}{h_{21}}$
$h_{11} = \frac{Z_{11}Z_{22} - Z_{12}Z_{21}}{Z_{22}}$	$h_{11} = \frac{1}{Y_{11}}$	$h_{11} = \frac{B}{D}$
$h_{12} = \frac{Z_{12}}{Z_{22}}$	$h_{12} = \frac{-Y_{12}}{Y_{11}}$	$h_{12} = \frac{AD - BC}{D}$
$h_{21} = \frac{-Z_{21}}{Z_{22}}$	$h_{21} = \frac{Y_{21}}{Y_{11}}$	$h_{21} = \frac{-1}{D}$
$h_{22} = \frac{1}{Z_{22}}$	$h_{22} = \frac{Y_{11}Y_{22} - Y_{12}Y_{21}}{Y_{11}}$	$h_{22} = \frac{C}{D}$

7.6 SCATTERING PARAMETERS

As illustrated in the preceding sections, Z-parameters are useful in analyzing series circuits while Y-parameters simplify the analysis of parallel (shunt) connected circuits. Similarly, transmission parameters are useful for chain or cascade circuits.

However, the characterization procedure of these parameters requires an open or short circuit at the other port. This extreme reflection makes it very difficult (and in certain cases, impossible) to determine the parameters of a network at radio and microwave frequencies. Therefore, a new representation, based on traveling waves, is defined. This is known as the *scattering matrix* of the network. Elements of this matrix are known as the *scattering parameters*.

Figure 7.2 shows a network along with incident and reflected waves at its two ports. We adopt a convention of representing the incident wave by a_i and the reflected wave by b_i at the ith port. Hence, a_1 is an incident wave while b_1 is reflected wave at port-1. Similarly, a_2 and b_2 represent incident and reflected waves at port-2, respectively. Assume that a source is connected at port-1 that produces the incident wave a_1. A part of this wave is reflected back at the input (due to impedance mismatch) while the remaining signal is transmitted through the network. It may change in magnitude as well as in phase before emerging at port-2. Depending on the termination at this port, part of the signal is reflected back as input to port-2. Hence, reflected wave b_1 depends on incident signals a_1 and a_2 at the two ports. Similarly, emerging wave b_2 also depends on a_1 and a_2. Mathematically,

$$b_1 = S_{11}a_1 + S_{12}a_2 \tag{7.6.1}$$

$$b_2 = S_{21}a_1 + S_{22}a_2 \tag{7.6.2}$$

Using the matrix notation, we can write,

$$\begin{bmatrix} b_1 \\ b_2 \end{bmatrix} = \begin{bmatrix} S_{11} & S_{12} \\ S_{21} & S_{22} \end{bmatrix} \begin{bmatrix} a_1 \\ a_2 \end{bmatrix} \tag{7.6.3}$$

or,

$$[b] = [S][a] \tag{7.6.4}$$

where $[S]$ is called the *scattering matrix* of the two-port network; S_{ij} are known as the *scattering parameters* of this network; and a_i represents the incident wave at the ith port while b_i represents the reflected wave at the ith port.

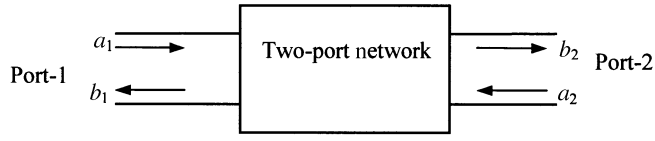

Figure 7.2 Two-port network with associated incident and reflected waves.

If port-2 is matched terminated while a_1 is incident at port-1, then a_2 is zero. In this condition, (7.6.1) and (7.6.2) give

$$S_{11} = \left.\frac{b_1}{a_1}\right|_{a_2=0} \tag{7.6.5}$$

and,

$$S_{21} = \left.\frac{b_2}{a_1}\right|_{a_2=0} \tag{7.6.6}$$

Similarly, with a source connected at port-2 while port-1 is terminated by a matched load, we find that

$$S_{12} = \left.\frac{b_1}{a_2}\right|_{a_1=0} \tag{7.6.7}$$

and,

$$S_{22} = \left.\frac{b_2}{a_2}\right|_{a_1=0} \tag{7.6.8}$$

Hence, S_{ii} is reflection coefficient Γ_i at the ith port when the other port is matched terminated. S_{ij} is the forward transmission coefficient of the jth port if i is greater than j, whereas it represents the reverse transmission coefficient if i is less than j with the other port terminated by a matched load.

We have not yet defined a_i and b_i in terms of voltage, current, or power. To that end, we write steady-state total voltage and current at the ith port as follows:

$$V_i = V_i^{\text{in}} + V_i^{\text{ref}} \tag{7.6.9}$$

and,

$$I_i = \frac{1}{Z_{\text{o}i}}(V_i^{\text{in}} - V_i^{\text{ref}}) \tag{7.6.10}$$

where superscripts "in" and "ref" represent the incident and reflected voltages, respectively. $Z_{\text{o}i}$ is characteristic impedance at ith port.

Equations (7.6.9) and (7.6.10) can be solved to find incident and reflected voltages in terms of total voltage and current at the ith port. Hence,

$$V_i^{\text{in}} = \frac{1}{2}(V_i + Z_{\text{o}i}I_i) \tag{7.6.11}$$

and,

$$V_i^{\text{ref}} = \frac{1}{2}(V_i - Z_{\text{o}i} I_i) \tag{7.6.12}$$

Assuming both of the ports to be lossless so that $Z_{\text{o}i}$ is a real quantity, the average power incident at the ith port is

$$P_i^{\text{in}} = \frac{1}{2}\text{Re}\{V_i^{\text{in}}(I_i^{\text{in}})^*\} = \frac{1}{2}\text{Re}\left\{V_i^{\text{in}}\left(\frac{V_i^{\text{in}}}{Z_{\text{o}i}}\right)^*\right\} = \frac{1}{2Z_{\text{o}i}}|V_i^{\text{in}}|^2 \tag{7.6.13}$$

and average power reflected from the ith port is

$$P_i^{\text{ref}} = \frac{1}{2}\text{Re}\left\{V_i^{\text{ref}}(I_i^{\text{ref}})^*\right\} = \frac{1}{2}\text{Re}\left\{V_i^{\text{ref}}\left(\frac{V_i^{\text{ref}}}{Z_{\text{o}i}}\right)^*\right\} = \frac{1}{2Z_{\text{o}i}}|V_i^{\text{ref}}|^2 \tag{7.6.14}$$

The a_i and b_i are defined in such a way that the squares of their magnitudes represent the power flowing in respective directions. Hence,

$$a_i = \frac{V_i^{\text{in}}}{\sqrt{2Z_{\text{o}i}}} = \frac{1}{2}\left(\frac{V_i + Z_{\text{o}i} I_i}{\sqrt{2Z_{\text{o}i}}}\right) = \frac{1}{2\sqrt{2}}\left(\frac{V_i}{\sqrt{Z_{\text{o}i}}} + \sqrt{Z_{\text{o}i}} I_i\right) \tag{7.6.15}$$

and,

$$b_i = \frac{V_i^{\text{ref}}}{\sqrt{2Z_{\text{o}i}}} = \frac{1}{2}\left(\frac{V_i - Z_{\text{o}i} I_i}{\sqrt{2Z_{\text{o}i}}}\right) = \frac{1}{2\sqrt{2}}\left(\frac{V_i}{\sqrt{Z_{\text{o}i}}} - \sqrt{Z_{\text{o}i}} I_i\right) \tag{7.6.16}$$

Therefore, units of a_i and b_i are

$$\sqrt{\text{Watt}} = \frac{\text{Volt}}{\sqrt{\text{Ohm}}} = \text{Amp} \cdot \sqrt{\text{Ohm}}$$

Power available from the source, P_{avs}, at port-1 is

$$P_{\text{avs}} = |a_1|^2;$$

power reflected from port-1, P_{ref}, is

$$P_{\text{ref}} = |b_1|^2;$$

and power delivered to the port (and hence, to the network), P_d, is

$$P_d = P_{\text{avs}} - P_{\text{ref}} = |a_1|^2 - |b_1|^2$$

Consider the circuit arrangement shown in Figure 7.3. There is a voltage source V_{S1} connected at port-1 while port-2 is terminated by load impedance Z_L. The source impedance is Z_S. Various voltages, currents, and waves are as depicted at the two ports of this network. Further, it is assumed that the characteristic impedances at port-1 and port-2 are Z_{o1} and Z_{o2}, respectively. Input impedance Z_1 at port-1 of the network is defined as the impedance across its terminals when port-2 is terminated by load Z_L while source V_{S1} along with Z_S are disconnected. Similarly, output impedance Z_2 at port-2 of the network is defined as the impedance across its terminals with load Z_L disconnected and voltage source V_{S1} replaced by a short circuit. Hence, source-impedance Z_S terminates port-1 of the network in this case. Input impedance Z_1 and output impedance Z_2 are responsible for input reflection coefficient Γ_1 and output reflection coefficient Γ_2, respectively. Hence, the ratio of b_1 to a_1 represents Γ_1 while that of b_2 to a_2 is Γ_2. For the two-port network, we can write

$$b_1 = S_{11}a_1 + S_{12}a_2 \tag{7.6.17}$$

and,

$$b_2 = S_{21}a_1 + S_{22}a_2 \tag{7.6.18}$$

Load reflection coefficient Γ_L is

$$\Gamma_L = \frac{Z_L - Z_{o2}}{Z_L + Z_{o2}} = \frac{a_2}{b_2} \tag{7.6.19}$$

Note that b_2 leaves port-2 and, therefore, it is incident on the load Z_L. Similarly, the wave reflected back from the load enters port-2 as a_2.

Source reflection coefficient Γ_S is found as

$$\Gamma_S = \frac{Z_S - Z_{o1}}{Z_S + Z_{o1}} = \frac{a_1}{b_1} \tag{7.6.20}$$

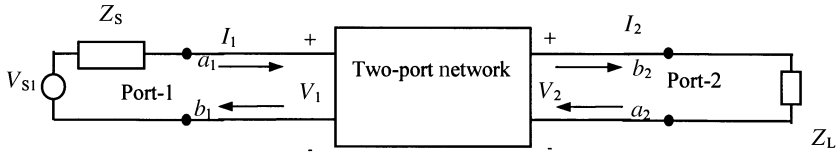

Figure 7.3 Two-port network with a voltage source connected at port-1 while port-2 is terminated.

Since b_1 leaves port-1 of the network, it is the incident wave on Z_S while a_1 is the reflected wave.

Input and output reflection coefficients are

$$\Gamma_1 = \frac{Z_1 - Z_{o1}}{Z_1 + Z_{o1}} = \frac{b_1}{a_1} \tag{7.6.21}$$

and,

$$\Gamma_2 = \frac{Z_2 - Z_{o2}}{Z_2 + Z_{o2}} = \frac{b_2}{a_2} \tag{7.6.22}$$

Dividing (7.6.17) by a_1 and then using (7.6.21), we find

$$\frac{b_1}{a_1} = \Gamma_1 = \frac{Z_1 - Z_{o1}}{Z_1 + Z_{o1}} = S_{11} + S_{12}\left(\frac{a_2}{a_1}\right) \tag{7.6.23}$$

Now, dividing (7.6.18) by a_2 and then combining with (7.6.19), we get

$$\frac{b_2}{a_2} = S_{22} + S_{21}\left(\frac{a_1}{a_2}\right) = \frac{1}{\Gamma_L} \Rightarrow \frac{a_1}{a_2} = \frac{1 - S_{22}\Gamma_L}{S_{21}\Gamma_L} \tag{7.6.24}$$

From (7.6.23) and (7.6.24),

$$\Gamma_1 = S_{11} + \frac{S_{12}S_{21}\Gamma_L}{1 - S_{22}\Gamma_L} \tag{7.6.25}$$

If a matched load is terminating port-2 then $\Gamma_L = 0$, and (7.6.25) simplifies to $\Gamma_1 = S_{11}$.

Similarly, from (7.6.18) and (7.6.22),

$$\frac{b_2}{a_2} = \Gamma_2 = \frac{Z_2 - Z_{o2}}{Z_2 + Z_{o2}} = S_{22} + S_{21}\left(\frac{a_1}{a_2}\right) \tag{7.6.26}$$

From (7.6.17) and (7.6.20), we have

$$\frac{b_1}{a_1} = S_{11} + S_{12}\left(\frac{a_2}{a_1}\right) = \frac{1}{\Gamma_S} \Rightarrow \frac{a_2}{a_1} = \frac{1 - S_{11}\Gamma_S}{S_{12}\Gamma_S} \tag{7.6.27}$$

Substituting (7.6.27) into (7.6.26) we get,

$$\Gamma_2 = S_{22} + \frac{S_{21}S_{12}\Gamma_S}{1 - S_{11}\Gamma_S} \tag{7.6.28}$$

If Z_S is equal to Z_{o1} then port-1 is matched and $\Gamma_S = 0$. Therefore, (7.6.28) simplifies to

$$\Gamma_2 = S_{22}$$

Hence, S_{11} and S_{22} can be found by evaluating the reflection coefficients at respective ports while the other port is matched terminated.

Let us determine the other two parameters, namely S_{21} and S_{12}, of the two-port network. Starting with (7.6.6) for S_{21}, we have

$$S_{21} = \left.\frac{b_2}{a_1}\right|_{a_2=0} \tag{7.6.6}$$

Now, a_2 is found from (7.6.15) with i as 2 and forcing it to zero we get

$$a_2 = \frac{1}{2}\left(\frac{V_2 + Z_{o2}I_2}{\sqrt{2Z_{o2}}}\right) = 0 \Rightarrow V_2 = -Z_{o2}I_2 \tag{7.6.29}$$

Substituting (7.6.29) in the expression for b_2 that is obtained from (7.6.16) with i as 2, we find that

$$b_2 = \frac{1}{2}\left(\frac{V_2 - Z_{o2}I_2}{\sqrt{2Z_{o2}}}\right) = -I_2\sqrt{\frac{Z_{o2}}{2}} \tag{7.6.30}$$

An expression for a_1 is obtained from (7.6.15) with $i = 1$. It simplifies for Z_S equal to Z_{o1}, as follows.

$$a_1 = \frac{1}{2}\left(\frac{V_1 + Z_{o1}I_1}{\sqrt{2Z_{o1}}}\right) = \frac{V_{S1}}{2\sqrt{2Z_{o1}}} \tag{7.6.31}$$

S_{21} is obtained by substituting (7.6.30) and (7.6.31) into (7.6.6), as follows.

$$S_{21} = \left.\frac{b_2}{a_1}\right|_{a_2=0} = \frac{\left(\frac{-\sqrt{Z_{o2}}I_2}{\sqrt{2}}\right)}{\left(\frac{V_{S1}}{2\sqrt{2Z_{o1}}}\right)} = \frac{2V_2}{V_{S1}}\sqrt{\frac{Z_{o1}}{Z_{o2}}} \tag{7.6.32}$$

Following a similar procedure, S_{12} may be found as

$$S_{12} = \left.\frac{b_1}{a_2}\right|_{a_1=0} = \frac{2V_1}{V_{S2}}\sqrt{\frac{Z_{o2}}{Z_{o1}}} \tag{7.6.33}$$

An analysis of S-parameters indicates that

$$|S_{11}|^2 = \frac{|b_1|^2}{|a_1|^2}\bigg|_{a_2=0} = \frac{P_{\text{avs}} - P_d}{P_{\text{avs}}} \tag{7.6.34}$$

where P_{avs} is power available from the source and P_d is power delivered to port-1. These two powers will be equal if the source impedance is conjugate of Z_1, that is, the source is matched with port-1.

Similarly, from (7.6.32),

$$|S_{21}|^2 = \frac{Z_{o2}\left(\frac{I_2}{\sqrt{2}}\right)^2}{\frac{1}{4Z_{o1}}\left(\frac{V_{S1}}{\sqrt{2}}\right)^2} = \frac{Z_{o2}\left(\frac{I_2}{\sqrt{2}}\right)^2}{\frac{1}{2}\left\{\frac{1}{2Z_{o1}}\left(\frac{V_{S1}}{\sqrt{2}}\right)^2\right\}} = \frac{P_{\text{AVN}}}{P_{\text{avs}}} \tag{7.6.35}$$

where P_{AVN} is power available at port-2 of the network. It will be equal to power delivered to a load that is matched to the port. This power ratio of (7.6.35) may be called the *transducer power gain*.

Following a similar procedure, it may be found that $|S_{22}|^2$ represents the ratio of power reflected from port-2 to power available from the source at port-2 while port-1 is terminated by a matched load Z_S, and $|S_{12}|^2$ represents a reverse transducer power gain.

Shifting the Reference Planes

Consider the two-port network shown in Figure 7.4. Assume that a_i and b_i are incident and reflected waves, respectively, at unprimed reference planes of the ith port. We use unprimed S-parameters for this case. Next, consider that plane A-A is shifted by a distance ℓ_1 to A′-A′. At this plane, a_1' and b_1' represent inward and outward traveling waves, respectively. Similarly, a_2' and b_2' represent inward and outward traveling waves, respectively, at plane B′-B′. We denote the scattering parameters at primed planes by a prime on each as well. Hence,

$$\begin{bmatrix} b_1 \\ b_2 \end{bmatrix} = \begin{bmatrix} S_{11} & S_{12} \\ S_{21} & S_{22} \end{bmatrix} \begin{bmatrix} a_1 \\ a_2 \end{bmatrix} \tag{7.6.36}$$

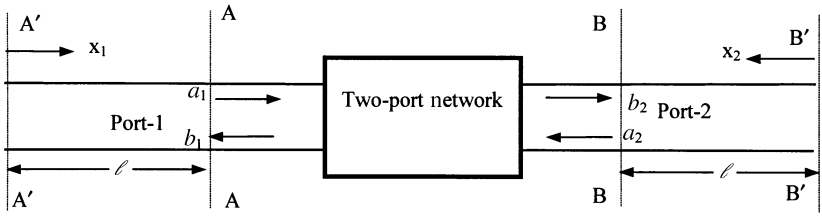

Figure 7.4 A two-port network with two reference planes on each side.

and,

$$\begin{bmatrix} b_1' \\ b_2' \end{bmatrix} = \begin{bmatrix} S_{11}' & S_{12}' \\ S_{21}' & S_{22}' \end{bmatrix} \begin{bmatrix} a_1' \\ a_2' \end{bmatrix} \tag{7.6.37}$$

Wave b_1 is delayed in phase by $\beta\ell_1$ as it travels from A to A′. That means b_1 is ahead in phase with respect to b_1'. Hence,

$$b_1 = b_1' e^{j\beta\ell_1} \tag{7.6.38}$$

Wave a_1 comes from A′ to plane A. Therefore, it has a phase delay of $\beta\ell_1$ with respect to a_1'. Mathematically,

$$a_1 = a_1' e^{-j\beta\ell_1} \tag{7.6.39}$$

On the basis of similar considerations at port-2, we can write

$$b_2 = b_2' e^{j\beta\ell_2} \tag{7.6.40}$$

and,

$$a_2 = a_2' e^{-j\beta\ell_2} \tag{7.6.41}$$

Substituting for b_1, a_1, b_2, and a_1 from (7.6.38)–(7.6.41) into (7.6.36), we get

$$\begin{bmatrix} b_1' e^{j\beta\ell_1} \\ b_2' e^{j\beta\ell_2} \end{bmatrix} = \begin{bmatrix} S_{11} & S_{12} \\ S_{21} & S_{22} \end{bmatrix} \begin{bmatrix} a_1' e^{-j\beta\ell_1} \\ a_2' e^{-j\beta\ell_2} \end{bmatrix} \tag{7.6.42}$$

We can rearrange this equation as follows.

$$\begin{bmatrix} b_1' \\ b_2' \end{bmatrix} = \begin{bmatrix} S_{11} e^{-j2\beta\ell_1} & S_{12} e^{-j\beta(\ell_1+\ell_2)} \\ S_{21} e^{-j\beta(l_1+\ell_2)} & S_{22} e^{-j2\beta\ell_2} \end{bmatrix} \begin{bmatrix} a_1' \\ a_2' \end{bmatrix} \tag{7.6.43}$$

Now, on comparing (7.6.43) with (7.6.37), we find that

$$\begin{bmatrix} S_{11}' & S_{12}' \\ S_{21}' & S_{22}' \end{bmatrix} = \begin{bmatrix} S_{11} e^{-j2\beta\ell_1} & S_{12} e^{-j\beta(\ell_1+\ell_2)} \\ S_{21} e^{-j\beta(\ell_1+\ell_2)} & S_{22} e^{-j2\beta\ell_2} \end{bmatrix} \tag{7.6.44}$$

Following a similar procedure, one can find the other relation as follows.

$$\begin{bmatrix} S_{11} & S_{12} \\ S_{21} & S_{22} \end{bmatrix} = \begin{bmatrix} s_{11}' e^{j2\beta\ell_1} & S_{12}' e^{j\beta(\ell_1+\ell_2)} \\ S_{21}' e^{j(\ell_1+\ell_2)} & S_{22}' e^{j2\beta\ell_2} \end{bmatrix} \tag{7.6.45}$$

Example 7.14: Total voltages and currents at two ports of a network are found as follows:

$$V_1 = 10\angle 0^\circ \text{ V}, \quad I_1 = 0.1\angle 40^\circ \text{ A}, \quad V_2 = 12\angle 30^\circ \text{ V}, \quad \text{and} \quad I_2 = 0.15\angle 100^\circ \text{ A}$$

Determine incident and reflected voltages, assuming that the characteristic impedance is $50\,\Omega$ at both its ports.

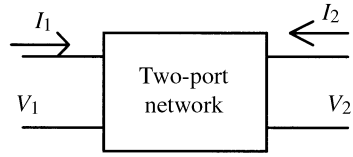

From (7.6.11) and (7.6.12) with $i = 1$, we find that

$$V_1^{\text{in}} = \frac{1}{2}(10\angle 0^\circ + 50 \times 0.1\angle 40^\circ) = 6.915 + j1.607 \text{ V}$$

and,

$$V_1^{\text{ref}} = \frac{1}{2}(10\angle 0^\circ - 50 \times 0.1\angle 40^\circ) = 3.085 - j1.607 \text{ V}$$

Similarly, with $i = 2$, incident and reflected voltages at port-2 are found to be

$$V_2^{\text{in}} = \frac{1}{2}(12\angle 30^\circ + 50 \times 0.15\angle 100^\circ) = 4.545 + j6.695 \text{ V}$$

and,

$$V_2^{\text{ref}} = \frac{1}{2}(12\angle 30^\circ - 50 \times 0.15\angle 100^\circ) = 5.845 - j0.691 \text{ V}$$

Example 7.15: Find S-parameters of a series impedance Z connected between the two ports, as shown here.

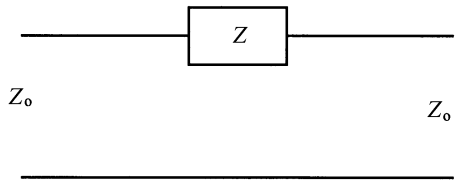

From (7.6.25), with $\Gamma_L = 0$ (i.e., port-2 is terminated by a matched load), we find that

$$S_{11} = \Gamma_1|_{a_2=0} = \frac{(Z + Z_o) - Z_o}{(Z + Z_o) + Z_o} = \frac{Z}{Z + 2Z_o}$$

Similarly, from (7.6.28), with $\Gamma_S = 0$ (i.e., port-1 is terminated by a matched load),

$$S_{22} = \Gamma_2|_{a_1=0} = \frac{(Z + Z_o) - Z_o}{(Z + Z_o) + Z_o} = \frac{Z}{Z + 2Z_o}$$

S_{21} and S_{12} are determined from (7.6.32) and (7.6.33), respectively. For evaluating S_{21}, we connect a voltage source V_{S1} at port-1 while port-2 is terminated by Z_o, as shown here. The source impedance is Z_o.

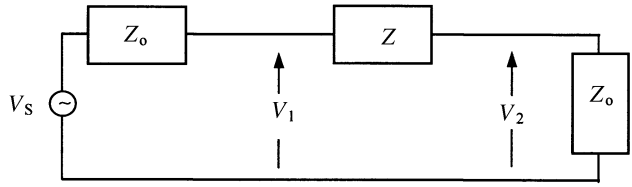

Using the voltage divider formula, we can write

$$V_2 = \frac{Z_o}{Z + 2Z_o} V_{S1}$$

Hence, from (7.6.32),

$$S_{21} = \frac{2V_2}{V_{S1}} = \frac{2Z_o}{Z + 2Z_o} = \frac{2Z_o + Z - Z}{Z + 2Z_o} = 1 - \frac{Z}{Z + 2Z_o}$$

For evaluating S_{12}, we connect a voltage source V_{S2} at port-2 while port-1 is terminated by Z_o, as shown here. The source impedance is Z_o.

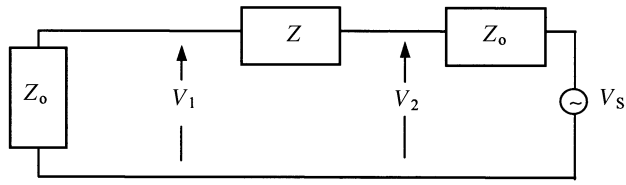

Using the voltage divider rule again, we find that

$$V_1 = \frac{Z_o}{Z + 2Z_o} V_{S2}$$

Now, from (7.6.33),

$$S_{12} = \frac{2V_1}{V_{S2}} = \frac{2Z_o}{Z + 2Z_o} = \frac{2Z_o + Z - Z}{Z + 2Z_o} = 1 - \frac{Z}{Z + 2Z_o}$$

Therefore,

$$\begin{bmatrix} S_{11} & S_{12} \\ S_{21} & S_{22} \end{bmatrix} = \begin{bmatrix} \Gamma_1 & 1-\Gamma_1 \\ 1-\Gamma_1 & \Gamma_1 \end{bmatrix}$$

where

$$\Gamma_1 = \frac{Z}{Z + 2Z_o}$$

An analysis of the S-parameters indicates that S_{11} is equal to S_{22}. It is because the given two-port network is symmetrical. Further, its S_{12} is equal to S_{21} as well. This happens because this network is reciprocal.

Consider a special case where the series impedance Z is a purely reactive element, that means Z equal to jX. In that case, Γ_1 can be written as

$$\Gamma_1 = \frac{jX}{jX + 2Z_o}$$

Therefore,

$$\begin{aligned} |S_{11}|^2 + |S_{21}|^2 &= \left| \frac{jX}{jX + 2Z_o} \right|^2 + \left| 1 - \frac{jX}{jX + 2Z_o} \right|^2 \\ &= \frac{X^2}{X^2 + (2Z_o)^2} + \frac{(2Z_o)^2}{X^2 + (2Z_o)^2} = 1 \end{aligned}$$

Similarly,

$$|S_{12}|^2 + |S_{22}|^2 = 1$$

On the other hand,

$$S_{11}S_{12}^* + S_{21}S_{22}^* = \frac{jX}{jX + 2Z_o} \times \frac{2Z_o}{-jX + 2Z_o} + \frac{2Z_o}{jX + 2Z_o} \times \frac{-jX}{-jX + 2Z_o} = 0$$

and,

$$S_{12}S_{11}^* + S_{22}S_{21}^* = \frac{2Z_o}{jX + 2Z_o} \times \frac{-jX}{-jX + 2Z_o} + \frac{jX}{jX + 2Z_o} \times \frac{2Z_o}{-jX + 2Z_o} = 0$$

These characteristics of the scattering matrix can be summarized as follows.

$$\sum S_{ij}S_{ik}^* = \delta_{jk} = \begin{cases} 1 & \text{if } j = k \\ 0 & \text{otherwise} \end{cases}$$

When elements of a matrix satisfy this condition, it is called the *unitary matrix*. Hence, the scattering matrix of a reactance circuit is unitary.

Example 7.16: Find S-parameters of a shunt admittance Y connected between the two ports, as shown here.

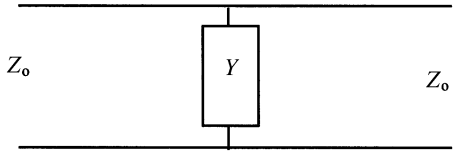

From (7.6.25),

$$S_{11} = \Gamma_1|_{\Gamma_L=0} = \frac{Z_1 - Z_{o1}}{Z_1 + Z_{o1}} = \frac{\frac{1}{Y_1} - \frac{1}{Y_o}}{\frac{1}{Y_1} + \frac{1}{Y_o}} = \frac{Y_o - Y_1}{Y_o + Y_1} = \frac{Y_o - (Y + Y_o)}{Y_o + (Y + Y_o)} = \frac{-Y}{2Y_o + Y}$$

Similarly, from (7.6.28),

$$S_{22} = \Gamma_2|_{\Gamma_S=0} = \frac{Z_2 - Z_{o2}}{Z_2 + Z_{o2}} = \frac{\frac{1}{Y_2} - \frac{1}{Y_o}}{\frac{1}{Y_2} + \frac{1}{Y_o}} = \frac{Y_o - Y_2}{Y_o + Y_2} = \frac{Y_o - (Y + Y_o)}{Y_o + (Y + Y_o)} = \frac{-Y}{2Y_o + Y}$$

For evaluating S_{21}, voltage source V_{S1} is connected at port-1 and port-2 is terminated by a matched load, as shown here.

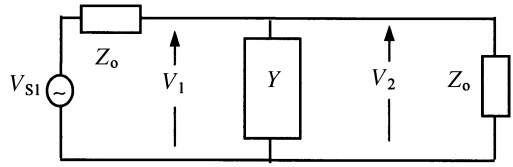

Using the voltage divider rule,

$$V_2 = \frac{\frac{1}{Y + Y_o}}{Z_o + \frac{1}{Y + Y_o}} V_{S1} = \frac{1}{Z_o(Y + Y_o) + 1} V_{S1} = \frac{Y_o}{Y + 2Y_o} V_{S1}$$

Now, from (7.6.32),

$$S_{21} = \frac{2V_2}{V_{S1}}\bigg|_{\Gamma_L=0} = \frac{2Y_o}{Y + 2Y_o} = 1 - \frac{Y}{Y + 2Y_o}$$

Similarly, when V_{S2} in series with Z_o is connected at port-2 while port-1 is matched terminated, S_{12} can be found from (7.6.33) as follows:

$$S_{12} = \frac{2V_1}{V_{S2}}\bigg|_{\Gamma_S=0} = \frac{2Y_o}{Y+2Y_o} = 1 - \frac{Y}{Y+2Y_o} = 1 + \Gamma_1$$

where

$$\Gamma_1 = -\frac{Y}{Y+2Y_o}$$

As expected, $S_{11} = S_{22}$ and $S_{12} = S_{21}$, because this circuit is symmetrical as well as reciprocal. Further, for $Y = jB$, the network becomes lossless. In that case,

$$|S_{11}|^2 + |S_{21}|^2 = \frac{B^2}{B^2 + (2Y_o)^2} + \frac{(2Y_o)^2}{B^2 + (2Y_o)^2} = 1$$

and,

$$S_{11}S_{12}^* + S_{21}S_{22}^* = \frac{-jB}{jB+2Y_o} \times \frac{2Y_o}{-jB+2Y_o} + \frac{2Y_o}{jB+2Y_o} \times \frac{jB}{-jB+2Y_o} = 0$$

Hence, with Y as jB, the scattering matrix is unitary. In fact, it can be easily proved that the scattering matrix of any lossless two-port network is unitary.

Example 7.17: An ideal transformer is designed to operate at 500 MHz. It has 1000 turns on its primary and 100 turns on its secondary side. Assuming that it has a 50-Ω connector on each side, determine its S-parameters (see illustration).

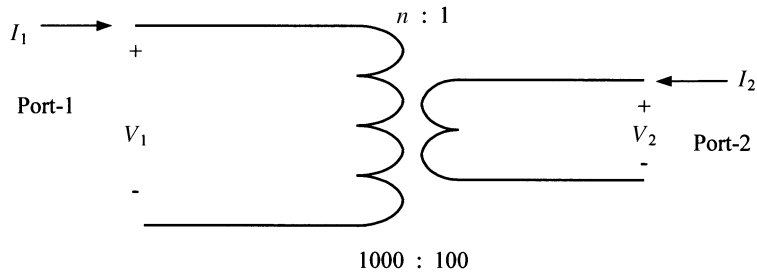

For an ideal transformer,

$$\frac{V_1}{V_2} = \frac{-I_2}{I_1} = n \quad \text{and} \quad \frac{V_1}{V_2}\,\frac{(-I_2)}{I_1} = \frac{V_1/I_1}{V_2/(-I_2)} = \frac{Z_1}{Z_2} = n^2$$

Now, following the procedure used in preceding examples, we find that

$$S_{11} = \left.\frac{b_1}{a_1}\right|_{a_2=0} = \Gamma_1|_{a_2=0} = \frac{Z_o n^2 - Z_o}{Z_o n^2 + Z_o} = \frac{n^2 - 1}{n^2 + 1} = \frac{99}{101}$$

and, voltage V_1 on the primary side of the transformer due to a voltage source V_{S1} with its internal impedance Z_o, can be determined by the voltage divider rule as follows.

$$V_1 = \frac{Z_o n^2}{Z_o n^2 + Z_o} V_{S1} \Rightarrow \frac{V_1}{V_{S1}} = \frac{n^2}{n^2 + 1} = \frac{nV_2}{V_{S1}}$$

Hence,

$$S_{21} = \left.\frac{2V_2}{V_{S1}}\right|_{a_2=0} = \frac{2n}{n^2 + 1} = \frac{20}{101}$$

Similarly, S_{22} and S_{12} are determined after connecting a voltage source V_{S2} with its internal impedance Z_o at port-2. Port-1 is terminated by a matched load this time. Therefore,

$$S_{22} = \left.\frac{b_2}{a_2}\right|_{a_1=0} = \Gamma_2|_{a_1=0} = \frac{\dfrac{Z_o}{n^2} - Z_o}{\dfrac{Z_o}{n^2} + Z_o} = \frac{1 - n^2}{1 + n^2} = -\frac{99}{101}$$

and,

$$V_2 = \frac{(Z_o/n^2)}{(Z_o/n^2) + Z_o} V_{S2} \Rightarrow \frac{V_2}{V_{S2}} = \frac{(1/n^2)}{(1/n^2) + 1} = \frac{1}{1 + n^2} = \frac{(V_1/n)}{v_{S2}}$$

Hence,

$$S_{12} = \left.\frac{2V_1}{V_{S2}}\right|_{a_1=0} = \frac{2n}{n^2 + 1} = \frac{20}{101}$$

Thus,

$$\begin{bmatrix} S_{11} & S_{12} \\ S_{21} & S_{22} \end{bmatrix} = \begin{bmatrix} \frac{99}{101} & \frac{20}{101} \\ \frac{20}{101} & -\frac{99}{101} \end{bmatrix}$$

This time, S_{11} is different from S_{22} because the network is not symmetrical. However, S_{12} is equal to S_{21} because it is reciprocal. Further, an ideal transformer is lossless. Hence, its scattering matrix must be unitary. Let us verify if that is the case:

$$|S_{11}|^2 + |S_{21}|^2 = \left(\frac{99}{101}\right)^2 + \left(\frac{20}{101}\right)^2 = \frac{10201}{10201} = 1$$

$$|S_{12}|^2 + |S_{22}|^2 = \left(\frac{20}{101}\right)^2 + \left(-\frac{99}{101}\right)^2 = \frac{10201}{10201} = 1$$

$$S_{11}S_{12}^* + S_{21}S_{22}^* = \frac{99}{101} \times \frac{20}{101} + \frac{20}{101} \times \left(-\frac{99}{11}\right) = 0$$

and,

$$S_{12}S_{11}^* + S_{22}S_{21}^* = \frac{20}{101} \times \frac{99}{101} + \left(-\frac{99}{101}\right) \times \frac{20}{101} = 0$$

Hence, the scattering matrix is indeed unitary.

Example 7.18: Find scattering parameters of the transmission line network shown here.

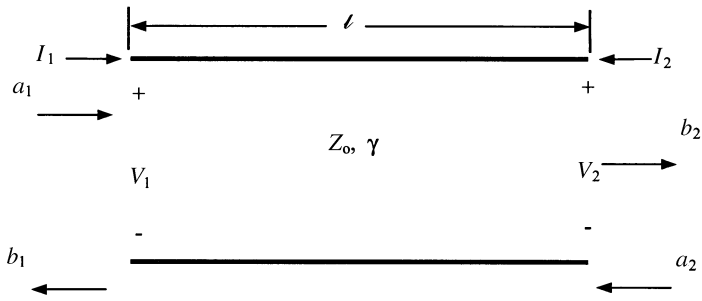

With port-2 matched terminated, wave a_1 entering port-1 emerges as $a_1\, e^{-\gamma\ell}$ at port-2. This wave is absorbed by the termination, making a_2 zero. Further, b_1 is zero as well because Z_1 is equal to Z_o in this case. Hence,

$$b_2 = a_1 e^{-\gamma\ell}$$

Similarly, when a source is connected at port-2 while port-1 is matched terminated, we find that a_1 and b_2 are zero and

$$b_1 = a_2 e^{-\gamma\ell}$$

Hence,

$$\begin{bmatrix} S_{11} & S_{12} \\ S_{21} & S_{22} \end{bmatrix} = \begin{bmatrix} 0 & e^{-\gamma\ell} \\ e^{-\gamma\ell} & 0 \end{bmatrix}$$

As expected, $S_{11} = S_{22}$ and $S_{12} = S_{21}$, because this circuit is symmetrical as well as reciprocal. Further, for $\gamma = j\beta$, the network becomes lossless. In that case,

$$\begin{bmatrix} S_{11} & S_{12} \\ S_{21} & S_{22} \end{bmatrix} = \begin{bmatrix} 0 & e^{-j\beta\ell} \\ e^{-j\beta\ell} & 0 \end{bmatrix}$$

Obviously, it is a unitary matrix now.

Example 7.19: Find scattering parameters of the two-port network shown here.

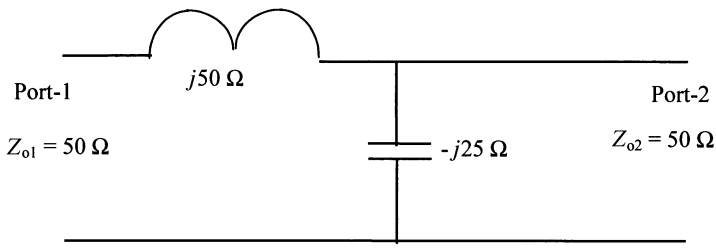

With port-2 matched terminated by a 50-Ω load, impedance Z_1 at port-1 is

$$Z_1 = j50 + \frac{50 \cdot (-j25)}{50 - j25} = j50 + 10 - j20 = 10 + j30\ \Omega$$

Therefore,

$$S_{11} = \Gamma_1|_{a_2=0} = \frac{Z_1 - Z_{o1}}{Z_1 + Z_{o1}} = \frac{10 + j30 - 50}{10 + j30 + 50} = 0.74536\angle 116.565^\circ$$

Similarly, output impedance Z_2 at port-2 while port-1 is matched terminated by a 50-Ω load is

$$Z_2 = \frac{(50 + j50)(-j25)}{50 + j50 - j25} = 10 - j30\,\Omega$$

and, from (7.6.32),

$$S_{22} = \Gamma_2|_{a_1=0} = \frac{Z_2 - Z_{o2}}{Z_1 + Z_{o2}} = \frac{10 - j30 - 50}{10 - j30 + 50} = 0.74536\angle -116.565^\circ$$

Now, let us connect a voltage source V_{S1} with its impedance at 50 Ω at port-1 while port-2 is matched, as shown here.

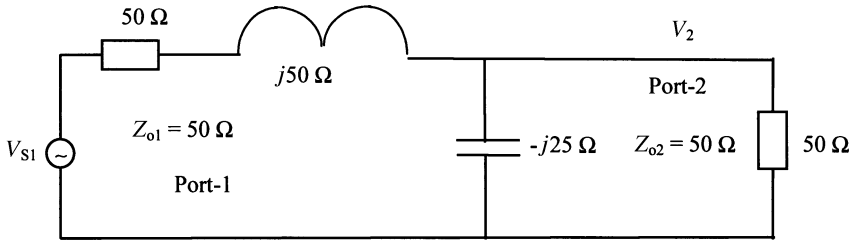

Using the voltage divider rule, we find that

$$V_2 = \frac{10 - j20}{50 + j50 + 10 - j20} V_{S1}$$

Therefore,

$$S_{21} = \frac{2V_2}{V_{S1}}\bigg|_{a_2=0} = 2\frac{10 - j20}{60 + j30} = 0.66666\angle -90^\circ$$

Now connect the voltage source at port-2 while port-1 is match terminated as shown here.

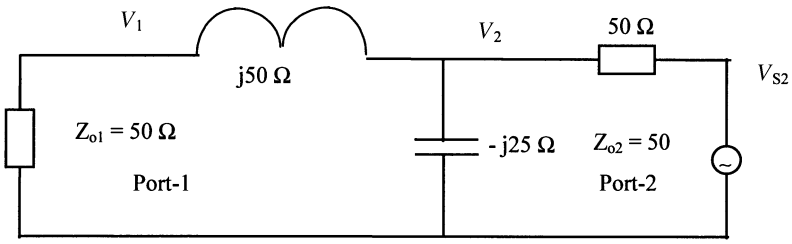

Using the voltage divider rule again, we find that

$$V_2 = \frac{10 - j30}{50 + 10 - j30} V_{S2} = 0.4714\angle -45^\circ \text{ V}$$

Using it one more time, V_1 is found as follows:

$$V_1 = \frac{50}{50 + j50} V_2 = \frac{1}{1 + j1} 0.4714\angle -45^\circ = 0.33333\angle -90^\circ \text{ V}$$

and now, from (7.6.33) we get

$$S_{12} = \left.\frac{2V_1}{V_{S2}}\right|_{a_1=0} = 2 \cdot 0.33333\angle -90^\circ = 0.66666\angle -90^\circ$$

Hence,

$$\begin{bmatrix} S_{11} & S_{12} \\ S_{21} & S_{22} \end{bmatrix} = \begin{bmatrix} 0.74536\angle 116.565^\circ & 0.66666\angle -90^\circ \\ 0.66666\angle -90^\circ & 0.74536\angle -116.565^\circ \end{bmatrix}$$

In this case, S_{11} is different from S_{22} because the network is not symmetrical. However, S_{12} is equal to S_{21} because the network is reciprocal. Further, this network is lossless. Hence, its scattering matrix must be unitary. It can be verified as follows:

$$|S_{11}|^2 + |S_{21}|^2 = (0.74536)^2 + (0.66666)^2 = 0.99999 = 1$$
$$|S_{12}|^2 + |S_{22}|^2 = (0.66666)^2 + (0.74536)^2 = 0.99999 = 1$$

$$\begin{aligned} S_{11}S_{12}^* + S_{21}S_{22}^* &= (0.74536\angle 116.565^\circ) \times (0.66666\angle 90^\circ) + (0.66666\angle -90^\circ) \\ &\quad \times (0.74536\angle 116.565^\circ) \\ &= 0 \end{aligned}$$

and,

$$\begin{aligned} S_{12}S_{11}^* + S_{22}S_{21}^* &= (0.66666\angle -90^\circ) \times (0.74536\angle -116.565^\circ) \\ &\quad + (0.74536\angle -116.565^\circ) \times (0.66666\angle 90^\circ) \\ &= 0 \end{aligned}$$

Hence, this scattering matrix is indeed unitary.

Table 7.2 summarizes the characteristics of parameter matrices of the reciprocal and symmetrical two-port networks. Properties of scattering parameters of lossless junctions are listed in Table 7.3.

TABLE 7.2 Properties of Parameters of Reciprocal and Symmetrical Two-Port Networks

Parameter Matrix	Properties
$\begin{bmatrix} Z_{11} & Z_{12} \\ Z_{21} & Z_{22} \end{bmatrix}$	$Z_{12} = Z_{21}$ $Z_{11} = Z_{22}$
$\begin{bmatrix} Y_{11} & Y_{12} \\ Y_{21} & Y_{22} \end{bmatrix}$	$Y_{12} = Y_{21}$ $Y_{11} = Y_{22}$
$\begin{bmatrix} A & B \\ C & D \end{bmatrix}$	$AD - BC = 1$ $A = D$
$\begin{bmatrix} S_{11} & S_{12} \\ S_{21} & S_{22} \end{bmatrix}$	$S_{12} = S_{21}$ $S_{11} = S_{22}$

TABLE 7.3 Properties of Scattering Matrix of Lossless Junctions

Properties	Explanations
Matrix $[S]$ is symmetrical.	$[S]^{\mathrm{t}} = [S]$, where $[S]^{\mathrm{t}}$ is the tranpose matrix of $[S]$. Consequently $$S_{ij} = S_{ji}$$
Matrix $[S]$ is unitary.	$[S]^{\mathrm{a}} = [S^*]^{\mathrm{t}} = [S]^{-1}$, where $[S]^{\mathrm{a}}$ is the adjoint matrix of $[S]$; $[S^*]^{\mathrm{t}}$ is the conjugate of $[S]^t$, and $[S]^{-1}$ is the inverse matrix of $[S]$. Consequently, $$\sum_{i=1}^{N} S_{ij}S_{ik}^* = \delta_{jk} = \begin{cases} 1 & \text{for } j = k \\ 0 & \text{otherwise} \end{cases}$$ Therefore, $$\sum_{i=1}^{N} S_{ij}S_{ij}^* = \sum_{i=1}^{N} \lvert S_{ij}\rvert^2 = 1, \quad j = 1, 2, 3, \ldots, N$$

7.7 CONVERSION FORM IMPEDANCE, ADMITTANCE, CHAIN, AND HYBRID PARAMETERS TO SCATTERING PARAMETERS OR VICE VERSA

From (7.1.3) we can write

$$\frac{V_i}{\sqrt{2Z_{oi}}} = \frac{1}{\sqrt{2Z_{oi}}} \sum_{k=1}^{2} Z_{ik}I_k = \sum_{k=1}^{2} \frac{Z_{ik}}{Z_{oi}} \sqrt{\frac{Z_{oi}}{2}} I_k = \sum_{k=1}^{2} \bar{Z}_{ik} \sqrt{\frac{Z_{oi}}{2}} I_k, \qquad \text{where } i = 1, 2$$

Therefore, from (7.6.15) and (7.6.16), we have

$$a_i = \frac{1}{2} \sum_{k=1}^{2} (\bar{Z}_{ik} + \delta_{ik}) \sqrt{\frac{Z_{oi}}{2}} I_k \tag{7.7.1}$$

and,

$$b_i = \frac{1}{2}\sum_{k=1}^{2}(\bar{Z}_{ik} - \delta_{ik})\sqrt{\frac{Z_{oi}}{2}}I_k \tag{7.7.2}$$

where,

$$\delta_{ik} = \begin{cases} 1 & \text{for } i = k \\ 0 & \text{otherwise} \end{cases}$$

Equations (7.7.1) and (7.7.2) can be written in matrix form as follows:

$$[a] = \frac{1}{2}\{[\bar{Z}] + [U]\}[\bar{I}] \tag{7.7.3}$$

$$[b] = \frac{1}{2}\{[\bar{Z}] - [U]\}[\bar{I}] \tag{7.7.4}$$

where

$$\bar{I} = \sqrt{\frac{Z_{oi}}{2}}I_k$$

and $[U]$ is the unit matrix.

From (7.7.3) and (7.7.4), we have

$$[b] = \{[\bar{Z}] - [U]\}\{[\bar{Z}] + [U]\}^{-1}[a] \tag{7.7.5}$$

Hence,

$$[S] = \{[\bar{Z}] - [U]\}\{[\bar{Z}] + [U]\}^{-1} \tag{7.7.6}$$

or,

$$[\bar{Z}] = \{[U] + [S]\}\{[U] - [S]\}^{-1} \tag{7.7.7}$$

Similarly, other conversion relations can be developed. Table 7.4 lists these equations when the two ports have different complex characteristic impedances. Characteristic impedance at port-1 is assumed Z_{o1}, with its real part as R_{o1}. Similarly, characteristic impedance at port-2 is Z_{o2}, with its real part as R_{o2}.

7.8 CHAIN SCATTERING PARAMETERS

Chain scattering parameters are also known as the *scattering transfer parameters* or *T-parameters* and are useful for networks in cascade. These are defined on the basis of waves a_1 and b_1 at port-1 as dependent variables and waves a_2 and b_2 at port-2 as independent variables. Hence,

$$\begin{bmatrix} a_1 \\ b_1 \end{bmatrix} = \begin{bmatrix} T_{11} & T_{12} \\ T_{21} & T_{22} \end{bmatrix}\begin{bmatrix} b_2 \\ a_2 \end{bmatrix}$$

TABLE 7.4 Conversion From (To) Impedance, Admittance, Chain, or Hybrid To (From) Scattering Parameters

$$S_{11} = \frac{(Z_{11} - Z_{01}^*)(Z_{22} + Z_{02}) - Z_{12}Z_{21}}{(Z_{11} + Z_{01})(Z_{22} + Z_{02}) - Z_{12}Z_{21}} \qquad Z_{11} = \frac{(Z_{01}^* + S_{11}Z_{01})(1 - S_{22}) + S_{12}S_{21}Z_{01}}{(1 - S_{11})(1 - S_{22}) - S_{12}S_{21}}$$

$$S_{12} = \frac{2Z_{12}\sqrt{R_{01}R_{02}}}{(Z_{11} + Z_{01})(Z_{22} + Z_{02}) - Z_{12}Z_{21}} \qquad Z_{12} = \frac{2S_{12}\sqrt{R_{01}R_{02}}}{(1 - S_{11})(1 - S_{22}) - S_{12}S_{21}}$$

$$S_{21} = \frac{2Z_{21}\sqrt{R_{01}R_{02}}}{(Z_{11} + Z_{01})(Z_{22} + Z_{02}) - Z_{12}Z_{21}} \qquad Z_{21} = \frac{2S_{21}\sqrt{R_{01}R_{02}}}{(1 - S_{11})(1 - S_{22}) - S_{12}S_{21}}$$

$$S_{22} = \frac{(Z_{11} + Z_{01})(Z_{22} - Z_{02}^*) - Z_{12}Z_{21}}{(Z_{11} + Z_{01})(Z_{22} + Z_{02}) - Z_{12}Z_{21}} \qquad Z_{22} = \frac{(Z_{02}^* + S_{22}Z_{02})(1 - S_{11}) + S_{12}S_{21}Z_{02}}{(1 - S_{11})(1 - S_{22}) - S_{12}S_{21}}$$

$$S_{11} = \frac{(1 - Y_{11}Z_{01}^*)(1 + Y_{22}Z_{02}) + Y_{12}Y_{21}Z_{01}^*Z_{02}}{(1 + Y_{11}Z_{01})(1 + Y_{22}Z_{02}) - Y_{12}Y_{21}Z_{01}Z_{02}} \qquad Y_{11} = \frac{(1 - S_{11})(Z_{02}^* + S_{22}Z_{02}) + S_{12}S_{21}Z_{02}}{(Z_{01}^* + S_{11}Z_{01})(Z_{02}^* + S_{22}Z_{02}) - S_{12}S_{21}Z_{01}Z_{02}}$$

$$S_{12} = \frac{-2Y_{12}\sqrt{R_{01}R_{02}}}{(1 + Y_{11}Z_{01})(1 + Y_{22}Z_{02}) - Y_{12}Y_{21}Z_{01}Z_{02}} \qquad Y_{12} = \frac{-2S_{12}\sqrt{R_{01}R_{02}}}{(Z_{01}^* + S_{11}Z_{01})(Z_{02}^* + S_{22}Z_{02}) - S_{12}S_{21}Z_{01}Z_{02}}$$

$$S_{21} = \frac{-2Y_{21}\sqrt{R_{01}R_{02}}}{(1 + Y_{11}Z_{01})(1 + Y_{22}Z_{02}) - Y_{12}Y_{21}Z_{01}Z_{02}} \qquad Y_{21} = \frac{-2S_{21}\sqrt{R_{01}R_{02}}}{(Z_{01}^* + S_{11}Z_{01})(Z_{02}^* + S_{22}Z_{02}) - S_{12}S_{21}Z_{01}Z_{02}}$$

$$S_{22} = \frac{(1 + Y_{11}Z_{01})(1 - Y_{22}Z_{02}^*) + Y_{12}Y_{21}Z_{01}^*Z_{02}^*}{(1 + Y_{11}Z_{01})(1 + Y_{22}Z_{02}) - Y_{12}Y_{21}Z_{01}Z_{02}} \qquad Y_{22} = \frac{(Z_{01}^* + S_{11}Z_{01})(1 - S_{22}) + S_{12}S_{21}Z_{01}}{(Z_{01}^* + S_{11}Z_{01})(Z_{02}^* + S_{22}Z_{02}) - S_{12}S_{21}Z_{01}Z_{02}}$$

$$S_{11} = \frac{AZ_{02} + B - CZ_{01}^*Z_{02} - DZ_{01}^*}{AZ_{02} + B + CZ_{01}Z_{02} + DZ_{01}} \qquad A = \frac{(Z_{01}^* + S_{11}Z_{01})(1 - S_{22}) + S_{12}S_{21}Z_{01}}{2S_{21}\sqrt{R_{01}R_{02}}}$$

$$S_{12} = \frac{2(AD - BC)(\sqrt{R_{01}R_{02}})}{AZ_{02} + B + CZ_{01}Z_{02} + DZ_{01}} \qquad B = \frac{(Z_{01}^* + S_{11}Z_{01})(Z_{02}^* + S_{22}Z_{02}) - S_{12}S_{21}Z_{01}Z_{02}}{2S_{21}\sqrt{R_{01}R_{02}}}$$

$$S_{21} = \frac{2\sqrt{R_{01}R_{02}}}{AZ_{02} + B + CZ_{01}Z_{02} + DZ_{01}} \qquad C = \frac{(1 - S_{11})(1 - S_{22}) - S_{12}S_{21}}{2S_{21}\sqrt{R_{01}R_{02}}}$$

$$S_{22} = \frac{-AZ_{02}^* + B - CZ_{01}Z_{02}^* + DZ_{01}}{AZ_{02} + B + CZ_{01}Z_2 + DZ_{01}} \qquad D = \frac{(1 - S_{11})(Z_{02}^* + S_{22}Z_{02}) + S_{12}S_{21}Z_{02}}{2S_{21}\sqrt{R_{01}R_{02}}}$$

$$S_{11} = \frac{(h_{11} - Z_{01}^*)(1 + h_{22}Z_{02}) - h_{12}h_{21}Z_{02}}{(Z_{01} + h_{11})(1 + h_{22}Z_{02}) - h_{12}h_{21}Z_{02}} \qquad h_{11} = \frac{(Z_{01}^* + S_{11}Z_{01})(Z_{02}^* + S_{22}Z_{02}) + S_{12}S_{21}Z_{01}Z_{02}}{(1 - S_{11})(Z_{02}^* + S_{22}Z_{02}) + S_{12}S_{21}Z_{02}}$$

$$S_{12} = \frac{2h_{12}\sqrt{R_{01}R_{02}}}{(Z_{01} + h_{11})(1 + h_{22}Z_{02}) - h_{12}h_{21}Z_{02}} \qquad h_{12} = \frac{2S_{12}\sqrt{R_{01}R_{02}}}{(1 - S_{11})(Z_{02}^* + S_{22}Z_{02}) + S_{12}S_{21}Z_{02}}$$

$$S_{21} = \frac{-2h_{21}\sqrt{R_{01}R_{02}}}{(Z_{01} + h_{11})(1 + h_{22}Z_{02}) - h_{12}h_{21}Z_{02}} \qquad h_{21} = \frac{-2S_{21}\sqrt{R_{01}R_{02}}}{(1 - S_{11})(Z_{02}^* + S_{22}Z_{02}) + S_{12}S_{21}Z_{02}}$$

$$S_{22} = \frac{(Z_{01} + h_{11})(1 - h_{22}Z_{02}^*) + h_{12}h_{21}Z_{02}^*}{(Z_{01} + h_{11})(1 + h_{22}Z_{02}) - h_{12}h_{21}Z_{02}} \qquad h_{22} = \frac{(1 - S_{11})(1 - S_{22}) - S_{12}S_{21}}{(1 - S_{11})(Z_{02}^* + S_{22}Z_{02}) + S_{12}S_{21}Z_{02}}$$

TABLE 7.5 Conversion Between Scattering and Chain Scattering Parameters

$S_{11} = \dfrac{T_{21}}{T_{11}}$	$T_{11} = \dfrac{1}{S_{21}}$
$S_{12} = \dfrac{T_{11}T_{22} - T_{12}T_{21}}{T_{11}}$	$T_{12} = \dfrac{-S_{22}}{S_{21}}$
$S_{21} = \dfrac{1}{T_{11}}$	$T_{21} = \dfrac{S_{11}}{S_{21}}$
$S_{22} = \dfrac{-T_{12}}{T_{11}}$	$T_{22} = \dfrac{-(S_{11}S_{22} - S_{12}S_{21})}{S_{21}}$

Conversion relations of chain scattering parameters with others can be easily developed. Conversions between S- and T-parameters are listed in Table 7.5.

SUGGESTED READING

I. Bahl and P. Bhartia, *Microwave Solid State Circuit Design*. New York: Wiley, 1988.

R. E. Collin, *Foundations for Microwave Engineering*. New York: McGraw Hill, 1992.

R. S. Elliott, *An Introduction to Guided Waves and Microwave Circuits*. Englewood Cliffs, NJ: Prentice Hall, 1993.

V. F. Fusco, *Microwave Circuits*. Englewood Cliffs, NJ: Prentice Hall, 1987.

G. Gonzalez, *Microwave Transistor Amplifiers*. Englewood Cliffs, NJ: Prentice Hall, 1997.

D. M. Pozar, *Microwave Engineering*. New York: Wiley, 1998.

S. Ramo. J. R. Whinnery, and T. Van Duzer. *Fields and Waves in Communication Electronics*, New York: Wiley, 1994.

Peter A. Rizzi, *Microwave Engineering*. Englewood Cliffs, NJ: Prentice Hall, 1988.

PROBLEMS

1. Determine Z- and Y-matrices for the following two-port network. The signal frequency is 500 MHz.

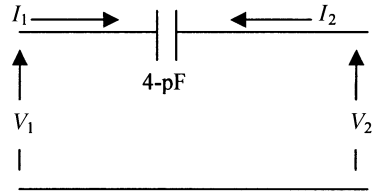

2. Determine Z-parameters of the following two-port network:

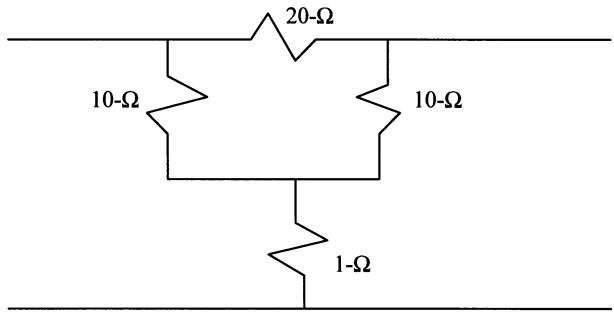

3. Determine the Z-parameters of the following two-port network operating at 800 MHz.

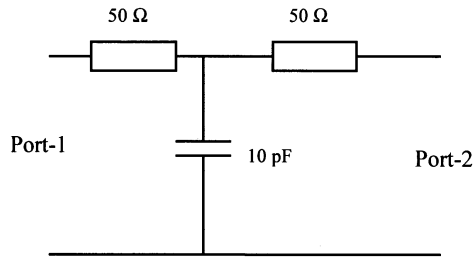

4. Determine the Z-matrix for the following two-port network.

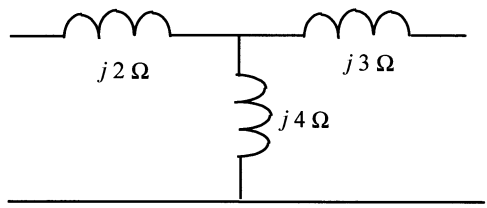

5. The following two-port network represents a high-frequency equivalent model of the transistor. If the transistor is operating at 10^8 rad/s then find its Z-parameters.

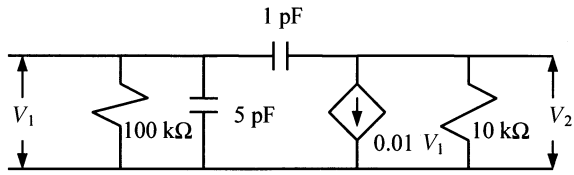

6. Find the Y-parameters of the two-port network given below.

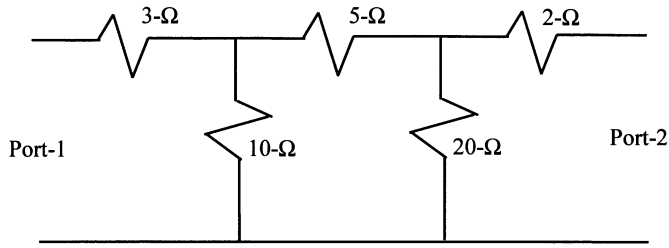

7. Measurements are performed with a two-port network as shown below. The observed voltages and currents are tabulated. However, there are a few blank entries in this table. Fill in those blanks and also find Y- as well as Z-parameters of this two-port network.

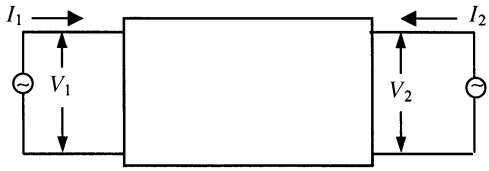

Experiment	V_1 (V)	V_2 (V)	I_1 (A)	I_2 (A)
1	20	0	4	−8
2	50	100	−20	−5
3	?	?	5	0
4	100	50	?	?
5	?	?	5	15

8. The Y-matrix of a two-port network is given as follows:

$$[Y] = \begin{bmatrix} 10 & -5 \\ 50 & 20 \end{bmatrix} \text{mS}$$

It is connected in a circuit as shown below. Find the voltages V_1 and V_2.

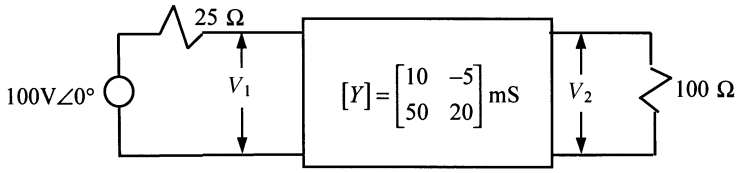

9. Determine the transmission and hybrid parameters for the following networks:

(a)

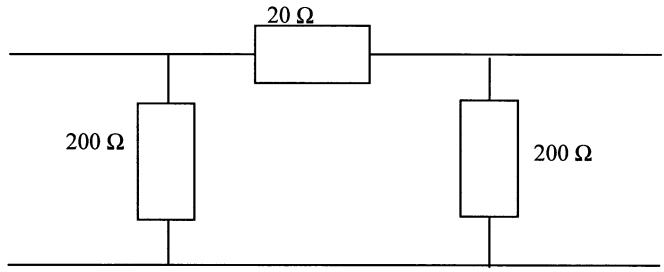

(b)

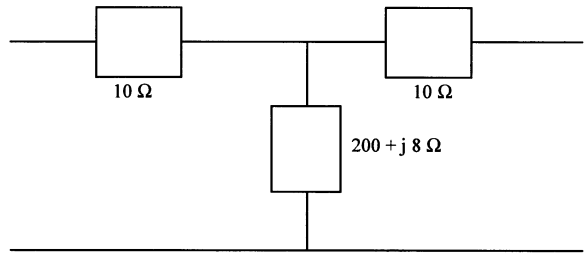

10. Calculate Z- and S-parameters for the following circuit at 4 GHz. Both ports of the network have characteristic impedance of 50 ohm.

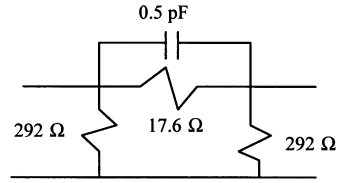

11. Determine S-parameters of the following two-port T-network:

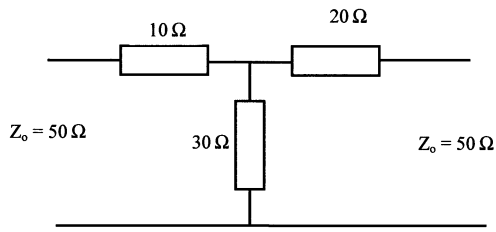

12. Determine S-parameters of the following two-port network:

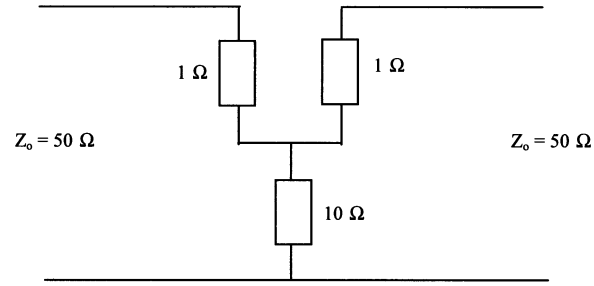

13. Determine S-parameters of the following two-port network:

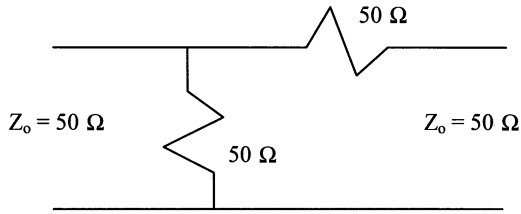

14. Determine S-parameters of the two-port pi-network shown below:

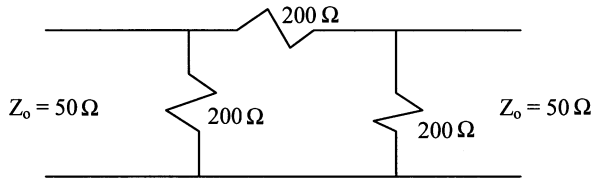

15. Scattering variables measured at a port are found as follows:

$$a = 8 - j5, \text{ and } b = 2 + j5$$

Normalizing impedance is $Z_o = 50\ \Omega$. Calculate the corresponding voltage and current.

16. Scattering variables measured at a port are:

$$a = 0.85\angle 45^\circ \text{ and } b = 0.25\angle 65^\circ$$

Normalizing impedance is $Z_o = 50\ \Omega$. Calculate the corresponding voltage and current.

17. Calculate power flow into a port in each case for the following sets of scattering variables at the port:

(a) $a = 3 + j5,\ b = 0.2 - j0.1$
(b) $a = 40 - j30,\ b = 5 - j5$

18. Calculate the power flow into a port in each case for the following sets of scattering variables at the port:
(a) $a = \angle 60^\circ,\ b = 2\angle -45^\circ$
(b) $a = 50\angle 0^\circ,\ b = 10\angle 0^\circ$

19. Calculate scattering variables a and b in each of the following cases:
(a) $V = 4 - j3\,\text{V},\ I = 0.3 + j0.4\,\text{A}$
(b) $V = 10\angle -30^\circ\text{V},\ I = 0.6\angle 70^\circ\text{A}$
Assume that characteristic impedance at the port is $100\,\Omega$.

20. Find the reflection coefficient for each of the following sets of scattering variables:
(a) $a = 0.3 + j0.4,\ b = 0.1 - 0.2$
(b) $a = -0.5 + j0.2,\ b = 0 - j0.1$
(c) $a = 0.5\angle -70^\circ,\ b = 0.3\angle 20^\circ$
(d) $a = 5\angle 0^\circ,\ b = 0.3\angle 90^\circ$

21. The scattering parameters of a two-port network are given as follows:

$$S_{11} = 0.687\angle 107^\circ, S_{21} = 1.72\angle -59^\circ, S_{12} = 0.114\angle -81^\circ, S_{22} = 0.381\angle 153^\circ$$

A source of 3 mV with internal resistance of $50\,\Omega$ is connected at port-1. Assuming the characteristic impedance at its ports as $50\,\Omega$, determine the scattering variable a_1, b_1, a_2, and b_2 for the following load conditions:
(a) $50\,\Omega$
(b) $100\,\Omega$

Radio-Frequency and Microwave Communication Circuits: Analysis and Design
Devendra K. Misra

ISBNs: 0-471-41253-8 (Hardback); 0-471-22435-9 (Electronic)

8

FILTER DESIGN

A circuit designer frequently requires filters to extract the desired frequency spectrum from a wide variety of electrical signals. If a circuit passes all signals from dc through a frequency ω_c but stops the rest of the spectrum, then it is known as a *low-pass filter*. The frequency ω_c is called its cutoff frequency. Conversely, a *high-pass filter* stops all signals up to ω_c and passes those at higher frequencies. If a circuit passes only a finite frequency band that does not include zero (dc) and infinite frequency, then it is called a *band-pass filter*. Similarly, a *band-stop filter* passes all signals except a finite band. Thus, band-pass and band-stop filters are specified by two cutoff frequencies to set the frequency band. If a filter is designed to block a single frequency, then it is called a *notch-filter*.

The ratio of the power delivered by a source to a load with and without a two-port network inserted in between is known as the *insertion loss* of that two-port. It is generally expressed in dB. The fraction of the input power that is lost due to reflection at its input port is called the *return loss*. The ratio of the power delivered to a matched load to that supplied to it by a matched source is called the *attenuation* of that two-port network. Filters have been designed using active devices such as transistors and operational amplifiers, as well as with only passive devices (inductors and capacitors only). Therefore, these circuits may be classified as *active* or *passive filters*. Unlike passive filters, active filters can amplify the signal besides blocking the undesired frequencies. However, passive filters are economical and easy to design. Further, passive filters perform fairly well at higher frequencies. This chapter presents the design procedure of these passive circuits.

There are two methods available to synthesize passive filters. One of them is known as the *image parameter method* and the other as the *insertion-loss method*. The former provides a design that can pass or stop a certain frequency band but its

frequency response cannot be shaped. The insertion-loss method is more powerful in the sense that it provides a specified response of the filter. Both of these techniques are included in this chapter. It concludes with a design overview of microwave filters.

8.1 IMAGE PARAMETER METHOD

Consider the two-port network shown in Figure 8.1. V_1 and V_2 represent voltages at its ports. Currents I_1 and I_2 are assumed as indicated in the figure. It may be noted that I_1 is entering port-1 while I_2 is leaving port-2. Further, Z_{in} is input impedance at port-1 when Z_{i2} terminates port-2. Similarly, Z_o is output impedance with Z_{i1} connected at port-1. Z_{i1} and Z_{i2} are known as the image impedance of the network. Following the transmission parameter description of the two-port, we can write

$$V_1 = AV_2 + BI_2 \tag{8.1.1}$$

and,

$$I_1 = CV_2 + DI_2 \tag{8.1.2}$$

Therefore, impedance Z_{in} at its input can be found as

$$Z_{in} = \frac{V_1}{I_1} = \frac{AV_2 + BI_2}{CV_2 + DI_2} = \frac{AZ_{i2} + B}{CZ_{i2} + D} \tag{8.1.3}$$

Alternatively, (8.1.1) and (8.1.2) can be rearranged as follows after noting that $AD - BC$ must be unity for a reciprocal network. Hence,

$$V_2 = DV_1 - BI_1 \tag{8.1.4}$$

and,

$$I_2 = -CV_1 + AI_1 \tag{8.1.5}$$

Therefore, output impedance Z_o is found to be

$$Z_o = -\frac{V_2}{I_2} = -\frac{DV_1 - BI_1}{-CV_1 + AI_1} = \frac{DZ_{i1} + B}{CZ_{i1} + A} \tag{8.1.6}$$

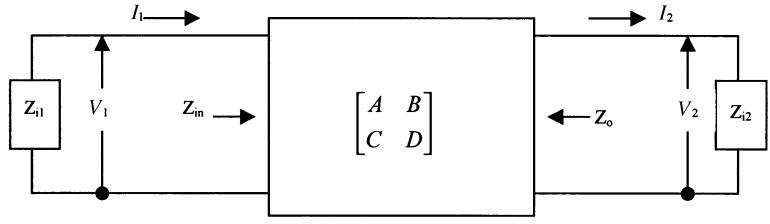

Figure 8.1 A two-port network with terminations.

Note that

$$Z_{i1} = -\frac{V_1}{I_1}$$

For $Z_{in} = Z_{i1}$ and $Z_o = Z_{i2}$, equations (8.1.3) and (8.1.6) give

$$Z_{i1}(CZ_{i2} + D) = AZ_{i2} + B \tag{8.1.7}$$

and,

$$Z_{i2}(CZ_{i1} + A) = DZ_{i1} + B \tag{8.1.8}$$

Subtracting equation (8.1.8) from (8.1.7), we find that

$$Z_{i2} = \frac{D}{A} Z_{i1} \tag{8.1.9}$$

Now, substituting (8.1.9) into (8.1.7), we have

$$Z_{i1} = \sqrt{\frac{AB}{CD}} \tag{8.1.10}$$

Similarly, substituting (8.1.10) into (8.1.9)

$$Z_{i2} = \sqrt{\frac{BD}{AC}} \tag{8.1.11}$$

Transfer characteristics of the network can be formulated as follows. From (8.1.1),

$$\frac{V_1}{V_2} = A + B\frac{I_2}{V_2} = A + \frac{B}{Z_{i2}}$$

or,

$$\frac{V_1}{V_2} = \sqrt{\frac{A}{D}}\,(\sqrt{AD} + \sqrt{BC})$$

For a reciprocal two-port network, $AD - BC$ is unity. Therefore,

$$\frac{V_2}{V_1} = \sqrt{\frac{D}{A}}\left(\frac{AD - BC}{\sqrt{AD} + \sqrt{BC}}\right) = \sqrt{\frac{D}{A}}\,(\sqrt{AD} - \sqrt{BC}) \tag{8.1.12}$$

Similarly, from (8.1.2),

$$\frac{I_2}{I_1} = \sqrt{\frac{A}{D}}\,(\sqrt{AD} - \sqrt{BC}) \tag{8.1.13}$$

Note that equation (8.1.12) is similar to (8.1.13) except that the multiplying coefficient in one is the reciprocal of the other. This coefficient may be interpreted as the transformer turn ratio. It is unity for symmetrical T and Pi networks. Propagation factor γ (equal to $\alpha + j\beta$, as usual) of the network can be defined as

$$e^{-\gamma} = \sqrt{AD} - \sqrt{BC}$$

Since $(AD - BC) = 1$, we find that

$$\cosh(\gamma) = \sqrt{AD} \tag{8.1.14}$$

Characteristic parameters of π- and T-networks are summarized in Table 8.1; corresponding low-pass and high-pass circuits are illustrated in Table 8.2.

TABLE 8.1 Parameters of T and Pi Networks

	π-Network	T-Network
	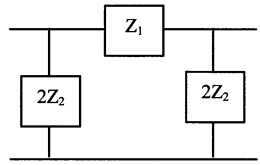	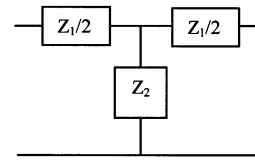
ABCD parameters	$A = 1 + \dfrac{Z_1}{2Z_2}$	$A = 1 + \dfrac{Z_1}{2Z_2}$
	$B = Z_1$	$B = Z_1 + \dfrac{Z_1^2}{4Z_2}$
	$C = \dfrac{1}{Z_2} + \dfrac{Z_1}{4Z_2^2}$	$C = \dfrac{1}{Z_2}$
	$D = 1 + \dfrac{Z_1}{2Z_2}$	$D = 1 + \dfrac{Z_1}{2Z_2}$
Image impedance	$Z_{i\pi} = \sqrt{\dfrac{Z_1 Z_2}{1 + \dfrac{Z_1}{4Z_2}}} = \dfrac{Z_1 Z_2}{Z_{iT}}$	$Z_{iT} = \sqrt{Z_1 Z_2\left(1 + \dfrac{Z_1}{4Z_2}\right)}$
Propagation constant, γ	$\cosh(\gamma) = 1 + \dfrac{Z_1}{2Z_2}$	$\cosh(\gamma) = 1 + \dfrac{Z_1}{2Z_2}$

TABLE 8.2 Constant-k Filter Sections

Filter Type	T-Section	π-Section
Low-pass	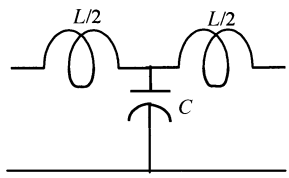	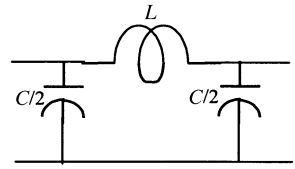
High-pass	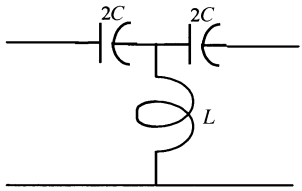	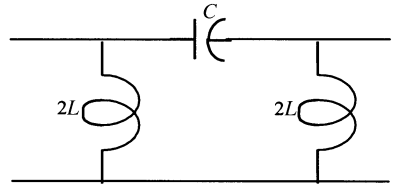

For a low-pass T-section as illustrated in Table 8.2,

$$Z_1 = j\omega L \tag{8.1.15}$$

and,

$$Z_2 = \frac{1}{j\omega C} \tag{8.1.16}$$

Therefore, its image impedance can be found from Table 8.1 as follows:

$$Z_{iT} = \sqrt{\frac{L}{C}}\left(1 - \frac{\omega^2 LC}{4}\right)^{0.5} \tag{8.1.17}$$

In the case of a dc signal, the second term inside the parentheses will be zero and the resulting image impedance is generally known as the nominal impedance, Z_o. Hence,

$$Z_o = \sqrt{\frac{L}{C}}$$

Note that the image impedance goes to zero if $\omega^2 LC/4 = 1$. The frequency that satisfies this condition is known as the *cutoff frequency*, ω_c. Hence,

$$\omega_c = \frac{2}{\sqrt{LC}} \tag{8.1.18}$$

Similarly, for a high-pass T-section,

$$Z_1 = \frac{1}{j\omega C} \tag{8.1.19}$$

and,

$$Z_2 = j\omega L \tag{8.1.20}$$

Therefore, its image impedance is found to be

$$Z_{\mathrm{iT}} = \sqrt{\frac{L}{C}}\left(1 - \frac{1}{4\omega^2 LC}\right)^{0.5} \tag{8.1.21}$$

The cutoff frequency of this circuit will be given as follows.

$$\omega_{\mathrm{c}} = \frac{1}{2\sqrt{LC}} \tag{8.1.22}$$

Example 8.1: Design a low-pass constant-k T-section that has a nominal impedance of 75 Ω and a cut-off frequency of 2 MHz. Plot its frequency response in the frequency band of 100 kHz to 10 MHz.

Since the nominal impedance Z_{o} must be 75 Ω,

$$Z_{\mathrm{o}} = 75 = \sqrt{\frac{L}{C}}$$

The cutoff frequency ω_{c} of a low-pass T-section is given by (8.1.18). Therefore,

$$\omega_{\mathrm{c}} = 2\pi \times 2 \times 10^6 = \frac{2}{\sqrt{LC}}$$

These two equations can be solved for the inductance L and the capacitance C, as follows.

$$L = 11.9366\,\mu\mathrm{H}$$

and,

$$C = 2.122\,\mathrm{nF}$$

This circuit is illustrated in Figure 8.2. Note that inductance L calculated here is twice the value needed for a T-section. Propagation constant γ of this circuit is

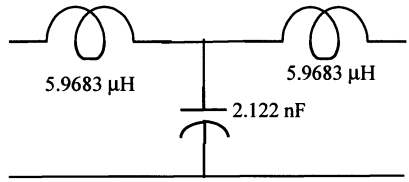

Figure 8.2 A low-pass constant-k T-section.

determined from the formula listed in Table 8.1. Transfer characteristics are then found as $e^{-\gamma}$.

The frequency response of the designed circuit is shown in Figure 8.3. The magnitude of the transfer function (ratio of the output to input voltages) remains constant at 0 dB for frequencies lower than 2 MHz. Therefore, the output magnitude will be equal to the input in this range. It falls by 3 dB if the signal frequency approaches 2 MHz. It falls continuously as the frequency increases further. Note that the phase angle of the transfer function remains constant at -180° beyond 2 MHz. However, it shows a nonlinear characteristic in the pass-band.

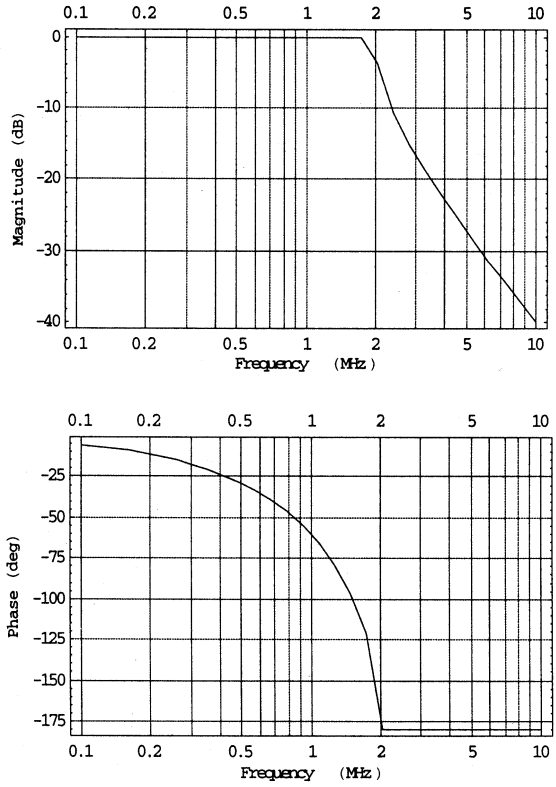

Figure 8.3 Frequency response of the T-section shown in Figure 8.2.

The image impedance Z_{iT} of this T-section can be found from (8.1.17). Its characteristics (magnitude and phase angle) with frequency are displayed in Figure 8.4. The magnitude of Z_{iT} continuously reduces as frequency is increased and becomes zero at the cutoff. The phase angle of Z_{iT} is zero in pass-band and it changes to 90° in the stop-band. Thus, image impedance is a variable resistance in the pass-band, whereas it switches to an inductive reactance in the stop-band.

Frequency characteristics illustrated in Figures 8.3 and 8.4 are representative of any constant-k filter. There are two major drawbacks to this kind of filter:

1. Signal attenuation rate after the cutoff point is not very sharp.
2. Image impedance is not constant with frequency. From a design point of view, it is important that it stays constant at least in its pass-band.

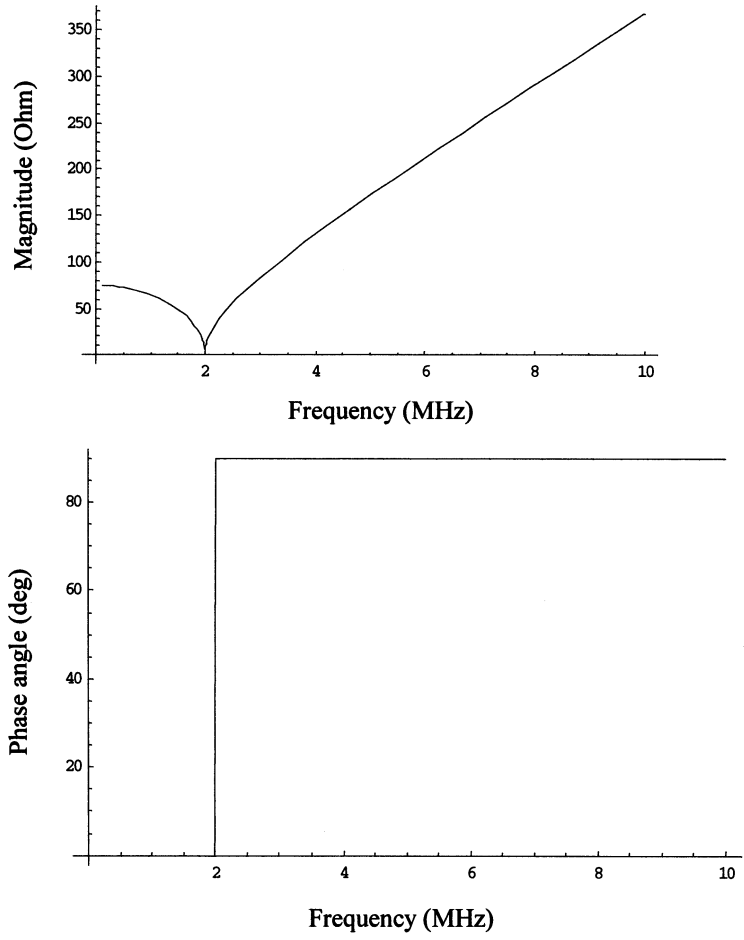

Figure 8.4 Image impedance of the constant-k filter of Figure 8.2 as a function of frequency.

These problems can be remedied using the techniques described in the following section.

m-Derived Filter Sections

Consider two T-sections shown in Figure 8.5. The first network represents the constant-k filter that is considered in the preceding section, and the second is a new *m*-derived section. It is assumed that the two networks have the same image impedance.

From Table 8.1, we can write

$$Z'_{iT} = Z_{iT} = \sqrt{Z'_1 Z'_2\left(1 + \frac{Z'_1}{4Z'_2}\right)} = \sqrt{Z_1 Z_2\left(1 + \frac{Z_1}{4Z_2}\right)}$$

It can be solved for Z'_2 as follows.

$$Z'_2 = \frac{1}{Z'_1}\left(Z_1 Z_2 + \frac{Z_1^2 - Z_1'^2}{4}\right) \tag{8.1.23}$$

Now, assume that

$$Z'_1 = mZ_1 \tag{8.1.24}$$

Substituting (8.1.24) in to (8.1.23) we get

$$Z'_2 = \frac{Z_2}{m} + \left(\frac{1 - m^2}{4m}\right)Z_1 \tag{8.1.25}$$

Thus, an *m*-derived section is designed from values of components determined for the corresponding constant-k filter. The value of m is selected to sharpen the attenuation at cutoff or to control image impedance characteristics in the pass-band.

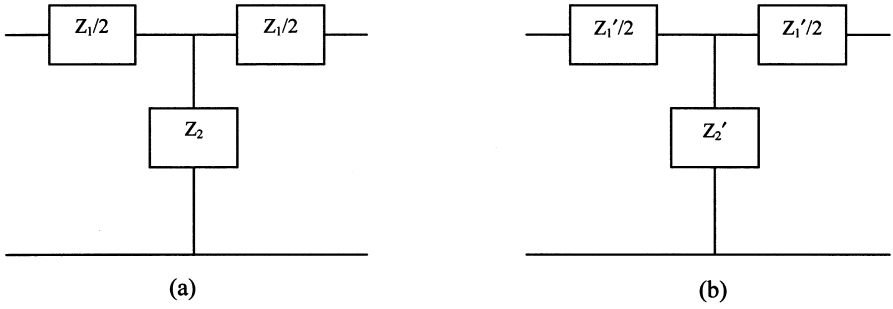

Figure 8.5 A constant-k T-section (a) and an *m*-derived section (b).

For a low-pass filter, the *m*-derived section can be designed from the corresponding constant-k filter using (8.1.24) and (8.1.25), as follows:

$$Z_1' = j\omega mL \tag{8.1.26}$$

and,

$$Z_2' = \left(\frac{1-m^2}{4m}\right) \times j\omega L + \frac{1}{j\omega mC} \tag{8.1.27}$$

Now we need to find its propagation constant γ and devise some way to control its attenuation around the cutoff. Expression for the propagation constant of a T-section is listed in Table 8.1. In order to find γ of this T-section, we first divide (8.1.26) by (8.1.27):

$$\frac{Z_1'}{Z_2'} = -\frac{\omega^2 m^2 LC}{1-\left(\frac{1-m^2}{4}\right)\omega^2 LC} = -\frac{\frac{4\omega^2 m^2}{\omega_c^2}}{1-(1-m^2)\frac{\omega^2}{\omega_c^2}} \tag{8.1.28}$$

where,

$$\omega_c = \frac{2}{\sqrt{LC}} \tag{8.1.29}$$

Using the formula listed in Table 8.1 and (8.1.28), propagation constant γ is found as follows:

$$\cosh(\gamma) = 1 + \frac{Z_1'}{2Z_2'} = 1 - \frac{2\left(\frac{m\omega}{\omega_c}\right)^2}{1-(1-m^2)\left(\frac{\omega}{\omega_c}\right)^2}$$

or,

$$\cosh(\gamma) = \frac{\omega_c^2 - \omega^2 - (m\omega)^2}{\omega_c^2 - (1-m^2)\omega^2} \tag{8.1.30}$$

Hence, the right-hand side of (8.1.30) is dependent on frequency ω. It will go to infinity (and therefore, γ) if the following condition is satisfied.

$$\omega = \frac{\omega_c}{\sqrt{1-m^2}} = \omega_\infty \tag{8.1.31}$$

This condition can be used to sharpen the attenuation at cutoff. A small m will place ω_∞ close to ω. In other words, ω_∞ is selected a little higher than ω_c and the fractional value of m is then determined from (8.1.31). Z_1' and Z_2' of the m-derived section are subsequently found using (8.1.24) and (8.1.25), respectively.

Note that the image impedance of an m-derived T-section is the same as that of the corresponding constant-k network. However, it will be a function of m in case of a π-network. Therefore, this characteristic can be utilized to design input and output networks of the filter so that the image-impedance of the composite circuit stays almost constant in its pass-band. Further, an infinite cascade of T-sections can be considered as a π-network after splitting its shunt arm as illustrated in Figure 8.6. Note that the impedance Z_2' of the T-network is replaced by 2 Z_2', while two halves of the series arms of the T-network give Z_1' of the π-network. Image impedance $Z_{i\pi}$ is found from Table 8.1, as follows.

$$Z_{i\pi} = \frac{Z_1' Z_2'}{Z_{iT}} = \frac{Z_1 Z_2 + \left(\frac{1 - m^2}{4}\right) Z_1^2}{Z_{iT}} \tag{8.1.32}$$

For the low-pass constant-k filter, we find from (8.1.15)–(8.1.18) that

$$Z_1 Z_2 = \frac{L}{C} = Z_o^2$$

$$Z_1^2 = -\omega^2 L^2 = \left(\frac{2 Z_o \omega}{\omega_c}\right)^2$$

and,

$$Z_{iT} = Z_o \sqrt{1 - \left(\frac{\omega}{\omega_c}\right)^2}$$

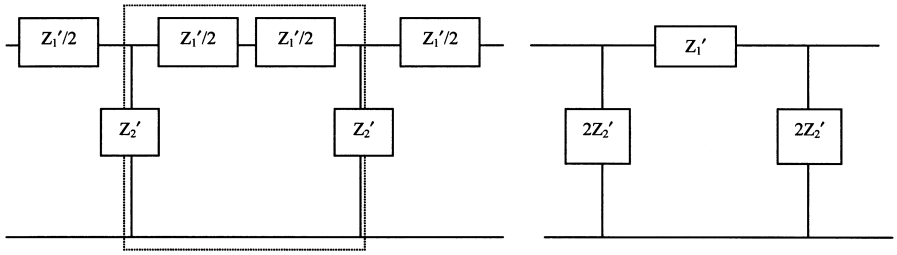

Figure 8.6 De-embedding of a π-network (b) from a cascaded T-network (a).

Therefore,

$$Z_{i\pi} = \frac{1 - (1 - m^2)\left(\frac{\omega}{\omega_c}\right)^2}{\sqrt{1 - \left(\frac{\omega}{\omega_c}\right)^2}} Z_o$$

or,

$$\bar{Z}_{i\pi} = \frac{1 - (1 - m^2)\bar{\omega}^2}{\sqrt{(1 - \bar{\omega}^2)}} \tag{8.1.33}$$

where $\bar{Z}_{i\pi} = \frac{Z_{i\pi}}{Z_o}$ may be called the *normalized image impedance* of π-network and $\bar{\omega} = \frac{\omega}{\omega_c}$ the *normalized frequency.*

Equation (8.1.33) is graphically displayed in Figure 8.7. The normalized image impedance is close to unity for nearly 90 per cent of the pass-band if m is kept around 0.6. Therefore, it can be used as pre- and post-stages of the composite filter (after bisecting it) to control the input impedance. These formulas will be developed later in this section.

Example 8.2: Design an m-derived T-section low-pass filter with cutoff frequency of 2 MHz and nominal impedance of 75 Ω. Assume that $f_\infty = 2.05$ MHz. Plot the response of this filter in the frequency band of 100 kHz to 10 MHz.

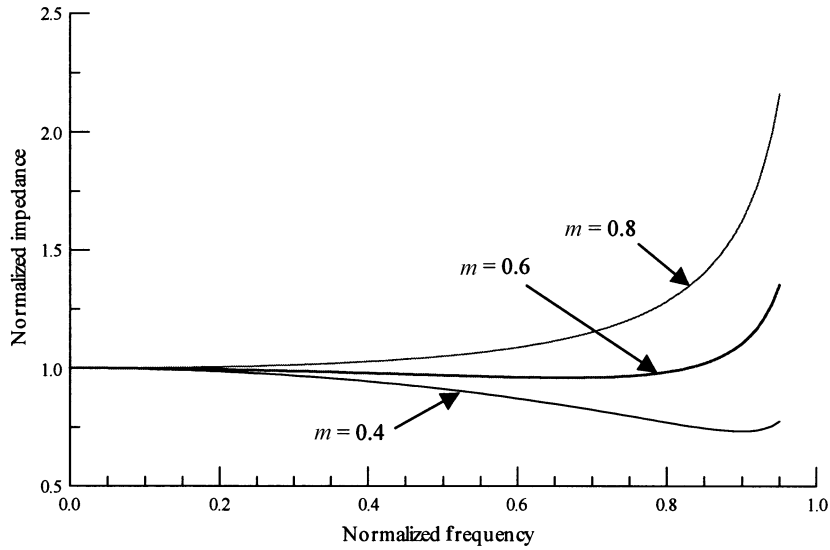

Figure 8.7 Normalized image impedance of π-network versus normalized frequency for three different values of m.

From (8.1.31),

$$1 - m^2 = \left(\frac{f_c}{f_\infty}\right)^2$$

Therefore,

$$m = \sqrt{1 - \left(\frac{f_c}{f_\infty}\right)^2} = \sqrt{1 - \left(\frac{2}{2.05}\right)^2} = 0.2195$$

Using (8.1.24) and (8.1.25) or Table 8.3 (on page 310) and component values of the constant-k section obtained earlier in Example 8.1, the *m*-derived filter is designed as follows:

$$mL/2 = 0.2195 \times 5.9683 = 1.31\ \mu\text{H}$$

$$mC = 0.2195 \times 2.122 = 465.78\ \text{nF}$$

and,

$$\frac{1 - m^2}{4m} L = 12.94\ \mu\text{H}$$

This filter circuit is illustrated in Figure 8.8.

As noted earlier, the image impedance of this circuit will be the same as that of the corresponding constant-k section. Hence, it will vary with frequency as illustrated earlier in Figure 8.4. Propagation constant γ of this circuit is determined from the formula listed in Table 8.1. The transfer characteristics are then found as $e^{-\gamma}$. Its magnitude and phase characteristics versus frequency are illustrated in Figure 8.9.

The transfer characteristics illustrated in Figure 8.9 indicate that the *m*-derived filter has a sharp change at cutoff frequency of 2 MHz. However, the output signal rises to −4dB in its stop-band. On the other hand, the constant-k filter provides higher attenuation in its stop-band. For example, the *m*-derived filter characteristic in

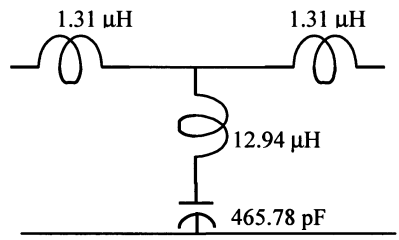

Figure 8.8 An *m*-derived T-section for Example 8.2.

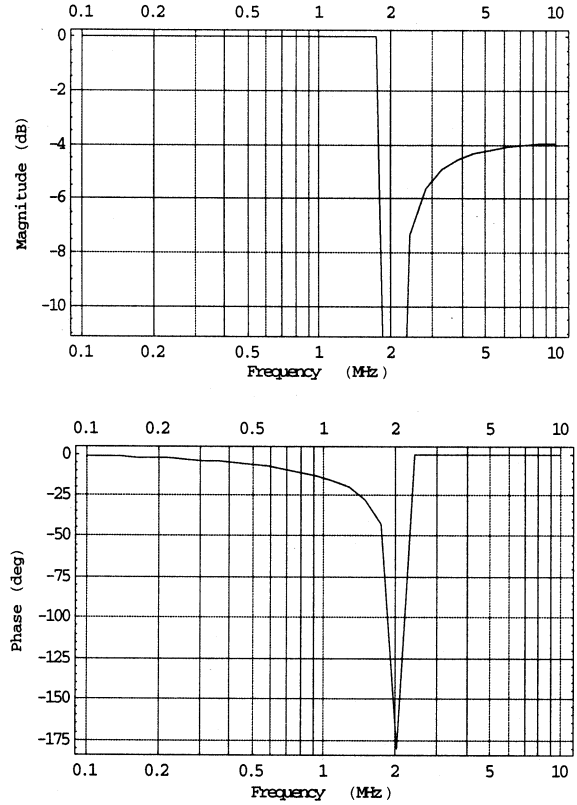

Figure 8.9 Frequency response of the *m*-derived T-section shown in Figure 8.8.

Figure 8.9 shows only 4 dB attenuation at 6 MHz, whereas the corresponding constant-k T-section has an attenuation of more than 30 dB at this frequency, as depicted in Figure 8.3.

Composite Filters

As demonstrated through the preceding examples, the *m*-derived filter provides an infinitely sharp attenuation right at its cutoff. However, the attenuation in its stop-band is unacceptably low. Contrary to this, the constant-k filter shows higher attenuation in its stop-band although the change is unacceptably gradual at the transition from pass-band to stop-band. One way to solve the problem is to cascade these two filters. Since image impedance stays the same in two cases, this cascading will not create a new impedance matching problem. However, we still need to address the problem of image impedance variation with frequency at the input and output ports of the network.

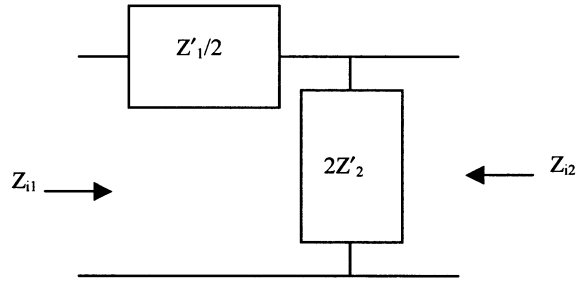

Figure 8.10 Right-hand side of the bisected π-section shown in Figure 8.6.

As illustrated in Figure 8.7, image impedance of the π-section with $m = 0.6$ remains almost constant over 90 per cent of the pass-band. If this network is bisected to connect on either side of the cascaded constant-k and *m*-derived sections, then it should provide the desired impedance characteristics. In order to verify these characteristics, let us consider a bisected π-section as shown in Figure 8.10. Its transmission parameters can be easily found following the procedure described in Chapter 7.

From (7.4.4)–(7.4.7), we find that

$$A = 1 + \frac{Z_1'}{4Z_2'} \tag{8.1.34}$$

$$B = \frac{Z_1'}{2} \tag{8.1.35}$$

$$C = \frac{1}{2Z_2'} \tag{8.1.36}$$

and,

$$D = 1 \tag{8.1.37}$$

Image impedance Z_{i1} and Z_{i2} can now be found from (8.1.10) and (8.1.11) as follows:

$$Z_{i1} = \sqrt{Z_1'Z_2' + \frac{Z_1'^2}{4}} = Z_{iT} \tag{8.1.38}$$

and,

$$Z_{i2} = \sqrt{\frac{Z_1'Z_2'}{1 + \dfrac{Z_1'}{4Z_2'}}} = \frac{Z_1'Z_2'}{Z_{iT}} = Z_{i\pi} \tag{8.1.39}$$

Thus, the bisected π-section can be connected at the input and output ports of cascaded constant-k and *m*-derived sections to obtain a composite filter that solves

TABLE 8.3 Design Relations for the Composite Filters

Low-Pass	High-Pass
Constant-k T-Filter 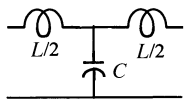 $Z_o = \sqrt{L/C}$ $\omega_c = 2/\sqrt{LC}$ $L = 2Z_o/\omega_c$ $C = 2/Z_o\omega_c$	*Constant-k T-filter* 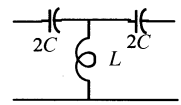 $Z_o = \sqrt{L/C}$ $\omega_c = 1/2\sqrt{LC}$ $L = 0.5Z_o/\omega_c$ $C = 0.5/Z_o\omega_c$
m-derived T-Section *(Values of L and C are same as above)* $m = \sqrt{1 - \left(\frac{f_c}{f_\infty}\right)^2}$ 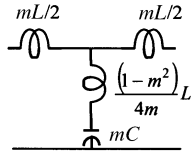 	*m-derived T-Section* *(Values of L and C are same as above)* $m = \sqrt{1 - \left(\frac{f_\infty}{f_c}\right)^2}$ 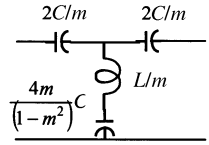
Input and Output Matching Sections 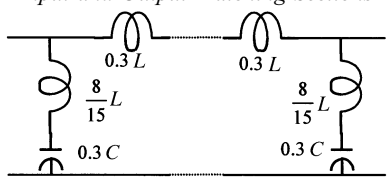 	*Input and Output Matching Sections* 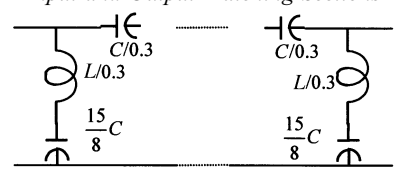

the impedance problem as well. Relations for design of these circuits are summarized in Table 8.3.

Example 8.3: Design a low-pass composite filter with a cutoff frequency of 2 MHz and image impedance of 75 Ω in its pass-band. Assume that $f_\infty = 2.05$ MHz. Plot its response in the frequency range of 100 kHz to 10 MHz.

Constant-k and *m*-derived sections of this filter are already designed in Examples 8.1 and 8.2, respectively. Its input and output matching sections can be designed as follows. With $m = 0.6$, we find that

$$\frac{mL}{2} = 3.581\,\mu\text{H}$$

$$\frac{mC}{2} = 636.6\,\text{pF}$$

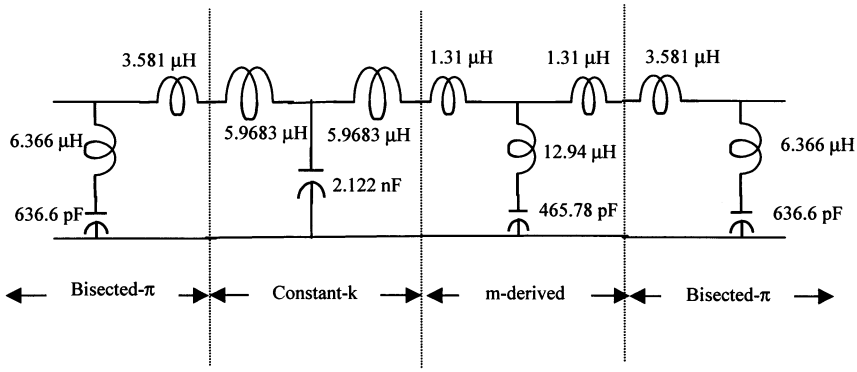

Figure 8.11 Composite filter of Example 8.3.

and,

$$\frac{1-m^2}{2m}L = 6.366\,\mu\text{H}$$

This composite filter is depicted in Figure 8.11.

Figure 8.12 illustrates the frequency response of this composite filter. As it indicates, there is a fairly sharp change in output signal as frequency changes from its pass-band to the stop-band. At the same time, output stays well below −40 dB in its stop-band. Figure 8.13 shows variation in the image impedance of this filter as the signal frequency changes. This indicates that the image impedance stays at 75 Ω (pure real, because the phase angle is zero) over most of its pass-band.

Example 8.4: Design a high-pass composite filter with nominal impedance of 75 Ω. It must pass all signals over 2 MHz. Assume that $f_\infty = 1.95$ MHz. Plot its characteristics in the frequency range of 1 MHz to 10 MHz.

From Table 8.3 we find the components of its constant-k section as follows:

$$L = \frac{75}{2 \times 2 \times \pi \times 2 \times 10^6}\text{H} = 2.984\,\mu\text{H}$$

and,

$$C = \frac{1}{2 \times 2 \times \pi \times 2 \times 10^6 \times 75}\text{F} = 530.5\,\text{pF}$$

Similarly, the component values for its *m*-derived filter section are determined as follows:

$$m = \sqrt{1-\left(\frac{f_\infty}{f_c}\right)^2} = \sqrt{1-\left(\frac{1.95}{2}\right)^2} = 0.222$$

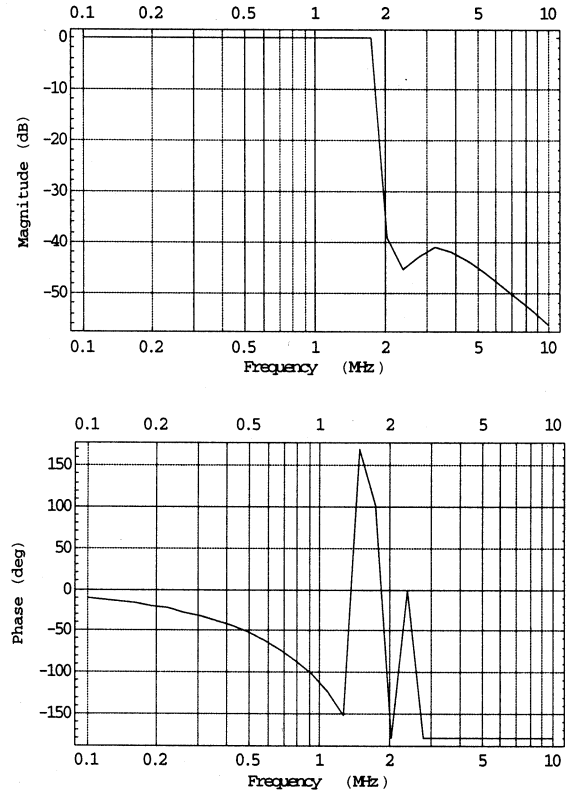

Figure 8.12 Frequency response of the composite filter of Figure 8.11.

Hence,

$$\frac{2C}{m} = 4.775\,\text{nF}$$

$$\frac{L}{m} = 13.43\ \mu\text{H}$$

and,

$$\frac{4m}{1-m^2}C = 0.496\,\text{nF}$$

Component values for the bisected π-section to be used at its input and output ports are found as

$$\frac{C}{0.3} = 1.768\,\text{nF}$$

$$\frac{L}{0.3} = 9.947\,\mu\text{H}$$

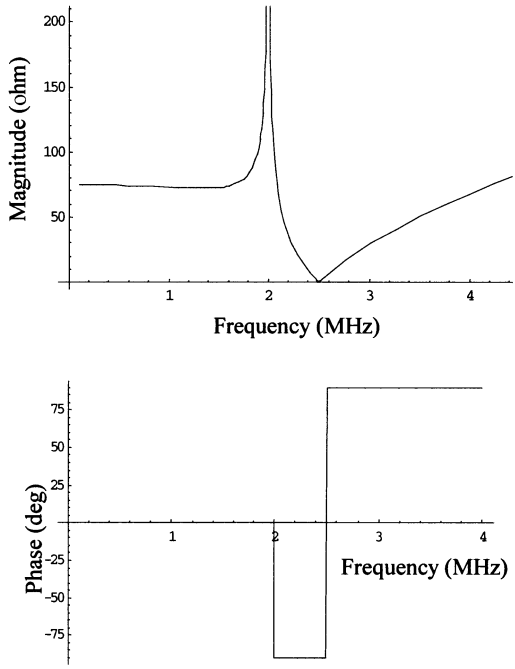

Figure 8.13 Image impedance of the composite filter of Figure 8.11 versus frequency.

and,

$$\frac{15}{8}C = 0.9947\,\text{nF}$$

The composite filter (after simplifying for the series capacitors in various sections) is illustrated in Figure 8.14. Frequency response of this composite filter is depicted in Figure 8.15. It shows that the attenuation in its stop-band stays below −40 dB, and the switching to pass-band is fairly sharp. As usual with this kind of circuit, its phase

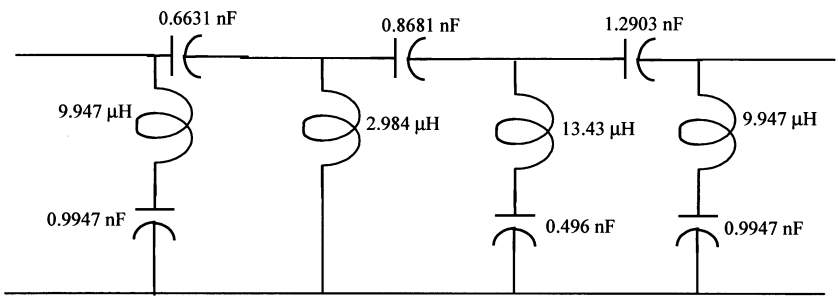

Figure 8.14 The composite high-pass filter with 2 MHz cutoff frequency.

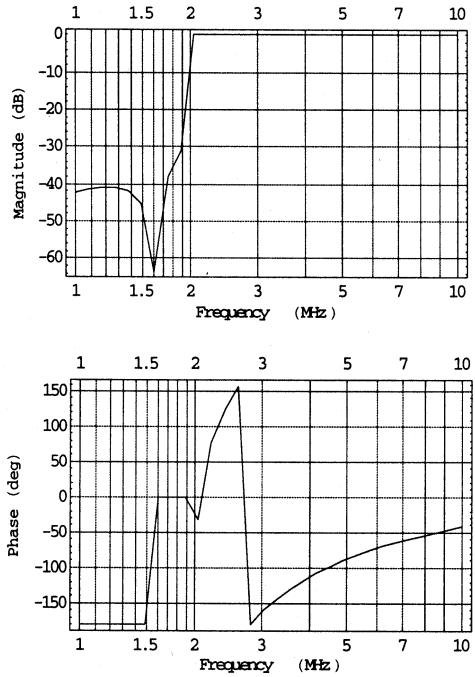

Figure 8.15 Frequency response of the composite high-pass filter of Figure 8.14.

characteristics may not be acceptable for certain applications because of inherent distortion.

As depicted in Figure 8.16, image impedance of this composite filter is almost constant at 75 Ω. Note that its magnitude varies over a wide range in the stop-band while its phase angle seems to remain constant at 90°. Phase angle of the image impedance is zero in the pass-band.

8.2 INSERTION LOSS METHOD

The output of an ideal filter would be the same as its input in the pass-band while it would be zero in the stop-band. Phase response of this filter must be linear to avoid signal distortion. In reality, such circuits do not exist and a compromise is needed to design the filters. The image parameter method described in the preceding section provides a simple design procedure. However, transfer characteristics of this circuit cannot be shaped as desired. On the other hand, the insertion loss method provides ways to shape pass- and stop-bands of the filter although its design theory is much more complex.

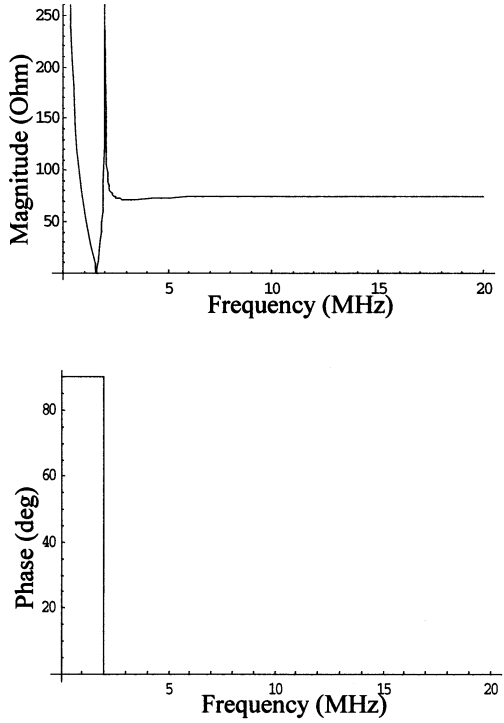

Figure 8.16 Image impedance of the composite high-pass filter of Figure 8.14 as a function of signal frequency.

The power-loss ratio of a two-port network is defined as the ratio of the power that is delivered to the load when it is directly connected at the generator to the power delivered when the network is inserted in between the two. In other words,

$$P_{\mathrm{LR}} = \frac{\text{Power incident at port} - 1}{\text{Power delivered to the load connected at port} - 2} = \frac{1}{1 - |\Gamma(\omega)|^2} \tag{8.2.1}$$

The power-loss ratio, P_{LR}, expressed in dB, is generally known as the insertion-loss of the network. It can be proved that $|\Gamma(\omega)|^2$ must be an even function of ω for a physically realizable network. Therefore, polynomials of ω^2 can represent it as follows:

$$|\Gamma(\omega)|^2 = \frac{f_1(\omega^2)}{f_1(\omega^2) + f_2(\omega^2)} \tag{8.2.2}$$

and,

$$P_{\mathrm{LR}} = 1 + \frac{f_1(\omega^2)}{f_2(\omega^2)} \tag{8.2.3}$$

where $f_1(\omega^2)$ and $f_2(\omega^2)$ are real polynomials in ω^2.

Alternatively, the magnitude of the voltage-gain of the two-port network can be found as

$$|G(\omega)| = \frac{1}{\sqrt{P_{\mathrm{LR}}}} = \frac{1}{\sqrt{1 + \dfrac{f_1(\omega^2)}{f_2(\omega^2)}}} \tag{8.2.4}$$

Hence, if P_{LR} is specified then $\Gamma(\omega)$ is fixed. Therefore, the insertion-loss method is similar to the impedance matching methods discussed earlier in Chapter 6.

Traditionally, the filter design begins with a lumped-element low-pass network that is synthesized by using normalized tables. It is subsequently scaled to the desired cutoff frequency and the impedance. Also, the low-pass prototype can be transformed to obtain a high-pass, a band-pass, or a band-stop filter. These lumped-element filters are used as a starting point to design the transmission line filter. This section presents the design procedure for two different kinds of lumped-element low-pass filters. It is followed by the transformation techniques used to design high-pass, band-pass, and band-stop filters.

Low-Pass Filters

As illustrated in Figure 8.17, an ideal low-pass filter will pass the signals below its cutoff frequency$\omega_c$without attenuation while it will stop those with higher frequencies. Further, the transition from its pass-band to its stop-band will be sharp. In reality, this kind of filter cannot be designed. Several approximations to these characteristics are available that can be physically synthesized. Two of these are presented below.

Maximally Flat Filter As its name suggests, this kind of filter provides the flattest possible pass-band response. However, its transition from pass-band to stop-band is

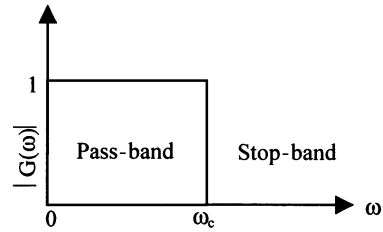

Figure 8.17 Characteristics of an ideal low-pass filter.

gradual. This is also known as a *binomial* or *Butterworth filter*. The magnitude of its voltage-gain (and hence, its frequency response) is given as follows:

$$|G(\omega)| = \frac{1}{\sqrt{1+\varsigma\bar{\omega}^{2n}}}, \qquad n = 1, 2, 3, \ldots \tag{8.2.5}$$

where ς is a constant that controls the power-loss ratio at its band edge; n is the order; and $\bar{\omega}$ is normalized frequency. For $|G(\omega| = 0.7071$ (i.e., -3 dB) at the band edge, ς is unity.

Note that derivatives of $|G(\omega)|$ at normalized frequencies much below the band edge are close to zero. This guarantees maximum flatness in the pass-band. Further, (8.2.5) indicates that $|G(\omega)|$ will be a fractional number for $\bar{\omega}$ greater than zero. Therefore, it is generally known as insertion loss, L, of the network when expressed in dB. Hence,

$$L = -20\log_{10}\left[\frac{1}{\sqrt{1+\varsigma\left(\frac{\omega}{\omega_c}\right)^{2n}}}\right] = 10\log_{10}\left[1+\varsigma\left(\frac{\omega}{\omega_c}\right)^{2n}\right]\text{dB} \tag{8.2.6}$$

or,

$$\frac{L}{10} = \log_{10}\left[1+\varsigma\left(\frac{\omega}{\omega_c}\right)^{2n}\right]$$

or,

$$\varsigma\left(\frac{\omega}{\omega_c}\right)^{2n} = 10^{\frac{L}{10}} - 1 \tag{8.2.7}$$

Figure 8.18 illustrates the pass-band characteristics of this kind of filter for three different values of n. Power-loss ratio at its band edge is assumed to be -3 dB, and therefore, ς is equal to unity. It shows that the pass-band becomes flatter with a sharper cutoff when its order n is increased. However, this relationship is not a linear one. This change in characteristics is significant for lower values of n in comparison with higher orders.

Equation (8.2.7) can be used for determining ς and n of a filter as follows. If insertion loss at the band edge ($\omega = \omega_c$) is specified as $L = L_c$ then (8.2.7) yields

$$\varsigma = 10^{\frac{L_c}{10}} - 1 \tag{8.2.8}$$

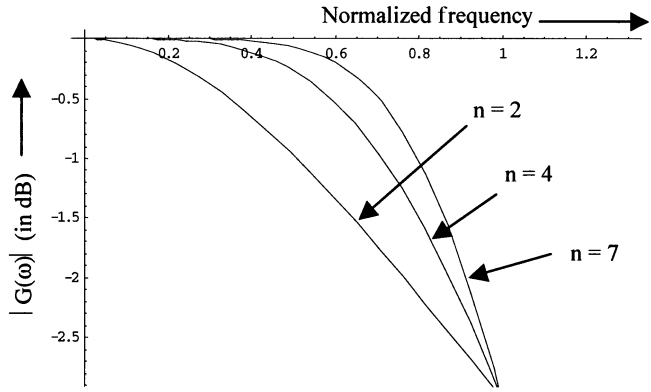

Figure 8.18 Characteristics of maximally flat low-pass filters.

Similarly, the required order n (and hence, number of elements required) of a filter can be determined for the specified L at a given stop-band frequency. It is found as follows.

$$n = \frac{1}{2} \times \frac{\log_{10}\left(10^{\frac{L}{10}} - 1\right)}{\log_{10}\left(\frac{\omega}{\omega_c}\right) + \log_{10}(\varsigma)} \tag{8.2.9}$$

Chebyshev Filter A filter with sharper cutoff can be realized at the cost of flatness in its pass-band. Chebyshev filters possess ripples in the pass-band but provide a sharp transition into the stop-band. In this case, Chebyshev polynomials are used to represent the insertion loss. Mathematically,

$$|G(\omega)| = \frac{1}{\sqrt{1 + \varsigma T_m^2(\bar{\omega})}}, \qquad m = 1, 2, 3, \ldots \tag{8.2.10}$$

where ς is a constant; $\bar{\omega}$ is normalized frequency: and $T_m(\omega)$ is a Chebyshev polynomial of the first kind and degree m. It is defined earlier in Chapter 6 by (6.5.2).

Figure 8.19 shows the frequency response of a typical Chebyshev filter for $m = 7$. It assumes that ripples up to -3 dB in its pass-band are acceptable. A comparison of this characteristic to that for a seventh order Butterworth filter shown in Figure 8.18 indicates that it has a much sharper transition from pass-band to stop-band. However, it is achieved at the cost of ripples in its pass-band.

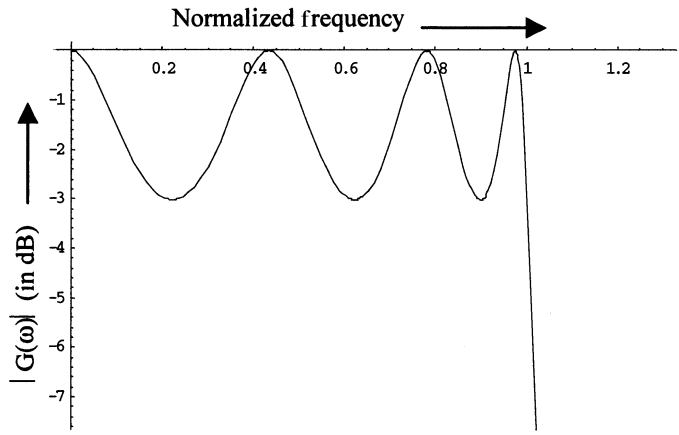

Figure 8.19 Characteristics of a low-pass Chebyshev filter for $n = 7$.

As before, the insertion loss of a Chebyshev filter is found as follows:

$$L = -20\log_{10}\left[\frac{1}{\sqrt{1+\varsigma T_m^2\left(\frac{\omega}{\omega_c}\right)}}\right] = 10\log_{10}\left[1+\varsigma T_m^2\left(\frac{\omega}{\omega_c}\right)\right]$$

or,

$$L = \begin{cases} 10\log_{10}\left[1+\varsigma\cos^2\left\{m\cos^{-1}\left(\frac{\omega}{\omega_c}\right)\right\}\right] & 0 \le \omega \le \omega_c \\ 10\log_{10}\left[1+\varsigma\cosh^2\left\{m\cosh^{-1}\left(\frac{\omega}{\omega_c}\right)\right\}\right] & \omega_c < \omega \end{cases} \tag{8.2.11}$$

where

$$\varsigma = 10^{0.1\times G_r} - 1 \tag{8.2.12}$$

G_r is ripple amplitude in dB.

The order m (and hence, number of elements) of a Chebyshev filter can be found from its specified characteristics as follows:

$$m = \frac{\cosh^{-1}\left[\sqrt{\frac{10^{0.1\times L}-1}{10^{0.1\times G_r}-1}}\right]}{\cosh^{-1}\left(\frac{\omega}{\omega_c}\right)} \tag{8.2.13}$$

where L is required insertion loss in dB at a specified frequency ω.

Example 8.5: It is desired to design a maximally flat low-pass filter with at least 15 dB attenuation at $\omega = 1.3\ \omega_c$ and -3 dB at its band edge. How many elements will be required for this filter? If a Chebyshev filter is used with 3-dB ripple in its pass-band then find the number of circuit elements.

From (8.2.8),

$$\varsigma = 10^{\frac{L_r}{10}} - 1 = 10^{0.3} - 1 = 1$$

And from (8.2.9) we have

$$n = \frac{1}{2} \times \frac{\log_{10}\left(10^{\frac{L}{10}} - 1\right)}{\log_{10}\left(\frac{\omega}{\omega_c}\right) + \log_{10}(\varsigma)} = 0.5 \times \frac{\log_{10}(10^{1.5} - 1)}{\log_{10}(1.3)} = 6.52$$

Therefore, 7 elements will be needed for this maximally flat filter.

In the case of a Chebyshev filter, (8.2.13) gives

$$m = \frac{\cosh^{-1}\left[\sqrt{\frac{10^{0.1\times L} - 1}{10^{0.1\times G_r} - 1}}\right]}{\cosh^{-1}\left(\frac{\omega}{\omega_c}\right)} = \frac{\cosh^{-1}[\sqrt{10^{1.5} - 1}]}{\cosh^{-1}(1.3)} = 2.49$$

Hence, it will require only 3 elements. Characteristics of these two filters are illustrated in Figure 8.20.

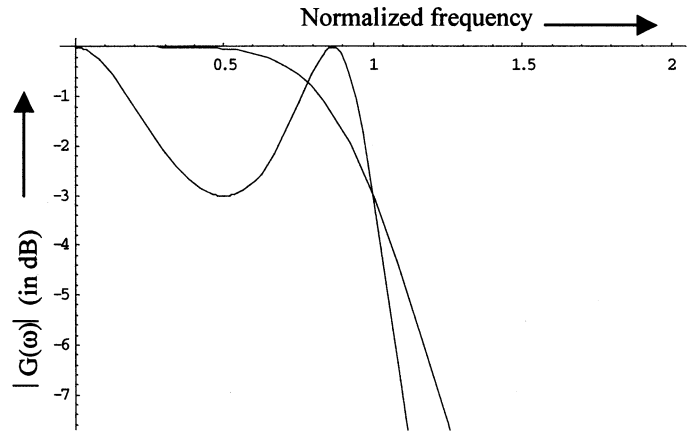

Figure 8.20 Characteristics of low-pass Butterworth and Chebyshev filters.

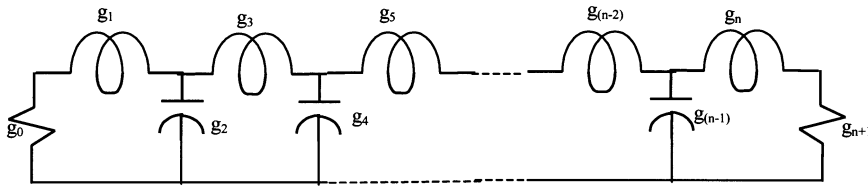

Figure 8.21 A low-pass ladder network prototype.

Low-Pass Filter Synthesis

The scope of this book does not include the theory of passive filter synthesis. There are several excellent references available in the literature for those who may be interested in this. The design procedure presented here is based on a doubly terminated low-pass ladder network as shown in Figure 8.21.

The g notation used in Figure 8.21 signifies roots of an nth order transfer function that govern its characteristics. These represent the normalized reactance values of filter elements with a cutoff frequency $\omega_c = 1$. Source resistance is represented by g_0 while the load is g_{n+1}. The filter is made up of series inductors and shunt capacitors that are in the form of cascaded T-networks. Another possible configuration is the cascaded π-network that is obtained after replacing g_1 by a short circuit, connecting a capacitor across the load g_{n+1}, and renumbering filter elements 1 through n. Elements of this filter are determined from n roots of the transfer function.

The transfer function is selected according to desired pass- and stop-band characteristics. Normalized values of elements are then found from the roots of that transfer function. These values are then adjusted according to desired cutoff frequency, and source and load resistance. Design procedures for the maximally flat and the Chebyshev filters can be summarized as follows.

Assume that the cut off frequency is given as follows:

$$\omega_c = 1 \tag{8.2.14}$$

Butterworth and Chebyshev filters can then be designed using the following formulas.

- For a Butterworth filter,

$$g_0 = g_{n+1} = 1 \tag{8.2.15}$$

and,

$$g_p = 2\sin\left[\frac{(2p-1)\pi}{2n}\right] \qquad p = 1, 2, \ldots, n \tag{8.2.16}$$

Element values computed from (8.2.15) and (8.2.16) are given in Table 8.4 for n up to 7.

TABLE 8.4 Element Values for Low-Pass Binomial Filter Prototypes ($g_0 = 1$, $\omega_c = 1$)

n	g_1	g_2	g_3	g_4	g_5	g_6	g_7	g_8
1	2.0000	1.0000						
2	1.4142	1.4142	1					
3	1.0000	2.0000	1.0000	1.0000				
4	0.7654	1.8478	1.8478	0.7654	1.0000			
5	0.6180	1.6180	2.0000	1.6180	0.6180	1		
6	0.5176	1.4142	1.9319	1.9319	1.4142	0.5176	1	
7	0.4450	1.2470	1.8019	2.0000	1.8019	1.2470	0.445	1.0000

- For a Chebyshev filter,

$$g_0 = 1 \tag{8.2.17}$$

$$g_{m+1} = \begin{cases} 1, & m \text{ is an odd number} \\ \cosh\left(\dfrac{\xi}{4}\right), & m \text{ is an even number} \end{cases} \tag{8.2.18}$$

$$g_1 = \frac{2a_1}{\chi} \tag{8.2.19}$$

and,

$$g_p = \frac{4a_{(p-1)}a_p}{b_{(p-1)}g_{(p-1)}}, \qquad p = 2, 3, \ldots, m \tag{8.2.20}$$

where,

$$\xi = \ln\left[\coth\left(\frac{G_r}{17.37}\right)\right] \tag{8.2.21}$$

$$\chi = \sinh\left(\frac{\xi}{2m}\right) \tag{8.2.22}$$

$$a_p = \sin\left[\frac{(2p-1)\pi}{2m}\right] \tag{8.2.23}$$

and,

$$b_p = \chi^2 + \sin^2\left(\frac{p\pi}{m}\right) \tag{8.2.24}$$

Element values for several low-pass Chebyshev filters that are computed from (8.2.17)–(8.2.24) are given in Tables 8.5–8.9.

TABLE 8.5 Element Values for Low-Pass Chebyshev Filter Prototypes ($g_0 = 1, \omega_c = 1$, and 0.1 dB ripple)

m	g_1	g_2	g_3	g_4	g_5	g_6	g_7	g_8
1	0.3053	1.0000						
2	0.8431	0.6220	1.3554					
3	1.0316	1.1474	1.0316	1.0000				
4	1.1088	1.3062	1.7704	0.8181	1.3554			
5	1.1468	1.3712	1.9750	1.3712	1.1468	1.0000		
6	1.1681	1.4040	2.0562	1.5171	1.9029	0.8618	1.3554	
7	1.1812	1.4228	2.0967	1.5734	2.0967	1.4228	1.1812	1.0000

TABLE 8.6 Element Values for Low-Pass Chebyshev Filter Prototypes ($g_0 = 1, \omega_c = 1$, and 0.5 dB ripple)

m	g_1	g_2	g_3	g_4	g_5	g_6	g_7	g_8
1	0.6987	1.0000						
2	1.4029	0.7071	1.9841					
3	1.5963	1.0967	1.5963	1.0000				
4	1.6703	1.1926	2.3662	0.8419	1.9841			
5	1.7058	1.2296	2.5409	1.2296	1.7058	1.0000		
6	1.7254	1.2479	2.6064	1.3136	2.4759	0.8696	1.9841	
7	1.7373	1.2582	2.6383	1.3443	2.6383	1.2582	1.7373	1.0000

TABLE 8.7 Element Values for Low-Pass Chebyshev Filter Prototypes ($g_0 = 1, \omega_c = 1$, and 1.0 dB ripple)

m	g_1	g_2	g_3	g_4	g_5	g_6	g_7	g_8
1	1.0178	1.0000						
2	1.8220	0.6850	2.6599					
3	2.0237	0.9941	2.0237	1.0000				
4	2.0991	1.0644	2.8312	0.7892	2.6599			
5	2.1350	1.0911	3.0010	1.0911	2.1350	1.0000		
6	2.1547	1.1041	3.0635	1.1518	2.9368	0.8101	2.6599	
7	2.1666	1.1115	3.0937	1.1735	3.0937	1.1115	2.1666	1.0000

TABLE 8.8 Element Values for Low-Pass Chebyshev Filter Prototypes ($g_0 = 1, \omega_c = 1$, and 2.0 dB ripple)

m	g_1	g_2	g_3	g_4	g_5	g_6	g_7	g_8
1	1.5297	1.0000						
2	2.4883	0.6075	4.0957					
3	2.7108	0.8326	2.7108	1.0000				
4	2.7926	0.8805	3.6064	0.6818	4.0957			
5	2.8311	0.8984	3.7829	0.8984	2.8311	1.0000		
6	2.8522	0.9071	3.8468	0.9392	3.7153	0.6964	4.0957	
7	2.8651	0.9120	3.8776	0.9536	3.8776	0.9120	2.8651	1.0000

TABLE 8.9 Element Values for Low-Pass Chebyshev Filter Prototypes ($g_o = 1, \omega_c = 1$, and 3.0 dB ripple)

m	g_1	g_2	g_3	g_4	g_5	g_6	g_7	g_8
1	1.9954	1.0000						
2	3.1014	0.5339	5.8095					
3	3.3489	0.7117	3.3489	1.0000				
4	3.4391	0.7483	4.3473	0.5920	5.8095			
5	3.4815	0.7619	4.5378	0.7619	3.4815	1.0000		
6	3.5047	0.7685	4.6063	0.7929	4.4643	0.6033	5.8095	
7	3.5187	0.7722	4.6392	0.8038	4.6392	0.7722	3.5187	1.0000

Scaling the Prototype to the Desired Cutoff Frequency and Load:

- *Frequency scaling:* For scaling the frequency from 1 to ω_c, divide all normalized g values that represent capacitors or inductors by the desired cutoff frequency expressed in radians per second. Resistors are excluded from this operation.
- *Impedance scaling:* To scale g_0 and g_{n+1} to X Ω from unity, multiply all g values that represent resistors or inductors by X. On other hand, divide those g values representing capacitors by X.

Example 8.6: Design a Butterworth filter with cutoff frequency of 10 MHz and an insertion loss of 30 dB at 40 MHz. It is to be used between a 50-Ω load and a generator with internal resistance of 50 Ω.

From (8.2.9), we have

$$n = \frac{1}{2} \times \frac{\log_{10}\left(10^{\frac{30}{10}} - 1\right)}{\log_{10}\left(\frac{40}{10}\right) + \log_{10}\left(10^{\frac{3}{10}} - 1\right)} = \frac{1}{2} \times \frac{\log_{10}(10^3 - 1)}{\log_{10}(4) + \log_{10}(1.9953 - 1)}$$

$$\approx \frac{0.5 \times 3}{0.6} \approx 2.5$$

Since the number of elements must be an integer, selecting $n = 3$ will provide more than the specified attenuation at 40 MHz. From (8.2.15) and (8.2.16),

$$g_0 = g_4 = 1$$

$$g_1 = 2\sin\left(\frac{\pi}{6}\right) = 1$$

$$g_2 = 2\sin\left(\frac{\pi}{2}\right) = 2$$

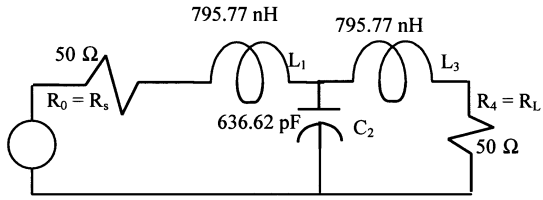

Figure 8.22 A maximally flat low-pass filter obtained in Example 8.6.

and,

$$g_3 = 2\sin\left(\frac{5\pi}{6}\right) = 1$$

If we use the circuit arrangement illustrated in Figure 8.22 then element values can be scaled to match the frequency and load resistance. Using the two rules, these values are found as follows:

$$L_1 = L_3 = 50 \times \frac{1}{2\pi \times 10^7}\text{H} = 795.77\text{ nH}$$

and,

$$C_2 = \frac{1}{50} \times \frac{2}{2\pi \times 10^7}\text{F} = 636.62\text{ pF}$$

The frequency response of this filter is shown in Figure 8.23. It indicates a 6-dB insertion-loss in the pass-band of the filter. This happens because the source resistance is considered a part of this circuit. In other words, this represents voltage across R_L with respect to source voltage, not to input of the circuit. Since source resistance is equal to the load, there is equal division of source voltage that results in −6 dB. Another 3-dB loss at the band edge shows a total of about 9 dB at 10 MHz. This characteristic shows that there is an insertion loss of over 40 dB at 40 MHz. It is clearly more than 30 dB from the band edge, as required by the example. Also, there is a nonlinear phase variation in its pass-band.

Alternatively, we can use a circuit topology as shown in Figure 8.24. In that case, component values are found by using the scaling rules, as follows:

$$L_2 = 50 \times \frac{1}{2\pi \times 10^7} \times 2 = 0.15915 \times 10^{-5}\text{ H} = 1591.5\text{ nH}$$

and,

$$C_1 = C_3 = \frac{1}{50} \times \frac{1}{2\pi \times 10^7} \times 1 = \frac{10^{-9}}{\pi}\text{F} = 318.31\text{ pF}$$

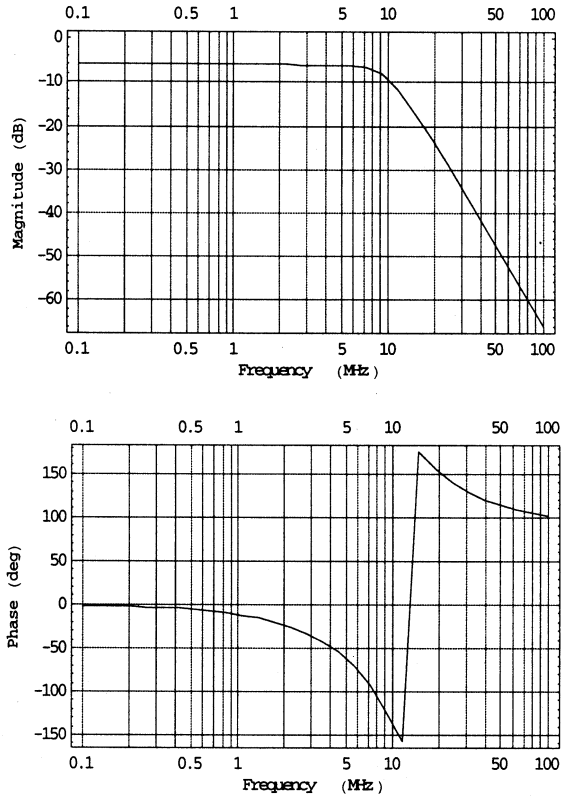

Figure 8.23 Characteristics of the low-pass filter shown in Figure 8.22.

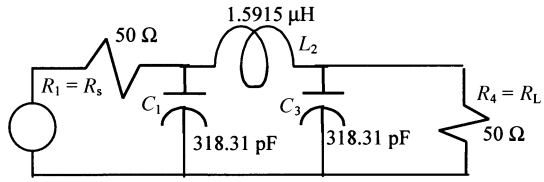

Figure 8.24 An alternative circuit for Example 8.6.

Frequency response of this circuit is illustrated in Figure 8.25. It is identical to that shown in Figure 8.23 for earlier circuit.

Example 8.7: Design a low-pass Chebyshev filter that may have ripples no more than 0.01 dB in its pass-band. The filter must pass all frequencies up to 100 MHz and attenuate the signal at 400 MHz by at least 5 dB. The load and the source resistance are of 75 Ω each.

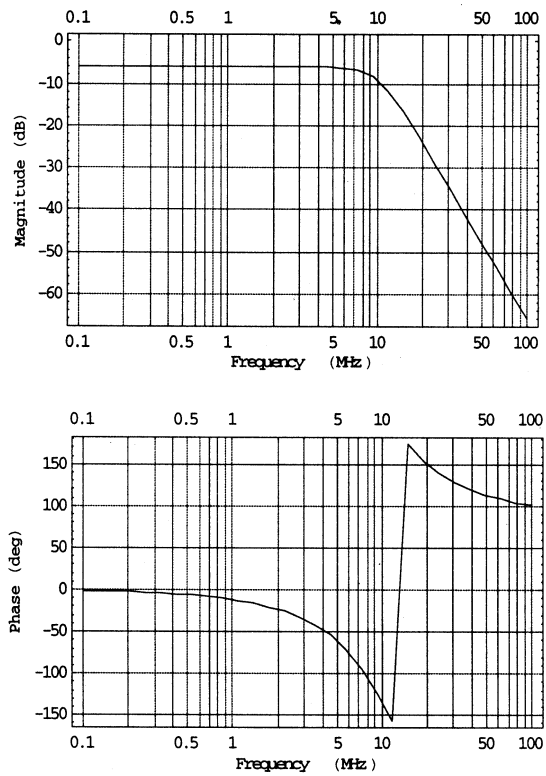

Figure 8.25 Characteristics of the low-pass filter shown in Figure 8.24.

Since,

$$G_r = 0.01\,\text{dB}$$

and

$$L\left(\frac{400}{100}\right) = 5\,\text{dB}$$

(8.2.13) gives,

$$m = \frac{\cosh^{-1}\left[\sqrt{\dfrac{(10^{0.5}-1)}{(10^{0.001}-1)}}\right]}{\cosh^{-1}(4)} = 2$$

Since we want a symmetrical filter with 75 Ω on each side, we select $m = 3$ (an odd number). It will provide more than 5 dB of insertion loss at 400 MHz. The g values can now be determined from (8.2.17) to (8.2.24), as follows. From (8.2.23),

$$a_1 = \sin\left(\frac{\pi}{6}\right) = 0.5$$

$$a_2 = \sin\left(\frac{\pi}{2}\right) = 1$$

and,

$$a_3 = \sin\left(\frac{5\pi}{6}\right) = 0.5$$

Next, from (8.2.21), (8.2.22), and (8.2.24) we get

$$\xi = \ln\left[\coth\left(\frac{0.01}{17.37}\right)\right] = 7.5$$

$$\chi = \sinh\left(\frac{7.5}{6}\right) = 1.6019$$

$$b_1 = 1.6019^2 + \sin^2\left(\frac{\pi}{3}\right) = 3.316$$

$$b_2 = 1.6019^2 + \sin^2\left(\frac{2\pi}{3}\right) = 3.316$$

and,

$$b_3 = 1.6019^2 + \sin^2\left(\frac{3\pi}{3}\right) = 2.566$$

However, b_3 is not needed in further calculations.

Finally, from (8.2.17) and (8.2.20),

$$g_0 = g_4 = 1$$

$$g_1 = \frac{2 \times 0.5}{1.6019} = 0.62425$$

$$g_2 = \frac{4 \times 0.5 \times 1}{3.316 \times 0.62425} = 0.9662$$

and,

$$g_3 = \frac{4 \times 1 \times 0.5}{3.316 \times 0.9662} = 0.62425$$

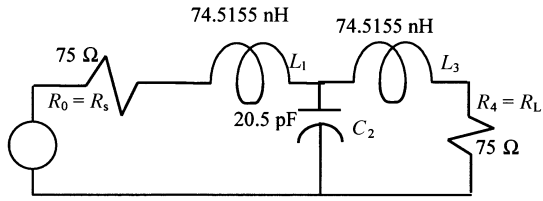

Figure 8.26 Low-pass Chebyshev filter circuit obtained in Example 8.7.

For the circuit topology of Figure 8.26, element values are found after applying the scaling rules as follows:

$$L_1 = L_3 = \frac{75 \times 0.62425}{2\pi \times 10^8}\text{H} = 74.5155\,\text{nH}$$

and,

$$C_2 = \frac{1}{75} \times \frac{1}{2\pi \times 10^8} \times 0.9662\,\text{F} = 20.5\,\text{pF}$$

Frequency response of this filter is illustrated in Figure 8.27. As expected, there is over 20-dB insertion loss at 400 MHz in comparison with its pass-band. Note that the magnitude of allowed ripple is so small that it does not show up in this figure. However, it is present there as shown on an expanded scale in Figure 8.28.

Figure 8.28 shows the pass-band characteristics of this Chebyshev filter. Since now the scale of magnitude plot is expanded, pass-band ripple is clearly visible. As expected, the ripple stays between -6.02 dB and -6.03 dB. Phase variation in this pass-band ranges from 0° and -70°.

The band edge of this filter can be sharpened further either by using a higher-order filter or by allowing larger magnitudes of the ripple in its pass-band. The higher-order filter will require more elements because the two are directly related. The next example illustrates that a sharper transition between the bands can be obtained even with a three-element filter if ripple magnitudes up to 3 dB are acceptable.

Example 8.8: Reconsider Example 8.7 to design a low-pass filter that exhibits the Chebyshev response with 3-dB ripple in its pass-band, $m = 3$, and a cutoff frequency of 100 MHz. The filter must have 75 Ω at both its input and output ports.

From (8.2.23),

$$a_1 = \sin\left(\frac{\pi}{6}\right) = 0.5$$

$$a_2 = \sin\left(\frac{\pi}{2}\right) = 1$$

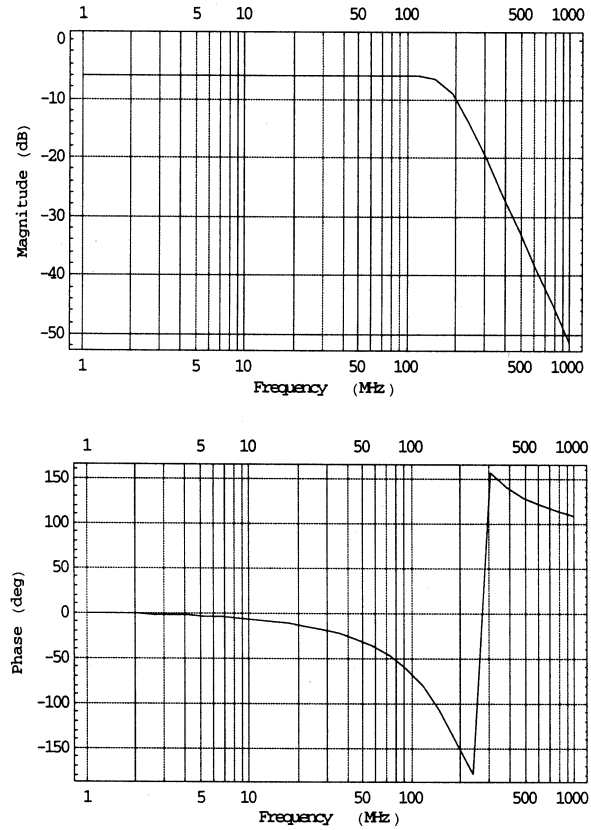

Figure 8.27 Characteristics of the low-pass Chebyshev filter shown in Figure 8.26.

and,

$$a_3 = \sin\left(\frac{5\pi}{6}\right) = 0.5$$

Now, from (8.2.21), (8.2.22), and (8.2.24),

$$\xi = \ln\left[\coth\left(\frac{3}{17.37}\right)\right] = 1.7661$$

$$\chi = \sinh\left(\frac{1.7661}{6}\right) = 0.2986$$

$$b_1 = 0.2986^2 + \sin^2\left(\frac{\pi}{3}\right) = 0.8392$$

$$b_2 = 0.2986^2 + \sin^2\left(\frac{2\pi}{3}\right) = 0.8392$$

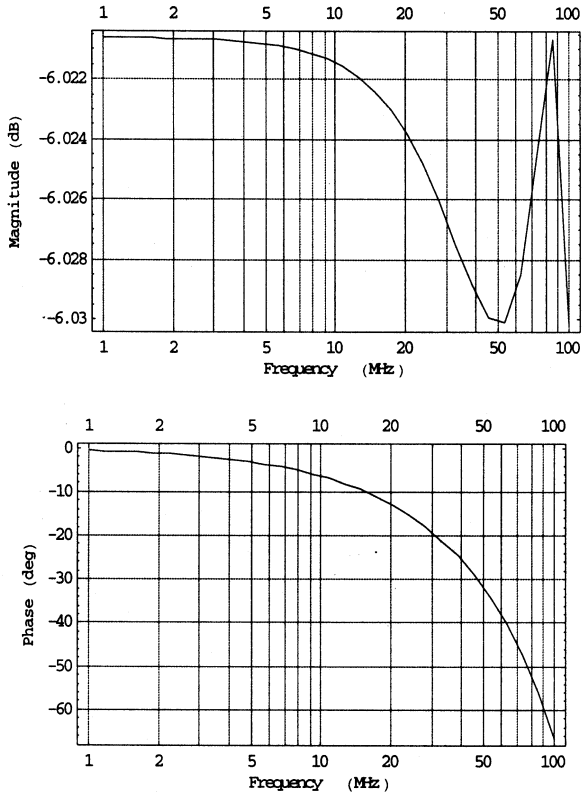

Figure 8.28 Pass-band characteristics of the filter shown in Figure 8.26.

and,

$$b_3 = 0.2986^2 + \sin^2\left(\frac{3\pi}{3}\right) = 0.0892$$

However, b_3 is not needed.

The g values for the filter can now be determined from (8.2.17)–(8.2.20), as follows:

$$g_0 = g_4 = 1$$

$$g_1 = \frac{2 \times 0.5}{0.2986} = 3.349$$

$$g_2 = \frac{4 \times 0.5 \times 1}{3.349 \times 0.8392} = 0.7116$$

and,

$$g_3 = \frac{4 \times 1 \times 0.5}{0.7116 \times 0.8392} = 3.349$$

These g-values are also listed in Table 8.9 for $m = 3$.

Elements of the circuit shown in Figure 8.29 are determined using the scaling rules, as follows (see Figure 8.30):

$$L_1 = L_3 = \frac{75 \times 3.349}{2\pi \times 10^8}\text{H} = 0.4\,\mu\text{H}$$

and,

$$C_2 = \frac{1}{75} \times \frac{1}{2\pi \times 10^8} \times 0.7116\,\text{F} = 15.1\,\text{pF}$$

High-Pass Filter

As mentioned earlier, a high-pass filter can be designed by transforming the low-pass prototype. This frequency transformation is illustrated in Figure 8.31. As illustrated, an ideal low-pass filter passes all signals up to the normalized frequency of unity with zero insertion loss whereas it completely attenuates higher frequencies. On the other hand, a high-pass filter must pass all signals with frequencies higher than its cutoff frequency ω_c and stop the signals that have lower frequencies. Therefore, the following frequency transformation formula will transform a low-pass filter to a high-pass.

$$\bar{\omega} = -\frac{\omega_c}{\omega} \tag{8.2.25}$$

Thus, inductors and capacitors will change their places. Inductors will replace the shunt capacitors of the low-pass filter and capacitors will be connected in series, in place of inductors. These elements are determined as follows:

$$C_{HP} = \frac{1}{\omega_c g_L} \tag{8.2.26}$$

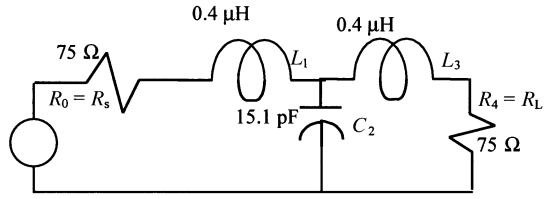

Figure 8.29 Low-pass Chebyshev filter circuit obtained in Example 8.8.

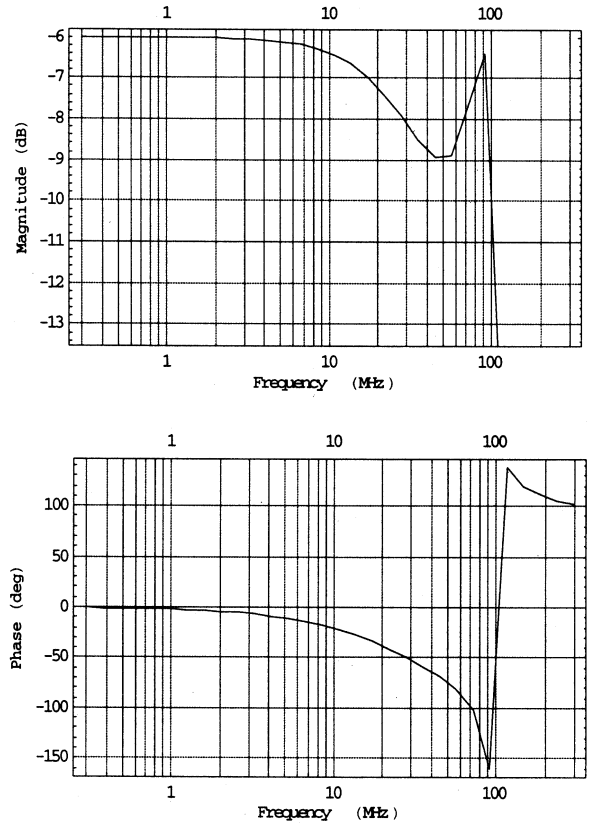

Figure 8.30 Characteristics of the low-pass filter of Example 8.8.

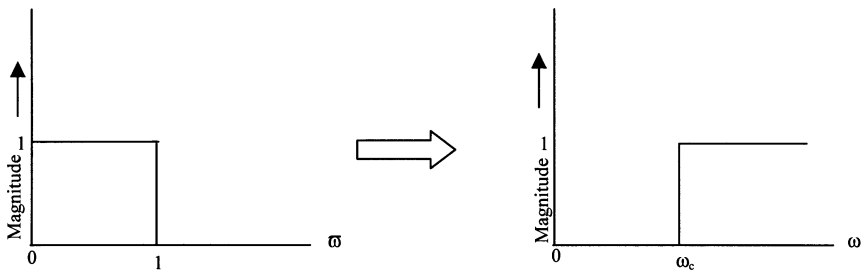

Figure 8.31 Transformation from a low-pass to high-pass characteristic.

and,

$$L_{HP} = \frac{1}{\omega_c g_C} \tag{8.2.27}$$

Capacitor C_{HP} and inductor L_{HP} can now be scaled as required by the load and source resistance.

Example 8.9: Design a high-pass Chebyshev filter with pass-band ripple magnitude less than 0.01 dB. It must pass all frequencies over 100 MHz and exhibit at least 5-dB attenuation at 25 MHz. Assume that the load and source resistances are at 75 Ω each.

The low-pass filter designed in Example 8.7 provides the initial data for this high-pass filter. With $m = 3, g_L = 0.62425$, and $g_C = 0.9662$, we find from (8.2.26) and (8.2.27) that

$$C_{HP} = \frac{1}{2\pi \times 10^8 \times 0.62425}\text{F} = 2.5495\,\text{nF}$$

and,

$$L_{HP} = \frac{1}{2\pi \times 10^8 \times 0.9662}\text{H} = 1.6472\,\text{nH}$$

Now, applying the resistance scaling, we get

$$C_1 = C_3 = \frac{2.5495}{75}\text{nF} = 33.9933\,\text{pF} = 34\,\text{pF}$$

and,

$$L_2 = 75 \times 1.6472 = 123.5\,\text{nH}$$

The resulting high-pass Chebyshev filter is shown in Figure 8.32. Its frequency response is illustrated in Figure 8.33. As before, source resistance is considered a part of the filter circuit, and therefore, its pass-band shows a 6-dB insertion loss.

Band-Pass Filter

A band-pass filter can be designed by transforming the low-pass prototype as illustrated in Figure 8.34. Here, an ideal low-pass filter passes all signals up to the normalized frequency of unity with zero insertion loss whereas it completely attenuates higher frequencies. On the other hand, a band-pass filter must pass all

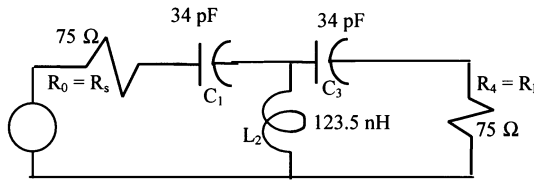

Figure 8.32 High-pass Chebyshev filter obtained for Example 8.8.

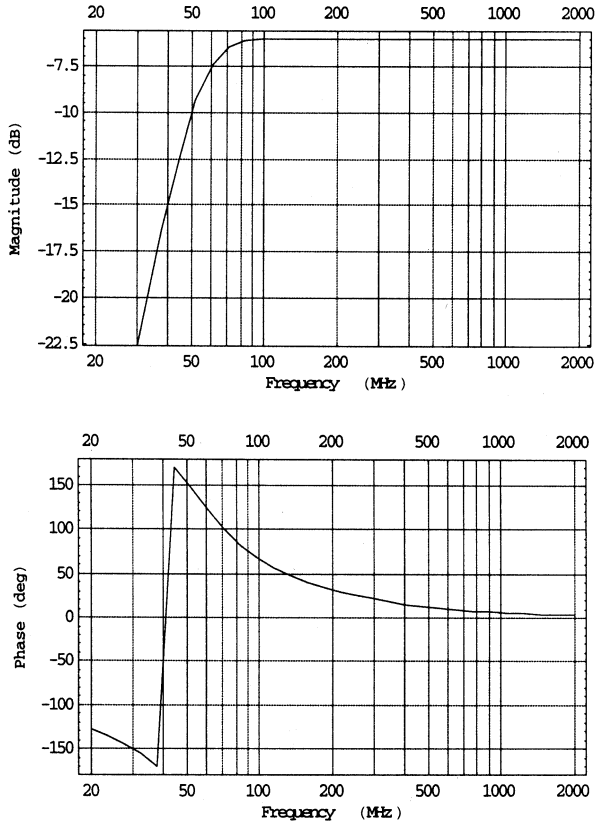

Figure 8.33 Characteristics of the high-pass Chebyshev filter shown in Figure 8.32.

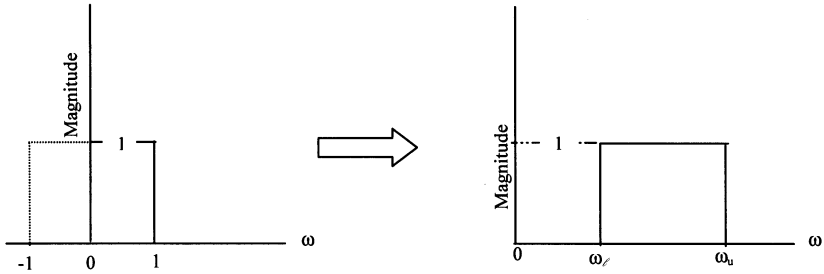

Figure 8.34 Transformation from a low-pass to band-pass characteristic.

signals with frequencies between ω_l and ω_u and stop the signals that are outside this frequency band. Hence, the following frequency relation transforms the response of a low-pass filter to a band-pass:

$$\bar{\omega} = \frac{1}{(\omega_u - \omega_\ell)} \left(\frac{\omega^2 - \omega_0^2}{\omega} \right) \tag{8.2.28}$$

where,

$$\omega_{\mathrm{o}} = \sqrt{\omega_{\ell} \times \omega_{\mathrm{u}}} \tag{8.2.29}$$

This transformation replaces the series inductor of low-pass prototype with an inductor L_{BP1} and a capacitor C_{BP1} that are connected in series. The component values are determined as follows:

$$C_{\mathrm{BP1}} = \frac{\omega_{\mathrm{u}} - \omega_{\ell}}{\omega_{\mathrm{o}}^2 g_{\mathrm{L}}} \tag{8.2.30}$$

and,

$$L_{\mathrm{BP1}} = \frac{g_{\mathrm{L}}}{\omega_{\mathrm{u}} - \omega_{\ell}} \tag{8.2.31}$$

Also, the capacitor C_{BP2} that is connected in parallel with an inductor L_{BP2} will replace the shunt capacitor of the low-pass prototype. These elements are found as follows:

$$L_{\mathrm{BP2}} = \frac{\omega_{\mathrm{u}} - \omega_{\ell}}{\omega_{\mathrm{o}}^2 g_{\mathrm{C}}} \tag{8.3.32}$$

and,

$$C_{\mathrm{BP2}} = \frac{g_{\mathrm{C}}}{\omega_{\mathrm{u}} - \omega_{\ell}} \tag{8.2.33}$$

These elements need to be further scaled as desired by the load and source resistance.

Example 8.10: Design a band-pass Chebyshev filter that exhibits no more than 0.01 dB ripples in its pass-band. It must pass signals in the frequency band of 10 MHz to 40 MHz with zero insertion loss. Assume that the load and source resistances are at 75 Ω each.

From (8.2.29), we have

$$f_{\mathrm{o}} = \sqrt{f_{\ell} \times f_{\mathrm{u}}} = \sqrt{10^7 \times 40 \times 10^6} = 20 \times 10^6 \text{ Hz}$$

Now, using (8.2.30)–(8.2.33) with $g_L = 0.62425$ and $g_C = 0.9662$ from Example 8.7, we get

$$C_{BP1} = \frac{2\pi \times 10^6(40-10)}{(2\pi \times 20 \times 10^6)^2 \times 0.62424}\text{F} = 19.122\,\text{nF}$$

$$L_{BP1} = \frac{0.62424}{2\pi \times 30 \times 10^6}\text{H} = 3.3116\,\text{nH}$$

$$L_{BP2} = \frac{2\pi \times 10^6(40-10)}{(2\pi \times 20 \times 10^6)^2 \times 0.9662}\text{H} = 12.354\,\text{nH}$$

and,

$$C_{BP2} = \frac{0.9662}{2\pi \times 30 \times 10^6}\text{F} = 5.1258\,\text{nF}$$

Next, values of elements are determined after applying the load and source resistance scaling. Hence,

$$C_1 = C_3 = \frac{19.122}{75}\text{nF} = 254.96\,\text{pF} \approx 255\,\text{pF}$$

$$L_1 = L_3 = 75 \times 3.3116\,\text{nH} = 0.2484\,\mu\text{H}$$

$$L_2 = 75 \times 12.354\,\text{nH} = 0.9266\,\mu\text{H}$$

and,

$$C_2 = \frac{5.1258}{75}\text{nF} = 68.344\,\text{pF}$$

The resulting filter circuit is shown in Figure 8.35, and its frequency response is depicted in Figure 8.36. It illustrates that we indeed have transformed the low-pass prototype to a band-pass filter for the 10-MHz to 40-MHz frequency band. As

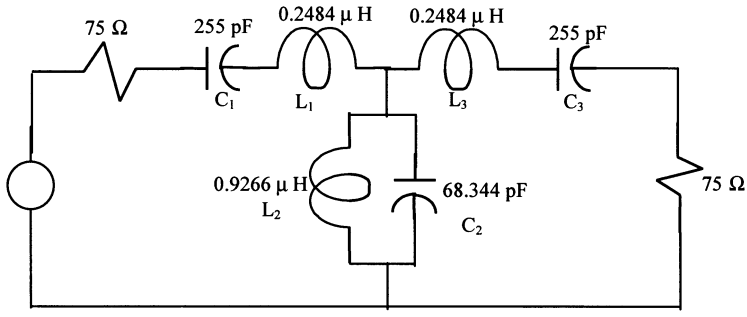

Figure 8.35 A band-pass filter circuit for Example 8.10.

before, the source resistance is considered a part of the filter circuit, and therefore, its pass-band shows a 6-dB insertion loss. Figure 11.37 shows its pass-band characteristics with expanded scales. It indicates that the ripple magnitude is limited to 0.01 dB, as desired.

Band-Stop Filter

A band-stop filter can be realized by transforming the low-pass prototype as illustrated in Figure 8.38. Here, an ideal low-pass filter passes all signals up to the normalized frequency of unity with zero insertion loss whereas it completely attenuates higher frequencies. On the other hand, a band-stop filter must stop all signals with frequencies between ω_ℓ and ω_u and pass the signals that are outside this frequency band. Hence, its characteristics are opposite to that of the band-pass filter considered earlier. The following frequency relation transforms the response of a low-pass filter to a band-stop.

$$\bar{\omega} = (\omega_u - \omega_\ell)\left(\frac{\omega}{\omega^2 - \omega_o^2}\right) \tag{8.2.34}$$

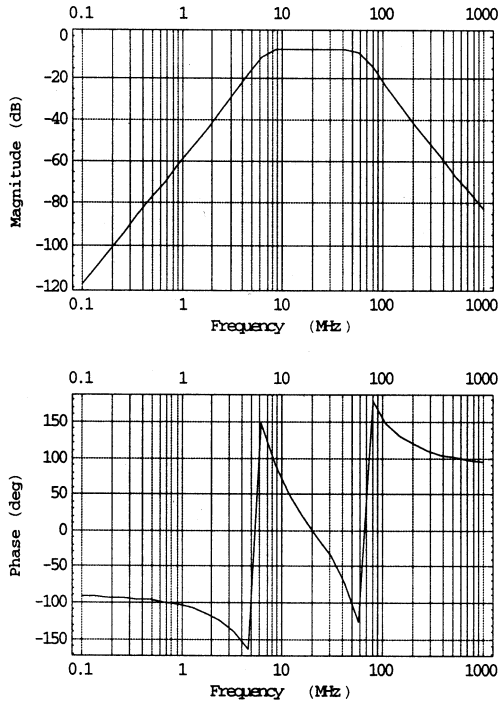

Figure 8.36 Transformation from a low-pass to band-pass characteristic.

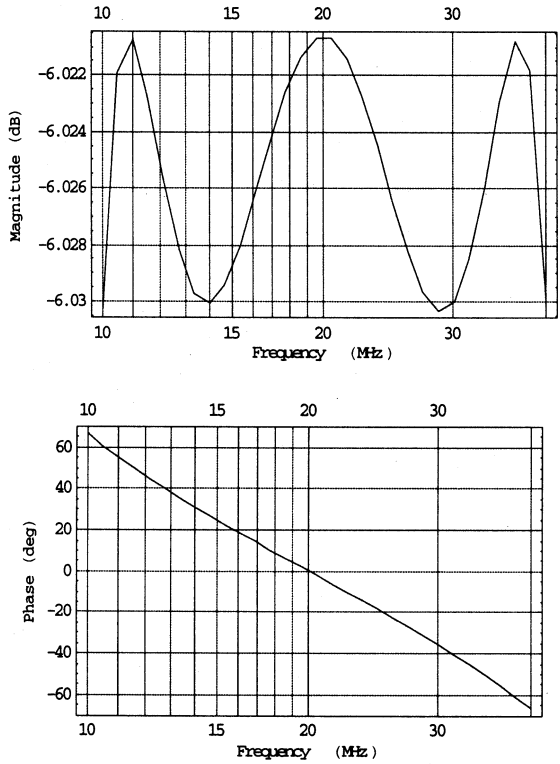

Figure 8.37 Pass-band characteristics of the band-pass filter shown in Figure 8.35.

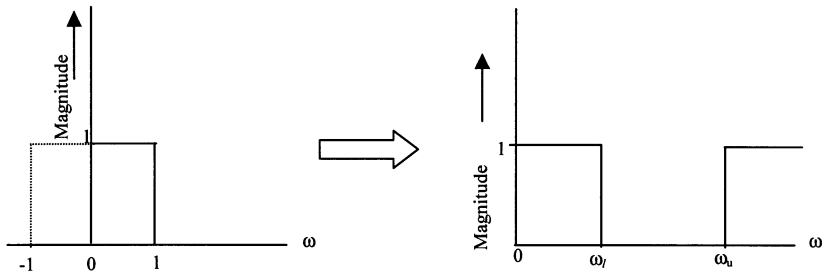

Figure 8.38 Transformation from a low-pass to band-stop characteristic.

This transformation replaces the series inductor of low-pass prototype with an inductor L_{BS1} and a capacitor C_{BS1} that are connected in parallel. Component values are determined as follows:

$$L_{BS1} = \frac{(\omega_u - \omega_\ell) g_L}{\omega_o^2} \tag{8.2.35}$$

and,

$$C_{\mathrm{BS1}} = \frac{1}{(\omega_{\mathrm{u}} - \omega_{\ell}) g_{\mathrm{L}}} \tag{8.2.36}$$

Also, capacitor C_{BS2}, which is connected in series with an inductor L_{BS2}, will replace the shunt capacitor of low-pass prototype. These elements are found as follows:

$$L_{\mathrm{BS2}} = \frac{1}{(\omega_{\mathrm{u}} - \omega_{\ell}) g_{\mathrm{C}}} \tag{8.2.37}$$

and,

$$C_{\mathrm{BS2}} = \frac{(\omega_{\mathrm{u}} - \omega_{\ell}) g_{\mathrm{C}}}{\omega_{\mathrm{o}}^2} \tag{8.2.38}$$

These elements need to be further scaled as desired by the load and source resistance. Table 8.10 summarizes these transformations for the low-pass prototype filter.

Example 8.11: Design a maximally flat band-stop filter with $n = 3$. It must stop signals in the frequency range from 10 MHz to 40 MHz and pass rest of the frequencies. Assume that the load and source resistances are at 75 Ω each.

From (8.2.29), we have

$$f_{\mathrm{o}} = \sqrt{f_{\ell} \times f_{\mathrm{u}}} = \sqrt{10^7 \times 40 \times 10^6} = 20 \times 10^6 \,\mathrm{Hz}$$

Now, using (8.2.35)–(8.2.38) with $g_{\mathrm{L}} = 1$ and $g_{\mathrm{C}} = 2$ from Example 8.6, we get

$$L_{\mathrm{BS1}} = \frac{2\pi \times 10^6 (40 - 10)}{(2\pi \times 20 \times 10^6)^2} \times 1\,\mathrm{H} = 11.94\,\mathrm{nH}$$

$$C_{\mathrm{BS1}} = \frac{1}{2\pi \times 10^6 (40 - 10) \times 1}\mathrm{F} = 5.305\,\mathrm{nF}$$

$$L_{\mathrm{BS2}} = \frac{1}{2\pi \times 10^6 (40 - 10) \times 2}\mathrm{H} = 2.653\,\mathrm{nH}$$

and,

$$C_{\mathrm{BS2}} = \frac{2\pi \times 10^6 (40 - 10)}{(2\pi \times 20 \times 10^6)^2} \times 2\,\mathrm{F} = 23.87\,\mathrm{nF}$$

TABLE 8.10 Filter Transformations

Filter	Circuit Elements	
Low-pass	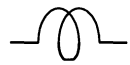 g_L	 g_C
High-pass	 $\frac{1}{\omega_c g_L}$	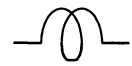 $\frac{1}{\omega_c g_C}$
Band-pass	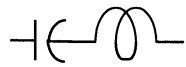 $\frac{\omega_u - \omega_\ell}{\omega_o^2 g_L}$ $\frac{g_L}{\omega_u - \omega_\ell}$	$\frac{\omega_u - \omega_\ell}{\omega_o^2 g_C}$ 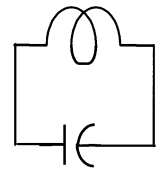 $\frac{g_C}{\omega_u - \omega_\ell}$
Band-stop	$\frac{(\omega_u - \omega_\ell) g_L}{\omega_o^2}$ 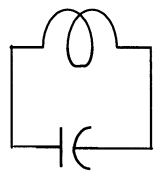 $\frac{1}{(\omega_u - \omega_\ell) g_L}$	$\frac{1}{(\omega_u - \omega_\ell) g_C}$ 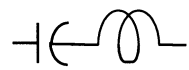 $\frac{(\omega_u - \omega_\ell) g_C}{\omega_o^2}$

Values of required elements are determined next following the load and source resistance scaling. Hence,

$$C_1 = C_3 = \frac{5.305}{75}\,\text{nF} = 70.73\,\text{pF}$$

$$L_1 = L_3 = 75 \times 11.94\,\text{nH} = 0.8955\,\mu\text{H}$$

$$L_2 = 75 \times 2.653\,\text{nH} = 0.1989\,\mu\text{H} \approx 0.2\,\mu\text{H}$$

and,

$$C_2 = \frac{23.87}{75}\text{nF} = 318.3\ \text{pF}$$

The resulting filter circuit is shown in Figure 8.39. Its frequency response depicted in Figure 8.40 indicates that we have transformed the low-pass prototype to a band-stop filter for the 10-MHz to 40-MHz frequency band. As before, source resistance is considered a part of the filter circuit, and therefore, its pass-band shows a 6-dB insertion loss.

8.3 MICROWAVE FILTERS

The filter circuits presented so far in this chapter use lumped elements. However, these may have practical limitations at microwave frequencies. When the signal wavelength is short, distances between the filter components need to be taken into account. Further, discrete components at such frequencies may cease to operate due to associated parasitic elements and need to be approximated with distributed components. As found in Chapter 3, transmission line stubs can be used in place of lumped elements. However, there may be certain practical problems in implementing the series stubs. This section begins with a technique to design a low-pass filter with only parallel connected lines of different characteristic impedance values. It is known as the *stepped impedance* (or high-Z, low-Z) *filter*. Since this technique works mainly for low-pass filters, the procedure to transform series reactance to shunt that utilizes Kuroda's identities is summarized next. Redundant sections of the transmission line are used to separate filter elements; therefore, this procedure is known as *redundant filter synthesis*. Nonredundant circuit synthesis makes use of these sections to improve the filter response as well. Other methods of designing microwave filters include coupled transmission lines and resonant cavities. Impedance transformers, discussed in Chapter 6, are essentially band-pass filters with

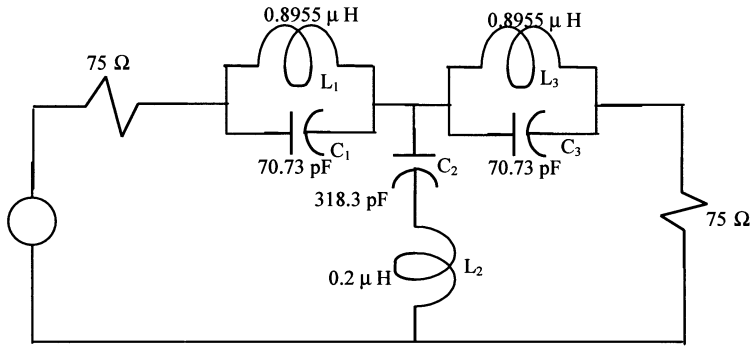

Figure 8.39 A band-stop circuit for Example 8.11.

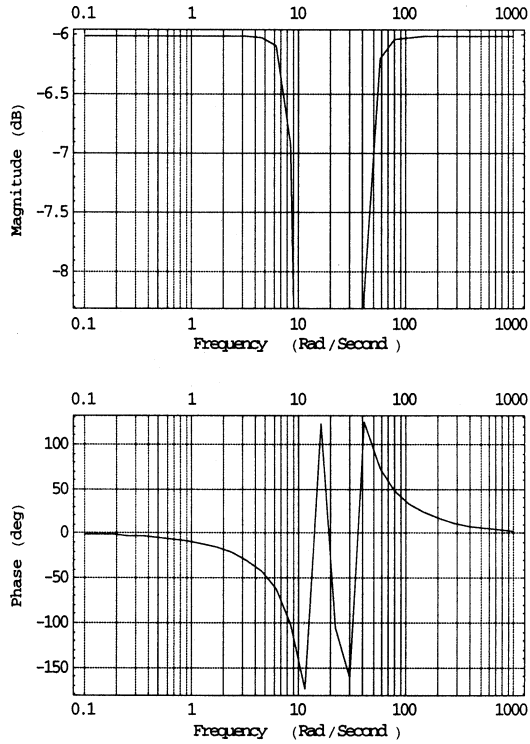

Figure 8.40 Characteristics of the band-stop filter shown in Figure 8.39.

different impedance at the two-ports. Interested readers can find detailed design procedures of all these filters in the references listed at the end of this chapter.

Low-Pass Filter Design Using Stepped Impedance Distributed Elements

Consider a lossless transmission line of length d and characteristic impedance Z_o, as shown in Figure 8.41 (a). If it is equivalent to the T-network shown in Figure 8.41 (b), these two must have the same network parameters. The impedance matrix of the transmission line was determined earlier in Example 7.4, as follows.

$$[Z]_{\text{line}} = \begin{bmatrix} -jZ_o \cot(\beta d) & -j\dfrac{Z_o}{\sin(\beta d)} \\ -j\dfrac{Z_o}{\sin(\beta d)} & -jZ_o \cot(\beta d) \end{bmatrix} \tag{8.3.1}$$

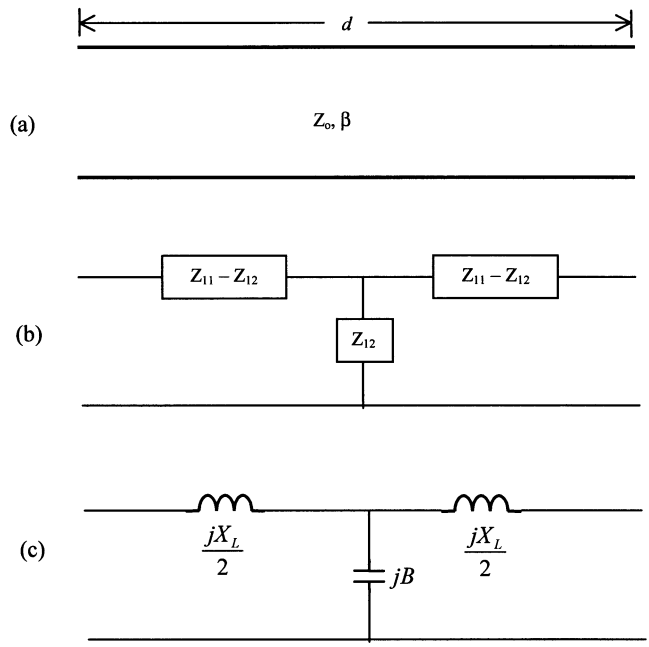

Figure 8.41 A lossless transmission line (a), equivalent symmetrical T-network (b), and (c) elements of T-networks.

The impedance matrix of the T-network, $[Z]_T$, may be found as follows.

$$[Z]_T = \begin{bmatrix} Z_{11} & Z_{12} \\ Z_{12} & Z_{11} \end{bmatrix} \tag{8.3.2}$$

Therefore, if this T-network represents the transmission line then we can write

$$Z_{11} = -jZ_o \cot(\beta d) \tag{8.3.3}$$

and,

$$Z_{12} = -j\frac{Z_o}{\sin(\beta d)} \tag{8.3.4}$$

Hence, Z_{12} is a capacitive reactance. Circuit elements in the series arm of the T-network are found to be inductive reactance. This is found as follows.

$$Z_{11} - Z_{12} = -jZ_o\left(\frac{\cos(\beta d) - 1}{\sin(\beta d)}\right) = jZ_o\frac{\sin\left(\frac{\beta d}{2}\right)}{\cos\left(\frac{\beta d}{2}\right)} = jZ_o \tan\left(\frac{\beta d}{2}\right) \tag{8.3.5}$$

Therefore, the series element of the T-network is an inductive reactance while its shunt element is capacitive, provided that $\beta d < \pi/2$.

For $\beta d < \pi/4$, (8.3.4) and (8.3.5) give

$$B \approx \frac{\beta d}{Z_o} \tag{8.3.6}$$

and,

$$X_L \approx Z_o \beta d \tag{8.3.7}$$

Special Cases:

- For Z_o very large, (8.3.6) becomes negligible in comparison with (8.3.7). Therefore, the equivalent T-network (and hence, the transmission line) represents an inductor that is given by

$$L = \frac{Z_o \beta d}{\omega} \tag{8.3.8}$$

- For Z_o very small, (8.3.6) dominates over (8.3.7). Therefore, the transmission line is effectively representing a shunt capacitance in this case. It is given by:

$$C = \frac{\beta d}{\omega Z_o} \tag{8.3.9}$$

Hence, high-impedance sections ($Z_o = Z_h$) of the transmission line can replace the inductors and low-impedance sections ($Z_o = Z_m$) can replace the capacitors of a low-pass filter. In a design, these impedance values must be selected as far apart as possible and the section lengths are determined to satisfy (8.3.8) and (8.3.9). When combined with the scaling rules, electrical lengths of the inductive and capacitive sections are found as

$$(\beta d)_L = \frac{R_o L}{Z_h} \text{rad} \tag{8.3.10}$$

and,

$$(\beta d)_C = \frac{Z_m C}{R_o} \text{ rad} \tag{8.3.11}$$

where L and C are normalized element values (g values) of the filter and R_o is the filter impedance.

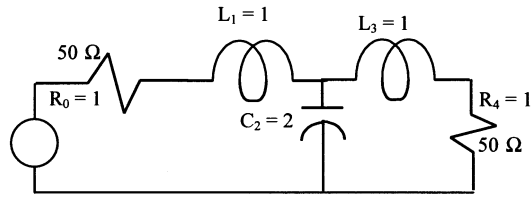

Figure 8.42 A maximally flat low-pass filter with normalized elements' values for Example 8.12.

Example 8.12: Design a three-element maximally flat low-pass filter with its cutoff frequency at 1 GHz. It is to be used between a 50-Ω load and a generator with its internal impedance at 50 Ω. Assume that $Z_h = 150\ \Omega$ and $Z_m = 30\ \Omega$.

From (8.2.15) and (8.2.16),

$$g_0 = g_4 = 1$$

$$g_1 = 2\sin\left(\frac{\pi}{6}\right) = 1$$

$$g_2 = 2\sin\left(\frac{\pi}{2}\right) = 2$$

and,

$$g_3 = 2\sin\left(\frac{5\pi}{6}\right) = 1$$

If we use a circuit arrangement as illustrated in Figure 8.42, then element values can be scaled for the frequency and the impedance. Using the scaling rules, these values are found as follows (see Figure 8.43):

$$\theta_1 = \theta_3 = (\beta d)_{\mathrm{L}} = \frac{1 \cdot 50}{150} = 0.3333 \text{ rad} = 19.1^\circ$$

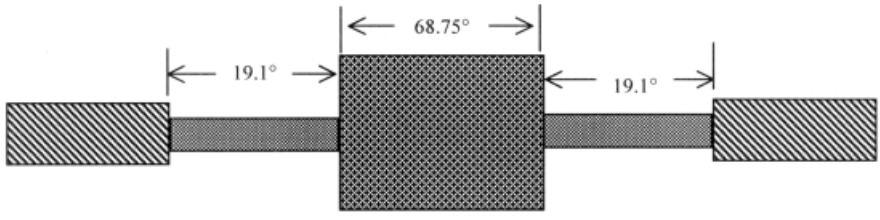

Figure 8.43 A maximally flat low-pass filter for Example 8.12.

and,

$$\theta_2 = (\beta d)_C = \frac{30 \cdot 2}{50} = 1.2 \text{ rad} = 68.75^\circ$$

Filter Synthesis Using the Redundant Elements

As mentioned earlier, transmission line sections can replace the lumped-elements of a filter circuit. Richard's transformation provides the tools needed in such a design. Further, Kuroda's identities are used to transform series elements to a shunt configuration that facilitates the design.

Richard's Transformation Richard proposed that open- and short-circuited lines could be synthesized like lumped elements through the following transformation:

$$\Omega = \tan(\beta d) = \tan\left(\frac{\omega d}{v_p}\right) \tag{8.3.12}$$

where v_p is the phase velocity of signal propagating on the line.

Since tangent function is periodic with a period of 2π, (8.3.12) is a periodic transformation. Substituting Ω in place of ω, reactance of the inductor L and of the capacitor C may be written as follows:

$$jX_L = j\Omega L = jL\tan(\beta d) \tag{8.3.13}$$

and,

$$jX_C = -j\frac{1}{\Omega C} = -j\frac{1}{C\tan(\beta d)} = -j\frac{1}{C}\cot(\beta d) \tag{8.3.14}$$

A comparison of (8.3.13) and (8.3.14) with the special cases considered in section 3.2 indicates that the former represents a short-circuited line with its characteristic impedance as L while the latter is an open-circuited with Z_o as $1/C$. Filter impedance is assumed to be unity. In order to obtain the cutoff of a low-pass filter prototype at unity frequency, the following must hold.

$$\Omega = \tan(\beta d) = 1 \rightarrow \beta d = \frac{\pi}{4} \rightarrow d = \frac{\lambda}{8} \tag{8.3.15}$$

Note that the transformation holds only at the cutoff frequency ω_c (frequency corresponding to λ), and therefore, the filter response will differ from that of its prototype. Further, the response repeats every 4 ω_c.

These transformations are illustrated in Figure 8.44. These stubs are known as the *commensurate lines* because of their equal lengths.

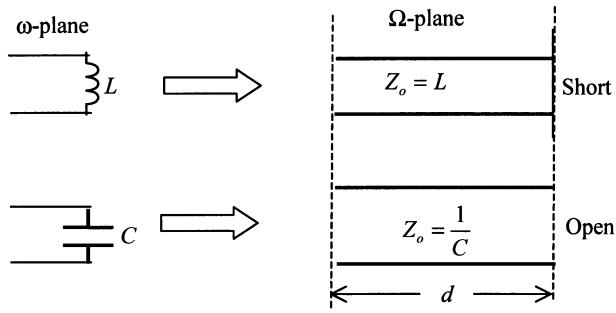

Figure 8.44 Distributed inductor and capacitor obtained from Richard's transformation.

Kuroda's Identities As mentioned earlier, Kuroda's identities facilitate the design of distributed element filters, providing the means to transform the series stubs into shunt or vice versa, to physically separate the stubs, and to render the characteristic impedance realizable. Figure 8.45 illustrates four identities that are useful in such transformation of networks. These networks employ the unit element (U.E.) that is basically a $\lambda/8$-long line at the cutoff frequency ω_c, with specified characteristic

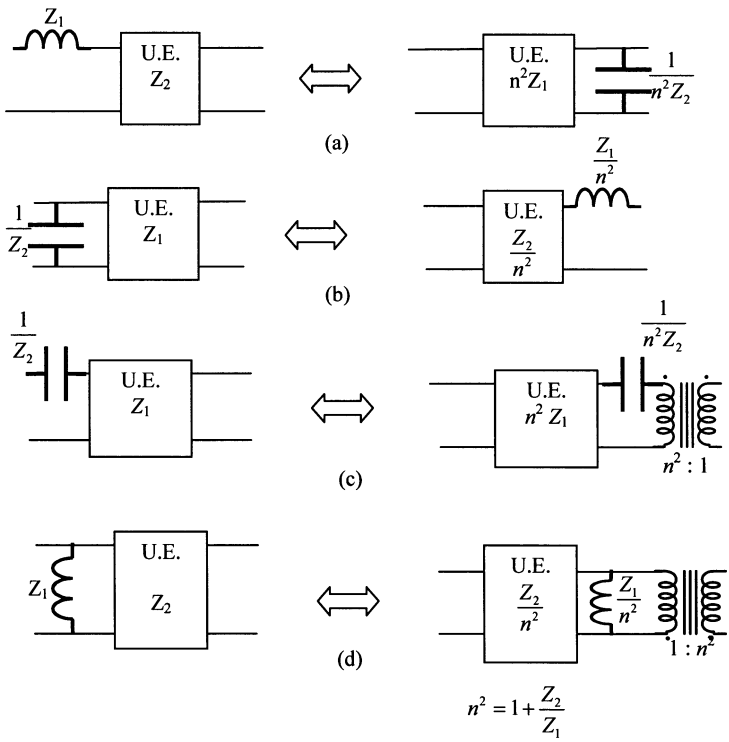

Figure 8.45 Kuroda's identities.

impedance. Inductors represent short-circuited stubs and capacitors open-circuited stubs. Obviously, its equivalent in lumped circuit theory does not exist.

The first identity is proved below. A similar procedure can be used to verify others. The circuits associated with the first identity can be redrawn as shown in Figure 8.46. A short-circuited stub of characteristic impedance Z_1 replaces the series inductor that is followed by a unit element transmission line of characteristic impedance Z_2. Its transformation gives a unit element transmission line of characteristic impedance n^2Z_1 and an open-circuited stub of characteristic impedance n^2Z_2 in place of a shunt capacitor.

Following Example 7.10, the transmission matrix of a short-circuited series stub with input impedance Z_S, can be found as follows. Impedance Z_S of the series stub is given as

$$Z_S = jZ_1 \tan(\beta d) = j\Omega Z_1 \tag{8.3.16}$$

$$\begin{bmatrix} A & B \\ C & D \end{bmatrix}_S = \begin{bmatrix} 1 & j\Omega Z_1 \\ 0 & 1 \end{bmatrix} \tag{8.3.17}$$

Following Example 7.13, transmission matrix of the unit element is found to be

$$\begin{bmatrix} A & B \\ C & D \end{bmatrix}_{\text{U.E.}} = \begin{bmatrix} \cos(\beta d) & jZ_2 \sin(\beta d) \\ \dfrac{j\sin(\beta d)}{Z_2} & \cos(\beta d) \end{bmatrix} = \cos(\beta d) \begin{bmatrix} 1 & jZ_2 \tan(\beta d) \\ \dfrac{j\tan(\beta d)}{Z_2} & 1 \end{bmatrix}$$

or,

$$\begin{bmatrix} A & B \\ C & D \end{bmatrix}_{\text{U.E.}} = \frac{1}{\sqrt{1+\Omega^2}} \begin{bmatrix} 1 & j\Omega Z_2 \\ \dfrac{j\Omega}{Z_2} & 1 \end{bmatrix} \tag{8.3.18}$$

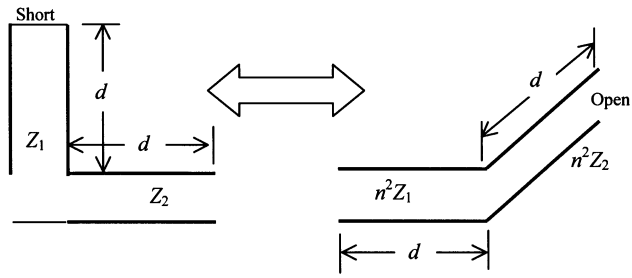

Figure 8.46 Illustration of Kuroda's first identity shown in Figure 8.45.

Since these two elements are connected in cascade, the transmission matrix for the first circuit in Figure 8.46 is found from (8.3.17) and (8.3.18) as follows.

$$\begin{bmatrix} A & B \\ C & D \end{bmatrix}_a = \begin{bmatrix} A & B \\ C & D \end{bmatrix}_S \cdot \begin{bmatrix} A & B \\ C & D \end{bmatrix}_{\text{U.E.}} = \frac{1}{\sqrt{1+\Omega^2}} \begin{bmatrix} 1 - \dfrac{\Omega^2 Z_1}{Z_2} & j\Omega(Z_1 + Z_2) \\ \dfrac{j\Omega}{Z_2} & 1 \end{bmatrix} \tag{8.3.19}$$

Now for the second circuit shown in Figure 8.46, the transmission matrix for the unit element is

$$\begin{bmatrix} A & B \\ C & D \end{bmatrix}_{\text{U.E.}} = \cos(\beta d) \begin{bmatrix} 1 & jn^2 Z_1 \tan(\beta d) \\ \dfrac{j\tan(\beta d)}{n^2 Z_1} & 1 \end{bmatrix} = \frac{1}{\sqrt{1+\Omega^2}} \begin{bmatrix} 1 & j\Omega n^2 Z_1 \\ \dfrac{j\Omega}{n^2 Z_1} & 1 \end{bmatrix} \tag{8.3.20}$$

Since impedance Z_{p} of the shunt stub is given as

$$Z_{\text{p}} = -jn^2 Z_2 \cot(\beta d) = -j\frac{n^2 Z_2}{\Omega} \tag{8.3.21}$$

its transmission matrix may be found by following Example 7.11, as

$$\begin{bmatrix} A & B \\ C & D \end{bmatrix}_{\text{p}} = \begin{bmatrix} 1 & 0 \\ \dfrac{j\Omega}{n^2 Z_2} & 1 \end{bmatrix} \tag{8.3.22}$$

Hence, the transmission matrix of the circuit shown on right-hand side is found as

$$\begin{bmatrix} A & B \\ C & D \end{bmatrix}_b = \begin{bmatrix} A & B \\ C & D \end{bmatrix}_{\text{U.E.}} \cdot \begin{bmatrix} A & B \\ C & D \end{bmatrix}_{\text{p}} = \frac{1}{\sqrt{1+\Omega^2}} \begin{bmatrix} 1 - \dfrac{\Omega^2 Z_1}{Z_2} & j\Omega n^2 Z_1 \\ \dfrac{j\Omega}{n^2}\left(\dfrac{1}{Z_1} + \dfrac{1}{Z_2}\right) & 1 \end{bmatrix} \tag{8.3.23}$$

On substituting for n^2, it is easy to show that this matrix is equal to that found in (8.3.19).

Example 8.13: Design a three-element maximally flat low-pass filter with its cutoff frequency as 1 GHz. It is to be used between a 50-Ω load and a generator with its internal impedance at 50 Ω.

A step-by-step procedure to design this filter is as follows:

- *Step 1:* As before, g values for the filter are found from (8.2.15) and (8.2.16) as

$$g_0 = g_4 = 1$$

$$g_1 = 2\sin\left(\frac{\pi}{6}\right) = 1$$

$$g_2 = 2\sin\left(\frac{\pi}{2}\right) = 2$$

and,

$$g_3 = 2\sin\left(\frac{5\pi}{6}\right) = 1$$

The circuit is drawn with normalized values as illustrated in Figure 8.47 (a).

- *Step 2:* Using Richard's transformation, the filter elements are replaced by

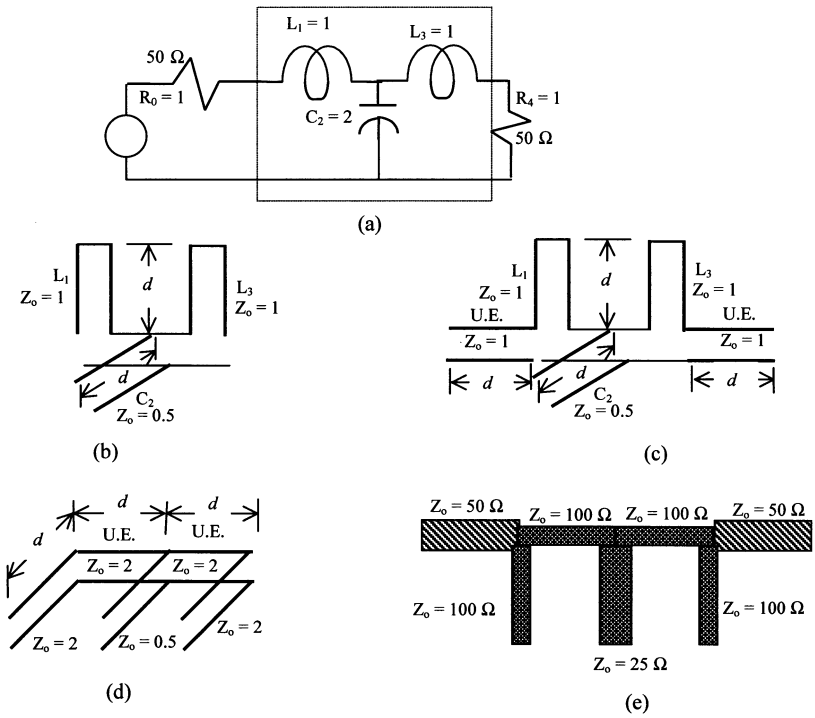

Figure 8.47 A maximally flat low-pass filter for Example 8.13.

stubs. Hence, short-circuited series stubs replace inductors L_1 and L_3 while an open-circuited shunt stub replaces the capacitor C_2. This is illustrated in Figure 8.47 (b).

- *Step 3:* Since the circuit found in step 2 cannot be fabricated in its present form, unit elements are added on its two sides. This is shown in Figure 8.47 (c).
- *Step 4:* Using Kuroda's identity shown in Figure 8.45 (a), series stub and unit element combinations are transformed to an open-circuited shunt stub and the unit element. Since $Z_1 = Z_2 = 1$, equivalent capacitance C and the characteristic impedance of the corresponding stub are found to be

$$C = \frac{1}{2} = 0.5$$

and,

$$Z_o = 2$$

Also, the characteristic impedance of each unit element is found to be 2. This circuit is illustrated in Figure 8.47 (d).

- *Step 5:* Now for impedance and frequency scaling, all normalized characteristic impedances are multiplied by 50 Ω, and the stub lengths are selected as $\lambda/8$ at 1 GHz. This is illustrated in Figure 8.47 (e).

SUGGESTED READING

I. Bahl and P. Bhartia, *Microwave Solid State Circuit Design*. New York: Wiley, 1988.

R. E. Collin, *Foundations for Microwave Engineering*. New York: McGraw Hill, 1992.

W. A. Davis, *Microwave Semiconductor Circuit Design*. New York: Van Nostrand Reinhold, 1984.

R. S. Elliott, *An Introduction to Guided Waves and Microwave Circuits*. Englewood Cliffs, NJ: Prentice Hall, 1993.

V. F. Fusco, *Microwave Circuits*. Englewood Cliffs, NJ: Prentice Hall, 1987.

G. L. Matthaei, L. Young, and E. M. T. Jones. *Microwave Filters, Impedance-Matching Networks, and Coupling Structures*. Dedham, MA: Artech House, 1980.

D. M. Pozar, *Microwave Engineering*. New York: Wiley, 1998.

PROBLEMS

1. Design a low-pass composite filter with nominal impedance of 50 Ω. It must pass all signals up to 10 MHz. Assume that $f_\infty = 10.05$ MHz. Plot its characteristics in the frequency range of 1 MHz to 100 MHz.

2. Design a high-pass T-section constant-k filter that has a nominal impedance of 50 Ω and a cutoff frequency of 10 MHz. Plot its frequency response in the frequency band of 100 kHz to 100 MHz.

3. Design an m-derived T-section high-pass filter with a cutoff frequency of 10 MHz and nominal impedance of 50 Ω. Assume that $f_\infty = 9.95$ MHz. Plot the response of this filter in the frequency band of 100 kHz to 100 MHz.

4. Design a high-pass composite filter with a cutoff frequency of 10 MHz and image impedance of 50 Ω in its pass-band. Assume that $f_\infty = 9.95$ MHz. Plot its response in the frequency range of 100 kHz to 100 MHz.

5. It is desired to design a maximally flat low-pass filter with at least 25 dB attenuation at $\omega = 2\ \omega_c$ and -1.5 dB at its band edge. How many elements will be required for this filter? If a Chebyshev filter is used with 1.5 dB ripple in its pass-band then find the number of circuit elements.

6. Design a Butterworth filter with a cutoff frequency of 150 MHz and an insertion loss of 50 dB at 400 MHz. It is to be used between a 75-Ω load and a generator with its internal resistance as 75 Ω.

7. Design a low-pass Chebyshev filter that exhibits ripples no more than 2 dB in its pass-band. The filter must pass all frequencies up to 50 MHz and attenuate the signal at 100 MHz by at least 15 dB. The load and the source resistance are of 50-Ω each.

8. Reconsider Problem 7 to design a low-pass filter that exhibits the Chebyshev response with 3-dB ripple in its pass-band. The filter must have 50 Ω at both its input and output ports.

9. Design a high-pass Chebyshev filter with pass-band ripple magnitude less than 3 dB. It must pass all frequencies over 50 MHz. A minimum of 15-dB insertion loss is required at 25 MHz. Assume that the load and source resistances are of 75 Ω each.

10. Design a band-pass Chebyshev filter that exhibits no more than 2 dB ripples in its pass-band. It must pass the signals that are in the frequency band of 50 MHz to 80 MHz with zero insertion loss. Assume that the load and source resistances are of 50 Ω each.

11. Design a maximally flat band-stop filter with $n = 5$. It must stop the signals in the frequency range from 50 MHz to 80 MHz and pass the rest of the frequencies. Assume that the load and source resistances are of 50 Ω each.

12. Design a fifth-order Butterworth filter with a cutoff frequency of 5 GHz. It is to be used between a 75-Ω load and a generator with its internal resistance as 75 Ω.

13. Design a third-order low-pass Chebyshev filter that exhibits ripples no more than 1 dB in its pass-band. The filter must pass all frequencies up to 1 GHz. The load and the source resistance are of 50 Ω each.

14. Design a fifth-order high-pass Chebyshev filter with pass-band ripple magnitude less than 3 dB. It must pass all frequencies over 5 GHz. Assume that the load and source resistances are of 75 Ω each.

Radio-Frequency and Microwave Communication Circuits: Analysis and Design
Devendra K. Misra

ISBNs: 0-471-41253-8 (Hardback); 0-471-22435-9 (Electronic)

9

SIGNAL-FLOW GRAPHS AND APPLICATIONS

A signal-flow graph is a graphical means of portraying the relationship among the variables of a set of linear algebraic equations. S. J. Mason originally introduced it to represent the cause-and-effect of linear systems. Associated terms are defined in this chapter along with the procedure to draw the signal-flow graph for a given set of algebraic equations. Further, signal-flow graphs of microwave networks are obtained in terms of their S-parameters and associated reflection coefficients. The manipulation of signal-flow graphs is summarized to find the desired transfer functions. Finally, the relations for transducer power gain, available power gain, and operating power gain are formulated in this chapter.

Consider a linear network that has N input and output ports. It is described by a set of linear algebraic equations as follows:

$$V_i = \sum_{j=1}^{N} Z_{ij} I_j \qquad i = 1, 2, \ldots, N \tag{9.1}$$

This says that the effect V_i at the ith port is a sum of gain times causes at its N ports. Hence, V_i represents the dependent variable (effect) while I_j are the independent variables (cause). *Nodes* or *junction points* of the signal-flow graph represent these variables. The nodes are connected together by line segments called *branches* with an arrow on each directed toward the dependent node. Coefficient Z_{ij} is the gain of a branch that connects the ith dependent node with jth independent node. Signal can be transmitted through a branch only in the direction of the arrow.

Basic properties of the signal-flow graph can be summarized as follows:

- A signal-flow graph can be used only when the given system is linear.
- A set of algebraic equations must be in the form of effects as functions of causes before its signal-flow graph can be drawn.
- A node is used to represent each variable. Normally, these are arranged from left to right, following a succession of inputs (causes) and outputs (effects) of the network.
- Nodes are connected together by branches with an arrow directed toward the dependent node.
- Signals travel along the branches only in the direction of the arrows.
- Signal I_k traveling along a branch that connects nodes V_i and I_k is multiplied by the branch-gain Z_{ik}. Dependent node (effect) V_i is equal to the sum of the branch gain times corresponding independent nodes (causes).

Example 9.1: Output b_1 of a system is caused by two inputs a_1 and a_2 as represented by the following algebraic equation. Find its signal-flow graph.

$$b_1 = S_{11}a_1 + S_{12}a_2$$

There are two independent variables and one dependent variable in this equation. Locate these three nodes and then connect node a_1 and a_2 with b_1, as shown in Figure 9.1. Arrows on two branches are directed toward effect b_1. Coefficients of input (cause) are shown as the gain of that branch.

Example 9.2: Output b_2 of a system is caused by two inputs a_1 and a_2 as represented by the following algebraic equation. Find its signal-flow graph.

$$b_2 = S_{21}a_1 + S_{22}a_2$$

There are again two independent variables and one dependent variable in this equation. Locate these three nodes and then connect node a_1 with b_2 and a_2 with b_2, as shown in Figure 9.2. Arrows on two branches are directed toward effect b_2. Coefficients of input (cause) are shown as the gain of that branch.

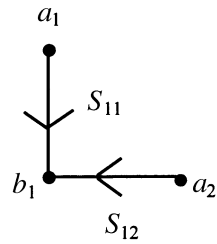

Figure 9.1 Signal-flow graph representation of Example 9.1.

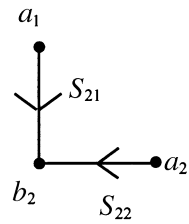

Figure 9.2 Signal-flow graph representation of Example 9.2.

Example 9.3: Input–output characteristics of a two-port network are given by the following set of linear algebraic equations. Find its signal-flow graph.

$$b_1 = S_{11}a_1 + S_{12}a_2$$
$$b_2 = S_{21}a_1 + S_{22}a_2$$

There are two independent variables a_1 and a_2 and two dependent variables b_1 and b_2 in this set of equations. Locate these four nodes and then connect node a_1 and a_2 with b_1. Similarly, connect a_1 and a_2 with b_2, as shown in Figure 9.3. Arrows on the branches are directed toward effects b_1 and b_2. Coefficients of each input (cause) are shown as the gain of that branch.

Example 9.4: The following set of linear algebraic equations represents the input–output relations of a multiport network. Find the corresponding signal-flow graph.

$$X_1 = R_1 + \frac{1}{2+s}X_2$$
$$X_2 = -4X_1 + R_2 - 7Y_1 - \frac{1}{s+4}X_2$$
$$Y_1 = \frac{s}{s^2+3}X_2$$
$$Y_2 = 10X_1 - sY_1$$

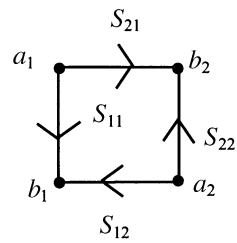

Figure 9.3 Signal-flow graph representation of Example 9.3.

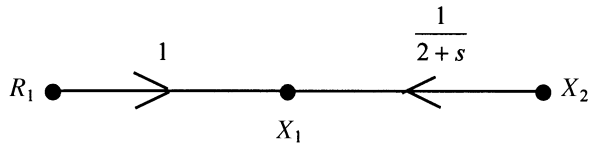

Figure 9.4 Signal-flow graph representation of the first equation of Example 9.4.

In the first equation, R_1 and X_2 represent the causes while X_1 is the effect. Hence, the signal-flow graph representing this equation can be drawn as illustrated in Figure 9.4.

Now, consider the second equation. X_1 is the independent variable in it. Further, X_2 appears as cause as well as effect. This means that a branch must start and finish at the X_2 node. Hence, when this equation is combined with the first one, the signal-flow graph will look as illustrated in Figure 9.5.

Next, we add to it the signal-flow graph of the third equation. It has Y_1 as the effect and X_2 as the cause. It is depicted in Figure 9.6.

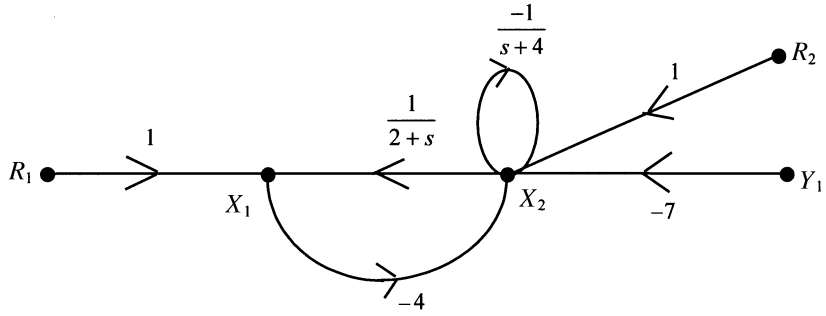

Figure 9.5 Signal-flow graph representation of the first two equations of Example 9.4.

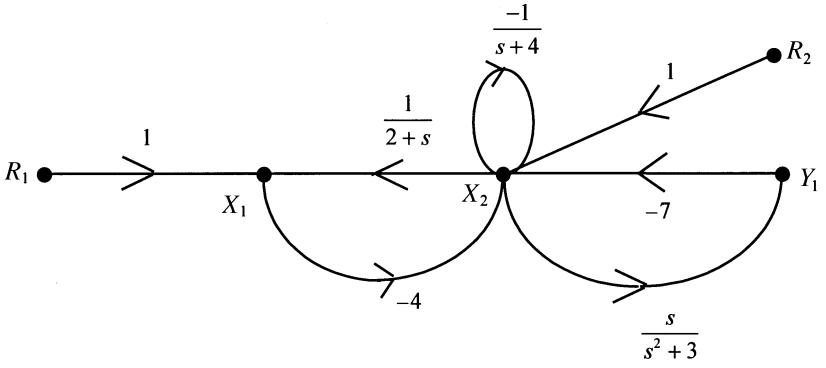

Figure 9.6 Signal-flow graph representation of the first three equations of Example 9.4.

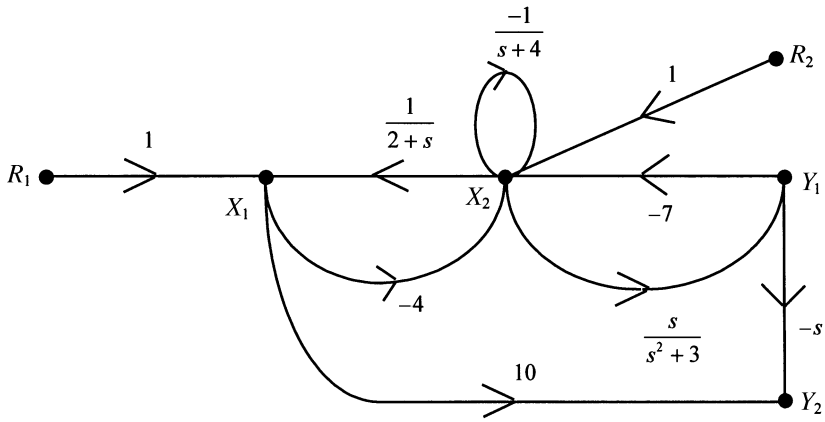

Figure 9.7 Complete signal-flow graph representation of Example 9.4.

Finally, the last equation has Y_2 as a dependent variable, and X_1 and Y_1 are two independent variables. A complete signal-flow graph representation is obtained after superimposing it as shown in Figure 9.7.

9.1 DEFINITIONS AND MANIPULATION OF SIGNAL-FLOW GRAPHS

Before we proceed with manipulation of signal-flow graphs, it will be useful to define a few remaining terms.

Input and Output Nodes: A node that has only outgoing branches is defined as an *input node* or *source*. Similarly, an *output node* or *sink* has only incoming branches. For example, R_1, R_2, and Y_1 are the input nodes in the signal-flow graph shown in Figure 9.8. This corresponds to the first two equations of Example 9.4. There is no output node (exclude the dotted branches) in it because X_1 and X_2 have both

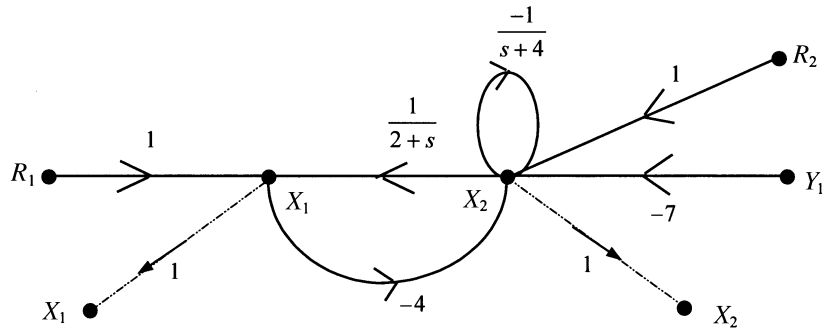

Figure 9.8 Signal-flow graph with R_1, R_2, and Y_1 as input nodes.

outgoing as well as incoming branches.

Nodes X_1 and X_2 in Figure 9.8 can be made the output nodes by adding an outgoing branch of unity gain to each one. This is illustrated in Figure 9.8 with dotted branches. It is equivalent to adding $X_1 = X_1$ and $X_2 = X_2$ in the original set of equations. Thus, any non-output node can be made an output node in this way. However, this procedure cannot be used to convert these nodes to input nodes because that changes the equations. If an incoming branch of unity gain is added to node X_1 then the corresponding equation is modified as follows:

$$X_1 = X_1 + R_1 + \frac{1}{2+s}X_2$$

However, X_1 can be made an input node by rearranging it as follows. The corresponding signal-flow graph is illustrated in Figure 9.9. It may be noted that now R_1 is an output node:

$$R_1 = X_1 - \frac{1}{2+s}X_2$$

Path: A continuous succession of branches traversed in the same direction is called the *path*. It is known as a *forward* path if it starts at an input node and ends at an output node without hitting a node more than once. The product of branch gains along a path is defined as the *path gain*. For example, there are two forward paths between nodes X_1 and R_1 in Figure 9.9. One of these forward paths is just one branch connecting the two nodes with path gain of 1. The other forward path is X_1 to X_2 to R_1. Its path gain is $4/(2+s)$.

Loop: A loop is a path that originates and ends at the same node without encountering other nodes more than once along its traverse. When a branch originates and terminates at the same node, it is called a *self-loop*. The path gain of a loop is defined as the *loop gain*.

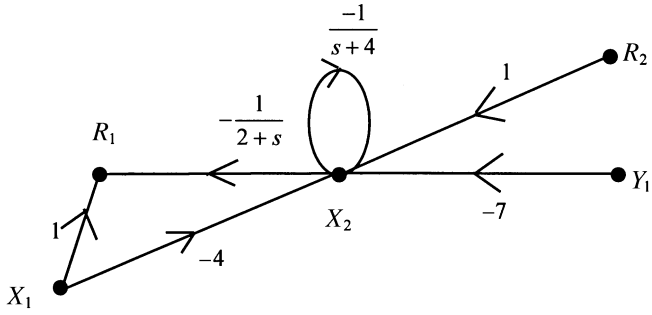

Figure 9.9 Signal-flow graph with R_1 as an output, and X_1, R_2, and Y_1 as the input nodes.

Once the signal-flow graph is drawn, the ratio of an output to input node (while other inputs, if there are more than one, are assumed to be zero) can be obtained by using *rules of reduction*. Alternatively, *Mason's rule* may be used. However, the latter rule is prone to errors if the signal-flow graph is too complex. The reduction rules are generally recommended for such cases, and are given as follows.

Rule 1: When there is only one incoming and one outgoing branch at a node (i.e., two branches are connected in series), it can be replaced by a direct branch with branch gain equal to the product of the two. This is illustrated in Figure 9.10.

Rule 2: Two or more parallel paths connecting two nodes can be merged into a single path with a gain that is equal to the sum of the original path gains, as depicted in Figure 9.11.

Rule 3: A self-loop of gain G at a node can be eliminated by multiplying its input branches by $1/(1 - G)$. This is shown graphically in Figure 9.12.

Rule 4: A node that has one output and two or more input branches can be split in such a way that each node has just one input and one output branch, as shown in Figure 9.13.

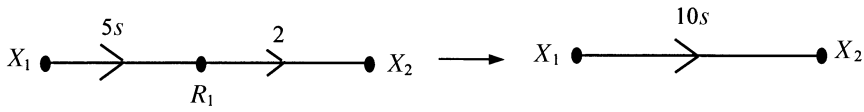

Figure 9.10 Graphical illustration of Rule 1.

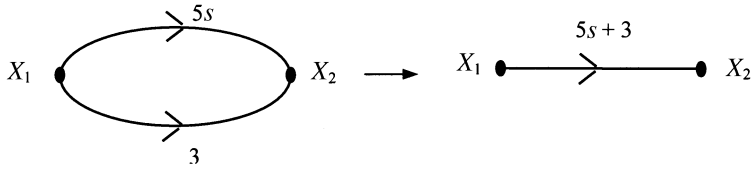

Figure 9.11 Graphical illustration of Rule 2.

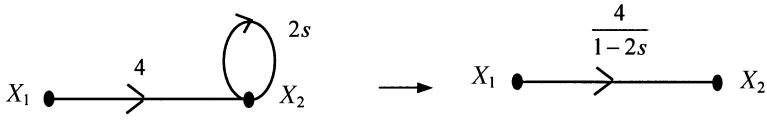

Figure 9.12 Graphical illustration of Rule 3.

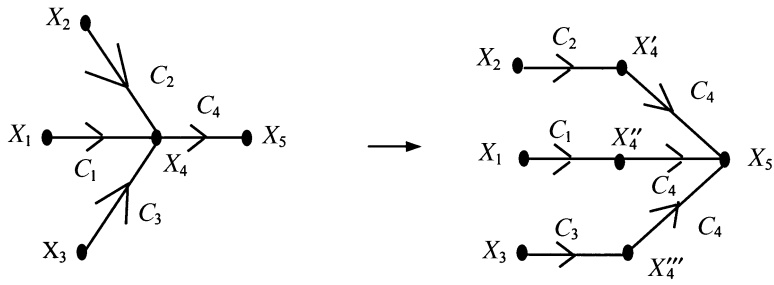

Figure 9.13 Graphical illustration of Rule 4.

Rule 5: It is similar to Rule 4. A node that has one input and two or more output branches can be split in such a way that each node has just one input and one output branch. This is shown in Figure 9.14.

Mason's Gain Rule: Ratio T of the effect (output) to that of the cause (input) can be found using Mason's rule as follows:

$$T(s) = \frac{P_1\Delta_1 + P_2\Delta_2 + P_3\Delta_3 + \cdots}{\Delta} \tag{9.1.1}$$

where P_i is the gain of the ith forward path,

$$\Delta = 1 - \sum L(1) + \sum L(2) - \sum L(3) + \cdots \tag{9.1.2}$$

$$\Delta_1 = 1 - \sum L(1)^{(1)} + \sum L(2)^{(1)} - \sum L(3)^{(1)} + \cdots \tag{9.1.3}$$

$$\Delta_2 = 1 - \sum L(1)^{(2)} + \sum L(2)^{(2)} - \sum L(3)^{(2)} + \cdots \tag{9.1.4}$$

$$\Delta_3 = 1 - \sum L(1)^{(3)} + \cdots \tag{9.1.5}$$

$$\vdots$$

$\sum L(1)$ stands for the sum of all first-order loop gains; $\sum L(2)$ is the sum of all second-order loop gains, and so on. $\sum L(1)^{(1)}$ denotes the sum of those first-order loop gains that do not touch path P_1 at any node; $\sum L(2)^{(1)}$ denotes the sum of those

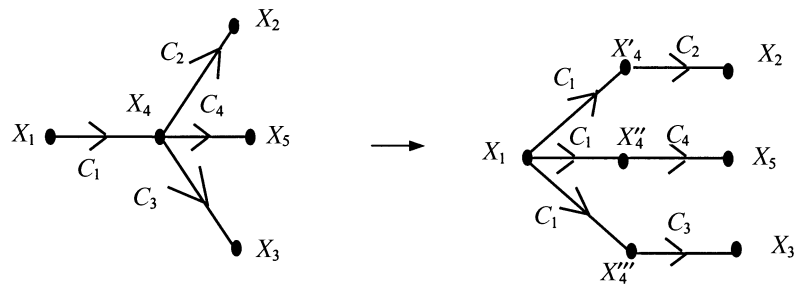

Figure 9.14 Graphical illustration of Rule 5.

second-order loop gains that do not touch the path of P_1 at any point; $\sum L(1)^{(2)}$ consequently denotes the sum of those first-order loops that do not touch path P_2 at any point, and so on.

First-order loop gain was defined earlier. Second-order loop gain is the product of two first-order loops that do not touch at any point. Similarly, third-order loop gain is the product of three first-order loops that do not touch at any point.

Example 9.5: A signal-flow graph of a two-port network is given in Figure 9.15. Using Mason's rule, find its transfer function Y/R.

There are three forward paths from node R to node Y. Corresponding path gains are found as follows:

$$P_1 = 1 \cdot 1 \cdot \frac{1}{s+1} \cdot 1 \cdot \frac{s}{s+2} \cdot 3 \cdot 1 = \frac{3s}{(s+1)(s+2)}$$

$$P_2 = 1 \cdot 6 \cdot 1 = 6$$

and,

$$P_3 = 1 \cdot 1 \cdot \frac{1}{s+1} \cdot (-4) \cdot 1 = -\frac{4}{s+1}$$

Next, it has two loops. The loop gains are

$$L_1 = -\frac{3}{s+1}$$

and,

$$L_2 = -\frac{5s}{s+2}$$

Using Mason's rule, we find that

$$\frac{Y}{R} = \frac{P_1 + P_2(1 - L_1 - L_2 + L_1L_2) + P_3(1 - L_2)}{1 - L_1 - L_2 + L_1L_2}$$

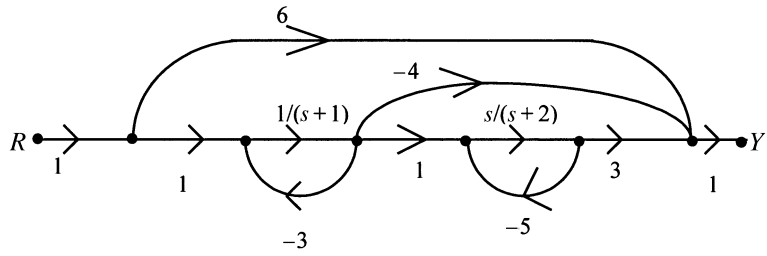

Figure 9.15 Signal-flow graph of Example 9.5.

9.2 SIGNAL-FLOW GRAPH REPRESENTATION OF A VOLTAGE SOURCE

Consider an ideal voltage source $E_S\angle 0^\circ$ in series with source impedance Z_S, as shown in Figure 9.16. It is a single-port network with terminal voltage and current V_S and I_S, respectively. It is to be noted that the direction of current-flow is assumed as entering the port, consistent with that of the two-port networks considered earlier. Further, the incident and reflected waves at this port are assumed to be a_S and b_S, respectively. Characteristic impedance at the port is assumed to be Z_o.

Using the usual circuit analysis procedure, total terminal voltage V_S can be found as follows:

$$V_S = V_S^{in} + V_S^{ref} = E_S + Z_S I_S = E_S + Z_S(I_S^{in} + I_S^{ref}) = E_S + Z_S\left(\frac{V_S^{in} - V_S^{ref}}{Z_o}\right) \tag{9.2.1}$$

where superscripts "in" and "ref" on V_S and I_S are used to indicate the corresponding incident and reflected quantities. This equation can be rearranged as follows:

$$\left(1 + \frac{Z_S}{Z_o}\right)V_S^{ref} = E_S - \left(1 - \frac{Z_S}{Z_o}\right)V_S^{in}$$

or,

$$V_S^{ref} = \frac{Z_o}{Z_o + Z_S}E_S - \frac{Z_o - Z_S}{Z_o + Z_S}V_S^{in}$$

Dividing it by $\sqrt{2Z_o}$, we find that

$$\frac{V_S^{ref}}{\sqrt{2Z_o}} = \frac{Z_o}{Z_o + Z_S}\frac{E_S}{\sqrt{2Z_o}} - \frac{Z_o - Z_S}{Z_o + Z_S}\frac{V_S^{in}}{\sqrt{2Z_o}}$$

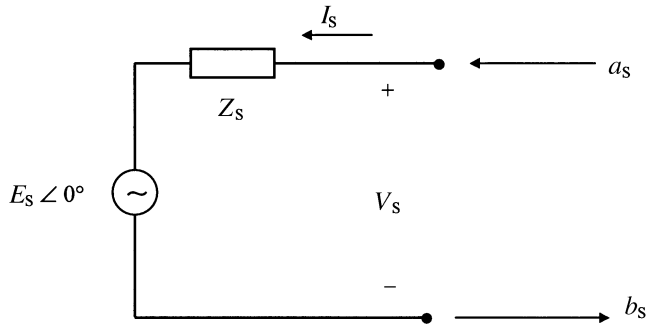

Figure 9.16 Incident and reflected waves at the output port of a voltage source.

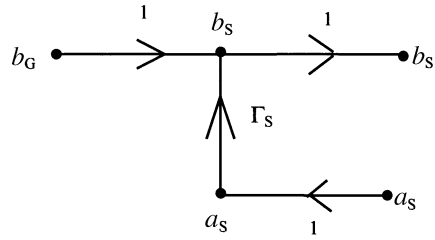

Figure 9.17 Signal-flow graph representation for a voltage source.

Using (7.6.15) and (7.6.16), this can be written as follows:

$$b_S = b_G + \Gamma_S a_S \tag{9.2.2}$$

where,

$$b_S = \frac{V_S^{ref}}{\sqrt{2Z_o}} \tag{9.2.3}$$

$$b_G = \frac{\sqrt{Z_o}E_S}{\sqrt{2}(Z_o + Z_S)} \tag{9.2.4}$$

$$a_S = \frac{V_S^{in}}{\sqrt{2Z_o}} \tag{9.2.5}$$

and,

$$\Gamma_S = \frac{Z_S - Z_o}{Z_S + Z_o} \tag{9.2.5}$$

From (9.2.2), the signal flow graph for a voltage source can be drawn as shown in Figure 9.17.

9.3 SIGNAL-FLOW GRAPH REPRESENTATION OF A PASSIVE SINGLE-PORT DEVICE

Consider load impedance Z_L as shown in Figure 9.18. It is a single-port device with port voltage and current V_L and I_L, respectively. The incident and reflected waves at the port are assumed to be a_L and b_L, respectively. Further, characteristic impedance at the port is Z_o.

Following the usual circuit analysis rules, we find that

$$V_L = V_L^{in} + V_L^{ref} = Z_L I_L = Z_L(I_L^{in} + I_L^{ref}) = Z_L\left(\frac{V_L^{in} - V_L^{ref}}{Z_o}\right)$$

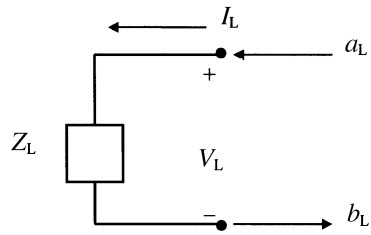

Figure 9.18 A passive one-port circuit.

or,

$$\left(1+\frac{Z_L}{Z_o}\right)V_L^{ref}=\left(\frac{Z_L}{Z_o}-1\right)V_L^{in} \tag{9.3.1}$$

or,

$$V_L^{ref}=\left(\frac{Z_L-Z_o}{Z_L+Z_o}\right)V_L^{in}=\Gamma_L V_L^{in} \tag{9.3.2}$$

After dividing it by $\sqrt{2Z_o}$, we then use (7.6.15) and (7.6.16) to find that

$$b_L=\Gamma_L a_L \tag{9.3.3}$$

where,

$$b_L=\frac{V_L^{ref}}{\sqrt{2Z_o}} \tag{9.3.4}$$

$$a_L=\frac{V_L^{in}}{\sqrt{2Z_o}} \tag{9.3.5}$$

and,

$$\Gamma_L=\frac{Z_L-Z_o}{Z_L+Z_o} \tag{9.3.6}$$

A signal-flow graph can be drawn on the basis of (9.3.3), as shown in Figure 9.19.

Example 9.6: Impedance Z_L terminates port-2 (output) of a two-port network as shown below in Figure 9.20. Draw the signal-flow graph and determine the reflection coefficient at its input port using Mason's rule.

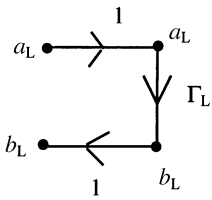

Figure 9.19 Signal-flow graph of a one-port passive device.

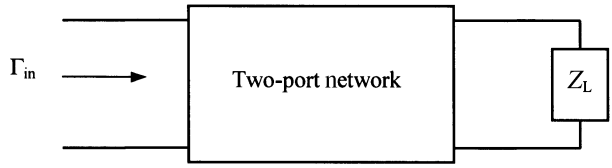

Figure 9.20 Two-port network with termination.

As shown in Figure 9.21, combining the signal-flow graphs of a passive load and that of the two-port network obtained in Example 9.3, we can get the representation for this network.

Its input reflection coefficient is given by the ratio of b_1 to a_1. For Mason's rule, we find that there are two forward paths, $a_1 \rightarrow b_1$ and $a_1 \rightarrow b_2 \rightarrow a_L \rightarrow b_L \rightarrow a_2 \rightarrow b_1$. There is one loop, $b_2 \rightarrow a_L \rightarrow b_L \rightarrow a_2 \rightarrow b_2$, which does not touch the former path. The corresponding path and loop gains are

$$P_1 = S_{11}$$
$$P_2 = S_{21} \cdot 1 \cdot \Gamma_L \cdot 1 \cdot S_{12} = \Gamma_L S_{21} S_{12}$$

and,

$$L_1 = 1 \cdot \Gamma_L \cdot 1 \cdot S_{22} = \Gamma_L S_{22}$$

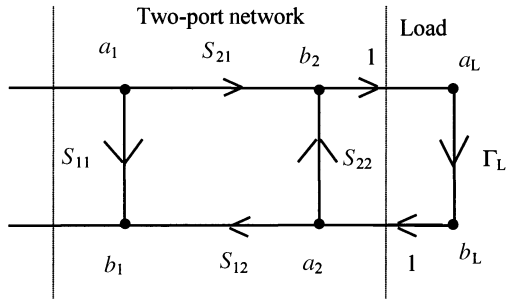

Figure 9.21 Signal-flow graph representation of the network shown in Figure 9.20.

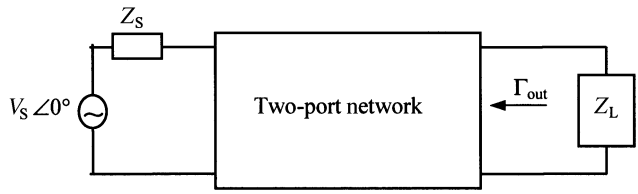

Figure 9.22 Two-port network with the source and the termination.

Hence,

$$\Gamma_{in} = \frac{b_1}{a_1} = \frac{P_1(1 - L_1) + P_2}{1 - L_1} = \frac{S_{11}(1 - \Gamma_L S_{22}) + \Gamma_L S_{21} S_{12}}{1 - \Gamma_L S_{22}} = S_{11} + \frac{\Gamma_L S_{21} S_{12}}{1 - \Gamma_L S_{22}}$$

Example 9.7: A voltage source is connected at the input port of a two-port network while load impedance Z_L terminates its output, as shown in Figure 9.22. Draw its signal-flow graph and find the output reflection coefficient Γ_{out}.

A signal-flow graph of this circuit can be drawn by combining the results of the previous example with those of a voltage source representation obtained in section 9.2. This is illustrated below in Figure 9.23.

The output reflection coefficient is defined as the ratio of b_2 to a_2 with load disconnected and the source impedance Z_S terminates port-1 (the input). Hence, there are two forward paths from a_2 to b_2, $a_2 \rightarrow b_2$ and $a_2 \rightarrow b_1 \rightarrow a_S \rightarrow b_S \rightarrow a_1 \rightarrow b_2$. There is only one loop (because the load is disconnected), $b_1 \rightarrow a_S \rightarrow b_S \rightarrow a_1 \rightarrow b_1$. The path and loop gains are found as follows:

$$P_1 = S_{22}$$
$$P_2 = S_{12} \cdot 1 \cdot \Gamma_S \cdot 1 \cdot S_{21} = \Gamma_S S_{12} S_{21}$$

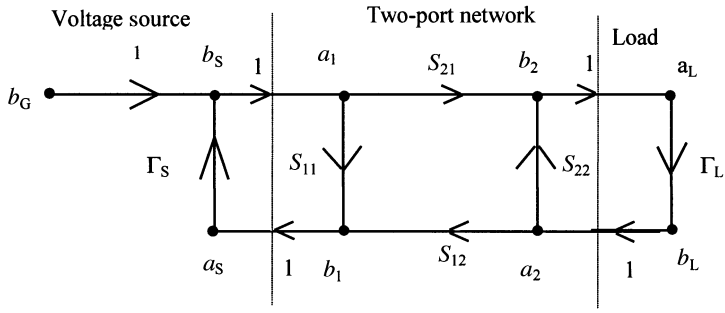

Figure 9.23 Signal-flow graph representation of the network shown in Figure 9.22.

and,

$$L_1 = 1 \cdot \Gamma_S \cdot 1 \cdot S_{11} = \Gamma_S S_{11}$$

Therefore, from Mason's rule, we have

$$\Gamma_{out} = \frac{b_2}{a_2} = \frac{P_1(1 - L_1) + P_2}{1 - L_1} = \frac{S_{22}(1 - S_{11}\Gamma_S) + S_{21}S_{12}\Gamma_S}{1 - S_{11}\Gamma_S} = S_{22} + \frac{S_{21}S_{12}\Gamma_S}{1 - S_{11}\Gamma_S}$$

Example 9.8: The signal-flow graph shown in Figure 9.24 represents a voltage source that is terminated by a passive load. Analyze the power transfer characteristics of this circuit and establish the conditions for maximum power transfer.

Using the defining equations of a_i and b_i, we can develop the following relations.

$$\text{Power output of the source} = |b_S|^2$$
$$\text{Power reflected back into the source} = |a_S|^2$$

Hence, power delivered by the source, P_d, is

$$P_d = |b_S|^2 - |a_S|^2$$

Similarly, we can write the following relations for power at the load:

$$\text{Power incident on the load} = |a_L|^2$$
$$\text{Power reflected from the load} = |b_L|^2 = |\Gamma_L|^2|a_L|^2$$

where Γ_L is the load reflection coefficient.

Hence, power absorbed by the load, P_L, is given by

$$P_L = |a_L|^2 - |b_L|^2 = |a_L|^2(1 - |\Gamma_L|^2) = |b_S|^2(1 - |\Gamma_L|^2)$$

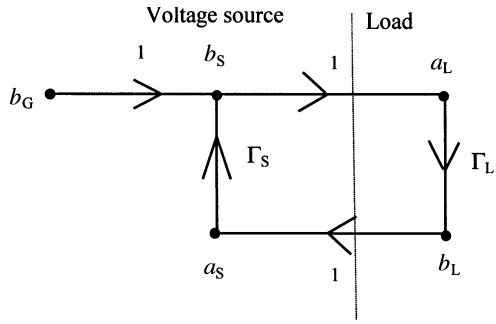

Figure 9.24 Signal-flow graph for Example 9.8.

Since

$$b_S = b_G + \Gamma_S a_S = b_G + \Gamma_S b_L = b_G + \Gamma_S \Gamma_L a_L = b_G + \Gamma_S \Gamma_L b_S$$

we find that

$$b_S = \frac{b_G}{1 - \Gamma_S \Gamma_L}$$

and,

$$a_S = \frac{1}{\Gamma_S}(b_S - b_G) = \frac{1}{\Gamma_S}\left(\frac{b_G}{1 - \Gamma_S \Gamma_L} - b_G\right) = \frac{\Gamma_L b_G}{1 - \Gamma_S \Gamma_L}$$

Hence,

$$\begin{aligned} P_d &= |b_S|^2 - |a_S|^2 = \left|\frac{b_G}{1 - \Gamma_S \Gamma_L}\right|^2 - \left|\frac{\Gamma_L b_G}{1 - \Gamma_S \Gamma_L}\right|^2 = \left|\frac{b_G}{1 - \Gamma_S \Gamma_L}\right|^2 (1 - |\Gamma_L|^2) \\ &= |b_S|^2 (1 - |\Gamma_L|^2) = P_L \end{aligned}$$

This simply says that the power delivered by the source is equal to the power absorbed by the load. We can use this equation to establish the load condition under which the source delivers maximum power. For that, we consider ways to maximize the following.

$$P_L = \left|\frac{b_G}{1 - \Gamma_S \Gamma_L}\right|^2 (1 - |\Gamma_L|^2)$$

For P_L to be a maximum, its denominator $1 - \Gamma_S \Gamma_L$ is minimized. Let us analyze this term more carefully using the graphical method. It says that there is a phasor $\Gamma_S \Gamma_L$ at a distance of unity from the origin that rotates with a change in Γ_L (Γ_S is assumed constant), as illustrated in Figure 9.25. Hence, the denominator has an

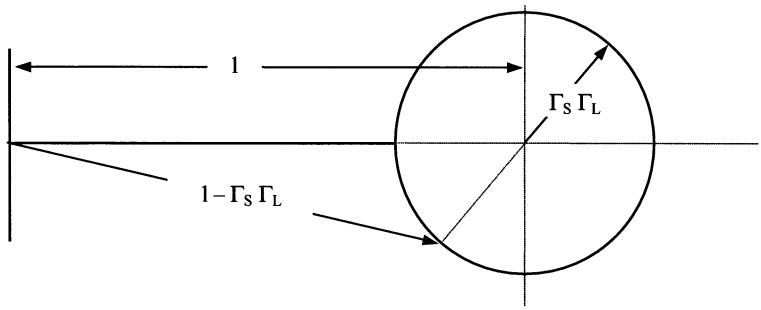

Figure 9.25 Graphical representation of $(1 - \Gamma_S \Gamma_L)$.

extreme value whenever $\Gamma_S\Gamma_L$ is a pure real number. If this number is positive real then the denominator is minimum. On the other hand, the denominator is maximized when $\Gamma_S\Gamma_L$ is a negative real number.

In order for $\Gamma_S\Gamma_L$ to be a positive real number, the load reflection coefficient Γ_L must be complex conjugate of the source reflection coefficient Γ_S. In other words,

$$\Gamma_L = \Gamma_S \Rightarrow \frac{Z_L - Z_o}{Z_L + Z_o} = \left(\frac{Z_S - Z_o}{Z_S + Z_o}\right)^*$$

For a real Z_o, it reduces to

$$Z_L = Z_S$$

The value of this maximum power is

$$P_L = \frac{|b_G|^2}{(1 - |\Gamma_S|^2)} = P_{avs}$$

where P_{avs} is maximum power available from the source. It is a well-known maximum power transfer theorem of electrical circuit theory.

Example 9.9: Draw the signal-flow graph of the three-port network shown in Figure 9.26. Find the transfer characteristics b_3/b_S using the graph.

For a three-port network, the scattering equations are given as follows:

$$\begin{aligned} b_1 &= S_{11}a_1 + S_{12}a_2 + S_{13}a_3 \\ b_2 &= S_{21}a_1 + S_{22}a_2 + S_{23}a_3 \\ b_3 &= S_{31}a_1 + S_{32}a_2 + S_{33}a_3 \end{aligned}$$

For the voltage source connected at port-1, we have

$$b_S = b_G + \Gamma_S a_S$$

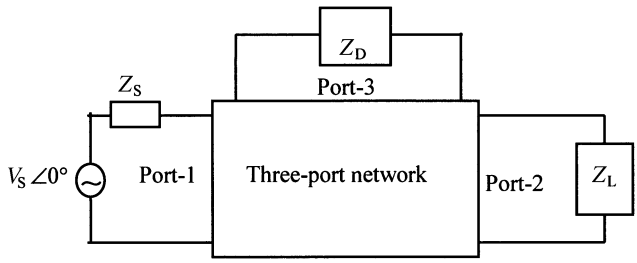

Figure 9.26 Three-port network of Example 9.9.

Since the wave coming out from the source is incident on port-1, b_S is equal to a_1. Therefore, we can write

$$a_1 = b_G + \Gamma_S b_1$$

For the load Z_L connected at port-2,

$$b_L = \Gamma_L a_L$$

Again, the wave emerging from port-2 of the network is incident on the load. Similarly, the wave reflected back from the load is incident on port-2 of the network. Hence,

$$b_2 = a_L$$

and,

$$b_L = a_2$$

Therefore, the above relation at the load Z_L can be modified as follows:

$$a_2 = \Gamma_L b_2$$

Following a similar procedure for the load Z_D connected at port-3, we find that

$$b_D = \Gamma_D a_D \Rightarrow a_3 = \Gamma_D b_3$$

Using these equations, a signal-flow graph can be drawn for this circuit as shown in Figure 9.27.

For b_3/b_S, there are two forward paths and eight loops in this flow graph. Path gains P_i and loop gains L_i are found as follows:

$$P_1 = S_{31}$$
$$P_2 = S_{21}S_{32}\Gamma_L$$
$$L_1 = S_{11}\Gamma_S$$
$$L_2 = S_{22}\Gamma_L$$

$$L_3 = S_{33}\Gamma_D$$
$$L_4 = S_{21}S_{12}\Gamma_L\Gamma_S$$
$$L_5 = S_{31}S_{23}S_{12}\Gamma_D\Gamma_L\Gamma_S$$
$$L_6 = S_{13}S_{21}S_{32}\Gamma_D\Gamma_L\Gamma_S$$
$$L_7 = S_{23}S_{32}\Gamma_D\Gamma_L$$

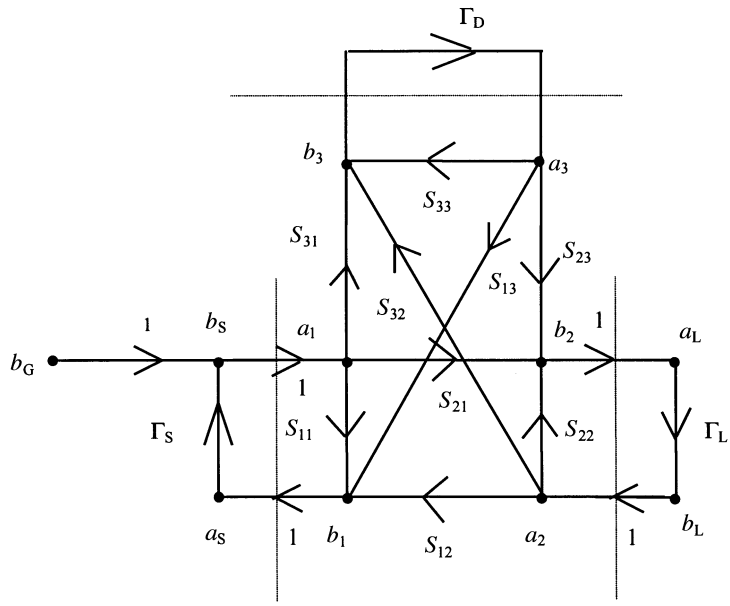

Figure 9.27 Signal-flow graph of the network shown in Figure 9.26.

and,

$$L_8 = S_{13}S_{31}\Gamma_D\Gamma_S$$

Therefore, various terms of Mason's rule can be evaluated as follows:

$$\Delta_1 = 1 - S_{22}\Gamma_L$$
$$\Delta_2 = 1$$
$$\sum L(1) = L_1 + L_2 + L_3 + L_4 + L_5 + L_6 + L_7 + L_8$$
$$\sum L(2) = L_1L_2 + L_1L_3 + L_2L_3 + L_3L_4 + L_1L_7 + L_2L_8$$
$$\sum L(3) = L_1L_2L_3$$

Using Mason's rule we can find

$$\frac{b_3}{b_S} = \frac{P_1\Delta_1 + P_2\Delta_2}{1 - \sum L(1) + \sum L(2) - \sum L(3)}$$

Note that this signal-flow graph is too complex, and therefore, one can easily miss a few loops. In cases like this, it is prudent to simplify the signal-flow graph using the five rules mentioned earlier.

9.4 POWER GAIN EQUATIONS

We have seen in the preceding section that maximum power is transferred when load reflection coefficient Γ_L is conjugate of the source reflection coefficient Γ_S. It can be generalized for any port of the network. In the case of an amplifier, maximum power will be applied to its input port if its input reflection coefficient Γ_{in} is complex conjugate of the source reflection coefficient Γ_S. If this is not the case then input will be less than the maximum power available from source. Similarly, maximum amplified power will be transferred to the load only if load reflection coefficient Γ_L is complex conjugate of output reflection coefficient Γ_{out}. Part of the power available at the output of the amplifier will be reflected back if there is a mismatch. Therefore, the power gain of an amplifier can be defined in at least three different ways as follows:

$$\text{Transducer power gain, } G_T = \frac{P_L}{P_{avs}} = \frac{\text{Power delivered to the load}}{\text{Power available from the source}}$$

$$\text{Operating power gain, } G_P = \frac{P_L}{P_{in}} = \frac{\text{Power delivered to the load}}{\text{Power input to the network}}$$

$$\text{Available power gain, } G_A = \frac{P_{AVN}}{P_{avs}} = \frac{\text{Power available from the network}}{\text{Power available from the source}}$$

where

P_{avs} = Power available from the source
P_{in} = Power input to the network
P_{AVN} = Power available from the network
P_L = Power delivered to the load

Therefore, the transducer power gain will be equal to that of operating power gain if the input reflection coefficient Γ_{in} is complex conjugate of the source reflection coefficient Γ_S. That is,

$$P_{avs} = P_{in}|_{\Gamma_{in}=\Gamma_S^*}$$

Similarly, the available power gain will be equal to the transducer power gain if the following condition holds at the output port

$$P_{AVN} = P_L|_{\Gamma_L=\Gamma_{out}^*}$$

In this section, we formulate these power gain relations in terms of scattering parameters and reflection coefficients of the circuit. In order to facilitate the formulation, we reproduce in Figure 9.28 the signal-flow graph obtained earlier in Example 9.7.

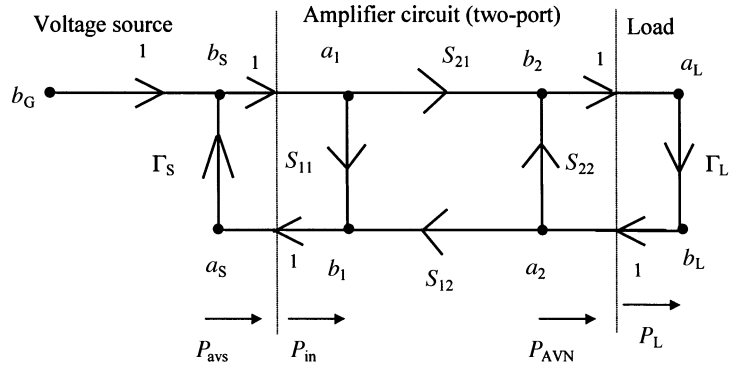

Figure 9.28 Signal-flow graph for an amplifier circuit with voltage source and terminating load.

Transducer Power Gain

In order to develop the relation for transducer power gain, we first determine the power delivered to load P_L and the power available from the source P_{avs}, as follows:

$$P_L = |a_L|^2 - |b_L|^2 = |a_L|^2(1 - |\Gamma_L|^2) = |b_2|^2(1 - |\Gamma_L|^2) \tag{9.4.1}$$

We have already derived an expression for P_{avs} in Example 9.7. That is rewritten here

$$P_{avs} = |b_S|^2 - |a_S|^2 = \frac{|b_G|^2}{1 - |\Gamma_S|^2} \tag{9.4.2}$$

Therefore, the transducer power gain is

$$G_T = \frac{|b_2|^2}{|b_G|^2}(1 - |\Gamma_L|^2)(1 - |\Gamma_S|^2) \tag{9.4.3}$$

We now need to find an expression for b_2/b_G. Mason's rule can be used to formulate it. There is only one forward path in this case. However, there are three loops. Path gain P_1 and the loop gains L_i are

$$P_1 = S_{21}$$
$$L_1 = S_{11}\Gamma_S$$
$$L_2 = S_{22}\Gamma_L$$

and,

$$L_3 = S_{12}S_{21}\Gamma_S\Gamma_L$$

Therefore,

$$\frac{b_2}{b_G} = \frac{P_1}{1-(L_1+L_2+L_3)+L_1L_2}$$
$$= \frac{S_{21}}{1-(S_{11}\Gamma_S + S_{22}\Gamma_L + S_{21}\Gamma_L S_{12}\Gamma_S) + S_{11}\Gamma_S S_{22}\Gamma_L} \quad (9.4.4)$$

Substituting (9.4.4) into (9.4.3), we get

$$G_T = \frac{|S_{21}|^2(1-|\Gamma_L|^2)(1-|\Gamma_S|^2)}{|1-(S_{11}\Gamma_S + S_{22}\Gamma_L + S_{21}\Gamma_L S_{12}\Gamma_S) + S_{11}\Gamma_S S_{22}\Gamma_L|^2} \quad (9.4.5)$$

It can be simplified as follows:

$$G_T = \frac{|S_{21}|^2(1-|\Gamma_L|^2)(1-|\Gamma_S|^2)}{|(1-S_{11}\Gamma_S)(1-S_{22}\Gamma_L) - S_{21}S_{12}\Gamma_L\Gamma_S|^2}$$

or,

$$G_T = \frac{|S_{21}|^2(1-|\Gamma_L|^2)(1-|\Gamma_S|^2)}{\left|(1-S_{22}\Gamma_L)\left(1-S_{11}\Gamma_S - \frac{S_{21}S_{12}\Gamma_L\Gamma_S}{1-S_{22}\Gamma_L}\right)\right|^2}$$

or,

$$G_T = \frac{|S_{21}|^2(1-|\Gamma_L|^2)(1-|\Gamma_S|^2)}{|(1-S_{22}\Gamma_L)(1-\Gamma_{in}\Gamma_S)|^2} = \frac{1-|\Gamma_S|^2}{|1-\Gamma_{in}\Gamma_S|^2} \cdot |S_{21}|^2 \cdot \frac{1-|\Gamma_L|^2}{|1-S_{22}\Gamma_L|^2} \quad (9.4.6)$$

where,

$$\Gamma_{in} = S_{11} + \frac{S_{21}S_{12}\Gamma_L}{1-S_{22}\Gamma_L} \quad (9.4.7)$$

This is the input reflection coefficient formulated earlier in Example 9.6.

Alternatively, (9.4.5) can be written as follows:

$$G_T = \frac{|S_{21}|^2(1-|\Gamma_L|^2)(1-|\Gamma_S|^2)}{|(1-S_{11}\Gamma_S)(1-\Gamma_{out}\Gamma_L)|^2} = \frac{1-|\Gamma_S|^2}{|1-S_{11}\Gamma_S|^2} \cdot |S_{21}|^2 \cdot \frac{1-|\Gamma_L|^2}{|1-\Gamma_{out}\Gamma_L|^2} \quad (9.4.8)$$

where,

$$\Gamma_{out} = S_{22} + \frac{S_{21}S_{12}\Gamma_S}{1-S_{11}\Gamma_S} \quad (9.4.9)$$

This is the output reflection coefficient formulated in Example 9.7.

Special Case: Consider a special case when the two-port network is unilateral. This means that there is an output signal at port-2 when a source is connected at port-1. However, a source (cause) connected at port-2 does not show its response (effect) at port-1. In terms of scattering parameters of the two-port, S_{12} is equal to zero in this

case, and therefore, the input and output reflection coefficients in (9.4.7) and (9.4.9) simplify as follows:

$$\Gamma_{\text{in}} = S_{11}$$

and,

$$\Gamma_{\text{out}} = S_{22}$$

The transducer power gain G_{T} as given by (9.4.6) or (9.4.8) simplifies to

$$G_{\text{T}}|_{S_{12}=0} = G_{\text{TU}} = \frac{1-|\Gamma_{\text{S}}|^2}{|1-S_{11}\Gamma_{\text{S}}|^2} \cdot |S_{21}|^2 \cdot \frac{1-|\Gamma_{\text{L}}|^2}{|1-S_{22}\Gamma_{\text{L}}|^2} = G_{\text{S}} \cdot G_{\text{o}} \cdot G_{\text{L}} \quad (9.4.10)$$

where G_{TU} may be called the *unilateral transducer power gain*, while

$$G_{\text{S}} = \frac{1-|\Gamma_{\text{S}}|^2}{|1-S_{11}\Gamma_{\text{S}}|^2} \quad (9.4.11)$$

$$G_{\text{o}} = |S_{21}|^2 \quad (9.4.12)$$

and,

$$G_{\text{L}} = \frac{1-|\Gamma_{\text{L}}|^2}{|1-S_{22}\Gamma_{\text{L}}|^2} \quad (9.4.13)$$

Equation (9.4.10) indicates that maximum G_{TU} is obtained when the input and output ports are conjugate matched. Hence,

$$G_{\text{TU}_{\text{max}}} = G_{\text{S}_{\text{max}}} \cdot G_{\text{o}} \cdot G_{\text{L}_{\text{max}}} \quad (9.4.14)$$

where,

$$G_{\text{S}_{\text{max}}} = G_{\text{S}|_{\Gamma_{\text{S}}=S_{11}^*}} \quad (9.4.15)$$

and,

$$G_{\text{L}_{\text{max}}} = G_{\text{L}|_{\Gamma_{\text{L}}=S_{22}^*}} \quad (9.4.16)$$

Operating Power Gain

In order to find the operating power gain, we require the power delivered to the load and power input to the circuit. We have already evaluated the power delivered to the load earlier in (9.4.1). Power input to the circuit is found as follows:

$$P_{\text{in}} = |a_1|^2 - |b_1|^2 = |a_1|^2(1-|\Gamma_{\text{in}}|^2)$$

Hence,

$$G_P = \frac{P_L}{P_{in}} = \frac{|b_2|^2(1-|\Gamma_L|^2)}{|a_1|^2(1-|\Gamma_{in}|^2)} \tag{9.4.17}$$

Now we evaluate b_2/a_1 using Mason's rule. With the source disconnected, we find that there is only one forward path and one loop with gains S_{21}, and $S_{22}\Gamma_L$, respectively. Hence,

$$\frac{b_2}{a_1} = \frac{S_{21}}{1-S_{22}\Gamma_L} \tag{9.4.18}$$

Substituting (9.4.18) into (9.4.17), we find that

$$G_P = \frac{1}{1-|\Gamma_{in}|^2} \cdot |S_{21}|^2 \cdot \frac{1-|\Gamma_L|^2}{|1-S_{22}\Gamma_L|^2} \tag{9.4.19}$$

Available Power Gain

Expressions for maximum powers available from the network and the source are needed to determine the available power gain. Maximum power available from the network P_{AVN} is delivered to the load if the load reflection coefficient is complex conjugate of the output. Using (9.4.1), we find that

$$P_{AVN} = P_{L|_{\Gamma_L=\Gamma_{out}^*}} = |b_2|^2(1-|\Gamma_L|^2) = |b_2|^2(1-|\Gamma_{out}|^2) \tag{9.4.20}$$

Power available from the source is given by (9.4.2). Hence,

$$G_A = \frac{P_{AVN}}{P_{avs}} = \frac{|b_2|^2}{|b_G|^2}(1-|\Gamma_{out}|^2)(1-|\Gamma_S|^2) \tag{9.4.21}$$

Next, using Mason's rule in the signal-flow graph of Figure 9.28, we find that

$$\begin{aligned}\frac{b_2}{b_G} &= \frac{S_{21}}{1-(S_{11}\Gamma_S + S_{22}\Gamma_L + S_{21}\Gamma_L S_{12}\Gamma_S) + S_{11}\Gamma_S S_{22}\Gamma_L} \\ &= \frac{S_{21}}{(1-S_{11}\Gamma_S)(1-\Gamma_{out}\Gamma_L)}\end{aligned}$$

and,

$$\left.\frac{b_2}{b_G}\right|_{\Gamma_L=\Gamma_{out}^*} = \frac{S_{21}}{(1-S_{11}\Gamma_S)(1-|\Gamma_{out}|^2)} \tag{9.4.22}$$

Now, substituting (9.4.22) into (9.4.21), we get

$$G_A = \frac{1 - |\Gamma_S|^2}{|1 - S_{11}\Gamma_S|^2} \cdot |S_{21}|^2 \cdot \frac{1}{1 - |\Gamma_{out}|^2} \tag{9.4.23}$$

Example 9.10: Scattering parameters of a microwave amplifier are found at 800 MHz as follows ($Z_o = 50\,\Omega$):

$$S_{11} = 0.45\angle 150^\circ, \quad S_{12} = 0.01\angle -10^\circ, \quad S_{21} = 2.05\angle 10^\circ, \quad S_{22} = 0.4\angle -150^\circ$$

Source and load impedances are $20\,\Omega$ and $30\,\Omega$, respectively. Determine transducer power gain, operating power gain, and available power gain.

First of all, we determine the source reflection coefficient Γ_S and the load reflection coefficient Γ_L as follows:

$$\Gamma_S = \frac{Z_S - Z_o}{Z_S + Z_o} = \frac{20 - 50}{20 + 50} = -\frac{30}{70} = -0.429$$

and,

$$\Gamma_L = \frac{Z_L - Z_o}{Z_L + Z_o} = \frac{30 - 50}{30 + 50} = -\frac{20}{80} = -0.25$$

Now, the input reflection coefficient Γ_{in} and the output reflection coefficient Γ_{out} can be calculated from (9.4.7) and (9.4.9), respectively:

$$\Gamma_{in} = S_{11} + \frac{S_{21}S_{12}\Gamma_L}{1 - S_{22}\Gamma_L} = 0.45\angle 150^\circ + \frac{(0.01\angle -10^\circ)(2.05\angle 10^\circ)(-0.25)}{1 - (0.4\angle -150^\circ)(-0.25)}$$

or,

$$\Gamma_{in} = -0.3953 + j0.2253 = 0.455\angle 150.32^\circ$$

and,

$$\Gamma_{out} = S_{22} + \frac{S_{21}S_{12}\Gamma_S}{1 - S_{11}\Gamma_S} = 0.4\angle -150^\circ + \frac{(0.01\angle -10^\circ)(2.05\angle 10^\circ)(-0.429)}{1 - (0.45\angle 150^\circ)(-0.429)}$$

or,

$$\Gamma_{out} = -0.3568 - j0.1988 = 0.4084\angle -150.87^\circ$$

The transducer power gain G_T can be calculated now from (9.4.6) or (9.4.8), as follows:

$$G_T = \frac{|S_{21}|^2(1-|\Gamma_L|^2)(1-|\Gamma_S|^2)}{|(1-S_{22}\Gamma_L)(1-\Gamma_{in}\Gamma_S)|^2} = \frac{|S_{21}|^2(1-|\Gamma_L|^2)(1-|\Gamma_S|^2)}{|(1-S_{11}\Gamma_S)(1-\Gamma_{out}\Gamma_L)|^2}$$

Hence,

$$G_T = \frac{1-(0.429)^2}{|1-(0.45\angle 150^\circ)(-0.429)|^2}(2.05)^2\frac{1-(0.25^2)}{|1-(0.4084\angle -150.87^\circ)(-0.25)|^2}$$
$$= 5.4872$$

Similarly, from (9.4.19),

$$G_P = \frac{1}{1-|\Gamma_{in}|^2}\cdot|S_{21}|^2\cdot\frac{1-|\Gamma_L|^2}{|1-S_{22}\Gamma_L|^2}$$

Therefore,

$$G_P = \frac{1}{1-(0.455^2)}(2.05)^2\frac{1-(0.25^2)}{|1-(0.4\angle -150^\circ)(-0.25)|^2} = 5.9374$$

The available power gain is calculated from (9.4.23) as follows.

$$G_A = \frac{1-|\Gamma_S|^2}{|1-S_{11}\Gamma_S|^2}\cdot S_{21}|^2\cdot\frac{1}{1-|\Gamma_{out}|^2}$$

Hence,

$$G_A = \frac{1-(0.429)^2}{|1-(0.45\angle 150^\circ)(-0.429)|^2}(2.05^2)\frac{1}{1-(0.4084)^2} = 5.8552$$

The three power gains can be expressed in dB as follows:

$$G_T\ (\text{dB}) = 10\log(5.4872) \approx 7.4\ \text{dB}$$
$$G_P\ (\text{dB}) = 10\log(5.9374) \approx 7.7\ \text{dB}$$

and,

$$G_A\ (\text{dB}) = 10\log(5.8552) \approx 7.7\ \text{dB}$$

Example 9.11: Scattering parameters of a microwave amplifier are found at 2 GHz as follows ($Z_o = 50\,\Omega$):

$$S_{11} = 0.97\angle -43^\circ, \quad S_{12} = 0.0, \quad S_{21} = 3.39\angle 140^\circ, \quad S_{22} = 0.63\angle -32^\circ$$

Source and load reflection coefficients are $0.97\angle 43^\circ$ and $0.63\angle 32^\circ$, respectively. Determine transducer power gain, operating power gain, and available power gain.

Since S_{12} is zero, this amplifier is unilateral. Therefore, its input and output reflection coefficients from (9.4.7) and (9.4.9) may be found as follows:

$$\text{Input reflection coefficient } \Gamma_{in} = S_{11} = 0.97\angle -43^\circ$$
$$\text{Output reflection coefficient } \Gamma_{out} = S_{22} = 0.63\angle -32^\circ$$

On comparing the input reflection coefficient with that of the source we find that one is complex conjugate of the other. Hence, the source is matched with the input port, and therefore, power available from the source is equal to the power input. Similarly, we find that the load reflection coefficient is conjugate of the output reflection coefficient. Hence, power delivered to the load will be equal to power available from the network at port-2. As may be verified from (9.4.10), (9.4.19), and (9.4.23), these conditions make all three power gains equal.

From (9.4.10),

$$\begin{aligned} G_{TU} &= \frac{1-|\Gamma_S|^2}{|1-S_{11}\Gamma_S|^2} \cdot |S_{21}|^2 \cdot \frac{1-|\Gamma_L|^2}{|1-S_{22}\Gamma_L|^2} = \frac{1-(0.97)^2}{|1-(0.97)^2|^2} \\ &\quad \cdot (3.39)^2 \cdot \frac{1-(0.63)^2}{|1-(0.63)^2|^2} \\ &= 322.42 \end{aligned}$$

From (9.4.19),

$$\begin{aligned} G_P &= \frac{1}{1-|\Gamma_{in}|^2} \cdot |S_{21}|^2 \cdot \frac{1-|\Gamma_L|^2}{|1-S_{22}\Gamma_L|^2} = \frac{1}{1-(0.97)^2} \cdot (3.39)^2 \cdot \frac{1-(0.63)^2}{|1-(0.63)^2|^2} \\ &= 322.42 \end{aligned}$$

From (9.4.23),

$$\begin{aligned} G_A &= \frac{1-|\Gamma_S|^2}{|1-S_{11}\Gamma_S|} \cdot |S_{21}|^2 \cdot \frac{1}{1-|\Gamma_{out}|^2} = \frac{1-(0.97)^2}{|1-(0.97)^2|^2} \cdot (3.39)^2 \cdot \frac{1}{1-(0.63)^2} \\ &= 322.42 \end{aligned}$$

SUGGESTED READING

R. E. Collin, *Foundations for Microwave Engineering*. New York: McGraw Hill, 1992.

W. A. Davis, *Microwave Semiconductor Circuit Design*. New York: Van Nostrand Reinhold, 1984.

V. F. Fusco, *Microwave Circuits*. Englewood Cliffs, NJ: Prentice Hall, 1987.

G. Gonzalez, *Microwave Transistor Amplifiers*. Englewood Cliffs, NJ: Prentice Hall, 1997.

D. M. Pozar, *Microwave Engineering*. New York: Wiley, 1998.

E. A. Wolff and R. Kaul, *Microwave Engineering and Systems Applications*. New York: Wiley, 1988.

PROBLEMS

1. Use Mason's rule to find $Y(S)/R(S)$ for the following signal-flow graph.

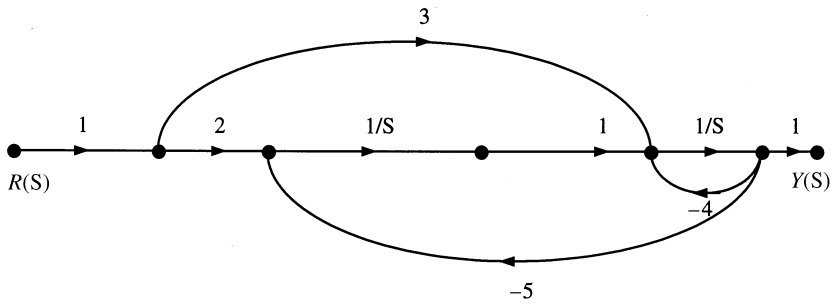

2. Use Mason's gain rule to find $\frac{Y_5(S)}{Y_1(S)}$ and $\frac{Y_2(S)}{Y_1(S)}$ for the following system:

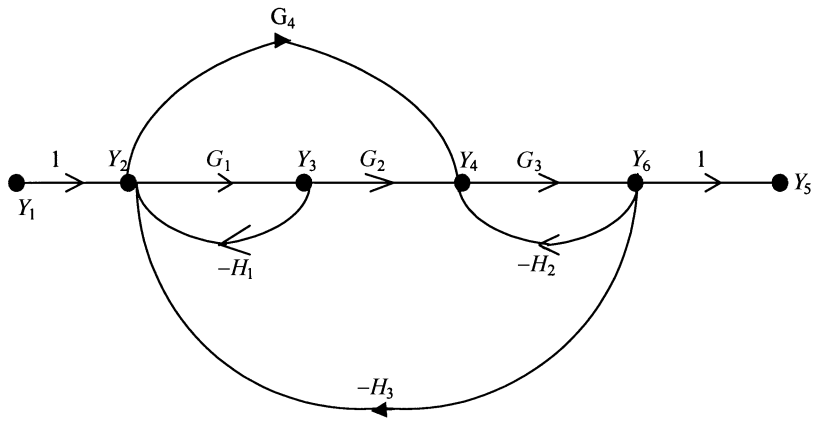

3. Use Mason's gain rule to find $\dfrac{Y_2(S)}{R_3(S)}$ for the following system:

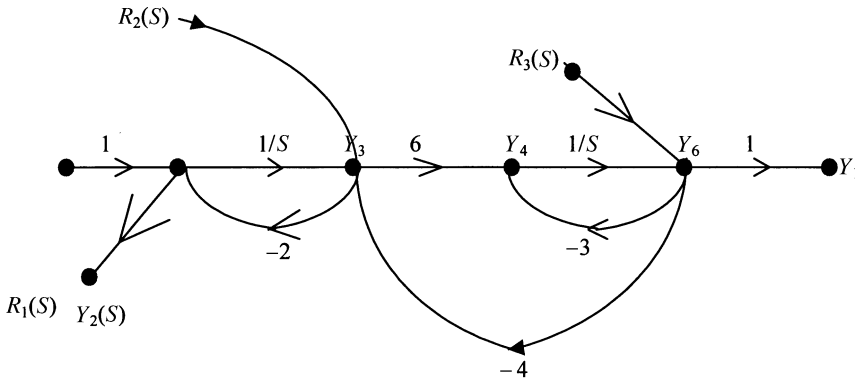

4. Use Mason's gain rule to find $Y(S)/R(S)$ for the following signal-flow graph.

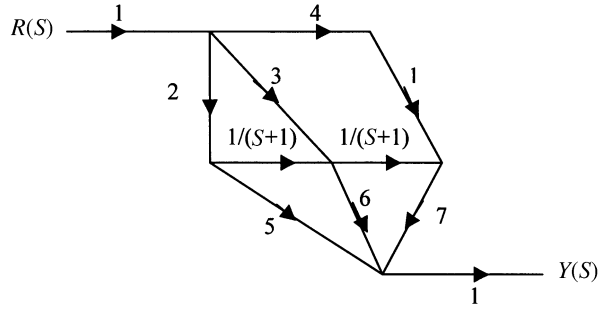

5. Draw the signal-flow graph for the following circuit. Use Mason's gain rule to determine the power ratios P_2/P_1 and P_3/P_1.

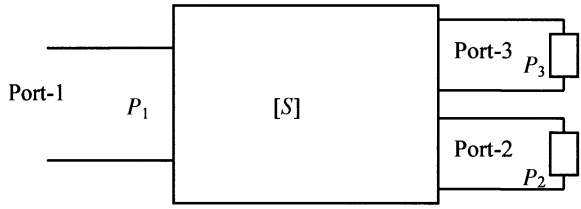

$$[S] = \begin{bmatrix} 0 & S_{12} & 0 \\ S_{21} & 0 & S_{23} \\ 0 & S_{32} & 0 \end{bmatrix}$$

Γ_{in} = reflection coefficient at port-1; Γ_2 and Γ_3 = reflection coefficients at ports 2 and 3, respectively.

6. A voltage source has an internal impedance of 100 Ω, and an EMF of 3 V. Using $Z_o = 50\,\Omega$, find the reflection coefficient and scattering variables a and b for the source.

7. A 10-mV voltage source has an internal impedance of $100 + j50\,\Omega$. Assuming the characteristic impedance Z_o is 50 Ω, find the reflection coefficient and scattering variables a and b for the source. Draw its signal-flow graph.

8. A voltage source of $1\angle 0^\circ$ V has an internal resistance of 80 Ω. It is connected to a load of $30 + j40\,\Omega$. Assuming the characteristic impedance is 50 Ω, find the scattering variables and draw its signal-flow graph.

9. The scattering parameters of a two-port network are given as follows:

$$S_{11} = 0.26 - j0.16, \quad S_{12} = S_{21} = 0.42, \quad \text{and} \quad S_{22} = 0.36 - j0.57$$

(a) Determine the input reflection coefficient and transducer power loss for $Z_S = Z_L = Z_o$.

(b) Do the same for $Z_S = Z_o$ and $Z_L = 3Z_o$.

10. Two two-port networks are connected in cascade. The scattering parameters of the first two-port network are

$$S_{11} = 0.28, \quad S_{12} = S_{21} = 0.56, \quad S_{22} = 0.28 - j0.56$$

For the second network, $S_{11} = S_{22} = -j0.54$ and $S_{12} = S_{21} = 0.84$. Determine the overall scattering and transmission parameters.

11. Draw the flow graph representation for the two cascaded circuits of the above problem. Using Mason's rule determine the following:

(a) Input reflection coefficient when the second network is matched terminated

(b) Forward transmission coefficient of the overall network

12. A GaAs MESFET has the following S-parameters measured at 8 GHz with a 50-Ω reference.

$$S_{11} = 0.26\angle -55^\circ, \quad S_{12} = 0.08\angle 80^\circ, \quad S_{21} = 2.14\angle 65^\circ, \quad \text{and } S_{22} = 0.82\angle -30^\circ$$

For $Z_L = 40 + j160\,\Omega$ and $\Gamma_S = 0.31\angle -76.87^\circ$, determine the operating power gain of the circuit.

13. S-parameters of a certain microwave transistor measured at 3 GHz with a 50-Ω reference are

$$S_{11} = 0.406\angle -100^\circ, \quad S_{12} = 0, \quad S_{21} = 5.0\angle 50^\circ, \quad \text{and} \quad S_{22} = 0.9\angle -60^\circ$$

Calculate the maximum unilateral power gain.

14. (a) Find the value of the source impedance that results in maximum power delivered to the load in the circuit shown below. Evaluate the maximum power delivered to the load.

(b) Using the value of Z_s from part (a), find the Thevenin equivalent circuit at the load end and evaluate the power delivered to the load.

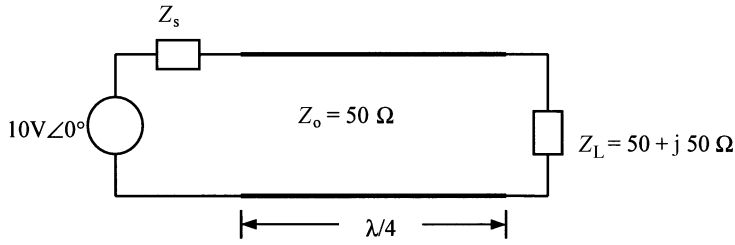

Radio-Frequency and Microwave Communication Circuits: Analysis and Design
Devendra K. Misra

ISBNs: 0-471-41253-8 (Hardback); 0-471-22435-9 (Electronic)

10

TRANSISTOR AMPLIFIER DESIGN

Amplifiers are among the basic building blocks of an electronic system. While vacuum tube devices are still used in high-power microwave circuits, transistors—silicon bipolar junction devices, GaAs MESFET, heterojunction bipolar transistors (HBT), and high-electron mobility transistors (HEMT)—are common in many RF and microwave designs. This chapter begins with the stability considerations for a two-port network and the formulation of relevant conditions in terms of its scattering parameters. Expressions for input and output stability circles are presented next to facilitate the design of amplifier circuits. Design procedures for various small-signal single-stage amplifiers are discussed for unilateral as well as bilateral transistors. Noise figure considerations in amplifier design are discussed in the following section. An overview of broadband amplifiers is included. Small-signal equivalent circuits and biasing mechanisms for various transistors are also summarized in subsequent sections.

10.1 STABILITY CONSIDERATIONS

Consider a two-port network that is terminated by load Z_L as shown in Figure 10.1. A voltage source V_S with internal impedance Z_S is connected at its input port. Reflection coefficients at its input and output ports are Γ_{in} and Γ_{out}, respectively. The source reflection coefficient is Γ_S while the load reflection coefficient is Γ_L. Expressions for input and output reflection coefficients were formulated in the preceding chapter (Examples 9.6 and 9.7).

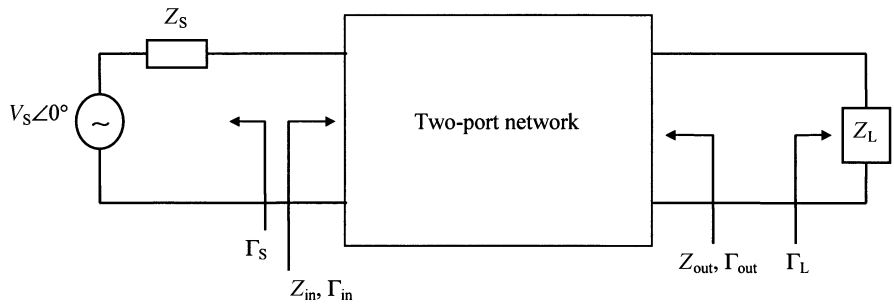

Figure 10.1 A two-port network with voltage source at its input and a load terminating the output port.

For this two-port to be unconditionally stable at a given frequency, the following inequalities must hold:

$$|\Gamma_S| < 1 \tag{10.1.1}$$

$$|\Gamma_L| < 1 \tag{10.1.2}$$

$$|\Gamma_{in}| = \left| S_{11} + \frac{S_{21}S_{12}\Gamma_L}{1 - S_{22}\Gamma_L} \right| < 1 \tag{10.1.3}$$

and,

$$|\Gamma_{out}| = \left| S_{22} + \frac{S_{21}S_{12}\Gamma_S}{1 - S_{11}\Gamma_S} \right| < 1 \tag{10.1.4}$$

Condition (10.1.3) can be rearranged as follows:

$$\left| S_{11} + \frac{S_{22}S_{21}S_{12}\Gamma_L + (S_{12}S_{21} - S_{12}S_{21})}{S_{22}(1 - S_{22}\Gamma_L)} \right| < 1$$

or,

$$\left| \frac{1}{S_{22}} \left(\Delta + \frac{S_{21}S_{12}}{1 - S_{22}\Gamma_L} \right) \right| < 1 \tag{10.1.5}$$

where,

$$\Delta = S_{11}S_{22} - S_{12}S_{21} \tag{10.1.6}$$

Since

$$1 - S_{22}\Gamma_L \xrightarrow[\Gamma_L = 1]{} 1 - S_{22} = 1 - |S_{22}| \exp(j\theta) = A \tag{10.1.7}$$

This traces a circle on the complex plane as θ varies from zero to 2π. It is illustrated in Figure 10.2. Further, $1/1 - |S_{22}| \exp(j\theta)$ represents a circle of radius r with its center located at d, where

$$r = \frac{1}{2}\left(\frac{1}{1 - |S_{22}|} - \frac{1}{1 + |S_{22}|}\right) = \frac{|S_{22}|}{1 - |S_{22}|^2} \tag{10.1.8}$$

and,

$$d = \frac{1}{2}\left(\frac{1}{1 + |S_{22}|} + \frac{1}{1 - |S_{22}|}\right) = \frac{1}{1 - |S_{22}|^2} \tag{10.1.9}$$

Hence, for $|\Gamma_L| \leq 1$ and $\angle \Gamma_L = \theta$, condition (10.1.5) may be written as follows:

$$\left|\frac{1}{|S_{22}|}\left(\Delta + S_{21}S_{12}\left\{\frac{1 + |S_{22}| \exp(j\theta)}{1 - |S_{22}|^2}\right\}\right)\right| < 1$$

or,

$$\frac{1}{|S_{22}|}\left|\Delta + \frac{S_{12}S_{21}}{1 - |S_{22}|^2} + \frac{S_{12}S_{21}|S_{22}| \exp(j\theta)}{1 - |S_{22}|^2}\right| < 1 \tag{10.1.10}$$

Now, using the Minkowski inequality,

$$\left(\sum_{k=1}^{n} |a_k + b_k|^p\right)^{1/p} \leq \left(\sum_{k=1}^{n} |a_k|^p\right)^{1/p} + \left(\sum_{k=1}^{n} |b_k|^p\right)^{1/p} \tag{10.1.11}$$

we find that (10.1.10) is satisfied if

$$\frac{1}{|S_{22}|}\left|\Delta + \frac{S_{12}S_{21}}{1 - |S_{22}|^2}\right| + \frac{|S_{12}S_{21}|}{1 - |S_{22}|^2} < 1$$

or,

$$\frac{1}{|S_{22}|}\left|\Delta + \frac{S_{12}S_{21}}{1 - |S_{22}|^2}\right| < 1 - \frac{|S_{12}S_{21}|}{1 - |S_{22}|^2} \tag{10.1.12}$$

Since the left-hand side of (10.1.12) is always a positive number, this inequality will be satisfied if the following is true

$$1 - |S_{22}|^2 - |S_{12}S_{21}| > 0 \tag{10.1.13}$$

Similarly, stability condition (10.1.4) will be satisfied if

$$1 - |S_{11}|^2 - |S_{12}S_{21}| > 0 \tag{10.1.14}$$

Adding (10.1.13) and (10.1.14), we get

$$2 - |S_{11}|^2 - |S_{22}|^2 - 2|S_{12}S_{21}| > 0$$

or,

$$1 - \tfrac{1}{2}(|S_{11}|^2 + |S_{22}|^2) > |S_{12}S_{21}| \tag{10.1.15}$$

From (10.1.6) and (10.1.15), we have

$$|\Delta| < |S_{11}S_{22}| + |S_{12}S_{21}| < |S_{11}S_{22}| + 1 - \tfrac{1}{2}(|S_{11}|^2 + |S_{22}|^2)$$

or,

$$|\Delta| < 1 - \tfrac{1}{2}(|S_{11}| - |S_{22}|)^2 \Rightarrow |\Delta| < 1 \tag{10.1.16}$$

Multiplying (10.1.13) and (10.1.14), we get

$$(1 - |S_{22}|^2 - |S_{12}S_{21}|)(1 - |S_{11}|^2 - |S_{12}S_{21}|) > 0$$

or,

$$1 - |S_{11}|^2 - |S_{22}|^2 - 2|S_{12}S_{21}| + \zeta > 0 \tag{10.1.17}$$

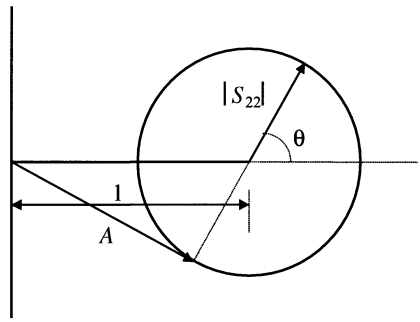

Figure 10.2 A graphical representation of (10.1.7).

where,

$$\zeta = |S_{11}|^2|S_{22}|^2 + |S_{12}S_{21}|^2 + |S_{12}S_{21}|(|S_{11}|^2 + |S_{22}|^2)$$

From the self-evident identity,

$$|S_{12}S_{21}|(|S_{11}| - |S_{22}|)^2 \geq 0$$

it can be proved that

$$\zeta \leq |\Delta|^2$$

Therefore, (10.1.17) can be written as follows:

$$1 - |S_{11}|^2 - |S_{22}|^2 - 2|S_{12}S_{21}| + |\Delta|^2 > 0$$

or,

$$1 - |S_{11}|^2 - |S_{22}|^2 + |\Delta|^2 > 2|S_{12}S_{21}|$$

or,

$$\frac{1 - |S_{11}|^2 - |S_{22}|^2 + |\Delta|^2}{2|S_{12}S_{21}|} > 1$$

Therefore,

$$k = \frac{1 - |S_{11}|^2 - |S_{22}|^2 + |\Delta|^2}{2|S_{12}S_{21}|} > 1 \qquad (10.1.18)$$

If S-parameters of a transistor satisfy conditions (10.1.16) and (10.1.18) then it is stable for any passive load and generator impedance. In other words, this transistor is *unconditionally stable*. On the other hand, it may be *conditionally stable* (stable for limited values of load or source impedance) if one or both of these conditions are violated. It means that the transistor can provide stable operation for a restricted range of Γ_S and Γ_L. A simple procedure to find these stable regions is to test inequalities (10.1.3) and (10.1.4) for particular load and source impedances. An alternative graphical approach is to find the circles of instability for load and generator reflection coefficients on a Smith chart. This latter approach is presented below.

From the expression of input reflection coefficient (9.4.7), we find that

$$\Gamma_{in} = S_{11} + \frac{S_{21}S_{12}\Gamma_L}{1 - S_{22}\Gamma_L} \Rightarrow \Gamma_{in}(1 - S_{22}\Gamma_L) = S_{11}(1 - S_{22}\Gamma_L) + S_{21}S_{12}\Gamma_L$$

or,

$$\Gamma_{in} = S_{11} - \Gamma_L(S_{11}S_{22} - S_{12}S_{21} - \Gamma_{in}S_{22}) \Rightarrow \Gamma_L = \frac{S_{11} - \Gamma_{in}}{\Delta - \Gamma_{in}S_{22}}$$

or,

$$\Gamma_L = \frac{S_{11} - \Gamma_{in}}{\Delta - \Gamma_{in}S_{22}} \frac{S_{22}}{S_{22}} = \frac{1}{S_{22}}\left(\frac{S_{11}S_{22} - \Gamma_{in}S_{22} - S_{12}S_{21} + S_{12}S_{21}}{\Delta - \Gamma_{in}S_{22}}\right)$$

or,

$$\Gamma_L = \frac{1}{S_{22}}\left(1 + \frac{S_{12}S_{21}}{\Delta - \Gamma_{in}S_{22}}\right) = \frac{1}{\Delta S_{22}}\left(\Delta + \frac{S_{12}S_{21}}{1 - \Gamma_{in}\Delta^{-1}S_{22}}\right) \tag{10.1.19}$$

As before, $1 - \Gamma_{in}S_{22}\Delta^{-1}$ represents a circle on the complex plane. It is centered at 1 with radius $|\Gamma_{in}S_{22}\Delta^{-1}|$; the reciprocal of this expression is another circle with center at

$$\frac{1}{2}\left(\frac{1}{1 + |\Delta^{-1}S_{22}|} + \frac{1}{1 - |\Delta^{-1}S_{22}|}\right) = \frac{1}{1 - |\Delta^{-1}S_{22}|^2}$$

and radius

$$\frac{1}{2}\left(\frac{1}{1 - |\Delta^{-1}S_{22}|} = \frac{1}{1 + |\Delta^{-1}S_{22}|}\right) = \frac{|\Delta^{-1}S_{22}|}{1 - |\Delta^{-1}S_{22}|^2}$$

Since $|\Gamma_{in}| < 1$, the region of stability will include all points on the Smith chart outside this circle. From (10.1.19), the center of the load impedance circle, C_L, is

$$C_L = \frac{1}{\Delta S_{22}}\left(\Delta + \frac{S_{12}S_{21}}{1 - |\Delta^{-1}S_{22}|^2}\right) = \frac{1}{\Delta S_{22}}\left(\Delta + \frac{S_{12}S_{21}|\Delta|^2}{|\Delta|^2 - |S_{22}|^2}\right)$$

or,

$$C_L = \frac{1}{S_{22}}\left(1 + \frac{S_{12}S_{21}\Delta^*}{|\Delta|^2 - |S_{22}|^2}\right) = \frac{1}{S_{22}}\left(\frac{|\Delta|^2 - |S_{22}|^2 + S_{12}S_{21}\Delta^*}{|\Delta|^2 - |S_{22}|^2}\right)$$

or,

$$C_L = \frac{1}{S_{22}}\left(\frac{\Delta^*(\Delta + S_{12}S_{21}) - |S_{22}|^2}{|\Delta|^2 - |S_{22}|^2}\right) = \frac{1}{S_{22}}\left(\frac{\Delta^* S_{11}S_{22} - |S_{22}|^2}{|\Delta|^2 - |S_{22}|^2}\right)$$

Therefore,

$$C_L = \frac{\Delta^* S_{11} - S_{22}^*}{|\Delta|^2 - |S_{22}|^2} = \frac{(S_{22} - \Delta S_{11}^*)^*}{|S_{22}|^2 - |\Delta|^2} \tag{10.1.20}$$

Its radius, r_L, is given by

$$r_L = \frac{1}{|\Delta S_{22}|}\left|\frac{S_{12}S_{21}|\Delta^{-1}S_{22}|}{1 - |\Delta^{-1}S_{22}|^2}\right| = \left|\frac{S_{12}S_{21}}{|\Delta|^2 - |S_{22}|^2}\right| \tag{10.1.21}$$

As explained following (10.1.19), this circle represents the locus of points over which the input reflection coefficient Γ_{in} is equal to unity. On one side of this circle, the input reflection coefficient is less than unity (stable region) while on its other side it exceeds 1 (unstable region). When load reflection coefficient Γ_L is zero (i.e., a matched termination is used), Γ_{in} is equal to S_{11}. Hence, the center of the Smith chart (reflection coefficient equal to zero) represents a stable point if $|S_{11}|$ is less than unity. On the other hand, it represents unstable impedance for $|S_{11}|$ greater than unity. If $\Gamma_L = 0$ is located outside the stability circle and is found stable then all outside points are stable. Similarly, if $\Gamma_L = 0$ is inside the stability circle and is found stable then all enclosed points are stable. If $\Gamma_L = 0$ is unstable then all points on that side of the stability circle are unstable.

Similarly, the locus of Γ_S can be derived from (10.1.4), with its center C_S and its radius r_S given as follows:

$$C_S = \frac{\Delta^* S_{22} - S_{11}^*}{|\Delta|^2 - |S_{11}|^2} = \frac{(S_{11} - \Delta S_{22}^*)^*}{|S_{11}|^2 - |\Delta|^2} \tag{10.1.22}$$

and,

$$r_S = \frac{1}{|\Delta S_{11}|}\left|\frac{S_{12}S_{21}|\Delta^{-1}S_{11}|}{1 - |\Delta^{-1}S_{11}|^2}\right| = \left|\frac{S_{12}S_{21}}{|\Delta|^2 - |S_{11}|^2}\right| \tag{10.1.23}$$

This circle represents the locus of points over which output reflection coefficient Γ_{out} is equal to unity. On one side of this circle, output reflection coefficient is less than unity (stable region) while on its other side it exceeds 1 (unstable region). When the source reflection coefficient Γ_S is zero then Γ_{out} is equal to S_{22}. Hence, the center of the Smith chart (reflection coefficient equal to zero) represents a stable point if $|S_{22}|$ is less than unity. On the other hand, it represents an unstable impedance point for $|S_{22}|$ greater than unity. If $\Gamma_S = 0$ is located outside the stability circle and is

found stable then all outside source-impedance points are stable. Similarly, if $\Gamma_S = 0$ is inside the stability circle and is found stable then all enclosed points are stable. If $\Gamma_S = 0$ is unstable then all points on that side of the stability circle are unstable.

Example 10.1: *S*-parameters of a properly biased transistor are found at 2 GHz as follows (50-Ω reference impedance):

$$S_{11} = 0.894\angle -60.6^\circ,\ S_{12} = 0.02\angle 62.4^\circ,\ S_{21} = 3.122\angle 123.6^\circ,$$
$$S_{22} = 0.781\angle -27.6^\circ$$

Determine its stability and plot the stability circles if the transistor is potentially unstable (see Figure 10.3).

From (10.1.16) and (10.1.18), we get

$$|\Delta| = |S_{11}S_{22} - S_{12}S_{21}| = 0.6964$$

and,

$$k = \frac{1 + |\Delta|^2 - |S_{11}|^2 - |S_{22}|^2}{2|S_{12}S_{21}|} = 0.6071$$

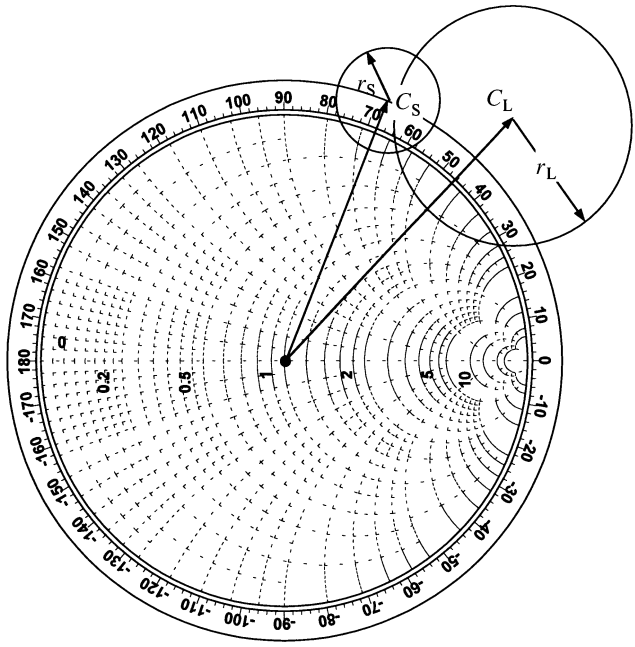

Figure 10.3 Input and output stability circles for Example 10.1.

Since one of the conditions for stability failed above, this transistor is potentially unstable.

Using (10.1.20)–(10.1.23), we can determine the stability circles as follows. For the output stability circle:

$$C_L = 1.36\angle 46.7^\circ$$

and,

$$r_L = 0.5$$

Since $|S_{11}|$ is 0.894, $\Gamma_L = 0$ represents a stable load point. Further, this point is located outside the stability circle, and therefore, all points outside this circle are stable.

For the input stability circle:

$$C_S = 1.13\angle 68.5^\circ$$

and,

$$r_S = 0.2$$

Since $|S_{22}|$ is 0.781, $\Gamma_S = 0$ represents a stable source impedance point. Further, this point is located outside the stability circle, and therefore, all points outside this circle are stable.

For the output stability circle, draw a radial line at 46.7°. With the radius of the Smith chart as unity, locate the center at 1.36 on this line. It can be done as follows. Measure the radius of the Smith chart using a ruler scale. Supposing that it is d mm. Location of the stability circle is then at 1.36 d mm away on this radial line. Similarly, the radius of the stability circle is 0.5 d mm. Load impedance must lie outside this circle for the circuit to be stable. Following a similar procedure, the input stability circle is drawn with its radius as 0.2 d mm and center at 1.13 d mm on the radial line at 68.5°. In order to have a stable design, the source impedance must lie outside this circle.

10.2 AMPLIFIER DESIGN FOR MAXIMUM GAIN

In this section, first we consider the design of an amplifier that uses a unilateral transistor ($S_{12} = 0$) and has maximum possible gain. A design procedure using a bilateral transistor ($S_{12} \neq 0$) is developed next that requires simultaneous conjugate matching at its two ports.

Unilateral Case

When S_{12} is zero, the input reflection coefficient Γ_{in} reduces to S_{11} while the output reflection coefficient Γ_{out} simplifies to S_{22}. In order to obtain maximum gain, source and load reflection coefficients must be equal to S_{11}^* and S_{22}^*, respectively. Further, the stability conditions for a unilateral transistor simplify to

$$|S_{11}| < 1$$

and,

$$|S_{22}| < 1$$

Example 10.2: S-parameters of a properly biased BJT are found at 1 GHz as follows (with $Z_o = 50\,\Omega$):

$$S_{11} = 0.606\angle -155^\circ, \quad S_{22} = 0.48\angle -20^\circ, \quad S_{12} = 0, \quad \text{and} \quad S_{21} = 6\angle 180^\circ$$

Determine the maximum gain possible with this transistor and design an RF circuit that can provide this gain.

(i) Stability check:

$$k = \frac{1 - |S_{11}|^2 - |S_{22}|^2 + |\Delta|^2}{2|S_{12}S_{21}|} = \infty; \qquad \because S_{12} = 0$$

and,

$$|\Delta| = |S_{11}S_{22} - S_{12}S_{21}| = |S_{11}S_{22}| = 0.2909$$

Since both of the conditions are satisfied, the transistor is unconditionally stable.

(ii) Maximum possible power gain of the transistor is found as

$$G_{TU} = \frac{1 - |\Gamma_S|^2}{|1 - \Gamma_{11}\Gamma_S|^2} \cdot |S_{21}|^2 \cdot \frac{1 - |\Gamma_L|^2}{|1 - S_{22}\Gamma_L|^2}$$

and

$$\begin{aligned} G_{TU_{max}} &= \frac{1 - |S_{11}^*|^2}{|1 - |S_{11}|^2|^2} \cdot |S_{21}|^2 \cdot \frac{1 - |S_{22}^*|^2}{|1 - |S_{22}|^2|^2} \\ &= \frac{1}{1 - 0.606^2} \cdot 6^2 \cdot \frac{1}{1 - 0.48^2} = 73.9257 \end{aligned}$$

or,

$$G_{\mathrm{TU}_{\max}} = 10\log_{10}(73.9257)\mathrm{dB} = 18.688\ \mathrm{dB}$$

(iii) For maximum unilateral power gain,

$$\Gamma_{\mathrm{S}} = S_{11}^{*} = 0.606\angle 155^{\circ}, \text{ and } \Gamma_{\mathrm{L}} = S_{22}^{*} = 0.48\angle 20^{\circ}$$

Component values are determined from the Smith chart as illustrated in Figure 10.4.

Corresponding to the reflection coefficient's magnitude 0.606, VSWR is 4.08. Hence, point D in Figure 10.4 represents the source impedance Z_{S}. Similarly, point B can be identified as the load impedance Z_{L}. Alternatively, the normalized impedance can be computed from the reflection coefficient. Then, points D and B can be located on the Smith chart. Now, we need to transform the zero reflection coefficient (normalized impedance of 1) to Γ_{S} (point D) at the input and to Γ_{L} (point B) at the output. One way to achieve this is to move first on the unity conductance circle from the center of the chart to point C and then on the constant resistance circle to reach point D. Thus, it requires a shunt capacitor and then a series inductor to match at the input. Similarly, we can follow the unity resistance circle from 1 to point A and then the constant conductance circle to reach point B. Thus, a capacitor is connected in series with the load and then an inductor in shunt to match its output side. Actual values of the components are determined as follows.

Normalized susceptance at point C is estimated as $j1.7$. Hence, the shunt capacitor on the source side must provide a susceptance of $1.7/50 = 0.034$ S.

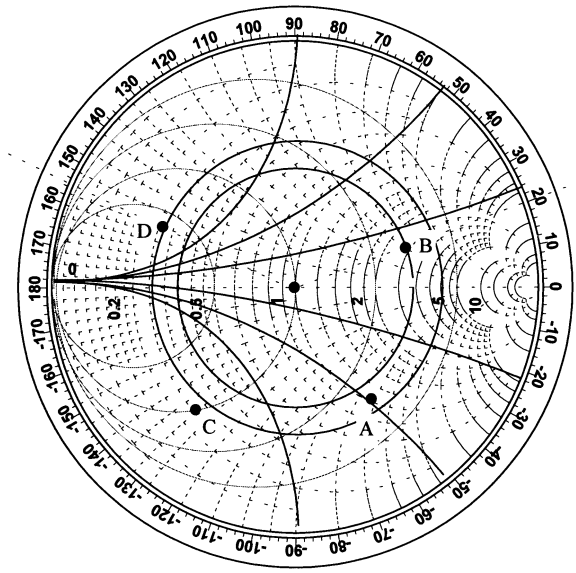

Figure 10.4 Smith chart illustrating the design of Example 10.2.

Since the signal frequency is 1 GHz, this capacitance must be 5.411 pF. Now, the change in normalized reactance from point C to point D is determined as $j0.2 - (-j0.45) = j0.65$. The positive sign indicates that it is an inductor of reactance $0.65 \cdot 50 = 32.5\,\Omega$. The corresponding inductance is found as 5.1725 nH.

Similarly, the normalized reactance at point A is estimated as $-j1.38$. Hence, the load requires a series capacitor of 2.307 pF. For transforming the susceptance of point A to that of point B, we need an inductance of $(-0.16 - 0.48)/50 = -0.0128$ S. It is found to be a shunt inductor of 12.434 nH. This circuit is illustrated in Figure 10.5.

Bilateral Case (Simultaneous Conjugate Matching)

In order to obtain the maximum possible gain, a bilateral transistor must be matched at both its ports simultaneously. This is illustrated in Figure 10.6. While its output port is properly terminated, the input side of the transistor is matched with the source such that $\Gamma_{in} = \Gamma_S^*$. Similarly, the output port of transistor is matched with the load while its input is matched terminated.

Mathematically,

$$\Gamma_{in} = \Gamma_S^*$$

and

$$\Gamma_{out} = \Gamma_L^*$$

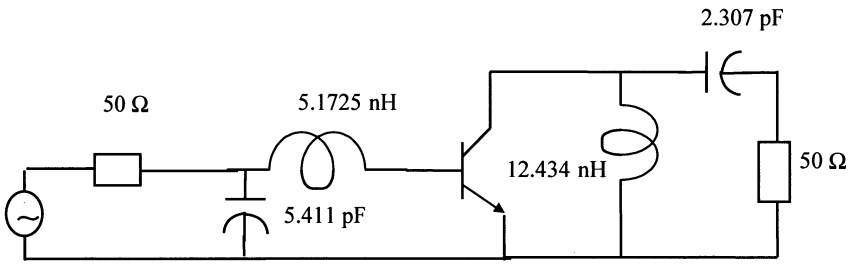

Figure 10.5 RF circuit designed for Example 10.2.

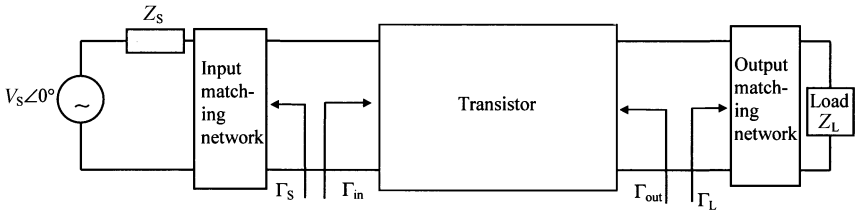

Figure 10.6 A bilateral transistor with input and output matching networks.

Therefore,

$$\Gamma_S^* = S_{11} + \frac{S_{12}S_{21}\Gamma_L}{1 - S_{22}\Gamma_L} \tag{10.2.1}$$

and,

$$\Gamma_L^* = S_{22} + \frac{S_{12}S_{21}\Gamma_S}{1 - S_{11}\Gamma_S} \tag{10.2.2}$$

From (10.2.1),

$$\Gamma_S = S_{11}^* + \frac{S_{12}^* S_{21}^*}{\frac{1}{\Gamma_L^*} - S_{22}^*} \tag{10.2.3}$$

and from (10.2.2),

$$\Gamma_L^* = \frac{S_{22} - (S_{11}S_{22} - S_{12}S_{21})\Gamma_S}{1 - S_{11}\Gamma_S} = \frac{S_{22} - \Gamma_S\Delta}{1 - S_{11}\Gamma_S} \tag{10.2.4}$$

Substituting (10.2.4) in (10.2.3), we have

$$\Gamma_S = S_{11}^* + \frac{S_{12}^* S_{21}^*}{\frac{1 - S_{11}\Gamma_S}{S_{22} - \Gamma_S\Delta} - S_{22}^*}$$

or,

$$\Gamma_S = S_{11}^* + \frac{S_{12}^* S_{21}^*(S_{22} - \Gamma_S\Delta)}{1 - S_{11}\Gamma_S - |S_{22}|^2 + \Gamma_S S_{22}^*\Delta} = S_{11}^* + \frac{S_{12}^* S_{21}^*(S_{22} - \Gamma_S\Delta)}{1 - |S_{22}|^2 - (S_{11} - S_{22}^*\Delta)\Gamma_S}$$

or,

$$\begin{aligned}(1 - |S_{22}|^2)\Gamma_S - (S_{11} - S_{22}^*\Delta)\Gamma_S^2 \\ = S_{11}^*(1 - |S_{22}|^2) - S_{11}^*(S_{11} - S_{22}^*\Delta)\Gamma_S + S_{12}^* S_{21}^*(S_{22} - \Gamma_S\Delta)\end{aligned}$$

or,

$$(S_{11} - S_{22}^*\Delta)\Gamma_S^2 + (|\Delta|^2 - |S_{11}|^2 + |S_{22}|^2 - 1)\Gamma_S + (S_{11}^* - S_{22}\Delta^*) = 0$$

This is a quadratic equation in Γ_S and its solution can be found as follows:

$$\Gamma_S = \frac{B_1 \pm \sqrt{B_1^2 - 4|C_1|^2}}{2C_1} = \Gamma_{MS} \tag{10.2.5}$$

where,

$$B_1 = 1 + |S_{11}|^2 - |S_{22}|^2 - |\Delta|^2$$

and

$$C_1 = S_{11} - S_{22}^* \Delta$$

Similarly, a quadratic equation for Γ_L can be formulated. Solutions to that equation are found to be

$$\Gamma_{ML} = \frac{B_2 \pm \sqrt{B_2^2 - 4|C_2|^2}}{2C_2} \tag{10.2.6}$$

where

$$B_2 = 1 + |S_{22}|^2 - |S_{11}|^2 - |\Delta|^2$$

and,

$$C_2 = S_{22} - S_{11}^* \Delta.$$

If $|B_1/2C_1| > 1$ and $B_1 > 0$ in equation (10.2.5) above, then the solution with a minus sign produces $|\Gamma_{MS}| < 1$ and that with a positive sign produces $|\Gamma_{MS}| > 1$. On other hand, if $|B_1/2C_1| > 1$ with $B_1 < 0$ in this equation, the solution with a plus sign produces $|\Gamma_{MS}| < 1$ and the solution with a minus sign produces $|\Gamma_{MS}| > 1$. Similar considerations apply to equation (10.2.6) as well.

OBSERVATION: $|B_i/2C_i| > 1$ implies that $|k| > 1$.

Proof:

$$\left|\frac{B_i}{2C_i}\right| > 1 \Rightarrow \left|\frac{1 + |S_{11}|^2 - |S_{22}|^2 - |\Delta|^2}{2(S_{11} - S_{22}^* \Delta)}\right| > 1$$

or,

$$|1 + |S_{11}|^2 - |S_{22}|^2 - |\Delta|^2| > 2|(S_{11} - S_{22}^*\Delta)|$$

Squaring on both sides of this inequality, we get

$$|1 + |S_{11}|^2 - |S_{22}|^2 - |\Delta|^2|^2 > 4|(S_{11} - S_{22}^*\Delta)|^2$$

and,

$$|S_{11} - S_{22}^*\Delta|^2 = (S_{11} - S_{22}^*\Delta)(S_{11}^* - S_{22}\Delta^*) = |S_{12}S_{21}|^2 + (1 - |S_{22}|^2)(|S_{11}|^2 - |\Delta|^2)$$

Therefore,

$$|1 + |S_{11}|^2 - |S_{22}|^2 - |\Delta|^2|^2 > 4|S_{12}S_{21}|^2 + 4(1 - |S_{22}|^2)(|S_{11}|^2 - |\Delta|^2)$$

or,

$$|1 + |S_{11}|^2 - |S_{22}|^2 - |\Delta|^2|^2 - 4(1 - |S_{22}|^2)(|S_{11}|^2 - |\Delta|^2) > 4|S_{12}S_{21}|^2$$

or,

$$(1 - |S_{22}|^2 - |S_{11}|^2 + |\Delta|^2)^2 > 4|S_{12}S_{21}|^2$$

or,

$$|1 - |S_{22}|^2 - |S_{11}|^2 + |\Delta|^2| > 2|S_{12}S_{21}|$$

Therefore,

$$\frac{|1 - |S_{22}|^2 - |S_{11}|^2 + |\Delta|^2|}{2|S_{12}S_{21}|} > 1 \Rightarrow k > 1$$

Also, it can be proved that $|\Delta| < 1$ implies that $B_1 > 0$ and $B_2 > 0$. Therefore, minus signs must be used in equations (10.2.5) and (10.2.6). Since,

$$G_{T_{max}} = \frac{(1 - |\Gamma_{MS}|^2)|S_{21}|^2(1 - |\Gamma_{ML}|^2)}{|(1 - S_{11}\Gamma_{MS})(1 - S_{22}\Gamma_{ML}) - S_{12}S_{21}\Gamma_{ML}\Gamma_{MS}|^2}$$

substituting equations (10.2.5), (10.2.6), and k from (10.1.18) gives

$$G_{T_{max}} = \frac{|S_{21}|}{|S_{12}|}(k - \sqrt{k^2 - 1}) \tag{10.2.7}$$

Maximum stable gain is defined as the value of $G_{T_{max}}$ when $k = 1$. Therefore,

$$G_{MSG} = \left|\frac{S_{21}}{S_{12}}\right| \tag{10.2.8}$$

Example 10.3: S-parameters of a properly biased GaAs FET HFET-1101 are measured using a 50-Ω network analyzer at 6 GHz as follows:

$$S_{11} = 0.614\angle -167.4^\circ,\ S_{21} = 2.187\angle 32.4^\circ,\ S_{12} = 0.046\angle 65^\circ,\ S_{22} = 0.716\angle -83^\circ$$

Design an amplifier using this transistor for a maximum possible gain.

First we need to test for stability using (10.1.16) and (10.1.18).

$$|\Delta| = |S_{11}S_{22} - S_{12}S_{21}| = 0.3419$$

and,

$$k = \frac{1 - |S_{11}|^2 - |S_{22}|^2 + |\Delta|^2}{2|S_{12}S_{21}|} = 1.1296$$

Since both of the conditions are satisfied, the transistor is unconditionally stable.

For the maximum possible gain, we need to use simultaneous conjugate matching. Therefore, the source and load reflection coefficients are determined from (10.2.5) and (10.2.6) as follows:

$$\Gamma_{MS} = \frac{B_1 - \sqrt{B_1^2 - 4|C_1|^2}}{2C_1} = 0.8673\angle 169.76^\circ$$

and,

$$\Gamma_{ML} = \frac{B_2 - \sqrt{B_2^2 - 4|C_2|^2}}{2C_2} = 0.9011\angle 84.48^\circ$$

There are many ways to synthesize these circuits. The design of one of the circuits is discussed here. As illustrated in Figure 10.7, normalized impedance points A and C are identified corresponding to Γ_{MS} and Γ_{ML}, respectively. The respective normalized admittance points B and D are next located. One way to transform the normalized admittance of unity to that of point B is to add a shunt susceptance (normalized) of about $j2.7$ at point E. This can be achieved with a capacitor or a stub of $0.194\,\lambda$ as shown in Figure 10.8. Now, for moving from point E to point B, we require a transmission line of about $0.065\,\lambda$. Similarly, an open-circuited shunt stub

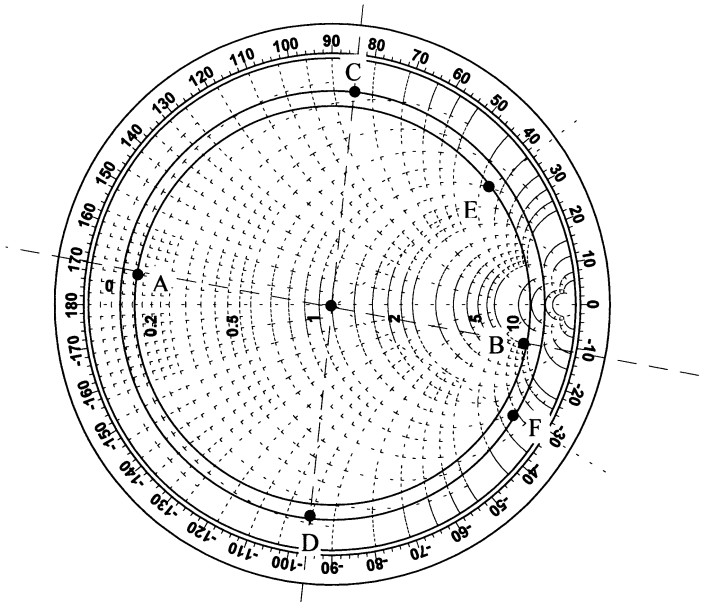

Figure 10.7 Design of input and output side matching networks.

of $0.297\,\lambda$ will transform the unity value to $1 - j3.4$ at point F and a transmission line length of $0.09\,\lambda$ will transform it to the desired value at point D.

Note that both of the shunt stubs are asymmetrical about the main line. A symmetrical stub is preferable. It can be achieved via two shunt-connected stubs of susceptance $j1.35$ at the input end and of $-j1.7$ at the output. This circuit is illustrated in Figure 10.9.

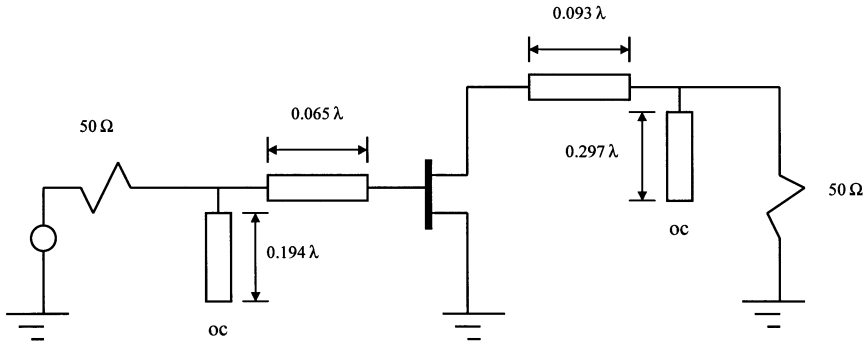

Figure 10.8 RF part of the amplifier circuit for Example 10.3.

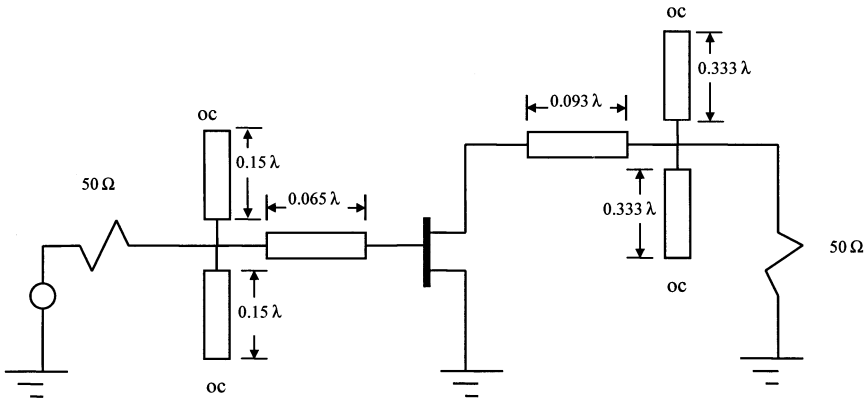

Figure 10.9 RF part of the amplifier circuit with symmetrical stubs.

The value of the gain is evaluated from (10.2.7) as follows:

$$G_{T_{max}} = \frac{|S_{21}|}{|S_{12}|}(k - \sqrt{k^2 - 1}) = 28.728 \Rightarrow 10 \cdot \log(28.728) = 14.58 \text{ dB}$$

***Unilateral Figure of Merit*:** In preceding examples, we find that the design with a bilateral transistor is a bit complex in comparison with a unilateral case. Procedure for the bilateral transistor becomes even more cumbersome when the specified gain is less than its maximum possible value. It can be simplified by assuming that a bilateral transistor is unilateral. The *unilateral figure of merit* provides an estimate of the error associated with this assumption. It can be formulated from (9.4.8) and (9.4.10) as follows:

$$\frac{G_T}{G_{TU}} = \frac{|1 - S_{22}\Gamma_L|^2}{|1 - \Gamma_{out}\Gamma_L|^2} = \left| \frac{1 - S_{22}\Gamma_L}{1 - S_{22}\Gamma_L - \dfrac{S_{12}S_{21}\Gamma_S\Gamma_L}{1 - S_{11}\Gamma_S}} \right|^2$$

$$= \left| \frac{1}{1 - \dfrac{S_{12}S_{21}\Gamma_S\Gamma_L}{(1 - S_{22}\Gamma_L)(1 - S_{11}\Gamma_S)}} \right|^2$$

or,

$$\frac{G_T}{G_{TU}} = \left| \frac{1}{1 - X} \right|^2$$

where

$$X = \frac{S_{12}S_{21}\Gamma_S\Gamma_L}{(1 - S_{22}\Gamma_L)(1 - S_{11}\Gamma_S)}$$

Therefore, the bounds of this gain ratio are given by

$$\frac{1}{(1 + |X|)^2} < \frac{G_T}{G_{TU}} < \frac{1}{(1 - |X|)^2}$$

When $\Gamma_S = S_{11}^*$ and $\Gamma_L = S_{22}^*$, G_{TU} has a maximum value. In this case, the maximum error introduced by using G_{TU} in place of G_T ranges as follows:

$$\frac{1}{(1 + U)^2} < \frac{G_T}{G_{TU}} < \frac{1}{(1 - U)^2} \tag{10.2.9}$$

where,

$$U = \frac{|S_{12}\|S_{21}\|S_{11}\|S_{22}|}{(1 - |S_{11}|^2)(1 - |S_{22}|^2)} \tag{10.2.10}$$

The parameter U is known as the unilateral figure of merit.

Example 10.4: The scattering parameters of two transistors are given below. Compare the unilateral figures of merit of the two.

Transistor A

$$S_{11} = 0.45\angle 150^\circ, \quad S_{12} = 0.01\angle -10^\circ$$
$$S_{21} = 2.05\angle 10^\circ, \quad S_{22} = 0.4\angle -150^\circ$$

Transistor B

$$S_{11} = 0.641\angle -171.3^\circ, \quad S_{12} = 0.057\angle 16.3^\circ$$
$$S_{21} = 2.058\angle 28.5^\circ, \quad S_{22} = 0.572\angle -95.7^\circ$$

From (10.2.10), we find that

$$U = \frac{0.01 * 2.05 * 0.45 * 0.4}{(1 - 0.45^2)(1 - 0.4^2)} = 0.00551 = U_A$$

for transistor A.

Similarly, for transistor B,

$$U = \frac{0.057 * 2.058 * 0.641 * 0.572}{(1 - 0.641^2)(1 - 0.572^2)} = 0.1085 = U_{\mathrm{B}}$$

Hence, the error bounds for these two transistors can be determined from (10.2.9) as follows. For transistor A,

$$0.9891 < \frac{G_{\mathrm{T}}}{G_{\mathrm{TU}}} < 1.0055$$

and for transistor B,

$$0.8138 < \frac{G_{\mathrm{T}}}{G_{\mathrm{TU}}} < 1.2582$$

Alternatively, these two results can be expressed in dB as follows:

$$-0.0476 \text{ dB} < \frac{G_{\mathrm{T}}}{G_{\mathrm{TU}}} < 0.0238 \text{ dB}$$

and,

$$-0.8948 \text{ dB} < \frac{G_{\mathrm{T}}}{G_{\mathrm{TU}}} < 0.9976 \text{ dB}$$

CONCLUSION: If $S_{12} = 0$ can be assumed for a transistor without introducing significant error, the design procedure will be much simpler in comparison with that of a bilateral case.

10.3 CONSTANT GAIN CIRCLES

In the preceding section, we considered the design of amplifiers for maximum possible gains. Now, let us consider the design procedure for other amplifier circuits. We split it again into two cases, namely, the unilateral and the bilateral transistors.

Unilateral Case

We consider two different cases of the unilateral transistors. In one case, it is assumed that the transistor is unconditionally stable because $|S_{11}|$ and $|S_{22}|$ are less than unity. In the other case, one or both of these parameters may be greater than unity. Thus, it makes $|\Delta|$ greater than 1.

From (9.4.10)

$$G_{TU} = \frac{1 - |\Gamma_S|^2}{|1 - S_{11}\Gamma_S|^2} \cdot |S_{21}|^2 \cdot \frac{1 - |\Gamma_L|^2}{|1 - S_{22}\Gamma_L|^2} = G_S \cdot G_o \cdot G_L$$

Expressions of G_S and G_L in this equation are similar in appearance. Therefore, we can express them by the following general form:

$$G_i = \frac{1 - |\Gamma_i|^2}{|1 - S_{ii}\Gamma_i|^2}; \qquad \begin{cases} i = S, & ii = 11 \\ i = L, & ii = 22 \end{cases} \tag{10.3.1}$$

Now, let us consider two different cases of unilateral transistors. In one case the transistor is unconditionally stable and in the other case it is potentially unstable.

(i) If the unilateral transistor is unconditionally stable then $|S_{ii}| < 1$. Therefore, maximum G_i in (10.3.1) will be given as

$$G_{imax} = \frac{1}{1 - |S_{ii}|^2} \tag{10.3.2}$$

Impedances that produce $G_{imax}(\Gamma_i = S_{ii}^*)$ are called *optimum terminations*. Therefore,

$$0 \le G_i \le G_{imax}$$

Values of Γ_i that produce a constant gain G_i lie in a circle on the Smith chart. These circles are called *constant gain circles*.

We define the normalized gain factor g_i as follows:

$$g_i = \frac{G_i}{G_{imax}} = G_i(1 - |S_{ii}|^2) \tag{10.3.3}$$

Hence,

$$0 \le g_i \le 1$$

From (10.3.1) and (10.3.2), we can write

$$g_i = \frac{1 - |\Gamma_i|^2}{|1 - S_{ii}\Gamma_i|^2}(1 - |S_{ii}|^2) \Rightarrow g_i|1 - S_{ii}\Gamma_i|^2 = (1 - |\Gamma_i|^2)(1 - |S_{ii}|^2)$$

or,

$$g_i(1 - S_{ii}\Gamma_i)(1 - S_{ii}^*\Gamma_i^*) = 1 - |S_{ii}|^2 - |\Gamma_i|^2 + |\Gamma_i|^2|S_{ii}|^2$$

or,

$$g_i(1 - S_{ii}\Gamma_i - S_{ii}^*\Gamma_i^* + |S_{ii}|^2|\Gamma_i|^2) = 1 - |S_{ii}|^2 - |\Gamma_i|^2(1 - |S_{ii}|^2)$$

or,

$$(g_i|S_{ii}^*|^2 + 1 - |S_{ii}|^2)|\Gamma_i|^2 - g_i(S_{ii}\Gamma_i + S_{ii}^*\Gamma_i^*) = 1 - g_i - |S_{ii}|^2$$

or,

$$\Gamma_i\Gamma_i^* - g_i\frac{(S_{ii}\Gamma_i + S_{ii}^*\Gamma_i^*)}{1 - (1 - g_i)|S_{ii}|^2} + \frac{g_i^2|S_{ii}|^2}{(1 - (1 - g_i)|S_{ii}|^2)^2} = \frac{1 - g_i - |S_{ii}|^2}{1 - (1 - g_i)|S_{ii}|^2} + \frac{g_i^2|S_{ii}|^2}{(1 - (1 - g_i)|S_{ii}|^2)^2}$$

Therefore,

$$\left|\Gamma_i - \frac{g_i S_{ii}^*}{1 - (1 - g_i)|S_{ii}|^2}\right|^2 = \frac{(1 - g_i - |S_{ii}|^2)(1 - (1 - g_i)|S_{ii}|^2) + |S_{ii}|^2 g_i^2}{(1 - (1 - g_i)|S_{ii}|^2)^2} \quad (10.3.4)$$

which is the equation of a circle, with its center d_i and radius R_i given as follows:

$$d_i = \frac{g_i S_{ii}^*}{1 - (1 - g_i)|S_{ii}|^2} \quad (10.3.5)$$

and,

$$R_i = \frac{(1 - |S_{ii}|^2)\sqrt{1 - g_i}}{1 - (1 - g_i)|S_{ii}|^2} \quad (10.3.6)$$

Example 10.4: S-parameters of a MESFET are given in the table below ($Z_o = 50\,\Omega$). Plot the constant gain circles at 4 GHz for $G_L = 0$ dB and 1 dB, and $G_S = 2$ dB and 3 dB. Using these plots, design an amplifier for a gain of 11 dB. Calculate and plot its transducer power gain and input return loss in the frequency band of 3 GHz to 5 GHz.

f (GHz)	S_{11}	S_{21}	S_{12}	S_{22}
3	$0.8\angle -90^\circ$	$2.8\angle 100^\circ$	0	$0.66\angle -50^\circ$
4	$0.75\angle -120^\circ$	$2.5\angle 80^\circ$	0	$0.6\angle -70^\circ$
5	$0.71\angle -140^\circ$	$2.3\angle 60^\circ$	0	$0.68\angle -85^\circ$

Since S_{12} is zero, this transistor is unilateral. Hence,

$$k = \infty, \text{ and } |\Delta| < 1, \text{ (because } |S_{11}| < 1 \text{ and } |S_{22}| < 1)$$

Therefore, it is unconditionally stable. From (9.4.14)–(9.4.16) we have

$$G_{\text{Smax}} = \frac{1}{1 - |S_{11}|^2} = \frac{1}{1 - 0.75^2} = 2.28857 = 3.59 \text{ dB}$$
$$G_{\text{Lmax}} = \frac{1}{1 - |S_{22}|^2} = \frac{1}{1 - 0.6^2} = 1.5625 = 1.92 \text{ dB}$$

and,

$$G_{\text{o}} = |S_{21}|^2 = 2.5^2 = 6.25 = 7.96 \text{ dB}$$
$$\therefore G_{\text{TUmax}} = 3.59 + 1.92 + 7.96 = 13.47 \text{ dB}$$

Thus, maximum possible gain is 2.47 dB higher than the desired value of 11 dB. Obviously, this transistor can be used for the present design.

The constant gain circles can be determined from (10.3.5) and (10.3.6). These results are tabulated here.

$G_{\text{S}} = 3 \text{ dB} \approx 2$	$g_{\text{S}} = 0.875$	$d_{\text{S}} = 0.706\angle 120^\circ$	$R_{\text{S}} = 0.166$
$G_{\text{S}} = 2 \text{ dB} = 1.58$	$g_{\text{S}} = 0.691$	$d_{\text{S}} = 0.627\angle 120^\circ$	$R_{\text{S}} = 0.294$
$G_{\text{L}} = 1 \text{ dB} = 1.26$	$g_{\text{L}} = 0.8064$	$d_{\text{L}} = 0.52\angle 70^\circ$	$R_{\text{L}} = 0.303$
$G_{\text{L}} = 0 \text{ dB} = 1$	$g_{\text{L}} = 0.64$	$d_{\text{L}} = 0.44\angle 70^\circ$	$R_{\text{L}} = 0.44$

As illustrated in Figure 10.10, the gain circles are drawn from this data. Since G_{o} is found as 8 dB (approximately), the remaining 3 dB need to be obtained through G_{S} and G_{L}. If we select G_{S} as 3 dB then G_{L} must be 0 dB. Alternatively, we can use G_{S} and G_{L} as 2 dB and 1 dB, respectively, to obtain a transducer power gain of $7.96 + 2 + 1 \approx 11$ dB.

Let us select point A on a 2-dB G_{S} circle and design the input side network. The corresponding admittance is found at point B, and therefore, a normalized capacitive susceptance of $j0.62$ is needed in parallel with the source admittance to reach the input VSWR circle. An open-ended, 0.09-λ-long shunt-stub can be used for this. The normalized admittance is now $1 + j0.62$. This admittance can be transformed to that of point B by a 0.183-λ-long section of transmission line. Similarly, point C can be used to obtain $G_{\text{L}} = 1$ dB. A normalized reactance of $j0.48$ in series with a 50-Ω load can be used to synthesize this impedance. Alternatively, the corresponding admittance point D is identified. Hence, a shunt susceptance of $-j0.35$ (an open-circuit stub of 0.431 λ) and then a transmission line length of 0.044 λ can provide the desired admittance. This circuit is illustrated in Figure 10.11.

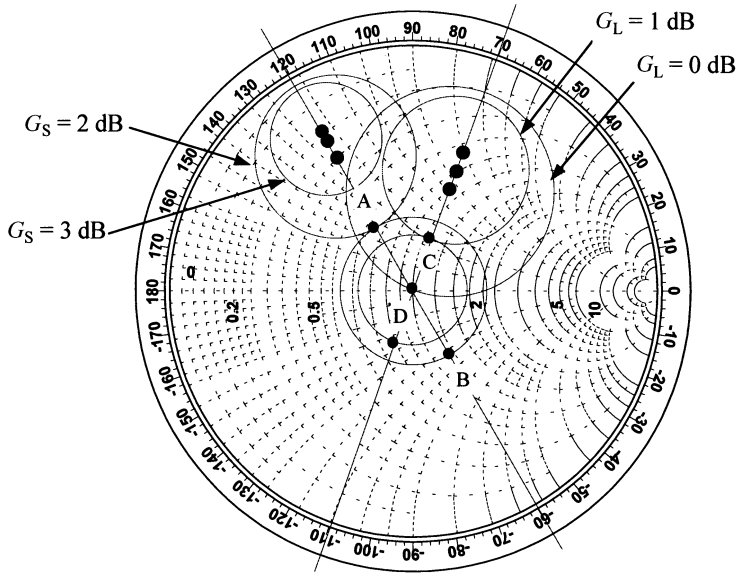

Figure 10.10 Constant gain circles and the network design for Example 10.4.

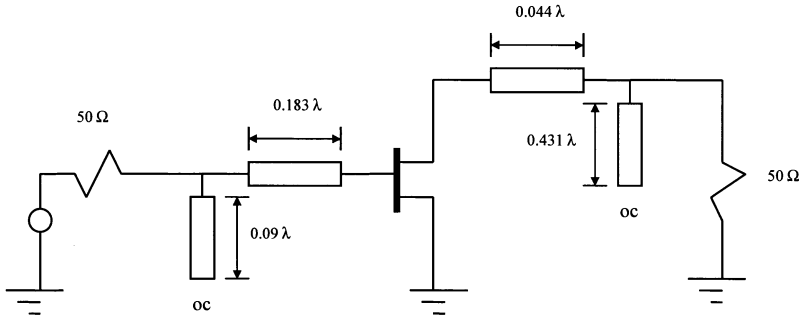

Figure 10.11 RF circuit designed for Example 10.4.

The return-loss is found by expressing $|\Gamma_{in}|$ in dB. Since

$$\Gamma_{in} = S_{11} + \frac{S_{12}S_{21}\Gamma_L}{1 - S_{22}\Gamma_L}$$

and $S_{12} = 0$, $\Gamma_{in} = S_{11}$, therefore, $|\Gamma_{in}(3\text{ GHz})| = 0.8$, $|\Gamma_{in}(4\text{ GHz})| = 0.75$, and $|\Gamma_{in}(5\text{ GHz})| = 0.71$.

Return loss at 3 GHz $= 20\log_{10}(0.8) = -1.94$ dB.
Return loss at 4 GHz $= 20\log_{10}(0.75) = -2.5$ dB.

Return loss at 5 GHz $= 20\log_{10}(0.71) = -2.97$ dB.

Transducer power gain at 4 GHz is 11 dB (because we designed the circuit for this gain). However, it will be different at other frequencies. We can evaluate it from (9.4.16) as follows.

$$G_{\mathrm{TU}} = \frac{1-|\Gamma_{\mathrm{S}}|^2}{|1-S_{11}\Gamma_{\mathrm{S}}|^2} \cdot |S_{21}|^2 \cdot \frac{1-|\Gamma_{\mathrm{L}}|^2}{|1-S_{22}\Gamma_{\mathrm{L}}|^2}$$

Note that Γ_{S}, Γ_{L}, and S-parameters of the transistor are frequency dependent. Therefore, we need to determine reflection coefficients at other frequencies before using the above formula. For a circuit designed with reactive discrete components, the new reactances can be easily evaluated. The corresponding reflection coefficients can, in turn, be determined using the appropriate formula. However, we used transmission lines in our design. Electrical lengths of these lines will be different at other frequencies. We can calculate new electrical lengths by replacing λ as follows:

$$\lambda \rightarrow \frac{f_{\mathrm{new}}}{f_{\mathrm{design}}}\lambda_{\mathrm{new}}$$

At 3 GHz, original lengths must be multiplied by $3/4 = 0.75$ to adjust for the change in frequency. Similarly, it must be multiplied by $5/4 = 1.25$ for 5 GHz. The new reflection coefficients can be determined using the Smith chart. The results are summarized below.

Γ_{S} CALCULATIONS:

Lengths at 4 GHz	3 GHz Lengths and Γ_{S}		5 GHz Lengths and Γ_{S}	
0.09	0.068	$0.24\angle 158^\circ$	0.113	$0.41\angle 81^\circ$
0.183	0.137		0.229	

Γ_{L} CALCULATIONS:

Lengths at 4 GHz	3 GHz Lengths and Γ_{L}		5 GHz Lengths and Γ_{L}	
0.044	0.033	$0.72\angle 109^\circ$	0.055	$0.15\angle -151^\circ$
0.431	0.323		0.539	

Therefore,

$$G_{TU}(3\text{ GHz}) = \frac{1-0.24^2}{|1-(0.24\angle 158^\circ)(0.8\angle -90^\circ)|^2}\cdot 2.8^2 \cdot \frac{1-0.72^2}{|1-(0.72\angle 109^\circ)(0.66\angle -50^\circ)|^2}$$

or,

$$G_{TU}(3\text{ GHz}) = 5.4117 = 10\log(5.4117) = 7.33\text{ dB}$$

Similarly,

$$G_{TU}(5\text{ GHz}) = \frac{1-0.41^2}{|1-(0.71\angle -140^\circ)(0.41\angle 81^\circ)|^2}\cdot 2.3^2 \cdot \frac{1-0.15^2}{|1-(0.58\angle -85^\circ)(0.15\angle -141^\circ)|^2}$$

or,

$$G_{TU}(5\text{ GHz}) = \frac{4.4008}{0.7849\cdot 1.1284} = 4.9688 = 6.96\text{ dB}$$

These return-loss and gain characteristics are displayed in Figure 10.12.

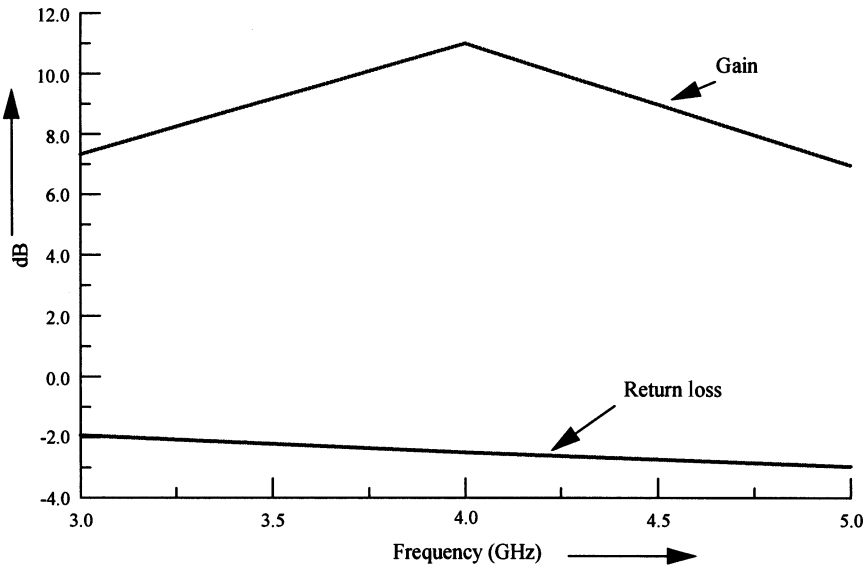

Figure 10.12 Gain and return loss versus frequency.

(ii) If a unilateral transistor is potentially unstable then $|S_{ii}| > 1$.

For $|S_{ii}| > 1$, the real part of the corresponding impedance will be negative. Further, G_i in (10.3.1) will be infinite for $\Gamma_i = 1/S_{ii}$. In other words, total loop-resistance on the input side (for $i = S$) or on the output side (for $i = L$) is zero. This is the characteristic of an oscillator. Hence, this circuit can oscillate. We can still use the same Smith chart to determine the corresponding impedance provided that the magnitude of reflection coefficient is assumed as $1/|S_{ii}|$, instead of $|S_{ii}|$ while its phase angle is the same as that of S_{ii}, and the resistance scale is interpreted as negative. The reactance scale of the Smith chart is not affected.

It can be shown that the location and radii of constant gain circles are still given by (10.3.5) and (10.3.6). The centers of these circles are located along a radial line passing through $1/S_{ii}$ on the Smith chart. In order to prevent oscillations, Γ_i must be selected such that the loop resistance is a positive number.

Example 10.5: A GaAs FET is biased at $V_{ds} = 5\,\text{V}$ and $I_{ds} = 10\,\text{mA}$. A 50-Ω ANA is used to determine its S-parameters at 1 GHz. These are found as follows:

$$S_{11} = 2.27\angle -120^\circ, \quad S_{21} = 4\angle 50^\circ, \quad S_{12} = 0, \text{ and } S_{22} = 0.6\angle -80^\circ$$

(a) Use a Smith chart to determine its input impedance and indicate on it the source impedance region(s) where the circuit is unstable.

(b) Plot the constant gain circles for $G_S = 3\,\text{dB}$ and $G_S = 5\,\text{dB}$ on the same Smith chart.

(c) Find a source impedance that provides $G_S = 3\,\text{dB}$ with maximum possible degree of stability. Also, determine the load impedance that gives maximum G_L. Design the input and output networks.

(d) Find the gain (in dB) of your amplifier circuit.

(a) First we locate $1/2.27 = 0.4405$ at $\angle -120^\circ$ on the Smith chart. It is depicted as point P in Figure 10.13. This point gives the corresponding impedance if the resistance scale is interpreted as negative. Thus, the normalized input impedance is about $-0.49 - j0.46$. Hence,

$$Z_{in} = 50(-0.49 - j0.46) = -24.5 - j23$$

Therefore, if we use a source that has impedance with its real part less than 24.5 Ω, the loop resistance on the input side will stay negative. That means one has to select a source impedance that lies inside the resistive circle of 0.49. Outside this circle is unstable.

(b) From (10.3.5) and (10.3.6),

$$d_S = \frac{g_S S_{11}^*}{1 - (1 - g_S)|S_{11}|^2} \qquad \text{and} \qquad R_S = \frac{(1 - |S_{11}|^2)\sqrt{1 - g_S}}{1 - (1 - g_S)|S_{11}|^2}$$

where $g_S = G_S(1 - |S_{11}|^2)$; the locations and radii of constant G_S circles are found as tabulated here.

$G_S = 5$ dB $\Rightarrow 10^{0.5} = 3.1623$	$G_S = 3$ dB $\Rightarrow 10^{0.3} = 2$
$g_S = 3.1623(1 - 2.27^2) = -13.1327$	$g_S = 2(1 - 2.27^2) = -8.3058$
$R_S = \dfrac{(1 - 2.27^2)\sqrt{1 + 13.1327}}{1 - (1 + 13.1327)2.27^2} = 0.2174$	$R_S = \dfrac{(1 - 2.27^2)\sqrt{1 + 8.3058}}{1 - (1 + 8.3058)2.27^2} = 0.2698$
$d_S = \dfrac{-13.1327 \cdot (2.27\angle 120^\circ)}{1 - (1 + 13.1327)2.27^2} = 0.45\angle 120^\circ$	$d_S = \dfrac{-8.3058 \cdot (2.27\angle 120^\circ)}{1 - (1 + 8.3058)2.27^2} = 0.4015\angle 120^\circ$

These constant G_S circles are shown on the Smith chart in Figure 10.13.

(c) In order to obtain $G_S = 3$ dB with maximum degree of stability, we select point A for the source impedance because it has a maximum possible real part.

$$\therefore \quad \bar{Z}_S \approx 1 + j0.5 \qquad \text{or} \qquad \Gamma_S = 0.24\angle 76^\circ$$

With $Z_S = 50 + j25\,\Omega$, loop resistance in the input side is $50 - 24.5 = 25.5\,\Omega$. It is a positive value, and therefore, the input circuit will be stable.

For maximum G_L, we select $\Gamma_L = S_{22}^* = 0.6\angle 80^\circ$. It is depicted as point C in Figure 10.13. The corresponding impedance Z_L is found to be

$$Z_L = 50(0.55 + j1.03) = 27.5 + j51.5$$

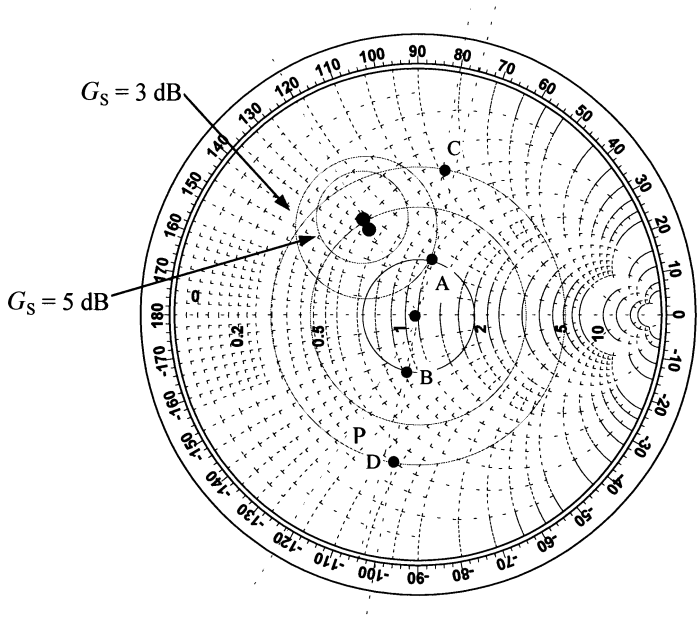

Figure 10.13 Amplifier design for Example 10.5.

Now, the input and output circuits can be designed for these values. One such circuit is shown in Figure 10.14.

(d) As designed, $G_S = 3$ dB. From (9.4.16),

$$G_{Lmax} = \frac{1}{1 - |S_{22}|^2} = \frac{1}{1 - 0.6^2} = 1.5625 = 1.9382 \text{ dB}$$

and,

$$G_o = |S_{21}|^2 = 4^2 = 16 = 12.0412 \text{ dB}$$

Therefore,

$$G_{TU} = 3 + 1.9382 + 12.0412 = 16.9794 \text{ dB}$$

Bilateral Case

If a microwave transistor cannot be assumed to be unilateral, the design procedure becomes tedious for a less than maximum possible transducer power gain. In this case, the operating or available power gain approach is preferred because of its simplicity. The design equations for these circuits are developed in this section.

***Unconditionally Stable Case*:** The operating power gain of an amplifier is given by (9.4.19). For convenience, it is reproduced here:

$$G_P = \frac{(1 - |\Gamma_L|^2)|S_{21}|^2}{(|1 - S_{22}\Gamma_L|^2)(1 - |\Gamma_{in}|^2)} \tag{9.4.19}$$

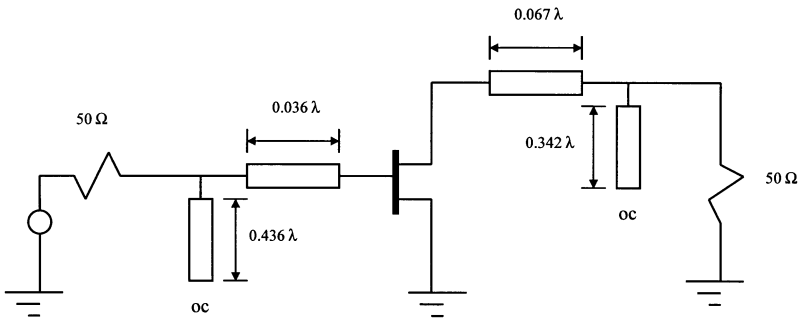

Figure 10.14 RF circuit for the amplifier of Example 10.5.

and the input reflection coefficient is

$$\Gamma_{\text{in}} = S_{11} + \frac{S_{12}S_{21}\Gamma_{\text{L}}}{1 - S_{22}\Gamma_{\text{L}}} = \frac{S_{11} - \Gamma_{\text{L}}\Delta}{1 - S_{22}\Gamma_{\text{L}}}$$

Therefore,

$$G_{\text{P}} = \frac{(1 - |\Gamma_{\text{L}}|^2)|S_{21}|^2}{(|1 - S_{22}\Gamma_{\text{L}}|^2) - (|S_{11} - \Gamma_{\text{L}}\Delta|^2)} = |S_{21}|^2 g_{\text{p}} \tag{10.3.7}$$

where,

$$g_{\text{p}} = \frac{(1 - |\Gamma_{\text{L}}|^2)}{(|1 - S_{22}\Gamma_{\text{L}}|^2) - (|S_{11} - \Gamma_{\text{L}}\Delta|^2)} \tag{10.3.8}$$

The equation for g_{p} can be simplified and rearranged as follows:

$$\left|\Gamma_{\text{L}} - \frac{g_{\text{p}}C_2^*}{1 + g_{\text{p}}(|S_{22}|^2 - |\Delta|^2)}\right|^2 = \frac{(1 - g_{\text{p}}(1 - |S_{11}|^2))(1 + g_{\text{p}}(|S_{22}|^2 - |\Delta|^2) + g_{\text{p}}^2|C_2|^2)}{(1 + g_{\text{p}}(|S_{22}|^2 - |\Delta|^2))^2} \tag{10.3.9}$$

where,

$$C_2 = S_{22} - S_{11}^*\Delta \tag{10.3.10}$$

Equation (10.3.9) can be simplified further as follows:

$$\left|\Gamma_{\text{L}} - \frac{g_{\text{p}}C_2^*}{1 + g_{\text{p}}(|S_{22}|^2 - |\Delta|^2)}\right|^2 = \frac{(1 - 2k|S_{12}S_{21}|g_p + |S_{12}S_{21}|^2 g_{\text{p}}^2)}{(1 + g_{\text{p}}(|S_{22}|^2 - |\Delta|^2))^2}$$

This represents a circle with its center c_{p} and radius R_{p} given as follows:

$$c_{\text{p}} = \frac{g_{\text{p}}C_2^*}{1 + g_{\text{p}}(|S_{22}|^2 - |\Delta|^2)} \tag{10.3.11}$$

and,

$$R_{\text{p}} = \frac{\sqrt{(1 - 2k|S_{12}S_{21}|g_{\text{p}} + |S_{12}S_{21}|^2 g_{\text{p}}^2)}}{1 + g_{\text{p}}(|S_{22}|^2 - |\Delta|^2)} \tag{10.3.12}$$

For $R_p = 0$, (10.3.12) can be solved for g_p, which represents its maximum value. It is given as follows:

$$g_p = g_{pmax} = \frac{1}{|S_{12}S_{21}|}(k - \sqrt{k^2 - 1})$$

and from (10.3.7) we have

$$G_{pmax} = \frac{|S_{21}|}{|S_{12}|}(k - \sqrt{k^2 - 1}) \tag{10.3.13}$$

A comparison of (10.3.13) with (10.2.7) indicates that the maximum operating power gain is equal to that of the maximum transducer power gain.

Following a similar procedure, expressions for center c_a and radius R_a of the constant available power gain circle can be formulated. These relations are,

$$c_a = \frac{g_a C_1^*}{1 + g_a(|S_{11}|^2 - |\Delta|^2)} \tag{10.3.14}$$

and,

$$R_a = \frac{\sqrt{(1 - 2k|S_{12}S_{21}|g_a + |S_{12}S_{21}|^2 g_a^2)}}{1 + g_a(|S_{11}|^2 - |\Delta|^2)} \tag{10.3.15}$$

where,

$$C_1 = S_{11} - S_{22}^*\Delta \tag{10.3.16}$$

and,

$$g_a = \frac{(1 - |\Gamma_s|^2)}{(|1 - S_{11}\Gamma_S|^2) - (|S_{22} - \Gamma_S\Delta|^2)} \tag{10.3.17}$$

Example 10.6: A GaAs FET is biased at $V_{ds} = 4\,\text{V}$ and $I_{ds} = 0.5I_{dss}$. Its S-parameters are given at 6 GHz as follows:

$$S_{11} = 0.641\angle -171.3^\circ, \qquad S_{12} = 0.057\angle 16.3^\circ,$$
$$S_{21} = 2.058\angle 28.5^\circ, \text{ and } S_{22} = 0.572\angle -95.7^\circ$$

Using this transistor, design an amplifier that provides an operating power gain of 9 dB.

Since $k = 1.5037$ and $|\Delta| = 0.3014$, this transistor is unconditionally stable. Further, G_{pmax} is found to be 11.38 dB. Hence, it can be used to get a gain of 9 dB. The corresponding circle data is found from (10.3.11) and (10.3.12) as follows:

$$c_{\text{p}} = 0.5083\angle 103.94^\circ \quad \text{and} \quad R_{\text{p}} = 0.4309$$

This circle is drawn on the Smith chart (Figure 10.15) and the load reflection coefficient is selected as $0.36\angle 50^\circ$. The corresponding input reflection coefficient is calculated as $0.63\angle -175.6^\circ$. Hence, Γ_{S} must be equal to $0.63\angle 175.6^\circ$ (i.e., conjugate of input reflection coefficient). These load- and source-impedance points are depicted in Figure 10.15 as C and A, respectively. The corresponding admittance points are identified as D and B on this chart. The load side network is designed by moving from point O to point F and then to point D. It is achieved by adding an open-circuited shunt stub of length $0.394\,\lambda$ and then a transmission line of $0.083\,\lambda$. For the source side, we can follow the path O–E–B, and therefore, an open-circuited shunt stub of $0.161\,\lambda$ followed by a $0.076\,\lambda$-long transmission line can provide the desired admittance. The designed circuit is shown in Figure 10.16.

***Potentially Unstable Case*:** Operating power gain circles for a bilateral potentially unstable transistor still can be found from (10.3.9) and (10.3.10). However, the load impedance point is selected such that it is in the stable region. Further, the conjugate of its input reflection coefficient must be a stable point because it represents the source reflection coefficient. Similarly, the available power gain circles can be drawn

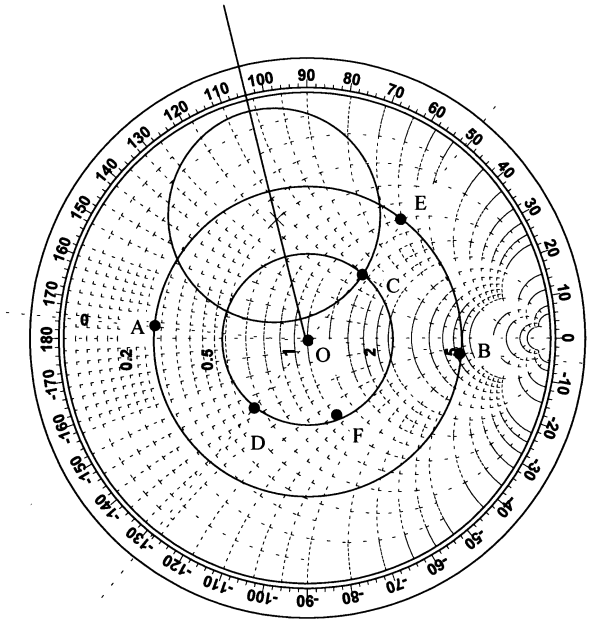

Figure 10.15 Matching network design for Example 10.6.

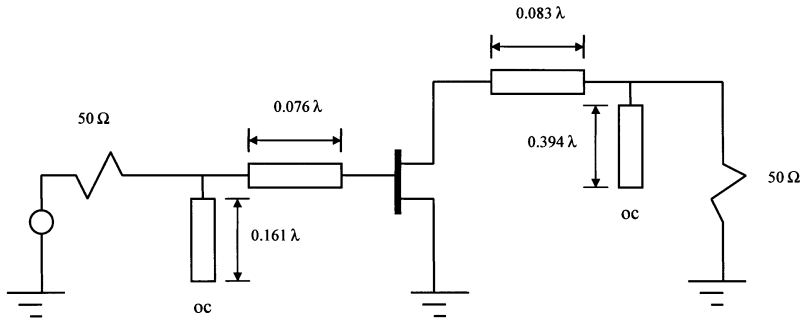

Figure 10.16 RF circuit of the amplifier for Example 10.6.

on a Smith chart using (10.3.12) and (10.3.13) along with the stability circles of the transistor. The source impedance point is selected such that it is in the stable region and provides the desired gain. Further, conjugate of the corresponding output reflection coefficient must lie in the stable region as well because it represents the load.

Example 10.7: A GaAs FET is biased at $I_{ds} = 5\,\text{mA}$ and $V_{ds} = 5\,\text{V}$ to measure its scattering parameters at 8 GHz. Using a 50-Ω system, this data is found as follows:

$$S_{11} = 0.5\angle -180^\circ, \quad S_{12} = 0.08\angle 30^\circ,$$
$$S_{21} = 2.5\angle 70^\circ, \text{ and } S_{22} = 0.8\angle -100^\circ$$

Design an amplifier using this transistor for an operating power gain of 10 dB.

From (10.1.16) and (10.1.18), we find that

$$|\Delta| = 0.2228$$

and

$$k = 0.3991$$

Since k is less than 1, this transistor is potentially unstable. The input and output stability circles are determined from (10.1.20)–(10.1.23) as follows. For the input stability circle:

$$C_S = 1.6713\angle 170.59^\circ$$

and,

$$r_S = 0.9983$$

Since $|S_{22}|$ is 0.8, $\Gamma_S = 0$ represents a stable source impedance point. Further, this point is located outside the stability circle, and therefore, all points outside this circle are stable.

For the output stability circle:

$$C_L = 1.1769\angle 97.17^\circ$$

and,

$$r_L = 0.3388$$

Since $|S_{11}|$ is 0.5, $\Gamma_L = 0$ represents a stable load impedance point. Further, this point is located outside the stability circle, and therefore, all points outside this circle are stable.

The data for a 10-dB gain circle is found from (10.3.11) and (10.3.12) as

$$c_p = 0.5717\angle 97.2^\circ \qquad \text{and} \qquad R_p = 0.4733$$

These circles are drawn on the Smith chart illustrated in Figure 10.17. Since this transistor is potentially unstable for certain load and input impedances, we need to avoid those regions. If we select $\Gamma_L = 0.1\angle 97^\circ$ (point C in Figure 10.17), the corresponding input reflection coefficient is calculated as $0.5209\angle -179.3^\circ$. There-

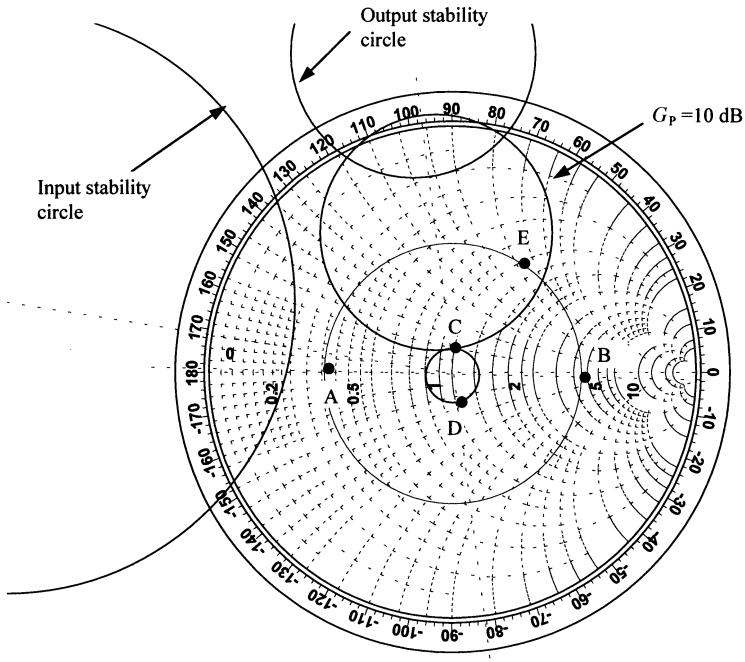

Figure 10.17 Design of input and output matching networks for Example 10.7.

fore, Γ_S is $0.5209\angle 179.3^\circ$. We find that this point lies in the stable region. One of the possible designs is illustrated in Figure 10.18.

Example 10.8: Design an amplifier for maximum possible transducer power gain, G_{Tmax}, using a BJT that is biased at $V_{CE} = 10\,V$, $I_C = 4\,mA$. Its S-parameters are found as follows using a 50-Ω system at 750 MHz.

$$S_{11} = 0.277\angle -59^\circ, \qquad S_{12} = 0.078\angle 93^\circ,$$
$$S_{21} = 1.92\angle 64^\circ, \text{ and } S_{22} = 0.848\angle -31^\circ$$

From (10.1.16) and (10.1.18),

$$k = 1.0325$$

and,

$$|\Delta| = 0.3242$$

Hence, the transistor is unconditionally stable.

For a maximum possible transducer power gain, we need to look for a simultaneous conjugate matching. From (10.2.5) and (10.2.6), we find that

$$\Gamma_{MS} = 0.7298\angle 135.44^\circ$$

and,

$$\Gamma_{ML} = 0.9511\angle 33.85^\circ$$

The corresponding normalized impedances are identified in Figure 10.19 as $0.1818 + j0.398$ (point A) and $0.2937 + j3.2619$ (point C), respectively. Points B and D represent respective normalized admittances on this Smith chart. For the load side, move from 1 to point E on the unity conductance circle and then from E to D on the constant VSWR circle. Hence, an open-circuited shunt stub of $0.278\,\lambda$ followed by a 0.176-λ-long transmission line is needed for the load side. Similarly, a

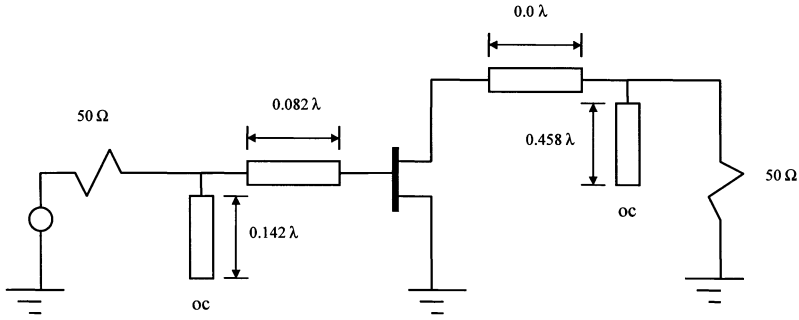

Figure 10.18 RF circuit of the amplifier for Example 10.7.

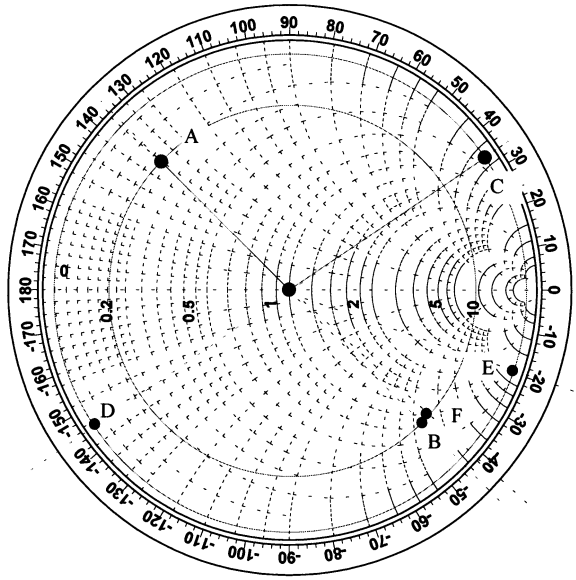

Figure 10.19 Design of input and output matching networks for Example 10.8.

shunt stub of 0.315 λ and a 0.004-λ-long section of the transmission line transform the normalized admittance of 1 to point F and then to B on the source side. The final circuit is illustrated in Figure 10.20.

Example 10.9: Using the BJT of the preceding example, design an amplifier for $G_p = 10\,\text{dB}$ at 750 MHz. Also, determine the reflection coefficients required to obtain maximum operating power gain and show that they are identical to those obtained in Example 10.8 for the simultaneous conjugate match.

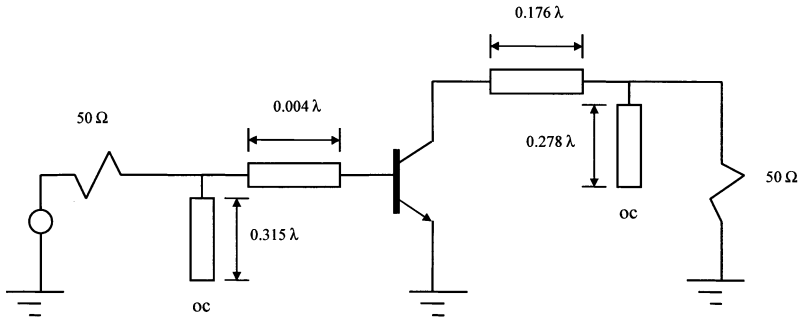

Figure 10.20 RF circuit of the amplifier for Example 10.8.

From the preceding example, we know that the transistor is unconditionally stable. For an operating power gain of 10 dB, location and radius of the constant gain circle are determined from (10.3.11) and (10.3.12) as follows:

$$c_p = 0.7812\angle 33.85^\circ \quad \text{and} \quad R_p = 0.2142$$

This gain circle is drawn on a Smith chart as shown in Figure 10.21. For an operating power gain of 10 dB, the load impedance must be selected on this circle. If we select a normalized impedance of $1.8 + j1.6$ (point C) then the load reflection coefficient is $0.56\angle 34^\circ$. The corresponding input reflection coefficient is found at $0.3455\angle -56.45^\circ$. Therefore, the source reflection coefficient Γ_S must be equal to $0.3455\angle 56.45^\circ$. Further, for a maximum operating power gain (that is, 12.8074 dB), the gain circle converges to a point that is located at $0.9511\angle 33.85^\circ$. Hence, this point represents the load reflection coefficient that is needed to obtain maximum operating power gain. Further, the corresponding input reflection coefficient is found to be $0.7298\angle -135.44^\circ$. Therefore, $\Gamma_S = 0.7298\angle 135.44^\circ$. A comparison of these results with those obtained in Example 10.8 indicates that the results are identical in both cases.

One of the possible RF circuits for obtaining an operating power gain of 10 dB can be designed as follows. After locating the load and source impedance points C and A, respectively, constant VSWR circles are drawn. The corresponding normalized admittance points D and B are then found. A normalized shunt susceptance of $-j1.3$ will transform the 50-Ω load impedance (normalized admittance of 1) to

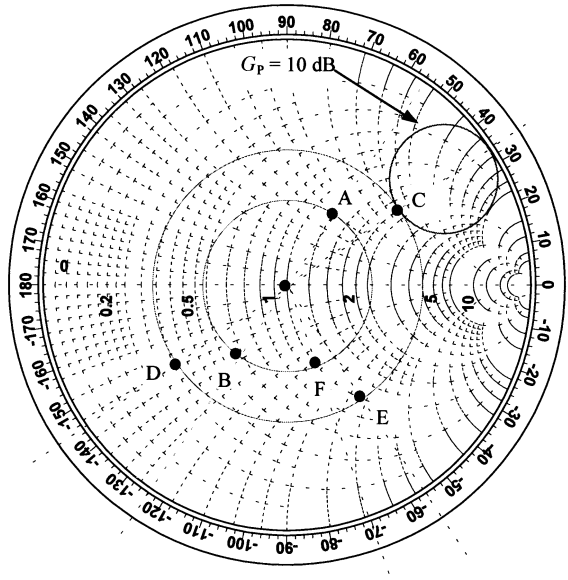

Figure 10.21 Design of input and output matching networks for Example 10.9.

$1 - j1.3$ (point E), then a 0.124-λ-long transmission line will move it to point D. An open-circuited 0.356-λ-long stub can be used to obtain a $-j1.3$ susceptance.

For the design of an input matching network, a normalized shunt susceptance of $-j0.75$ may be used to transform a 50-Ω source impedance (normalized admittance of 1) to $1 - j0.75$ (point F). A 0.075-λ-long transmission line is then connected to transform this admittance to that of point B. A 0.397-λ-long open-circuited stub can be used to obtain the desired susceptance of $-j0.75$. The final circuit is illustrated in Figure 10.22.

Example 10.10: A suitably biased GaAs FET has the following *S*-parameters measured at 2 GHz with a 50-Ω system:

$$S_{11} = 0.7\angle -65^\circ, \quad S_{12} = 0.03\angle 60^\circ, \quad S_{21} = 3.2\angle 110^\circ, \text{ and } S_{22} = 0.8\angle -30^\circ.$$

Determine the stability and design an amplifier for $G_p = 10$ dB.

From (10.1.16) and (10.1.18),

$$|\Delta| = 0.5764$$

and,

$$k = 1.053$$

Hence, the transistor is unconditionally stable.

The circle parameters for an operating power gain of 10 dB are found from (10.3.11) and (10.3.12) as follows:

$$c_p = 0.3061\angle 39.45^\circ$$

and,

$$R_p = 0.6926$$

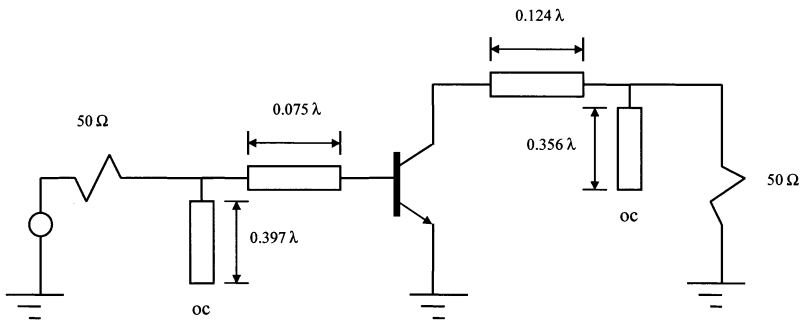

Figure 10.22 RF circuit of the amplifier for Example 10.9.

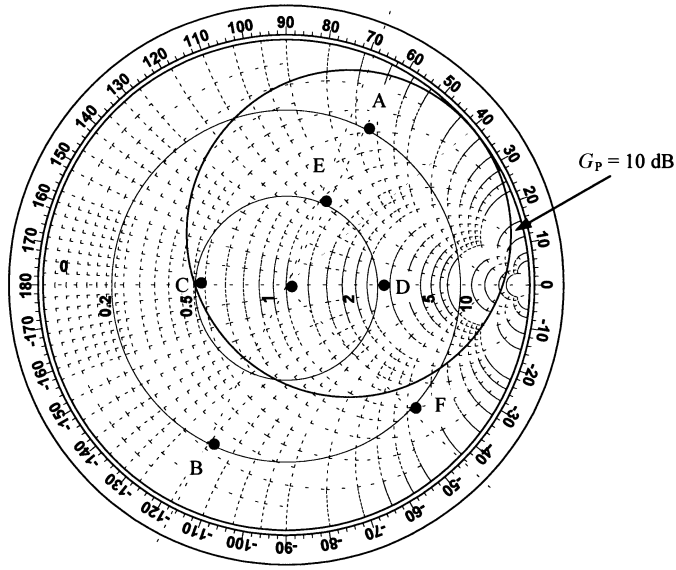

Figure 10.23 Design of input and output matching networks for Example 10.10.

This circle is drawn on the Smith chart as shown in Figure 10.23. If we select a normalized load of $0.45 + j0$ (point C), the corresponding load reflection coefficient will be $0.38\angle 180°$. This gives an input reflection coefficient of $0.714\angle -63°$. That means the source reflection coefficient Γ_S must be $0.714\angle 63°$. The corresponding normalized impedance may be found as $0.569 + j1.4769$ (point A). This data is used to draw the VSWR circles, as shown in the figure. Matching networks can be designed to synthesize the normalized admittances of points D (for the load side) and B (for the source side). A normalized shunt susceptance of $j0.8$ moves 50 Ω (center of the chart) to point E and then a 0.094-λ-long transmission line can transform it to the desired value at point D. The shunt susceptance of $j0.8$ can be obtained via a capacitor of 1.27 pF. Similarly, a shunt inductor of 1.89 nH adds a normalized susceptance of $-j2.1$ at the source side (point F) and then a 0.101-λ-long

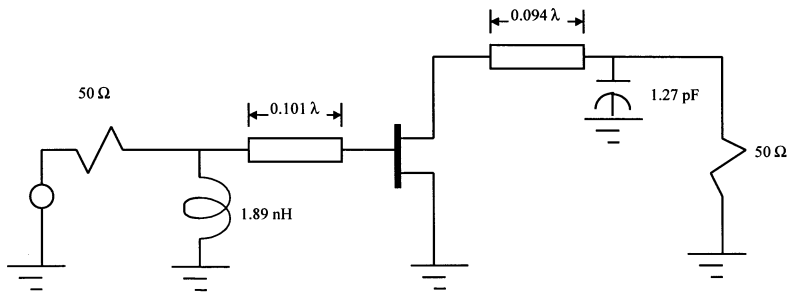

Figure 10.24 RF circuit of the amplifier for Example 10.10.

transmission line can transform that to the desired value of $0.22 - j0.6$ (point B). The final circuit is illustrated in Figure 10.24.

10.4 CONSTANT NOISE FIGURE CIRCLES

Noise characteristics of the two-port networks are considered in Chapter 2. We found that the noise factor of an amplifier can be expressed via (2.5.21) as follows:

$$F = F_{\min} + \frac{R_n}{G_S}|Y_S - Y_{opt}|^2 \tag{10.4.1}$$

where,

$F_{\min}$ = Minimum noise factor of the transistor (attained for $Y_S = Y_{opt}$)
R_n = Equivalent noise resistance of the transistor
G_S = Real part of the source admittance
$Y_S = G_S + jB_S = \dfrac{1}{Z_o}\dfrac{1-\Gamma_S}{1+\Gamma_S}$ = Source admittance presented to the transistor
Γ_S = Source reflection coefficient seen by the transistor
$Y_{opt} = \dfrac{1}{Z_o}\dfrac{1-\Gamma_{opt}}{1+\Gamma_{opt}}$ = Optimum source admittance that results in minimum noise figure.

Γ_{opt} = Optimum source reflection coefficient that results in minimum noise figure.

Since

$$|Y_S - Y_{opt}|^2 = \left|\frac{1}{Z_o}\cdot\frac{1-\Gamma_S}{1+\Gamma_S} - \frac{1}{Z_o}\cdot\frac{1-\Gamma_{opt}}{1+\Gamma_{opt}}\right|^2 = \frac{4}{|Z_o|^2}\cdot\frac{|\Gamma_S - \Gamma_{opt}|^2}{|1+\Gamma_S|^2\cdot|1+\Gamma_{opt}|^2} \tag{10.4.2}$$

and,

$$G_S = \mathrm{Re}(Y_S) = \frac{1}{2Z_o}\left(\frac{1-\Gamma_S}{1+\Gamma_S} + \frac{1-\Gamma_S^*}{1+\Gamma_S^*}\right) = \frac{1-|\Gamma_S|^2}{Z_o\cdot|1+\Gamma_S|^2} \tag{10.4.3}$$

(10.4.1) can be written as follows:

$$F = F_{\min} + \frac{4R_n}{Z_o}\cdot\frac{|\Gamma_S - \Gamma_{opt}|^2}{(1-|\Gamma_S|^2)\cdot|1+\Gamma_{opt}|^2}$$

or,

$$\frac{|\Gamma_S - \Gamma_{opt}|^2}{(1 - |\Gamma_S|^2)} = \frac{F - F_{min}}{4(R_n/Z_o)} \cdot |1 + \Gamma_{opt}|^2 = N \tag{10.4.4}$$

where N is called the *noise figure parameter.*

From (10.4.4), we have

$$|\Gamma_S - \Gamma_{opt}|^2 = N(1 - |\Gamma_S|^2)$$

or,

$$(\Gamma_S - \Gamma_{opt})(\Gamma_S^* - \Gamma_{opt}^*) = \Gamma_S\Gamma_S^* - (\Gamma_S^*\Gamma_{opt} + \Gamma_S\Gamma_{opt}^*) + \Gamma_{opt}\Gamma_{opt}^* = N - N|\Gamma_S|^2$$

or,

$$\Gamma_S\Gamma_S^* - \frac{(\Gamma_S^*\Gamma_{opt} + \Gamma_S\Gamma_{opt}^*)}{N+1} + \frac{|\Gamma_{opt}|^2}{(N+1)^2} = \frac{N - \Gamma_{opt}\Gamma_{opt}^*}{N+1} + \frac{|\Gamma_{opt}|^2}{(N+1)^2}$$

or,

$$\left|\Gamma_S - \frac{\Gamma_{opt}}{N+1}\right|^2 = \frac{N(N+1) - N|\Gamma_{opt}|^2}{(N+1)^2}$$

Hence,

$$\left|\Gamma_S - \frac{\Gamma_{opt}}{N+1}\right| = \frac{\sqrt{N(N+1) - N|\Gamma_{opt}|^2}}{(N+1)} \tag{10.4.5}$$

Equation (10.4.5) represents a circle on the complex Γ_S-plane. Its center C_{NF} and radius R_{NF} are given by

$$C_{NF} = \frac{\Gamma_{opt}}{N+1} \tag{10.4.6}$$

and,

$$R_{NF} = \frac{\sqrt{N(N+1) - N|\Gamma_{opt}|^2}}{(N+1)} \tag{10.4.7}$$

Using (10.4.6) and (10.4.7), constant noise figure circles can be drawn on a Smith chart. The source reflection coefficient Γ_S is selected inside this circle to keep the noise figure of the amplifier within a specified noise factor F.

Example 10.11: A bipolar junction transistor is biased at $V_{CE} = 4\,\text{V}$, and $I_{CE} = 30\,\text{mA}$. Its scattering and noise parameters are measured at 1 GHz with a 50-Ω system as follows:

$$S_{11} = 0.707\angle -155^\circ, \quad S_{21} = 5.0\angle 180^\circ, \quad S_{12} = 0,$$
$$S_{22} = 0.51\angle -20^\circ, \quad F_{\min} = 3\text{ dB}, \quad R_n = 4\text{-}\Omega, \text{ and } \Gamma_{\text{opt}} = 0.45\angle 180^\circ$$

Design the input and output matching networks for this transistor so that it produces a power gain of 16 dB and a noise figure of less than 3.5 dB.

From (10.1.16) and (10.1.18), we find that

$$k = \infty$$

and,

$$|\Delta| = 0.3606$$

Therefore, the transistor is unconditionally stable.

From (9.4.14)–(9.4.16),

$$G_{\text{Smax}} = 3\text{ dB}$$
$$G_{\text{Lmax}} = 1.31\text{ dB}$$

and,

$$G_{\text{o}} = 13.98\text{ dB}$$

Hence,

$$G_{\text{TUmax}} = 3 + 1.31 + 13.98 = 18.29\text{ dB}$$

Therefore, this transistor can be used for a power gain of 16 dB. Since G_{o} is approximately 14 dB, the remaining 2 dB can be set via G_{S} and G_{L}. If we design an input-matching network that provides G_{S} as 1.22 dB then we need an output-matching network for a G_{L} of 0.78 dB. The G_{S} and G_{L} circles are found from (10.3.5) and (10.3.6) as follows:

$$d_{\text{S}} = 0.5634\angle 155^\circ$$
$$R_{\text{S}} = 0.3496$$
$$d_{\text{L}} = 0.4655\angle 20^\circ$$

and,

$$R_{\text{L}} = 0.2581$$

The 3.5-dB noise figure circle is found from (10.4.6) and (10.4.7) as follows:

$$C_{\mathrm{NF}} = 0.3658 \angle 180^{\circ}$$

and,

$$R_{\mathrm{NF}} = 0.3953$$

These gain and noise circles are drawn on the Smith chart illustrated in Figure 10.25. If we select point B on 1.22-dB G_{S} circle as Γ_{S} then the noise figure will stay within 3.5 dB. The load-side matching network is designed so that it provides G_{L} as 0.78 dB. We select point D for Γ_{L}. The two matching networks are designed below using discrete components.

For the design of a source-side network, we can move on the unity conductance circle from 1 to point A. It requires a shunt capacitor for a normalized susceptance of $+j0.75$. A capacitor of 2.39 pF can provide this susceptance at 1 GHz. The next step is to reach point B from A by moving on the constant resistance circle of 0.65 that requires an inductive reactance of normalized value $+j0.56$, and hence, an inductor of 4.46 nH. Similarly, the load-side network can be designed following the unity resistance circle from 1 to point C. It requires a capacitor of 2.27 pF in series with 50-Ω output. Next, move from point C to D on the conductance circle of 0.35. Hence, it requires an inductor of 19.89 nH. The complete RF circuit is shown in Figure 10.26.

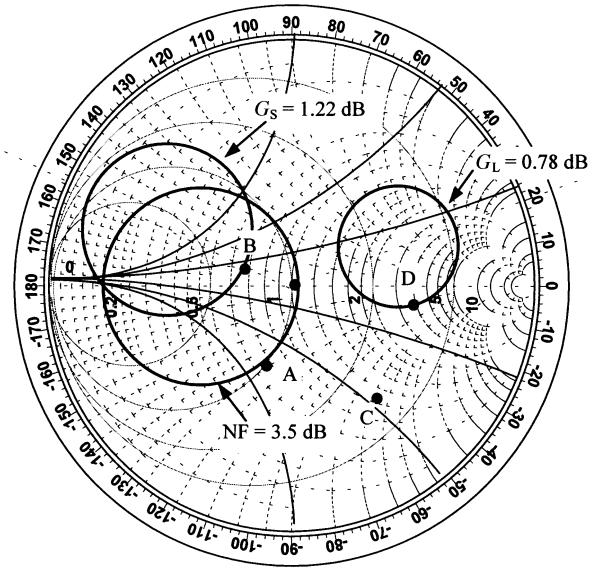

Figure 10.25 Design of input and output matching networks for Example 10.11.

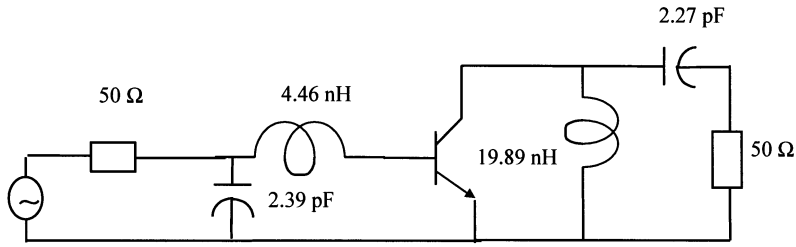

Figure 10.26 RF circuit design for Example 10.11.

Example 10.12: A GaAs FET has the following scattering and noise parameters at 4 GHz, measured with a 50-Ω system:

$$S_{11} = 0.6\angle -60^\circ, \quad S_{21} = 1.9\angle 81^\circ, \quad S_{12} = 0.05\angle 26^\circ,$$
$$S_{22} = 0.5\angle -60^\circ, \quad F_{\min} = 1.6 \text{ dB}, \quad R_n = 20\ \Omega, \text{ and } \Gamma_{\text{opt}} = 0.62\angle 100^\circ$$

(a) Assuming the FET to be unilateral, design an amplifier for a maximum possible gain and a noise figure no more than 2.0 dB. Estimate the error introduced in G_T due to this assumption.

(b) Redesign the amplifier in (a), with FET being bilateral.

From (10.1.16) and (10.1.18),

$$|\Delta| = 0.3713$$

and,

$$k = 2.778$$

Hence, the transistor is unconditionally stable.

(a) The unilateral figure of merit is found from (10.2.10) as 0.0594. Therefore,

$$-0.501 \text{ dB} < \frac{G_T}{G_{TU}} < 0.5938 \text{ dB}$$

This means that the maximum error in the gain of the amplifier due to this assumption will be of the order of ±0.5 dB.

Using (9.4.14)–(9.4.16), we find that

$$G_{\text{Smax}} = 1.9382 \text{ dB}$$
$$G_{\text{Lmax}} = 1.25 \text{ dB}$$

and,

$$G_o = 5.5751 \text{ dB}$$

Therefore,

$$G_{TUmax} = 1.9382 + 1.25 + 5.5751 = 8.7627 \text{ dB}$$

Since we are looking for a maximum possible gain with a noise figure less than 2 dB, we should use load impedance that provides a conjugate match. Note that this selection does not influence the noise figure. Thus, we select $\Gamma_L = S_{22}^* = 0.5\angle 60^\circ$. It is depicted by point C on the Smith chart in Figure 10.27. For the design of the source side, we first determine the relevant gain and noise circles.

From (10.3.5) and (10.3.6), the constant gain circles for $G_S = 1.5$ dB and 1.7 dB are determined as follows. For $G_S = 1.5$ dB,

$$d_S = 0.5618\angle 60^\circ, \quad R_S = 0.2054$$

For $G_S = 1.7$ dB,

$$d_S = 0.5791\angle 60^\circ, \quad R_S = 0.1507$$

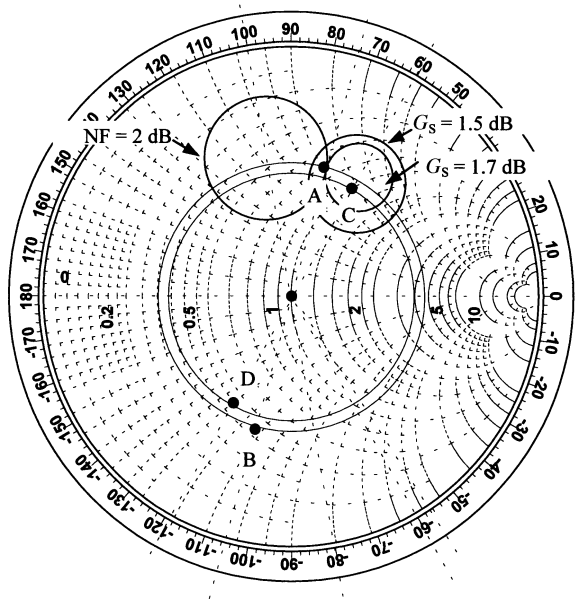

Figure 10.27 Design of input and output matching networks for Example 10.12(a).

The 2-dB noise figure circle is found from (10.4.6) and (10.4.7) as follows:

$$C_{\mathrm{NF}} = 0.5627\angle 100^{\circ}$$

and,

$$R_{\mathrm{NF}} = 0.2454$$

These circles are drawn on the Smith chart as shown in Figure 10.27. We find that the 2-dB noise figure circle almost touches the $G_{\mathrm{S}} = 1.7$-dB circle at a point. Further, the 1.5-dB gain circle has a larger radius. It suggests that a gain larger than 1.7 dB will have higher noise figure. As illustrated, the optimum Γ_{S} for this problem is point A. A circuit designed with short-circuited shunt stubs and transmission line lengths is shown in Figure 10.28.

(b) When the transistor is bilateral, we need to use the operating power gain or available power gain approach for the design. The operating power gain approach provides information about the load impedance. Source impedance is determined subsequently as complex conjugate of the input impedance. If this value of the source impedance does not satisfy the noise figure specification then one needs to select a different load impedance. Thus, several iterations may be needed before the noise and gain requirements are satisfied. On the other hand, the available power gain approach provides the source impedance. The load impedance is then determined as a complex conjugate of the output impedance. Hence, a suitable source impedance can be determined that simultaneously satisfies the gain as well as the noise characteristics. Hence, the available power gain approach does not require iterative calculations, and therefore, it is preferable in the present case.

From (10.3.14) and (10.3.15), the 8-dB gain circle is found as follows:

$$c_{\mathrm{a}} = 0.5274\angle 64.76^{\circ}, \quad R_{\mathrm{a}} = 0.2339$$

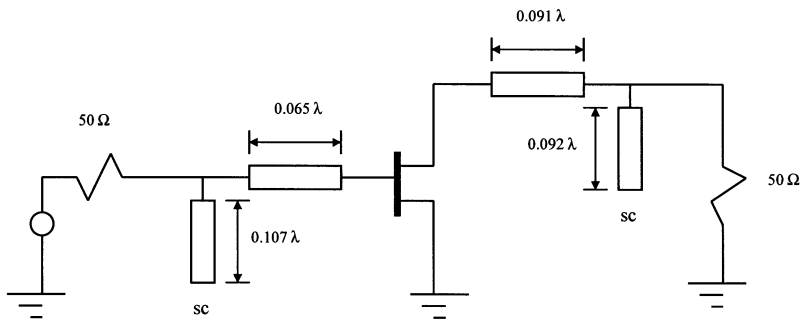

Figure 10.28 RF circuit of the amplifier for Example 10.12(a).

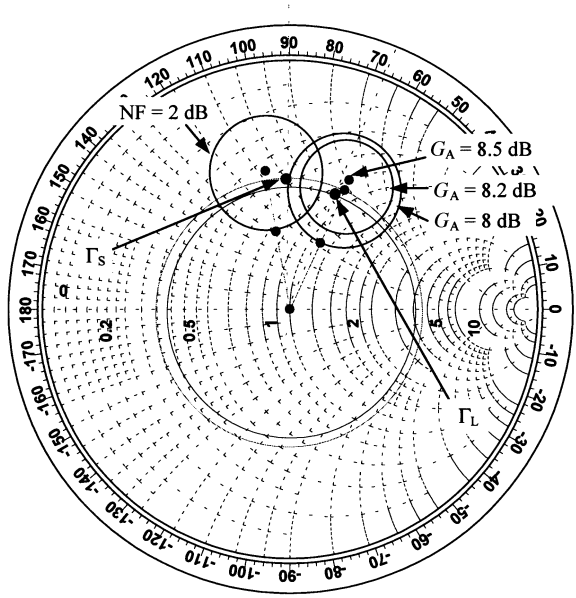

Figure 10.29 Available power gain circles and RF circuit design for Example 10.12(b).

Further, the maximum possible available power gain is found to be 8.5 dB. It represents a point at $0.5722\angle 64.76^\circ$. The noise circle stays the same as in (a) above. These circles are drawn on a Smith chart as shown in Figure 10.29. If we select Γ_S as $0.535\angle 90^\circ$ then the noise figure stays well below 2 dB. The corresponding output reflection coefficient is found to be $0.5041\angle -67.83^\circ$. Hence, the load reflection coefficient must be $0.5041\angle 67.83^\circ$. Now, the input and output matching networks can be easily designed. The transducer power gain of this circuit is found from (9.4.8) to be 8 dB.

A comparison of the gain obtained in (b) with that in (a) shows that the two differ by 0.76 dB. However, the uncertainty predicted in (a) is about ± 0.5 dB. The 8.2-dB gain circle shown in Figure 10.29 indicates that the gain in (b) can be increased to a little over 8.2 dB. That will bring the two values within the predicted range.

Example 10.13: An Avantek low-noise silicon bipolar transistor, AT-41410, is biased at $V_{CE} = 8$ V and $I_C = 10$ mA. Its scattering and noise parameters are measured at 1 GHz with a 50-Ω system. The results are found as follows:

$$S_{11} = 0.6\angle -163^\circ, \quad S_{21} = 7.12\angle 86^\circ, \quad S_{12} = 0.039\angle 35^\circ,$$
$$S_{22} = 0.5\angle -38^\circ, \quad F_{\min} = 1.3 \text{ dB}, \quad R_n = 8\ \Omega, \text{ and } \Gamma_{opt} = 0.06\angle 49^\circ$$

Design the input and output matching networks of an amplifier that provides a power gain of 16 dB with noise figure less than 2.5 dB.

From (10.1.16) and (10.1.18),

$$|\Delta| = 0.1892$$

and,

$$k = 0.7667$$

Hence, the transistor is potentially unstable.

The input stability circle is determined from (10.1.22) and (10.1.23) as follows:

$$C_S = 1.7456\angle 171.69^\circ$$

and,

$$r_S = 0.8566$$

Since $|C_S|$ is larger than r_S, this circle does not enclose the center of the Smith chart ($\Gamma_S = 0$). Further, the output reflection coefficient Γ_{out} is equal to S_{22} for $\Gamma_S = 0$. Hence, $|\Gamma_{out}|$ is 0.5 at this point and provides a stable circuit with this transistor. Therefore, the stability circle encloses the unstable region (i.e., the inside is unstable).

Similarly, the output stability circle is found from (10.1.20) and (10.1.21) as follows:

$$C_L = 2.1608\angle 50.8^\circ$$

and,

$$r_L = 1.2965$$

Again, the center of the Smith chart ($\Gamma_L = 0$) is outside this circle because $|C_L|$ is larger than r_L. Since input reflection coefficient Γ_{in} is equal to S_{11} at this point, $|\Gamma_{in}|$ is 0.6. Hence, it represents load impedance that will provide a stable operation for this transistor. Therefore, all impedances on the Smith chart that are outside the stability circle represent the stable region and those enclosed by the stability circle are unstable.

Since the transistor is bilateral and we want a noise figure below 2.5 dB, we use the available power gain approach. The 16-dB gain circle is found from (10.3.14)

and (10.3.15) as follows:

$$c_a = 0.3542\angle 171.69^\circ$$

and,

$$R_a = 0.6731$$

The 2.5-dB noise figure circle is found from (10.4.6) and (10.4.7) as follows:

$$C_{NF} = 0.0346\angle 40^\circ$$

and,

$$R_{NF} = 0.6502$$

These circles are drawn on the Smith chart as illustrated in Figure 10.30. If we select Γ_S at point B ($\Gamma_S = 0.13\angle 0^\circ$) then Γ_{out} is found to be $0.469\angle -36.45^\circ$. Hence, the load reflection coefficient Γ_L must be equal to $0.469\angle 36.45^\circ$ (point D).

For an input-side network, we can move from point E to A on the unity resistance circle by adding a normalized reactance of about $-j0.55$ (i.e., $-j27.5\,\Omega$) in series

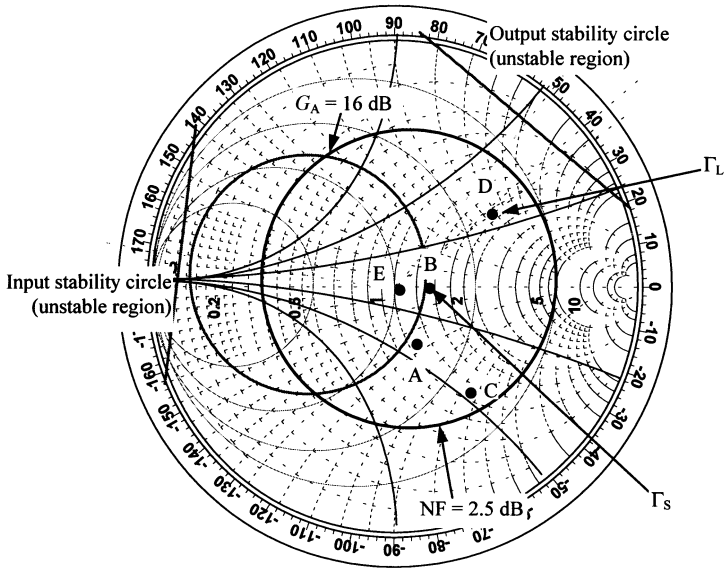

Figure 10.30 Design of input and output matching networks for Example 10.13.

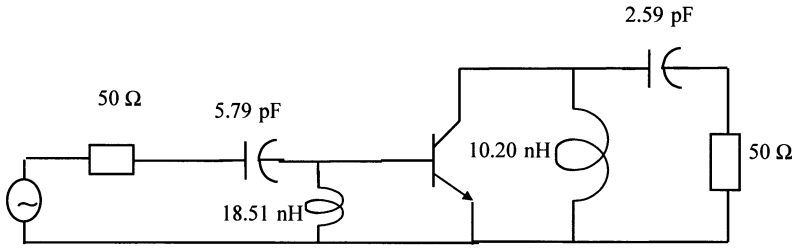

Figure 10.31 RF circuit for Example 10.13.

with 50 Ω. It requires a capacitor of 5.7874 pF at 1 GHz. We then move on the conductance circle of 0.77 to reach point B from A. It means that we need a normalized susceptance of $-j0.43$ (i.e., $-j0.0086$ S). Hence, an inductor of 18.5064 nH connected in shunt will suffice.

Similarly, an output matching network can be designed following the path from E to C on the unity resistance circle and then from C to D along the conductance circle of 0.4. It requires a series reactance of about $-j1.23$ (i.e., $-j61.5\,\Omega$) and then a shunt susceptance of approximately $-j0.78$ (i.e., $-j0.0156$ S). Hence, a capacitor of 2.59 pF in series with the 50-Ω load and then a shunt inductor of 10.20 nH are needed, as illustrated in Figure 10.31.

10.5 BROADBAND AMPLIFIERS

Signals carrying information generally possess a finite bandwidth, and therefore, the electronics employed to process such signals need to have characteristics constant over that bandwidth. The amplifier designs presented in preceding sections are valid only at a single frequency. This is mainly because the design of matching networks is frequency sensitive and governed by the Bode-Fano constraints discussed in Chapter 6. Some of the techniques used to broaden the bandwidth of amplifiers are summarized below.

Resistive Matching

As discussed in Chapter 5 (section 5.3), the resistive matching networks are independent of frequency and hence can be used to design broadband amplifiers. The upper limit will be determined from the frequencies when the resistances cease to work due to associated parasitic elements. Further, the noise figure of such amplifiers may be unacceptable.

Compensating Networks

Since the reactance of a capacitor is inversely related with frequency, it will have a higher value at lower frequencies in comparison with the higher end of the band. On

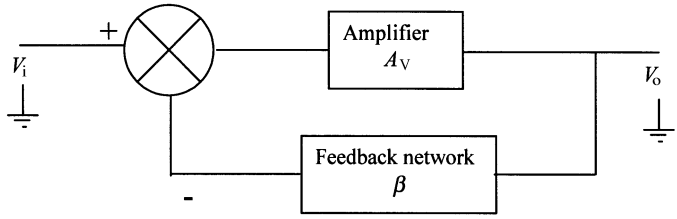

Figure 10.32 Simplified feedback system for an amplifier.

the other hand, the inductive reactance exhibits a direct relation with frequency, providing low reactance at the lower end of the band. Hence, these components can be used to devise compensating networks that are effective at the two edges of the frequency band. However, the design may be too complex and can adversely affect matching at the input and the output.

Negative Feedback

Negative feedback can widen the bandwidth of amplifier and improve the matching at its input and output. However, the gain of the amplifier is reduced and also it may adversely affect the noise figure unless another relatively low-noise amplifier is added in the forward path before the original amplifier. Figure 10.32 illustrates a simplified feedback arrangement of the amplifier. If V_i and V_o are voltages at its input and output, respectively, A_v is voltage gain of the amplifier, and β is the transfer function of the feedback network, then we can write

$$V_o = (V_i - \beta V_o)A_V \tag{10.5.1}$$

Rearranging this equation we find that

$$\frac{V_o}{V_i} = G_V = \frac{A_V}{1 + A_V\beta} \tag{10.5.2}$$

Since the voltage-gain characteristic of the amplifier at higher frequencies can be expressed as follows:

$$A_V = \frac{A_o}{1 + j\dfrac{f}{f_c}} \tag{10.5.3}$$

G_V is found to be

$$G_V = \frac{\dfrac{A_o}{1 + A_o\beta}}{1 + j\dfrac{f}{f_c(1 + A_o\beta)}} \tag{10.5.4}$$

A_o is the mid-band voltage gain; f_c is the corner frequency (3-dB frequency), and f is the signal frequency in Hz.

From (10.5.4), the new corner frequency, f_c', is found as

$$f_c' = f_c(1 + A_o\beta) \tag{10.5.5}$$

Hence, the cutoff frequency of the overall gain is increased by a factor of $(1 + A_o\beta)$. However, the new mid-band voltage gain, as given below, is also reduced by the same factor. Thus, the gain-bandwidth product of the circuit remains the same.

$$A_o' = \frac{A_o}{1 + A_o\beta} \tag{10.5.6}$$

Balanced Circuits

Another way to improve the matching over wider bandwidth is illustrated in Figure 10.33. It employs two amplifiers in conjunction with two 90°-hybrid junctions. An ideal 90°-hybrid splits its input power equally in the forward direction while there is no power coupling to its fourth port. Further, the branched-out signal lags behind the direct path by 90°. Hence, the power input at port-3 of the first hybrid junction appears at port-1 and port-2 while it is not coupled at all to port-4. Similarly, the signal entering into port-1 divides equally between port-4 ($\angle -90°$) and port-3 ($\angle 0°$).

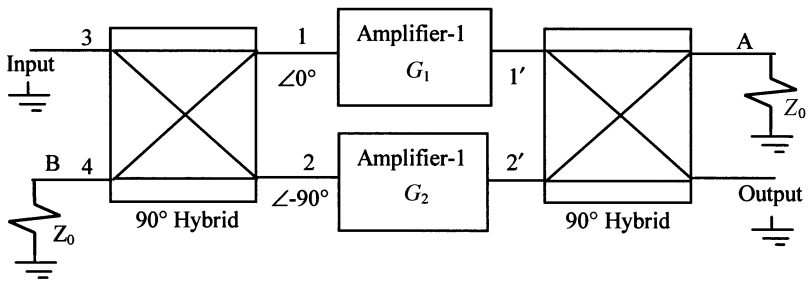

Figure 10.33 Block diagram of a balanced amplifier.

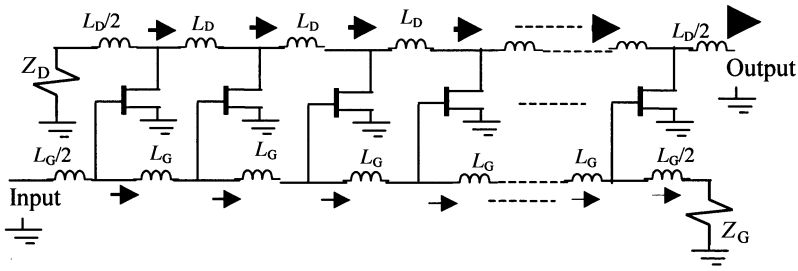

Figure 10.34 Schematic circuit of a traveling wave amplifier.

Now assume that the two amplifiers in Figure 10.33 have identical input impedance. Signals fed to these amplifiers have the same magnitudes but a phase difference of 90°. Therefore, the signals reflected back would have identical magnitudes but maintain the phase difference. The reflected signals enter port-1 and port-2, and split with equal powers at port-3 and port-4. Thus, two signals appearing back at port-3 are equal in magnitude but 180° out of phase with respect to each other and, therefore, cancel out. On the other hand, signals appearing at port-4 are in phase (since both went through the 90° delay). However, port-4 is matched terminated and this power is dissipated. Signals amplified by the two amplifiers are fed to a second hybrid that is matched terminated at port-A. Signals entering at its ports 1′ and 2′ appear at the output (only 50% power of each channel) while canceling out at port-A. Thus, the overall gain of an ideal balanced amplifier is equal to that of an amplifier connected in one of its channels.

Traveling Wave Amplifiers

Traveling wave amplifiers (also known as *distributed amplifiers*) use discrete transistors in a distributed manner, as illustrated in Figure 10.34. In this technique, lumped inductors form artificial transmission lines in conjunction with input and output capacitance of the transistors. The input signal travels through the gate line that is terminated by impedance Z_G at the end. An amplified signal is available via the drain line that is terminated by impedance Z_D at its other end. This arrangement provides the possibility of increasing the gain-bandwidth product of the amplifier.

The gate of each FET taps off the input signal traveling along the gate line and transfers it to the drain line through its transconductance. The remaining input signal is dissipated in terminating impedance Z_G. The drain line parameters are selected in such a way that the amplified signals available from each transistor are added in a forward traveling wave and an amplified signal is available at the output. This happens when the phase velocities on the drain and gate lines are same. Any signal propagating on the drain line in the opposite direction is dissipated in Z_D.

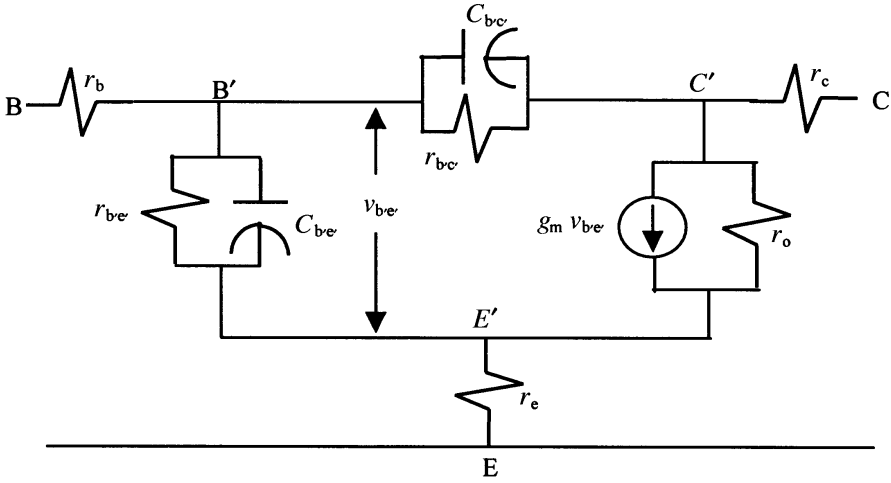

Figure 10.35 Small-signal equivalent circuit of a BJT.

10.6 SMALL-SIGNAL EQUIVALENT CIRCUIT MODELS OF TRANSISTORS

Bipolar Junction Transistor (BJT)

Figure 10.35 illustrates a small-signal equivalent model of the BJT. In this circuit, r_b is the resistance between its base terminal and the apparent base. It is created because of low doping of the base. $C_{b'e'}$ represents diffusion capacitance C_D and junction capacitance C_{je} connected in parallel; $r_{b'e'}$ is the resistance at the emitter-base junction while $r_{b'c'}$ is the resistance at the base-collector junction. $C_{b'c'}$ is capacitance between base and collector; r_c represents the collector resistance because the collector is lightly doped; r_o is output resistance representing the finite slope of its $I_c - V_{CE}$ characteristics. Ideally, r_o will be infinite. The resistance r_e represents emitter resistance, and g_m is the transconductance. Various parameters

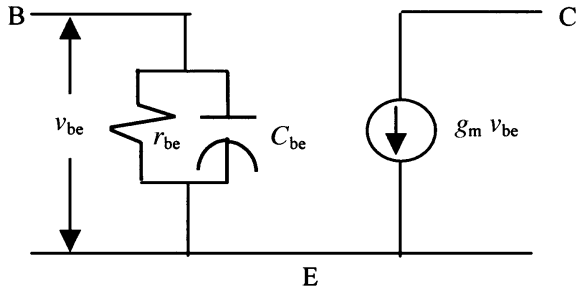

Figure 10.36 Simplified small-signal equivalent circuit of a BJT.

are related as follows:

$$\beta = h_{FE} = \frac{I_C}{I_B} \tag{10.6.1}$$

$$\alpha = \frac{I_C}{I_E} = \frac{\beta}{1+\beta} \tag{10.6.2}$$

$$g_m = \left.\frac{\delta i_C}{\delta v_{b'e'}}\right|_{V_{CE}} = \frac{q_e I_C}{kT} \tag{10.6.3}$$

$$r_{b'e'} = \left[\left.\frac{\delta i_b}{\delta v_{EB}}\right|_{V_{BC}}\right]^{-1} = \frac{\beta}{g_m} \tag{10.6.4}$$

$$r_{b'c'} = \left[\left.\frac{\delta i_b}{\delta v_{EC}}\right|_{V_{EB}}\right]^{-1} \approx \infty \tag{10.6.5}$$

$$C_{b'c'} = \frac{C_{b'c'o}}{\left[1 - \dfrac{v_{CB}}{V_{BIP}}\right]^m} \tag{10.6.6}$$

$$C_{je} = \frac{C_{jeo}}{\left[1 - \dfrac{v_{EB}}{V_{BIP}}\right]^m} \tag{10.6.7}$$

and,

$$C_D = \frac{q_e I_E}{kT}\tau_e \tag{10.6.8}$$

I_C, I_B, and I_E are collector, base, and emitter currents, respectively. T is temperature in K; q_e is electronic charge, and k is the Boltzmann constant. $C_{b'c'o}$ is zero-biased capacitance; V_{BIP} is built-in potential of the base-collector junction; m is equal to $\frac{1}{2}$ for uniform doping and 1/3 for graded doping. τ_e is the base transit time. A simplified small-signal equivalent of the BJT is shown in Figure 10.36.

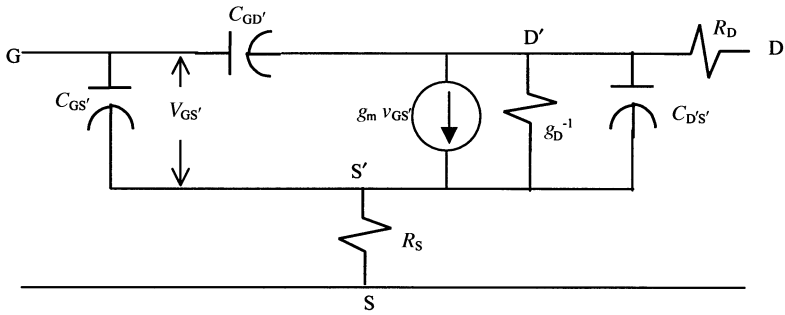

Figure 10.37 Small-signal equivalent circuit of a MOSFET.

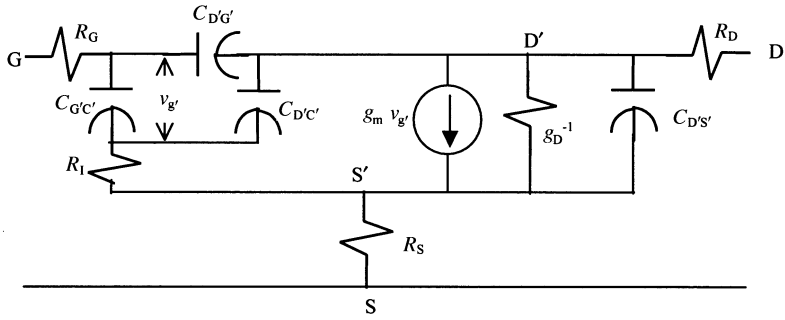

Figure 10.38 Small-signal equivalent circuit of a MESFET.

Metal-Oxide-Semiconductor Field-Effect Transistor (MOSFET)

The small-signal equivalent circuit of a MOSFET is illustrated in Figure 10.37. It is assumed that both the source and the substrate are grounded. R_s and R_D are the series resistance at the source and the drain, respectively. The oxide overlay gives rise to capacitance that degrades the high-frequency performance. It includes the source-gate and the drain-gate capacitances. $C_{GS'}$ and $C_{GD'}$ represent these as well as respective parasitic capacitances. $C_{D'S'}$ includes the capacitance between drain and substrate. Drain conductance g_D and transconductance g_m are defined as follows:

$$g_D = \left.\frac{\partial I_D}{\partial V_D}\right|_{V_G=\text{constant}} \tag{10.6.9}$$

and,

$$g_m = \left.\frac{\partial I_D}{\partial V_G}\right|_{V_D=\text{constant}} \tag{10.6.10}$$

Metal-Semiconductor Field-Effect Transistors (MESFET)

The small-signal equivalent circuit of a MESFET is illustrated in Figure 10.38. R_G, R_S, and R_D represent the extrinsic parasitic resistances that are in series with the gate, the source, and the drain, respectively. $C_{D'S'}$ is the drain-source capacitance. Transconductance g_m and drain conductance g_D are as defined earlier. R_I is the channel resistance that is responsible for a finite charging time to capacitor $C_{G'C'}$ between the gate and the channel. $C_{D'C'}$ represents the drain-to-channel capacitance.

10.7 DC BIAS CIRCUITS FOR TRANSISTORS

Transistor circuits require dc bias that provides the desired quiescent point. Further, it should hold the operation stable over a range of temperatures. Resistive circuits

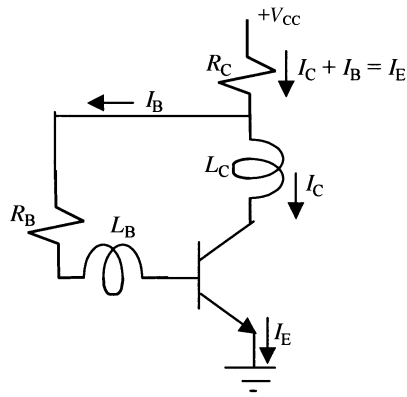

Figure 10.39 Transistor bias circuit with voltage feedback.

used at lower frequencies can be employed in the RF range as well. However, sometimes these circuits may not work satisfactorily at higher frequencies. For example, a resistance in parallel with a bypass capacitor is frequently used at the emitter to provide stable operation at lower frequencies. This circuit may not work at microwave frequencies because it can produce oscillation. Further, the resistance in an amplifier circuit can degrade the noise figure. Active bias networks provide certain advantages over the resistive circuits.

Figure 10.39 illustrates a resistive bias network with voltage feedback. Inductors L_C and L_B are used to block RF from going toward R_C and R_B. At the same time, dc bias passes through them to respective terminals of BJT without loss (assuming that the inductors have zero resistance). If V_{BE} represents base-emitter voltage of the transistor then

$$V_{BE} + R_B I_B + R_C I_E = V_{CC} \tag{10.7.1}$$

Since

$$I_B = I_E - I_C = (1 - \alpha) I_E = \frac{I_E}{1 + \beta} \tag{10.7.2}$$

(10.7.1) can be written as follows:

$$I_E = \frac{V_{CC} - V_{BE}}{R_C + \dfrac{R_B}{1 + \beta}} \tag{10.7.3}$$

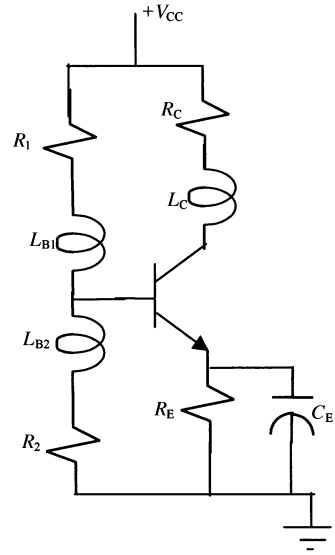

Figure 10.40 Transistor bias circuit with emitter bypassed resistor.

For I_E to be less sensitive to changes in V_{BE} and β, the following conditions must be satisfied:

$$V_{CC} \gg V_{BE} \tag{10.7.4}$$

and,

$$R_C \gg \frac{R_B}{1+\beta} \tag{10.7.5}$$

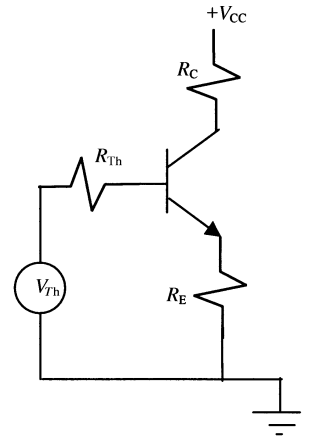

Figure 10.41 An equivalent of the circuit shown in Figure 10.40.

Hence, it is advisable to use high V_{CC} and R_C. However, there are practical limitations. Another option is to use a small R_B, but it will limit V_{CE} and, therefore, the swing in output. It is up to the circuit designer to weigh these options of the trade-off and to pick the components accordingly.

An alternative biasing network that uses a bypassed resistor at the emitter is illustrated in Figure 10.40. As before, inductors L_C, L_{B1}, and L_{B2} are used to block the RF. On the other hand, capacitor C_E is used to bypass RF. Figure 10.41 shows the Thevenin equivalent of this circuit for the dc condition where

$$V_{Th} = \frac{R_2}{R_1 + R_2} V_{CC} \tag{10.7.6}$$

and,

$$R_{Th} = \frac{R_1 R_2}{R_1 + R_2} \tag{10.7.7}$$

From the equivalent circuit shown in Figure 10.41,

$$V_{Th} = R_{Th} I_B + V_{BE} + R_E I_E = \left(\frac{R_{Th}}{1 + \beta} + R_E \right) I_E + V_{BE} \tag{10.7.8}$$

Hence,

$$I_E = \frac{V_{Th} - V_{BE}}{R_E + \dfrac{R_{Th}}{1 + \beta}} \tag{10.7.9}$$

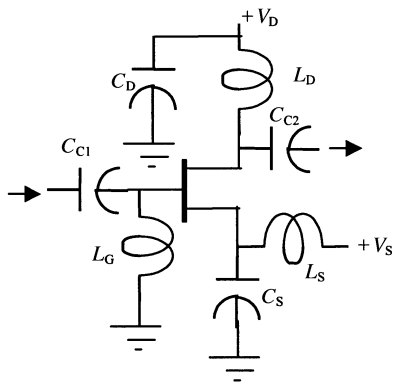

Figure 10.42 A bias circuit employing two unipolar (positive) dc sources.

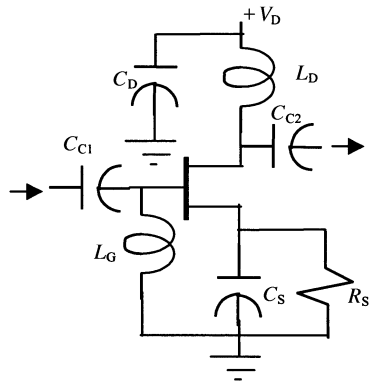

Figure 10.43 Transistor bias circuit employing a single power supply.

Therefore, the following conditions must be met for stable I_E:

$$V_{Th} \gg V_{BE} \tag{10.7.10}$$

and,

$$R_E \gg \frac{R_{Th}}{1+\beta} \tag{10.7.11}$$

Note that for a fixed V_{CC}, V_{Th} cannot be increased arbitrarily because it reduces V_{CB} and hence V_{CE}. Smaller V_{CE} means limited output swing. Further, large R_E will reduce V_{CE} as well. On the other hand, smaller R_{Th} will mean low input impedance of the circuit. It is up to the circuit designer to work within these contradictory requirements. As a rule of thumb, V_{Th} is selected no more than 15 to 20 percent of V_{CC}.

For a low-noise and low-power design, the drain current of the MESFET is selected around 0.15 I_{DSS} (I_{DSS} is the drain current in the saturation region with $V_{GS} = 0$) and V_{DS} just enough to keep it in saturation. A higher drain current point (generally around 0.95 I_{DSS}) is selected for low-noise, high-power design. Higher V_{DS} is used for high-efficiency and high-power applications. Figure 10.42 shows a bias circuit that requires a dual positive power supply. V_S is applied to the source terminal of the MESFET via inductor L_S. Capacitor C_S grounds the source at RF while L_S blocks it from the dc supply. Inductor L_G grounds the gate for dc while stopping the RF. Similarly, bias voltage V_D is applied to the drain terminal via inductor L_D. However, it stops the RF from going toward the bias supply that is further ensured by capacitor C_D. This circuit is recommended for low-noise, high-gain, high-power, and high-efficiency applications.

Another bias circuit that requires only a single power supply is illustrated in Figure 10.43. Voltage drop across R_S is applied to the gate via inductor L_G. This resistance can also be used to adjust the gain of this circuit. As mentioned earlier, it will be generating thermal noise as well.

Note that a quarter-wavelength-long line with a short circuit at one end can replace the RF-blocking inductors. The short circuit is generally achieved via a capacitor connected across the dc power supply.

SUGGESTED READING

I. J. Bahl and P. Bhartia, *Microwave Solid State Circuit Design*. New York: Wiley, 1988.

R. E. Collin, *Foundations for Microwave Engineering*. New York: McGraw Hill, 1992.

W. A. Davis, *Microwave Semiconductor Circuit Design*. New York: Van Nostrand Reinhold, 1984.

G. Gonzalez, *Microwave Transistor Amplifiers*. Englewood Cliffs, NJ: Prentice Hall, 1997.

D. M. Pozar, *Microwave Engineering*. New York: Wiley, 1998.

G. D. Vendelin, A. Pavio, and U. L. Rhode, *Microwave Circuit Design Using Linear and Nonlinear Techniques*. New York: Wiley, 1990.

E. A. Wolff and R. Kaul, *Microwave Engineering and Systems Applications*. New York: Wiley, 1988.

PROBLEMS

1. S-parameters of a certain microwave transistor are measured at 3 GHz with a 50-Ω reference resistance and found as

$$S_{11} = 0.505\angle -150^\circ, \quad S_{12} = 0,$$
$$S_{21} = 7\angle 180^\circ, \text{ and } S_{22} = 0.45\angle -20^\circ$$

Calculate the maximum unilateral power gain and design an amplifier using this transistor for maximum power gain.

2. NE868495-4 GaAs power FET has the following S-parameters measured at $V_{ds} = 9\,\text{V}$ and $I_{ds} = 600\,\text{mA}$ at 5 GHz with a 50-Ω line:

$$S_{11} = 0.45\angle 163^\circ, \quad S_{12} = 0.04\angle 40^\circ,$$
$$S_{21} = 2.55\angle -106^\circ, \text{ and } S_{22} = 0.46\angle -65^\circ$$

Use this transistor to design an amplifier for the maximum power gain at 5 GHz.

3. Design an amplifier for maximum possible gain at 600 MHz, using a M/ACOM MA4T64435 bipolar junction transistor in the common-emitter configuration.

Its S-parameters, measured at $V_{CE} = 8\,\text{V}$ and $I_C = 10\,\text{mA}$ ($Z_o = 50\,\Omega$), are as follows:

$$S_{11} = 0.514\angle -101^\circ, \quad S_{21} = 9.562\angle 112.2^\circ,$$
$$S_{12} = 0.062\angle 49^\circ, \text{ and } S_{22} = 0.544\angle -53^\circ$$

Calculate the gain in dB for your circuit.

4. Design an amplifier for a maximum possible transducer power gain at 2 GHz, using an Avantek ATF-45171 GaAs FET with following common-source S-parameters measured at $V_{DS} = 9\,\text{V}$ and $I_{DS} = 250\,\text{mA}$ ($Z_o = 50\,\Omega$):

$$S_{11} = 0.83\angle -137^\circ, \quad S_{21} = 3.45\angle 83^\circ,$$
$$S_{12} = 0.048\angle 19^\circ, \text{ and } S_{22} = 0.26\angle -91^\circ$$

Calculate the gain in dB for your circuit.

5. NE720 GaAs MESFET biased at $V_{ds} = 4\,\text{V}$ and $I_{ds} = 30\,\text{mA}$ has the following S-parameters at 4 GHz:

$$S_{11} = 0.70\angle -127^\circ, \quad S_{12} = 0,$$
$$S_{21} = 3.13\angle 76^\circ, \text{ and } S_{22} = 0.47\angle -30^\circ$$

Plot (a) the input constant gain circles for 3, 2, 1, 0, −1, and −2 dB, and (b) the output constant gain circles for the same decibel levels.

6. NE41137 GaAs FET has the following S-parameters measured at $V_{ds} = 5\,\text{V}$ and $I_{ds} = 10\,\text{mA}$ at 3 GHz with a 50-Ω resistance:

$$S_{11} = 038\angle -169^\circ, \quad S_{12} = 0,$$
$$S_{21} = 1.33\angle -39^\circ, \text{ and } S_{22} = 0.95\angle -66^\circ$$

Design an amplifier using this transistor for a power gain of 6 dB.

7. An Avantek ATF-13036 GaAs FET in common-source configuration has the following S-parameters measured at $V_{DS} = 2.5\,\text{V}$ and $I_{DS} = 20\,\text{mA}$ at 6 GHz with a 50-Ω line:

$$S_{11} = 0.55\angle -137^\circ, \quad S_{21} = 3.75\angle 52^\circ,$$
$$S_{12} = 0.112\angle 14^\circ, \text{ and } S_{22} = 0.3\angle -80^\circ$$

Design an amplifier using this transistor for an available power gain of 10 dB.

8. NE868898-7 GaAs FET has the following S-parameters measured at $V_{ds} = 9\,\text{V}$ and $I_{ds} = 1.2\,\text{A}$ at 7 GHz:

$$S_{11} = 0.42\angle 155^\circ, \quad S_{12} = 0.13\angle -10^\circ,$$
$$S_{21} = 2.16\angle 25^\circ, \text{ and } S_{22} = 0.51\angle -70^\circ$$

(a) Draw the input and output stability circles if the transistor is potentially unstable.

(b) Find the maximum operating power gain.

(c) Plot the power-gain circles for 8 and 6 dB.

9. The DXL 3503A (chip) Ku-band medium-power GaAs FET has the following S-parameters measured at $V_{ds} = 6\,\text{V}$ and $I_{ds} = 0.5I_{dss}$ at 18 GHz with a 50-Ω line:

$$S_{11} = 0.64\angle -160^\circ, \quad S_{12} = 0.08\angle 127^\circ,$$
$$S_{21} = 0.81\angle 23^\circ, \text{ and } S_{22} = 0.77\angle -78^\circ$$

This transistor is to be used for a high-gain amplifier. Design the input and output matching networks using balanced stubs for a maximum possible power gain at 18 GHz.

10. A M/ACOM BJT, MA4T64433 in common-emitter configuration has the following S-parameters measured at $V_{CE} = 8\,\text{V}$ and $I_C = 25\,\text{mA}$ at 1 GHz with a 50-Ω line:

$$S_{11} = 0.406\angle -155^\circ, \quad S_{21} = 6.432\angle 89.6^\circ,$$
$$S_{12} = 0.064\angle 53.1^\circ, \text{ and } S_{22} = 0.336\angle -57.1^\circ$$

Design an amplifier using this transistor for an available power gain of 10 dB.

11. The S-parameters of a BJT at 2 GHz in a 50-Ω system are:

$$S_{11} = 1.5\angle -100^\circ, \quad S_{21} = 5.0\angle 50^\circ,$$
$$S_{12} = 0.0\angle 0^\circ, \text{ and } S_{22} = 0.9\angle -60^\circ$$

(a) Calculate the input impedance and the optimum output termination.

(b) Determine the unstable region on the Smith chart and construct constant gain circles for $G_s = 3\,\text{dB}$ and $G_s = 4\,\text{dB}$.

(c) Design the input matching network for $G_s = 4\,\text{dB}$ with the greatest degree of stability.

(d) Determine G_{TU} in dB for your design.

12. An Avantek low-noise silicon bipolar transistor, AT-41470, has the following S-parameters measured at $V_{CE} = 8\,\text{V}$ and $I_C = 25\,\text{mA}$ at 100 MHz with a 50-Ω line:

$$S_{11} = 0.64\angle -62^\circ, \quad S_{21} = 42.11\angle 147^\circ, \quad S_{12} = 0.009\angle 75^\circ,$$
$$S_{22} = 0.85\angle -19^\circ, \quad F_{\min} = 1.2\ \text{dB}, \quad \Gamma_{\text{opt}} = 0.12\angle 5^\circ, \text{ and } R_n = 8.5\ \Omega$$

Design input and output matching networks of the amplifier for $G_T = 35\,\text{dB}$ and a low-noise figure of 2 dB. For design purposes, assume that the device is unilateral, and calculate the maximum error in G_T resulting from this assumption.

13. An Avantek low-noise GaAs FET, ATF-13100 has the following S-parameters measured at $V_{DS} = 2.5\,\text{V}$ and $I_{DS} = 20\,\text{mA}$ at 4 GHz with a 50-Ω line:

$$S_{11} = 0.85\angle -58^\circ, \quad S_{21} = 4.54\angle 126^\circ, \quad S_{12} = 0.085\angle 59^\circ,$$
$$S_{22} = 0.49\angle -33^\circ, \quad F_{\min} = 0.5\ \text{dB}, \quad \Gamma_{\text{opt}} = 0.60\angle 30^\circ, \text{ and } R_n = 16\ \Omega$$

Design input and output matching networks of the amplifier for $G_T = 12\,\text{dB}$ and a low-noise figure of 2 dB. For design purposes, assume that the device is unilateral, and calculate the maximum error in G_T resulting from this assumption.

14. HP HXTR-6101 microwave transistor has the following parameters measured at 4 GHz with a reference resistance of 50-Ω:

$$\text{Minimum noise figure} = 2.5\ \text{dB}, \quad \Gamma_{\text{opt}} = 0.475\angle 155^\circ, \text{ and } R_n = 3.5\ \Omega$$

Plot the noise-figure circles for given values of F at 2.5, 3.0, 3.5, 4.0, and 5.0 dB.

15. A transistor has the following parameters:

$$S_{11} = 0.5\angle 160^\circ, \quad S_{12} = 0.06\angle 50^\circ, \quad S_{21} = 3.6\angle 60^\circ, \quad S_{22} = 0.5\angle -45^\circ,$$
$$\Gamma_{\text{opt}} = 0.4\angle 145^\circ, \quad R_n = 0.4 \text{ ohm, and } F_{\min} = 1.6\ \text{dB}$$

Design an amplifier with the best possible noise figure for a power gain of 10 dB. Also, the VSWR on either side should be less than 2.

16. A DXL 1503A-P70 X-band low-noise GaAs FET is biased at $V_{ds} = 3.5\,\text{V}$ and $I_{ds} = 12\,\text{mA}$. Its S-parameters are measured at 12 GHz with a 50-Ω line as follows:

$$S_{11} = 0.48\angle -130^\circ, \ S_{12} = 0.01\angle 92^\circ, \ S_{21} = 2.22\angle 75^\circ, \ S_{22} = 0.52\angle -65^\circ$$
$$\Gamma_{\text{opt}} = 0.45\angle 175^\circ, \quad R_n = 3.5\ \Omega, \text{ and } F_{\min} = 2.5\ \text{dB}$$

Design input and output matching networks using discrete components for a maximum amplifier gain of 9 dB and a low-noise figure of 3 dB.

Radio-Frequency and Microwave Communication Circuits: Analysis and Design
Devendra K. Misra

ISBNs: 0-471-41253-8 (Hardback); 0-471-22435-9 (Electronic)

11

OSCILLATOR DESIGN

Oscillator circuits are used for generating the periodic signals that are needed in various applications. These circuits convert a part of dc power into the periodic output and do not require a periodic signal as input. This chapter begins with the basic principle of sinusoidal oscillator circuits. Several transistor circuits are subsequently analyzed in order to establish their design procedures. Ceramic resonant circuits are frequently used to generate reference signals while the voltage-controlled oscillators are important in modern frequency synthesizer design using the phase-lock loop. Fundamentals of these circuits are discussed in this chapter. Diode-oscillators used at microwave frequencies are also summarized. The chapter ends with a description of the microwave transistor circuits using S- parameters.

11.1 FEEDBACK AND BASIC CONCEPTS

Solid-state oscillators use a diode or a transistor in conjunction with the passive circuit to produce sinusoidal steady-state signals. Transients or electrical noise triggers oscillations initially. A properly designed circuit sustains these oscillations subsequently. This process requires a nonlinear active device. In addition, since the device is producing RF power, it must have a negative resistance.

The basic principle of an oscillator circuit can be explained via a linear feedback system as illustrated in Figure 11.1. Assume that a part of output Y is fed back to the system along with input signal X. As indicated, the transfer function of the forward-

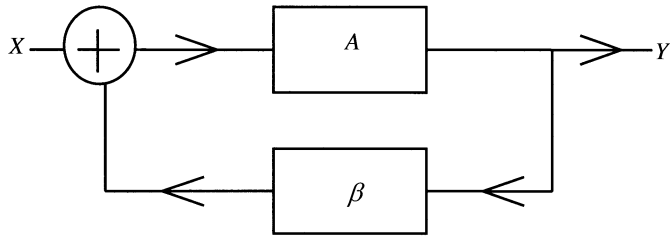

Figure 11.1 A simple feedback system.

connected subsystem is A while the feedback path has a subsystem with its transfer function as β. Therefore,

$$Y = A(X + \beta Y)$$

Closed-loop gain T (generally called the *transfer function*) of this system is found from this equation as

$$T = \frac{Y}{X} = \frac{A}{1 - A\beta} \tag{11.1.1}$$

Product $A\beta$ is known as the *loop gain*. It is a product of the transfer functions of individual units in the loop. Numerator A is called the *forward path gain* because it represents the gain of a signal traveling from input to output.

For the loop gain of unity, T becomes infinite. Hence, the circuit has an output signal Y without an input signal X and the system oscillates. The condition, $A\beta = 1$, is known as the *Barkhausen criterion*. Note that if the signal $A\beta$ is subtracted from X before it is fed to A then the denominator of (11.1.1) changes to $1 + A\beta$. In this case, the system oscillates for $A\beta = -1$. This is known as the *Nyquist criterion*. Since the output of an amplifier is generally 180° out of phase with its input, it may be a more appropriate description for that case.

A Generalized Oscillator Circuit

Consider a transistor circuit as illustrated in Figure 11.2. Device T in this circuit may be a bipolar transistor or a FET. If it is a BJT then terminals 1, 2, and 4 represent the base, emitter, and collector, respectively. On the other hand, these may be the gate, source, and drain terminals if it is a FET. Its small-signal equivalent circuit is shown in Figure 11.3. The boxed part of this figure represents the transistor's equivalent, with g_m being its transconductance, and Y_{i} and Y_{o} its input and output admittances, respectively.

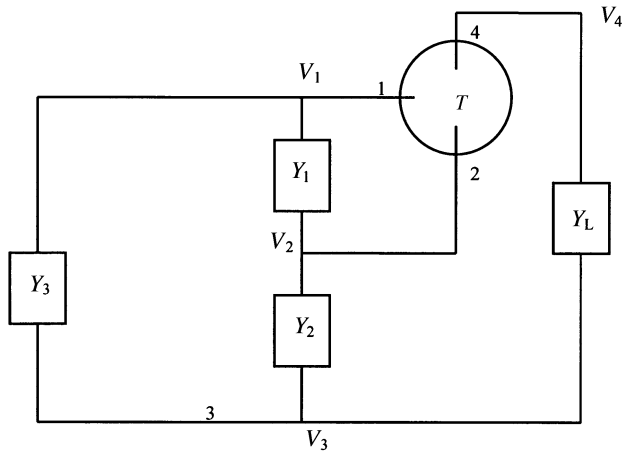

Figure 11.2 A schematic oscillator circuit.

Application of Kirchhoff's current law at nodes 1, 2, 3, and 4 gives

$$Y_3(V_1 - V_3) + Y_1(V_1 - V_2) + Y_i(V_1 - V_2) = 0 \tag{11.1.2}$$

$$-Y_1(V_1 - V_2) - Y_2(V_3 - V_2) - Y_i(V_1 - V_2) - g_m(V_1 - V_2) - Y_o(V_4 - V_2) = 0 \tag{11.1.3}$$

$$-Y_3(V_1 - V_3) - Y_2(V_2 - V_3) - Y_L(V_4 - V_3) = 0 \tag{11.1.4}$$

and

$$g_m(V_1 - V_2) + Y_o(V_4 - V_2) + Y_L(V_4 - V_3) = 0 \tag{11.1.5}$$

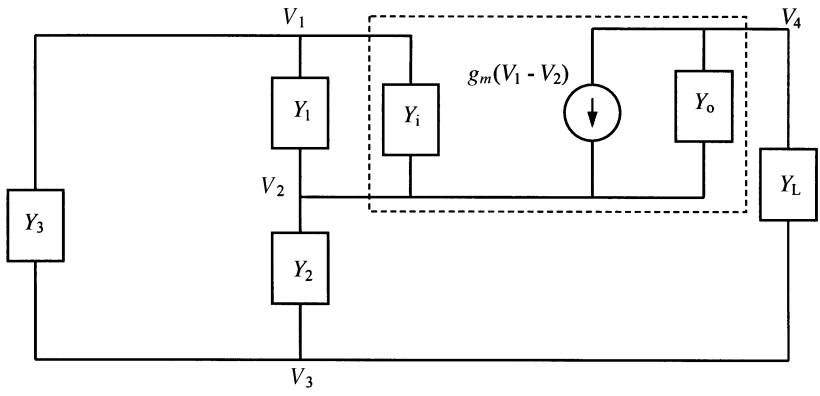

Figure 11.3 An electrical equivalent of the schematic oscillator circuit.

Simplifying (11.1.2)–(11.1.5), we have

$$(Y_1 + Y_3 + Y_\mathrm{i})V_1 - (Y_1 + Y_\mathrm{i})V_2 - Y_3V_3 = 0 \tag{11.1.6}$$

$$-(Y_1 + Y_\mathrm{i} + g_m)V_1 + (Y_1 + Y_2 + Y_\mathrm{i} + g_m + Y_\mathrm{o})V_2 - Y_2V_3 - Y_\mathrm{o}V_4 = 0 \tag{11.1.7}$$

$$-Y_3V_1 - Y_2V_2 + (Y_2 + Y_3 + Y_\mathrm{L})V_3 - Y_\mathrm{L}V_4 = 0 \tag{11.1.8}$$

and

$$g_mV_1 - (g_m + Y_\mathrm{o})V_2 - Y_\mathrm{L}V_3 + (Y_\mathrm{o} + Y_\mathrm{L})V_4 = 0 \tag{11.1.9}$$

These equations can be written in matrix form as follows:

$$\begin{bmatrix} (Y_1 + Y_3 + Y_\mathrm{i}) & -(Y_1 + Y_\mathrm{i}) & -Y_3 & 0 \\ -(Y_1 + Y_\mathrm{i} + g_m) & (Y_1 + Y_2 + Y_\mathrm{i} + g_m + Y_\mathrm{o}) & -Y_2 & -Y_\mathrm{o} \\ -Y_3 & -Y_2 & (Y_2 + Y_3 + Y_\mathrm{L}) & -Y_\mathrm{L} \\ g_m & -(g_m + Y_\mathrm{o}) & -Y_\mathrm{L} & (Y_\mathrm{o} + Y_\mathrm{L}) \end{bmatrix} \times \begin{bmatrix} V_1 \\ V_2 \\ V_3 \\ V_4 \end{bmatrix} = 0 \tag{11.1.10}$$

For a nontrivial solution to this system of equations, the determinant of the coefficient matrix must be zero. It sets constraints on the nature of circuit components that will be explained later.

Equation (11.1.10) represents the most general formulation. It can be simplified for specific circuits as follows:

1. If a node is connected to ground then that column and row are removed from (11.1.10). For example, if node 1 is grounded then the first row as well as the first column will be removed from (11.1.10).
2. If two nodes are connected together then the corresponding columns and rows of the coefficient matrix are added together. For example, if nodes 3 and 4 are connected together then rows 3 and 4 as well as columns 3 and 4 are replaced by their sums as follows:

$$\begin{bmatrix} (Y_1 + Y_3 + Y_\mathrm{i}) & -(Y_1 + Y_\mathrm{i}) & -Y_3 \\ -(Y_1 + Y_\mathrm{i} + g_m) & (Y_1 + Y_2 + Y_\mathrm{i} + g_m + Y_\mathrm{o}) & -(Y_2 + Y_\mathrm{o}) \\ -Y_3 + g_m & -(g_m + Y_2 + Y_\mathrm{o}) & (Y_2 + Y_3 + Y_\mathrm{o}) \end{bmatrix} \begin{bmatrix} V_1 \\ V_2 \\ V_3 \end{bmatrix} = 0 \tag{11.1.11}$$

If output impedance of the device is very high then Y_o is approximately zero. In this case, (11.1.11) can be simplified further. For a nontrivial solution, the determinant of its coefficient matrix must be zero. Hence,

$$\begin{vmatrix} (Y_1 + Y_3 + Y_i) & -(Y_1 + Y_i) & -Y_3 \\ -(Y_1 + Y_i + g_m) & (Y_1 + Y_2 + Y_i + g_m) & -Y_2 \\ -Y_3 + g_m & -(g_m + Y_2) & (Y_2 + Y_3) \end{vmatrix} = 0 \qquad (11.1.12)$$

For a common-emitter BJT (or a common-source FET) circuit, $V_2 = 0$, and therefore, row 2 and column 2 are removed from (11.1.12). Hence, it simplifies further as follows:

$$\begin{vmatrix} (Y_1 + Y_3 + Y_i) & -Y_3 \\ -Y_3 + g_m & (Y_2 + Y_3) \end{vmatrix} = 0 \qquad (11.1.13)$$

Therefore,

$$(Y_2 + Y_3)(Y_1 + Y_3 + Y_i) + Y_3(-Y_3 + g_m) = 0 \qquad (11.1.14)$$

or,

$$g_m Y_3 + Y_1 Y_2 + Y_2 Y_3 + Y_2 Y_i + Y_1 Y_3 + Y_3 Y_i = 0 \qquad (11.1.15)$$

If the input admittance $Y_i = G_i$ (pure real) and the other three admittances (Y_1, Y_2, and Y_3) are purely susceptive then (11.1.15) produces

$$g_m jB_3 - B_1 B_2 - B_2 B_3 + jB_2 G_i - B_1 B_3 + jB_3 G_i = 0 \qquad (11.1.16)$$

On separating its real and imaginary parts, we get

$$B_1 B_2 + B_2 B_3 + B_1 B_3 = 0 \qquad (11.1.17)$$

and,

$$g_m B_3 + B_2 G_i + B_3 G_i = 0 \qquad (11.1.18)$$

Equation (11.1.17) is satisfied only when at least one susceptance is different from the other two (i.e., if one is capacitive then other two must be inductive or vice versa). Similarly, (11.1.18) requires that B_2 and B_3 must be of different kinds. An exact relation between the two reactances can be established using (11.1.18) as follows:

$$(g_m + G_i)B_3 + G_i B_2 = 0 \qquad (11.1.19)$$

or

$$\left(\frac{g_m}{G_i}+1\right)B_3+B_2=0=B_2+(1+\beta)B_3 \tag{11.1.20}$$

or,

$$X_3=-(1+h_{fe})X_2 \tag{11.1.21}$$

Here, h_{fe} represents the small signal current gain of common-emitter circuit. It is given by

$$h_{fe}=g_m/G_i \tag{11.1.22}$$

Equation (11.1.21) indicates that if X_2 is an inductor then X_3 is a capacitor or vice versa.

Further, dividing (11.1.17) by $B_1B_2B_3$, the corresponding reactance relation is found as

$$X_1+X_2+X_3=0 \tag{11.1.23}$$

Hence, at least one of the reactance is different from the other two. That is, if X_3 is an inductor then the other two must be capacitors or vice versa. From (11.1.21) and (11.1.23),

$$X_1+X_2-(1+h_{fe})X_2=0 \tag{11.1.24}$$

or,

$$X_1=h_{fe}X_2 \tag{11.1.25}$$

Since h_{fe} is a positive number, X_1 and X_2 must be of the same kind.

If B_1 and B_2 are inductive then B_3 must be a capacitive susceptance. This kind of oscillator circuit is called the *Hartley oscillator*. On the other hand, B_3 is an inductor if capacitors are used for B_1 and B_2. This circuit is called the *Colpitts oscillator*. Figure 11.4 illustrates the RF sections of these two circuits (excluding the transistor's

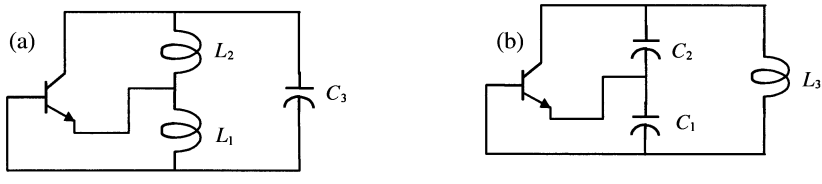

Figure 11.4 Simplified circuits of (a) Hartley and (b) Colpitts oscillators.

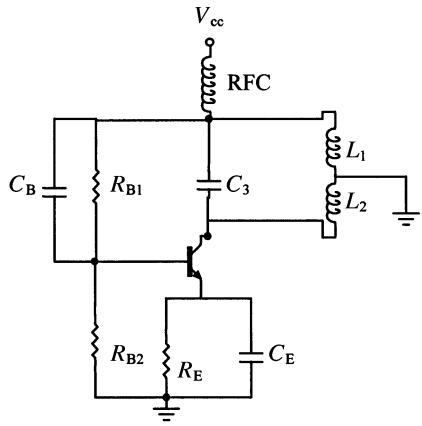

Figure 11.5 A biased BJT Hartely oscillator circuit.

biasing network). A BJT Hartley oscillator with its bias arrangement is shown in Figure 11.5.

Resonant frequency of the Hartley oscillator is obtained from (11.1.23) as follows:

$$\omega L_1 + \omega L_2 - \frac{1}{\omega C_3} = 0$$

or,

$$\omega^2 = \frac{1}{C_3(L_1 + L_2)} \tag{11.1.26}$$

Similarly, the resonant frequency of a Colpitts oscillator is found to be

$$-\frac{1}{\omega C_1} - \frac{1}{\omega C_2} + \omega L_3 = 0$$

or,

$$\omega^2 = \frac{C_1 + C_2}{C_1 C_2 L_3} \tag{11.1.27}$$

Resistors R_{B1}, R_{B2} and R_E in Figure 11.5 are determined according to the bias point selected for a transistor. Capacitors C_B and C_E must bypass the RF, and therefore, these should have relatively high values. C_E is selected such that its reactance at the design frequency is negligible in comparison with R_E. Similarly, the parallel combination of R_{B1} and R_{B2} must be infinitely large in comparison with the reactance of C_B. The RF choke (RFC) offers an infinitely large reactance at the RF

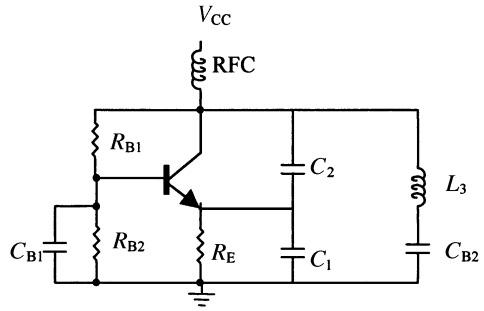

Figure 11.6 A biased BJT Colpitts oscillator circuit.

while it passes dc with almost zero resistance. Thus, it blocks the ac signal from reaching the dc supply. Since capacitors C_B and C_E have almost zero reactance at RF, the node that connects L_1 and C_3 is electrically connected to the base of BJT. Also, the grounded junction of L_1 and L_2 is effectively connected to the emitter. Hence, the circuit depicted in Figure 11.5 is essentially the same for the RF as that shown in Figure 11.4 (a).

Capacitor C_3 and total inductance $L_1 + L_2$ are determined such that (11.1.26) is satisfied at the desired frequency of oscillations. L_1 and L_2 satisfy (11.1.25) as well when the oscillator circuit operates.

A BJT-based Colpitts oscillator is shown in Figure 11.6. Resistors R_{B1}, R_{B2}, and R_E are determined from the usual procedure of biasing a transistor. Reactance of the capacitor C_{B1} must be negligible in comparison with parallel resistances R_{B1} and R_{B2}. Similarly, the reactance of C_{B2} must be negligible in comparison with that of the inductor L_3. The purpose of capacitor C_{B2} is to protect the dc supply from short-circuiting via L_3 and RFC.

Since capacitors C_{B1} and C_{B2} have negligible reactance, the ac equivalent of this circuit is same as that shown in Figure 11.4 (b). C_1, C_2, and L_3 are determined from the resonance condition (11.1.27). Also, (11.1.25) holds at the resonance.

As described in the preceding paragraphs, capacitor C_{B2} provides almost a short circuit in the desired frequency range and the inductor L_3 is selected such that

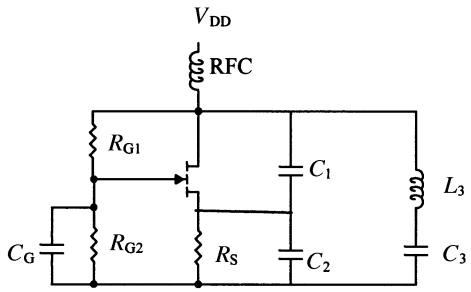

Figure 11.7 A FET-based Clapp oscillator circuit.

Figure 11.8 Resonant circuits for Colpitts (a) and Clapp (b) oscillators.

(11.1.27) is satisfied. An alternative design procedure that provides better stability of the frequency is as follows. L_3 is selected larger than needed to satisfy (11.1.27), and then C_{B2} is determined to bring it down to the desired value at resonance. This kind of circuit is called the *Clapp oscillator*. A FET-based Clapp oscillator circuit is shown in Figure 11.7. It is very similar to the Colpitts design and operation except for the selection of C_{B2} that is connected in series with the inductor. At the design frequency, the series inductor-capacitor combination provides the same inductive reactance as that of the Colpitts circuit. However, if there is a drift in frequency then the reactance of this combination changes rapidly. This can be explained further with the help of Figure 11.8.

Figure 11.8 illustrates the resonant circuits of Colpitts and Clapp oscillators. An obvious difference between the two circuits is the capacitor C_3 that is connected in series with L_3. Note that unlike C_3, the blocking capacitor C_{B2} shown in Figure 11.6 does not affect the RF operation.

Reactance X_1 of the series branch in the Colpitts circuit is ωL_3 whereas it is $X_2 = \omega L_3 - \dfrac{1}{\omega C_3}$ in the case of the Clapp oscillator. If inductor L_3 in the former case is selected as 1.59 μH and the circuit is resonating at 10 MHz, then the change in its reactance around resonance is as shown in Figure 11.9. The series branch of the Clapp circuit has the same inductive reactance at the resonance if $L_3 = 3.18\,\mu\text{H}$ and $C_3 = 159\,\text{pF}$. However, the rate of change of reactance with frequency is now higher in comparison with X_1. This characteristic helps in reducing the drift in oscillation frequency.

Another Interpretation of the Oscillator Circuit

Ideal inductors and capacitors store electrical energy in the form of magnetic and electric fields, respectively. If such a capacitor with initial charge is connected across an ideal inductor, it discharges through that. Since there is no loss in this system, the inductor recharges the capacitor back and the process repeats. However, real inductors and capacitors are far from being ideal. Energy losses in the inductor and the capacitor can be represented by a resistance r_1 in this loop. Oscillations die out because of these losses. As shown in Figure 11.10, if a negative resistance $-r_1$ can be introduced in the loop then the effective resistance becomes zero. In other words, if a circuit can be devised to compensate for the losses then oscillations can be sustained. This can be done using an active circuit, as illustrated in Figure 11.11.

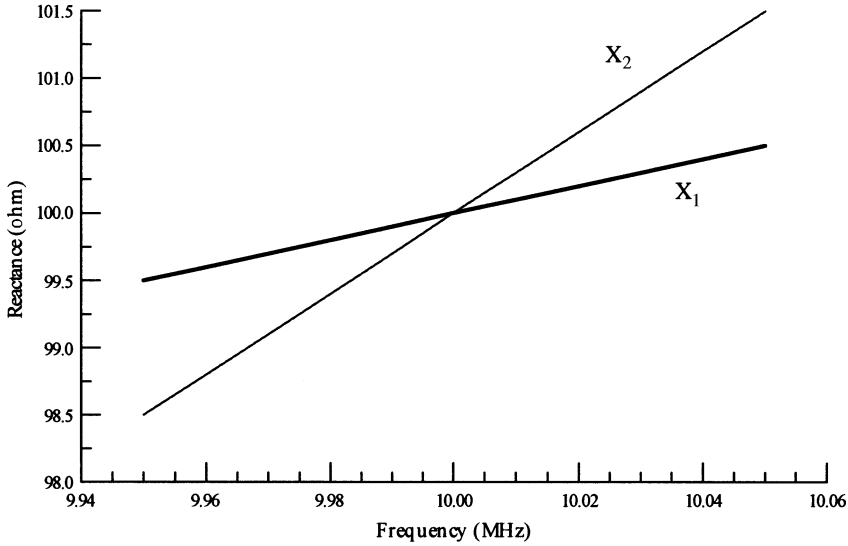

Figure 11.9 Reactance of inductive branch versus frequency for Colpitts (X_1) and Clapp (X_2) circuits.

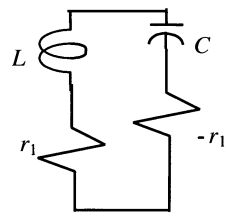

Figure 11.10 An ideal oscillator circuit.

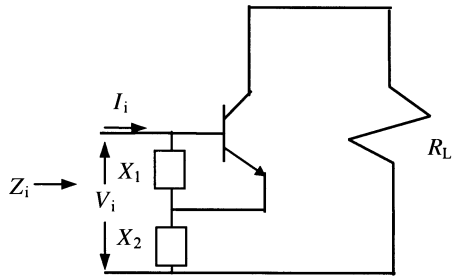

Figure 11.11 A BJT circuit to obtain negative resistance.

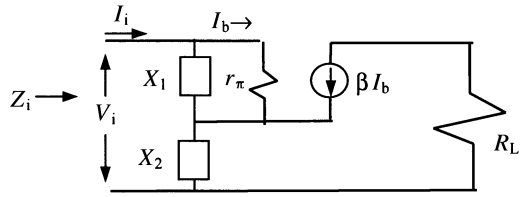

Figure 11.12 A small-signal equivalent of Figure 11.11 with output impedance of the BJT neglected.

Consider the transistor circuit shown in Figure 11.11. X_1 and X_2 are arbitrary reactance, and the dc bias circuit is not shown in this circuit for simplicity. For analysis, a small-signal equivalent circuit can be drawn as illustrated in Figure 11.12. Using Kirchhoff's voltage law, we can write

$$V_i = I_i(X_1 + X_2) - I_b(X_1 - \beta X_2) \tag{11.1.28}$$

and,

$$0 = I_i(X_1) - I_b(X_1 + r_\pi) \tag{11.1.29}$$

Equation (11.1.29) can be rearranged as follows:

$$I_b = \frac{X_1}{X_1 + r_\pi} I_i \tag{11.1.30}$$

Substituting (11.1.30) into (11.1.28), we find that

$$V_i = I_i\left(X_1 + X_2 - \frac{X_1 - \beta X_2}{X_1 + r_\pi} X_1\right) \tag{11.1.31}$$

Impedance Z_i across its input terminal can now be determined as follows:

$$Z_i = \frac{V_i}{I_i} = \left(X_1 + X_2 - \frac{X_1 - \beta X_2}{X_1 + r_\pi} X_1\right) = \frac{(1+\beta)X_1X_2 + (X_1 + X_2)r_\pi}{X_1 + r_\pi} \tag{11.1.32}$$

For $X_1 \ll r_\pi$, the following approximation can be made

$$Z_i \approx \frac{(1+\beta)X_1X_2}{r_\pi} + X_1 + X_2 \tag{11.1.33}$$

For X_1 and X_2 to be capacitive, it simplifies to

$$Z_i \approx -\frac{(1+\beta)}{r_\pi} \times \frac{1}{\omega^2 C_1 C_2} - j\left(\frac{C_1 + C_2}{\omega C_1 C_2}\right) \tag{11.1.34}$$

Since β, r_π, and g_m of a BJT are related as follows:

$$\frac{1+\beta}{r_\pi} \approx g_m$$

(11.1.34) can be further simplified. Hence,

$$Z_i \approx -\frac{g_m}{\omega^2 C_1 C_2} - \frac{j}{\omega}\left(\frac{C_1 + C_2}{C_1 C_2}\right) \tag{11.1.35}$$

Therefore, if this circuit is used to replace capacitor C of Figure 11.10 and the following condition is satisfied then the oscillations can be sustained

$$r_1 = \frac{g_m}{\omega^2 C_1 C_2} \tag{11.1.36}$$

The frequency of these oscillations is given as follows:

$$\omega = \frac{1}{\sqrt{\dfrac{LC_1C_2}{(C_1 + C_2)}}} \tag{11.1.37}$$

A comparison of this equation with (11.1.27) indicates that it is basically the Colpitts oscillator. On the other hand, if X_1 and X_2 are inductive then (11.1.33) gives the following relation

$$Z_i \approx -g_m \omega^2 L_1 L_2 + j\omega(L_1 + L_2) \tag{11.1.38}$$

Now, if this circuit replaces inductor L of Figure 11.10 and the following condition is satisfied then sustained oscillations are possible

$$r_1 = g_m \omega^2 L_1 L_2 \tag{11.1.39}$$

The frequency of these oscillations is given as follows:

$$\omega = \frac{1}{\sqrt{C(L_1 + L_2)}} \tag{11.1.40}$$

This is identical to (11.1.26), the Hartley oscillator frequency.

11.2 CRYSTAL OSCILLATORS

Quartz and ceramic crystals are used in the oscillator circuits for additional stability of frequency. They provide a fairly high Q (of the order of 100,000) that shows a small drift with temperature (on the order of 0.001 percent per °C). A simplified electrical equivalent circuit of a crystal is illustrated in Figure 11.13.

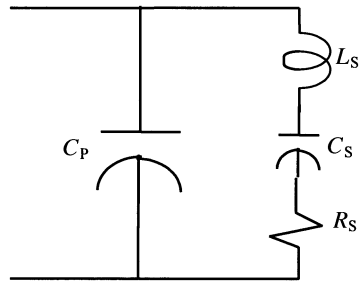

Figure 11.13 Equivalent circuit of a crystal.

As this equivalent circuit indicates, the crystal exhibits both series and parallel resonant modes. For example, the terminal impedance of a crystal with typical values of $C_P = 29\,\text{pF}$, $L_S = 58\,\text{mH}$, $C_S = 0.054\,\text{pF}$, and $R_S = 15\,\Omega$ exhibits a distinct minimum and maximum with frequency, as shown in Figure 11.14. Its main characteristics may be summarized as follows:

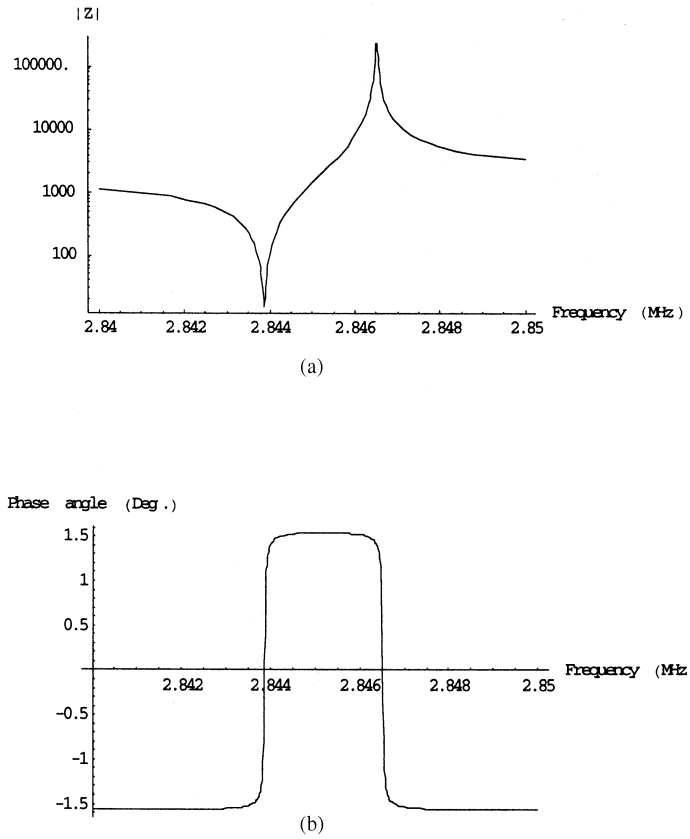

Figure 11.14 Magnitude (a) and phase angle (b) of the terminal impedance as a function of frequency.

- Magnitude of the terminal impedance decreases up to around 2.844 MHz while its phase angle remains constant at -90°. Hence, it is effectively a capacitor in this frequency range.
- Magnitude of the impedance dips around 2.844 MHz and its phase angle goes through a sharp change from -90° to 90°. It has series resonance at this frequency.
- Magnitude of the impedance has a maximum around 2.8465 MHz where its phase angle changes back to -90° from 90°. It exhibits a parallel resonance around this frequency.
- Phase angle of the impedance remains constant at 90° in the frequency range of 2.844–2.8465 MHz while its magnitude increases. Hence, it is effectively an inductor.
- Beyond 2.8465 MHz, the phase angle stays at -90° while its magnitude goes down with frequency. Therefore, it is changed back to a capacitor.

Series resonant frequency ω_S and parallel resonant frequency ω_P of the crystal can be found from its equivalent circuit. These are given as follows:

$$\omega_S = \frac{1}{\sqrt{L_S C_S}} \tag{11.2.1}$$

and,

$$\omega_P = \omega_S \sqrt{\left(1 + \frac{C_S}{C_P}\right)} \tag{11.2.2}$$

Hence, the frequency range $\Delta\omega$ over which the crystal behaves as an inductor can be determined as follows:

$$\omega_P - \omega_S = \Delta\omega = \omega_S \left\{ \sqrt{\left(1 + \frac{C_S}{C_P}\right)} - 1 \right\} \approx \frac{C_S}{2C_P} \omega_S \tag{11.2.3}$$

$\Delta\omega$ is known as the *pulling figure* of the crystal. Typically, ω_P is less than 1 percent higher than ω_S. For an oscillator design, a crystal is selected such that the frequency of oscillation falls between ω_S and ω_P. Therefore, the crystal operates basically as an inductor in the oscillator circuit. A BJT oscillator circuit using the crystal is shown in Figure 11.15. It is known as the *Pierce oscillator*. A comparison of its RF equivalent circuit with that shown in Figure 11.4 (b) indicates that the Pierce circuit is similar to the Colpitts oscillator with inductor L_3 replaced by the crystal.

As mentioned earlier, the crystal provides very stable frequency of oscillation over a wide range of temperature. The main drawback of a crystal oscillator circuit is that its tuning range is relatively small. It is achieved by adding a capacitor in

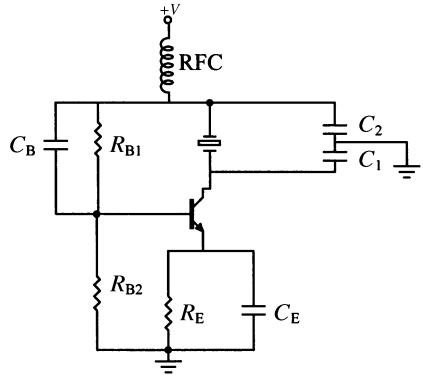

Figure 11.15 Pierce oscillator circuit.

parallel with the crystal. This way, the parallel resonant frequency ω_P can be decreased up to the series resonant frequency ω_S.

11.3 ELECTRONIC TUNING OF OSCILLATORS

In most of the circuits considered so far, capacitance of the tuned circuit can be varied to change the frequency of oscillation. It can be done electronically by using a varactor diode and controlling its bias voltage.

There are two basic types of varactors—abrupt and hyperabrupt junctions. Abrupt junction diodes provide very high Q and also operate over a very wide tuning voltage range (typically, 0 to 60 V). These diodes provide an excellent phase noise performance because of their high Q.

Hyperabrupt-type diodes exhibit a quadratic characteristic of the capacitance with applied voltage. Therefore, these varactors provide a much more linear tuning characteristic than the abrupt type. These diodes are preferred for tuning over a wide frequency band. An octave tuning range can be covered in less than 20 V. The main disadvantage of these diodes is that they have a much lower Q, and therefore, the phase noise is higher than that obtained from the abrupt junction diodes.

The capacitance of a varactor diode is related to its bias voltage as follows:

$$C = \frac{A}{(V_R + V_B)^n} \tag{11.3.1}$$

A is a constant; V_R is the applied reverse bias voltage; and V_B is the built-in potential that is 0.7 V for silicon diodes and 1.2 V for GaAs diodes. For the following analysis, we can write

$$C = \frac{A}{V^n} \tag{11.3.2}$$

In this equation, A represents capacitance of the diode when V is one volt. Also, n is a number between 0.3 and 0.6, but can be as high as 2 for a hyperabrupt junction. The resonant circuit of a typical voltage-controlled oscillator (VCO) has a parallel tuned circuit consisting of inductor L, fixed capacitor C_f, and the varactor diode with capacitance C. Therefore, its frequency of oscillation can be written as follows:

$$\omega = \frac{1}{\sqrt{L(C_f + C)}} = \frac{1}{\sqrt{L\left(C_f + \frac{A}{V^n}\right)}} \tag{11.3.3}$$

Let ω_o be the angular frequency of an unmodulated carrier and V_o and C_o be the corresponding values of V and C. Then

$$\omega_o^2 = \frac{1}{L(C_f + C_o)} = \frac{1}{L\left(C_f + \frac{A}{V_o^n}\right)} \tag{11.3.4}$$

Further, the carrier frequency deviates from ω_o by $\delta\omega$ for a voltage change of δV. Therefore,

$$(\omega_o + \delta\omega)^2 = \frac{1}{L\left(C_f + \frac{A}{(V_o + \delta V)^n}\right)} \Rightarrow (\omega_o + \delta\omega)^{-2} = L(C_f + A(V_o + \delta V)^{-n}) \tag{11.3.5}$$

Dividing (11.3.5) by (11.3.4), we have

$$\left(\frac{\omega_o + \delta\omega}{\omega_o}\right)^2 = \frac{C_f + C_o}{C_f + A(V_o + \delta V)^{-n}} = \frac{C_f + C_o}{C_f + AV_o^{-n}\left(1 + \frac{\delta V}{V_o}\right)^{-n}}$$

or,

$$\left(1 + \frac{\delta\omega}{\omega_o}\right)^2 = \frac{C_f + C_o}{C_f + C_o\left(1 + \frac{\delta V}{V_o}\right)^{-n}} \Rightarrow \left(1 + \frac{\delta\omega}{\omega_o}\right)^{-2} = \frac{C_f + C_o\left(1 + \frac{\delta V}{V_o}\right)^{-n}}{C_f + C_o}$$

or,

$$1 - 2\frac{\delta\omega}{\omega_o} \approx \frac{C_f + C_o\left(1 - n\frac{\delta V}{V_o}\right)}{C_f + C_o} = 1 - n\frac{\delta V}{V_o} \times \frac{C_o}{C_f + C_o}$$

Hence,

$$\frac{\delta\omega}{\delta V} = \frac{n\omega_o}{2V_o}\left(\frac{C_o}{C_f + C_o}\right) = K_1 \tag{11.3.6}$$

K_1 is called the *tuning sensitivity* of the oscillator. It is expressed in radians per second per volt.

11.4 PHASE-LOCKED LOOP

Phase-locked loop (PLL) is a feedback system that is used to lock the output frequency and phase to the frequency and phase of a reference signal at its input. The reference waveform can be of many different types, including sinusoidal and digital. The PLL has been used for various applications that include filtering, frequency synthesis, motor speed control, frequency modulation, demodulation, and signal detection.

The basic PLL consists of a voltage-controlled oscillator (VCO), a phase detector (PD), and a filter. In its most general form, the PLL may also contain a mixer and a frequency divider as shown in Figure 11.16.

In steady state, the output frequency is expressed as follows:

$$f_o = f_m + Nf_r \tag{11.4.1}$$

Hence, the output frequency can be controlled by varying N, f_r, or f_m.

It is helpful to consider the PLL in terms of phase rather than frequency. This is done by replacing f_o, f_m, f_r with θ_o, θ_m, and θ_r, respectively. Further, the transfer characteristics of each building block need to be formulated before the PLL can be analyzed.

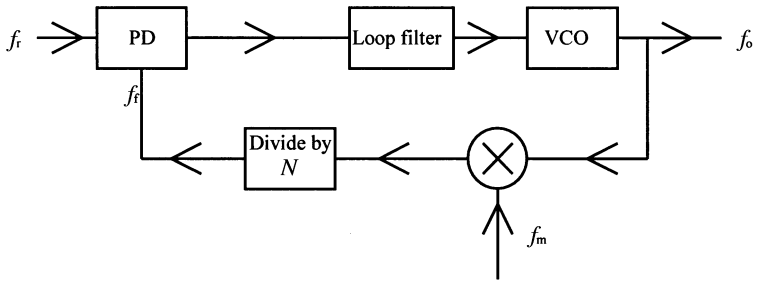

Figure 11.16 Block-diagram of a PLL system.

Phase Detector

With loop in lock, the output of the phase detector is a direct voltage V_e that is a function of the phase difference $\theta_d = \theta_r - \theta_f$. If input frequency f_r is equal to f_f then V_e must be zero. In commonly used analog phase detectors, V_e is a sinusoidal, triangular, or sawtooth function of θ_d. It is equal to zero when θ_d is equal to $\pi/2$ for the sinusoidal and triangular types, and π for the sawtooth type. Therefore, it is convenient to plot V_e versus a shifted angle θ_e as shown in Figures 11.17–11.19 for a direct comparison of these three types of detectors. Hence, the transfer characteristic of a sinusoidal-type phase detector can be expressed as follows:

$$V_e = A\sin(\theta_e) \qquad -\frac{\pi}{2} \le \theta_e \le \frac{\pi}{2} \tag{11.4.2}$$

This can be approximated around $\theta_e \approx 0$ by the following expression

$$V_e \approx A\theta_e$$

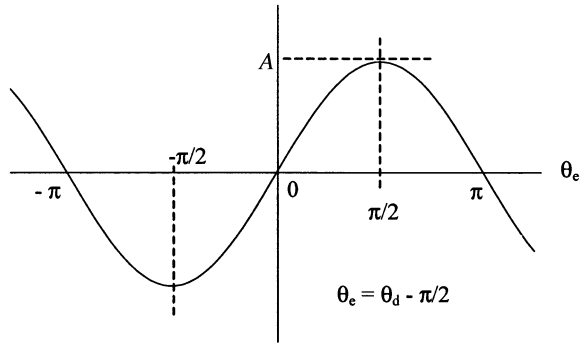

Figure 11.17 Sinusoidal output of the PD.

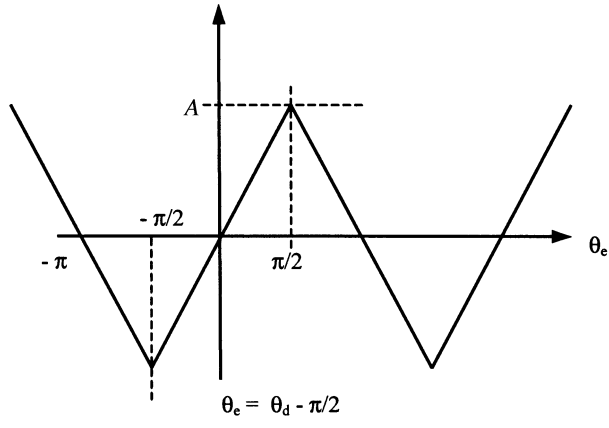

Figure 11.18 Triangular wave.

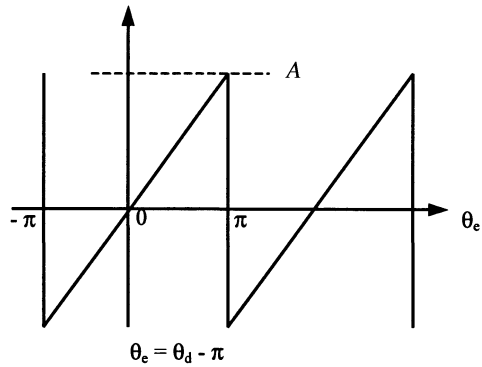

Figure 11.19 Sawtooth wave.

In the case of a triangular output of the phase detector, the transfer characteristic can be expressed as follows:

$$V_e = \frac{2A}{\pi}\theta_e \qquad -\frac{\pi}{2} \le \theta_e \le \frac{\pi}{2} \tag{11.4.3}$$

From the transfer characteristic of the sawtooth-type phase detector illustrated in Figure 11.19, we can write

$$V_e = \frac{A}{\pi}\theta_e \qquad -\pi \le \theta_e \le \pi \tag{11.4.4}$$

Since V_e is zero in steady state, the gain factor K_d (volts per radians) in all three cases is

$$\frac{V_e}{\theta_e} = K_d \tag{11.4.5}$$

Voltage-Controlled Oscillator

As described earlier, a varactor diode is generally used in the resonant circuit of an oscillator. Its bias voltage is controlled to change the frequency of oscillation. Therefore, the transfer characteristic of an ideal voltage-controlled oscillator (VCO) has a linear relation, as depicted in Figure 11.20. Hence, the output frequency of a VCO can be expressed as follows:

$$f_o = f_S + k_o V_d \quad \text{(Hz)}$$

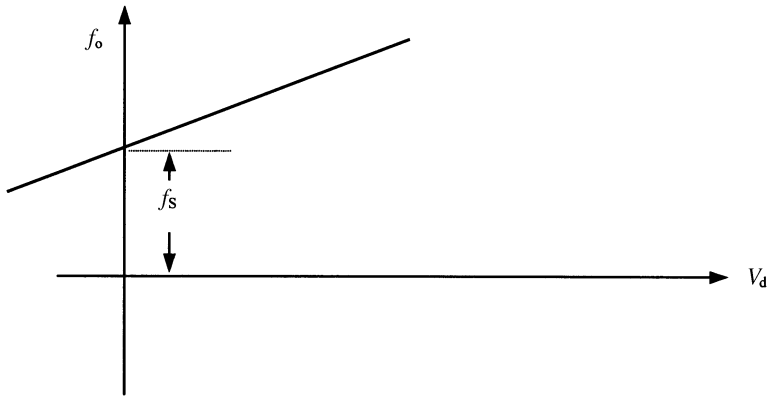

Figure 11.20 Characteristic of a voltage-controlled oscillator.

or,

$$\omega_o = \omega_S + K_o V_d \quad \text{(radian per sec.)}$$

or,

$$\omega_o = \omega_S + \delta\omega \quad \text{(radian per sec.)}$$

$$\theta(t) = \int_0^t \omega_o \, dt = \omega_S t + \int_0^t \delta\omega \, dt = \theta_S + \theta_o(t)$$

Therefore,

$$\theta_o(t) = \int_o^t \delta\omega \, dt \Rightarrow \frac{d\theta_o(t)}{dt} = \delta\omega = K_o V_d \tag{11.4.6}$$

In the s-domain,

$$s\theta_o(s) = K_o V_d(s) \Rightarrow \frac{\theta_o(s)}{V_d(s)} = \frac{K_o}{s}$$

Hence, VCO acts as an integrator.

Loop Filters

A low-pass filter is connected right after the phase detector to suppress its output harmonics. Generally, it is a simple first-order filter. Sometimes higher-order filters are also employed to suppress additional ac components. The transfer characteristics of selected loop-filters are summarized below.

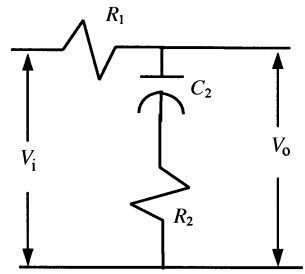

Figure 11.21 Lead-lag filter.

(i) *Lead-lag filter*: A typical lead-lag filter uses two resistors and a capacitor, as illustrated in Figure 11.21. Its transfer function, $F(s)$, can be found as follows:

$$\frac{V_o}{V_i} = \frac{R_2 + \dfrac{1}{sC_2}}{R_1 + R_2 + \dfrac{1}{sC_2}} = \frac{1 + sR_2C_2}{1 + s(R_1C_2 + R_2C_2)}$$

Hence,

$$F(s) = \frac{1 + \tau_2 s}{1 + \tau_1 s} \tag{11.4.7}$$

where,

$$\tau_2 = R_2C_2 \tag{11.4.8}$$

and,

$$\tau_1 = (R_1 + R_2)C_2 \tag{11.4.9}$$

Typical magnitude and phase characteristics versus frequency (the Bode plot) of a lead-lag filter are illustrated in Figure 11.22. The time constants τ_1 and τ_2 used to draw these characteristics were 0.1 s and 0.01 s, respectively. Note that the changes in these characteristics occur at $1/\tau_1$ and $1/\tau_2$.

(ii) *Integrator and lead filter*: This kind of filter generally requires an OPAMP along with two resistors and a capacitor. As illustrated in Figure 11.23, the feedback path of the OPAMP uses a capacitor in series with resistance. Assuming that the OPAMP is ideal and is being used in inverting configuration, the transfer characteristics of this filter can be found as follows:

$$\frac{V_o}{V_i} = -\frac{R_2 + \dfrac{1}{sC_2}}{R_1} = -\frac{1 + sR_2C_2}{sR_1C_2}$$

$$F(s) = \frac{1 + s\tau_2}{s\tau_1} \tag{11.4.10}$$

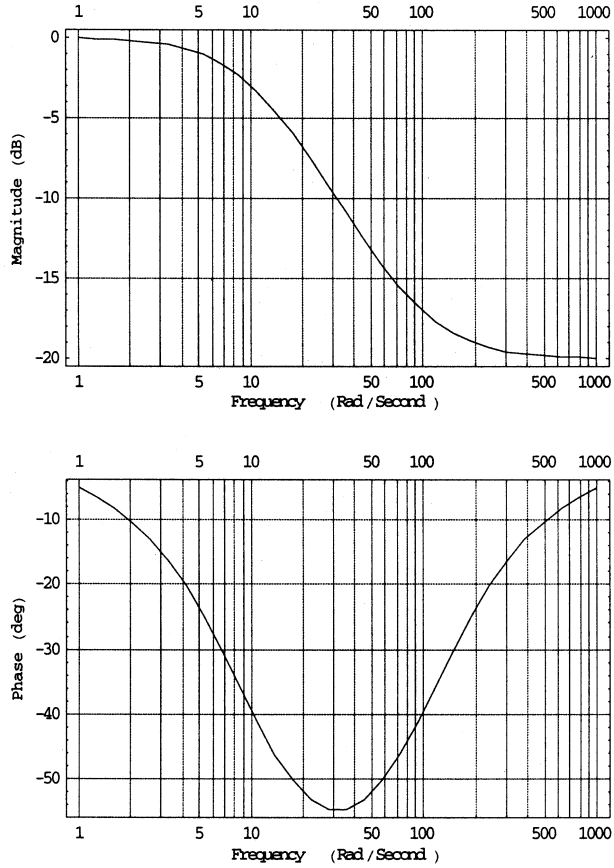

Figure 11.22 Frequency response (Bode plot) of lead-lag filter.

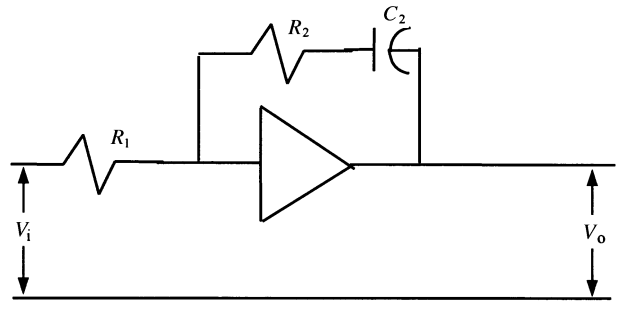

Figure 11.23 Integrator and lead filter.

where,

$$\tau_1 = R_1 C_2 \tag{11.4.11}$$

and,

$$\tau_2 = R_2 C_2 \tag{11.4.12}$$

Typical frequency response characteristics (the Bode plot) of an integrator and lead filter are illustrated in Figure 11.24. Time constants τ_1 and τ_2 used for this illustration are 0.1 s and 0.01 s, respectively.

Note again that there are significant changes occurring in these characteristics at frequencies that are equal to $1/\tau_1$ and $1/\tau_2$. For frequencies less than 10 rad/s phase angle is almost constant at -90° whereas the magnitude changes at a rate of 20 dB/s. It represents the characteristics of an integrator. Phase angle becomes zero

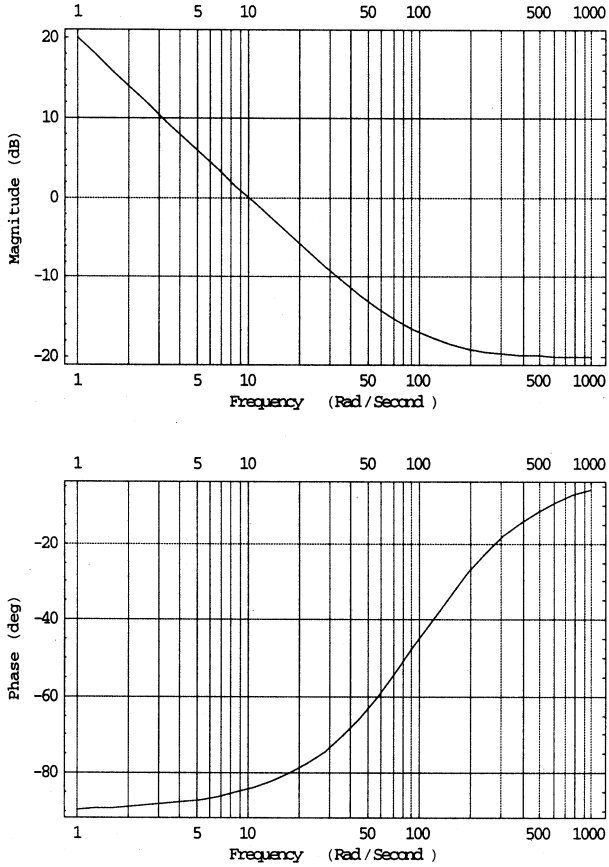

Figure 11.24 Frequency response (Bode plot) of integrator and lead filter.

for frequencies greater than 100 rad/s. The magnitude becomes constant at −20 dB as well.

(iii) *Integrator and lead-lag filter*: Another active filter that is used in the loop is shown in Figure 11.25. It employs two capacitors in the feedback loop of the OPAMP. Assuming again that the OPAMP is ideal and is connected in inverting configuration, the transfer function of this filter can be found as follows:

$$\frac{V_o}{V_i} = -\frac{1}{R_1}\left(\frac{\frac{R_2}{sC_2}}{R_2 + \frac{1}{sC_2}} + \frac{1}{sC_1}\right) = -\frac{1}{R_1}\left(\frac{R_2}{1 + sR_2C_2} + \frac{1}{sC_1}\right)$$

$$= -\frac{\frac{R_2}{R_1}}{1 + sR_2C_2} - \frac{1}{sR_1C_1}$$

or,

$$\frac{V_o}{V_i} = -\frac{sR_2C_1 + 1 + sR_2C_2}{sR_1C_1(1 + sR_2C_2)}$$

This can be rearranged as follows:

$$F(s) = -\frac{1}{s\tau_1} \times \frac{1 + s\tau_2}{1 + s\tau_3} \tag{11.4.13}$$

where,

$$\tau_1 = C_1R_1 \tag{11.4.14}$$

$$\tau_2 = R_2(C_1 + C_2) \tag{11.4.15}$$

$$\tau_3 = R_2C_2 \tag{11.4.16}$$

Frequency response of a typical integrator and lead-lag filter is shown in Figure 11.26. Time constants τ_1, τ_2, and τ_3 are assumed to be 1, 0.1, and 0.01 s, respectively. The corresponding frequencies are 1, 10, and 100 rad/s. At frequencies below 1 rad/s, magnitude of the transfer function reduces at the rate of 20 dB per decade while its phase angle stays at −90°. Similar characteristics may be observed higher than 100 rad/s. It is a typical integrator characteristic. Significant change in the frequency response may be observed at 10 rad/s as well.

An equivalent block diagram of the PLL can be drawn as shown in Figure 11.27. Output θ_o of the VCO can be controlled by voltage V, reference signal θ_r, or modulator input θ_m. In order to understand the working of the PLL when it is nearly locked, the transfer function for each case can be formulated with the help of this diagram.

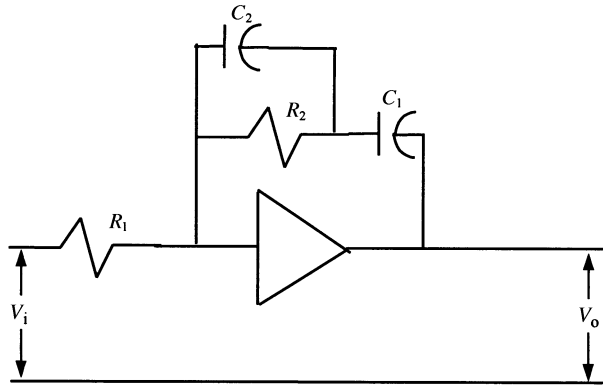

Figure 11.25 Integrator and lead-lag filter.

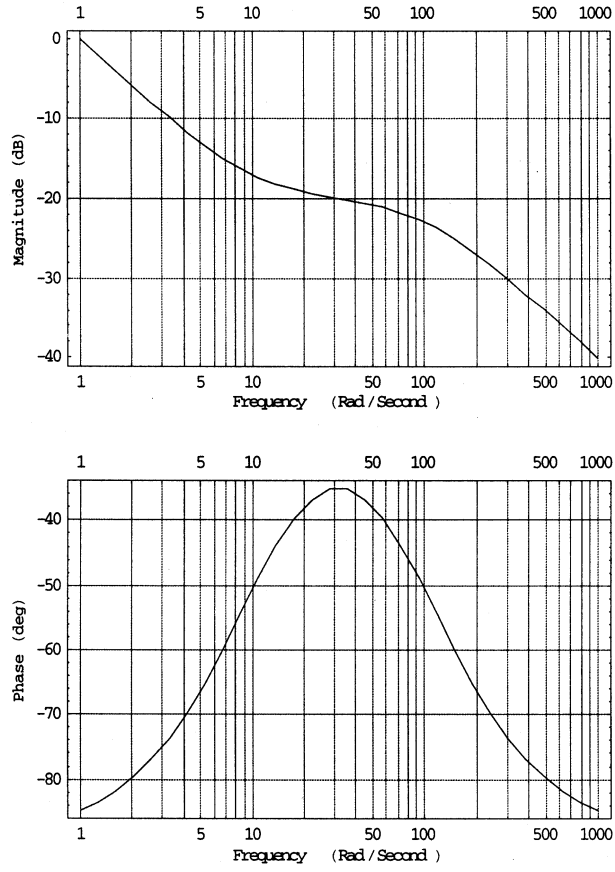

Figure 11.26 Frequency response (Bode plot) of integrator and lead-lag filter.

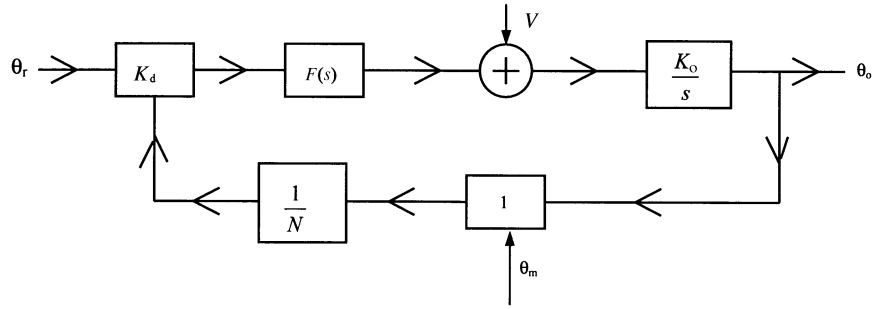

Figure 11.27 Equivalent block diagram of a PLL.

A general formula for the transfer function $T(s)$ of a single feedback loop system can be written with the help of Figure 11.1, as follows:

$$T(s) = \frac{\text{Forward gain}}{1 + \text{Loop gain}} \tag{11.4.17}$$

Since there are three different ways to control the phase of the VCO, the transfer function for each case can be found via (11.4.17), as follows.

1. When phase θ_m of the mixer input controls the VCO output θ_o, its transfer function $T_1(s)$ is found to be

$$T_1(s) = \frac{\theta_o(s)}{\theta_m(s)} = \frac{\frac{1}{N} \times K_d \times F(s) \times \frac{K_o}{s}}{1 + \frac{1}{N} \times K_d \times F(s) \times \frac{K_o}{s} \times 1} = \frac{KF(s)}{s + KF(s)} \tag{11.4.18}$$

where,

$$K = \frac{K_d K_o}{N} \tag{11.4.19}$$

2. When phase θ_r of the reference input controls the output θ_o of the VCO, its transfer function $T_2(s)$ will be as follows:

$$T_2(s) = \frac{\theta_o(s)}{\theta_r(s)} = \frac{K_d \times F(s) \times \frac{K_o}{s}}{1 + K\frac{F(s)}{s}} = \frac{NKF(s)}{s + KF(s)} \tag{11.4.20}$$

3. Similarly, for the case of input voltage V controlling θ_o, its transfer function $T_3(s)$ is found to be

$$T_3(s) = \frac{\theta_o(s)}{V} = \frac{\dfrac{K_o}{s}}{1 + K\dfrac{F(s)}{s}} = \frac{K_o}{s + KF(s)} \tag{11.4.21}$$

It is obvious from (11.4.18)–(11.4.21) that the transfer function $F(s)$ of the filter significantly affects the working of a PLL. Various kinds of loop filters have been used to obtain the desired PLL characteristics, including the three loop filters described earlier, namely, (i) the lead-lag filter, (ii) an integrator in combination with a lead network, and (iii) an integrator combined with a lead-lag network.

Equations (11.4.18)–(11.4.21) are used to analyze the stability of a PLL and to develop the relevant design procedures. As an example, consider the case where a lead-lag filter is being used and the frequency divider is excluded from the loop (that is, $N = 1$). The transfer function $T_2(s)$ for this PLL can be obtained by substituting (11.4.7) into (11.4.20) as follows:

$$T_2(s) = \frac{K_v(1 + \tau_2 s)}{s(1 + \tau_1 s) + K_v(1 + \tau_2 s)}$$

where $K_v = K_d K_o$ is the dc gain of the loop.

Generally, $T_2(s)$ is rearranged in the following form for further analysis of the PLL

$$T_2(s) = \frac{\omega_n^2 + \left(2\zeta\omega_n - \dfrac{\omega_n^2}{K_v}\right)s}{s^2 + 2\zeta\omega_n s + \omega_n^2}$$

Coefficients ω_n and ζ are called the *natural frequency* and the *damping factor*, respectively. These are defined as follows:

$$\omega_n = \sqrt{\frac{K_v}{\tau_1}}$$

and,

$$\zeta = \frac{\omega_n}{2}\left(\tau_2 + \frac{1}{K_v}\right)$$

These coefficients must be selected such that the PLL is stable and performs according to the specifications.

See Table 11.1 for a summary of PLL components.

TABLE 11.1 Summary of PLL Components

Element	Transfer Function	Remarks
VCO	$\frac{K_o}{s}$	K_o is the slope of the oscillator frequency to voltage characteristic. It is expressed in radians per second per volt.
Mixer	1	Change of output phase equals change of input phase.
Divider	$\frac{1}{N}$	N is the division ratio.
Phase detector	K_d	K_d is the slope of phase detector voltage to phase characteristic in volts per radian.
Filter	$F(s)$	Transfer function depends on the type of filter used.

Phase-Locked Loop Terminology

Hold-in Range: This is also called the *lock range*, the *tracking range*, or the *synchronization range*. If reference frequency f_r is slowly changed from the free-running frequency f_f then VCO frequency f_o tracks f_r until the phase error θ_e approaches $\pm\pi/2$ for sinusoidal and triangular phase detectors or $\pm\pi$ for the sawtooth-type phase detector. It is assumed here that the VCO is capable of sufficient frequency deviation, and loop filter and amplifier (if any) are not overdriven.

From the transfer function of a sinusoidal phase detector as given by (11.4.2), we find that

$$\sin(\theta_e) = \frac{V_e}{K_d}$$

Output voltage V_e of the phase detector is applied to the input of the voltage-controlled oscillator. Therefore, using (11.4.6) with $V_d = V_e$,

$$\sin(\theta_e) = \frac{V_e}{K_d} = \frac{\delta\omega}{K_o K_d} \tag{11.4.22}$$

Since θ_e ranges between -90° to $+90^\circ$, the hold-in range, $\delta\omega_H$, for this case is found to be

$$\delta\omega_H = \pm K_d K_o \tag{11.4.23}$$

Hence, if there is no frequency divider in the loop (i.e., $N = 1$) then the hold-in range is equal to dc loop gain.

Similarly, the hold-in range with a triangular or sawtooth-type phase detector with linear characteristics can be determined via (11.4.3)–(11.4.5). It may be found as

$$\delta\omega_H = \pm K_d K_o \theta_{emax} \tag{11.4.24}$$

Note that θ_{emax} is $\pi/2$ for the triangular and π for the sawtooth-type phase detectors.

Example 11.1: Free-running frequency and the gain factor of a voltage-controlled oscillator are given as 100 MHz and 100 kHz/V, respectively. It is being used in a PLL along with a sinusoidal phase detector with maximum output of 2 V at $\theta_e = \pi/2$ radians. If there are no amplifiers or frequency divider in the loop, what is its hold-in range?

From (11.4.2),

$$K_d = \frac{V_e}{\sin(\theta_e)} = 2$$

Similarly, from the voltage-controlled oscillator characteristics,

$$K_o = \frac{\delta\omega}{V_d} = 2\pi \times 100 \times 1000 \text{ rad/sec/V}$$

Hence,

$$\delta\omega_H = \pm 2 \times 2\pi \times 10^5 \text{ rad/sec}$$

or,

$$\delta f_H = \pm 200 \text{ KHz}$$

Example 11.2: If the phase detector in the preceding example is replaced by a triangular type with $V_{emax} = A = 2$ V at $\theta_{emax} = \pi/2$ radians, find the new holding range.

From (11.4.5),

$$K_{\mathrm{d}} = \frac{2}{\pi/2} = \frac{4}{\pi}$$

Since the voltage-controlled oscillator is still the same, $K_{\mathrm{o}} = 2\pi 10^5$ rad/sec/V. Hence, the new hold-in range will be given as follows:

$$\delta\omega_{\mathrm{H}} = \frac{4}{\pi} \times 2 \times \pi \times 10^5 \times \frac{\pi}{2} = 4\pi \times 10^5 \text{ rad/sec}$$

or,

$$\delta f_{\mathrm{H}} = 200 \text{ kHz}.$$

Acquisition of Lock: Suppose that a signal with frequency f_{r} is applied to the loop as shown in Figure 11.16. If this frequency is different from the feedback signal frequency f_{f}, the loop tries to capture or acquire the signal. Two frequencies are equalized if the initial difference is not too large. In general, maximum radian frequency difference $\pm(\omega_{\mathrm{r}} - \omega_{\mathrm{f}})$ must be smaller than the hold-in range. Acquisition of lock is a nonlinear process that is beyond the scope of this chapter. Some general conclusions based on a commonly used lead-lag filter are summarized below.

Lock-in Range: If frequency difference $|\omega_{\mathrm{r}} - \omega_{\mathrm{f}}|$ is less than 3-dB bandwidth of closed-loop transfer function $T_2(s)$, the loop locks up without slipping cycles. The maximum lock-in range, $\delta\omega_{\mathrm{L}}$, may be found by the following formula

$$\delta\omega_{\mathrm{L}} = \pm\frac{K\tau_2}{\tau_1} \tag{11.4.25}$$

K is the dc loop gain, $\tau_1 = (R_1 + R_2)C_2$, and $\tau_2 = R_2C_2$, as defined earlier.

The lock-in range can be expressed in terms of natural frequency ω_n and damping factor ζ of the closed-loop transfer function $T_2(s)$ with a lead-lag filter. It is given as follows:

$$\delta\omega_{\mathrm{L}} \approx \pm 2\zeta\omega_n \tag{11.4.26}$$

where

$$\omega_n = \sqrt{\frac{K}{\tau_1}} \tag{11.4.27}$$

and,

$$\zeta = \frac{\omega_n}{2}\left(\tau_2 + \frac{1}{K}\right) \tag{11.4.28}$$

Pull-in Range: Suppose that frequency difference $|\omega_r - \omega_f|$ is initially outside the lock-in range but it is inside the pull-in range. In this case, the difference frequency signal at output of the phase detector is nonlinear and contains a dc component that gradually shifts the VCO frequency $f_o (f_f = f_o/N)$ toward f_r until lock-in occurs. For high-gain loops, an approximate formula for the pull-in range is given as follows:

$$\delta\omega_P \approx \pm\sqrt{2(2\zeta\omega_n K - \omega_n^2)} \tag{11.4.29}$$

It is desirable for the loop to have a large bandwidth that helps in capture initially. However, it increases the transmission of noise. These contradictory conditions may be satisfied in two different ways:

1. Use larger bandwidth initially but reduce it after the lock is acquired.
2. Use small bandwidth but sweep the frequency of the voltage-controlled oscillator until the lock is acquired.

Example 11.3: In the PLL shown below, peak amplitudes of the reference input as well as the VCO output are both 0.75 V. An analog multiplier is being used as a phase detector that has a 2-V output when its reference input, V_{in}, and the oscillator signal, V_{osc}, are both 2 V. Free-running frequency of the VCO is 10 MHz, which reduces to zero when its control voltage V_{cntl} is reduced by 1 V. Find the phase difference between the input and the VCO output when it is in lock with input frequency of (a) 11 MHz, and (b) 9 MHz.

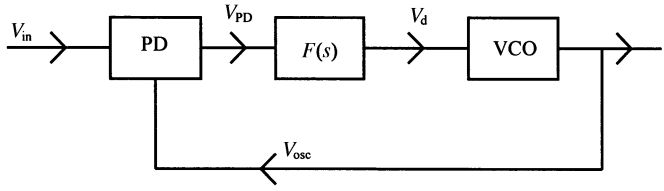

Since the output of an analog multiplier is proportional to the product of its two inputs, we can write

$$V_{PD} = K_m V_{in} V_{osc}$$

Hence, the proportionality constant K_m is

$$K_m = \frac{2}{2 \times 2} = 0.5 \text{ per V}$$

For,

$$V_{\text{in}} = E_{\text{in}} \sin(\omega t)$$

and,

$$V_{\text{osc}} = E_{\text{osc}} \cos(\omega t - \phi_{\text{d}})$$

$$V_{\text{PD}} = K_m E_{\text{in}} E_{\text{osc}} \sin(\omega t) \cos(\omega t - \phi_{\text{d}}) = 0.5 K_m E_{\text{in}} E_{\text{osc}} \{\sin(\phi_{\text{d}}) + \sin(2\omega t - \phi_{\text{d}})\}$$

Since the output of the phase detector is passed through a low-pass filter before it is applied to the voltage-controlled oscillator, the controlling voltage V_{d} may be written as follows:

$$V_{\text{d}} = 0.5 K_m E_{\text{in}} E_{\text{osc}} \sin(\phi_{\text{d}}) \approx 0.5 K_m E_{\text{in}} E_{\text{osc}} \phi_{\text{d}}$$

Hence, the transfer function K_{d} is

$$K_{\text{d}} = \frac{V_{\text{d}}}{\phi_{\text{d}}} = 0.5 K_m E_{\text{in}} E_{\text{osc}} = 0.5 \times 0.5 \times 0.75^2 = 0.1406 \text{ V/rad}$$

Transfer function K_{o} of the voltage-controlled oscillator can be found from (11.4.6) as follows:

$$K_{\text{o}} = \frac{\delta\omega}{V_{\text{d}}} = \frac{2\pi \times 10^7}{1} = 2\pi \times 10^7 \text{ radian per second per volt}$$

Since the output frequency of the voltage-controlled oscillator is given as follows:

$$\omega_{\text{o}} = K_{\text{o}} V_{\text{d}} + \omega_{\text{s}} = \omega_{\text{in}}$$

we can write

$$V_{\text{d}} = \frac{\omega_{\text{in}} - \omega_{\text{s}}}{K_{\text{o}}}$$

Hence,

$$\phi_{\text{d}} = \frac{V_{\text{d}}}{K_{\text{d}}} = \frac{\omega_{\text{in}} - \omega_{\text{s}}}{K_{\text{o}} K_{\text{d}}}$$

(a) The input signal frequency in this case is 11 MHz while the free-running frequency of the voltage-controlled oscillator is 10 MHz. Hence,

$$\phi_d = \frac{2\pi(11 \text{ MHz} - 10 \text{ MHz})}{K_o K_d} = 0.7111 \text{ rad} = 40.74^\circ$$

Since there is a constant phase shift of 90° that is always present, actual phase difference between the input signal and the output of VCO will be $90^\circ - 40.74^\circ = 49.26^\circ$.

(b) Since the input signal frequency in this case is 9 MHz, we find that

$$\phi_d = \frac{2\pi(9 \text{ MHz} - 10 \text{ MHz})}{K_o K_d} = -0.7111 \text{ rad} = -40.74^\circ$$

As before, because of a constant phase shift of 90°, actual phase difference between the input signal and the output of the VCO will be $90^\circ + 40.74^\circ = 130.74^\circ$.

Further Analysis of the PLL

Consider the simplified block diagram of the PLL as shown in Figure 11.28. It consists of only a phase detector, a low-pass filter, and a voltage-controlled oscillator. Assume that the reference and the output signals are v_r and v_o, respectively. Hence,

$$v_r(t) = A_r \sin\{\omega t + \theta_r(t)\} \tag{11.4.30}$$

and,

$$v_o(t) = A_o \cos\{\omega t + \theta_o(t)\} \tag{11.4.31}$$

Note that output frequency of the VCO varies with $v_2(t)$; therefore,

$$\theta_o(t) = K_o \int^t v_2(\tau)\, d\tau \tag{11.4.32}$$

K_o is in radians per second per volt, as defined earlier.

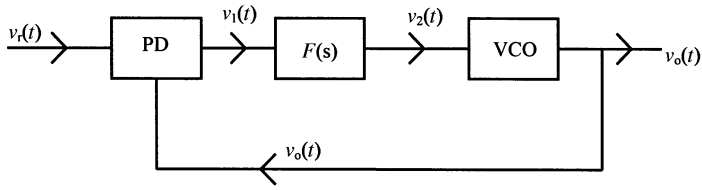

Figure 11.28 Simplified block diagram of a PLL.

Output of the phase detector is

$$v_1(t) = K_m v_r(t) v_o(t) = K_m A_r A_o \sin\{\omega t + \theta_r(t)\} \cos\{\omega t + \theta_o(t)\}$$

or,

$$v_1(t) = \frac{K_m A_r A_o}{2} (\sin\{\theta_r(t) - \theta_o(t)\} + \sin\{2\omega_o t + \theta_r(t) + \theta_o(t)\}) \tag{11.4.33}$$

The low-pass filter stops the sum frequency component (the second term). Hence,

$$v_2(t) = K_d \sin\{\theta_e(t)\} \otimes f(t) \tag{11.4.34}$$

where $\otimes$ represents the convolution of two terms; $\theta_e(t)$ is equal to $\theta_r(t) - \theta_o(t)$; and K_d is equal to $0.5 K_m A_r A_o$.

The overall equation describing the operation of the PLL may be found as follows:

$$\frac{d\theta_e(t)}{dt} = \frac{d\theta_r(t)}{dt} - \frac{d\theta_o(t)}{dt} = \frac{d\theta_r(t)}{dt} - \frac{d}{dt}\left(K_d K_o \int^t \sin\{\theta_e(\tau)\} \otimes f(\tau) d\tau\right)$$

or,

$$\frac{d\theta_e(t)}{dt} = \frac{d\theta_r(t)}{dt} - K_d K_o \sin\{\theta_e(t)\} \otimes f(t) \tag{11.4.35}$$

For $\sin\{\theta_e(t)\} \approx \theta_e(t)$, (11.4.35) can be approximated as follows:

$$\frac{d\theta_e(t)}{dt} \approx \frac{d\theta_r(t)}{dt} - K_d K_o \theta_e(t) \otimes f(t)$$

Taking the Laplace transform of this equation with initial conditions as zero, it can be transformed into the frequency domain. Hence,

$$s\theta_e(s) = s\theta_r(s) - K_d K_o \theta_e(s) F(s)$$

or,

$$\{s + K_d K_o F(s)\}\{\theta_r(s) - \theta_o(s)\} = s\theta_r(s)$$

or,

$$K_d K_o F(s) \theta_r(s) = \{s + K_d K_o F(s)\} \theta_o(s)$$

Hence, the closed-loop transfer function $T(s)$ is

$$T(s) = \frac{\theta_o(s)}{\theta_r(s)} = \frac{K_d K_o F(s)}{s + K_d K_o F(s)} \tag{11.4.36}$$

This is identical to (11.4.20) formulated earlier if the frequency division is assumed as unity.

Example 11.4: Analyze the PLL system shown below. By controlling the frequency divider, its output frequency can be changed from 2 MHz to 3 MHz in steps of 100 kHz. Transfer function of the phase detector, K_d, is 0.5 V per radian. Free-running frequency and gain factor of VCO are 2.5 MHz and 10^7 rad/sec/volt, respectively. Voltage gain of the amplifier is 10. Design a passive lead-lag-type low-pass filter that can be used in the loop.

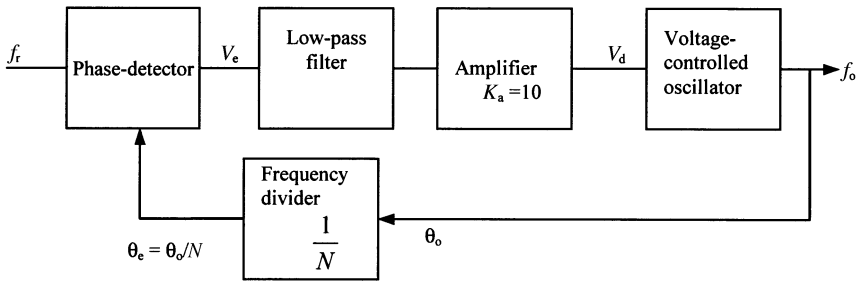

With f_m as zero (i.e., without the mixer), the output frequency is found from (11.4.1) as follows:

$$f_o = N f_r$$

Since it has a resolution of 100 kHz, its reference frequency must be the same. Next, the range of N is determined from the above equation and the desired frequency band. For f_o to be 2 MHz, N must be equal to 20. Similarly, it is 30 for an output frequency of 3 MHz. Hence,

$$20 \leq N \leq 30$$

From (11.4.6),

$$V_d = \frac{\omega_o - \omega_f}{K_o} = \frac{2\pi}{10^7}(2 \times 10^6 - 2.5 \times 10^6) = -\frac{\pi}{10} \text{ V}$$

Going back around the loop, input to the amplifier (or output of the phase detector) can be found as

$$V_e = \frac{V_d}{K_a} = -\frac{\pi}{100} \text{ V}$$

and output of the frequency divider may be found from (11.4.5) as follows:

$$\theta_e = \frac{V_e}{K_d} = -\frac{\pi}{50} \text{ rad}$$

Therefore, θ_o at the output frequency of 2 MHz is given as follows:

$$\theta_o = -\frac{2}{5}\pi = -1.2566 \text{ rad}$$

The dc loop gain K can be found via (11.4.19) as

$$K = \frac{K_d K_a K_o}{N} = \frac{0.5 \times 10 \times 10^7}{20} = 2.5 \times 10^6$$

The pull-in range $\delta\omega_p$ is given by (11.4.29) assuming that $K \gg \omega_n$.

For $\omega_n = 10^4$ rad/s and $\zeta = 0.8$, the pull-in range is

$$\delta\omega \approx 2.8249 \times 10^5 \text{ rad/s}$$

or,

$$\delta f_p = 4.5 \times 10^4 \text{ Hz} = 45 \text{ kHz}$$

A lag-lead filter can be designed as follows:

From (11.4.27) and (11.4.28)

$$\tau_1 = \frac{K}{\omega_n^2} = \frac{2.5 \times 10^6}{10^8} = 0.025 \text{ s} = (R_1 + R_2)C_2$$

$$\zeta = \frac{\omega_n}{2}\left(\tau_2 + \frac{1}{K}\right) \Rightarrow \tau_2 = \frac{2\zeta}{\omega_n} - \frac{1}{K} = \frac{2 \times 0.8}{10^4} - \frac{1}{2.5 \times 10^6}$$
$$= 1.596 \times 10^{-4} \text{ s} = R_2 C_2$$

For $C_2 = 0.5\,\mu\text{F}$,

$$R_2 = \frac{1.596 \times 10^{-4}}{0.5 \times 10^{-6}} = 319.2\ \Omega$$

and,

$$R_1 = \frac{\tau_1}{C_2} - R_2 = \frac{0.025}{0.5 \times 10^{-6}} - 319.2 = 50000 - 319.2 = 49680.8\ \Omega \approx 50\ \text{k}\Omega$$

11.5 FREQUENCY SYNTHESIZERS

The frequency of a reference oscillator can be multiplied and its harmonics can be generated with the help of a nonlinear device. The desired frequency component can then be filtered out. This kind of frequency generation is called *direct synthesis*. However, it has several limitations, including the constraints on the filter design. An alternative approach uses a PLL (analog or digital) to synthesize the desired signal. This is known as *indirect synthesis*. Another technique, known as *direct digital synthesis* (DDS), uses a digital computer and the digital-to-analog converter for generating the desired signal. In this section, we consider indirect frequency synthesis. Mixers and frequency multipliers are described in next chapter.

Example 11.4 illustrated the basic principle of an indirect frequency synthesizer. A simplified PLL frequency synthesizer is illustrated in Figure 11.29. As discussed in preceding section, the feedback signal frequency f_d is equal to the reference frequency f_r if the loop is in locked state. Since the frequency divider divides the output frequency by N, the output frequency f_o is equal to Nf_r. If N is an integer then the frequency step is equal to reference frequency f_r. For a fine resolution, the reference frequency should be very low. On the other hand, lower f_r increases the switching time. As a rule of thumb, the product of switching time t_s and the reference frequency f_r is equal to 25. Therefore, the switching time is 25 s for the reference frequency of 1 Hz. Since a shorter switching time is desired, it limits the frequency resolution of this system.

As illustrated in Figure 11.30, one way to improve the frequency resolution while keeping the switching time short (the reference frequency high) is to add another frequency divider at its output. Hence, the output frequency in this system will be given as follows:

$$f_o = N\frac{f_r}{M} \tag{11.5.1}$$

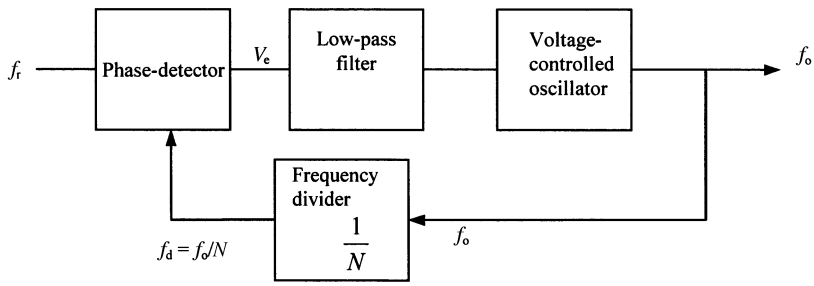

Figure 11.29 A PLL frequency synthesizer.

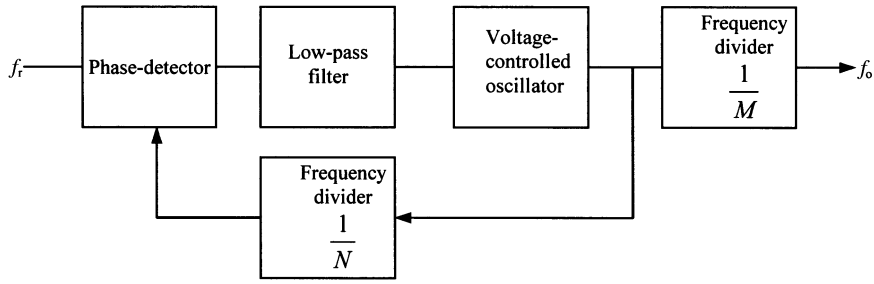

Figure 11.30 A PLL followed by a frequency divider.

Thus, the frequency resolution in this system is f_r/M, which shows an improvement over the previous arrangement. However, a close analysis of this system indicates that the signal frequency in its phase-locked loop section may become excessively large. This is explained further via the following example.

Example 11.5: Design a PLL frequency synthesizer that covers the frequency range from 100 MHz to 110 MHz with a resolution of 1 kHz.

With the single loop of Figure 11.29, the reference frequency must be equal to the resolution required. Hence,

$$f_r = 1 \text{ kHz}$$

Since the output frequency $f_o = Nf_r$, the range of N is given as follows:

$$10^5 \leq N \leq 11 \times 10^4$$

As explained earlier, the switching time in this case is on the order of 25 milliseconds. If this switching time is not acceptable and we want to keep it below 250 μsec then an arrangement similar to that illustrated in Figure 11.30 may be used. A reference frequency of 100 kHz provides the switching time of 250 μsec. In this case, setting M of the output frequency can be determined as follows:

$$M = \frac{f_r}{\text{Frequency resolution}} = \frac{100 \text{ kHz}}{1 \text{ kHz}} = 100$$

In order to cover the desired frequency range, the voltage-controlled oscillator must generate the frequencies from 10 GHz to 11 GHz. This is because the frequency divider divides output of the voltage-controlled oscillator by M before the signal appearing at the output.

Range of N can be determined after dividing the frequency of the voltage-controlled oscillator by the reference frequency. Hence,

$$10^5 \leq N \leq 11 \times 10^4$$

Thus, this may not be a good technique to get better frequency resolution. However, this concept is extended in practice where multiple loops are used to obtain fine resolution. It is illustrated through the following example.

Example 11.6: Design a PLL frequency synthesizer for the frequency range 1 MHz to 50 MHz with increments of 1 kHz.

Note that if a single-loop synthesizer is used in this case then its reference frequency should be of 1 kHz. That makes its switching time on the order of 0.025 sec and the setting of frequency divider ranges as follows:

$$1 \times 10^3 \leq N \leq 50 \times 10^3$$

An alternative design that uses three phase-locked loops is illustrated in Figure 11.31. Loops A and B use a higher-reference frequency (say, 100 kHz), while the output of A (f_A) works as the reference for loop C after it is divided by M. The following relation holds when the loops are in locked state

$$f_A = f_o - f_B$$

Therefore, output frequency f_o is equal to the sum of other two, namely, f_A and f_B.

If a mixer is used to combine f_A and f_B directly then its sum and difference frequency components may be too close to separate the two via a band-pass filter. However, the present technique of using a phase-locked loop C for this purpose accomplishes the desired separation.

Since the reference frequency is 100 kHz, the output frequency of loop A, f_a, can be varied in steps of 100 kHz and 1 kHz resolution in the output can be achieved with M as 100. Hence,

$$f_a = 10^5 N_A$$

and,

$$f_A = \frac{f_a}{100} = 10^3 \times N_A$$

Thus, f_A varies in 1-kHz steps. Loop A can generate increments of 1 and 10 kHz in the output frequency. Similarly, loop B produces 0.1 and 1 MHz steps in the output frequency. Reference frequency f_A to loop C should be selected in such a way that it keeps its switching time short. If, for example, f_A is equal to 1 kHz then the switching time of loop C is on the order of 0.025 sec. Since it is the longest time

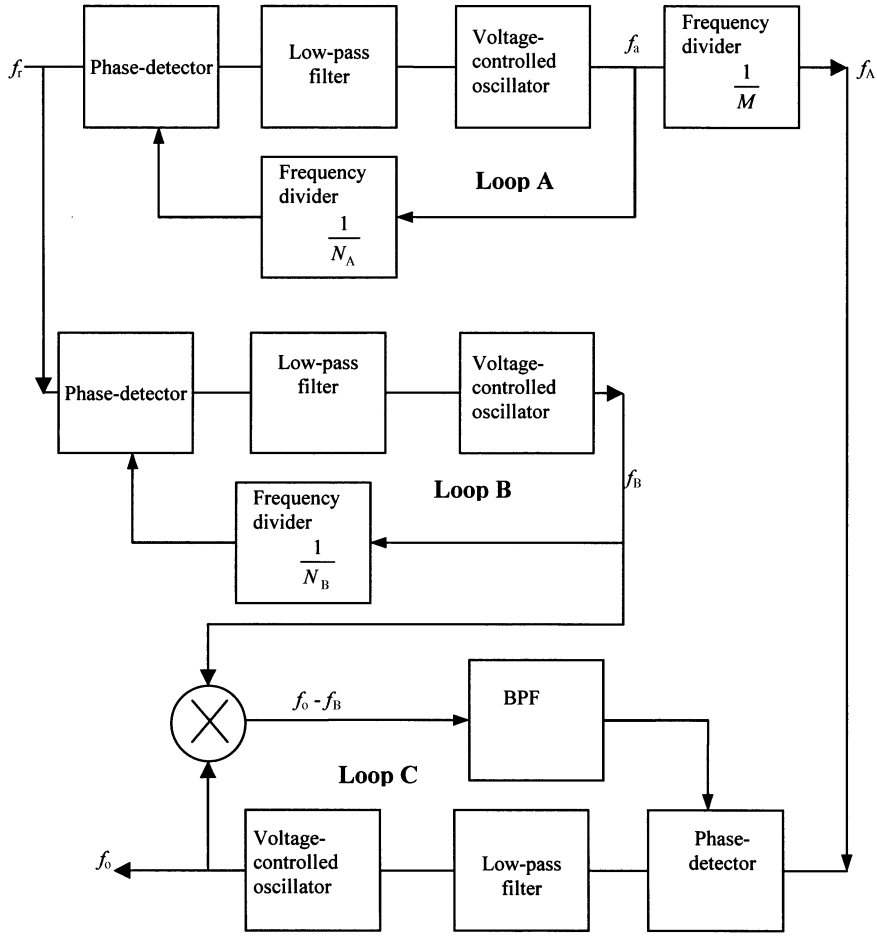

Figure 11.31 A multiloop frequency synthesizer system.

among the three loops, it sets the overall response time of the synthesizer. To reduce the response time of loop C, f_A may be increased to 500 kHz so that

$$500 \text{ kHz} \leq f_A \leq 599 \text{ kHz}$$

Therefore, the output frequency of loop A (that is, before dividing by 100) ranges as follows:

$$5 \times 10^7 \text{ Hz} \leq f_a \leq 5.99 \times 10^7 \text{ Hz}$$

The range of the frequency divider setting, N_A, can be determined easily as f_a/f_r. Hence,

$$500 \leq N_A \leq 599$$

Since $f_B = f_o - f_A$, f_B is reduced by 500 kHz so that

$$(1 - 0.5)\ \text{MHz} \leq f_B \leq (50 - 0.5)\ \text{MHz}$$

or,

$$0.5\ \text{MHz} \leq f_B \leq 49.5\ \text{MHz}$$

Hence, the frequency divider setting, N_B, in loop B ranges as follows:

$$5 \leq N_B \leq 495$$

Loops A and B use same reference frequency, and therefore, they have the same response time. It is on the order of 250 μsec. On the other hand, loop C has a response time on the order of 50 μsec. Thus, overall response time of the frequency synthesizer is approximately 250 μsec. At the same time, we achieved a frequency resolution of 1 kHz. This idea can be extended further to reduce the frequency resolution even below 1 kHz while keeping the overall response time short by using additional loops.

11.6 ONE-PORT NEGATIVE RESISTANCE OSCILLATORS

Properly biased Gunn and IMPATT (*imp*act ionization *a*valanche *t*ransit *t*ime) diodes exhibit negative resistance characteristics that can be utilized in conjunction with an external resonant circuit to design a solid-state microwave oscillator. The Gunn diode is a transferred-electron device that uses a bulk semiconductor (usually GaAs or InP) as opposed to a *p-n* junction. Its dc-to-RF conversion efficiency is generally less than 10 percent.

The IMPATT diode uses a reverse-biased *p-n* junction to generate microwave power. The diode material is usually silicon or GaAs, and it is operated with a relatively high voltage, on the order of 70 to 100 V, to achieve a reverse-biased avalanche breakdown current. When coupled with a high-Q resonator and biased at an appropriate operating point, the diode exhibits a negative resistance effect and sustained oscillations are obtained. Its output power is much higher (on the order of tens or hundreds of W) in comparison with that produced by a Gunn diode. On the other hand, Gunn diodes produce relatively low FM noise.

Figure 11.32 shows the RF equivalent circuits for a one-port negative resistance oscillator where Z_G is the input impedance (Y_G is the corresponding input admittance) of the active device (i.e., a biased diode). Figure 11.32 (b) is an equivalent parallel arrangement of the circuit shown in Figure 11.32 (a). In general, the impedance Z_G (or admittance Y_G) is current (or voltage) and frequency dependent.

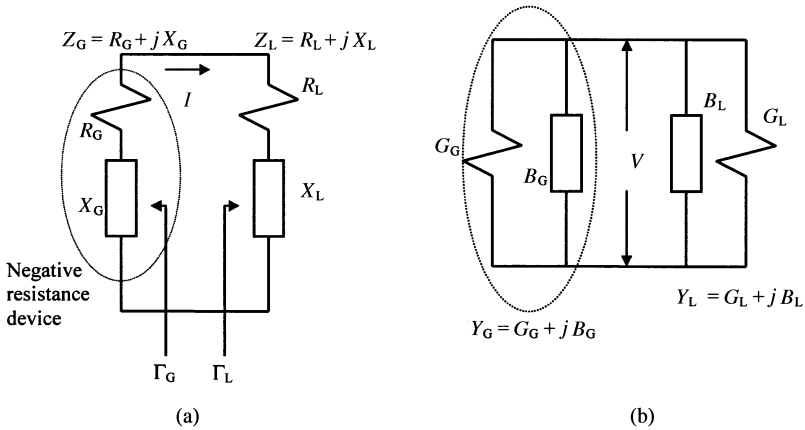

Figure 11.32 Series (a) and parallel (b) equivalent circuits for one-port negative resistance microwave oscillators.

Applying Kirchhoff's loop equation in the circuit shown in Figure 11.32 (a), we get

$$(Z_G + Z_L)I = 0$$

If oscillations are occurring then current I in the loop is nonzero. In such a situation, the following conditions must be satisfied:

$$R_G + R_L = 0 \tag{11.6.1}$$

and,

$$X_G + X_L = 0 \tag{11.6.2}$$

Similarly, applying Kirchhoff's node equation in the circuit shown in Figure 11.32 (b), we get

$$(Y_G + Y_L)V = 0$$

Again, voltage V across the circuit is not equal to zero if oscillations are occurring. Therefore, this condition is satisfied only if $Y_G + Y_L = 0$. Hence,

$$G_G + G_L = 0 \tag{11.6.3}$$

and,

$$B_G + B_L = 0 \tag{11.6.4}$$

Since R_L (or G_L) has a positive value that is greater than zero, the above conditions require a negative R_G (or $-G_G$). Negative resistance implies a source because a positive resistance dissipates the energy.

Note that the impedance Z_G is nonlinearly related with the current (or voltage) and the frequency. Conditions (11.6.1)–(11.6.4) represent the steady-state behavior of the circuit. Initially, it is necessary for the overall circuit to be unstable at a certain frequency (i.e., the sum of R_G and R_L is a negative number). Any transient excitation or noise then causes the oscillation to build up at a frequency ω. As the current (or voltage) increases, R_G (or G_G) becomes less negative until it reaches a value such that (11.6.1)–(11.6.4) are satisfied.

For the startup of oscillation, negative resistance of the active device in a series circuit must exceed the load resistance by about 20 percent (i.e., $R_G \approx -1.2R_L$). Similarly, G_G is approximately $-1.2G_L$ to start the oscillations in the parallel circuit. For the stability of an oscillator, high-Q resonant circuits, such as cavities and dielectric resonators are used.

Example 11.7: A 6-GHz oscillator is to be designed using a negative resistance diode with its reflection coefficient Γ_G as $1.25\angle 40^\circ$ (measured with $Z_o = 50\,\Omega$ as reference). Determine its load impedance.

From

$$\Gamma_G = \frac{\bar{Z}_G - 1}{\bar{Z}_G + 1}$$

$$\bar{Z}_G = \frac{1 + \Gamma_G}{1 - \Gamma_G} = \frac{1 + 1.25\angle 40^\circ}{1 - 1.25\angle 40^\circ} = \frac{1.9576 + j0.8035}{0.0424 - j0.8035} = \frac{2.1161\angle 22.32^\circ}{0.8046\angle -86.98^\circ}$$

or,

$$\bar{Z}_G = 2.63\angle 109.3^\circ = -0.8693 + j2.4822$$

If a given reflection coefficient has magnitude greater than unity then we can still use the Smith chart to find the corresponding impedance provided that we follow the procedure described in Chapter 10 (Section 10.3). Thus, the impedance point can be identified on the Smith chart, as shown in Figure 11.33. The corresponding value is found to be the same as obtained above through the formula. Hence,

$$Z_G = R_G + jX_G = -43.5 + j124.11\ \Omega$$

Therefore, the load impedance is given as follows:

$$Z_L = 43.5 - j124.11\ \Omega$$

The corresponding equivalent circuit is illustrated in Figure 11.34.

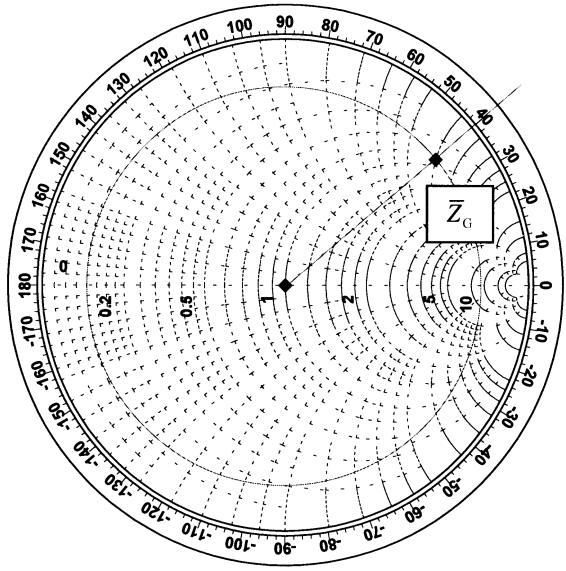

Figure 11.33 Graphical method of determining the input impedance of the diode.

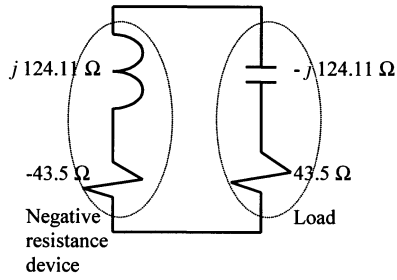

Figure 11.34 Equivalent circuit of Example 11.7.

11.7 MICROWAVE TRANSISTOR OSCILLATORS

Several oscillator circuits using transistors were considered in Section 11.1 along with the basic concepts. This section presents a design procedure that is based on the S-parameters of the transistor. RF circuit arrangement of a microwave transistor oscillator is shown in Figure 11.35. A field-effect transistor shown as the device in this figure is in common-source configuration, although any other terminal can be used in its place, provided that the corresponding S-parameters are known. Further, a BJT can also be used in its place. In other words, the design procedure described here is general and applies to any transistor circuit configuration as long as its S-parameters are known.

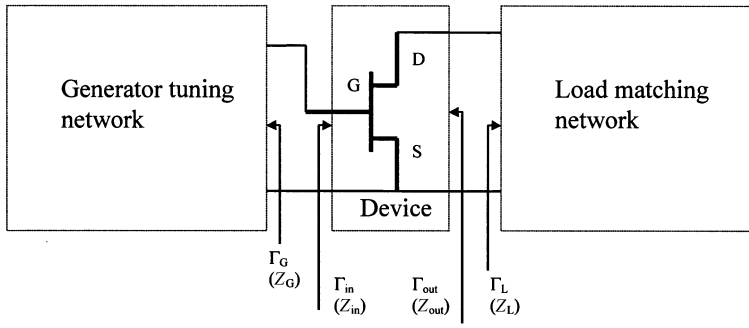

Figure 11.35 Microwave transistor oscillator circuit.

Unlike the amplifier circuit, the transistor for an oscillator design must be unstable. Therefore, the opposite of conditions (10.1.16) and (10.1.18) must hold in this case. If the stability parameter k is not less than unity (or $|\Delta|$ is not larger than unity) then an external positive feedback can be used to make the device unstable. Equations (11.6.1) to (11.6.4) of the preceding section can be recast as follows:

$$\Gamma_{in}\Gamma_G = 1 \tag{11.7.1}$$

or,

$$\Gamma_{out}\Gamma_L = 1 \tag{11.7.2}$$

These two conditions state that passive terminations Z_G and Z_L must be added for resonating the input and output ports of the active device at the frequency of oscillation. These two conditions are complementary to each other; i.e., if condition (11.7.1) is satisfied then (10.7.2) is also satisfied, and vice versa. It can be proved as follows.

From the expression for input reflection coefficient obtained in Example 9.6, we can write

$$\Gamma_{in} = S_{11} + \frac{S_{12}S_{21}\Gamma_L}{1 - S_{22}\Gamma_L} = \frac{S_{11} - \Delta\Gamma_L}{1 - S_{22}\Gamma_L} \Rightarrow \frac{1}{\Gamma_{in}} = \frac{1 - S_{22}\Gamma_L}{S_{11} - \Delta\Gamma_L} \tag{11.7.3}$$

where $\Delta = S_{11}S_{22} - S_{12}S_{21}$ as defined earlier in Chapter 10.

If (11.7.1) is satisfied, then

$$\Gamma_G = \frac{1}{\Gamma_{in}} = \frac{1 - S_{22}\Gamma_L}{S_{11} - \Delta\Gamma_L} \Rightarrow S_{11}\Gamma_G - \Delta\Gamma_L\Gamma_G = 1 - S_{22}\Gamma_L \Rightarrow \Gamma_L = \frac{1 - S_{11}\Gamma_G}{S_{22} - \Delta\Gamma_G} \tag{11.7.4}$$

and the output reflection obtained in Example 9.7 can be rearranged as follows:

$$\Gamma_{out} = S_{22} + \frac{S_{12}S_{21}\Gamma_G}{1 - S_{11}\Gamma_G} = \frac{S_{22} - \Delta\Gamma_G}{1 - S_{11}\Gamma_G} \tag{11.7.5}$$

From (11.7.4) and (11.7.5),

$$\Gamma_{out}\Gamma_L = 1$$

Similarly, it can be proved that if condition (11.7.2) is satisfied then (11.7.1) is also satisfied.

After a transistor configuration is selected, the output stability circle can be drawn on the Γ_L plane, and Γ_L is selected to produce a large value of negative resistance at the input of the transistor. Then, Γ_G (and hence Z_G) can be chosen to match the input impedance Z_{in}. If the small-signal S-parameters are used in such design, a fairly large negative value of R_{in} must be selected initially so that the sum of R_G and R_{in} is a negative number. As oscillations build up, R_{in} becomes less and less negative. If its initial value is less negative then the oscillation may cease when the power buildup increases R_{in} to the point where $R_G + R_{in}$ is greater than zero. In practice, a value of $R_G = -R_{in}/3$ is typically used. To resonate the circuit, the reactive part of Z_G is selected as $-X_{in}$.

Example 11.8: Using a GaAs FET in the common gate configuration, design an oscillator at 4 GHz. To provide the positive feedback, a 4-nH inductor is connected in series with its gate. S-parameters of the resulting circuit are given below ($Z_o = 50\,\Omega$).

$$S_{11} = 2.18\angle -35^\circ, \quad S_{21} = 2.75\angle 96^\circ, \quad S_{12} = 1.26\angle 18^\circ, \text{ and } S_{22} = 0.52\angle 155^\circ$$

From (10.1.16) and (10.1.18),

$$\Delta = S_{11}S_{22} - S_{21}S_{12} = 2.34\angle -68.9^\circ$$

and,

$$k = \frac{1 - |S_{11}|^2 - |S_{22}^*|^2 + |\Delta|^2}{2|S_{12}S_{21}|} = 0.21$$

Therefore, the transistor and inductor combination is potentially unstable, and it can be used for an oscillator design (see Figure 11.36).

From (10.1.22) and (10.1.23), the input stability circle is determined as follows:

$$\text{Center } C_s = \frac{(S_{11} - \Delta S_{22}^*)^*}{|S_{11}|^2 - |\Delta|^2} = 4.67\angle -141.8^\circ$$

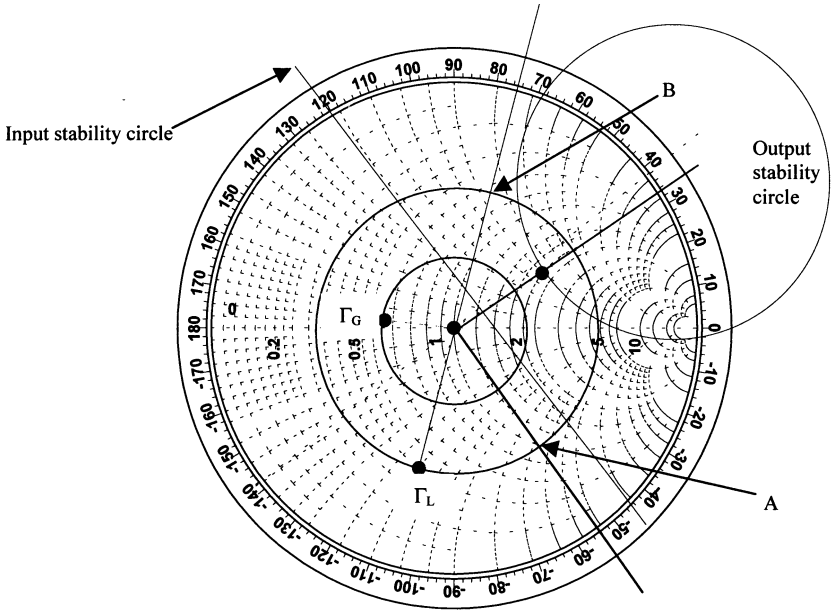

Figure 11.36 Input and output stability circles for Example 11.8.

and,

$$\text{Radius } r_s = \left|\frac{S_{12}S_{21}}{|S_{11}|^2 - |\Delta|^2}\right| = 4.77$$

Further, it may be found that the inside of this circle is stable.

Similarly, the output stability circle is determined from (10.1.20) and (10.1.21) as follows:

$$\text{Center } C_L = \frac{(S_{22} - \Delta S_{11}^*)^*}{|S_{22}|^2 - |\Delta|^2} = 1.08\angle 33.1^\circ$$

and,

$$\text{Radius } r_L = \left|\frac{S_{12}S_{21}}{|S_{22}|^2 - |\Delta|^2}\right| = 0.67$$

Again, the inside of this circle is determined as the stable region.

We want to select Z_L in the unstable region for which ρ_{in} is large. Thus, after several trials, we selected $\Gamma_L = 0.59\angle -104^\circ$. A single stub network can be designed for this Γ_L. A 0.096-λ-long shunt stub with a short circuit at its other end transforms 50 Ω to the admittance at point A and then a 0.321-λ-long line takes it to point B (the desired admittance).

Next, we calculate Γ_{in} for this Γ_L as follows:

$$\Gamma_{in} = S_{11} + \frac{S_{12}S_{21}\Gamma_L}{1 - S_{22}\Gamma_L} = 3.9644\angle -2.4252^\circ$$

$$\therefore \quad Z_{in} = 50 \times \frac{1 + \Gamma_{in}}{1 - \Gamma_{in}} = 50 \times (-1.6733 - j0.03815) = -83.67 - j1.91\ \Omega$$

$$\therefore \quad Z_G = \frac{83.67}{3} + j1.91 \approx 27.9 + j1.91\ \Omega \Rightarrow \Gamma_G = \frac{Z_G - 50}{Z_G + 1} = 0.2847\angle 173.6^\circ$$

$$\text{VSWR} = (1 + 0.2847)/(1 - 0.2847) = 1.796$$

Hence, Z_G can be synthesized via a 27.9-Ω resistance in series with a 0.01-λ-long line. The designed oscillator circuit is illustrated in Figure 11.37.

Example 11.9: Design a microwave oscillator at 2.75 GHz using a BJT in its common-base configuration. S-parameters of the transistor are given as follows:

$$S_{11} = 0.9\angle 150^\circ, \quad S_{21} = 1.7\angle -80^\circ, \quad S_{12} = 0.07\angle 120^\circ, \text{ and } S_{22} = 1.08\angle -56^\circ$$

Note that this transistor is potentially unstable ($k = -0.6447$). This unstable region on the Smith chart can be increased further using an external feedback. A 1.45-nH inductor in its base terminal, shown here, is found to provide optimum response.

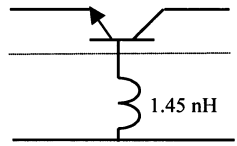

Before we proceed with the design, we need to determine the S-parameters of this transistor-inductor combination. Since these are connected in series, its impedance parameters can be easily found by adding impedance matrices of the two. The impedance matrix of the transistor can be determined from the corresponding S-parameters and the formulas tabulated in Chapter 7 (Table 7.4). The calculation proceeds as follows:

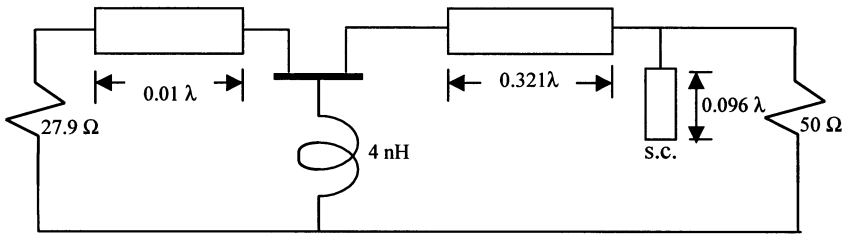

Figure 11.37 RF circuit of the GaAs FET oscillator for Example 11.8.

1. *Determination of the normalized Z-parameters of the BJT*:

$$\Delta_1 = (1 - S_{11})(1 - S_{22}) - S_{12}S_{21} = 1.0164 + j1.3386 = 1.6807\angle 52.79^\circ$$
$$\bar{Z}_{11} = \frac{(1 + S_{11})(1 - S_{22}) + S_{21}S_{12}}{\Delta_1} = 0.3005\angle 63.58^\circ = 0.1337 + j0.2691$$
$$\bar{Z}_{12} = \frac{2S_{12}}{\Delta_1} = 0.0833\angle 67.21^\circ = 0.0323 + j0.0768$$
$$\bar{Z}_{21} = \frac{2S_{21}}{\Delta_1} = 2.023\angle -132.79^\circ = -1.3743 - j1.4846$$

and,

$$\bar{Z}_{22} = \frac{(1 - S_{11})(1 + S_{22}) + S_{21}S_{12}}{\Delta_1} = 2.0154\angle -94.15^\circ = -0.1459 - j2.0101$$

2. *Z-matrix of the inductor section*: Impedance of the inductor,

$$Z_{\text{inductor}} = j2 \times \pi \times 2.75 \times 10^9 \times 1.45 \times 10^{-9}\ \Omega = j25.0542\ \Omega$$

or

$$\bar{Z}_{\text{inductor}} = \frac{j25.0542}{50} = j0.5011$$

Therefore, the Z-matrix of the inductor section will be given as follows:

$$[\bar{Z}_{\text{inductor}}] = \begin{bmatrix} j0.5011 & j0.5011 \\ j0.5011 & j0.5011 \end{bmatrix}$$

3. *Z-impedance of the BJT and inductor combination*:

$$\begin{bmatrix} \bar{Z}'_{11} & \bar{Z}'_{12} \\ \bar{Z}'_{21} & \bar{Z}'_{22} \end{bmatrix} = \begin{bmatrix} \bar{Z}_{11} & \bar{Z}_{12} \\ \bar{Z}_{21} & \bar{Z}_{22} \end{bmatrix} + [\bar{Z}_{\text{inductor}}]$$
$$= \begin{bmatrix} 0.1337 + j0.7702 & 0.0323 + j0.5779 \\ -1.3743 - j0.9067 & -0.1459 - j1.509 \end{bmatrix}$$

4. *Determination of S-matrix of the BJT and inductor combination*: The S-parameters of this circuit can be easily determined from its Z-parameters using

the formulas given in Table 7.4. Various steps of this calculation are given as follows:

$$\Delta = (\bar{Z}_{11}+1)(\bar{Z}_{22}+1) - \bar{Z}'_{12}\bar{Z}'_{21} = 1.651 - j0.2294 = 1.6669\angle -7.91^\circ$$

$$S'_{12} = \frac{2\bar{Z}'_{12}}{\Delta} = 0.6945\angle 94.71^\circ$$

$$S'_{21} = \frac{2\bar{Z}'_{21}}{\Delta} = 1.9755\angle -138.68^\circ$$

$$S'_{11} = \frac{(\bar{Z}'_{11}-1)(\bar{Z}'_{22}+1) - \bar{Z}'_{12}\bar{Z}'_{21}}{\Delta} = 1.6733\angle 99.1^\circ$$

and,

$$S'_{22} = \frac{(\bar{Z}'_{11}+1)(\bar{Z}'_{22}-1) - \bar{Z}'_{12}\bar{Z}'_{21}}{\Delta} = 1.13\angle -101.3^\circ$$

Now from (10.1.16) and (10.1.18),

$$\Delta = S_{11}S_{22} - S_{21}S_{12} = 1.2601\angle 44.29^\circ$$

and,

$$k = \frac{1 - |S_{11}|^2 - |S_{22}|^2 + |\Delta|^2}{2|S_{12}S_{21}|} = -0.5426$$

Therefore, the transistor and inductor combination is potentially unstable, and it can be used for an oscillator design. It may be interesting to know that without the feedback inductor (just for the transistor), Δ and k are $0.9072\angle 100.09^\circ$ and -0.6447, respectively.

From (10.1.22) and (10.1.23), the input stability circle is determined as follows:

$$\text{Center } C_s = \frac{(S_{11} - \Delta S^*_{22})^*}{|S_{11}|^2 - |\Delta|^2} = 1.0262\angle -42.96^\circ$$

and,

$$\text{Radius } r_s = \left|\frac{S_{12}S_{21}}{|S_{11}|^2 - |\Delta|^2}\right| = 1.132$$

Further, it may be found that the outside of this circle is stable.

Similarly, the output stability circle of the circuit is determined from (10.1.20) and (10.1.21) as follows:

$$\text{Center } C_{\text{L}} = \frac{(S_{22} - \Delta S_{11}^*)^*}{|S_{22}|^2 - |\Delta|^2} = 5.0241 \angle 23.18^\circ$$

and,

$$\text{Radius } r_{\text{L}} = \left| \frac{S_{12}S_{21}}{|S_{22}|^2 - |\Delta|^2} \right| = 4.4107$$

This time, the inside of this circle is found to be stable.

There are two output stability circles illustrated in Figure 11.38. Circle 1 encloses the unstable region for the BJT alone (i.e., the feedback inductor is not used). This means that the load impedance of the oscillator circle must be selected inside this circle. On the other hand, the range of impedance increases significantly with the feedback inductor. It is illustrated by circle 2, which encloses the stable region.

We want to select Z_{L} in the unstable region for which ρ_{in} is large. Thus, after several trials, we selected $\Gamma_{\text{L}} = 0.5689 \angle 167.8^\circ$. A single stub network can be designed for this Γ_{L}. A shunt stub of 0.147 λ with an open circuit at its other end transforms 50 Ω to point B and then a 0.1-λ-long line provides the desired admittance (point A).

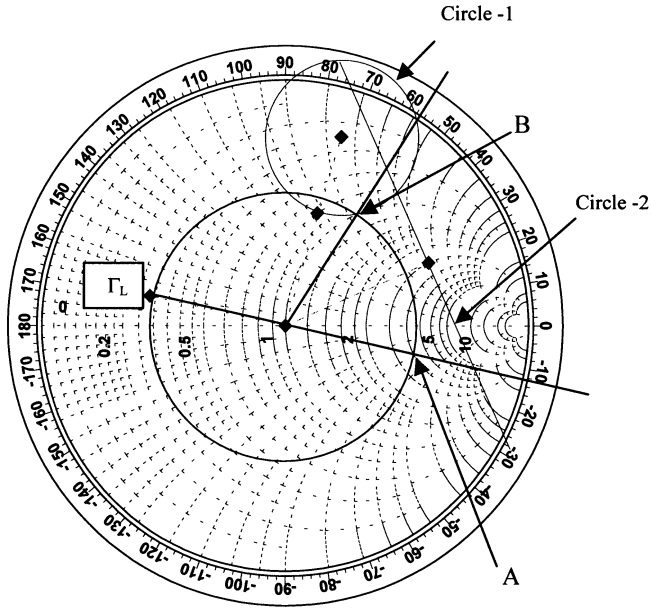

Figure 11.38 Input and output stability circles for Example 11.9.

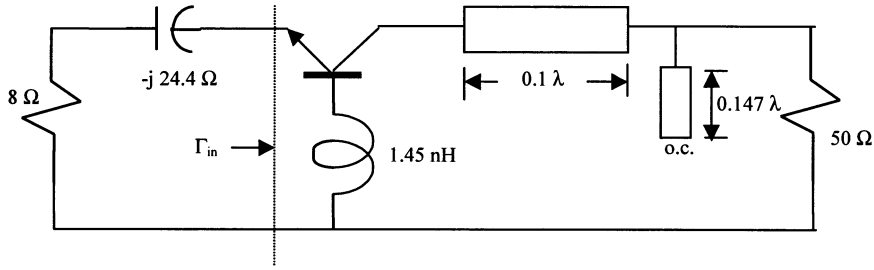

Figure 11.39 RF circuit of the BJT oscillator for Example 11.9.

Next, we calculate Γ_{in} for this Γ_L as follows (see Figure 11.39):

$$\Gamma_{in} = S_{11} + \frac{S_{12}S_{21}\Gamma_L}{1 - S_{22}\Gamma_L} = 2.1726\angle 118.8375^\circ$$

$$\therefore \quad Z_{in} = 50 \times \frac{1 + \Gamma_{in}}{1 - \Gamma_{in}} = -23.8 + j24.35\ \Omega$$

and,

$$\therefore \quad Z_G = \frac{23.8}{3} - j24.35 \approx 8 - j24.4\ \Omega$$

Three-Port S-Parameter Description of the Transistor

Transistor parameters are generally specified as a two-port device while keeping one of its terminals as a reference point (common emitter, common source, etc.). However, it may be advantageous in certain design instances to use a different terminal as a common electrode. Further, it may be prudent sometimes to add an external feedback that enhances the desired characteristics of a device. A three-port description of the transistor facilitates such design procedures. This section describes a computation method to determine three-port S-parameters of the transistor (or any other three-terminal circuit) from its two-port description. These parameters are subsequently used to design the feedback network for the device as well as for changing its common terminal.

Consider a three-port network as illustrated in Figure 11.40. Incident and reflected waves at the three ports are related through its S-parameters as follows:

$$\begin{bmatrix} b_1' \\ b_2' \\ b_3' \end{bmatrix} = \begin{bmatrix} S_{11}' & S_{12}' & S_{13}' \\ S_{21}' & S_{22}' & S_{23}' \\ S_{31}' & S_{32}' & S_{33}' \end{bmatrix} \begin{bmatrix} a_1' \\ a_2' \\ a_3' \end{bmatrix} \tag{11.7.6}$$

It can be shown that these S-parameters satisfy the following two conditions, and therefore, all nine elements of the scattering matrix are not independent:

$$\sum_{i=1}^{3} S_{ij}' = 1, \qquad j = 1, 2, 3 \tag{11.7.7}$$

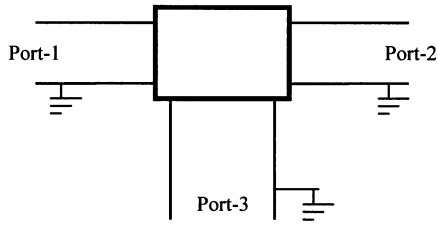

Figure 11.40 A three-port network.

and,

$$\sum_{j=1}^{3} S'_{ij} = 1, \qquad i = 1, 2, 3 \tag{11.7.8}$$

Condition (11.7.7) can be proved when there is negligible stray capacitance at each port. In that case, the algebraic sum of the currents entering these ports must be zero. Hence,

$$\sum_{n=1}^{3} i_n = 0$$

Using (7.6.15) and (7.6.16), we can write

$$\sum_{i=1}^{3} (a'_i - b'_i) = 0$$

or,

$$\sum_{i=1}^{3} \left(a'_i - \sum_{j=1}^{3} S'_{ij} a'_j \right) = 0 \tag{11.7.9}$$

If we select $a'_2 = a'_3 = 0$ then (11.7.9) simplifies to

$$a'_1 - \sum_{i=1}^{3} S'_{i1} a'_1 = 0$$

or,

$$\sum_{i=1}^{3} S'_{i1} = 1 \tag{11.7.10}$$

Similarly, for $a'_1 = a'_3 = 0$

$$\sum_{i=1}^{3} S'_{i2} = 1 \tag{11.7.11}$$

and, for $a'_1 = a'_2 = 0$

$$\sum_{i=1}^{3} S'_{i3} = 1 \tag{11.7.12}$$

Hence, condition (11.7.7) is verified.

Condition (11.7.8) can be verified as follows. When every port has the same voltage there will be no input current provided that the stray capacitance from each terminal to ground is zero. Since $i_i = a'_i - b'_i$, b'_i must be equal to a'_i. Consequently, $b'_1 = b'_2 = b'_3 = a'$ for $a'_1 = a'_2 = a'_3 = a'$. Hence,

$$b'_i = \sum_{j=1}^{3} S'_{ij} a'_j = a' \sum_{j=1}^{3} S'_{ij} = a', \qquad i = 1, 2, 3$$

or

$$\sum_{j=1}^{3} S'_{ij} = 1, \qquad i = 1, 2, 3$$

That proves condition (11.7.8).

Using (7.6.15) and (7.6.16), we find that the normalized voltage at port-3 is $V_3 = a'_3 + b'_3$. Let us now define new voltage waves at ports 1 and 2 as follows:

$$a_1 = a'_1 - \frac{V_3}{2} = a'_1 - \frac{a'_3 + b'_3}{2} \tag{11.7.13}$$

$$b_1 = b'_1 - \frac{V_3}{2} = b'_1 - \frac{a'_3 + b'_3}{2} \tag{11.7.14}$$

$$a_2 = a'_2 - \frac{V_3}{2} = a'_2 - \frac{a'_3 + b'_3}{2} \tag{11.7.15}$$

and

$$b_2 = b'_2 - \frac{V_3}{2} = b'_2 - \frac{a'_3 + b'_3}{2} \tag{11.7.16}$$

The new total voltages at ports 1 and 2 are now

$$V_1 = a_1 + b_1 = a'_1 + b'_1 - V_3 \tag{11.7.17}$$

and,

$$V_2 = a_2 + b_2 = a'_2 + b'_2 - V_3 \tag{11.7.18}$$

Thus, these voltages are referred to the port-3 voltage.

Note that these definitions of new incident and reflected waves do not change the port currents, i.e.,

$$b_1 - a_1 = b_1' - a_1' \tag{11.7.19}$$

and,

$$b_2 - a_2 = b_2' - a_2' \tag{11.7.20}$$

The two-port scattering matrix that relates b_1 and b_2 to a_1 and a_2 will now make the port-3 terminal common. Hence,

$$b_1 = S_{11}a_1 + S_{12}a_2 \tag{11.7.21a}$$

$$b_2 = S_{21}a_1 + S_{22}a_2 \tag{11.7.21b}$$

Combining (11.7.13)–(11.7.21), we have

$$b_1' - \frac{a_3' + b_3'}{2} = S_{11}\left(a_1' - \frac{a_3' + b_3'}{2}\right) + S_{12}\left(a_2' - \frac{a_3' + b_3'}{2}\right) \tag{11.7.22a}$$

and,

$$b_2' - \frac{a_3' + b_3'}{2} = S_{21}\left(a_1' - \frac{a_3' + b_3'}{2}\right) + S_{22}\left(a_2' - \frac{a_3' + b_3'}{2}\right) \tag{11.7.22b}$$

From Kirchhoff's current law, the sum of all currents flowing into the three terminals must be zero. Therefore, we can write

$$a_1' - b_1' + a_2' - b_2' + a_3' - b_3' = 0 \tag{11.7.23}$$

Rearranging (11.7.22) and (11.7.23) we get

$$b_1' = S_{11}a_1' + S_{12}a_2' + (1 - S_{11} - S_{12})\left(\frac{a_3' + b_3'}{2}\right) \tag{11.7.24a}$$

$$b_2' = S_{21}a_1' + S_{22}a_2' + (1 - S_{21} - S_{22})\left(\frac{a_3' + b_3'}{2}\right) \tag{11.7.24b}$$

and,

$$\begin{aligned} b_3' &= a_1' + a_2' + a_3' - b_1' - b_2' \\ &= a_1' + a_2' + a_3' - S_{11}a_1' - S_{12}a_2' - (1 - S_{11} - S_{12})\left(\frac{a_3' + b_3'}{2}\right) \\ &\quad - S_{21}a_1' - S_{22}a_2' - (1 - S_{21} - S_{22})\left(\frac{a_3' + b_3'}{2}\right) \end{aligned}$$

or,

$$b_3' = \frac{2\Delta_{12}}{4-\Delta}a_1' + \frac{2\Delta_{21}}{4-\Delta}a_2' + \frac{\Delta}{4-\Delta}a_3' \tag{11.7.25}$$

where,

$$\Delta_{12} = 1 - S_{11} - S_{21} \tag{11.7.26a}$$
$$\Delta_{21} = 1 - S_{12} - S_{22} \tag{11.7.26b}$$
$$\Delta = S_{11} + S_{22} + S_{12} + S_{21} = 2 - \Delta_{12} - \Delta_{21} = 2 - \Delta_{11} - \Delta_{22} \tag{11.7.26c}$$
$$\Delta_{11} = 1 - S_{11} - S_{12} \tag{11.7.26d}$$
$$\Delta_{22} = 1 - S_{21} - S_{22} \tag{11.7.26e}$$

Now from (11.7.24) and (11.7.25), we find that

$$b_1' = \left(S_{11} + \frac{\Delta_{11}\Delta_{12}}{4-\Delta}\right)a_1' + \left(S_{12} + \frac{\Delta_{11}\Delta_{21}}{4-\Delta}\right)a_2' + \frac{2\Delta_{11}}{4-\Delta}a_3' \tag{11.7.27a}$$

$$b_2' = \left(S_{21} + \frac{\Delta_{22}\Delta_{12}}{4-\Delta}\right)a_1' + \left(S_{22} + \frac{\Delta_{22}\Delta_{21}}{4-\Delta}\right)a_2' + \frac{2\Delta_{22}}{4-\Delta}a_3' \tag{11.7.27b}$$

Equations (11.7.25) and (11.7.27) can be expressed in matrix form as follows:

$$\begin{bmatrix} b_1' \\ b_2' \\ b_3' \end{bmatrix} = \begin{bmatrix} \left(S_{11} + \frac{\Delta_{11}\Delta_{12}}{4-\Delta}\right) & \left(S_{12} + \frac{\Delta_{11}\Delta_{21}}{4-\Delta}\right) & \frac{2\Delta_{11}}{4-\Delta} \\ \left(S_{21} + \frac{\Delta_{22}\Delta_{12}}{4-\Delta}\right) & \left(S_{22} + \frac{\Delta_{22}\Delta_{21}}{4-\Delta}\right) & \frac{2\Delta_{22}}{4-\Delta} \\ \frac{2\Delta_{12}}{4-\Delta} & \frac{2\Delta_{21}}{4-\Delta} & \frac{\Delta}{4-\Delta} \end{bmatrix} \begin{bmatrix} a_1' \\ a_2' \\ a_3' \end{bmatrix} \tag{11.7.28}$$

Therefore, if two-port S-parameters of a three-terminal device are given with terminal 3 common then the corresponding three-port scattering matrix can be found from (11.7.28). If we are given the scattering matrix of a transistor in its common emitter configuration then it can be converted to a three-port device (four-terminal device) where the fourth terminal is a common ground point and its nine scattering parameters can be found via (11.7.28).

Feedback Network Design Consideration

If a load impedance Z is connected between terminal 3 and the ground then $b'_3 = \Gamma^{-1} a'_3$, where

$$\Gamma = \frac{Z - Z_o}{Z + Z_o}$$

Therefore,

$$b'_3 = \Gamma^{-1} a'_3 = S'_{31} a'_1 + S'_{32} a'_2 + S'_{33} a'_3$$

or,

$$a'_3 = -\frac{S'_{31}}{S'_{33} - \Gamma^{-1}} a'_1 - \frac{S'_{32}}{S'_{33} - \Gamma^{-1}} a'_2 \tag{11.7.29}$$

Scattering parameters of the resulting two-port network can be found from (11.7.6) and (11.7.29) as follows:

$$b'_1 = \left(S'_{11} - \frac{S'_{13} S'_{31}}{S'_{33} - \Gamma^{-1}} \right) a'_1 + \left(S'_{12} - \frac{S'_{13} S'_{32}}{S'_{33} - \Gamma^{-1}} \right) a'_2 \tag{11.7.30}$$

and,

$$b'_2 = \left(S'_{21} - \frac{S'_{23} S'_{31}}{S'_{33} - \Gamma^{-1}} \right) a'_1 + \left(S'_{22} - \frac{S'_{23} S'_{32}}{S'_{33} - \Gamma^{-1}} \right) a'_2 \tag{11.7.31}$$

These two equations can be expressed in matrix form as follows and the corresponding new S_{ijn} can be identified

$$\begin{bmatrix} b'_1 \\ b'_2 \end{bmatrix} = \begin{bmatrix} \left(S'_{11} - \frac{S'_{13} S'_{31}}{S'_{33} - \Gamma^{-1}} \right) & \left(S'_{12} - \frac{S'_{13} S'_{32}}{S'_{33} - \Gamma^{-1}} \right) \\ \left(S'_{21} - \frac{S'_{23} S'_{31}}{S'_{33} - \Gamma^{-1}} \right) & \left(S'_{22} - \frac{S'_{23} S'_{32}}{S'_{33} - \Gamma^{-1}} \right) \end{bmatrix} \begin{bmatrix} a'_1 \\ a'_2 \end{bmatrix}$$
$$= \begin{bmatrix} S_{11n} & S_{12n} \\ S_{21n} & S_{22n} \end{bmatrix} \begin{bmatrix} a'_1 \\ a'_2 \end{bmatrix} \tag{11.7.32}$$

If port-3 is grounded (i.e., $V_3 = 0$) then Γ in (11.7.32) is -1.

A similar procedure may be adopted for the other ports as well. In other words, if port-1 is terminated by impedance Z then $b'_1 = \Gamma^{-1} a'_1$. S-parameters of this new two-port network that is formed by ports 2 and 3 of the original three-port network

can be determined from (11.7.6). Suppose that the common-source S-parameters of a FET are given whereas the design procedure requires its common-gate S-parameters; then the computation proceeds as follows. First, we determine its three-port S-parameters using (11.7.28). The source terminal forms the third port of the FET while its gate and drain terminals remain as ports 1 and 2 of the three-port network. Next, we switch back to a two-port network by short circuiting port-1. If a feedback network is needed then that impedance is used to terminate this port.

As (11.7.32) indicates, S-parameters of the new two-port network can be modified up to a certain extent by adjusting the terminating impedance Z. Note that its reflection coefficient Γ will satisfy the following two equations:

$$\Gamma = \frac{S_{11n} - S'_{11}}{S_{11n}S'_{33} - \Lambda_1} \tag{11.7.33}$$

and,

$$\Gamma = \frac{S_{22n} - S'_{22}}{S_{22n}S'_{33} - \Lambda_2} \tag{11.7.34}$$

where,

$$\Lambda_1 = S'_{11}S'_{33} - S'_{31}S'_{13} \tag{11.7.35}$$

and,

$$\Lambda_2 = S'_{22}S'_{33} - S'_{32}S'_{23} \tag{11.7.36}$$

In the case of a reactive termination at port-3, $|\Gamma| = 1$. It maps a circle in the S_{11n}-plane, the center C_1 and radius R_1 of which are given as follows:

$$C_1 = \frac{S'_{11} - \Lambda_1 S'^{*}_{33}}{1 - |S'_{33}|^2} \tag{11.7.37}$$

and,

$$R_1 = \frac{|S'_{31}S'_{13}|}{|1 - |S'_{33}|^2|} \tag{11.7.38}$$

Similarly, center C_2 and radius R_2 of the circle for S_{22n} are found as follows:

$$C_2 = \frac{S'_{22} - \Lambda_2 S'^{*}_{33}}{1 - |S'_{33}|^2} \tag{11.7.39}$$

and,

$$R_2 = \frac{|S'_{32}S'_{23}|}{|1 - |S'_{33}|^2|} \tag{11.7.40}$$

These circles are drawn on a Smith chart and S_{11n} and S_{22n} are optimized for the desired feedback. In the case of an oscillator design, a positive feedback is desired. In other words, the inverse of the conditions (10.1.16) and (10.1.18) must hold so that the transistor becomes potentially unstable. Alternatively, the μ-factor can be determined from the following equation and its magnitude should be kept to a small value that is less than unity.[1] The transistor is unconditionally stable for magnitudes greater than unity:

$$\mu = \frac{1 - |S_{22n}|^2}{|S_{11n} - \Delta_n S^*_{22n}| + |S_{21n}S_{12n}|} \tag{11.7.41}$$

where

$$\Delta_n = S_{11n}S_{22n} - S_{12n}S_{21n} \tag{11.7.42}$$

Example 11.10: Reconsider the BJT of Example 11.9. Find its three-port S-parameter description. Use the inductive termination at its base and verify whether that provides optimum feedback for the oscillator design.

From (11.7.28), the three-port S-parameters are found as follows:

$$\begin{bmatrix} S'_{11} & S'_{12} & S'_{13} \\ S'_{21} & S'_{22} & S'_{23} \\ S'_{31} & S'_{32} & S'_{33} \end{bmatrix} = \begin{bmatrix} 0.396\angle 84.4^\circ & 0.393\angle 29.3^\circ & 0.852\angle -43.5^\circ \\ 0.582\angle -79.1^\circ & 0.534\angle -54.7^\circ & 1.163\angle 60^\circ \\ 0.87\angle 11.8^\circ & 0.425\angle 34.9^\circ & 0.466\angle -115.4^\circ \end{bmatrix}$$

Reactance of a 1.45-nH inductor is $j25.0542\ \Omega$ and its reflection coefficient Γ can be found easily for $Z_o = 50\,\Omega$. S-parameters of the resulting two-port network are found from (11.7.32) as follows:

$$\begin{bmatrix} S_{11n} & S_{12n} \\ S_{21n} & S_{22n} \end{bmatrix} = \begin{bmatrix} 1.722\angle 100.1^\circ & 0.714\angle 94.8^\circ \\ 2.083\angle -136.4^\circ & 1.163\angle -102.5^\circ \end{bmatrix}$$

These results are very close to those obtained earlier in Example 11.9. Minor deviations are attributed to the roundoff errors involved.

[1] Les Besser, "Avoiding RF Oscillations," *Applied Microwave and Wireless*, pp. 44–55, Spring 1995.

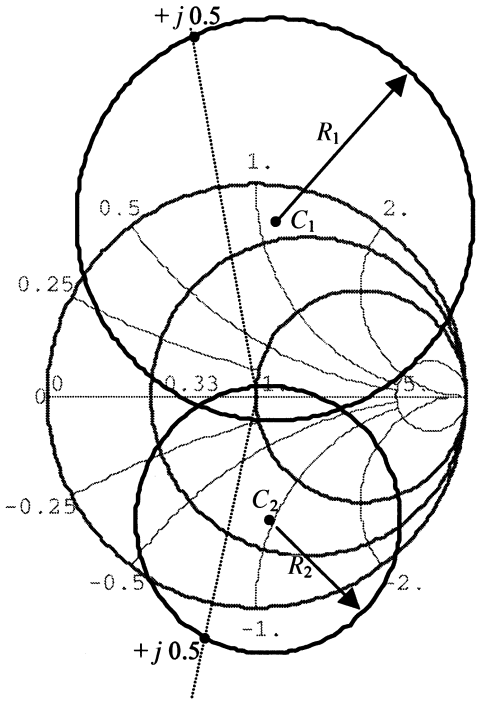

Figure 11.41 S_{11n} and S_{22n} circles on the Smith chart.

In order to verify the feedback provided by the inductor, we first plot S_{11n} and S_{22n} circles on a Smith chart. To that end, the information of these circles is found from (11.7.37)–(11.7.40). The results are:

$$C_1 = 0.837\angle 84^\circ, \quad R_1 = 0.947, \quad C_2 = 0.587\angle -84.6^\circ, \text{ and } R_2 = 0.631$$

These two circles are illustrated in Figure 11.41. It may be easily verified that the points indicated on these circles correspond to S_{11n} and S_{22n} of the two-port network obtained with an inductive termination of $j0.5$ at the base terminal. Further, the magnitude of the μ-factor of the transistor (without feedback inductor) in common-base configuration is 0.674. It means that the transistor is potentially unstable. When the inductor is added to its base, the magnitude of the μ-factor decreases to 0.126. Hence, the inductor enhances the positive feedback further to facilitate the oscillator design.

SUGGESTED READING

Bahl, I. J. and Bhartia, P., *Microwave Solid State Circuit Design*. New York: Wiley, 1988.

Collin, R. E., *Foundations for Microwave Engineering*. New York: McGraw Hill, 1992.

Davis, W. A., *Microwave Semiconductor Circuit Design*. New York: Van Nostrand Reinhold, 1984.

Gonzalez, G., *Microwave Transistor Amplifiers*. Englewood Cliffs, NJ: Prentice Hall, 1997.

Larson, L. E. (Editor), *RF and Microwave Circuit Design for Wireless Communications*. Boston: Artech House, 1996.

Pozar, D. M., *Microwave Engineering*. New York: Wiley, 1998.

Rohde, U. L., *Microwave and Wireless Synthesizers*. New York: Wiley, 1997.

Smith, J. R., *Modern Communication Circuits*. New York: McGraw Hill, 1998.

Vendelin, G. D., Pavio, A., and Rhode, U. L., *Microwave Circuit Design Using Linear and Non-linear Techniques*. New York: Wiley, 1990.

PROBLEMS

1. In the figure shown below, gain of the amplifier is constant with frequency (i.e., $A_v(j\omega) = A_o$) and

$$\beta(j\omega) = \frac{10^{-6}}{1 - j(\omega - 2\pi \times 10^9)}$$

Use the Barkhausen criteria to determine the frequency of oscillation and the required value of A_o.

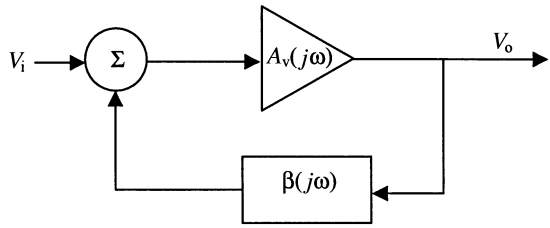

2. In the following circuit, the FET is biased such that its g_m is 4.5 mS. For this circuit to oscillate at 100 MHz, find C_1 and C_2. An open-loop gain of 5 ensures the beginning of oscillations and the unloaded Q of a 100-nH inductor is 1000.

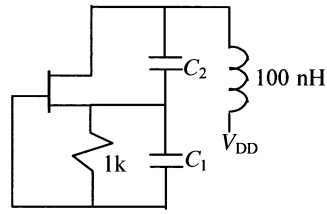

3. In the following circuit, the FET is biased such that its g_m is 4.5 mS. For this circuit to oscillate at 100 MHz, find L_1 and L_2. An open- loop gain of 5 ensures the beginning of oscillations.

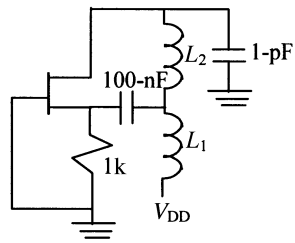

4. Free-running frequency and the gain factor of a voltage-controlled oscillator are given as 500 MHz and 150 kHz/V, respectively. It is being used in a PLL along with a sinusoidal phase detector with maximum output of 5 V at $\theta_e = \pi/2$ radians. If there are no amplifiers or frequency divider in the loop, what is its hold-in range?

5. If the phase detector in the preceding example is replaced by a triangular type with $V_{emax} = A = 5$ V at $\theta_{emax} = \pi/2$ radians, find the new holding range.

6. In the PLL shown below, peak amplitudes of the reference input as well as the VCO output are 1.5 V. An analog multiplier is being used as the phase detector that has 5-V output when its reference input, V_{in}, and the oscillator signal, V_{osc}, both are 2 V. Free-running frequency of the VCO is 50 MHz, which reduces to zero when its control voltage V_{cntl} is reduced by 5 V. Find the phase difference between the input and the VCO output when it is in lock with input frequency of

(a) 55 MHz

(b) 45 MHz

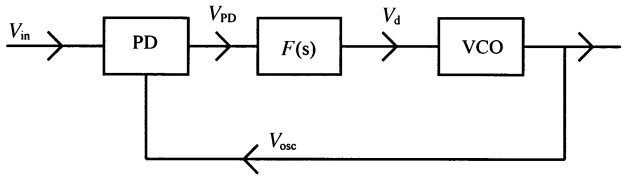

7. Analyze the PLL system shown below. By controlling the frequency divider, its output frequency can be changed from 4 MHz to 6 MHz in steps of 200 kHz. The transfer function of the phase detector, K_d, is 0.5 V per radian. Free-running frequency and gain factor of VCO are 5 MHz and 10^7 rad/sec/volt, respectively.

Voltage gain of the amplifier is 20. Design a passive lead-lag-type low-pass filter that can be used in the loop.

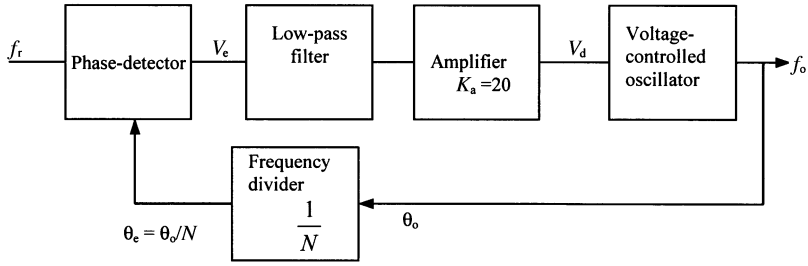

8. Design a multiple phase-locked loop synthesizer to cover the frequency range 35.40 to 40.0 MHz in 10-Hz increments. The reference frequency is to be 100 kHz. No loop should operate with a reference frequency below 100 kHz.

9. Design a three-loop synthesizer to cover the frequency range of 190 MHz to 200 MHz in steps of 10 Hz. The loop frequency switching time should not exceed 25 ms.

10. A 2 GHz oscillator is to be designed using a negative resistance diode with its reflection coefficient Γ_G as $2.05\angle -60^\circ$ (measured with $Z_o = 50\,\Omega$ as reference). Determine its load impedance.

11. S-parameters of a GaAs MESFET are measured in the common-source mode at $V_{ds} = 6$ V and $I_{ds} = 50$ mA at 8 GHz. The results are found as follows:

$$S_{11} = 0.63\angle -150^\circ, \quad S_{12} = 0.07\angle -30^\circ,$$
$$S_{21} = 3.10\angle 40^\circ, \text{ and } S_{22} = 0.70\angle -100^\circ$$

Determine its S-parameters in common-gate configuration.

12. A silicon BJT is biased at $V_{CE} = 18$ V and $I_C = 30$ mA. Its S-parameters measured at 5.0 GHz in the common-emitter configuration are found to be

$$S_{11} = 0.63\angle -150^\circ, \quad S_{12} = 0.007\angle -30^\circ,$$
$$S_{21} = 2.10\angle 40^\circ, \text{ and } S_{22} = 0.70\angle -100^\circ$$

Find its S-parameters in common-base configuration.

13. A silicon BJT is biased at $V_{CE} = 0$ V and $I_C = 40$ mA. Its S-parameters measured at 8.0 GHz in the common-base configuration are found to be

$$S_{11} = 1.32\angle 88^\circ, \quad S_{12} = 0.595\angle 99^\circ,$$
$$S_{21} = 1.47\angle 172^\circ, \text{ and } S_{22} = 1.03\angle -96^\circ$$

Find its S-parameters in common-emitter configuration.

14. Design an oscillator to operate at 8 GHz using the common-gate configuration of MESFET given in Problem 11. Use an inductor at its gate terminal to provide the positive feedback, if necessary. Determine the value of the feedback inductor.

15. Design an oscillator to operate at 5 GHz using the common-base configuration of BJT given in Problem 12. Use an inductor at its base terminal to provide the positive feedback, if necessary. Determine the value of the feedback inductor.

Radio-Frequency and Microwave Communication Circuits: Analysis and Design
Devendra K. Misra

ISBNs: 0-471-41253-8 (Hardback); 0-471-22435-9 (Electronic)

12

DETECTORS AND MIXERS

Detector and mixer circuits employ nonlinear electronic devices to process electrical information. For example, if a transmission line is being used to send only one voice signal at a given time then it can be directly connected without a problem. On the other hand, if two different voice signals are sent at the same time via this line then no information can be retrieved at the other end due to their interference. In practice, there may be a large number of telephone subscribers that need to be connected via a single long-distance communication line for economic reasons. This requires some means to move each voice channel to a different frequency band. The solution is *frequency division multiplexing* (FDM). A commonly used FDM hierarchy is illustrated in Figure 12.1. These multiplexing systems require mixers and detectors.

Similarly, wireless systems operate at higher frequencies to achieve efficient and directional radiation from an antenna. In this case, electrical information is generally superimposed on a high-frequency carrier signal via amplitude or frequency modulation. In *amplitude modulation* (AM), the amplitude of a radio-frequency signal (the carrier) varies according to information (the modulating) signal. In the case of *frequency modulation* (FM), the frequency of the carrier signal varies according to the modulating signal. Figure 12.2 illustrates various waveforms associated with these modulations.

This chapter begins with an overview of the characteristics of these modulations and their detection schemes. Several mixer circuits are then presented that can be designed using diodes or transistors as nonlinear electronic devices.

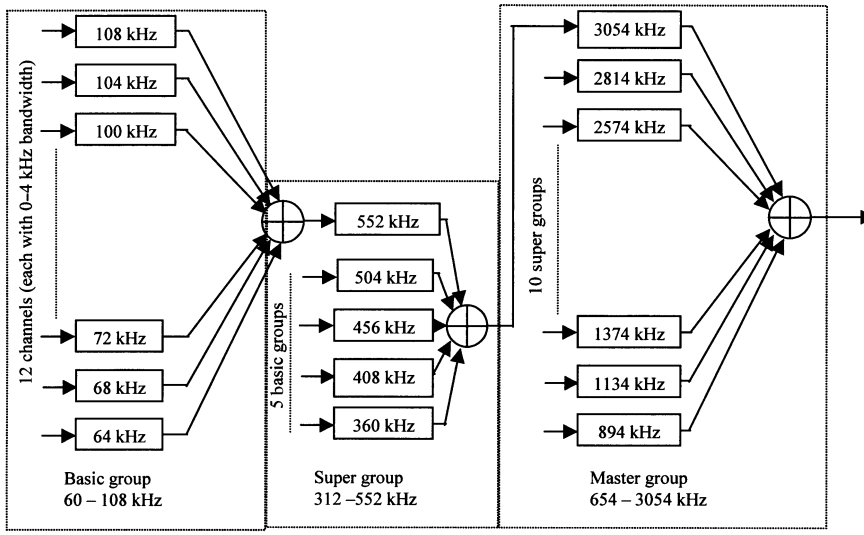

Figure 12.1 FDM hierarchy.

12.1 AMPLITUDE MODULATION

Consider the amplitude modulation system illustrated in Figure 12.3. Assume that two inputs to this circuit are $s(t) = a_o + b_o m(t)$ and $c(t) = \cos(\omega_c t + \psi)$. The output signal $c_{AM}(t)$ is then found as

$$c_{AM}(t) = s(t)c(t) = a_o\left[1 + \frac{b_o}{a_o}m(t)\right]\cos(\omega_c t + \psi) \tag{12.1.1}$$

An analysis of this expression shows that $c_{AM}(t)$ represents an amplitude-modulated signal with $s(t)$ as the modulating signal and $c(t)$ as the carrier. Further, the ratio b_o/a_o is called the *modulation index*.

If the modulating signal is $m(t) = \cos(\omega_m t)$ then (12.1.1) can be simplified as follows:

$$c_{AM}(t) = a_o\left[1 + \frac{b_o}{a_o}\cos(\omega_m)\right]\cos(\omega_c t + \psi)$$

or,

$$c_{AM}(t) = a_o\cos(\omega_c + \psi) + \frac{b_o}{2}[\cos\{(\omega_c + \omega_m)t + \psi\} + \cos\{(\omega_c - \omega_m)t + \psi\}] \tag{12.1.2}$$

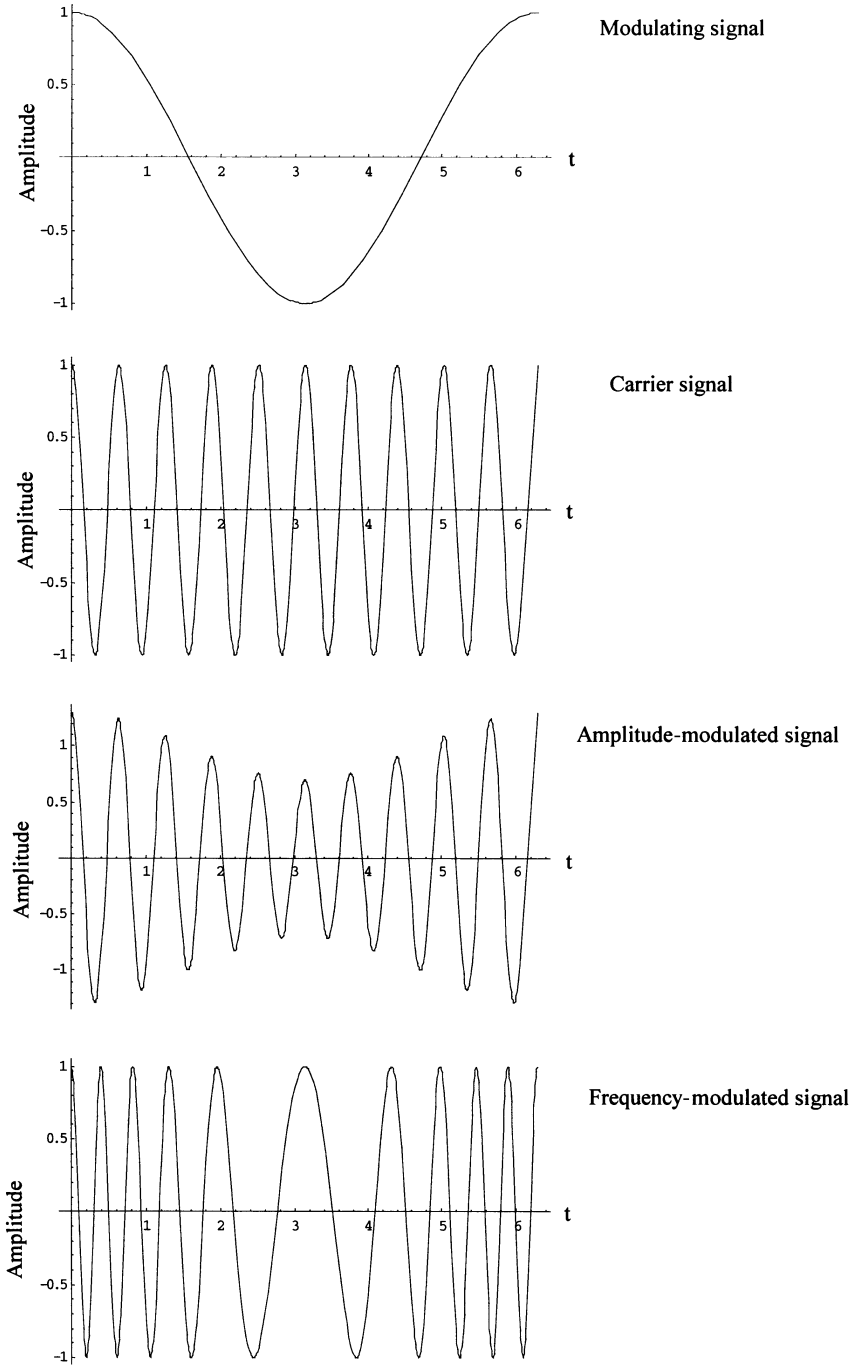

Figure 12.2. Amplitude- and frequency-modulated waveforms.

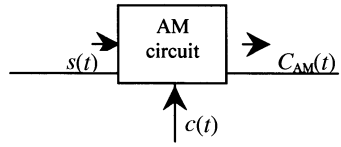

Figure 12.3 An amplitude-modulation system.

This can be easily graphed to verify that indeed it represents an amplitude-modulated signal as illustrated in Figure 12.2. Further, it shows that the output has three sinusoidal signals, each with different frequencies. Its frequency spectrum is shown in Figure 12.4. Besides the carrier frequency ω_c, there are two other frequencies $\omega_c \pm \omega_m$. The signal spectrum $\omega_c + \omega_m$ represents the upper side band while $\omega_c - \omega_m$ is the lower side band. Note that each sideband includes the information signal ω_m. When only one of these signals is used to send the information then it is called a *single-sideband* (SSB) AM transmission. On the other hand, complete $c_{AM}(t)$ represents a *double-sideband* (DSB) AM transmission. It is called the *suppressed carrier* AM if the carrier component of $c_{AM}(t)$ is filtered out before transmitting.

Example 12.1: A 100-MHz sinusoidal signal is being used as the carrier for an AM transmission. Its amplitude is 1000 V while the average power is 10 kW. The modulating signal is $s(t) = 3\cos(\omega_1 t) + 2\cos(2\omega_1 t) + \cos(3\omega_1 t)$, where $\omega_1 = 4\pi \times 10^6$ rad/s. The modulation index is 0.15.

(a) Determine the frequency spectrum of modulated signal. Also, find the amplitude of each sinusoidal component, power in the carrier and each pair of sidebands, and the total bandwidth of the AM signal.
(b) Determine peak amplitude and peak instantaneous power of this signal.

Since amplitude of the carrier signal is 1000 V and its power is 10 kW, the proportionality constant that relates the two can be determined. For $P = \alpha V^2$,

$$\alpha = \frac{P}{V^2} = \frac{10000}{1000000} = 0.01$$

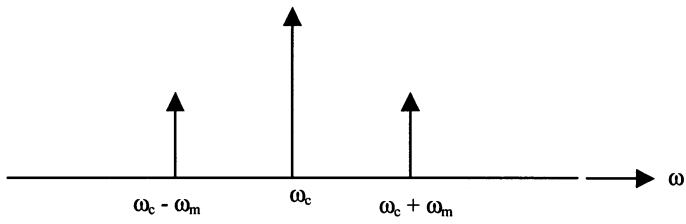

Figure 12.4 Frequency spectrum of $c_{AM}(t)$.

The amplitude-modulated signal can be determined from (12.1.1) as follows:

$$C_{\mathrm{AM}}(t) = 1000 \cdot [1 + 0.15\{3\cos\omega_1 t) + 2\cos(2\omega_1 t) + \cos(3\omega_1 t)\}]\cos(\omega_c t)\mathrm{V}$$

or,

$$\begin{aligned} C_{\mathrm{AM}}(t) = {} & 1000 \cdot \cos(\omega_c t) + 225 \cdot [\cos(\omega_c + \omega_1)t + \cos(\omega_c - \omega_1)t] \\ & + 150 \cdot [\cos(\omega_c + 2\omega_1)t + \cos(\omega_c - 2\omega_1)t] \\ & + 75 \cdot [\cos(\omega_c + 3\omega_1)t + \cos(\omega_c - 3\omega_1)t]\mathrm{V} \end{aligned}$$

where $\omega_1 = 4\pi \times 10^6$ rad/s and $\omega_c = 2\pi \times 10^8$ rad/s.

(a) From the above expression, results can be summarized as follows:

	Carrier	$\omega_c \pm \omega_1$	$\omega_c \pm 2\omega_1$	$\omega_c \pm 3\omega_1$
Frequency	100 MHz	(100 ± 2) MHz	(100 ± 4) MHz	(100 ± 6) MHz
Amplitude	1000 V	225 V	150 V	75 V
Power	10000 W	1012.5 W	450 W	112.5 W

(b) Peak amplitude, $A = 1000 + 2 \times (255) + 2 \times (150) + 2 \times (75) = 1900$ V; peak power $= \alpha A^2 = 36100$ W.

Frequency Converters

Frequency converters use nonlinear electronic devices that multiply the input signals. They can be used to generate high-frequency sinusoidal signals from a low-frequency reference. Consider the frequency converter shown in Figure 12.5. Let V_i and V_L be two sinusoidal inputs that produce V_o at its output.

Mathematically,

$$V_i = a\cos(\omega_1 t)$$

$$V_L = b\cos(\omega_2 t)$$

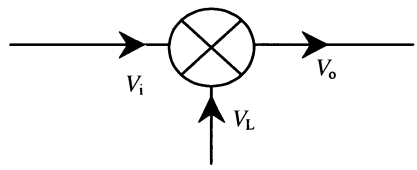

Figure 12.5 A frequency converter.

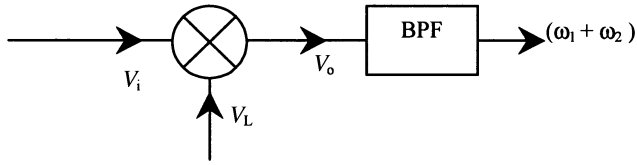

Figure 12.6 An up-converter circuit.

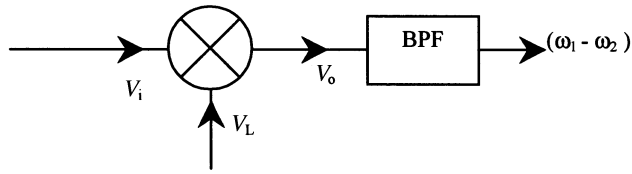

Figure 12.7 A down-converter circuit.

and,

$$V_o = ab\cos(\omega_1 t)\cos(\omega_2 t)$$

Output V_o can be rearranged as follows:

$$V_o = \frac{ab}{2}[\cos(\{\omega_1 + \omega_2\}t) + \cos(\{\omega_1 - \omega_2\}t)] \tag{12.1.3}$$

Hence, the output is a sum of two sinusoidal signals. These sum and difference frequency signals can be filtered out for up or down conversions as illustrated in Figures 12.6 and 12.7, respectively.

A Single-Diode Mixer Circuit Arrangement

Consider the circuit arrangement shown in Figure 12.8. Two inputs v_s and v_L are added together before applying to a diode. Capacitors C_1 and C_2 are used to block the dc bias of the diode from other sides of the circuit. Thus, these capacitors are selected such that there is negligible reactance for the ac signal. Similarly, inductors L_1 and L_2 are used to block ac from short circuiting via the dc source. Hence, these inductors should have very high reactance at ac whereas dc passes through with negligible loss. Thus, the voltage applied to the diode has both ac as well as dc components.

In order to analyze this circuit and determine its output signal, we need to consider the actual characteristics of the diode. The V-I characteristic of a typical forward-biased diode is illustrated in Figure 12.9. For the present case, bias-voltage V_b is assumed high enough to keep the diode forward biased.

If the current through this diode is i_d while voltage across its terminals is v_d then

$$i_d = I_s(e^{\alpha v_d} - 1) \tag{12.1.4}$$

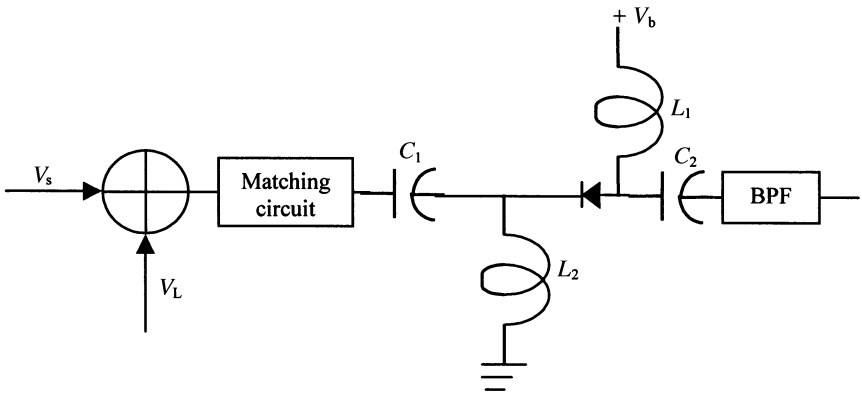

Figure 12.8 A single-diode mixer circuit.

where,

$$\alpha = \frac{q}{nkT} \tag{12.1.5}$$

I_s is called the *reverse-saturation current* (on the order of 10^{-8} to 10^{-15}A); q is the electronic charge (1.602×10^{-19} C); n is a number ranging between 1 and 2; k is the Boltzmann constant (1.38×10^{-23} J/K), and T is the temperature in Kelvin.

Since the diode has both alternating and direct voltage across it, we can write

$$v_d = V_b + v_{ac}$$

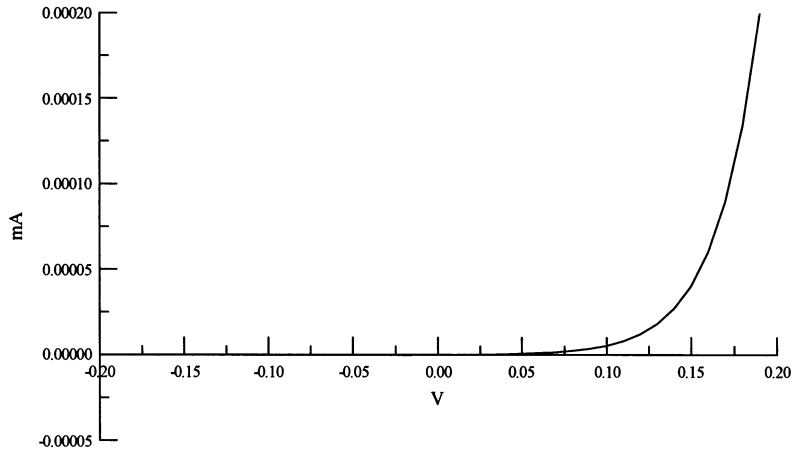

Figure 12.9 V-I characteristic of a typical diode.

where, $v_{ac} = v_s + v_L$. Therefore, current through the diode can be expressed as follows:

$$i_d = I_s(e^{\alpha(V_b + v_{ac})} - 1) = I_s(e^{\alpha V_b} e^{\alpha v_{ac}} - 1)$$

If $v_{ac} \ll V_b$ such that αv_{ac} is a small fraction then i_d can be expanded as follows. Further, it can be approximated only by a few terms of the series

$$i_d = I_s\left[e^{\alpha V_b} \cdot \left\{1 + \alpha v_{ac} + \frac{(\alpha v_{ac})^2}{2} + \cdots\right\} - 1\right]$$

After rearranging, we find that

$$i_d = I_s(e^{\alpha V_b} - 1) + I_s e^{\alpha V_b}\left\{\alpha v_{ac} + \frac{(\alpha v_{ac})^2}{2} + \cdots\right\} = I_b + i_{ac}$$

Thus, there are two components in the diode current—a dc, I_b and an ac, i_{ac}.

The ac component i_{ac} through the diode may be approximated as follows:

$$i_{ac} \approx I_s e^{\alpha V_b}\left\{\alpha v_{ac} + \frac{(\alpha v_{ac})^2}{2}\right\} = g_d v_{ac} + g'_d \frac{v_{ac}^2}{2} \tag{12.1.6}$$

where,

$$g_d = \alpha I_s e^{\alpha V_b} = \alpha(I_b + I_s) \tag{12.1.7}$$

and,

$$g'_d = \alpha g_d \tag{12.1.8}$$

Parameter g_d is known as the *dynamic conductance* of the diode. It is equal to the inverse of the junction resistance. Parameter g'_d has units of A per V^2. A small-signal equivalent circuit of the diode can be drawn as shown in Figure 12.10. Its junction capacitance C_j appears in parallel with the junction resistance R_j. The lead inductance L_p and bulk resistance R_s appear in series with this combination. As illustrated, packaging capacitance C_p between the two leads appears in parallel with the circuit:

Example 12.2: Equivalent circuit parameters of a diode in an axial lead package are given as follows:

$$C_p = 0.1 \text{ pF}, \quad L_p = 2.0 \text{ nH}, \quad C_j = 0.15 \text{ pF}, \quad R_s = 10\ \Omega, \text{ and } I_s = 10^{-8} \text{ A}$$

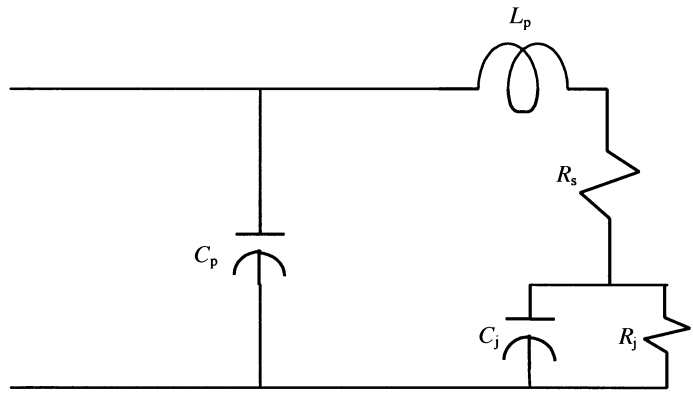

Figure 12.10 A small-signal equivalent circuit of the diode.

Determine its junction resistance if the bias current is (a) zero, and (b) 100 μA. Assume that the diode is at room temperature ($T = 290$ K) and $n = 1$.

From (12.1.7),

$$R_j = \frac{1}{g_d} = \frac{1}{\alpha(I_b + I_s)}$$

and,

$$\frac{kT}{q} = \frac{1.38 \times 10^{-23} \times 290}{1.602 \times 10^{-19}} = 0.025 \text{ V}$$

(a) $R_j = \dfrac{0.025}{10^{-8}} \Omega = 2500 \text{ k}\Omega.$

(b) $R_j = \dfrac{0.025}{(100 + 0.01) \times 10^{-6}} \Omega = 249.9 \ \Omega.$

Radio Frequency Detector

Diodes are used for the detection of radio frequency signals, to convert a part of RF input to dc. They are used for monitoring the power (relative power measurement), automatic gain control circuits, and the detection of AM signals.

Assume that the RF signal, $a_1 \cos(\omega t)$, is applied to a diode biased at V_b. Hence, total voltage V_t applied to it is

$$V_t = V_b + a_1 \cos(\omega t)$$

The corresponding diode current i_d can be expressed as follows:

$$i_d \approx I_b + g_d a_1 \cos(\omega t) + \frac{g_d'}{2} a_1^2 \cos^2(\omega t)$$

or,

$$i_d \approx I_b + g_d' \frac{a_1^2}{4} + g_d a_1 \cos(\omega t) + \frac{g_d'}{4} a_1^2 \cos(2\omega t) \tag{12.1.9}$$

Current sensitivity, β_i, of the diode is defined as a ratio of the change in output dc to that of RF input power. Hence,

$$\beta_i = \frac{\frac{g_d' a_1^2}{4}}{\frac{g_d a_1^2}{2}} = \frac{g_d'}{2g_d} \tag{12.1.10}$$

The current sensitivity has units of amps per watt or V^{-1}.

An open-circuit voltage sensitivity β_v of the diode is defined as the ratio of change in direct voltage across the junction to that of RF input power. Hence,

$$\beta_v = \frac{g_d'}{2g_d^2} = \beta_i R_j \tag{12.1.11}$$

Voltage sensitivity has units of volts per watt or A^{-1}. Its typical range is 400–1500 mA^{-1}. Consider a diode circuit that has no dc bias voltage as shown in Figure 12.11. If an amplitude-modulated signal V_{in} is applied to this circuit then current through the diode can be found through (12.1.6).

For $V_{in} = V_o[1 + m\cos(\omega_m t)]\cos(\omega_c t)$

$$i_{ac} \approx g_d V_o[1 + m\cos(\omega_m t)]\cos(\omega_c t) + \frac{g_d' V_o^2}{2}[1 + m\cos(\omega_m t)]^2 \cos^2(\omega_c t)$$

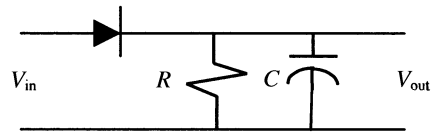

Figure 12.11 A zero-biased diode detector circuit.

or,

$$i_{ac} \approx g_d V_o \left[\cos(\omega_c t) + \frac{m}{2}\cos\{(\omega_m + \omega_c)t\} + \frac{m}{2}\cos\{(\omega_m - \omega_c)t\}\right] + \frac{g'_d V_o^2}{4}\left[1 + \frac{m^2}{2} + 2m\cos(\omega_m t) + \frac{m^2}{2}\cos(2\omega_m t) + \cos(2\omega_c t) + m\cos\{(2\omega_c + \omega_m)t\} + m\cos\{(2\omega_c - \omega_m)t\} + \frac{m^2}{2}\cos(2\omega_c t) + \frac{m^2}{4}\cos\{2(\omega_c + w_m)t\} + \frac{m^2}{4}\cos\{2(\omega_c - \omega_m)t\}\right] \quad (12.1.12)$$

Hence, the diode current has several frequency components that are graphically illustrated in Figure 12.12. It includes the modulating signal frequency ω_m. If this current flows through a resistance R then the corresponding voltage contains the same spectrum as well. A low-pass filter can be used to suppress the undesired high-frequency signals. Note that there is a second harmonic $2\omega_m$ of the modulating signal that sometimes may be difficult to suppress. However, it may have relatively negligible amplitude, especially when the modulation index m is less than unity.

As a special case, if an unmodulated radio frequency signal is applied to this circuit then m is zero in (12.1.12). Therefore, the expression for the diode current simplifies to

$$i_{ac} \approx \frac{g'_d V_o^2}{4} + g_d V_o \cos(\omega_c t) + \frac{g'_d V_o^2}{4}\cos(2\omega_c t)$$

Therefore, a capacitor C connected across the output can easily suppress its sinusoidal components while its first term represents a direct voltage that is proportional to the square of the RF amplitude V_o. This kind of circuit is used in practice to monitor radio frequency and microwave signals.

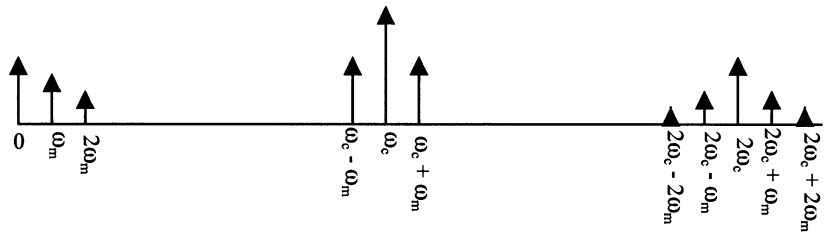

Figure 12.12 Spectrum of the diode current given by (12.1.12).

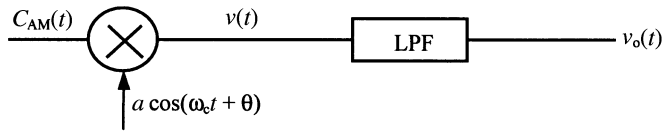

Figure 12.13 A simple coherent detector circuit.

Coherent Detection of AM

An alternative technique for detection of amplitude-modulated signals is illustrated in Figure 12.13. In this case, the amplitude-modulated signal is multiplied with a sinusoidal signal that has the same frequency as the carrier signal. Assume that

$$C_{AM}(t) = a_o\{1 + m(t)\}\cos(\omega_c t + \varphi)$$

Voltage $v(t)$ at the output of the multiplier is found to be,

$$v(t) = C_{AM}(t)a\cos(\omega_c t + \varphi) = aa_o\{1 + m(t)\}\cos(\omega_c t + \varphi)\cos(\omega_c t + \varphi)$$

or,

$$v(t) = \frac{aa_o}{2}\{1 + m(t)\}\{\cos(\theta - \varphi) + \cos(2\omega_c t + \theta + \varphi)\}$$

If the low-pass filter has a cutoff frequency that is less than $2\omega_c$ then its output voltage v_o is found to be as follows:

$$v_o(t) = \frac{aa_o}{2}\{1 + m(t)\}\cos(\theta - \varphi)$$

Hence, this circuit can provide a more efficient way to extract the information signal from the AM than the one considered earlier. However, the output voltage goes to zero if the argument of cosine function $(\theta - \varphi)$ is 0.5π (90°). To ensure maximum output voltage, this phase difference should be zero. In other words, the local oscillator signal should be phaselocked to the carrier. This can be done using a PLL scheme discussed earlier in Chapter 11. This circuit arrangement is illustrated in Figure 12.14.

Single-Sideband (SSB) Generation

As illustrated in Figure 12.4, the modulating signal is included in both of the sidebands of an amplitude-modulated signal. The precious frequency spectrum can be economized if only one of these is used to transmit the information. For example, the FDM hierarchy shown in Figure 12.1 employs only the lower sideband. It can be achieved with a low-pass filter that passes only the desired component. On the other hand, it can be done more efficiently using the circuit illustrated in Figure 12.15.

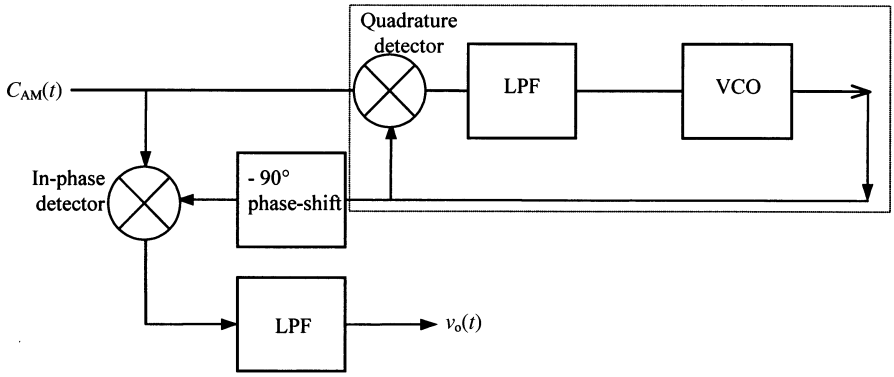

Figure 12.14 A PLL-based coherent detection scheme.

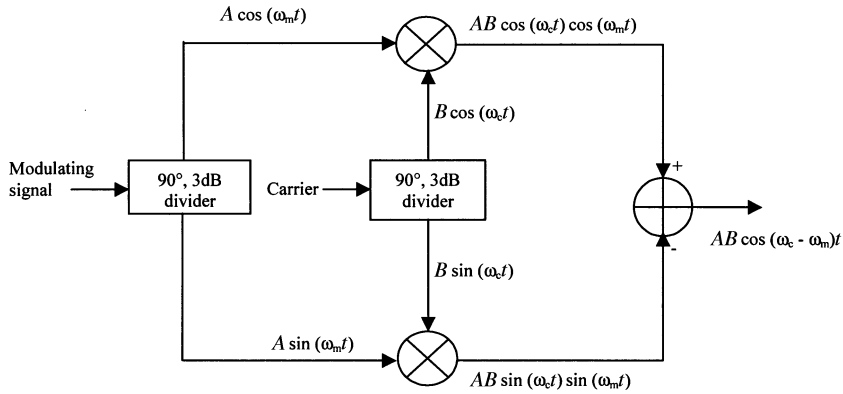

Figure 12.15 A SSB generation scheme.

This circuit uses two power dividers and two mixers. A power divider splits the input signal into two that are equal in amplitude but differ in phase by 90°. Thus, a power divider divides the modulating signal into $A\ \cos(\omega_m t)$ and $A\ \sin(\omega_m t)$. Similarly, the carrier is also divided into $B\ \cos(\omega_c t)$ and $B\ \sin(\omega_c t)$. These components are applied to corresponding mixers and the output of one is then subtracted from the other to get the single sideband.

12.2 FREQUENCY MODULATION

As illustrated in Figure 12.2, in frequency modulation, the carrier frequency changes according to the modulating signal. It can be expressed mathematically as follows:

$$c_{FM}(t) = A\cos\left[\omega_c t + \Delta\omega \int x(t)dt + \psi\right] \tag{12.2.1}$$

where A is amplitude of the carrier; $\Delta\omega$ is the frequency deviation coefficient in radians per second per volt, and $x(t)$ is the modulating signal in V. Therefore, the frequency of c_{FM}, $\omega(t)$, is

$$\omega(t) = \frac{d}{dt}\left[\omega_{\mathrm{c}}t + \Delta\omega \int x(t)dt + \psi\right] = \omega_{\mathrm{c}} + \Delta\omega\, x(t) \tag{12.2.2}$$

If the modulating signal is a sinusoidal wave that is given by the following expression

$$x(t) = a\cos(\omega_{\mathrm{m}}\mathrm{t} + \theta_{\mathrm{m}})$$

then,

$$\int x(t)dt = \frac{a}{\omega_{\mathrm{m}}}\sin(\omega_{\mathrm{m}}t + \theta_{\mathrm{m}})$$

Therefore, the frequency-modulated carrier in this case will be given as

$$c_{\mathrm{FM}}(t) = A\cos\left[\omega_{\mathrm{c}}t + \frac{a\Delta\omega}{\omega_{\mathrm{m}}}\sin(\omega_{\mathrm{m}}t + \theta_{\mathrm{m}}) + \psi\right] \tag{12.2.3}$$

Modulation index β of the frequency-modulated signal is defined as follows:

$$\beta = \frac{a\Delta\omega}{\omega_{\mathrm{m}}} \tag{12.2.4}$$

Note that the modulation index is a dimensionless quantity.

In order to determine the frequency spectrum of $c_{\mathrm{FM}}(t)$, we need to find an equivalent expression for the RHS of (12.2.3) as follows:

$$c_{\mathrm{FM}}(t) = A\ \mathrm{Re}\lfloor e^{\{j\omega_{\mathrm{c}}t + j\psi + j\beta\sin(\omega_{\mathrm{m}}t + \theta_{\mathrm{m}})\}}\rfloor$$

or,

$$c_{\mathrm{FM}}(t) = A\ \mathrm{Re}\lfloor e^{j(\omega_{\mathrm{c}}t + \psi)} \cdot e^{j\beta\sin(\omega_{\mathrm{m}}t + \theta_{\mathrm{m}})}\rfloor \tag{12.2.5}$$

From the mathematical tables,

$$e^{j\beta\sin(\alpha)} = \sum_{n=-\infty}^{\infty} J_n(\beta)e^{jn\alpha}$$

where $J_n(\beta)$ is the Bessel function of the first kind and order n. Therefore,

$$c_{\mathrm{FM}}(t) = A\ \mathrm{Re}\left[\sum_{n=-\infty}^{\infty} J_n(\beta) e^{j\{\omega_c t+\psi+n(\omega_m t+\theta_m)\}}\right]$$

or,

$$c_{\mathrm{FM}}(t) = A \sum_{n=-\infty}^{\infty} J_n(\beta) \cos[(\omega_c + n\omega_m)t + n\theta_m + \psi] \tag{12.2.6}$$

where,

$$J_{-n}(\beta) = (-1)^n J_n(\beta)$$

Therefore, the frequency spectrum of this frequency-modulated signal extends to infinity. This is illustrated in Figure 12.16. As may be observed, the amplitudes of these harmonics are going down for the higher-order terms. Since these amplitudes include the Bessel function, a meaningful conclusion can be drawn only after understanding its characteristics. As illustrated in Figure 12.17, the magnitude of a Bessel function is much smaller than unity if its order n is much larger than its argument β. In particular,

$$J_n(\beta) \ll 1, \qquad \text{for } n \gg \beta$$

Therefore, the infinite series of (12.2.6) can be terminated at a finite n. Bandwidth B_c determined this way is known as the *Carson rule bandwidth* which takes $n = (\beta + 1)$ terms of the infinite series into account. It is given by the following expression

$$B_c = 2(\beta + 1)\omega_n \text{ rad/s} \tag{12.2.7}$$

If β is very large then B_c occupies a bandwidth $(\beta + 1)$ times larger than that which would be produced by an amplitude-modulated signal. It is known as

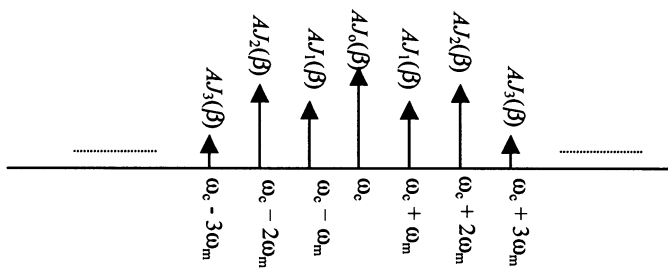

Figure 12.16 Spectrum of the FM signal with sinusoidal modulation.

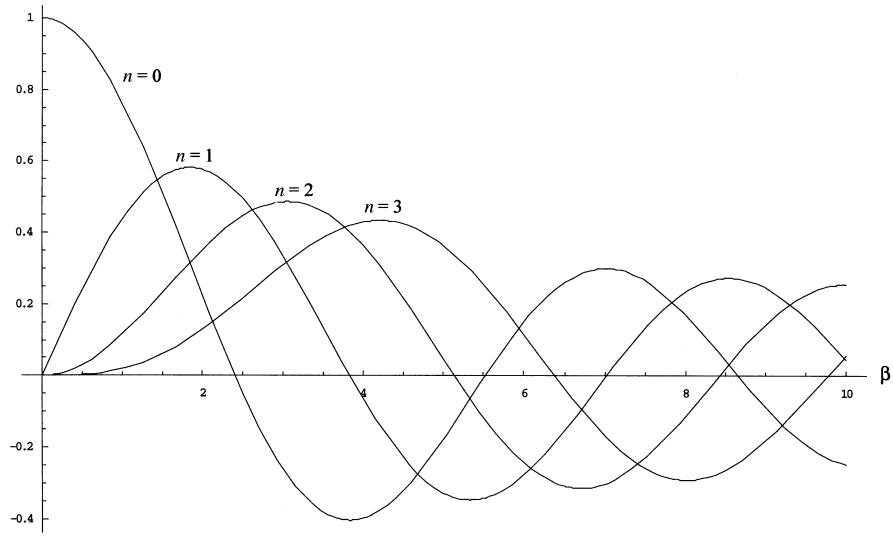

Figure 12.17 Bessel function of the first kind for $n = 0, 1, 2$, and 3.

wideband FM. On the other hand, if β is much smaller than unity then the FM bandwidth is comparable to that of an AM system. It is known as *narrowband FM*.

Example 12.3: A frequency modulator is connected with a carrier, $f_c = 5$ MHz, and an audio signal $V_m = 1$ V of $f_m = 1$ kHz. It produces frequency deviation of ± 10 kHz at the output of the modulator.

(a) FM wave from the modulator is passed through a series of frequency multipliers with a total multiplication factor of 12, that is, $f_o = 12\, f_{in}$. What is the frequency deviation at the output?
(b) Output of the modulator ($f_c = 5$ MHz, $\Delta f = 10$ kHz) is input to a mixer stage along with a 55-MHz signal from an oscillator. Find the sum frequency output f_o of the mixer and the frequency deviation Δf_o.
(c) What is the modulation index at the output of the modulator?
(d) Audio input to the modulator is changed to $V_m = 2$ V and $f_m = 500$ Hz. At the modulator output, what will be the modulation index and frequency deviation Δf?

The problem can be solved as follows:

(a) Since the input frequency is multiplied by a factor of 12, frequency deviation at the output of the multiplier will be ± 10 kHz $\times$ 12 $= \pm 120$ kHz.

(b) This arrangement is illustrated here.

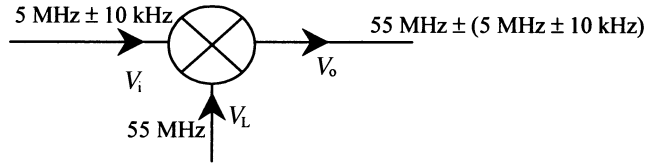

Therefore, the sum frequency in the output is given as

$$55 \text{ MHz} + 5 \text{ MHz} + 10 \text{ kHz} = 60.01 \text{ MHz}$$

The frequency deviation is ±5.01 MHz.

(c) From (12.2.4),

$$\beta = \frac{a\Delta\omega}{\omega_m} = \frac{a\Delta f}{f_m} = \frac{1 \times 10 \text{ kHz}}{1 \text{ kHz}} = 10$$

(d) Frequency deviation in this case increases by a factor of two. Therefore,

$$\beta = \frac{a\Delta\omega}{\omega_m} = \frac{a\Delta f}{f_m} = \frac{2 \times 10 \text{ kHz}}{500 \text{ Hz}} = 40$$

FM Detector

A PLL is frequently employed for the detection of frequency-modulated signals. Consider that the reference signal $v_r(t)$ in Figure 12.18 is an FM signal as given below:

$$v_r(t) = A_r \sin\left\{\omega_c t + \Delta\omega \int^t m(\tau)d\tau\right\}$$

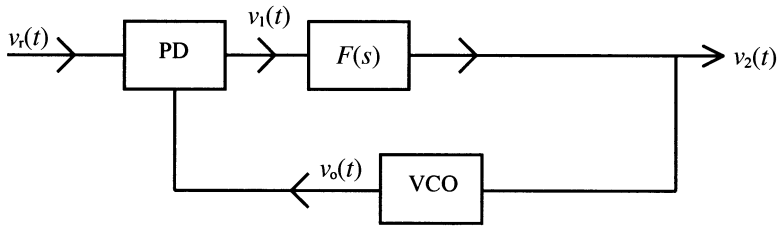

Figure 12.18 FM detection scheme using a PLL.

where,

$$\theta_r(t) = \Delta\omega \int^t m(\tau)d\tau$$

In the transform domain, it can be expressed as

$$\theta_r(s) = \Delta\omega \frac{M(s)}{s}$$

The transfer function of the system shown in Figure 12.18 is given as follows:

$$\frac{V_2(s)}{\theta_r(s)} = \frac{K_d F(s)}{1 + K_d \dfrac{K_o}{s} F(s)} = \frac{sK_d F(s)}{s + K_d K_o F(s)}$$

Hence, the output voltage in the frequency domain is found to be

$$V_2(s) = \frac{sK_d F(s)}{s + K_d K_o F(s)} \times \Delta\omega \times \frac{M(s)}{s} = \frac{\Delta\omega K_d F(s) M(s)}{s + K_d K_o F(s)}$$

Assuming that $M(s)$ has a bandwidth B and $|F(s)| = 1$ in the pass-band, this expression can be simplified as follows:

$$V_2(s) = \frac{\Delta\omega K_d M(s)}{s + K_d K_o} = \frac{\dfrac{\Delta\omega M(s)}{K_o}}{1 + \dfrac{s}{K_d K_o}} \approx \frac{\Delta\omega M(s)}{K_o}$$

Hence, for $K_d K_o$ very large such that

$$\left| \frac{s}{K_d K_o} \right| \ll 1$$

we have

$$V_2(s) \approx \frac{\Delta\omega M(s)}{K_o}$$

Switching back to the time-domain, we find that the output voltage will be given as follows:

$$v_2(t) \approx \frac{\Delta\omega}{K_o} m(t)$$

Hence, the output voltage $v_2(t)$ is proportional to the information signal $m(t)$.

12.3 SWITCHING-TYPE MIXERS

It can be easily shown from (12.1.9) that the output of a single-diode mixer circuit contains the local oscillator and the RF input frequencies as well. Sometimes it may be hard to filter these out from the desired signal. This section presents efficient ways to accomplish this. It is assumed for simplicity that the diodes used in these circuits are ideal. Hence, it turns the circuit on or off depending on whether it is forward or reverse biased. Because of this characteristic, these circuits are termed switching-type mixers.

Switching-type mixers can be divided into two categories. In single-balanced mixers, the local oscillator or the RF input can be balanced out such that it does not appear in the output. On other hand, the output of a double-balanced mixer contains neither of the input frequencies.

Consider the single-balanced mixer circuit shown in Figure 12.19. The transformer and the diodes are assumed ideal for simplicity. Further, it is assumed that the local oscillator voltage v_L is a square-wave with large amplitude in comparison with v_i. Therefore, only the local oscillator signal determines the conduction through a given diode. An equivalent of this circuit is shown in Figure 12.20. When v_L is

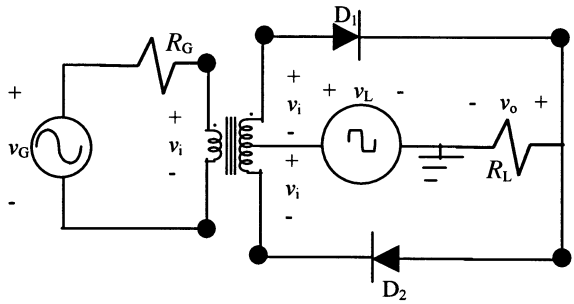

Figure 12.19 A switching-type single-balanced mixer.

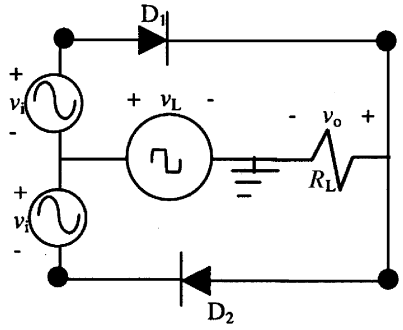

Figure 12.20 An equivalent of the circuit shown in Figure 12.19.

positive, diode D_1 is on and D_2 is off. The reverse is true if v_L switches to its negative polarity. Mathematically,

$$v_o = \begin{cases} v_L + v_i & v_L > 0 \\ v_L - v_i & v_L < 0 \end{cases}$$

or,

$$v_o = v_L + v_i' \tag{12.3.1}$$

where,

$$v_i' = v_i s(t) \tag{12.3.2}$$

$$s(t) = \begin{cases} 1 & v_L > 0 \\ -1 & v_L < 0 \end{cases} \tag{12.3.3}$$

Hence, the switching frequency of $s(t)$ is ω_L, same as the frequency of the local oscillator.

Using Fourier series representation, $s(t)$ may be expressed as follows:

$$s(t) = \frac{4}{\pi} \sum_{n=1}^{\infty} \frac{(-1)^{n+1}}{n} \sin\left(\frac{n\pi}{2}\right) \cos(n\omega_L t) \tag{12.3.4}$$

If v_i is a sinusoidal signal as given below

$$v_i = V \cos(\omega_i t)$$

then,

$$v_i' = \frac{2V}{\pi} \sum_{n=1}^{\infty} \frac{(-1)^{n+1}}{n} \sin\left(\frac{n\pi}{2}\right) [\cos\{(n\omega_L + \omega_i)t\} + \cos\{(n\omega_L - \omega_i)t\}] \tag{12.3.5}$$

Therefore, the output voltage can be expressed as follows:

$$v_o = v_L + v_i' = v_L + \frac{2V}{\pi} \sum_{n=1}^{\infty} \frac{(-1)^{n+1}}{n} \sin\left(\frac{n\pi}{2}\right) [\cos\{(n\omega_L + \omega_i)t\} + \cos\{(n\omega_L - \omega_i)t\}] \tag{12.3.6}$$

Thus, output consists of the local oscillator frequency ω_L and an infinite number of sum and difference frequencies of ω_i with odd multiples of ω_L. Frequency components $\omega_L + \omega_i$ and $\omega_L - \omega_i$ represent the upper and lower sidebands, respectively, each with amplitudes equal to $2V/\pi$. These components can be separated from the other higher-order terms, known as *spurious signals*.

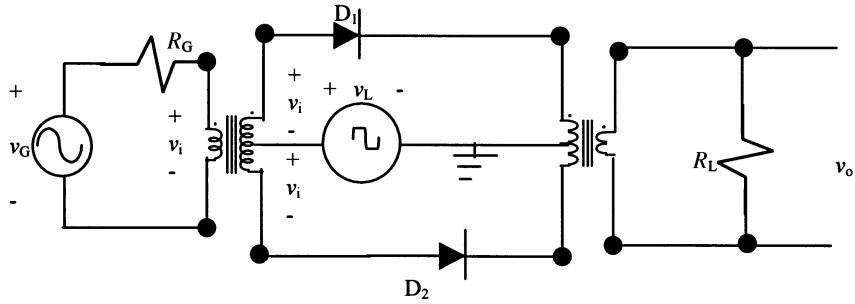

Figure 12.21 Another switching-type single-balanced mixer.

Note that this formulation is based on the ideal switching characteristic of the diode. In other words, it assumes that the local oscillator instantaneously switches the diode current. Deviation from this characteristic increases the distortion in its output. A major disadvantage of this mixer circuit is that the local oscillator signal appears in its output. Frequency components ω_L and $\omega_L \pm \omega_i$ may be very close if the local oscillator frequency is high. In this situation, it may be difficult to separate these signals.

An alternative circuit that blocks the local oscillator signal from appearing at its output is depicted in Figure 12.21. As before, it can be easily analyzed by assuming that the diodes are ideal and the local oscillator voltage controls its switching. A simplified equivalent of this circuit is shown in Figure 12.22. In this circuit, both diodes conduct (on) when the local oscillator voltage is positive and they do not conduct (off) otherwise.

Hence, the output voltage v_o can be written as follows:

$$v_o = v_i s(t) \tag{12.3.7}$$

where,

$$s(t) = \begin{cases} 1 & v_L > 0 \\ 0 & v_L < 0 \end{cases} \tag{12.3.8}$$

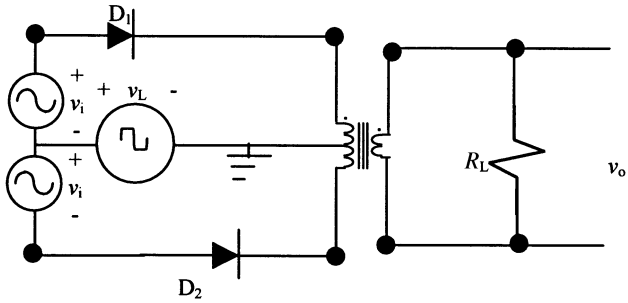

Figure 12.22 An equivalent of the single-balanced mixer shown in Figure 12.21.

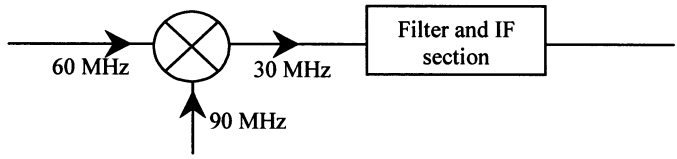

Figure 12.23 The single-balanced mixer of Figure 12.21 at the receiver.

This $s(t)$ can be expressed in terms of the Fourier series as follows:

$$s(t) = \frac{1}{2} + \sum_{n=1}^{\infty} \frac{2}{n\pi} \sin\left(\frac{n\pi}{2}\right) \cos(n\omega_L t) \tag{12.3.9}$$

For $v_i = V\cos(\omega_i t)$, the output voltage is found to be

$$v_o = \frac{V}{2}\cos(\omega_i t) + \frac{V}{\pi}\sum_{n=1}^{\infty} \frac{1}{n} \sin\left(\frac{n\pi}{2}\right)[\cos\{(n\omega_L + \omega_i)t\} + \cos\{(n\omega_L - \omega_i)t\}] \tag{12.3.10}$$

Thus, output of this mixer circuit does not contain the local oscillator signal. However, it includes the input signal frequency ω_i that appears with the sidebands and spurious signals. It can be a problem in certain applications. For example, consider a case where the input and the local oscillator signal frequencies at a receiver are 60 MHz and 90 MHz, respectively. As illustrated in Figure 12.23, the difference signal frequency at its output is 30 MHz. If there is a 30-MHz signal also present at the input, it will get through the mixer as well. A preselector (band-pass filter) may be used to suppress the undesired input.

Note from (12.3.10) that the amplitude of the sidebands is only V/π whereas it was twice this in (12.3.6). It influences the sensitivity of the receiver employing this mixer. In the following section, we consider another mixer circuit that solves most of these problems.

Double-Balanced Mixer

This mixer circuit requires four diodes and two transformers with secondary sides center-tapped, as shown in Figure 12.24. As before, it is assumed that the local oscillator voltage v_L is high in comparison with the input v. Hence, diodes D_1 and D_2 conduct when the local oscillator voltage is positive while the other two are in off state. This situation turns the other way around when the voltage v_L reverses its polarity.

Thus, diodes D_1 and D_2 conduct for positive half cycle of v_L while D_3 and D_4 conduct for the negative half. Equivalent circuits can be drawn separately for these two states. Figure 12.25 shows one such equivalent circuit that represents the case of positive v_L. Diode resistance in forward-biased condition is assumed to be r_d. The equivalent circuit can be simplified further to facilitate the analysis.

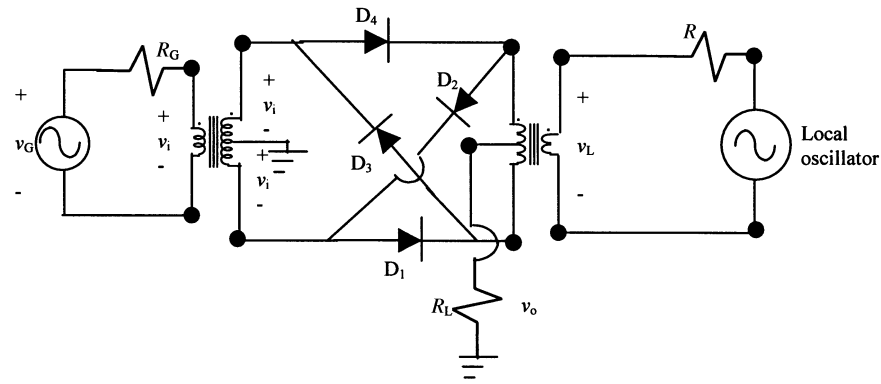

Figure 12.24 A switching-type double-balanced mixer.

Consider the simplified equivalent circuit shown in Figure 12.26. Currents in two loops are assumed as i_1 and i_2. Using Kirchhoff's voltage law, loop equations can be written as follows:

$$v_i = R_L(i_1 - i_2) + r_d i_1 - v_L \tag{12.3.11}$$

and,

$$v_i = R_L(i_1 - i_2) - r_d i_2 + v_L \tag{12.3.12}$$

Equations (12.3.11) and (12.3.12) can be solved for $i_1 - i_2$. Hence,

$$i_1 - i_2 = \frac{v_i}{R_L + \left(\frac{r_d}{2}\right)} \tag{12.3.13}$$

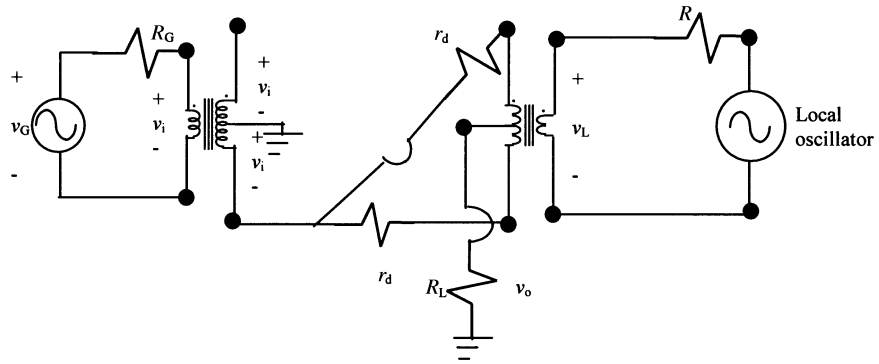

Figure 12.25 An equivalent of the double-balanced mixer with positive v_L.

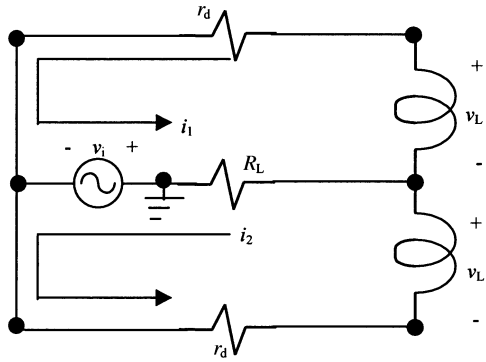

Figure 12.26 A simplified equivalent circuit of Figure 12.25.

But, from Ohm's law,

$$i_1 - i_2 = -\frac{v_o}{R_L} \tag{12.3.14}$$

Combining (12.3.13) and (12.3.14),

$$\frac{v_o}{v_i} = -\frac{R_L}{R_L + \left(\frac{r_d}{2}\right)} \tag{12.3.15}$$

Similarly, an equivalent circuit can be drawn for the negative half-cycle of v_L. Diodes D_3 and D_4 are conducting in this case, and following an identical analysis it may be easily found that

$$\frac{v_o}{v_i} = +\frac{R_L}{R_L + \left(\frac{r_d}{2}\right)} \tag{12.3.16}$$

Equations (12.3.15) and (12.3.16) can be expressed by a single equation after using the function $s(t)$ as defined earlier by (12.3.3). Hence,

$$v_o = \frac{R_L}{R_L + \left(\frac{r_d}{2}\right)} v_i' = \frac{R_L}{R_L + \left(\frac{r_d}{2}\right)} v_i s(t) \tag{12.3.17}$$

Now using the Fourier series representation for $s(t)$ as given in (12.3.4), (12.3.17) can be expressed as,

$$v_o = \frac{R_L}{R_L + \left(\frac{r_d}{2}\right)} v_i \frac{4}{\pi} \sum_{n=1}^{\infty} \frac{(-1)^{n+1}}{n} \sin\left(\frac{n\pi}{2}\right) \cos(n\omega_L t) \tag{12.3.18}$$

In case of a sinusoidal input, $v_i = V\cos(\omega_i t)$, the output voltage v_o can be found as

$$v_o = \frac{R_L}{R_L + \left(\frac{r_d}{2}\right)} \frac{2V}{\pi} \sum_{n=1}^{\infty} \frac{(-1)^{n+1}}{n} \sin\left(\frac{n\pi}{2}\right) [\cos\{(n\omega_L + \omega_i)t\} + \cos\{(n\omega_L - \omega_i)t\}] \tag{12.3.19}$$

Hence, this mixer circuit produces the upper and lower sidebands along with an infinite number of spurious signals. However, both ω_L and ω_i signals are isolated from the output. This analysis assumes that the diodes are perfectly matched and the transformers are ideal. Variations of these characteristics may not perfectly isolate the output from the input and the local oscillator. These double-balanced mixers are commercially available for application in audio through microwave frequency bands.

12.4 CONVERSION LOSS

Since mixers are used to convert the frequency of an input signal, a circuit designer would like to know if there is some change in its power as well. This information is especially important in receiver design where the received signal may be fairly weak. Conversion loss (or gain) of the mixer is defined as a ratio of the power output in one of the sidebands to the power of its input signal. It can be evaluated as follows.

Consider the double-balanced mixer circuit shown in Figure 12.24. Using its equivalent circuit as illustrated in Figure 12.26, the input resistance R_{in} can be found with the help of (12.3.13) as follows:

$$R_{in} = \frac{v_i}{i_1 - i_2} = R_L + \frac{r_d}{2} \approx R_L \tag{12.4.1}$$

It is assumed here that the resistance R_L is much larger in comparison with forward resistance r_d of the diode.

If there is maximum power transfer from the voltage source v_G at the input to the circuit then source resistance R_G must be equal to input resistance R_{in}. Since input resistance is equal to load R_L, the following condition must be satisfied

$$R_G = R_L$$

If the sinusoidal source voltage v_G has a peak value of V_P then it divides between two equal resistances R_G and R_{in}, and only half of voltage V_P appears across the transformer input. Hence,

$$P_i = \frac{V_P^2}{8R_L} \tag{12.4.2}$$

From (12.3.19), peak output voltage V_o of the sideband is

$$V_o\Big|_{\omega_L \pm \omega_i} = \frac{2V}{\pi} = \frac{V_P}{\pi} \tag{12.4.3}$$

Therefore, output power P_o is found as

$$P_o = \frac{V_P^2}{2\pi^2 R_L} \tag{12.4.4}$$

If G is defined as the conversion gain that is a ratio of its output to input power then from (12.4.2) and (12.4.4) we find that

$$G = \frac{P_o}{P_i} = \frac{V_P^2}{2\pi^2 R_L} \times \frac{8R_L}{V_P^2} = \frac{4}{\pi^2} \tag{12.4.5}$$

Since G is less than unity, it is really not a gain but a loss of power. Hence, the conversion loss, L, is

$$L = 10 \log\left(\frac{\pi^2}{4}\right) = 3.92 \text{ dB} \approx 4 \text{ dB} \tag{12.4.6}$$

Hence, approximately 40 per cent power of the input signal is transferred to the output of an ideal double-balanced mixer. Circuit loss and mismatch reduce it further.

In the case of a single-balanced mixer where the local oscillator is isolated from the output, the sideband voltage can be found from (12.3.10). Hence, the power output in one of the sidebands is given as follows:

$$P_o = \frac{1}{2R_L}\left(\frac{V}{\pi}\right)^2 = \frac{V_P^2}{8\pi^2 R_L} \tag{12.4.7}$$

Since the input power is still given by (12.4.2), its conversion gain may be found as follows:

$$G = \frac{P_o}{P_i} = \frac{V_s^2}{8\pi^2 R_L} \times \frac{8R_L}{V_s^2} = \frac{1}{\pi^2} \tag{12.4.8}$$

Again, the output is less than the input power, and therefore, it represents a loss of signal power. The conversion loss for this case is

$$L = 10 \log(\pi^2) = 9.943 \approx 10 \text{ dB} \tag{12.4.9}$$

Hence, the conversion loss in this single-balanced mixer is 6 dB (four times) larger than that of the double-balanced mixer considered earlier. It may be noted that the mixer circuit shown in Figure 12.19 has a conversion loss of only 4 dB.

These results show that maximum possible power transferred from the input to the output of a diode mixer is less than 40 per cent. Therefore, these circuits always have conversion loss. A conversion gain is possible only when a transistor (BJT or FET) circuit is used as the mixer. FET mixers are briefly described later in this chapter.

12.5 INTERMODULATION DISTORTION IN DIODE-RING MIXERS

As discussed in Chapter 2, the noise level defines the lower end of the dynamic range of a system whereas the distortion determines its upper end. Therefore, a circuit designer needs to know the distortion introduced by the mixer and whether there is some way to limit that. We consider here the mixer circuit depicted in Figure 12.27, which has a resistance R in series with each diode.

Assuming v_L is large enough such that the local oscillator solely controls the conduction through the diodes, an equivalent circuit can be drawn for each half cycle. In the case of a positive half period of v_L, the simplified equivalent circuit may be drawn as illustrated in Figure 12.28. Diodes D_1 and D_2 conduct for this duration while the other two are in off state. Assume that i_L is current due to v_L and i is due to v_i. Hence, currents through the diodes are given as follows:

Current through diode $D_1 = i_{d3} = i_L - i$.
Current through diode $D_2 = i_{d4} = i_L + i$.

Since the V–I characteristic of a diode is given as follows:

$$i_d = I_s(e^{\alpha v_d} - 1) \approx I_s e^{\alpha v_d} \tag{12.5.1}$$

where

$$\alpha = \frac{q}{nkT} \tag{12.5.2}$$

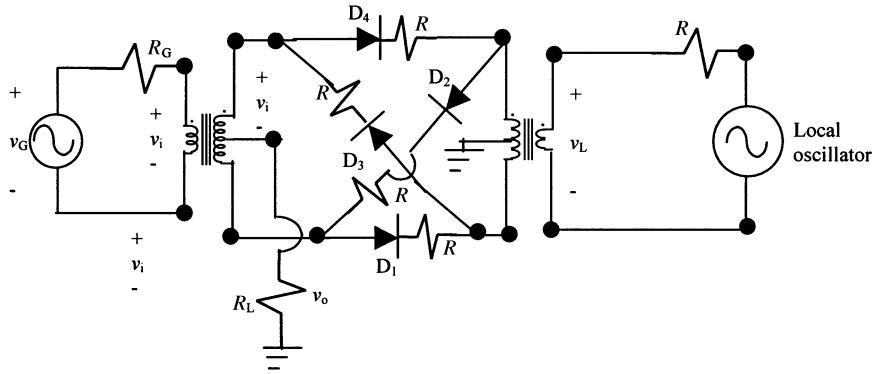

Figure 12.27 A mixer circuit with resistance R in each branch.

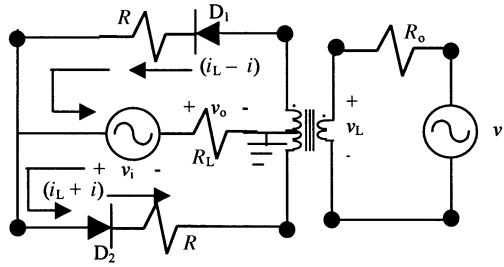

Figure 12.28 A simplified equivalent of the circuit shown in Figure 12.27 for $v_L > 0$.

we find that

$$v_d = \frac{1}{\alpha}\ln\left(\frac{i_d}{I_s}\right) \tag{12.5.3}$$

Note that net current flowing through the load resistance R_L is the difference of two loop currents, namely, $(i_L - i)$ and $(i_L + i)$. Hence, the LO current through R_L cancels out whereas two components of current due to v_i are added to make it $2i$. Loop equations for the circuit can be found to be

$$v_L = (i_L - i)R + v_{d3} + v_i - R_L 2i \tag{12.5.4}$$

and,

$$v_L = R_L 2i - v_i + R(i_L + i) + v_{d4} \tag{12.5.5}$$

Subtracting (12.5.5) from (12.5.4), we have,

$$0 = -2(R + 2R_L)i + 2v_i + v_{d3} - v_{d4}$$

or,

$$2(R + 2R_L)i - 2v_i = \frac{1}{\alpha}\left\{\ln\left(\frac{i_L - i}{I_s}\right) - \ln\left(\frac{i_L + i}{I_s}\right)\right\} = -\frac{1}{\alpha}\ln\left(\frac{i_L + i}{i_L - i}\right)$$

or,

$$v_i = (R + 2R_L)i + \frac{1}{2\alpha}\ln\left(\frac{i_L + i}{i_L - i}\right) \tag{12.5.6}$$

Since the LO current i_L is very large in comparison with i, it can be expanded as an infinite series

$$v_i = \left(R + 2R_L + \frac{1}{\alpha i_L}\right) i + \frac{1}{3\alpha i_L^3} i^3 + \frac{1}{5\alpha i_L^5} i^5 + \cdots \tag{12.5.7}$$

An inverse series solution to this can be easily found with the help of computer software (such as Mathematica®), as follows:

$$i = \frac{v_i}{R + 2R_L + \dfrac{1}{\alpha i_L}} - \frac{v_i^3}{3\alpha i_L^3 \left(R + 2R_L + \dfrac{1}{\alpha i_L}\right)^4} + \cdots \tag{12.5.8}$$

Therefore, the output voltage v_o can be written as follows.

$$v_o = 2R_L i = 2R_L \left[\frac{v_i}{R + 2R_L + \dfrac{1}{\alpha i_L}} - \frac{v_i^3}{3\alpha i_L^3 \left(R + 2R_L + \dfrac{1}{\alpha i_L}\right)^4} + \cdots \right] \tag{12.5.9}$$

On comparing it with (2.5.31), we find that the term responsible for the intermodulation distortion (IMD) is

$$k_3 = -\frac{2R_L}{3\alpha i_L^3 \left(R + 2R_L + \dfrac{1}{\alpha i_L}\right)^4} \tag{12.5.10}$$

Since the IMD is directly proportional to the cube of k_3, (12.5.10) must be minimized to reduce the intermodulation distortion. One way to achieve this objective is to use a large local oscillator current i_L. Another possible way is to employ the resistance R in series with each diode. Sometimes an additional diode is used in place of R. This permits higher local oscillator drive levels and a corresponding reduction in IMD.

Example 12.4: In the mixer circuit shown below, transformer and diodes are ideal. The transformer has 400 turns on its primary and 800 turns with a center-tap on its secondary side. Find the output voltage and the value of load R_L that provides

maximum power transfer from v_s.

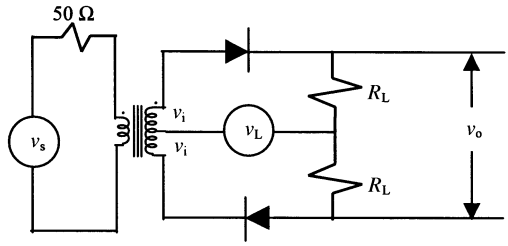

For maximum power transfer, the impedance when transformed to the primary side of the transformer must be equal to 50 Ω. Since number of turns on either side of the center-tap is the same as on its primary side and only one of the diodes is conducting at a given time, load resistance R_L must be 50 Ω as well. Under this condition, only half of the signal-voltage appears across the primary. Hence, $v_i = v_s/2$.

Assume that v_L is large in comparison with v_i such that the diode switching is controlled solely by the local oscillator. Therefore,

$$v_o = \begin{cases} (v_L + v_i) & \text{for } v_L > 0 \\ -(v_L + v_i) & \text{for } v_L < 0 \end{cases}$$

This output voltage can be expressed as follows:

$$v_o = (v_L + v_i)s(t)$$

where,

$$s(t) = \begin{cases} 1 & v_L > 0 \\ -1 & v_L < 0 \end{cases}$$

We already know the Fourier series representation for this $s(t)$, given by (12.3.4) as

$$s(t) = \frac{4}{\pi}\sum_{n=1}^{\infty}\frac{(-1)^{n+1}}{n}\sin\left(\frac{n\pi}{2}\right)\cos(n\omega_L t) \tag{12.3.4}$$

If v_i and v_s are sinusoidal voltages given as follows:

$$v_i = V_i\cos(\omega_i t)$$

and,

$$v_L = V_L\cos(\omega_L t)$$

then the output voltage will be

$$v_o = [V_i \cos(\omega_i t) + V_L \cos(\omega_L t)]\frac{4}{\pi}\sum_{n=1}^{\infty}\frac{(-1)^{n+1}}{n}\sin\left(\frac{n\pi}{2}\right)\cos(n\omega_L t)$$

or,

$$v_o = \frac{2}{\pi}\sum_{n=1}^{\infty}\frac{(-1)^{n+1}}{n}\sin\left(\frac{n\pi}{2}\right)\left[\begin{array}{c} V_i\{\cos(n\omega_L + \omega_i)t + \cos(n\omega_L - \omega_i)t\} \\ +V_L\{\cos(n\omega_L + \omega_L)t + \cos(n\omega_L - \omega_L)t\} \end{array}\right]$$

12.6 FET MIXERS

Diodes are commonly used in mixer circuits because of certain advantages, including a relatively low noise. A major disadvantage of these circuits is the conversion loss that cannot be reduced below 4 dB. On the other hand, transistor circuits can provide a conversion gain although they may be noisier. A well-designed FET mixer produces less distortion in comparison with BJT circuits. Further, the range of its input voltage is generally much higher (ten times or so) with respect to BJT mixers. The switching and resistive types of mixer have been designed using the FET. This section presents an overview of selected FET mixer circuits.

Figure 12.29 shows a FET mixer circuit. Local oscillator signal v_L is applied to the source terminal of the FET via a capacitor C_1 while the input v_i is connected to its gate. For the FET operating in saturation, we can write

$$i_D = I_{DSS}\left(1 - \frac{V_{gs}}{V_P}\right)^2 \tag{12.6.1}$$

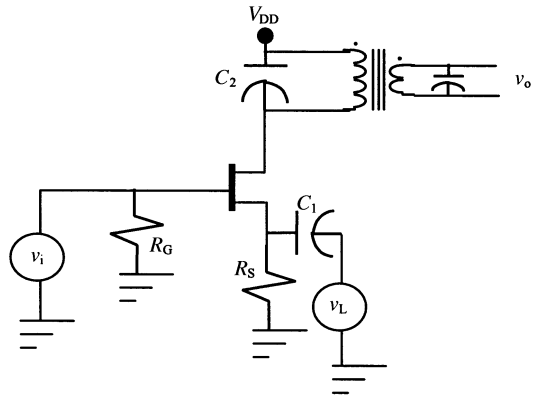

Figure 12.29 FET mixer circuit.

where i_D is the drain current of the FET; V_{gs} is the gate-to-source voltage; V_P is its pinch-off voltage; and I_{DSS} is drain current for $V_{gs} = 0$.

For the circuit shown in Figure 12.29, total gate voltage V_{gs} is given as follows:

$$V_{gs} = v_i - v_L + V_{GS}$$

where V_{GS} is gate-to-source dc bias voltage.

Therefore, the drain current i_D in this case is

$$i_D = I_{DSS}\left(1 - \frac{v_i - v_L + V_{GS}}{V_p}\right)^2 \tag{12.6.2}$$

For sinusoidal v_i and v_L given as follows:

$$v_i = V_i \cos(\omega_i t)$$

and,

$$v_L = V_L \cos(\omega_L t)$$

the drain current i_D can be found from (12.6.2). Hence,

$$i_D = I_{DSS}\left[1 - \frac{V_i \cos(\omega_i t) - V_L \cos(\omega_L t) + V_{GS}}{V_p}\right]^2$$

or,

$$\begin{aligned} i_D =& I_{DSS}\left[1 - \frac{2}{V_p}\{V_i \cos(\omega_i t) - V_L \cos(\omega_L t) + V_{GS}\}\right] \\ &+ \frac{I_{DSS}}{V_p^2}\{V_{GS}^2 + 2V_{GS}V_i \cos(\omega_i t) + V_i^2 \cos^2(\omega_i t) - 2V_L V_{GS} \cos(\omega_L t) \\ &+ V_L^2 \cos^2(\omega_L t) - 2V_i V_L \cos(\omega_i t)\cos(\omega_L t)\} \end{aligned} \tag{12.6.3}$$

Equation (12.6.3) can be rearranged in the following form and then the amplitudes of sum and difference frequency components can be easily identified as follows:

$$\begin{aligned} i_D = I_{DC} &+ a_1 \cos(\omega_i t) + a_2 \cos(\omega_L t) + b_1 \cos(2\omega_i t) + 2\cos(2\omega_L t) \\ &- c[\cos\{(\omega_L + \omega_i)t\} + \cos\{(\omega_L - \omega_i)t\}] \end{aligned}$$

where,

$$c = \frac{I_{DSS} V_i V_L}{V_p^2} \tag{12.6.4}$$

Ratio of amplitude c and input voltage V_i is defined as *conversion transconductance* g_c. Hence,

$$g_c = \frac{c}{V_i} = \frac{I_{DSS} V_L}{V_p^2} \tag{12.6.5}$$

For high conversion gain, g_c must be large. It appears from (12.6.5) that the FET with high I_{DSS} should be preferable, but that is generally not the case. I_{DSS} and V_p of a FET are related in such a way that the device with high I_{DSS} also has high V_P. Therefore, it may result in a lower g_c than a low I_{DSS} device. V_L is directly related to the conversion gain. Hence, higher local oscillator voltage increases the conversion gain. Since the FET is to be operated in its saturation mode (the constant current region), V_L must be less than the magnitude of the pinch-off voltage.

As a special case, if $V_L = |V_P|/2$ then the conversion transconductance may be found as

$$g_c = \frac{I_{DSS}}{2V_p} \tag{12.6.7}$$

Since the transconductance g_m of a JFET is given as

$$g_m = \frac{\partial i_D}{\partial V_{GS}} = -\frac{2I_{DSS}}{V_p}\left(1 - \frac{V_{GS}}{V_p}\right) \tag{12.6.8}$$

and,

$$g_m\Big|_{V_{GS}=0} = -\frac{2I_{DSS}}{V_p} \tag{12.6.9}$$

the conversion transconductance is one-fourth of the small-signal transconductance evaluated at $V_{GS} = 0$ (provided that $V_L = 0.5\ V_p$). For a MOSFET, it can be shown that the conversion transconductance cannot exceed one-half of the small-signal transconductance.

Note from (12.6.3) that there are fundamental terms of input as well as local oscillator frequencies, their second-order harmonics, and the desired $\omega_i \pm \omega_L$ components. Unlike the diode mixer, higher-order spurious signals are not present in this output. In reality, there is some possibility for those terms to be present because of the circuit imperfections.

An alternative to the circuit shown in Figure 12.29 combines the local oscillator signal with the input before applying it to the gate of FET. The analysis of this circuit is similar to the one presented above. In either case, one of the serious problems is the isolation among the three signals. There have been numerous attempts to address those problems.

Example 12.5: A given JFET has $I_{DSS} = 50$ mA and transconductance $g_m = 200$ mS when its gate voltage V_{GS} is zero. If it is being used in a mixer that has a 50-Ω load, find the conversion gain of the circuit.

Since

$$g_m\Big|_{V_{GS}=0} = -\frac{2I_{DSS}}{V_p}$$

then

$$V_p = \frac{2 \times 50 \times 10^{-3}}{200 \times 10^{-3}} = \frac{1}{2} = 0.5 \text{ V}$$

If the local oscillator voltage v_L is kept at approximately 0.25 V then the conversion transconductance g_c may be found as follows:

$$g_c = \frac{50 \times 10^{-3}}{2 \times 0.5} = 50 \times 10^{-3} \text{ S} = 50 \text{ mS}$$

Therefore, the magnitude of voltage gain A_v is

$$A_v \approx g_c R_L = 50 \times 10^{-3} \times 50 = 2.5$$

Since common-gate configuration of the FET is generally used in the mixer circuit, its current gain is close to unity. Therefore, the conversion power gain of this circuit is approximately 2.5.

The dual-gate FET is frequently employed in a mixer circuit. There are several circuit configurations and modes of operation of dual-gate FET mixers. Figure 12.30 illustrates a circuit that usually performs well in most receiver designs. The working of this circuit can be explained considering that a dual-gate FET represents two single-gate transistors connected in cascode. Hence, the upper FET works as a source follower and the lower one provides mixing. RF signal is applied to a gate that is close to the ground while the local oscillator is connected at the other gate (one close to the drain in common-source configuration). If RF is connected to the other gate then the drain resistance of the lower transistor section appears as source resistance and thus reduces the signal.

This circuit is used as a mixer when both transistors are operating in their triode (non saturation) mode. A bypass circuit is needed before its output to block the input (RF) and the local oscillator signals. Further, another bypass circuit may be needed

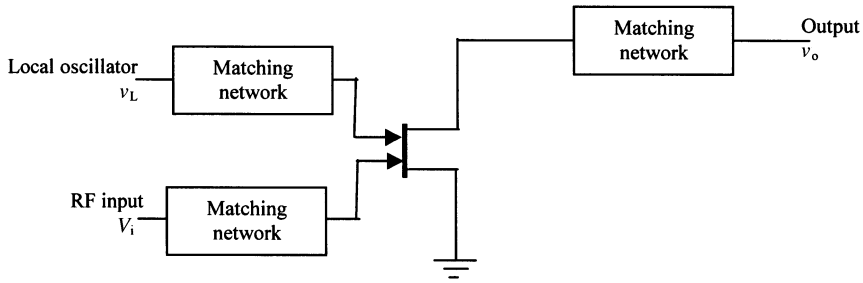

Figure 12.30 A dual-gate FET mixer.

across the local oscillator to block the output frequencies. This circuit has lower gain and higher noise but a properly designed mixer can achieve modestly higher third-harmonic intercept in comparison with the single-gate mixer.

Figure 12.31 shows a FET mixer circuit that employs two transistors and transformers. Local oscillator signal is applied to both transistors in the same phase while one RF input is out of phase with respect to the other. Resulting output is a differential of the two sides, and therefore, the local oscillator signal is canceled out while the RF is added. The nonlinear characteristic of the transistors generates the upper and the lower sideband signals.

If the dc bias voltage at the source is V_S; the RF input is $V_i \cos(\omega_i t)$, and the local oscillator voltage is $V_L \cos(\omega_L t)$, then the output voltage of this circuit is given as follows:

$$v_o = \left\{\frac{4R_L V_i}{V_P} + \frac{4R_L V_i V_S}{V_P^2}\right\} \cos(\omega_i t) + \frac{2R_L V_i V_L}{V_P^2} \{\cos(\omega_L + \omega_i)t + \cos(\omega_L - \omega_i)t\} \tag{12.6.10}$$

This shows that the output of this circuit contains the RF input frequency along with two sidebands. Asymmetry and other imperfection can add more frequency components as well.

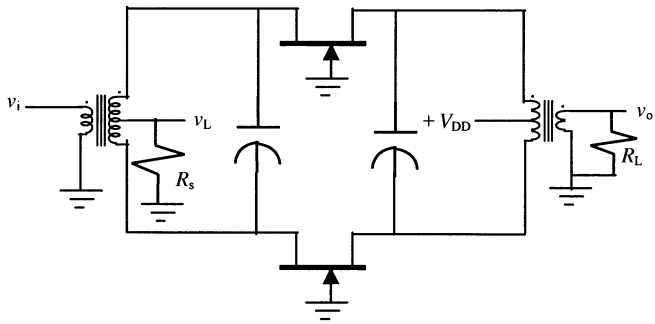

Figure 12.31 FET balanced mixer.

SUGGESTED READING

Bahl, I. J., and Bhartia, P., *Microwave Solid State Circuit Design*. New York: Wiley, 1988.

Collin, R. E., *Foundations for Microwave Engineering*. New York: McGraw Hill, 1992.

Larson, L. E. (Editor), *RF and Microwave Circuit Design for Wireless Communications*, Boston: Artech House, 1996.

Maas, S. A., *Microwave Mixers*. Boston: Artech House, 1993.

Pozar, D. M., *Microwave Engineering*. New York: Wiley, 1998.

Rohde, U. L., *Microwave and Wireless Synthesizers*. New York: Wiley, 1997.

Smith, J. R., *Modern Communication Circuits*. New York: McGraw Hill, 1998.

Vendelin, G. D., Pavio, A., and Rhode, U. L., *Microwave Circuit Design Using Linear and Non-linear Techniques*. New York: Wiley, 1990.

PROBLEMS

1. In the amplitude-modulated signal, the carrier output is 1-kW. If wave modulation is 100 per cent, determine the power in each sideband. How much power is being transmitted?

2. Assume that an AM transmitter is modulated with a video signal given by $m(t) = -0.15 + 0.7\sin(\omega_1 t)$ where f_1 is 4 MHz. Let the unmodulated carrier amplitude be 100 V. Evaluate and sketch the spectrum of the modulated signal.

3. An AM broadcast station that uses 95 per cent modulation is operating at total output power of 100 kW. Find the transmitted power in its sidebands.

4. With modulation index of 80 per cent, an AM transmitter produces 15 kW. How much of this is carrier power? Find the percentage power saving if the carrier and one of the sidebands are suppressed before transmission.

5. When an AM station transmits an unmodulated carrier, the current through its antenna is found to be 10 A. It increases to 12 A with a modulated signal. Determine the modulation index used by the station.

6. A 1-MHz carrier signal is simultaneously amplitude modulated with 300-Hz, 800-Hz, and 2-kHz sinusoidal signals. What are the frequencies present in the output?

7. An AM broadcast transmitter radiates 50 kW of carrier power. If the modulation index is 0.85 then find the radiated power.

8. A FM broadcast station uses a 10-kHz audio signal of 2-V peak value to modulate the carrier. If allowed frequency deviation is 20 kHz, determine its bandwidth requirement.

9. A frequency modulator is supplied with a carrier of 10 MHz and a 1.5-kHz audio signal of 1 V. The frequency deviation at its output is found to be ± 9 kHz.

(a) FM wave from the modulator is passed through a series of frequency multipliers with a total multiplication of 15 (i.e., $f_o = 15f_c$). Determine the frequency deviation at the output of the multiplier.

(b) Output of the modulator is mixed with a 58-MHz signal. Find the sum frequency output of the mixer and its frequency deviation.

(c) Find the modulation index at the output of the modulator.

(d) Audio input to the modulator is changed to 500 Hz with its amplitude at 2 V. Determine the modulation index and frequency deviation at the output of the modulator.

10. A frequency-modulated signal, given below, is applied to a 75-Ω antenna. Determine

(a) the carrier frequency

(b) the transmitted power

(c) the modulation index

(d) the frequency of the modulating signal.

$$v_{FM}(t) = 1500 \times \cos\{2\pi \times 10^9 t + 2\sin(3\pi \times 10^5)\}\ \text{V}$$

11. When the modulating frequency in FM is 400 Hz and the modulating voltage is 2.4 V, the modulation index is 60. Calculate the maximum deviation in frequency. What is the modulation index when the modulating frequency is reduced to 250 Hz and the modulating voltage is simultaneously raised to 3.2 V?

12. The $i_D - V_{gs}$ characteristics of a FET are given by the following equation. If it is being used in a mixer that has a 50-Ω load, find the conversion gain of the circuit

$$i_D = 7\left(1 - \frac{2 \cdot V_{gs}}{7}\right)^2 \text{ mA}$$

13. Calculate the conversion loss of the double-balanced mixer shown below. The diode on-resistance is much less than the load resistance R_L. What value of R_L is required for maximum power transfer if the transformer employed in the circuit has 400 turns in its primary and 800 turns with a center-tap on its secondary side?

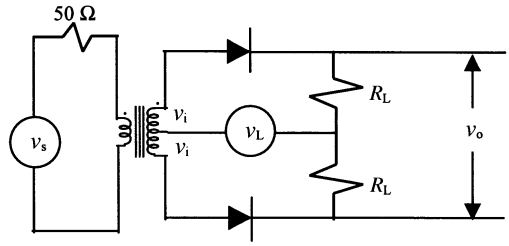

14. In the mixer circuit shown below, transformer and diodes are ideal. The transformer has 200 turns on each side. Find the value of R_L that provides maximum power transfer from the source

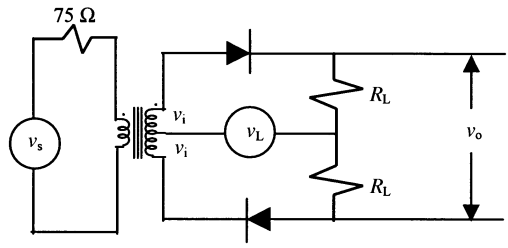

Radio-Frequency and Microwave Communication Circuits: Analysis and Design
Devendra K. Misra

ISBNs: 0-471-41253-8 (Hardback); 0-471-22435-9 (Electronic)

APPENDIX 1

DECIBELS AND NEPER

Consider a two-port network shown in Figure A1.1. Assume that V_1 and V_2 are the voltages at its ports. The voltage gain (or loss) G_v of this circuit is expressed in dB as follows:

$$G_v = 20 \log_{10}\left(\frac{V_2}{V_1}\right) \text{dB} \tag{A1.1}$$

Similarly, if P_1 and P_2 are the power levels at the two ports then the power gain (or loss) of this circuit in dB is given as

$$G_p = 10 \log_{10}\left(\frac{P_2}{P_1}\right) \text{dB} \tag{A1.2}$$

Thus, the dB unit provides a relative level of the signal. For example, if we are asked to find P_2 in watts for G_p as 3 dB then we also need P_1. Otherwise, the only information we can deduce is that P_2 is twice P_1.

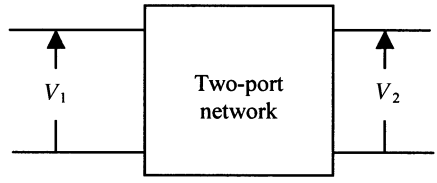

Figure A1.1 A two-port network.

Sometimes power is expressed in logarithmic units, such as dBW and dBm. These units are defined as follows. If P is power in watts then it can be expressed in dBW as

$$G = 10\log_{10}(P)\,\text{dBW} \tag{A1.3}$$

On the other hand, if P is in mW then the corresponding dBm power is found as

$$G = 10\log_{10}(P)\,\text{dBm} \tag{A1.4}$$

Thus, the dBW and dBm units represent power relative to 1 W and 1 mW, respectively.

Another decibel unit that is commonly used to specify phase noise of an oscillator or strengths of various sidebands of a modulated signal is dBc. It specifies the signal strength relative to the carrier. Consider a 100-MHz oscillator that has an output power of -10 dBm. Suppose that its output power is -30 dBm in the frequency range of 105 MHz to 106 MHz, then power per Hz in the output spectrum is -90 dBm and the phase noise is -80 dBc.

In general, if amplitudes of the sideband and the carrier are given as V_2 and V_c, respectively, then the sideband in dBc is found as follows:

$$G_2 = 20\log\left(\frac{V_2}{V_c}\right) \tag{A1.5}$$

Consider now a one-meter-long transmission line with its attenuation constant α. If V_1 is the signal voltage at its input port then voltage V_2 at its output is given as follows:

$$|V_2| = |V_1|e^{-\alpha} \tag{A1.6}$$

Therefore, the voltage gain G_v of this circuit in neper is

$$G_v(\text{neper}) = \ln\left(\frac{|V_2|}{|V_1|}\right) = -\alpha\,\text{neper} \tag{A1.7}$$

On the other hand, G_v in dB is found to be

$$G_v(\text{dB}) = 20\log\left(\frac{|V_2|}{|V_1|}\right) = 20\log(e^{-\alpha}) = -20\alpha\log(e) = -8.6859\alpha\,\text{dB}$$

Therefore,

$$1\,\text{neper} = 8.6859\,\text{dB} \tag{A1.8}$$

The negative sign indicates that V_2 is smaller than V_1 and there is loss of signal.

Radio-Frequency and Microwave Communication Circuits: Analysis and Design
Devendra K. Misra

ISBNs: 0-471-41253-8 (Hardback); 0-471-22435-9 (Electronic)

APPENDIX 2

CHARACTERISTICS OF SELECTED TRANSMISSION LINES

COAXIAL LINE

Consider a coaxial line with its inner and outer conductor radii a and b, respectively, as illustrated in Figure A2.1. Further, ε_r is the dielectric constant of insulating material. The line parameters L, R, C, and G of this coaxial line are found as follows:

$$C = \frac{55.63\varepsilon_r}{\ln(b/a)} \quad \text{pF/m} \tag{A2.1}$$

and,

$$L = 200\ln(b/a) \quad \text{nH/m} \tag{A2.2}$$

If the coaxial line has small losses due to imperfect conductor and insulator, its resistance and conductance parameters can be calculated as follows:

$$R \approx 10\left[\frac{1}{a}+\frac{1}{b}\right]\sqrt{\frac{f_{(\text{GHz})}}{\sigma}} \quad \text{ohm/m} \tag{A2.3}$$

and,

$$G = \frac{0.3495\varepsilon_r f_{(\text{GHz})}\tan(\delta)}{\ln(b/a)} \quad \text{S/m} \tag{A2.4}$$

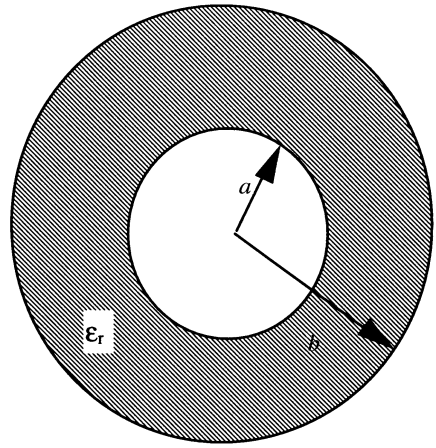

Figure A2.1 Coaxial line geometry.

where tan(δ) is loss-tangent of the dielectric material; σ is conductivity of the conductors in S/m; and $f_{(\mathrm{GHz})}$ is the signal frequency in GHz.

Characteristic impedance and propagation constant of the coaxial line can be easily calculated using the formulas given in Chapter 3.

Attenuation constants α_c and α_d due to conductor and dielectric losses, respectively, may be determined from the following formulas:

$$\alpha_c = \frac{R_s}{2\sqrt{\frac{\mu_o}{\varepsilon_o \varepsilon_r}} \ln\left(\frac{b}{a}\right)} \left(\frac{1}{a} + \frac{1}{b}\right) \tag{A2.5}$$

$$\alpha_d = \frac{\omega}{2} \sqrt{\mu_o \varepsilon_o \varepsilon_r} \tan \delta \tag{A2.6}$$

where,

$$R_s = \sqrt{\frac{\omega \mu_o}{2\sigma}} \tag{A2.7}$$

STRIP LINE

The strip line geometry is illustrated below in Figure A2.2. Insulating material of thickness h has a dielectric constant ε_r. Width and thickness of the central

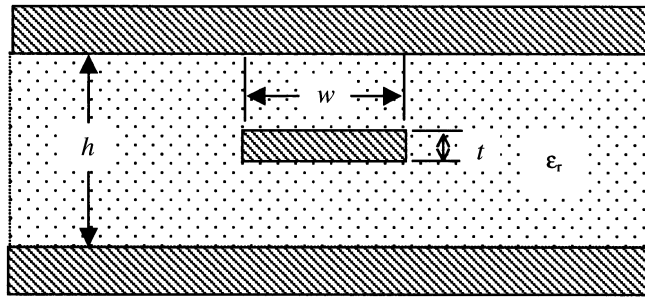

Figure A2.2 Strip line geometry.

conducting strip are w and t, respectively. For the case of $t = 0$, its characteristic impedance can be found as follows:

$$Z_o = \frac{1}{\sqrt{\varepsilon_r}} \begin{cases} 296.1\left(0.6931 + \ln\left[\dfrac{1+\sqrt{x'}}{1-\sqrt{x'}}\right]\right)^{-1} & 0 < x \le 0.7 \\ 30\left(0.6931 + \ln\left[\dfrac{1+\sqrt{x}}{1-\sqrt{x}}\right]\right) & 0.7 \le x < 1 \end{cases} \tag{A2.8}$$

$$x' = \tanh\left(\frac{\pi w}{2h}\right) \tag{A2.9}$$

and,

$$x = \sqrt{1 - x'^2} \tag{A2.10}$$

For the design of a strip line, the following convenient formulas can be used:

$$\frac{w}{h} = 0.6366 \tanh^{-1}(\sqrt{k}) \tag{A2.11}$$

where,

$$k = \begin{cases} \left(\dfrac{e^{\pi/y} - 2}{e^{\pi/y} + 2}\right)^2 & 0 \le y \le 1 \\ \sqrt{1 - \left(\dfrac{e^{\pi y} - 2}{e^{\pi y} + 2}\right)^4} & 1 \le y \end{cases} \tag{A2.12}$$

$$y = Z_o \frac{\sqrt{\varepsilon_r}}{94.18} \tag{A2.13}$$

For $t \neq 0$,

$$\frac{w}{h} = \Delta_1 - \Delta_2 \tag{A2.14}$$

$$\Delta_1 = 2.5465(1 - \Lambda)\frac{\sqrt{e^y + 0.568}}{e^y - 1} \tag{A2.15}$$

and

$$\Delta_2 = \frac{\Lambda}{\pi}\left[1 - 0.5 \ln\left\{\left(\frac{\Lambda}{2 - \Lambda}\right)^2 + \left(\frac{0.0796\Lambda}{\Delta_1 - 0.26\Lambda}\right)^{\delta}\right\}\right] \tag{A2.16}$$

where,

$$\Lambda = \frac{t}{h} \tag{A2.17}$$

$$\delta = \frac{2}{1 + \frac{2}{3}\frac{\Lambda}{1 - \Lambda}} \tag{A2.18}$$

and y is as defined in (A2.13).

MICROSTRIP LINE

The geometry of a microstrip line is illustrated in Figure A2.3. Dielectric substrate on the conducting ground is h meters high and its dielectric constant is ε_r. Width and

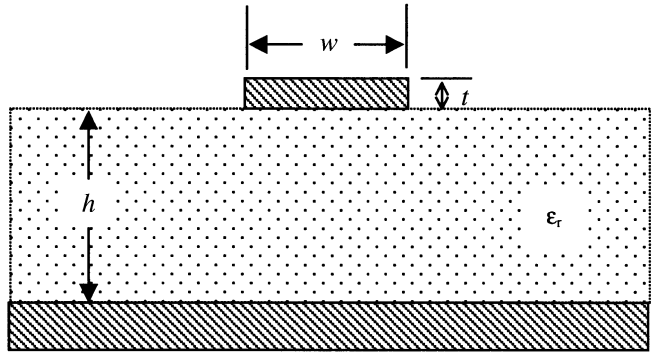

Figure A2.3 Microstrip line geometry.

thickness of the conducting strip on its top are w and t, respectively. Characteristic impedance of this line can be found as follows:

$$Z_o = \begin{cases} \dfrac{60}{\sqrt{\varepsilon_{re}}} \ln\left(\dfrac{8h}{w_e} + \dfrac{w_e}{4h}\right) & \text{for} \dfrac{w_e}{h} \le 1 \\ \dfrac{376.7}{\sqrt{\varepsilon_{re}}} \left[\dfrac{w_e}{h} + 1.393 + 0.667 \ln\left(\dfrac{w_e}{h} + 1.444\right)\right]^{-1} & \text{for} \dfrac{w_e}{h} \ge 1 \end{cases} \tag{A2.19}$$

where

$$\frac{w_e}{h} = \begin{cases} \dfrac{w}{h} + 0.3979 \dfrac{t}{h} \left\{1 + \ln\left(12.5664 \dfrac{w}{t}\right)\right\}, & \dfrac{w}{h} \le \dfrac{1}{2\pi} \\ \dfrac{w}{h} + 0.3979 \dfrac{t}{h} \left\{1 + \ln\left(2 \dfrac{h}{t}\right)\right\}, & \dfrac{w}{h} \ge \dfrac{1}{2\pi} \end{cases} \tag{A2.20}$$

The effective dielectric constant ε_{re} of a microstrip line ranges between ε_r and 1 because of its propagation characteristics. If the signal frequency is low such that the dispersion is not a problem then it can be determined as follows.

$$\varepsilon_{re} = 0.5\left[\varepsilon_r + 1 + (\varepsilon_r - 1) F\left(\frac{w}{h}\right)\right] - \frac{\varepsilon_r - 1}{4.6} \frac{t}{h} \sqrt{\frac{h}{w}} \tag{A2.21}$$

where,

$$F\left(\frac{w}{h}\right) = \begin{cases} \left(1 + 12 \dfrac{h}{w}\right)^{-0.5} + 0.04\left(1 - \dfrac{w}{h}\right)^2, & \dfrac{w}{h} \le 1 \\ \left(1 + 12 \dfrac{h}{w}\right)^{-0.5}, & \dfrac{w}{h} \ge 1 \end{cases} \tag{A2.22}$$

If dispersion cannot be ignored then the effective dielectric constant may be found as follows:

$$\varepsilon_{re}(f) = \left(\frac{\sqrt{\varepsilon_r} - \sqrt{\varepsilon_{re}}}{1 + 4F^{-1.5}} + \sqrt{\varepsilon_{re}}\right)^2 \tag{A2.23}$$

where,

$$F = \frac{40}{3} f_{(GHz)} h \sqrt{\varepsilon_r - 1} \left[0.5 + \left\{1 + 2 \log\left(1 + \frac{w}{h}\right)\right\}^2\right] \tag{A2.24}$$

The corresponding characteristic impedance is determined from the following formula

$$Z_o(f) = Z_o \frac{\varepsilon_{re}(f) - 1}{\varepsilon_{re} - 1} \sqrt{\frac{\varepsilon_{re}}{\varepsilon_{re}(f)}} \tag{A2.25}$$

Attenuation constants α_c and α_d for the conductor and dielectric losses, respectively, are determined as follows:

$$\alpha_c = \begin{cases} 9.9825 \dfrac{\zeta}{hZ_o} \sqrt{\dfrac{f_{(GHz)}}{\sigma}} \dfrac{32 - (w_e/h)^2}{32 + (w_e/h)^2} \quad \text{neper/m} & \dfrac{w}{h} \le 1 \\ 44.1255 \times 10^{-5} \dfrac{\zeta Z_o \varepsilon_{re}}{h} \sqrt{\dfrac{f_{(GHz)}}{\sigma}} \left\{ \dfrac{w_e}{h} + \dfrac{0.667\left(\dfrac{W_e}{h}\right)}{\dfrac{w_e}{h} = 1.444.} \right\} \quad \text{neper/m} & \dfrac{w}{h} \ge 1 \end{cases} \tag{A2.26}$$

where

$$\zeta = \begin{cases} 1 + \dfrac{h}{w_e}\left(1 + \dfrac{1.25t}{\pi w} + \dfrac{1.25}{\pi} \ln\left(4\pi \dfrac{w}{t}\right)\right) & \dfrac{w}{h} \le \dfrac{1}{2\pi} \\ 1 + \dfrac{h}{w_e}\left(1 - \dfrac{1.25t}{\pi h} + \dfrac{1.25}{\pi} \ln\left(2\dfrac{h}{t}\right)\right) & \dfrac{w}{h} \ge \dfrac{1}{2\pi} \end{cases} \tag{A2.27}$$

σ is conductivity of the conductor and $f_{(GHz)}$ is the signal frequency in GHz.

$$\alpha_d = 10.4766 \frac{\varepsilon_r}{\varepsilon_r - 1} \frac{\varepsilon_{re} - 1}{\sqrt{\varepsilon_{re}}} f_{GHz)} \tan\delta \quad \text{neper/m} \tag{A2.28}$$

For the design of a microstrip line that has negligible dispersion, the following formulas may be more convenient. For $A > 1.52$:

$$\frac{w}{h} = \frac{8e^A}{e^{2A} - 2} \tag{A2.29}$$

For $A \le 1.52$:

$$\frac{w}{h} = 0.6366\left[B - 1 - \ln(2B - 1) + \frac{\varepsilon_r - 1}{2\varepsilon_r}\left\{\ln(B - 1) + 0.39 - \frac{0.61}{\varepsilon_r}\right\}\right] \tag{A2.30}$$

where,

$$A = \frac{Z_o}{84.8528}\sqrt{(\varepsilon_r + 1)} + \frac{\varepsilon_r - 1}{(\varepsilon_r + 1)}\left(0.23 + \frac{0.11}{\varepsilon_r}\right) \tag{A2.31}$$

and

$$B = \frac{592.2}{Z_o\sqrt{\varepsilon_r}} \tag{A2.32}$$

Experimental verification indicates that (A2.29) and (A2.30) are fairly accurate as long as $\frac{t}{h} \leq 0.005$.

Radio-Frequency and Microwave Communication Circuits: Analysis and Design
Devendra K. Misra

ISBNs: 0-471-41253-8 (Hardback); 0-471-22435-9 (Electronic)

APPENDIX 3

SPECIFICATIONS OF SELECTED COAXIAL LINES AND WAVEGUIDES

TABLE A3.1 Selected Computer, Instrumentation, and Broadcast Cables

Cable type RG()	Insulation	Core O.D. (In.)	Cable O.D. (In.)	Z_o (Ω)	Capacitance (pF/ft)	Attenuation (dB/100 ft) at 400 MHz
8/U	Polyethylene	0.285	0.405	50	26.0	3.8
9/U	Polyethylene	0.280	0.420	51	30.0	4.1
11/U	Polyethylene	0.285	0.405	75	20.5	4.2
58/U	Polyethylene	0.116	0.195	53.5	28.5	9.5
59/U	Polyethylene	0.146	0.242	75	17.3	5.6
122/U	Polyethylene	0.096	0.160	50	30.8	16.5
141A/U	Teflon	0.116	0.190	50	29.0	9.0
142B/U	Teflon	0.116	0.195	50	29.0	9.0
174/U	Teflon	0.060	0.100	50	30.8	20.0
178B/U	Teflon	0.034	0.072	50	29.0	28.0
179B/U	Teflon	0.063	0.100	75	19.5	21.0
180B/U	Teflon	0.102	0.140	95	15.0	17.0
213/U	Polyethylene	0.285	0.405	50	30.8	4.7
214/U	Polyethylene	0.285	0.425	50	30.8	4.7
223/U	Polyethylene	0.116	0.206	50	30.8	10.0
316/U	Teflon	0.060	0.098	50	29.0	20.0

TABLE A3.2 Selected Semi-rigid Coaxial Lines

MIL-C-17F Designation	Nominal Impedance (Ω)	Dielectric Diameter (in)	Center Conductor Diameter (in)	Maximum Operating Frequency (GHz)	Capacitance (pF/ft)	Attenuation at 1 GHz (dB/100 ft)
129	50	0.209	0.0641	18	29.6	7.5
130	50	0.1175	0.0362	20	29.9	12
133	50	0.066	0.0201	20	32	22
151	50	0.037	0.0113	20	32	40
154	50	0.026	0.008	20	32	60

TABLE A3.3 Standard Rectangular Waveguides

EIA Nomenclature WR (−)	Inside Dimension (in.)	TE_{10} Mode Cutoff Frequency (GHz)	Recommended Frequency Band for TE_{10} Mode
2300	23.0 × 11.5	0.2565046	0.32–0.49
2100	21.0 × 10.5	0.2809343	0.35–0.53
1800	18.0 × 9.0	0.3277583	0.41–0.62
1500	15.0 × 7.5	0.3933131	0.49–0.75
1150	11.5 × 5.75	0.5130267	0.64–0.98
975	9.75 × 4.875	0.6051054	0.76–1.15
770	7.7 × 3.85	0.7662235	0.96–1.46
650	6.5 × 3.25	0.9077035	1.14–1.73
510	5.1 × 2.55	1.1569429	1.45–2.2
430	4.3 × 2.15	1.3722704	1.72–2.61
340	3.4 × 1.7	1.7357340	2.17–3.30
284	2.84 × 1.34	2.0782336	2.60–3.95
229	2.29 × 1.145	2.5779246	3.22–4.90
187	1.87 × 0.872	3.1530286	3.94–5.99
159	1.59 × 0.795	3.7125356	4.64–7.05
137	1.372 × 0.622	4.3041025	5.38–8.17
112	1.122 × 0.497	5.2660611	6.57–9.99
90	0.9 × 0.4	6.5705860	8.20–12.5
75	0.75 × 0.375	7.8899412	9.84–15.0
62	0.622 × 0.311	9.4951201	11.9–18.0
51	0.51 × 0.255	11.586691	14.5–22.0
42	0.42 × 0.17	14.088529	17.6–26.7
34	0.34 × 0.17	17.415732	21.7–33.0
28	0.28 × 0.14	21.184834	26.4–40.0
22	0.244 × 0.112	26.461666	32.9–50.1
19	0.188 × 0.094	31.595916	39.2–59.6
15	0.148 × 0.074	40.058509	49.8–75.8
12	0.122 × 0.061	48.54910	60.5–91.9
10	0.1 × 0.05	59.35075	73.8–112
8	0.08 × 0.04	74.44066	92.2–140
7	0.065 × 0.0325	91.22728	114–173
5	0.051 × 0.0255	116.47552	145–220
4	0.043 × 0.0215	137.93866	172–261
3	0.034 × 0.017	174.43849	217–330

Radio-Frequency and Microwave Communication Circuits: Analysis and Design
Devendra K. Misra

ISBNs: 0-471-41253-8 (Hardback); 0-471-22435-9 (Electronic)

APPENDIX 4

SOME MATHEMATICAL FORMULAS

$$\sin(A+B) = \sin A \cos B + \cos A \sin B$$

$$\sin(A-B) = \sin A \cos B - \cos A \sin B$$

$$\cos(A+B) = \cos A \cos B - \sin A \sin B$$

$$\cos((A-B) = \cos A \cos B + \sin A \sin B$$

$$\tan(A+B) = \frac{\tan A + \tan B}{1 - \tan A \tan B}$$

$$\tan(A-B) = \frac{\tan A - \tan B}{1 + \tan A \tan B}$$

$$\sin^2 A + \cos^2 A = 1$$

$$\tan^2 A + 1 = \sec^2 A$$

$$\cot^2 A + 1 = \mathrm{scs}^2 A$$

$$\sin A + \sin B = 2 \sin\left(\frac{A+B}{2}\right) \cos\left(\frac{A-B}{2}\right)$$

$$\sin A - \sin B = 2 \cos\left(\frac{A+B}{2}\right) \sin\left(\frac{A-B}{2}\right)$$

$$\cos A + \cos B = 2 \cos\left(\frac{A+B}{2}\right) \cos\left(\frac{A-B}{2}\right)$$

$$\cos A - \cos B = 2 \sin\left(\frac{A+B}{2}\right) \sin\left(\frac{B-A}{2}\right)$$

$$2\sin A\cos B = \sin(A+B) + \sin(A-B)$$
$$2\cos A\sin B = \sin(A+B) - \sin(A-B)$$
$$2\cos A\cos B = \cos(A+B) + \cos(A-B)$$
$$2\sin A\sin B = \cos(A-B) - \cos(A+B)$$

$$\sin\left(\frac{A}{2}\right) = \pm\sqrt{\frac{1-\cos A}{2}}$$
$$\sin 2A = 2\sin A\cos A$$
$$\cos 2A = \cos^2 A - \sin^2 A = 2\cos^2 A - 1 = 1 - 2\sin^2 A$$
$$\tan 2A = \frac{2\tan A}{1-\tan^2 A}$$

$$\cos\left(\frac{A}{2}\right) = \pm\sqrt{\frac{1+\cos A}{2}}$$

$$\tan\left(\frac{A}{2}\right) = \pm\sqrt{\frac{1-\cos A}{1+\cos A}} = \frac{\sin A}{1+\cos A} = \frac{1-\cos A}{\sin A}$$

$$e^{jA} = \cos A + j\sin A$$
$$e^{-jA} = \cos A - j\sin A$$
$$\sin A = \frac{e^{jA} - e^{-jA}}{2j} = A - \frac{A^3}{3!} + \frac{A^5}{5!} - \frac{A^7}{7!} + \cdots$$
$$\cos A = \frac{e^{jA} + e^{-jA}}{2j} = 1 - \frac{A^2}{2!} + \frac{A^4}{4!} - \frac{A^6}{6!} + \cdots$$
$$\tan A = j\frac{e^{jA} - e^{-jA}}{e^{jA} + e^{-jA}} = A + \frac{A^3}{3!} + 2\frac{A^5}{15!} + 17\frac{A^7}{315!} + \cdots$$

$$\sinh A = \frac{e^A - e^{-A}}{2}$$
$$\cosh A = \frac{e^A + e^{-A}}{2}$$
$$\tanh A = \frac{\sinh A}{\cos A} = \frac{e^A - e^{-A}}{e^A + e^{-A}}$$
$$\coth A = \frac{\cosh A}{\sinh A} = \frac{e^A + e^{-A}}{e^A - e^{-A}}$$
$$\sinh(A+B) = \sinh A\cosh B + \cosh A\sinh B$$
$$\cosh(A+B) = \cosh A\cosh B + \sinh A\sinh B$$
$$\sinh(A-B) = \sinh A\cosh B - \cosh A\sinh B$$

$$\cosh(A-B) = \cosh A \cosh B - \sinh A \sinh B$$

$$\tanh(A+B) = \frac{\tanh A + \tanh B}{1 + \tanh A \tanh B}$$

$$\tanh(A-B) = \frac{\tanh A - \tanh B}{1 - \tanh A \tanh B}$$

$$\cos(jA) = \cosh A$$

$$\sin(jA) = j \sinh A$$

$$\cosh^2 A - \sinh^2 A = 1$$

$$\sinh(jA) = j \sin A$$

$$\cosh(jA) = \cos A$$

$$\tanh(jA) = j \tan A$$

$$e^{A} = 1 + A + \frac{A^2}{2!} + \frac{A^3}{3!} + \frac{A^4}{4} + \cdots$$

$$e^{-A} = 1 - A + \frac{A^2}{2} - \frac{A^3}{3} + \frac{A^4}{4!} - \cdots$$

$$\sinh A = \frac{e^{A} - e^{-A}}{2} = A + \frac{A^3}{3!} + \frac{A^5}{5!} + \frac{A^7}{7!} + \cdots$$

$$\cosh A = \frac{e^{A} + e^{-A}}{2} = 1 + \frac{A^2}{2!} + \frac{A^4}{4!} + \frac{A^6}{6!} + \cdots$$

$$\log_a(xy) = \log_a(x) + \log_a(y)$$

$$\log_a\left(\frac{x}{y}\right) = \log_a(x) - \log_a(y)$$

$$\log_a(x^y) = y \log_a(x)$$

$$\log_a(x) = \log_b(x) \times \log_a(b) = \frac{\log_b(x)}{\log_b(a)}$$

$$\ln(x) = \log_{10}(x) \times \ln(10) = 2.302585 \times \log_{10}(x)$$

$$\log_{10}(x) = \ln(x) \times \log_{10}(e) = 0.434294 \times \ln(x)$$

$$e = 2.718281828$$

Radio-Frequency and Microwave Communication Circuits: Analysis and Design
Devendra K. Misra

ISBNs: 0-471-41253-8 (Hardback); 0-471-22435-9 (Electronic)

APPENDIX 5

PROPERTIES OF SOME MATERIALS

TABLE A5.1 Conductivity of Some Materials

Material	Conductivity in S/m
Aluminum	3.54×10^7
Brass	1.5×10^7
Bronze	1.0×10^7
Copper	5.813×10^7
Gold	4.1×10^7
Iron	1.04×10^7
Nichrome	0.09×10^7
Nickel	1.15×10^7
Silver	6.12×10^7
Stainless steel	0.11×10^7

TABLE A5.2 Dielectric Constant and Loss Tangent of Some Materials at 3 GHz

Material	Dielectric constant, ε_r	Loss tangent, $\tan \delta$
Alumina	9.6	0.0001
Glass (pyrex)	4.82	0.0054
Mica (ruby)	5.4	0.0003
Nylon (610)	2.84	0.012
Polystyrene	2.55	0.0003
Plexiglas	2.60	0.0057
Quartz (fused)	3.8	0.00006
Rexolite (1422)	2.54	0.00048
Styrofoam (103.7)	1.03	0.0001
Teflon	2.1	0.00015
Water (distilled)	77	0.157

Radio-Frequency and Microwave Communication Circuits: Analysis and Design
Devendra K. Misra

ISBNs: 0-471-41253-8 (Hardback); 0-471-22435-9 (Electronic)

APPENDIX 6

COMMON ABBREVIATIONS

ACTS:	advanced communication technology satellite
ADC:	analog-to-digital converter
ADPCM:	adaptive differential pulse code modulation
ADSL:	asymmetric digital subscriber line
AFC:	automatic frequency control
AGC:	automatic gain control
AM:	amplitude modulation
AMPS:	advanced mobile phone service
ARDIS:	advanced radio data information service
ATM:	asynchronous transfer mode
AWGN:	additive white Gaussian noise
B-CDMA:	broadcast CDMA
BER:	bit error rate
BIOS:	basic input-output system
BJT:	bipolar junction transistor
BPSK:	biphase shift keying
CCIR:	International Radio Consultative Committee
CDMA:	code division multiple access
CDPD:	cellular digital packet data
CIR:	carrier-over-interference ratio

CMOS: complementary metal-oxide semiconductor
CNR: carrier-over-noise ratio
Codec: coder-decoder
CRC: cyclic redundancy check
CSMA/CD: carrier sense multiple access with collision detection
CT: cordless telephone

DAC: digital-to-analog converter
DBS: direct broadcast satellite
DCE: data communication equipment
DCP: data communication protocol
DCS-1800: digital communication system 1800
DDS: direct digital synthesis
DECT: digital European cordless telecommunications
DIP: dual in-line package
DRO: dielectric resonator oscillator
DSMA: digital sensed multiple access

EIA: Electronics Industries Association
EIRP: effective isotropic radiated power
EMC: electromagnetic compatibility
ERC: European Radio Commission
ESDI: enhanced small device interface
ETN: electronic tandem network
ETSI: European Telecommunication Standard Institute

FCC: Federal Communications Commission
FDD: frequency division duplex
FDDI: fiber-distributed data interface
FDMA: frequency division multiple access
FET: field-effect transistor
FM: frequency modulation
FSK: frequency shift keying

GEO: geosynchronous satellite
GMSK: Gaussian-filtered minimum shift keying
GPIB: general-purpose interface bus
GPS: global positioning system
GSM: (Groupe Special Mobile) global system for mobile communication

HBT: heterojunction bipolar transistor
HDTV: high-definition television
HEMT: high-electron mobility transistor
HF: high frequency
HIPERLAN: high-performance radio LAN

IF: intermediate frequency
I and Q: in-phase and quadrature phase
IC: integrated circuits
IDE: integrated device electronics
IP: intermodulation product
IP: Internet protocol
IMPATT: impact ionization avalanche transit time diode
INTELSAT: International Telecommunication Satellite Consortium
ISDN: integrated services digital network
ISM: industrial, scientific, and medical bands
ITU: International Telecommunication Union

JDC: Japanese digital cellular standard
JFET: junction field-effect transistor
JPEG: Joint Photographic Experts Group

LAN: local area network
LATA: local access and transport area
LEOs: low-earth-orbit satellite
LHCP: left-hand circular polarization
LNA: 1ow noise amplifier
LO: local oscillator

MAN: metropolitan area network
MEOs: medium-earth-orbit satellite
MESFET: metal semiconductor field-effect transistor
MIDI: musical instrument digital interface
MMIC: monolithic microwave integrated circuit
MODFET: modulation doped field-effect transistor
MOSFET: metal-oxide semiconductor field-effect transistor
MPEG: Motion Picture Experts Group
MSS: mobile satellite service
MTI: moving target indicator

MTSO: mobile telephone switching office

NF: noise figure
NMT: Nordic Mobile Telephone
NTSC: National Television Standards Committee
NTT: Nippon Telephone and Telegraph

PAL: phase alternating line
PBX: private branch exchange
PCM: pulse code modulation
PCMCIA: Personal Computer Memory Card International Association
PCN: personal communication network
PCS: personal communication service
PHP: personal handy phone
PHS: personal handyphone system (formerly PHP)
PLL: phase-lock loop
POTS: plain old telephone service
PSTN: public switched telephone network
PVC: permanent virtual connection

QCELP: Qualcomm coded excited linear predictive coding
QDM: quadrature demodulator
QPSK: quadrature phase shift keying

RCS: radar cross section
RES: Radio Expert Systems Group
RF: radio frequency
RHCP: right-handed circular polarization
RMS: root mean square
RPE-LTP: regular pulse excitation long-term predictor
RTMS: radio telephone mobile system

SAW: surface acoustic wave
SCSI: small computer systems interface
SDH: synchronous digital hierarchy
SDN: switched digital network
SFDR: spur free dynamic range
SINAD: signal-over-noise and distortion
SMR: specialized mobile radio
SONET: synchronous optical network

TACS: total access communication system
TCP: transmission control protocol
TDD: time division duplex
TDMA: time division multiple access
TDR: time-domain reflectometry
TEM: transverse electromagnetic wave
TETRA: trans-European trunked radio system
TIA: Telecommunications Industry Association
TVRO: TV receive-only
TWTA: traveling wave tube amplifier

UDPC: universal digital personal communications
UHF: ultra-high frequency

VCO: voltage-controlled oscillator
VHF: very-high frequency
VLSI: very-large-scale integration
VSAT: very small aperture (satellite ground) terminal
VSELP: vector sum excited linear predictive coding
VSWR: voltage standing wave ratio

WAN: wide area network
WATS: wide area telecommunication network
WER: word error rate
WLAN: wireless local area network
WLL: wireless local loop

Radio-Frequency and Microwave Communication Circuits: Analysis and Design
Devendra K. Misra

ISBNs: 0-471-41253-8 (Hardback); 0-471-22435-9 (Electronic)

APPENDIX 7

PHYSICAL CONSTANTS

Permittivity of free-space, ε_o	8.8542×10^{-12} F/m
Permeability of free-space, μ_o	$4\pi \times 10^{-7}$ H/m
Impedance of free-space, η_o	376.7 Ω
Velocity of light in free space, c	2.997925×10^{8} m/s
Charge of electron, q_e	1.60210×10^{-19} C
Mass of electron, m_e	9.1091×10^{-31} kg
Boltzmann's constant, k	1.38×10^{-23} J/K
Planck's constant, h	6.6256×10^{-34} J-s

Radio-Frequency and Microwave Communication Circuits: Analysis and Design
Devendra K. Misra

ISBNs: 0-471-41253-8 (Hardback); 0-471-22435-9 (Electronic)

INDEX